EPA-650/2-73-033b

October 1973

Environmental Protection Technology Series

AERODYNAMIC CONTROL OF NITROGEN OXIDES AND OTHER POLLUTANTS FROM FOSSIL FUEL COMBUSTION

VOLUME II. RAW DATA AND EXPERIMENTAL EQUIPMENT

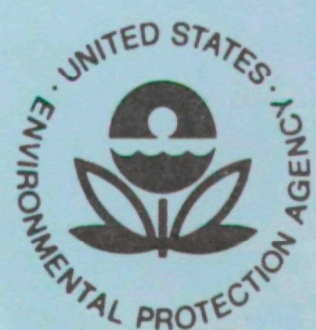

Office of Research and Development
U.S. Environmental Protection Agency
Washington, D.C. 20460

DISCLAIMER

This project has been funded at least in part with Federal funds from the Environmental Protection Agency under contract number 68-02-0216. The content of this publication does not necessarily reflect the views or policies of the U. S. Environmental Protection Agency, nor does mention of trade names, commercial products, or organizations imply endorsement by the U. S. Government.

EPA-650/2-73-033b

AERODYNAMIC CONTROL OF NITROGEN OXIDES AND OTHER POLLUTANTS FROM FOSSIL FUEL COMBUSTION

VOLUME II. RAW DATA AND EXPERIMENTAL EQUIPMENT

by

D.H. Larson and D.R. Shoffstall

Institute of Gas Technology
IIT Center, 3424 South State Street
Chicago, Illinois 60616

Contract No. 68-02-0216
Program Element No. 1A2014
ROAP No. 21ADG47

EPA Project Officer: David W. Pershing

Control Systems Laboratory
National Environmental Research Center
Research Triangle Park, North Carolina 27711

Prepared for

OFFICE OF RESEARCH AND DEVELOPMENT
U.S. ENVIRONMENTAL PROTECTION AGENCY
WASHINGTON, D.C. 20460

October 1973

This report has been reviewed by the Environmental Protection Agency and approved for publication. Approval does not signify that the contents necessarily reflect the views and policies of the Agency, nor does mention of trade names or commercial products constitute endorsement or recommendation for use.

TABLE OF CONTENTS

TABLE OF CONTENTS, Cont.

LIST OF FIGURES

LIST OF FIGURES, Cont.

LIST OF FIGURES, Cont.

LIST OF FIGURES, Cont.

LIST OF FIGURES, Cont.

LIST OF FIGURES, Cont.

LIST OF FIGURES, Cont.

LIST OF FIGURES, Cont.

LIST OF FIGURES, Cont.

LIST OF FIGURES, Cont.

LIST OF FIGURES, Cont.

LIST OF FIGURES, Cont.

LIST OF FIGURES, Cont.

LIST OF FIGURES, Cont.

LIST OF FIGURES, Cont.

LIST OF FIGURES, Cont.

LIST OF FIGURES, Cont.

LIST OF FIGURES, Cont.

LIST OF FIGURES, Cont.

LIST OF TABLES

LIST OF TABLES, Cont.

LIST OF TABLES, Cont.

LIST OF TABLES, Cont.

LIST OF TABLES, Cont.

LIST OF TABLES, Cont.

LIST OF TABLES, Cont.

INTRODUCTION

This volume of the final report for EPA Contract No. 68-02-0216 contains all of the raw data and data plots collected during the program. This volume also fully describes the experimental facilities. This includes dimensional descriptions of the hot-modeling furnace, the cold-modeling furnace simulator, sampling probes, instrumentation, and the test burners.

A companion publication (Volume I) presents a comparison of burner performance under varying operating conditions based on an analysis of the raw data. Volume I also contains specific recommendations for minimizing NO_x emissions from the burner types tested as well as for areas where further study will be required.

COLD-MODELING FURNACE SIMULATOR

A. Description of the Cold Test Chamber

A cold flow chamber was constructed which provided an aerodynamic simulation of flow in the hot test furnace. This facility provided a capability for examining the flow characteristics of each test burner under ambient temperature conditions. This information was necessary for determining the most effective sampling locations for the hot furnace test work.

The geometry and dimensions of the cold-modeling test facility were fixed by the dimensions of the available IGT hot-model furnace. This simplifies the similarity criteria necessary to apply cold-model results to the hot model. The cold-model facility has a cross-sectional area of 25 square feet (5 feet high and 5 feet wide). General aerodynamic considerations indicate that most of the pertinent flow phenomena should occur in the first 2-3 feet of the test chamber. However, the facility is specified as 10 feet long to allow studies to be made of potential downstream effects and to ensure that the gas exit stack will not influence the primary test area.

Figure II-1 shows the overall dimensions of the cold-model test facility, the type of construction used, and the location of the access ports for insertion of sampling probes. A lightweight steel framework was constructed to serve as support for the wall panels and various burners being tested. The framework is rigid and strong enough to ensure that the relative positions of the burner, confining walls, and sample probes remain constant to within 0.1 inch during testing. The floor of the cold-model facility was built of 0.250-inch-thick aluminum, supported every 24 inches by a steel channel superstructure. This construction enables the operator to work inside the test chamber without damage to the facility.

The sidewalls and roof panels of the first 6 feet of the facility were clear plastic (Plexiglas). The plastic walls provided good visibility where most of the test work was done. The plastic walls also provide the interior view of the chamber necessary for a photographic study of flow using tracers (smoke). The last 4 feet of the chamber sidewalls and

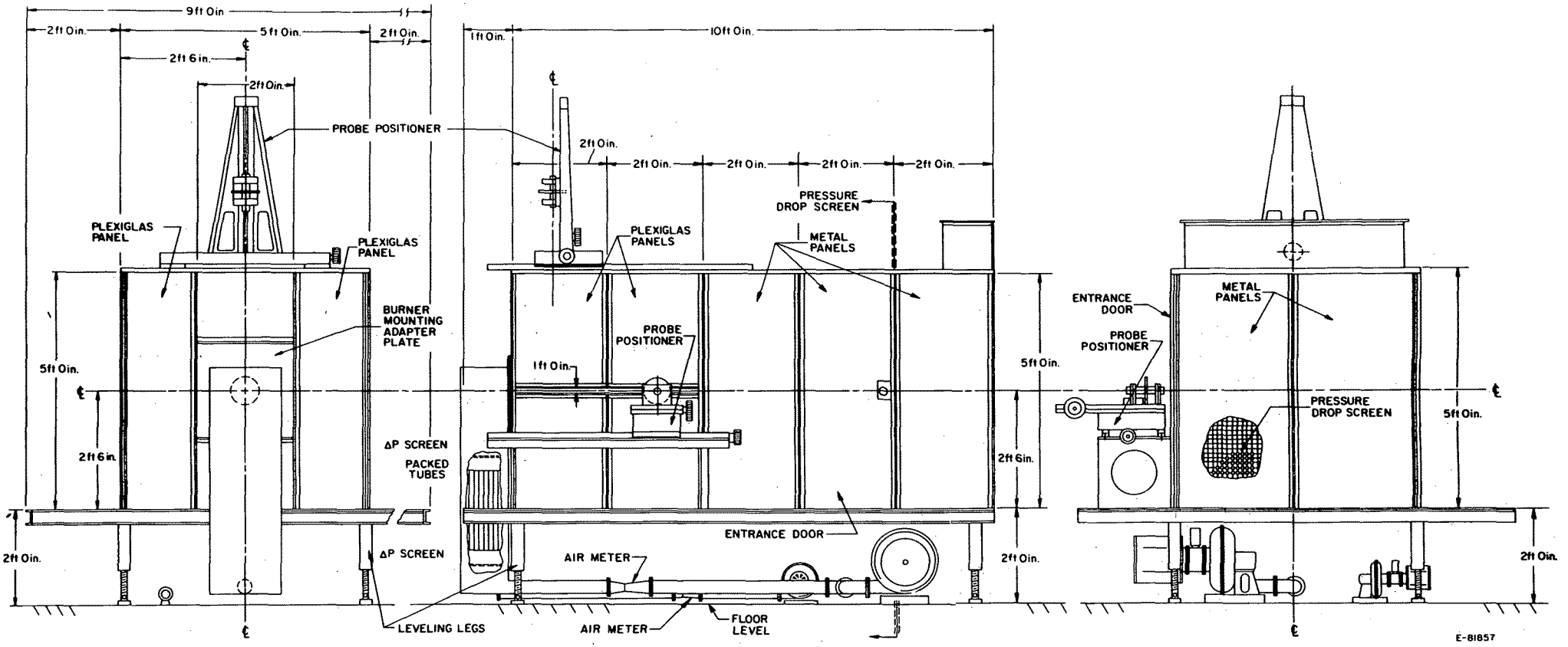

Figure II-1. COLD-MODEL TEST FACILITIES

roof were constructed of 0.250-inch-thick aluminum sheets. Also, the position of the aluminum and plastic panels are interchangeable. This feature provides flexibility in the location of visual studies in the chamber.

An access door placed in one sidewall of the chamber provides, when closed, a smooth, continuous interior wall surface. The interior of the cold-model facility does have projections inward from or distortion of the walls as they would upset the flow patterns and make analysis more difficult.

The burner end of the chamber is designed so that a variety of burner types can be installed using a standard-size adapter plate, as shown in Figure II-2

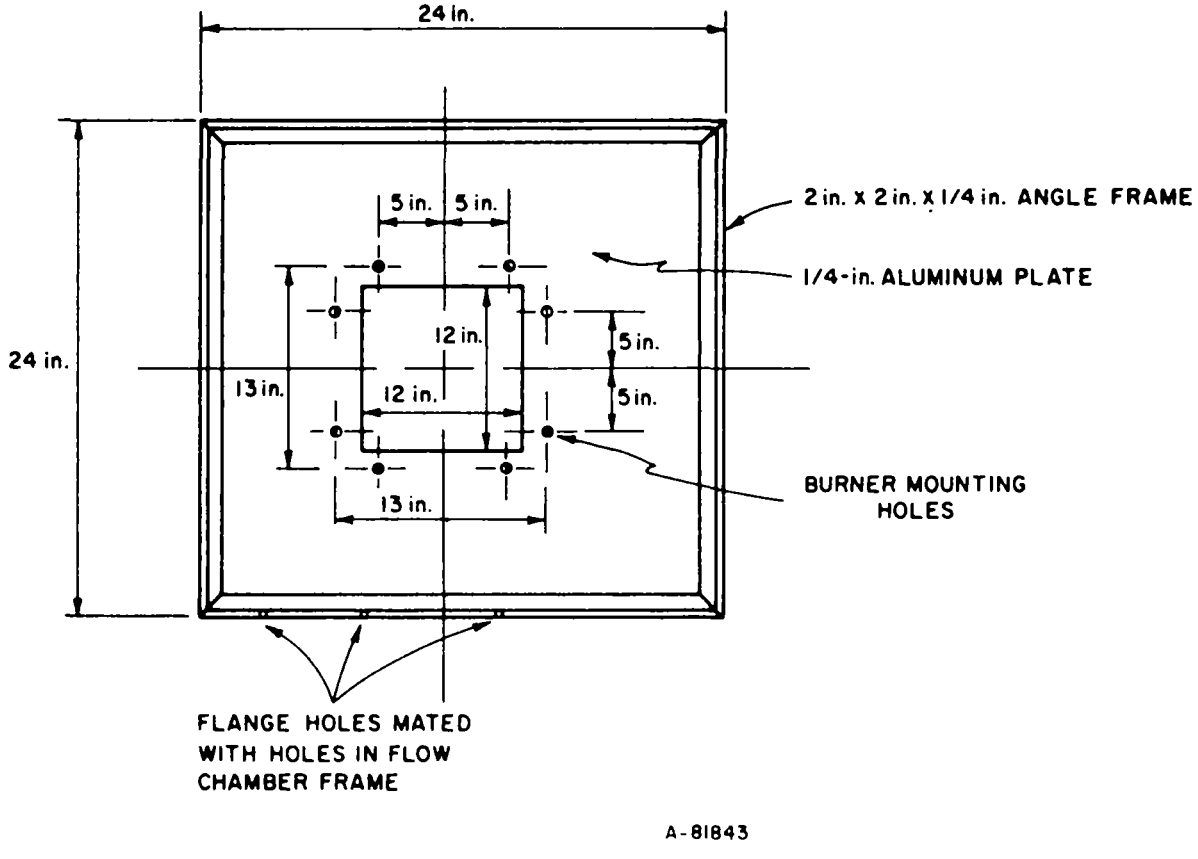

Figure II-2. COLD-MODEL BURNER ADAPTER PLATE

The adapter plate fits and bolts into a 24 by 24 inch hole framed in the end of the chamber.

The major criterion for design of the sampling probe access holes was maximum flexibility of probe position. The design selected (Figure II-1) uses two slots, one in the sidewall and one in the roof, running parallel to the center line of the test chamber. The sidewall slot enabled us to position the probe anywhere in a horizontal plane passing through the burner axis. The roof slot provides the same positional capabilities, but rotated 90 degrees about the burner axis. Figure II-3 shows the probe positions obtainable using the slot design. The panels in the model can be easily changed so that other slot configurations can readily be developed.

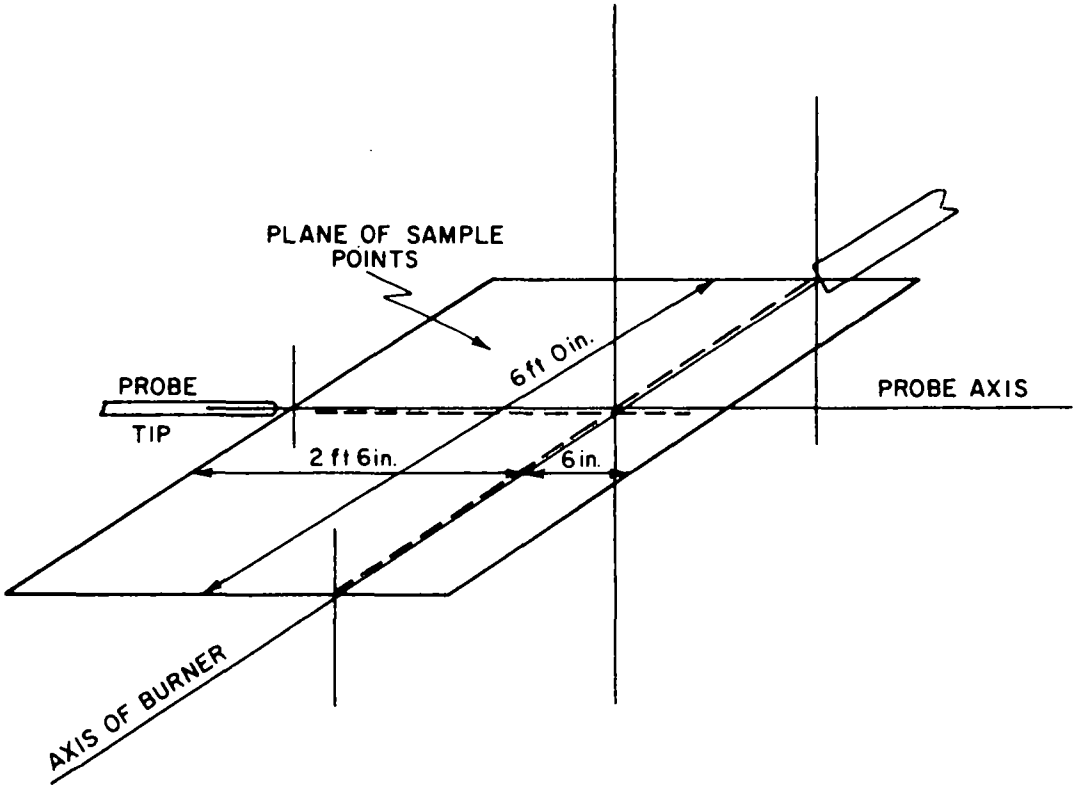

Figure II-3. PLANE OF SAMPLE POINTS ABOUT BURNER AXIS

The sampling slots are fitted with a sliding spring steel seal designed to maintain the chamber essentially "air tight" while allowing freedom of probe movement. Figure II-4 shows a cross-sectional view of the sliding seal. Grooves 0.025 inch deep and 0.5 inch wide are cut in the plastic

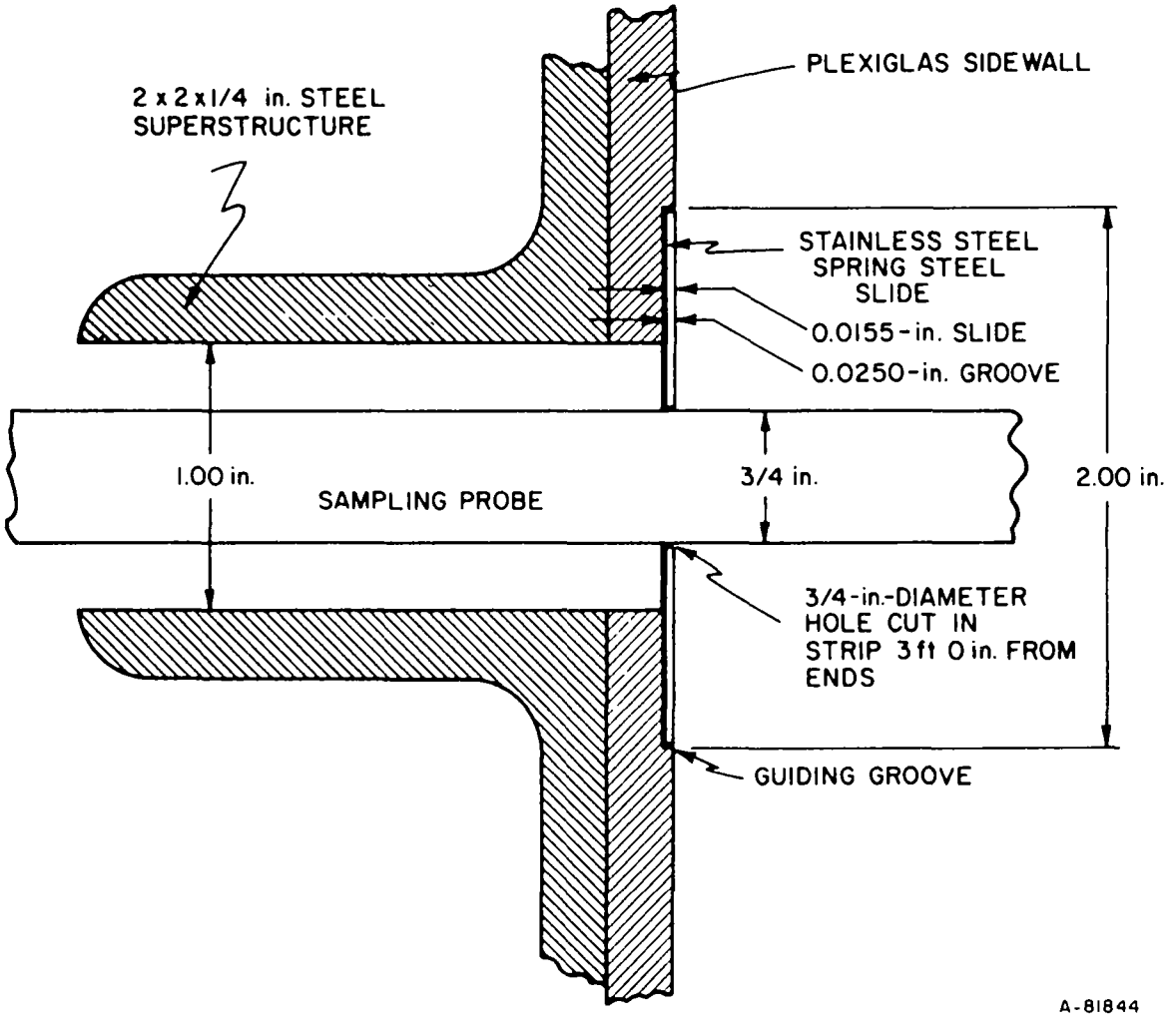

Figure II-4. SLIDING PROBE SEAL

edges of the chamber wall adjacent to the sampling slots. They act as guides to maintain the relative positions of the seal and the probe slot. A 0.015-inch-thick strip of stainless steel is stretched across the length of the test chamber covering the wall slot. The stainless steel strip seats are flush in the groove, machined into the plastic walls. At either end of the chamber the metal strip winds around a take-up cylinder (Figure II-5). These cylinders are constructed so that they apply an equal and oppositely directed force on the metal strip. The opposite forces applied to the strip put tension on the metal, which holds it back against the chamber walls. The tension supplied by each of the cylinders

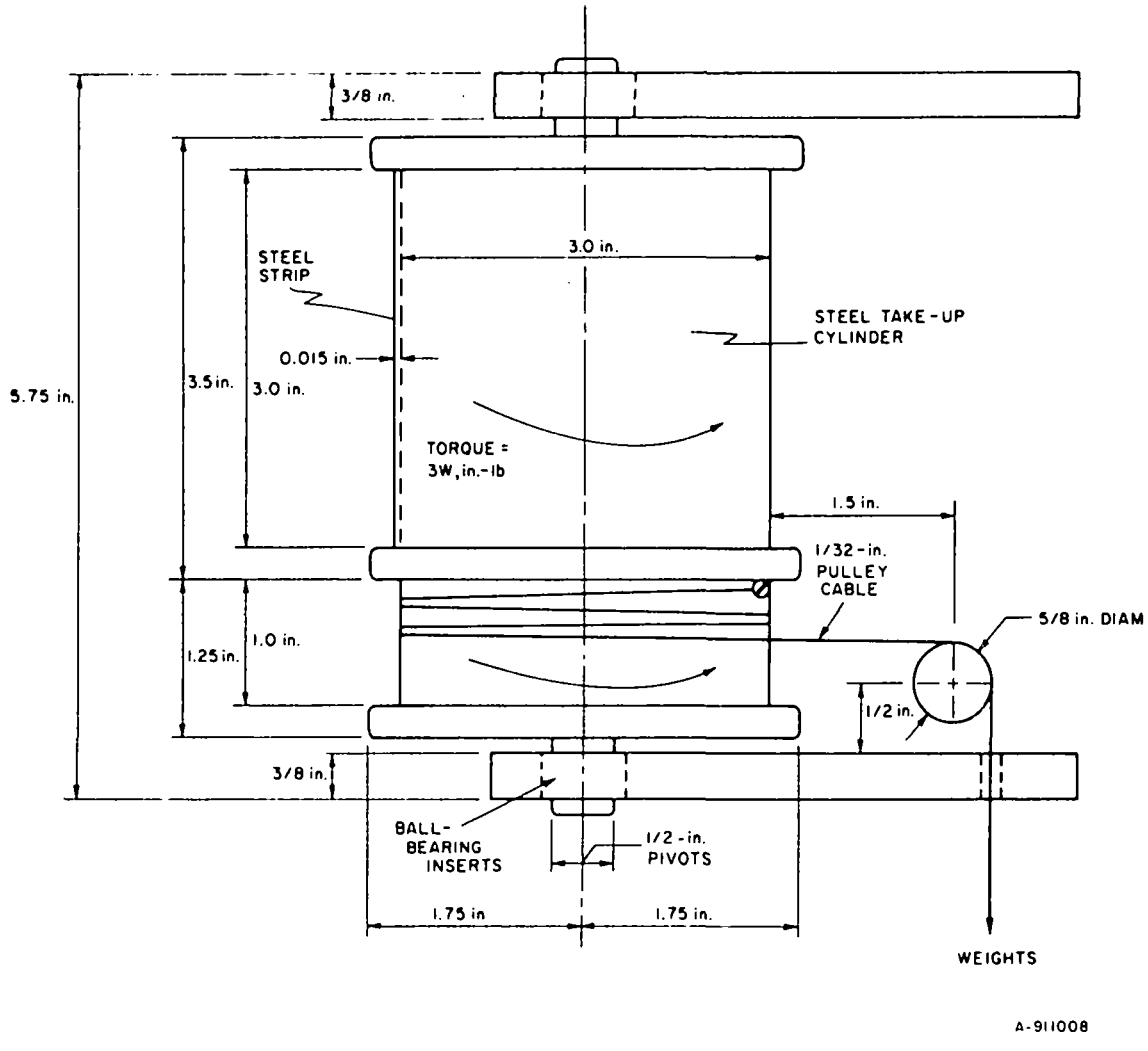

Figure II-5. PULLEY ARRANGEMENT FOR SLIDING PROBE HOLE SEAL

is achieved with weights. In this way, as the probe is moved down the length of the chamber, one cylinder "plays out" a portion of the metal strip while the other cylinder takes it up, maintaining a constant tension. The amount of weight necessary to provide the proper tension will be experimentally determined on the finished unit.

The blower selected to deliver the primary air flow in the test facility is a North American Model 2344-28-3-20 turbovane blower, which is capable of delivering 62,000 CF/hr at a pressure of 44 oz/sq in. This flow capacity was selected to match the amount of combustion air used by the hot-model furnace operating at its maximum gas input of 4000 CF/hr and 40% excess air. The high-pressure capability of this

fan is necessary to overcome the estimated pressure drop of our vane-induced swirl generator. The air is cleaned with a North American Model 14-MGV filter attached to the blower inlet. This filter used oil-impregnated paper which is capable of removing particles as small as several microns. The air flow is controlled by a butterfly valve located between the air filter and the blower inlet. Air flow measurement was made with calibrated orifices and controlled with "butterfly" valves on the fan inlets. The air ducts were fitted with a single position probe access (Figure II-6).

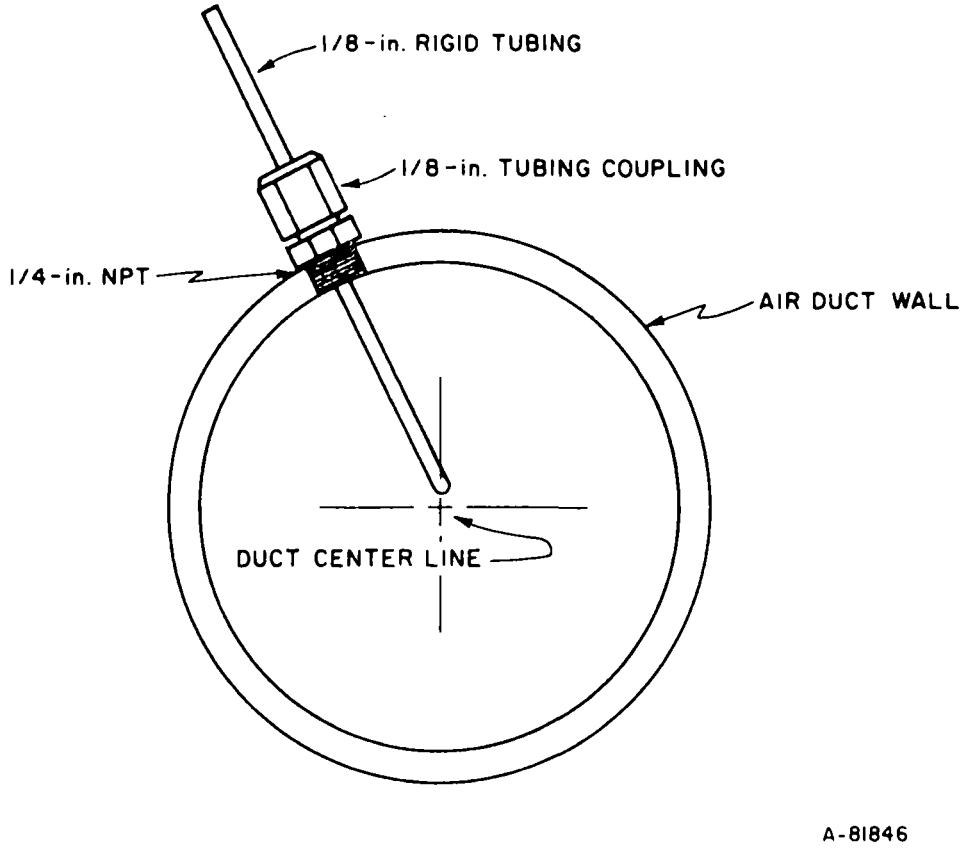

Figure II-6. SUPPLY AIR PRESSURE PROBE

This hole was used to insert a pressure probe attached to an electronic manometer capable of measuring high-frequency pressure pulsation. The air stream was spot-checked after each air flow setting for pulsation. Any pulsation of the air in the supply system potentially will result in a pulsation in the test chamber.

B. Cold-Model Probe Positioner

Each of the sampling probes inserted into the burner flow regions, through the sliding seal, were positioned and held in place by an accurate positioning device.

Figure II-7 shows the basic design of the device in three views. A level, supporting bed is formed by three fiber glass H-beams attached to the frame of the chamber. The H-beams are cross-connected by aluminum bars 1 inch thick and 3 inches wide (parts A1-A10). The bed was designed to have a deflection less than 0.001 inch under the weight of the probe-positioning device. Aluminum and fiber glass are used throughout the system wherever possible to reduce the weight.

The probe and other equipment are moved (axially) down the furnace length on two 3-square-inch "box rails" (parts B1 and B2). The box rails are securely mounted to the supporting bed by setscrews and were adjusted so that they were both parallel to the chamber axis to within 0.01 inch. Precision-machined vee-blocks (parts B1 and B2) ride on the outer edge of each box rail and provide lateral guidance as well as vertical support to the moving mechanism. A forced lubrication system is built into each vee-block to provide a constant oil film over all metal-to-metal contact areas. Mineral oil will be used to ensure a coefficient of friction, f_o, less than 0.3. The probe is positioned by an Acme threaded lead screw (not shown) sized to move the probe 0.1 inch per rotation. The position is read on a linear scale attached to the outer box rail; the vernier adjustment is provided by a circular scale on the lead screw. Using the linear scale for rough-positioning and the vernier scale for fine-positioning, the probe tip can be placed with an accuracy of 0.01 inch. The lead screw is equipped with an electric motor for rapid, rough probe placement and with a hand crank for final positioning. About 15.0 inch-pounds of motor torque is required to move the probe as calculated from the standard static friction equations for parallel surfaces and for screws with square threads.

The probe's radial movement is accomplished with the same box rail and vee-block arrangement used for its axial movement (parts C1, C2, E1, and E2). The probe tip has a full 5-foot movement, allowing it to completely traverse the chamber's width. Again, the probe is moved using an Acme threaded lead screw; its position is determined by combining readings from a linear and a circular scale.

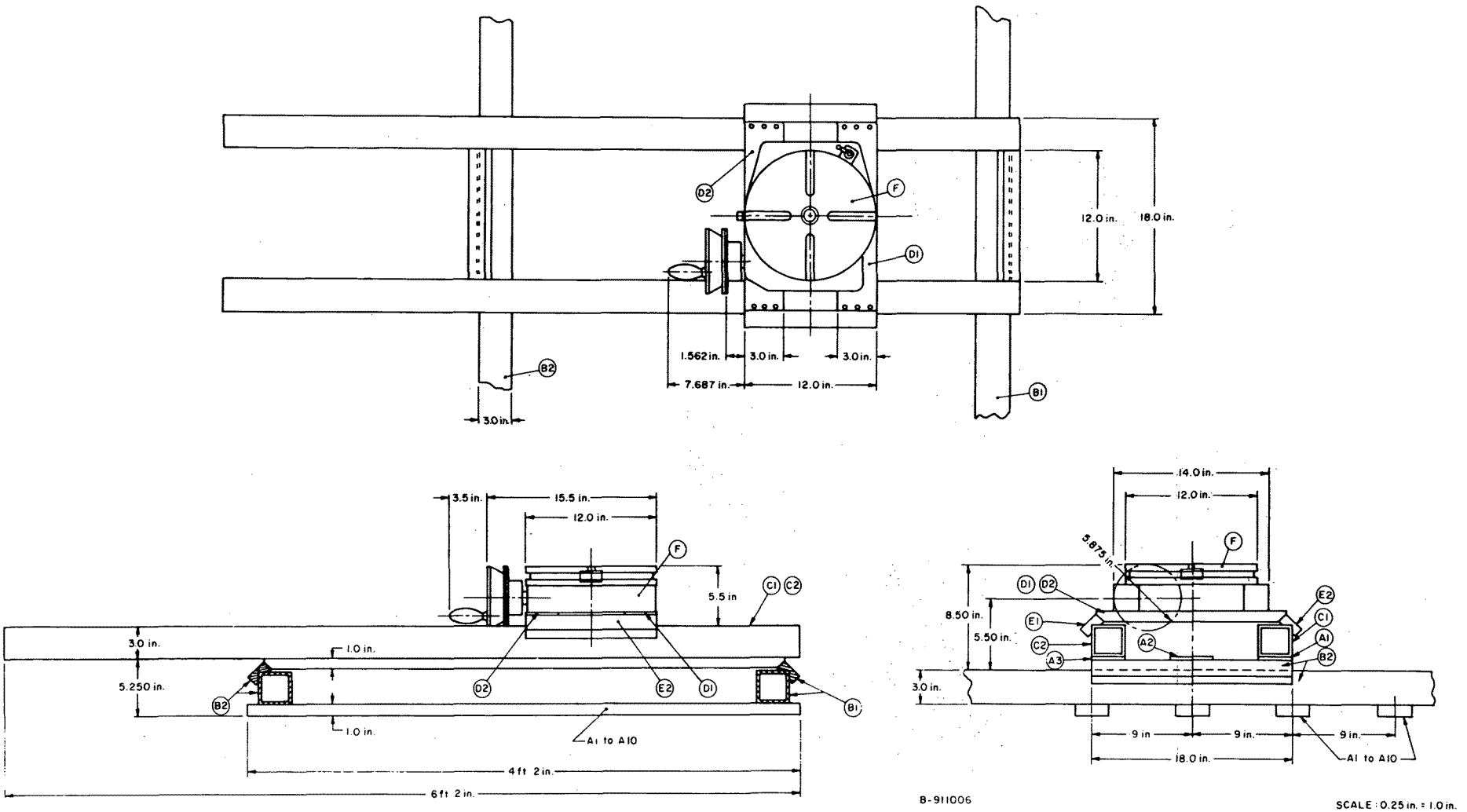

Figure II-7. GENERAL ASSEMBLY OF PROBE POSITIONER

A planetary turntable (part F, Figure II-7) provides the rotational motion of the probe tip shown in Figure II-8.

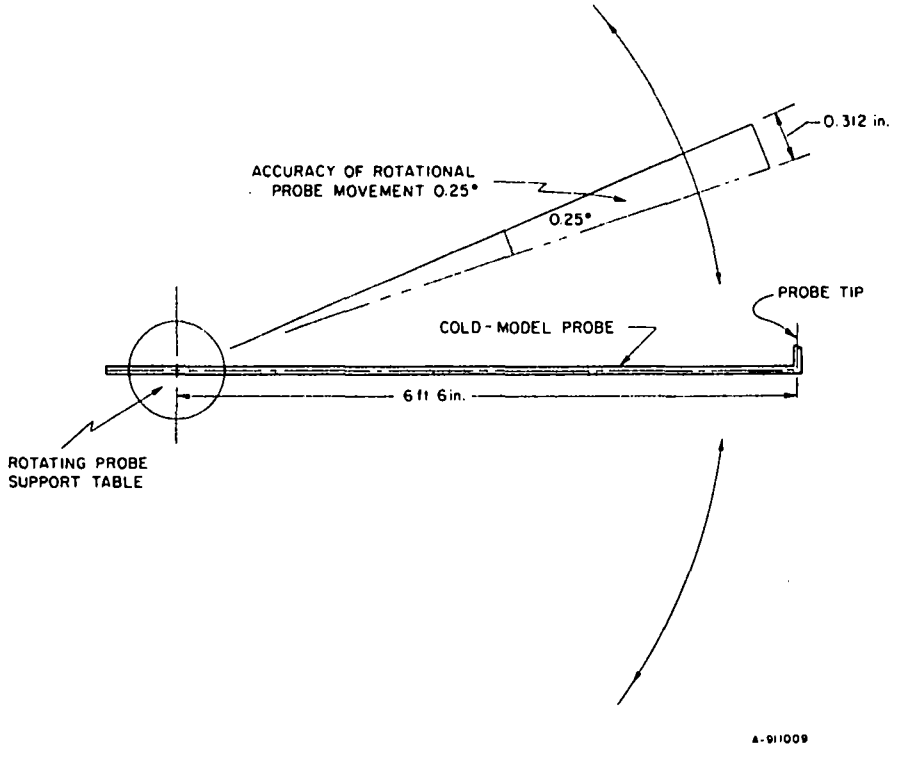

Figure II-8. ROTATIONAL MOTION ACCURACY OF COLD-MODEL PROBE POSITIONER

The rotational motion is required to null the five-hold, spherical, pitot tube used for velocity measurements. A circular scale attached around the periphery of the table is divided into 720 divisions (0.5 degree per division); therefore, the probe tip can be positioned with an accuracy of 0.312 inch.

The bracket that actually holds the probe is attached to the top of the turntable. (The top view is shown in Figure II-9.) This bracket consists of two 2-inch split-bushing pillow blocks (parts G1 and G2) and a steel adapter (part H). The steel adapter is based to match the outside diameter of the probe being used. A separate steel adapter is provided for each probe and securely clamped around the probe base. Each adapter has a 2-inch outside diameter which matches the base size of the split-bushing pillow blocks. To lock a probe in position, the pillow blocks are opened by removing four bolts and the adapter is snapped into place. Should it be necessary, the probe can be removed and reinstalled

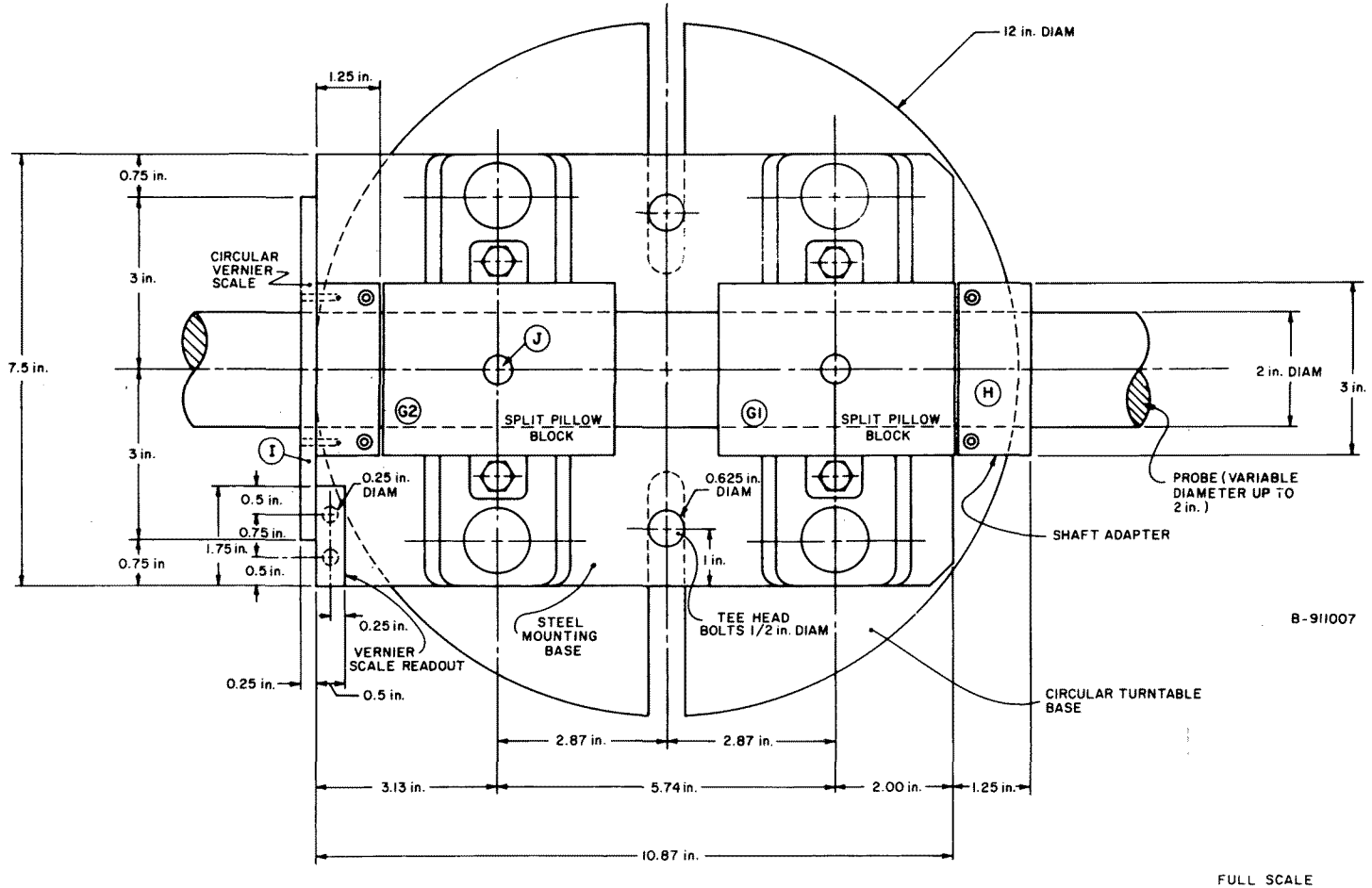

Figure II-9. AXIAL PROBE ROTATION GENERAL ASSEMBLY

easily, while ensuring that the tip will be positioned each time to within ±0.001 inch of its original position. The adapter/pillow block arrangements also allow probe rotation about its axis. Again, this particular motion is necessary to null the reading of a five-hole spherical pitot tube. The rotational position of the probe is read on a circular scale (part I) attached to each steel adapter. The probe is rotated manually and held in position by a blunt-nose setscrew (part J) in the rear pillow block. A forced lubrication system is built into each bearing to eliminate binding.

C. Cold-Model Instrumentation, Probes, and Calibration Methods

Three types of information were obtained from the cold-modeling facility: flow direction and magnitude as well as mixing rate. Flow direction and magnitude are measured with a five-hole, spherical head, pitot tube. Mixing rates were measured by monitoring the rate of tracer-gas dilution at some sampling point.

When using the five-hole pitot tube, normally, the probe is operated by rotating the tip until the pressure in two of the five holes is nulled. The stream velocity and direction is then determined by an established relationship between the pressure differences in the other holes and the probe's "yaw" and "pitch" angles. Mr. Wright of BCURA Industrial Laboratories recently developed a method of determining stream velocity and direction without the time-consuming job of nulling two probe holes. (See the 1970 Journal of Physics, Volume 3.) This method only requires positioning the probe at the point of interest and measuring the pressure difference between each combination of two holes. This requires four pressure readings, which can be made with switching valves in about 10 minutes. A computer is then used to solve for five simultaneous equations. We calibrated our probe using this method.

Very simply stated, BCURA calculated the relationship between the flow parameters and the pressure distribution over the pitot probe from potential flow theory. This results in the following equations:

$$p_\eta = p_s + 1/2\ K_\eta \rho v^2 \qquad \text{(II-1)}$$

$$p_{\eta_1} - p_{\eta_2} = 1/2\ \rho v^2 (K_{\eta_1} - K_{\eta_2}) \qquad \text{(II-2)}$$

where p_η is the pressure at some point η on the probe tip surface (Figure II-10); p_s is the free-stream static pressure; ρ, the fluid density; v, the free-stream velocity; and K_η, the pressure recovery factor.

They found experimentally that, for sufficiently high velocities ($N_{Re} > 4000$), K_η is practically independent of Reynolds number and is then only a function of the angle θ_η. By selecting appropriate reference axes the angle, θ_η, can be expressed in terms of measured angles using spherical trigonometric relations; BCURA uses the conical, Φ, and dihedral, δ, angles shown in Figure II-11.

By properly choosing certain combinations of recovery factors, expressions were derived for the angles Φ and δ and, hence, the velocity direction, the magnitude of the velocity, and the static pressure of the system. The relationships are expressed in the following equations:

- Angle or Direction

$$K_\Phi = \{1 - \sum_{\eta=1}^{4} (p_0 - p_\eta) \mid 2[\sum_{\eta=1}^{4} (p_0 - p_\eta)^2]^{1/2}\}^{1/2} \qquad \text{(II-3)}$$

- Velocity

$$K_v = \{\rho v^2[\sum_{\eta=1}^{4} (p_0 - p_\eta)^2]^{-1/2}\}^{1/2} \qquad \text{(II-4)}$$

- Pressure

$$K_p = 2(p_0 - p_s)/\rho v^2 \qquad \text{(II-5)}$$

Also

$$\tan \delta = -(p_1 - p_3)/(p_2 - p_4) \qquad \text{(II-6)}$$

The probe to be used is calibrated by inserting it in a circular free-stream jet containing a potential core representing an adequate cross-sectional area with a uniform velocity profile. The various pressures are measured over an appropriate range of chosen reference angles and flow velocities. The curves for K_Φ, K_v, and K_p versus Φ are obtained from these data.

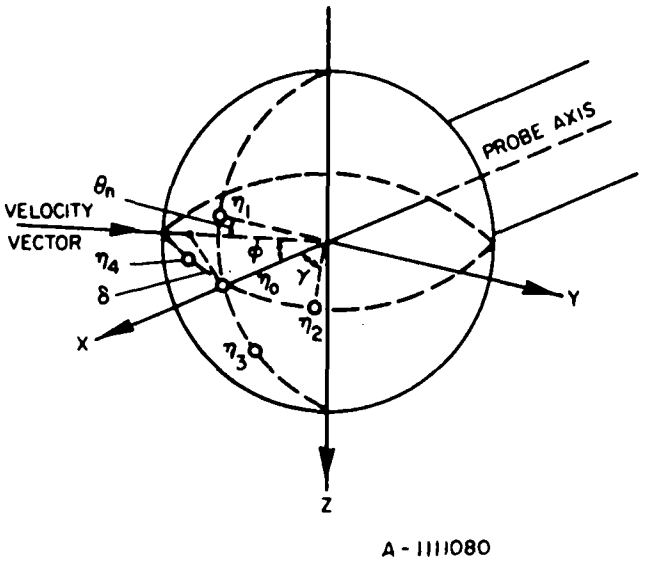

Figure II-10. SPHERICAL SENSING HEAD OF A FIVE-HOLE PITOT TUBE

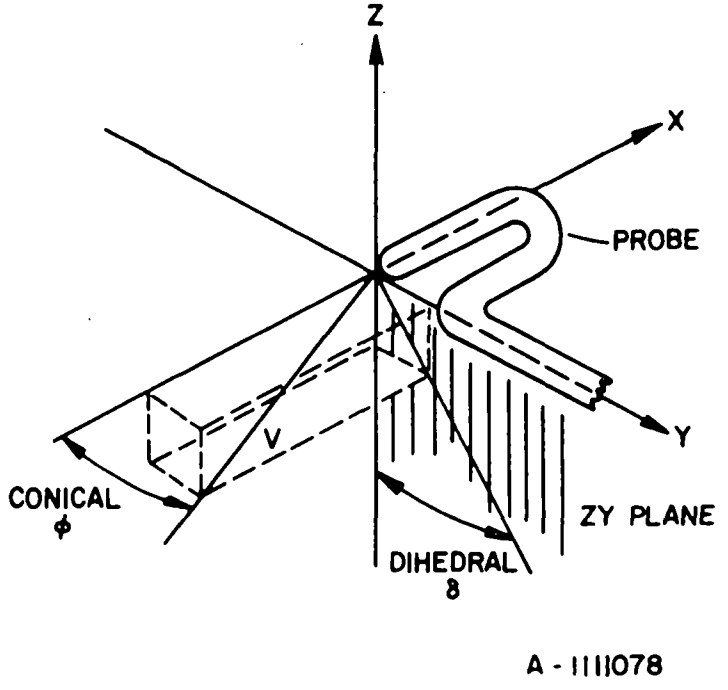

Figure II-11. CONICAL AND DIHEDRAL ANGLES

Once the calibration curves are obtained, the probe is ready for use in the experimental flow system. The pitot probe is placed at the required measuring point, and its position and inclination in the flow chamber are recorded. A set of pressure differentials are measured, and the calibration curves used to obtain the conical, Φ, and dihedral, δ, angles.

Once the conical and dihedral angles have been determined, values for K_v and K_p can be obtained from the calibration curves. (The complete process can be carried out on a computer if the equations for the calibration curves are determined.) Figure II-12 shows an example of calibration curves for a spherical probe.

The values of K_v and K_p are substituted into Equations II-4 and II-5 to calculate the velocity, v, and static pressure, p_s. In calculating the static pressure, Equation II-5 yields a value for $(p_0 - p_s)$ whereby –

$$p_s - p_{AT} = (p_0 - p_{AT}) - (p_0 - p_s) \qquad \text{(II-7)}$$

and $(p_0 - p_{AT})$ is one of the measured pressure differentials. Therefore,

$$p_s = (p_s - p_{AT}) + p_{AT} \qquad \text{(II-8)}$$

The authors of this method found that the maximum error in Φ is less than 0.33 degree. Comparing the theoretical and actual values, the error in K_v is less than 1%. However, practical calibrations are advisable because large deviations may arise from the influence of the probe stem, from the size of the holes in the sensing head, and from the constructional errors of slight misalignment of the holes.

A calibration assembly for the five-hole pitot probe consists of a source of constant velocity air, a differential pressure range selector panel, a differential pressure sensor, an electronic manometer, and the pitot tube to be calibrated. The general assembly is shown in Figure II-13.

The constant-velocity air stream is generated by a North American blower with a 740 CF/min capacity at a pressure of 24 oz/sq in. Flexible tubing connects the blower to a 12 x 12 x 16 inch plywood box (Figure II-14). A 6-inch-diameter aluminum disk is mounted inside the box directly in line with the blower inlet. This disk is used to break up the main air stream entering from the blower. A perforated aluminum

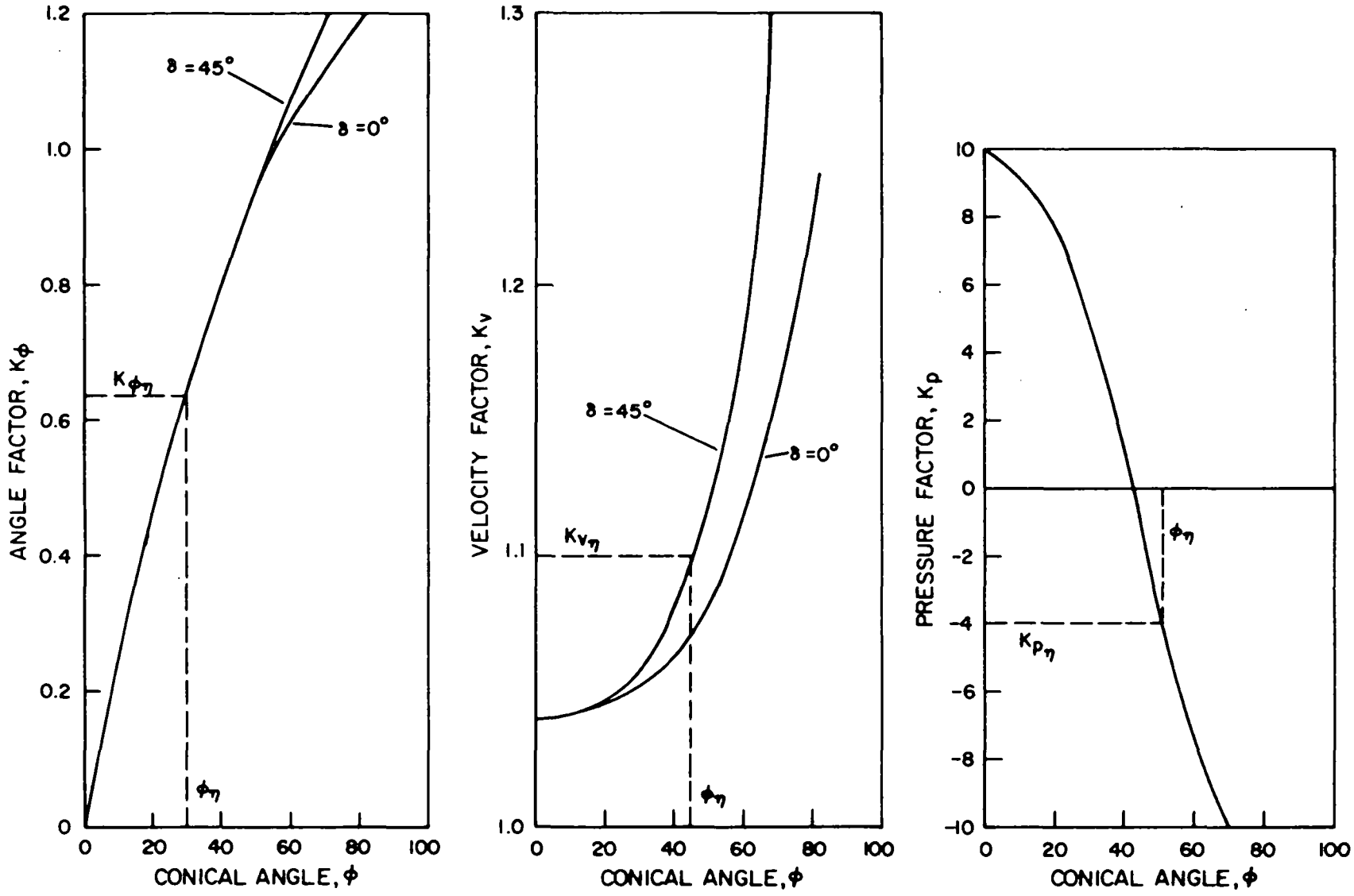

Figure II-12. EXAMPLES OF CALIBRATION CURVES FOR K_{Φ}, K_v AND K_p FOR A TYPICAL FIVE-HOLE, SPHERICAL HEAD, PITOT TUBE

A-1111079

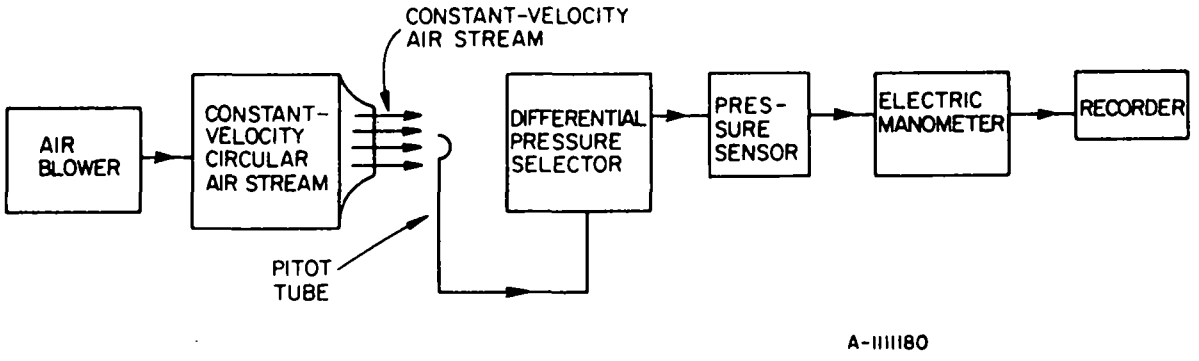

Figure II-13. CALIBRATION ASSEMBLY FOR FIVE-HOLE PITOT PROBE

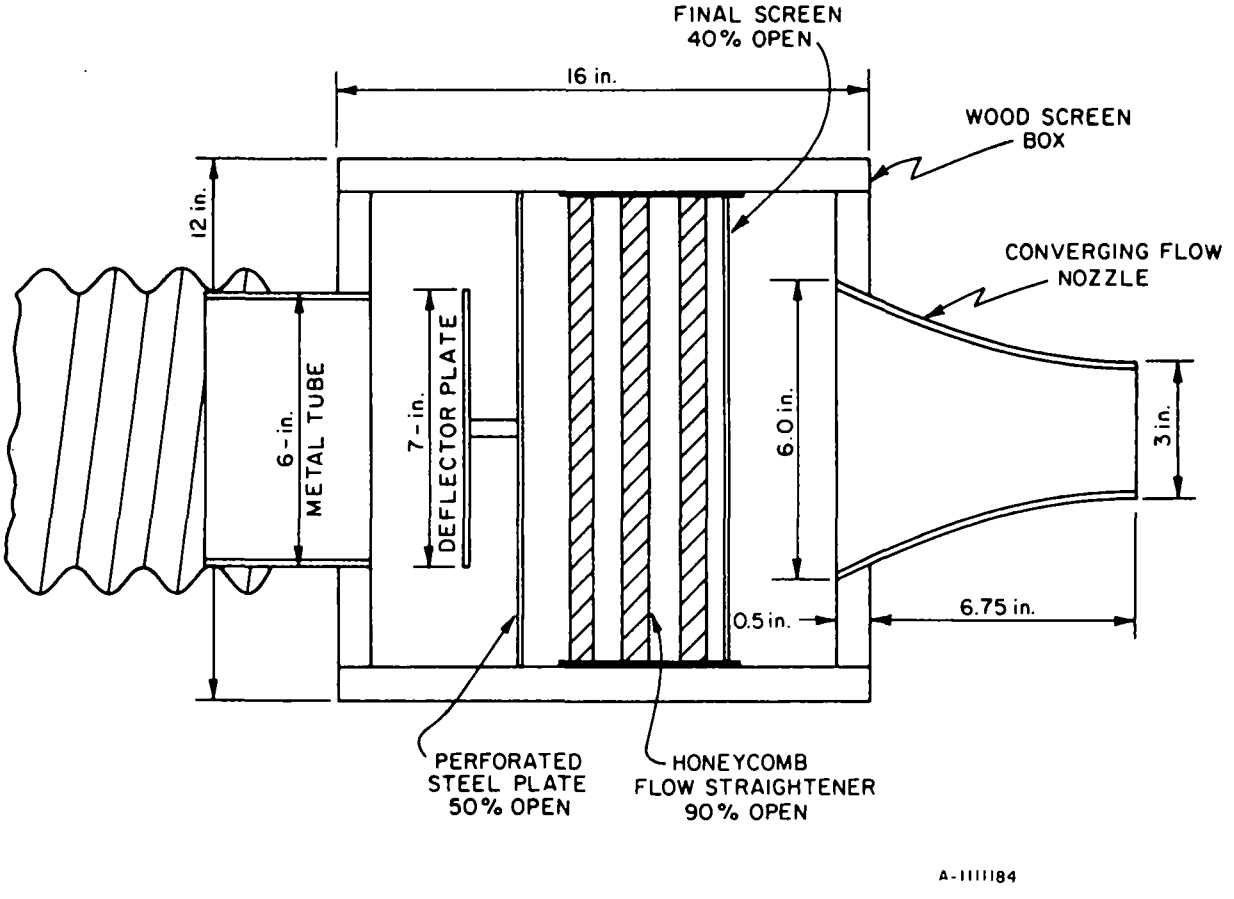

Figure II-14. PITOT TUBE FLOW CALIBRATION NOZZLE

plate, which uniformly distributes the air in a plane perpendicular to the direction of flow, follows the disk. The air is then passed through three layers of 5/8-inch honeycomb to break up any large turbulences. Two screens are used to break up any remaining turbulences. Mounted at the outlet of the box is a converging brass flow nozzle with a 3-inch-diameter outlet. The nozzle is used to produce the desired steady-state circular air stream.

The five-hole hemispherical pitot tube is mounted with the sensing head centered in the nozzle. The five holes in the pitot's head are connected to the differential pressure selector, which can be set to monitor the pressure difference between any two pressure holes or between any pressure hole and the atmosphere. The differential pressure being monitored is fed to a Barocel pressure transducer. The output from the transducer is amplified by a CGS electronic manometer and appears as a permanently recorded voltage on a fast-response Brush hot-wire strip recorder.

To calibrate the pitot for the factors K_{Φ}, K_v, and K_p discussed earlier, it must be rotated about the geometrical center of the sensing head. Since it would have been very cumbersome to rotate the 6-1/2-foot probes used in this project about their measuring points, we are holding the probes stationary and rotating the direction of the air stream. This is accomplished by mounting the air stream nozzle in a stand, which is simultaneously pivoted about the axes, which are perpendicular and parallel to the direction of flow. The maximum amount of rotation is 70 degrees in the conical and dihedral angles of the system. A diagram of the pivotal stand is shown in Figure II-15.

The values of the conical and dihedral angles are determined by using the trigonometric relationships for right triangles. Having a fixed coordinate system relative to the rotating air stream nozzle allows us to measure an angle of rotation relative to each coordinate (fixed) axis. The cosine of the angle relative to the direction of flow yields the conical angle. The angle of rotation in the plane perpendicular to the flow yields the cosine of the dihedral angle. The cosine of the angle of rotation is evaluated by taking the ratio of the length of the box along a fixed axis at a 0 degree rotation to its length at an arbitrary rotation.

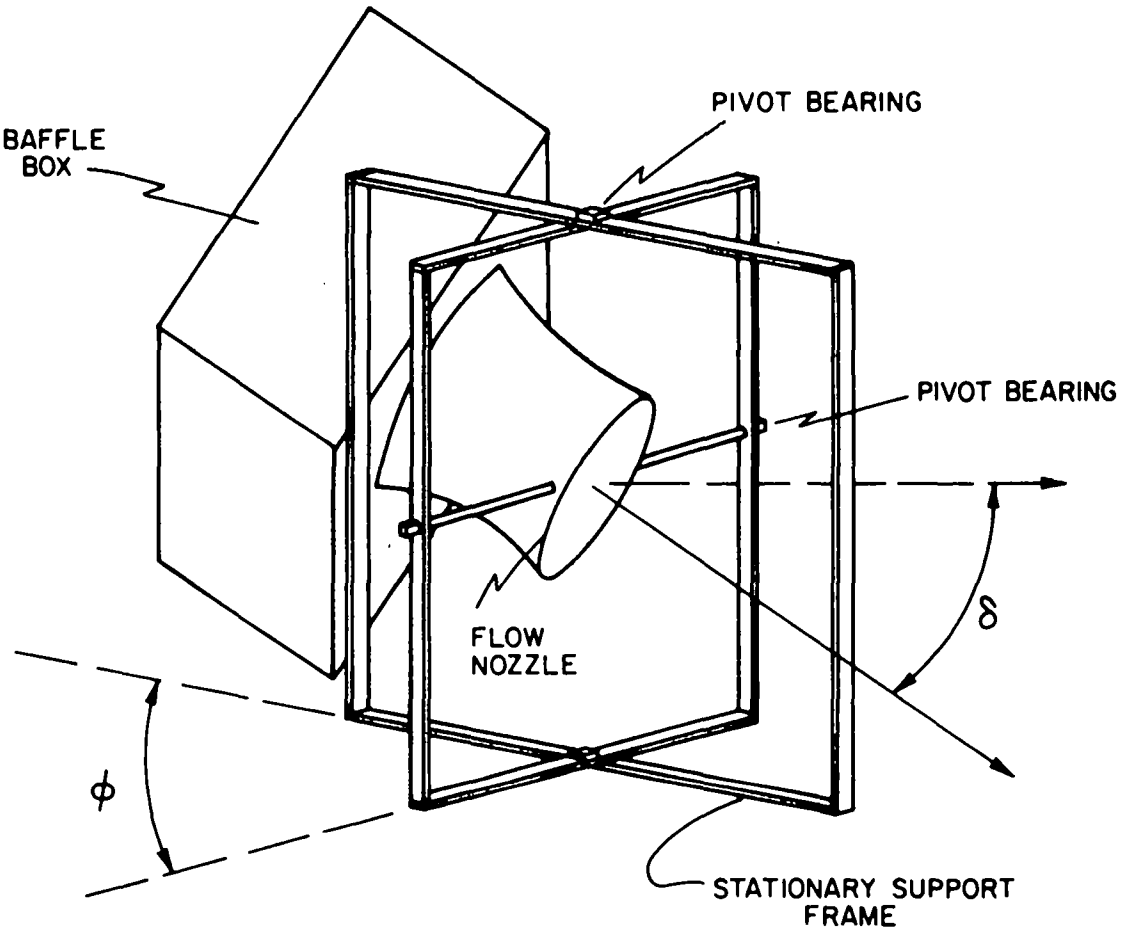

Figure II-15. PIVOTING NOZZLE MOUNT

Calibration of our probe was carried out for flow velocities of 25 ft/s and 50 ft/s, and conical angles between 0 and 65 degrees. To check consistency, two sets of data were collected for each velocity. The mean calibration curves for K_Φ, K_V, and K_p are shown in Figures II-16, II-17, and II-18, respectively, by the solid line. The theoretical values of these three factors were obtained from potential flow theory for a sphere having the outer ring of holes situated at a conical angle of 40 degrees, are shown by the dashed lines in Figures II-16, II-17, and II-18.

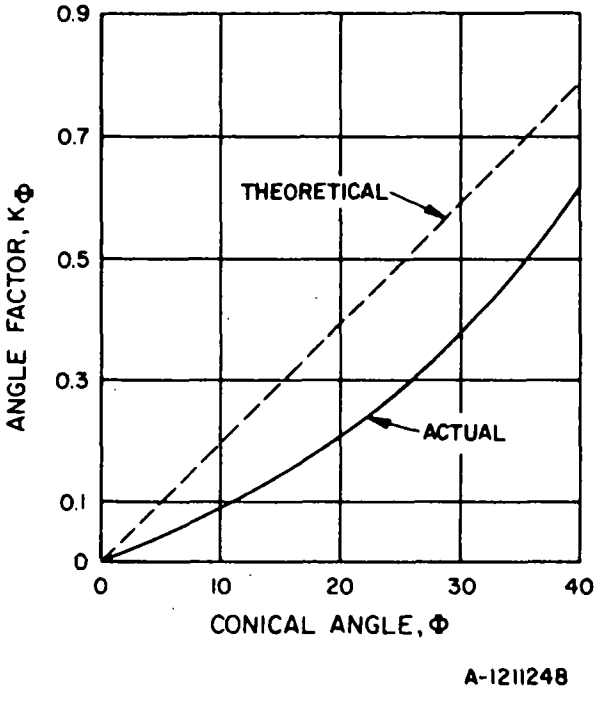

Figure II-16. K_Φ AS A FUNCTION OF CONICAL ANGLE FOR A FIVE-HOLE PITOT PROBE

The agreement between measured data and theory was reasonably good considering the substantial differences in tip configuration. Part of the deviation between curves arose because of the small influence of the stem of the probe and because of the size of the holes in the sensing head. However, most of the observed differences are believed to result because the probe is perfectly spherical.

Another factor in calibrating the five-hole pitot probe is that the flow patterns and mixing eddies change very rapidly in the areas of interest. Consequently, it is necessary to know the frequency response, amplitude shift, and maximum frequency of pressure change that can be detected by the five-hole pitot probe for any interruption of this type of data.

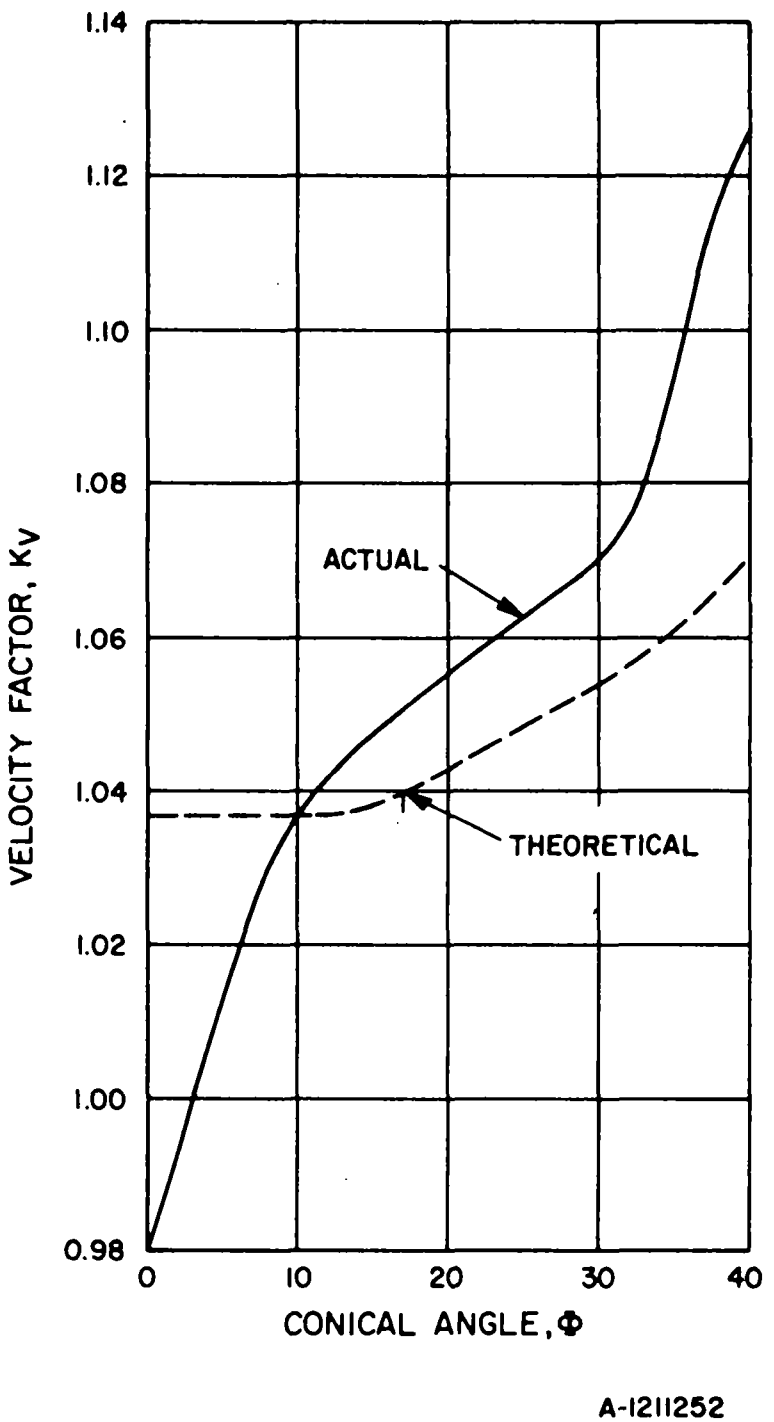

Figure II-17. K_V AS A FUNCTION OF CONICAL ANGLE FOR A FIVE-HOLE PITOT PROBE

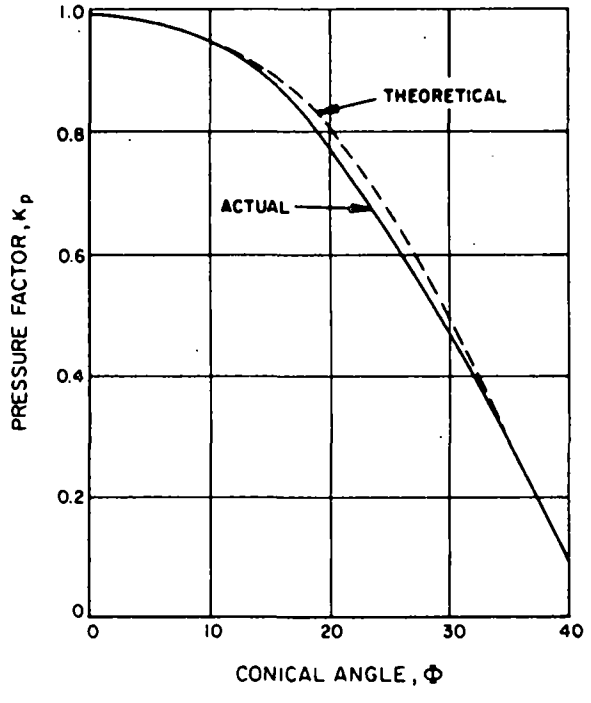

Figure II-18. K_p AS A FUNCTION OF CONICAL ANGLE FOR A FIVE-HOLE PITOT PROBE

To determine the change in amplitude of the measured pressure differentials as a function of frequency for the pitot probe, we built a pulsed air flow device. The experimental apparatus used for this calibration is shown in Figure II-19.

A disk with a pie-shaped section cut out of it was attached to a variable-speed motor. A constant air source was positioned below the disk and the five-hole pitot above the disk. When the disk was rotated by the motor, it would interrupt the air stream at any desired frequency, depending upon the motor speed. In this way we created a variable-frequency, pulsed, pressure signal. To achieve different turbulent conditions and magnitudes, disks were fabricated from solid plastic, perforated plate, and fine-mesh screen.

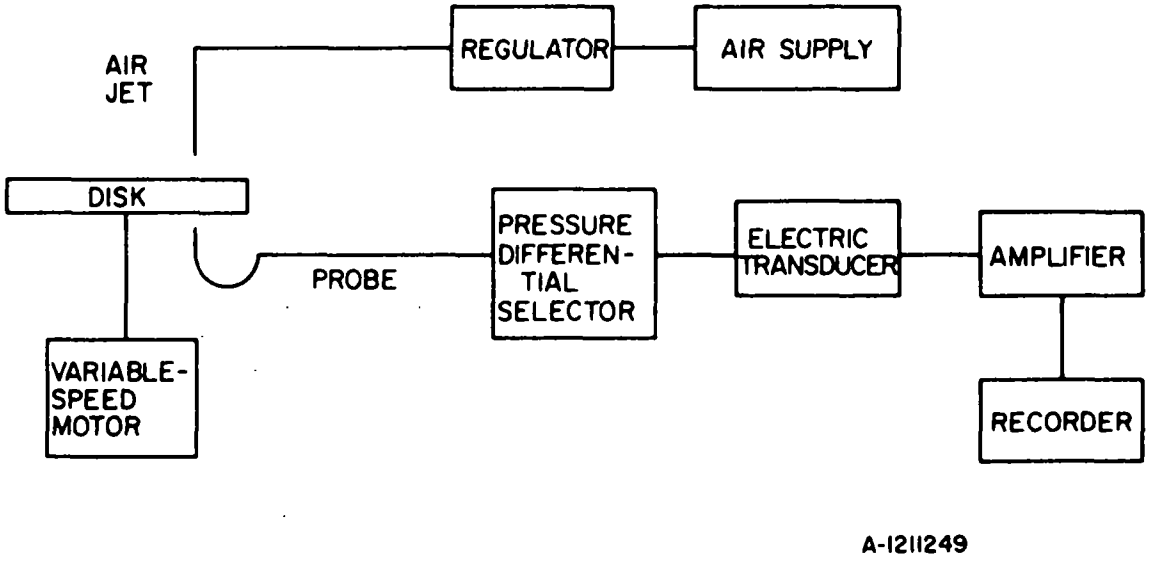

Figure II-19. EXPERIMENTAL APPARATUS FOR TRANSIENT CALIBRATION

We found that the electronic differential-pressure sensor alone could respond to pressure fluctuations as high as 500 Hz, but that the probe damped out fluctuations above 10 Hz, yielding only the mean velocity.

Graphical representatives of the difference between the actual and maximum measured pressures as a function of frequency for the Plexiglas and aluminum perforated plates are shown in Figures II-20 and II-21. A decrease in the amplitude of the pressure as a function of frequency for the different turbulent systems is observed. To determine the percentage change in amplitude, the ratio $\left(\frac{P_{max} - P_{min}}{P_{max}}\right)$ versus the actual pressure is plotted in Figures II-22 and II-23. Here we can observe that the fluctuations in the amplitude decrease rapidly with increase in frequency and degree of turbulence. For the thin gauge screen, which should most closely reproduce the turbulence to be expected in the cold-model furnace, the amplitude fluctuations for pressures less than 0.02 psia cannot be resolved with our equipment.

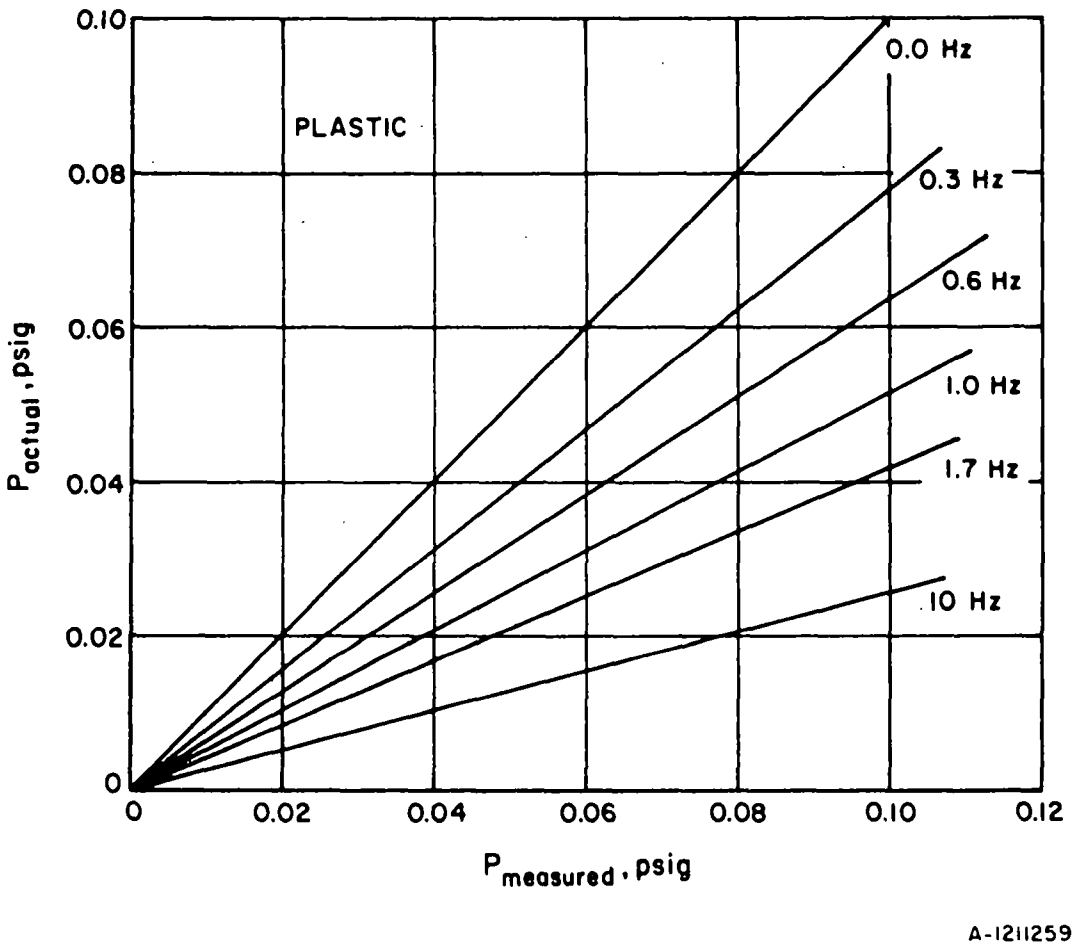

Figure II-20. PRESSURE MEASURED BY SENSOR VERSUS ACTUAL PRESSURE AS A FUNCTION OF PULSE FREQUENCY FOR THE SOLID (Plastic) DISK

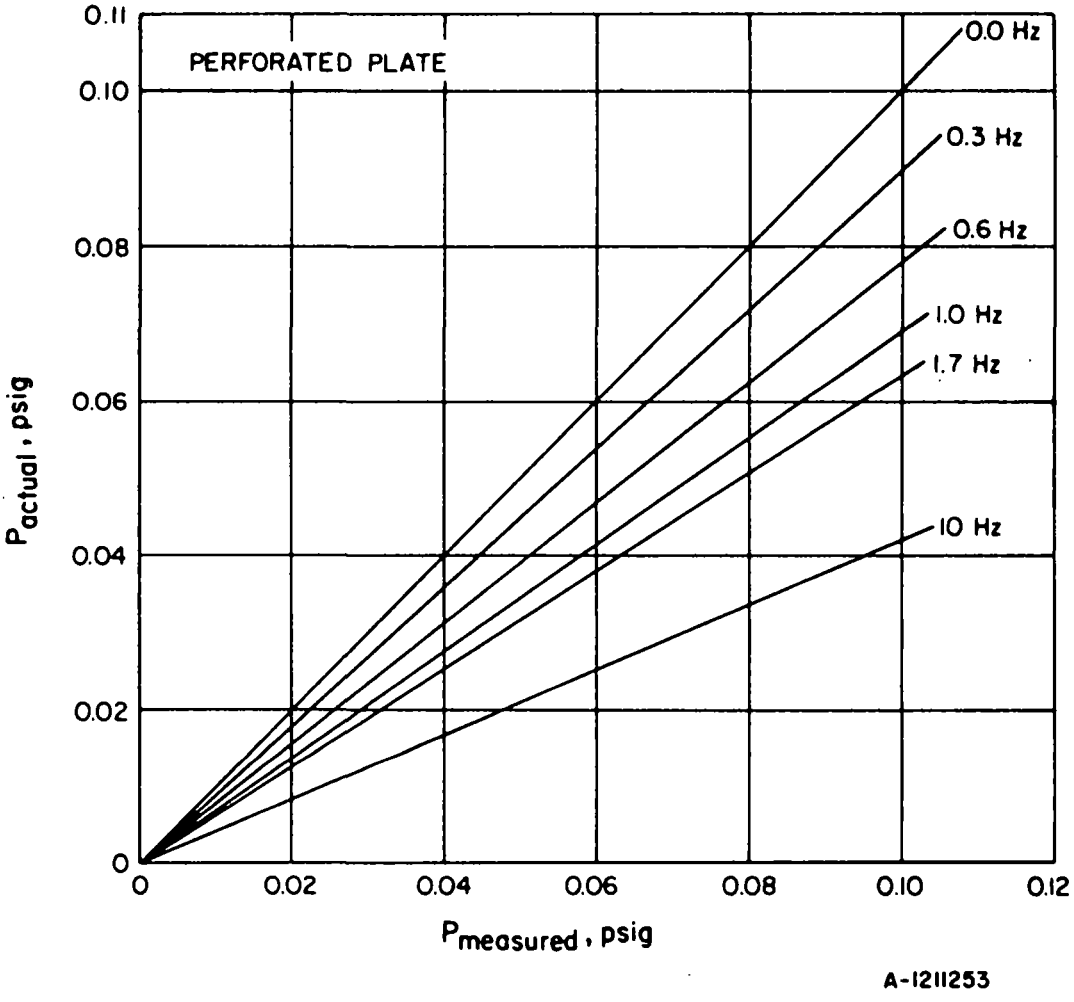

Figure II-21. PRESSURE MEASURED BY SENSOR VERSUS ACTUAL PRESSURE AS A FUNCTION OF PULSE FREQUENCY FOR THE PERFORATED DISK

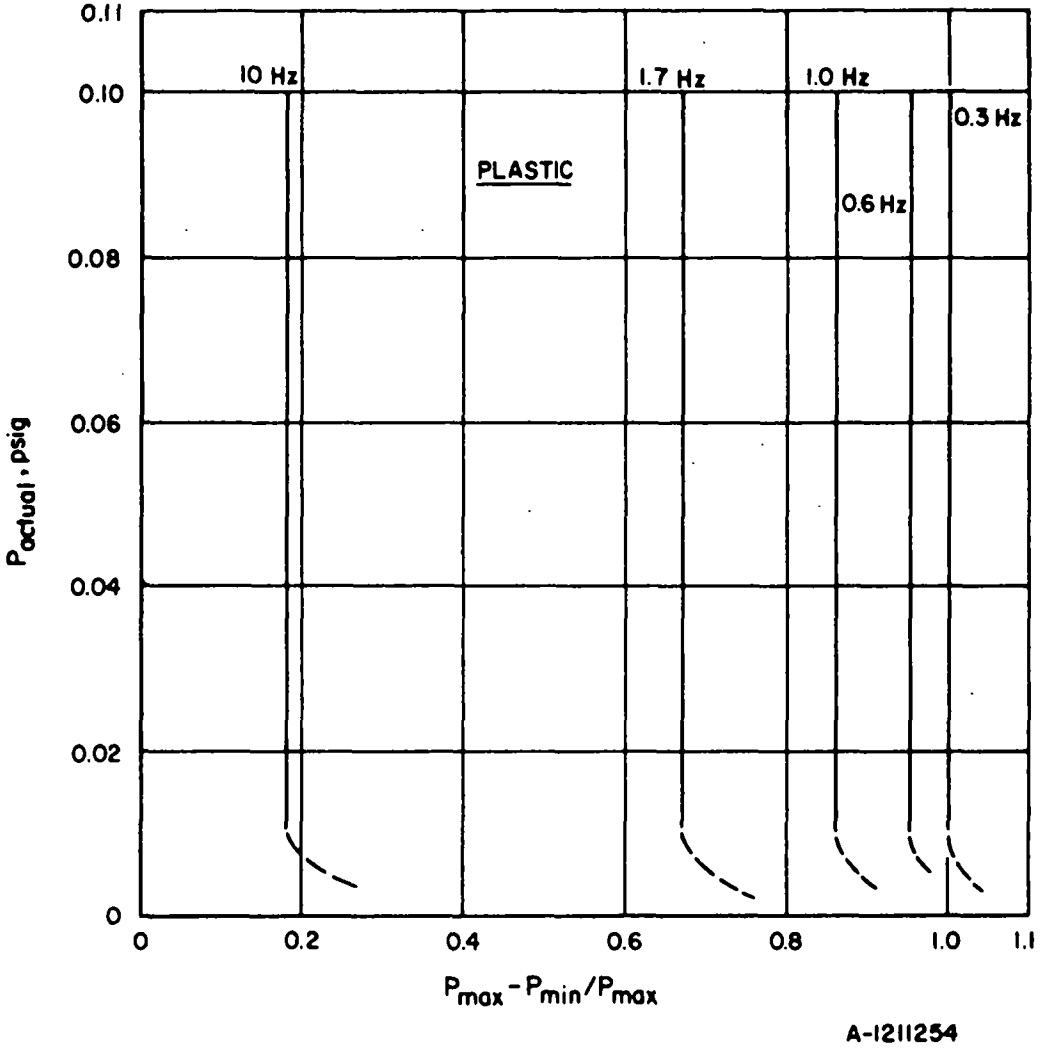

Figure II-22. PERCENTAGE CHANGE IN AMPLITUDE OF PRESSURE SIGNAL AS A FUNCTION OF FREQUENCY AND ACTUAL PRESSURE FOR THE SOLID DISK

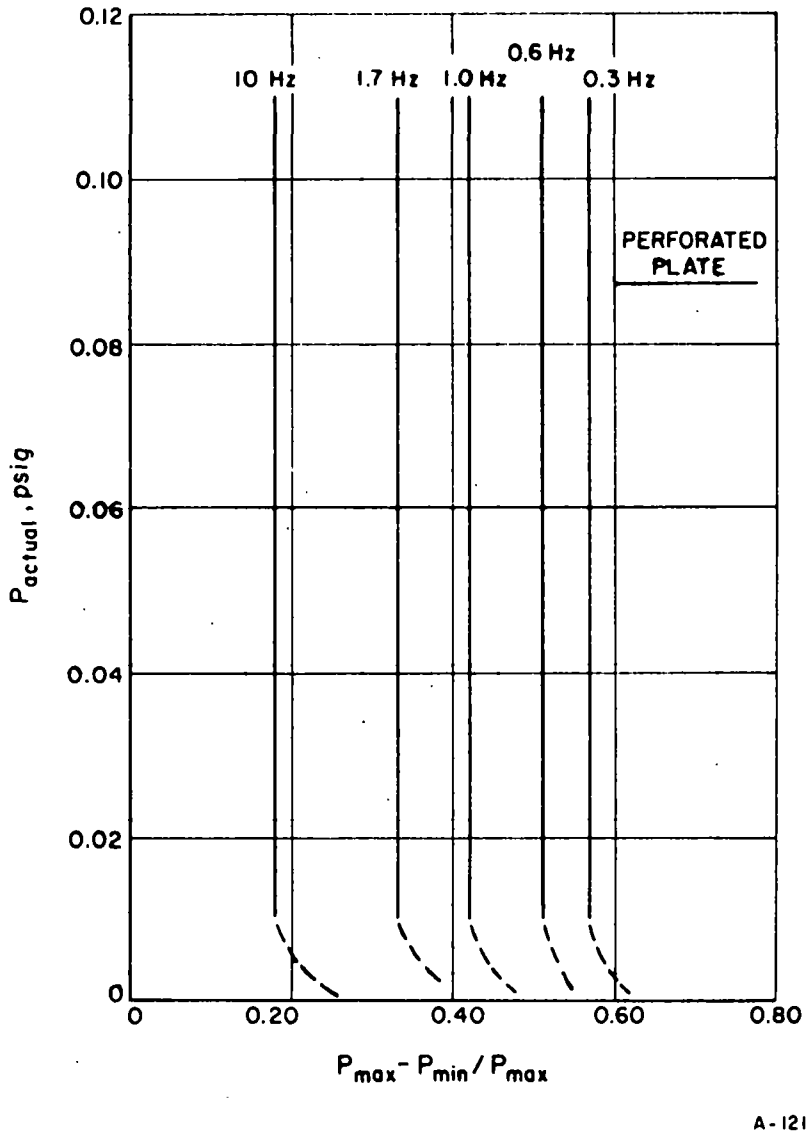

Figure II-23. PERCENTAGE CHANGE IN AMPLITUDE OF PRESSURE SIGNAL AS A FUNCTION OF FREQUENCY AND ACTUAL PRESSURE FOR PERFORATED DISK

We concluded that measuring flow changes having a frequency above 10 Hz is not practical with our present probe and that only mean velocity and direction can reliably be extracted from the data.

HOT-MODELING TEST FURNACE FACILITY

A. Furnace Test Chamber

The hot-model furnace facility used for this program has a cross-sectional area of 25 sq ft with a height of 5 feet, width of 5 feet, and length of 15 feet. The furnace is capable of operating at temperatures of up to 3000°F with gas inputs up to 3.5 million Btu/hr. A portion of this project involved designing three modifications to the basic furnace which were required to perform the specific tests of this program. These modifications were –

- Installing cast refractory water-cooled panels to simulate the thermal loading found in industrial furnaces.
- Installing a quick-change burner-mounting bracket.
- Installing a sliding seal device for inserting the probes into the furnace while preventing air leakage.

Figure II-24 shows general construction and dimensions of one of the cast refractory water-cooled panels.

Figure II-25 shows the water-cooled sliding seal installed in the south furnace wall.

The program's objectives required that the furnace operate with a maximum wall temperature of 2800°F, with a 3.5 million Btu/hr input, and that the wall temperature be lowered to approximately 1800°F using water loads. In addition, the furnace was to be fired from one end, whereas originally it was fired through the sidewall, simulating an industrial boiler system. To make these modifications, we prepared a complete heat balance on the system and selected the new wall materials and type of construction from the results. The finished furnace was completely made of cast refractory, except for the hearth, which was built of firebrick. The brick hearth gives the required flexibility to install water-cooled loads in the firing path, if necessary.

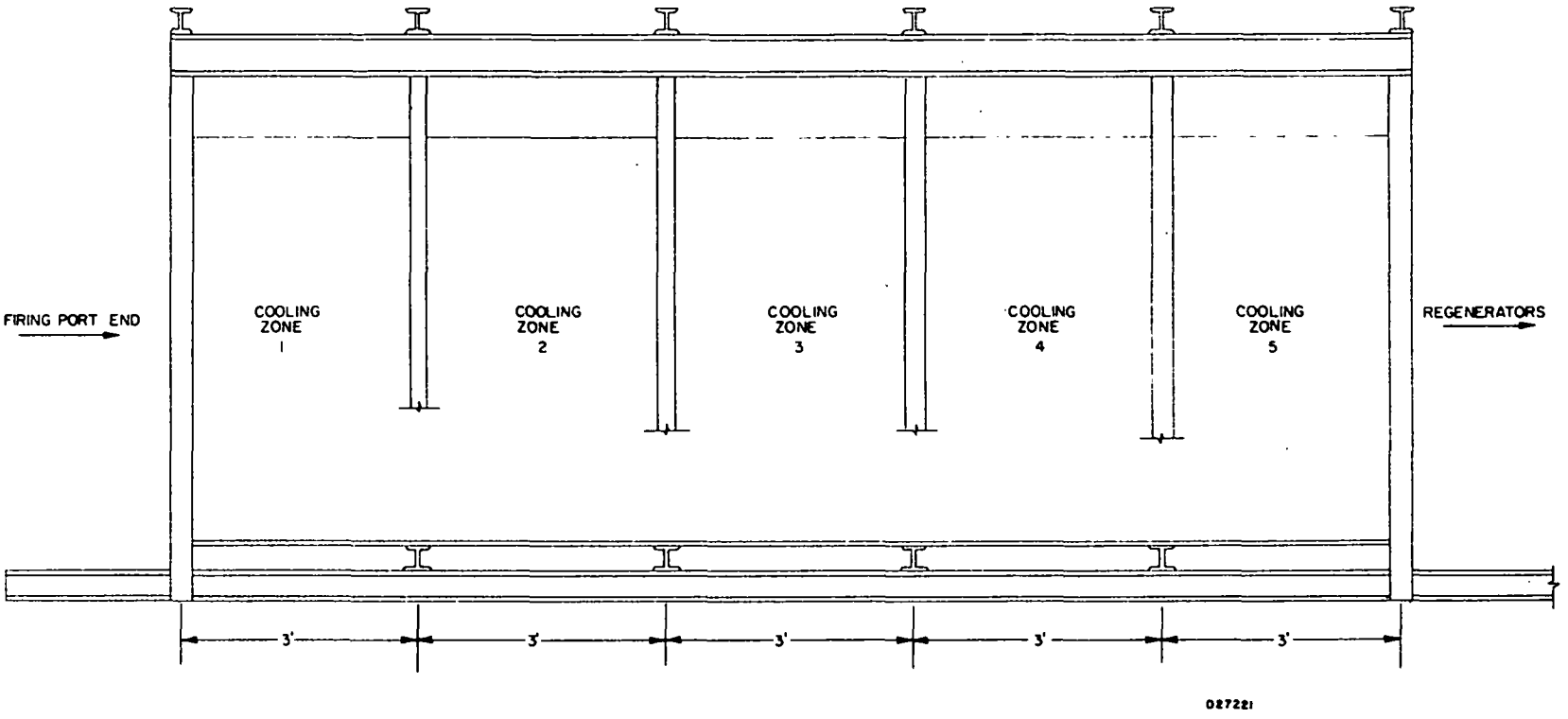

Figure II-24. SIDE VIEW OF MAIN FURNACE SHOWING STEEL STRUCTURE AND COOLING ZONES

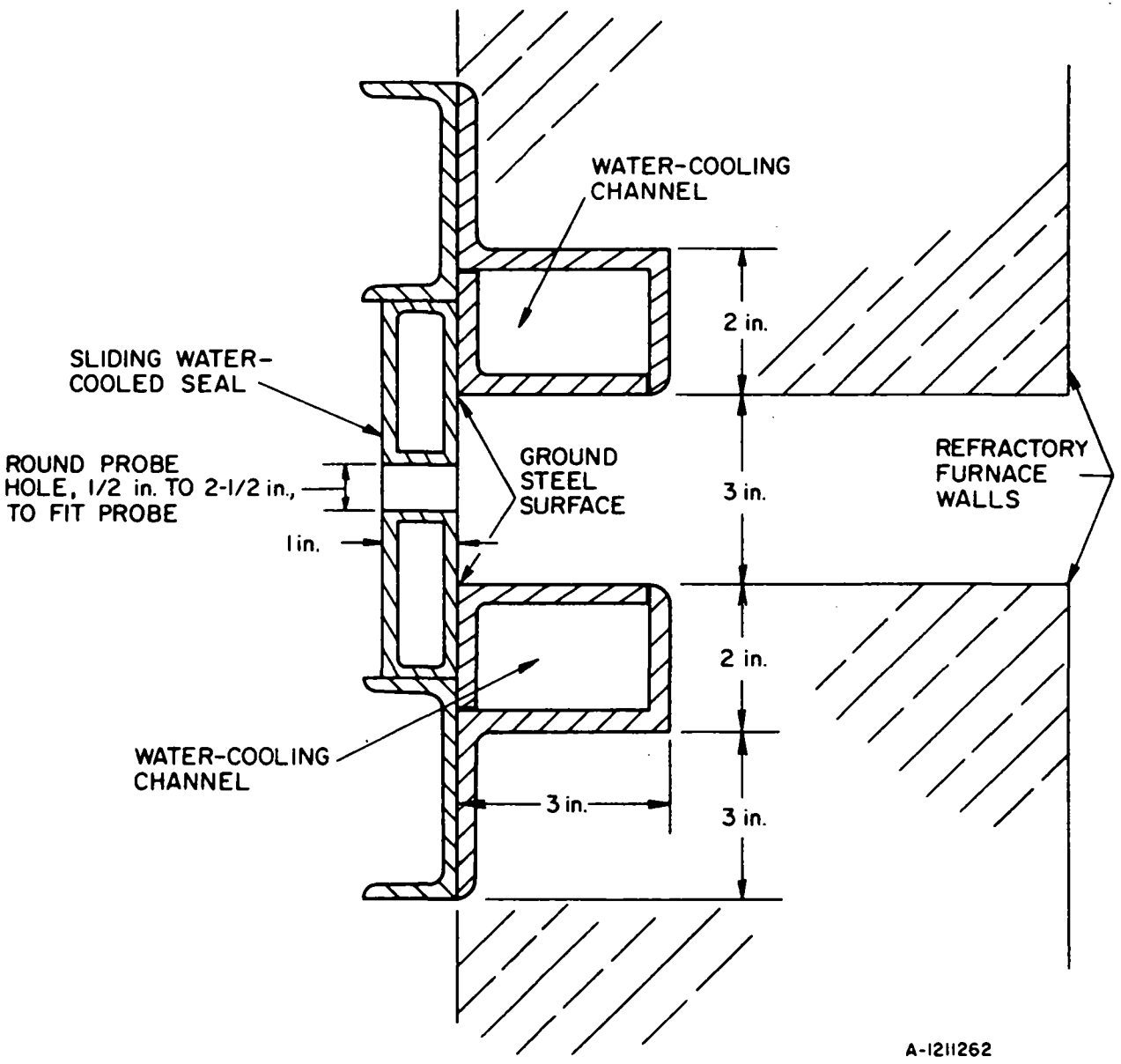

Figure II-25. PROBE SLOT-SEAL ASSEMBLY

1. Heat Losses Through Refractory Walls

The heat losses through the furnace walls are one of the most significant losses which determine the operating temperature of the furnace for a fixed gas input. The available gas and air supply to the furnace dictated a maximum energy input of 3.5 million Btu/hr. Figure II-26 illustrates the thermal conditions which must exist for steady operation.

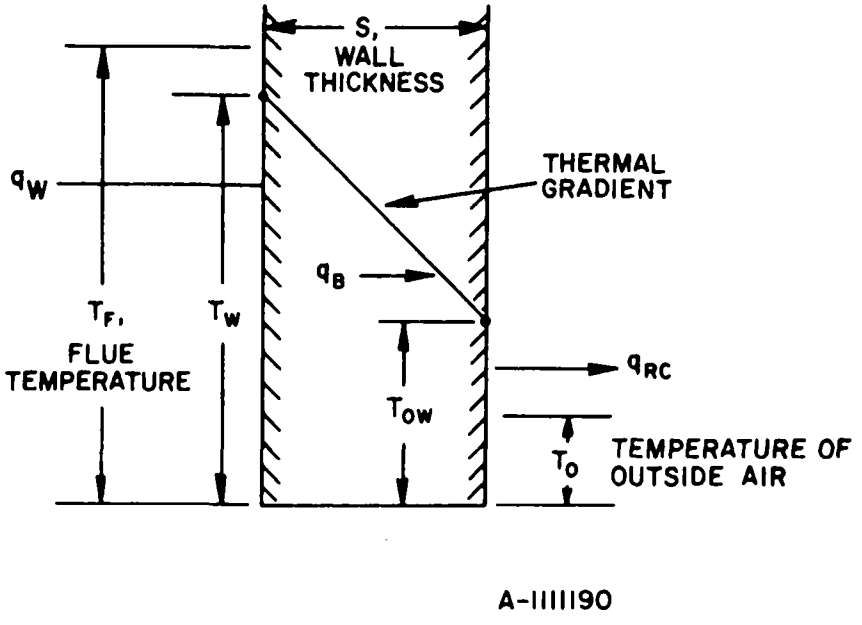

Figure II-26. TEMPERATURE GRADIENT FOR STEADY FLOW OF HEAT THROUGH A FURNACE WALL

The inside temperature of the wall drops steadily in the direction of its outer surface, where it exceeds the temperature of the surrounding air. The heat loss for a given expanse of wall and for a given furnace temperature becomes less if the wall is made thicker, if the thermal conductivity of the refractory is lowered, or if the outer surface of the furnace is of such a character that does not readily give up its heat to the surrounding media. These relationships are mathematically expressed by the following equations:

$$q_B = q_W = \frac{k(T_w - T_{ow})}{S} \qquad \text{(II-9)}$$

$$q_{RC} = q_W = C(T_{ow} - T_o) \qquad \text{(II-10)}$$

where –

q_W = heat transmitted, Btu/hr-sq ft

k = thermal conductivity of wall materials, Btu-in./hr-^{0}F-sq ft

S = thickness of walls, in.

C = coefficient of radiant and convective heat loss, Btu/hr-sq ft-^{0}F

T_w = inside wall temperature, ^{0}F

T_{ow} = outside wall temperature, ^{0}F

T_o = temperature of surrounding air, ^{0}F

Equations II-9 and II-10 are fundamental to heat transfer calculations for any furnace and were applied here for this program's furnace requirements. The unknown quantities in Equations II-9 and II-10 are q_W and T_{ow}. Our particular requirements for proper furnace operations fixed the values for the other variables (Table II-1).

Table II-1. REQUIRED OPERATING CONDITIONS OF EXPERIMENTAL FURNACE

Maximum Natural Gas Input: 3.5×10^6 Btu/hr

Maximum Inside Wall Temperature, T_w: 2800^{0}F

Average Surrounding Air Temperature,* T_o: 80^{0}F

Thermal Conductivity† of Refractories, k: 7.37 Btu-in./hr-^{0}F-sq ft

Thickness† of Walls, S: 9.0 in.

* The inside air of the building which houses the furnace is controlled by ventilating and heating units at a temperature of 80^{0}F.

† These values were based on the existing dimensions of the furnace and refractories currently being used in the roof, which were not structurally modified for the project.

Obtaining a value for q_W involves calculating the heat losses from Equations II-9 and II-10 for various assumed outside wall temperatures, and then comparing each to determine the outside wall temperature at which q_B equals q_{RC}. Substituting the values for k and S shown in Table II-1 into Equation II-9 yields –

$$q_B = q_W = \frac{7.37}{9}(T_w - T_{ow}) = 0.82(2800 - T_{ow}) \qquad \text{(II-11)}$$

Figure II-27 shows values of q_B for assumed outside wall temperatures that range between 0^0 and 1100^0F. The heat loss varies from 1400 to 2300 Btu/hr-sq ft over this temperature range.

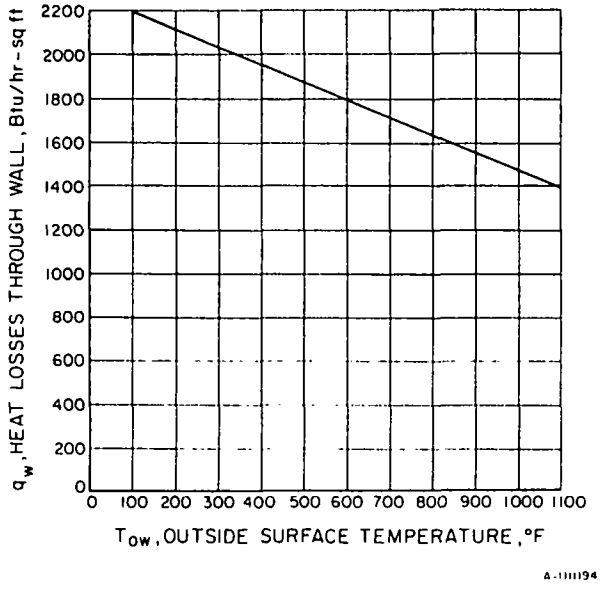

Figure II-27. HEAT LOSSES THROUGH WALLS AS A FUNCTION OF OUTSIDE WALL TEMPERATURES FOR A 2800^0F INSIDE WALL TEMPERATURE

Calculating q_{RC} from Equation II-10 is somewhat more difficult because C varies with the temperature of the outside wall, with its horizontal or vertical location, and with the physical condition of the surface. Although this coefficient is not a true coefficient of heat transfer, it accounts for the heat lost by both radiation and convection. For approximate calculations, the heat loss coefficient, C, can be determined from Equation II-12 and then substituted into Equation II-10.

$$C = 1.6 + 0.006\ T_{ow} \qquad \text{(II-12)}$$

For a more rigorous solution, we used Equation II-13 to account for the heat losses from radiation and convection separately from all vertical walls in still air.

$$q_{RC} = q_W = 0.155\ \left[\left(\frac{T_{ow} + 460}{100}\right)^4 - \left(\frac{T_o + 460}{100}\right)^4\right] + 0.28\ (T_{ow} - T_o)^{5/4} \qquad \text{(II-13)}$$

Figure II-28 again shows q_{RC} as a function of the assumed outside wall temperatures, T_{ow}, over the temperature range of 0^0-1000^0F. A sufficiently accurate estimate of the heat losses caused by radiation and convection from the furnace hearth can be obtained by dividing q_{RC} by 2.0.

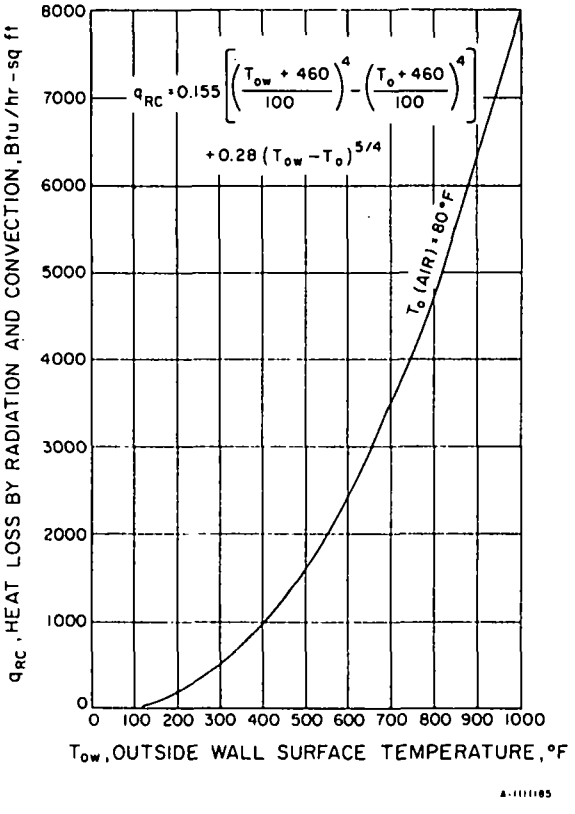

Figure II-28. HEAT LOSSES FROM VERTICAL WALLS IN STILL AIR AT 80^0F

By comparing Figures II-27 and II-28 and knowing that $q_{RC} = q_B = q_W$, we found that for the sidewalls and roof —

$$q_W = q_B = q_{RC} \tilde{=} 1850 \text{ Btu/hr-sq ft}$$

$$\text{when } T_{ow} = 535^0\text{F}$$

For the furnace hearth —

$$q_W = q_B = q_{RC} \tilde{=} 1750 \text{ Btu/hr-sq ft}$$

$$\text{when } T_{ow} = 700^0\text{F}$$

The values of q_W obtained for the sidewalls and hearth can be compared with the wall losses that can be tolerated for the available fixed gas input. These are obtained from the generalized overall heat balance on the furnace. Total heat losses through the walls can be calculated from Equation II-14, which is simply the conservation of energy.

$$Q_W = Q_I - Q_F - Q_S - Q_M \qquad \text{(II-14)}$$

where –

Q_I = total heat input, Btu/hr

Q_F = heat lost with flue products, Btu/hr

Q_S = heat lost to any furnace load, Btu/hr

Q_M = miscellaneous heat losses like radiation through openings, etc., Btu/hr

Since Q_W, Q_I, $Q_F >> Q_S$, Q_M, we assumed that $Q_S = Q_M = 0$. Therefore –

$$Q_W = Q_I - Q_F \qquad \text{(II-15)}$$

Heat input, Q_I, is the heat supplied by burning a certain quantity of natural gas, which we fixed earlier at 3.5 million Btu/hr.

Heat losses through hot flue products leaving the furnace are a fraction of the mass flow of products and the heat capacity of each flue component. However, we need not calculate Q_F because these values are standard and are published in a wide variety of textbooks and reference tables. For reference purposes, Figure II-29 gives the heat lost through flue products as a function of the flue gas temperature. Generally, the temperature of the flue products is about 200 degrees higher than the average furnace wall temperature when no load is present in the furnace. For our wall temperature of 2800°F, we assumed that the flue temperature was 3000°F. From Figure II-29, the heat losses are 75% of the gas input or 2.71 million Btu/hr.

Referring again to Equation II-15, the allowable total heat loss through the walls is –

$$Q_W = (3.5 \times 10^6) - (2.66 \times 10^6) = 790,000 \text{ Btu/hr}$$

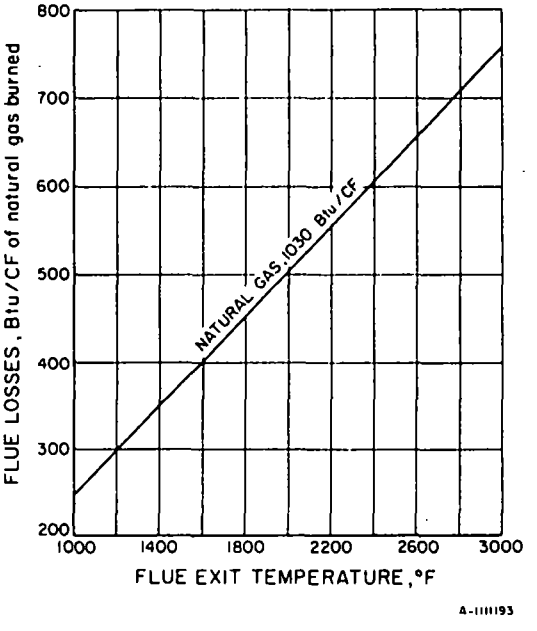

Figure II-29. HEAT LOSSES THROUGH FLUE AS A FUNCTION OF FLUE GAS TEMPERATURE (Fuel/Air = Stoich.)

When the total allowable wall losses, Q_W, are divided by the furnace surface area, we obtain the allowable wall losses per square foot, q'_W. The furnace-wall surface area, calculated in the following section, is 455 sq ft. Therefore —

$$q'_W = \frac{Q_W}{A} = \frac{790,000}{426} = 1845 \text{ Btu/hr-sq ft} \qquad \text{(II-16)}$$

If we choose a refractory wall with the proper thickness and a refractory material with the proper thermal conductivity, k, then the allowable wall losses, q'_W, should approximately equal the calculated wall losses, q_W. In our case these are reasonably close:

$$q_W = 1850 \text{ Btu/hr-sq ft}$$

$$q'_W = 1845 \text{ Btu/hr-sq ft}$$

2. Furnace Surface Area for Heat Transfer

The basic inside furnace dimensions (Figure II-30) are 5 x 5 x 15 feet long, with 9-inch-thick walls. Obviously, the area of the hot face is smaller than that of the cold (outside) surface; therefore, the true heat-transmitting surface lies somewhere between the inside and outside surface areas. Generally, the true heat-transmitting surface is assumed to be halfway between the inner and outer edges. Therefore –

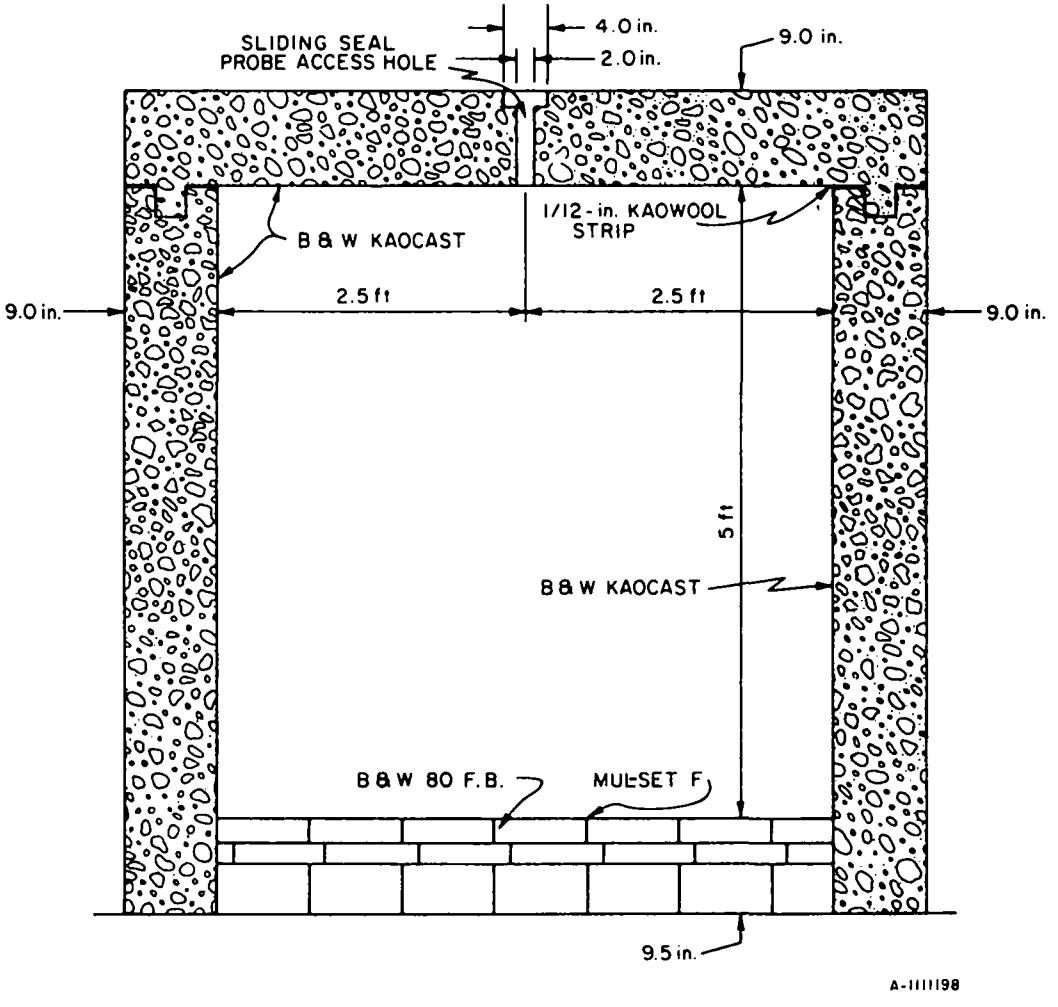

Figure II-30. END VIEW OF HOT-MODEL REFRACTORY CONSTRUCTION

$$A_s = (L + 9)(H + 9) \quad \text{(II-17)}$$

$$A_e = (W + 9)(H + 9) \quad \text{(II-18)}$$

$$A_h = (W + 9)(L + 9) \quad \text{(II-19)}$$

$$A_r = A_h = (W + 9)(L + 9) \quad \text{(II-20)}$$

$$A_{total} = 2A_s + 2A_e + 2A_h \quad \text{(II-21)}$$

where —

A_s = area of sidewalls, sq ft

A_e = area of endwalls, sq ft

A_h, A_r = area of hearth and roof, sq ft

Substituting the furnace's inside dimensions into Equations II-17 to II-21 yields —

$$A_s = 90.5 \text{ sq ft}$$

$$A_e = 32.0 \text{ sq ft}$$

$$A_h = A_r = 90.5 \text{ sq ft}$$

$$A_{total} = 426 \text{ sq ft}$$

3. Internal Water Load Calculations

Two types of wall cooling systems were used in the experimental furnace: The primary cooling control was provided by water tubes positioned in the refractory, and additional control could be obtained, when necessary, by inserting tubes directly into the combustion chamber.

The design calculations for the buried water load tubes indicated that 30 tubes were required in each wall with the tubes having a 1.0-inch outside diameter and a 12-gauge Type-304 stainless steel wall. The tubes contained flowing air during periods when the maximum refractory face temperature of 2800°F was necessary. When it became necessary to lower wall temperature to a minimum of 2400°F, water was substituted for the air. Table II-2 summarizes the flow and temperature conditions of the cooling system. The calculations leading to these values are not presented because the methods of calculation are widely published in most heat-transfer texts.

Table II-2. OPERATING CONDITIONS OF PRIMARY COOLING LOAD SYSTEM FOR VARIOUS FURNACE CONDITIONS

General (Fixed) Conditions	
Tube Diameter, inches	1.0
Tube Wall Thickness, inches	0.109
Number Tubes Per Wall	30
At Refractory Face Temperature of 2800°F	
Cooling Media	Air
Tube Wall Temperature, °F	1260 (Average)
Air Flow Per Tube, SCF/hr	750
Total Air Flow, SCF/hr*	66,000
Outlet Air Temperature, °F	850
Pressure Drop Per Tube, psia	0.1
Air Supply Fan	100,000 CF/hr at 1.5 psig
At Refractory Face Temperature of 2400°F	
Cooling Media	Water
Tube Wall Temperature, °F	200
Water Flow Per Tube, lb/hr	550
Total Water Flow, lb/hr*	50,000
Water Outlet Temperature, °F	135
Water Pump Design	150 gpm at 60 psig

* Ceiling not cooled.

Figure II-31 shows a schematic diagram of the cooling tube system piping. Air is supplied from a conventional high-pressure blower equipped with a butterfly valve and filter on the inlet. The air is piped to a 6-inch-diameter manifold to which the inlet of each cooling tube is connected. The air is metered with a standard orifice plate at the inlet to the manifold. The manifold is constructed of Schedule 40 steel pipe, and the air duct is Schedule 10 PVC plastic pipe. The heated air from each cooling tube is piped to an outlet manifold of Schedule 40 steel pipe. One end of the pipe terminates outside and serves as the vent for waste air. The vent end of the outlet manifold is equipped with a 6-inch-diameter blind plate that must be shut off when cooling with water. Water

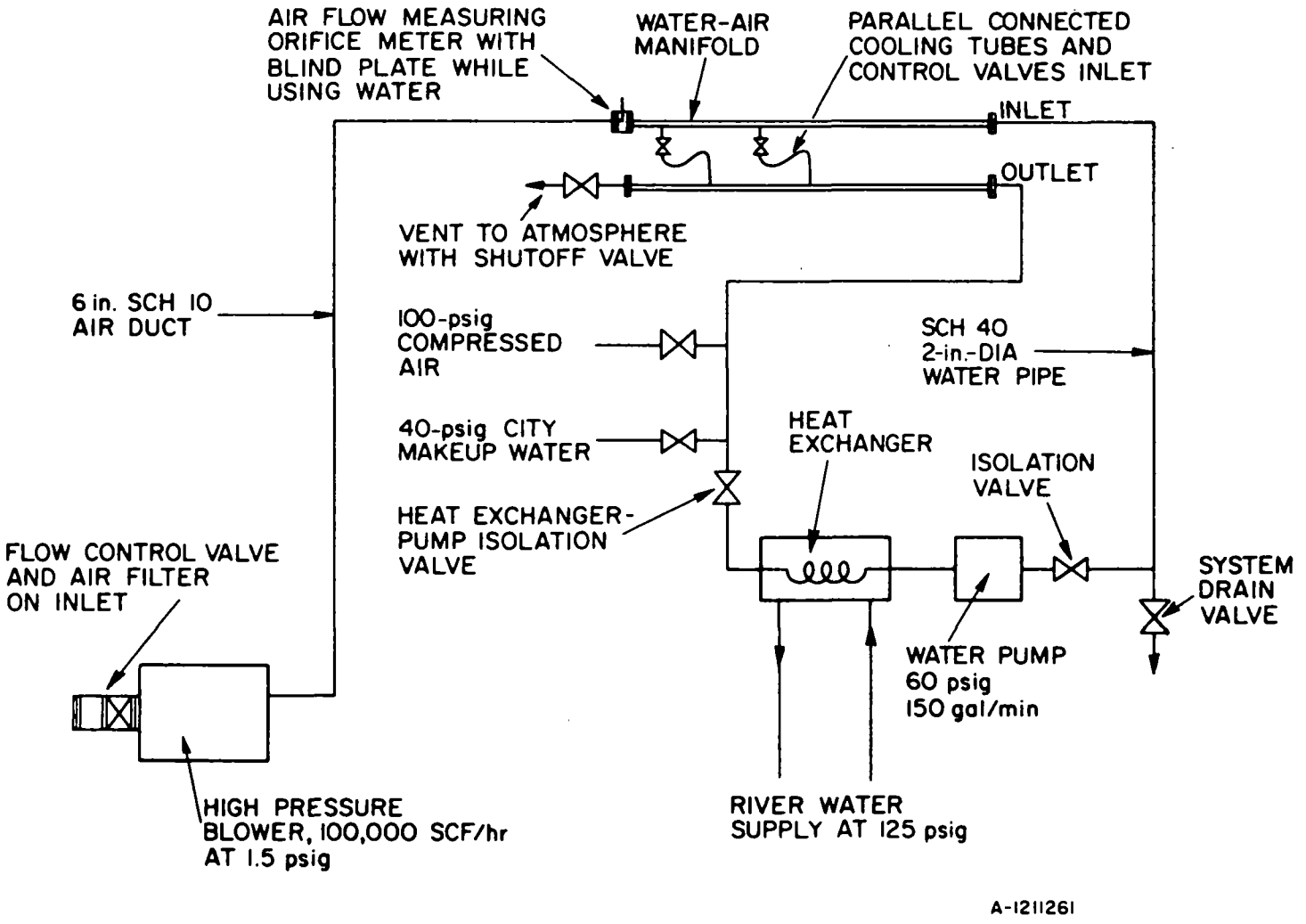

Figure II-31. SCHEMATIC DIAGRAM OF WATER-AIR COOLING SUPPLY SYSTEM

is supplied by a 60-psig pump capable of delivering 150 gallons per minute. Water is continuously recirculated through a heat exchanger. The heat exchanger is cooled by river water supplied by our pilot plant system at 125 psig. The water is piped to the cooling tubes through the same manifolds used for air. Therefore, to switch between air and water requires a somewhat complex valve arrangement. First, the air blower is isolated from the manifold by inserting a blind plate in place of the orifice plate and then closing the atmospheric vent. The water pump is started and the manifolds flooded by opening both isolation valves. When changing from water to air, the isolation valves are closed off and the water blown out of the system through the drain valve by the 100-psig compressed air. Whenever the water system is started up, it must be charged with makeup city water. The makeup water inlet is upstream of the heat exchanger and of a higher pressure than the heat exchanger inlet line. Therefore, the makeup water can be added while the high-pressure circulating pump is operating.

The "bayonet" type of cooling tube inserted directly into the combustion chamber was designed, in addition to the "buried" cooling tubes, for —

1. Lowering average wall temperature below 2400°F, if needed, which cannot be accomplished by the buried tubes.

2. Providing spot cooling in very high heat-release areas where the buried loads might not be effective enough to provide isothermal conditions.

The "bayonet" probes absorb heat by radiation and convection, thus cooling the refractories. The probe design we selected is shown in Figure II-32. This design is both effective and relatively inexpensive to fabricate.

The effective area for heat transfer of a single probe is —

$$A = \frac{2L\pi D}{24} = \frac{L\pi D}{12} \qquad \text{(II-22)}$$

where —

L = insertion depth into furnace, ft

D = diameter of tube, in.

A = effective area for heat transfer, sq ft

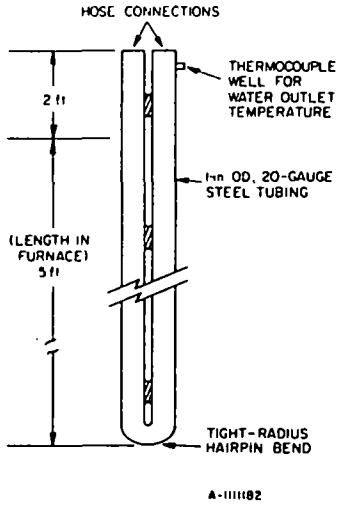

Figure II-32. WATER LOAD DESIGN

To simplify the following calculations, we must convert the dimensions of the double-tube probe into "equivalent" single-tube dimensions. The equivalent area of the single-tube probe, A_E, is –

$$A_E = \frac{\pi D_E L}{24} \qquad \text{(II-23)}$$

Since $A = A_E$, by design, then –

$$D_E = 2D = (2)(1.0 \text{ in.}) = 2.0 \text{ in.} \qquad \text{(II-24)}$$

and the equivalent area for heat transfer is –

$$A_E = \frac{\pi D_E L}{24} = \frac{(3.14)(2)(5)}{24} = 1.31 \text{ sq ft}$$

where L = 5 feet for the full insertion of the probe into the furnace enclosure.

Heat is transferred to the tube walls by radiation and convection and then to the water in the tubes by convection. The mathematical equation for heat transferred from the furnace walls to the tube surface (Figure II-33) is –

$$Q_{TRC} = AF_a F_\epsilon \sigma (T_1^4 - T_2^4) \qquad \text{(II-25)}$$

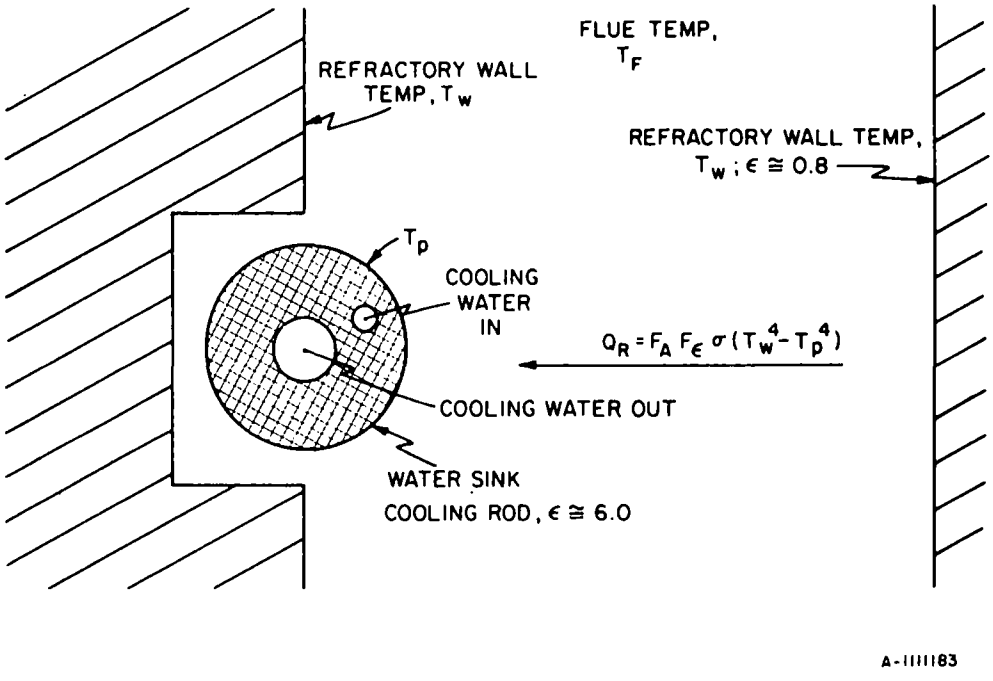

Figure II-33. NOMENCLATURE FOR RADIANT HEAT TRANSFER FROM FURNACE WALLS TO INTERNAL COOLING TUBES

where —

Q_{TRC} = heat transmitted to tubes by radiation and convection, Btu/hr

A = effective heat transfer area of the tube or tubes, sq ft

F_a = shape factor, dimensionless

F_ϵ = emissivity factor, dimensionless

σ = Stefan-Boltzmann constant, 0.1714 X 10^{-8} Btu/hr-$^0R^4$-sq ft

T_1 = temperature of furnace walls, ^0R

T_2 = temperature of tube walls, ^0R

The heat transfer from the tube walls to the water by convection is mathematically determined by Equation II-26.

$$Q_{TC} = hA'(T_2 - T_{mb}) \qquad \text{(II-26)}$$

where —

Q_{TC} = heat transmitted to water, Btu/hr

h = convective heat transfer coefficient, Btu/sq ft-^{0}F-hr

A' = surface area of tube walls, sq ft

T_2 = temperature of tube walls, ^{0}F

T_{mb} = mean temperature of water, ^{0}F

The convective heat transfer coefficient is determined by the empirical equation of Sieder and Tate.

$$\left(\frac{hD}{k}\right)_{mb} = \left(\frac{\mu_{mb}}{\mu_s}\right)^{0.14} \left(\frac{D}{L}\right)^{1/3} (N_{Pr})_{mb}^{1/3} (N_{Re})_{mb}^{1/3} U \qquad \text{(II-27)}$$

where the only variables are the mass flow of water in a tube and the temperature rise tolerable in the tubes, and —

D = tube diameter, ft

k = thermal conductivity of water at T_{mb}, Btu/sq ft-^{0}F-hr

μ = viscosity of water, lbf/s-sq ft (s, at tube surface; mb, average)

L = length of tube, ft

U = velocity of water in tubes, ft/s

N_{Pr} = Prandtl number

N_{Re} = Reynolds number

where —

$$N_{Pr} = \frac{C_p \mu}{k} \qquad \text{(II-28)}$$

and

$$N_{Re} = \frac{\rho UD}{\mu} \qquad \text{(II-29)}$$

and

C_p = heat capacity of water at T_{mb}, Btu/lbm-^{0}F

ρ = density, lbm/cu ft

The solution to this problem is similar to that for finding the steady-state wall temperature without water cooling. Q_{TRC} and Q_{TC} are solved simultaneously in terms of the variables; the operating conditions are found by comparing the results, where Q_{TRC} equals Q_{TC}.

To solve Q_{TRC}, let F_A equal 0.5. This value was determined from curves published in Engineering Heat Transfer by Hsu for 2-inch-diameter tubular cooling pipes, which are spaced 0.5-4.0 feet apart along one wall and receive the heat transferred from a surrounding enclosure.

F_ϵ the emissivity factor for a relatively small receiver area (compared with the radiating surface which is positioned approximately hemispherically around the receiver), is given by Equation II-30.

$$F_\epsilon = \epsilon_r \epsilon_e \qquad \text{(II-30)}$$

where —

ϵ_r = emissivity of receiver tubes

ϵ_e = emissivity of radiating furnace walls (assumed to equal 1.0)

Substituting the values of F_A and T_2 into Equation II-25 and assuming a maximum tube wall temperature (T_2) of 200°F to prevent the water from boiling, yields Figure II-34, which shows heat transferred by radiation per unit area (q_s) as a function of the tube emissivity and of the temperature of the furnace walls or radiating surface. Multiplying these data by the area yields Figure II-35.

Q_{TC} is solved by first solving for h from Equations II-27, II-28, and II-29. Values for the equations' constants at the mean water temperature, T_{mb}, are given in Table II-3. The mean water temperature is given by Equation II-31:

$$T_{mb} = 1/2(T_{inlet} + T_{outlet}) \qquad \text{(II-31)}$$

We chose a temperature rise of 30°F with an average inlet temperature of 70°F; therefore —

$$T_{mb} = 1/2(70 + 100) = 85^0F$$

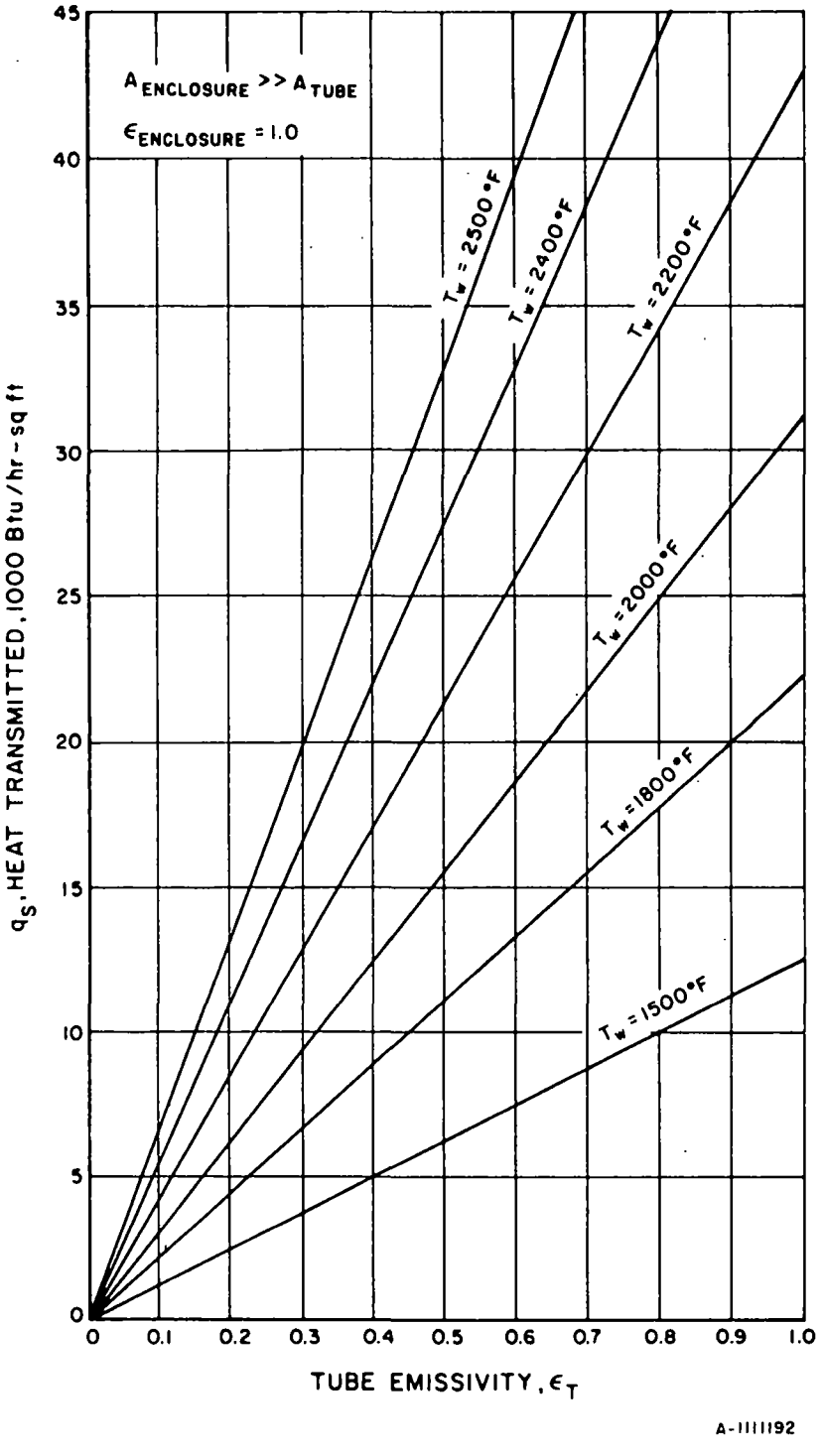

Figure II-34. HEAT TRANSMITTED PER UNIT AREA TO 2-INCH-DIAMETER TUBE (T_2 = 200°F) FROM AN ENCLOSURE SURROUNDING 180 DEGREES OF TUBE

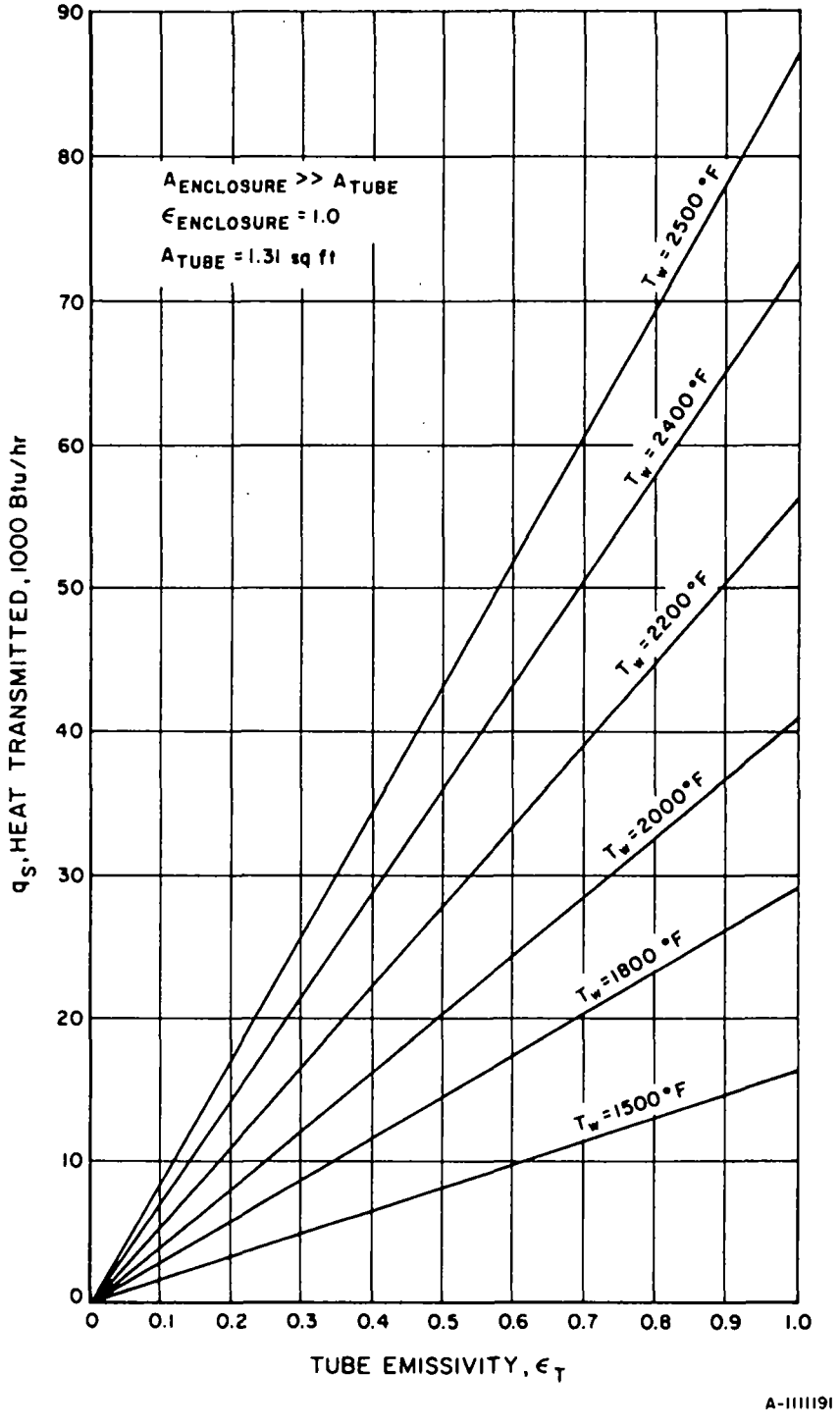

Figure II-35. TOTAL HEAT TRANSMITTED PER TUBE

Table II-3. VALUES FOR CONSTANTS OF EQUATIONS II-27, II-28, AND II-29 AT $T_{mb} = 85^0F$ FOR WATER

$$\mu_{mb} = 1.5 \times 10^{-5} \text{ lbf/s-sq ft}$$

$$k = 0.356 \text{ Btu/sq ft-}^0\text{F-hr}$$

$$C_p = 0.998 \text{ Btu/lbm-}^0\text{F}$$

$$\rho = 62.1 \text{ lbm/cu ft}$$

$$\mu_{at\ 200^0F} = 0.55 \times 10^{-5} \text{ lbf/s-sq ft}$$

$$A' = \pi DL = 2.61 \text{ sq ft}$$

To simplify the results we expressed the velocity of the water in terms of the weight flow, Equation II-32.

$$U = \frac{W}{\rho A} = \frac{W}{1220} \qquad \text{(II-32)}$$

where W = weight flow, lb/hr.

Using Equations II-26 to II-29 and the values in Table II-3, solved for Q_{TC}, as a function of the weight flow of water yields Figure II-36.

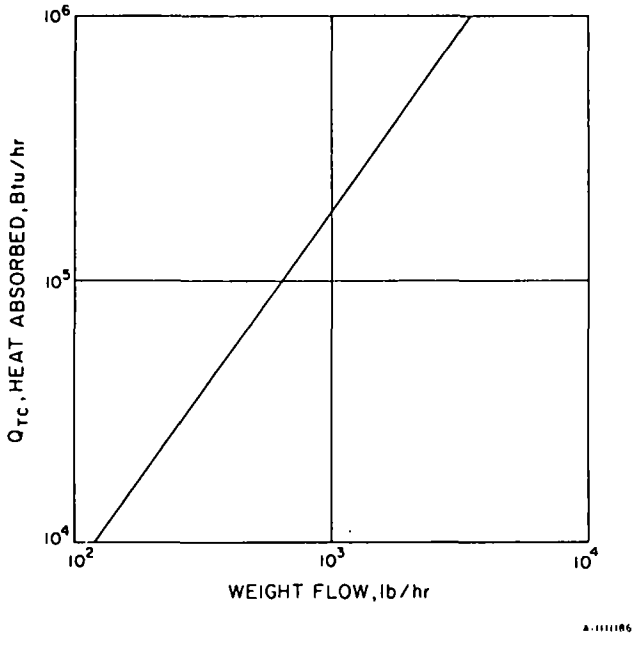

Figure II-36. WEIGHT FLOW OF WATER AS A FUNCTION OF HEAT TRANSFERRED FROM TUBE WALLS TO WATER

It is now possible to determine, from Figures II-35 and II-36, the water flow necessary to maintain a 200°F tube surface temperature as a function of the desired furnace wall temperature and the tube's emissivity. Figure II-37, compiled from Figures II-35 and II-36, shows the minimum amount of water necessary for any desired furnace wall temperature assuming a tube emissivity equal to 0.8.

The last remaining step of these design calculations is to determine the number of tubes necessary to remove enough heat from the furnace to maintain any desired wall temperature. This is done by recalculating the heat losses through the wall, Q_W, for wall temperatures other than 2800°F. These calculations are shown in Figure II-38. The procedure is now the same as that described earlier for heat losses at a 2800°F inside wall temperature. The data in Figures II-29 and II-38 are compared to determine the heat loss per square foot of wall (q_W) which, when multiplied by the area of the walls, yields their total heat loss as a function of the wall temperature. Substitute Q_W into Equation II-14, where Q_S now becomes the heat absorbed by the cooling tubes.

Figure II-39 shows Q_S, the amount of heat which must be removed by the water loads to hold a desired wall temperature, with a gas input of 3.5 million Btu/hr. We can now use Figures II-35 and II-39 to determine the number of water tubes necessary to hold a desired wall temperature. The heat load is determined from Figure II-39 for the desired temperature and divided by the heat sink capacity of a single tube as shown in Figure II-35. This yields the required number of cooling tubes, Figure II-40.

It is now possible to calculate from Figure II-37 the total amount of cooling water required by the system as a function of the inside wall temperature. Figure II-41 was plotted by multiplying the water required per tube by the total number of tubes required at various wall temperatures. From this information we learned that a larger water pump was necessary at the test site if wall temperatures lower than 1960°F are required: Our earlier system is only capable of delivering 1200 gph (~10,000 lb/hr) at 100 psig.

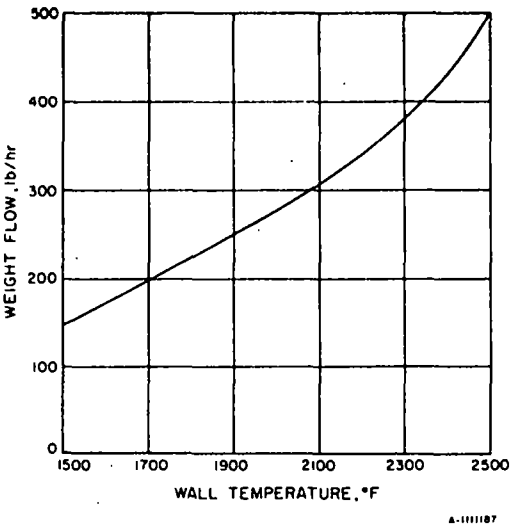

Figure II-37. MINIMUM WATER FLOW PER TUBE AS A FUNCTION OF INSIDE WALL TEMPERATURE

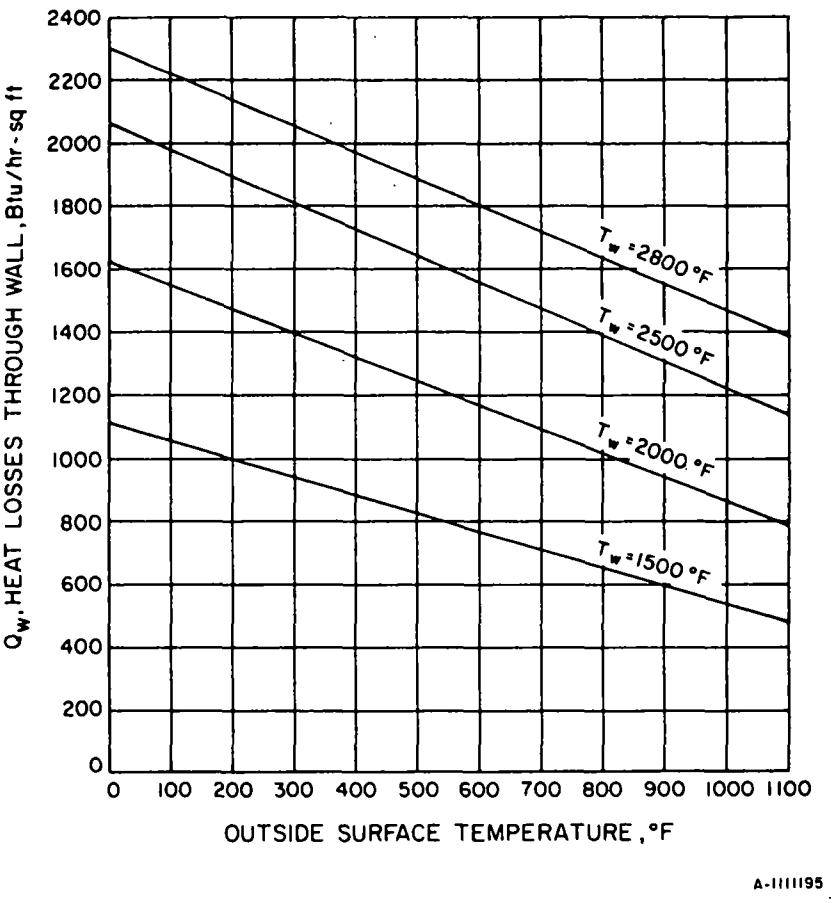

Figure II-38. HEAT LOSSES THROUGH WALLS AS A FUNCTION OF OUTSIDE WALL TEMPERATURE

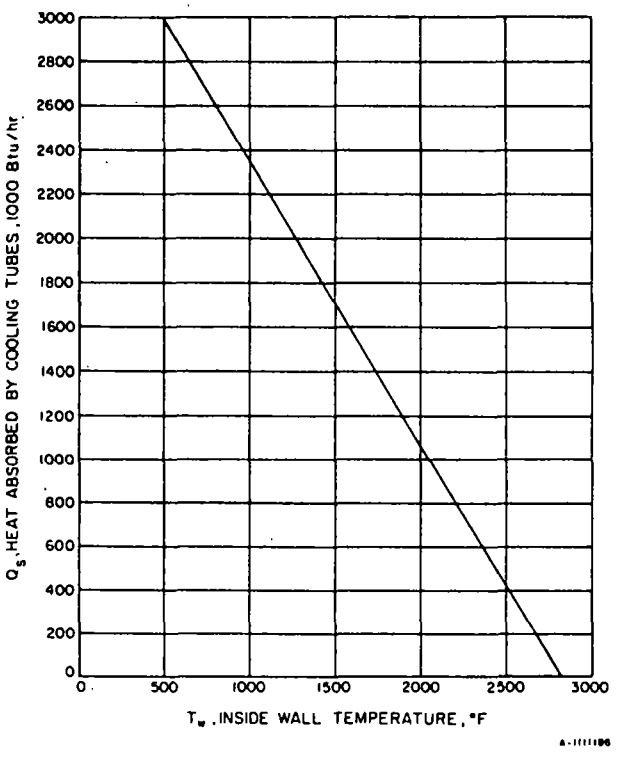

Figure II-39. AMOUNT OF HEAT THE WATER LOAD IS REQUIRED TO ABSORB TO MAINTAIN DESIRED WALL TEMPERATURE WITH GAS INPUT OF 3.5 MILLION Btu/hr

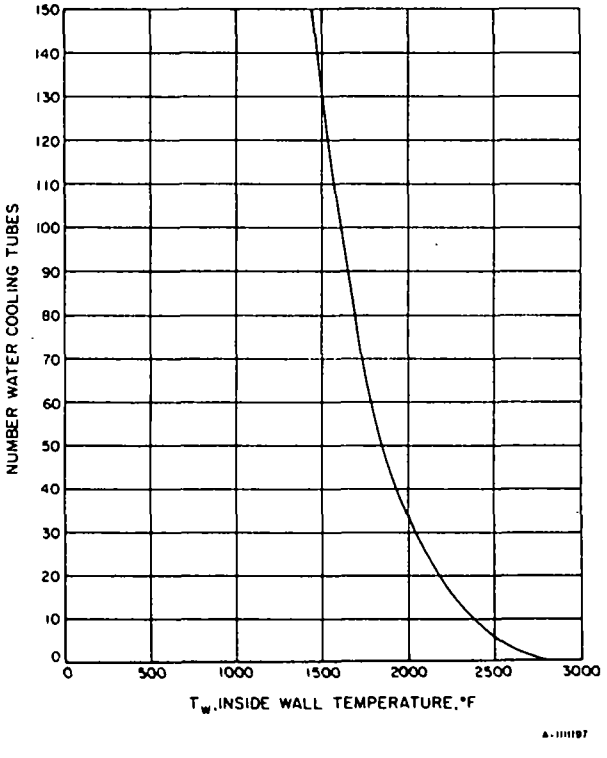

Figure II-40. REQUIRED NUMBER OF COOLING TUBES AS A FUNCTION OF INSIDE WALL TEMPERATURE

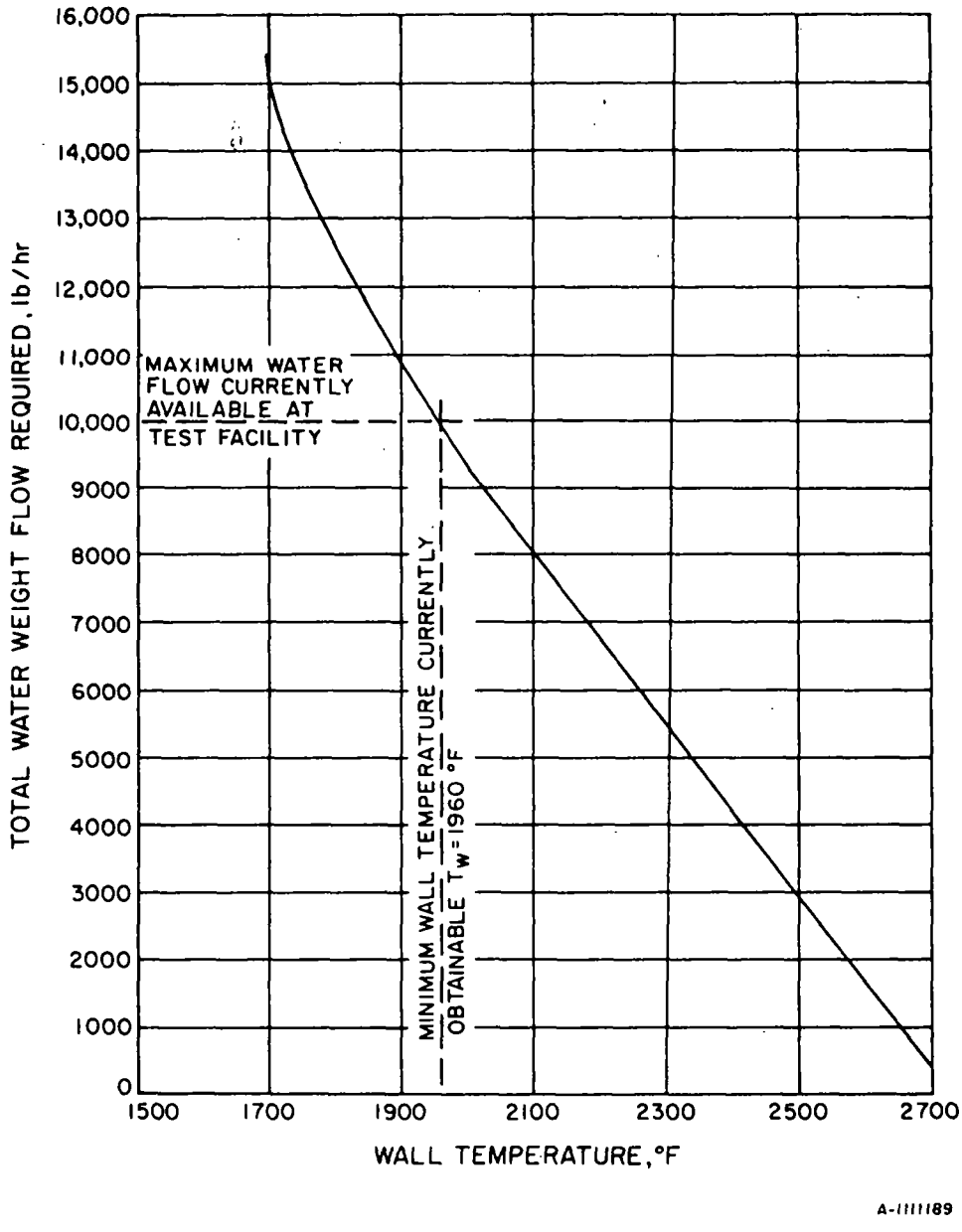

Figure II-41. TOTAL WATER CONSUMPTION REQUIRED BY COOLING LOAD AS A FUNCTION OF INSIDE WALL TEMPERATURE

The pressure drop through each probe was also considered in determining what pump pressure was required as a function of the desired inside wall temperature. The pressure drop through any tube can be mathematically determined by Equation II-33:

$$\Delta P = fL\rho U^2/288\ Dg \qquad \text{(II-33)}$$

where —

ΔP = pressure drop, psig
f = friction coefficient
L = tube length, ft
ρ = fluid density, lbm/cu ft
U = fluid velocity, ft/s
D = tube diameter, ft
g = acceleration of gravity (32.17 ft/sq s)

The velocity is expressed in terms of weight flow, assuming that the density of the fluid is 62.1 lbm/cu ft.

$$U^2 = 8.6 \times 10^{-7}\ W^2 \qquad \text{(II-34)}$$

where W = weight flow, lb/hr.

The values of the parameters in Equations II-33 and II-34 for the tube design and water that has a mean temperature of 85°F are given in Table II-4 (except for the friction factor, f).

Table II-4. PARAMETERS FOR PRESSURE DROP EQUATION FOR WATER AT 85°F

Tube Length, L = 10 ft

Tube Diameter, D = 8.34×10^{-2} ft

Fluid Density, ρ = 62.1 lbm/cu ft

Fluid Viscosity, $\mu = 0.56 \times 10^{-3}$ lbm/ft-s

Substituting Equation II-34 and the values from Table II-4 into Equation II-33 yields —

$$\Delta P = (6.4 \times 10^{-6})\ W^2 f \qquad \text{(II-35)}$$

The friction factor, f, is a function of the Reynolds number —

$$N_{Re} = \frac{\rho UD}{\mu} \qquad \text{(II-36)}$$

where μ = absolute fluid viscosity, lbm/ft-s. Therefore, the friction factor is a function of U or ultimately of weight flow. To solve for the pressure drop, we converted R. J. S. Pigott's data for Reynolds number versus friction factor to weight flow versus friction factor. This conversion is shown in Figure II-42. Solving Equation II-35, using the numbers in Figure II-42, yields the pressure drop per tube as a function of weight flow (Figure II-43).

B. High-Temperature Flame-Sampling Probes

One of the major tasks of this program was to map the profiles of temperature, chemical species, and flow magnitude and direction in the flame of each burner type. Modified designs of the International Flame Research Foundation were used to construct probes which would enable this type of data collection.

We constructed both a multidirectional impact tube (MDIT) and a gas sampling probe. Assembly drawings for these probes are shown in Figures II-44 and II-45. The MDIT probe (Figure II-44) has a hemispherical sensing head, which has passed the calibration standards of the International Flame Research Foundation. The tip construction and our calibration methods were described earlier in this report.

The 8-inch-long probe tip is 0.312 inch in diameter and constructed of Type-316 stainless steel. Each of the five tip holes is connected to thin-walled tubes, which pass through the probe body and are connected to the pressure differential measuring equipment. The probe tip is also water-cooled so that it can be used in the hot furnace environment. Water is brought into the tip through a 1/8-inch-diameter stainless-steel tube and returns along the walls of the outer tube and into the 1-1/2-inch-diameter collection chamber. The water leaves the collection chamber through a 3/8-inch-diameter tube. This type of water-cooling design keeps the cooling tubes as large as possible and, hence, pressure drop as small as possible. This is consistent with the physical size requirements of the tip.

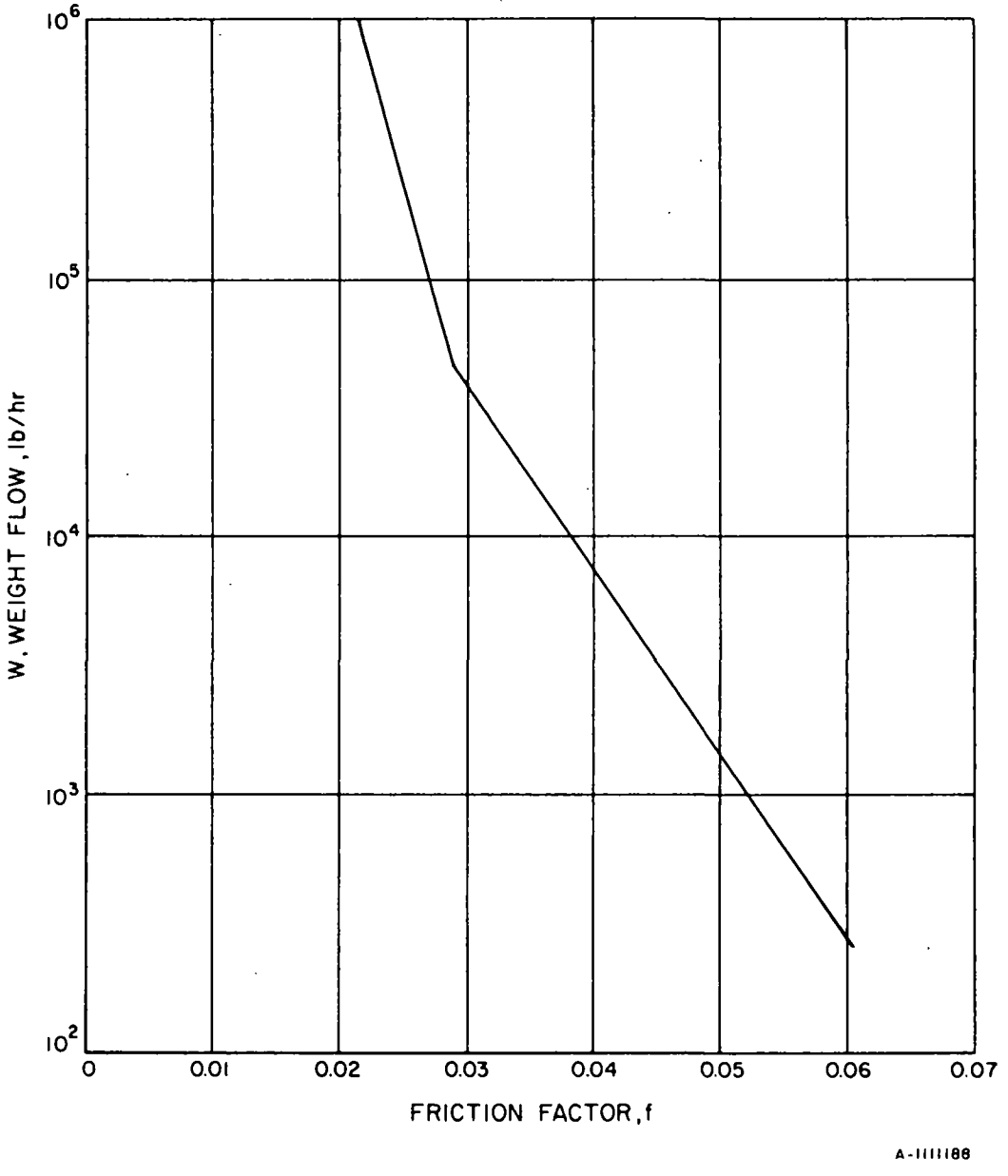

Figure II-42. FRICTION FACTOR AS A FUNCTION OF WEIGHT FLOW FOR 1-INCH-DIAMETER DRAWN STEEL TUBING CONTAINING FLOWING WATER AT 85°F

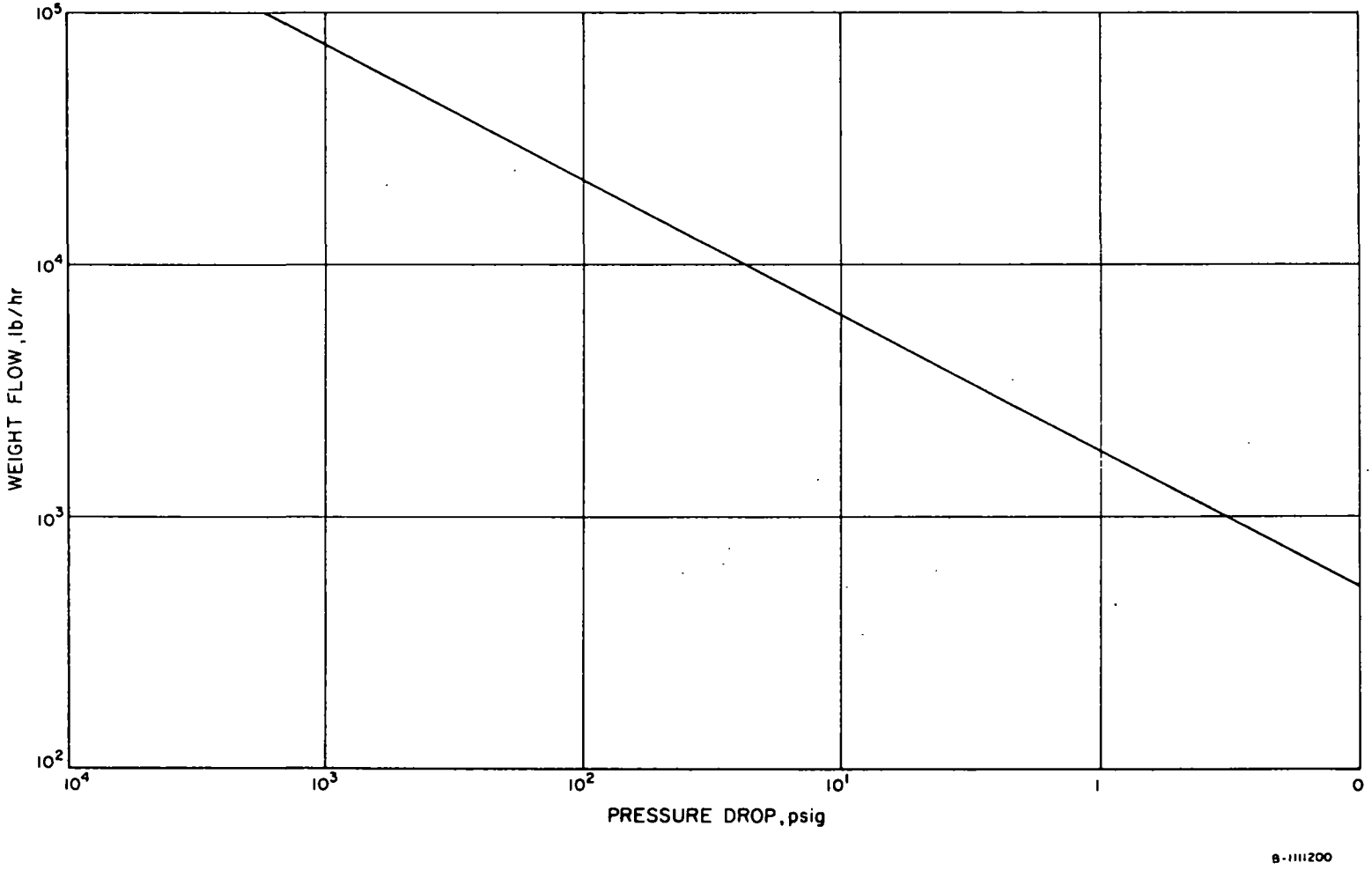

Figure II-43. SYSTEM PRESSURE DROP PER TUBE AS A FUNCTION OF WEIGHT FLOW OF WATER

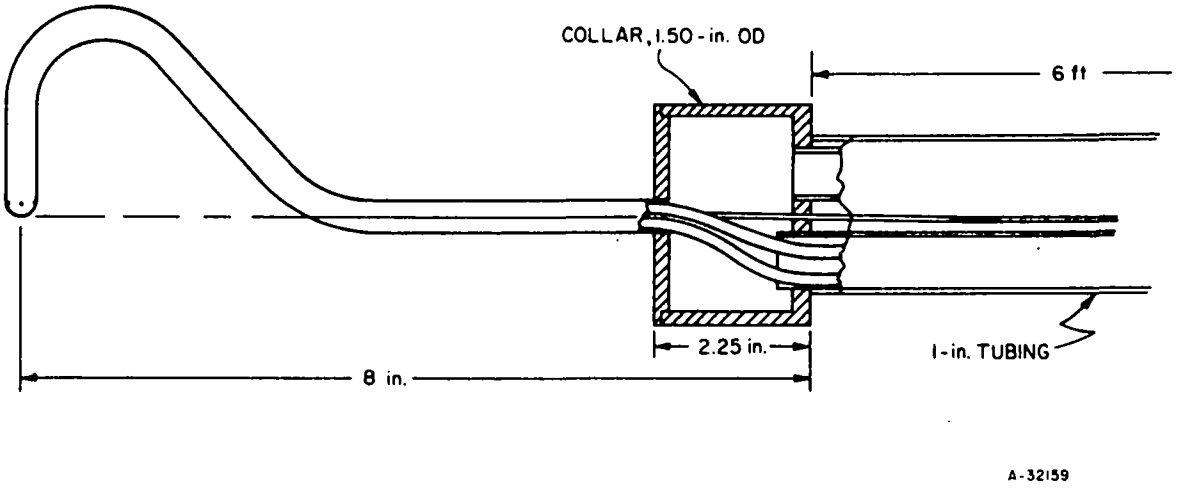

Figure II-44. FIVE-HOLE PITOT TUBE PROBE HEAD

The gas-sampling probe (Figure II-45) is constructed similarly to the five-hole pitot probe, except that the tip has only a single center hole, and it is slightly longer. Both of the probes are designed to be inserted into a water-cooled "general probe holder," which will allow the insertion of the probe tips into the hot model up to a depth of 5 feet. The general probe holder (Figure II-46) is a series of concentric tubes, with a center tube large enough to hold the water-collection chamber of both probe tips and the outer tubes carrying the water for cooling. The 2-1/2-inch-diameter holder is large in comparison to the probe tip. Its large size is necessary to maintain a reasonable water pressure drop of about 50 psig.

The probe positioner, described earlier in this report, supports the probes with two pillow blocks which allow the probes to rotate. Aluminum bushings are inserted into the blocks so that various sized probes can be used. The original bushing was made for the cold-model probe which had an outside diameter of 1.00 inch; therefore, a new bushing was needed to adapt the positioner to the 1.75-inch diameter of the probes used for hot-model testing.

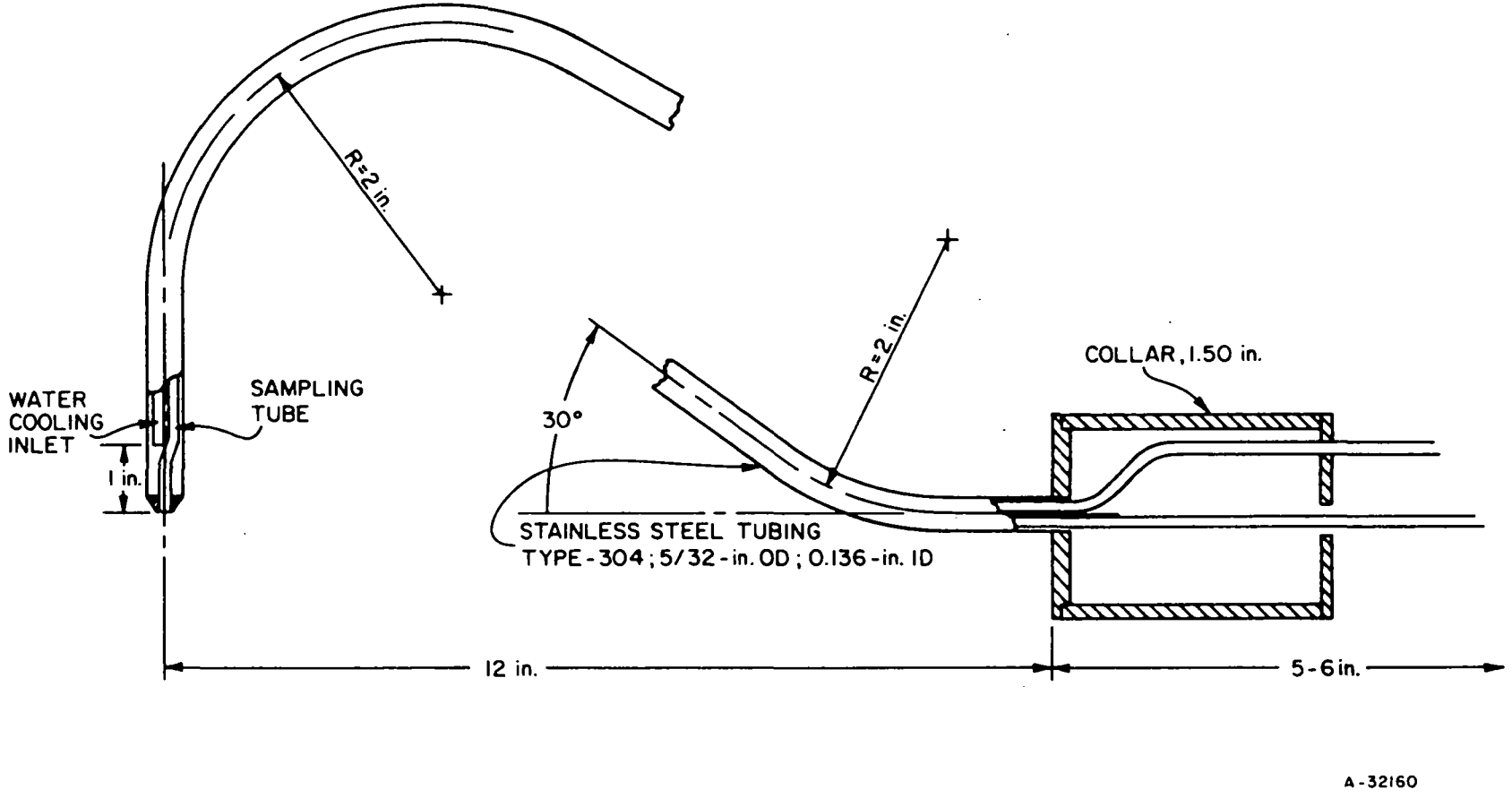

Figure II-45. GAS-SAMPLING PROBE HEAD

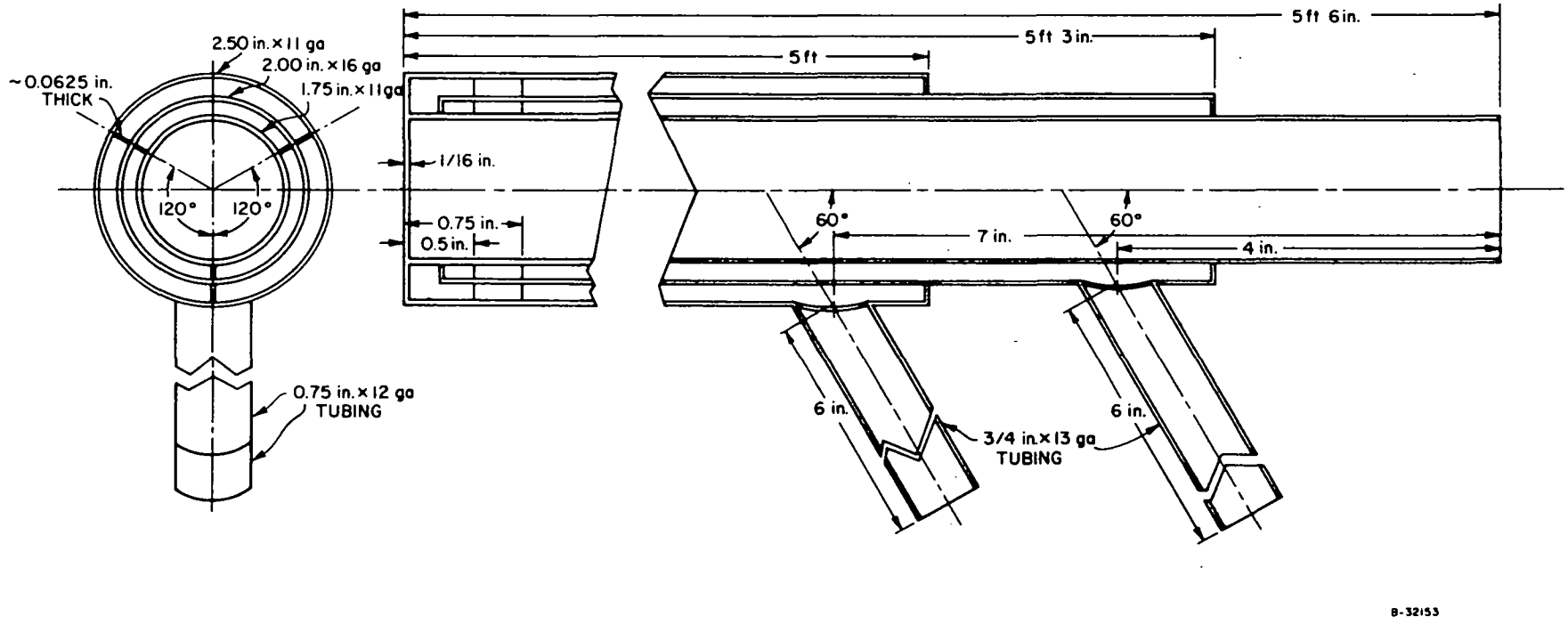

Figure II-46. GENERAL PROBE HOLDER

To facilitate the accurate rotation of both probes and to be able to return them to their original position, within 1/2 degree, we mounted an angular vernier scale to the rear of the adapter bushing (Figure II-47). Additional modifications included a probe support, which was added at the front of the probe positioner (Figure II-47) because of the heavier probes used for hot-model work.

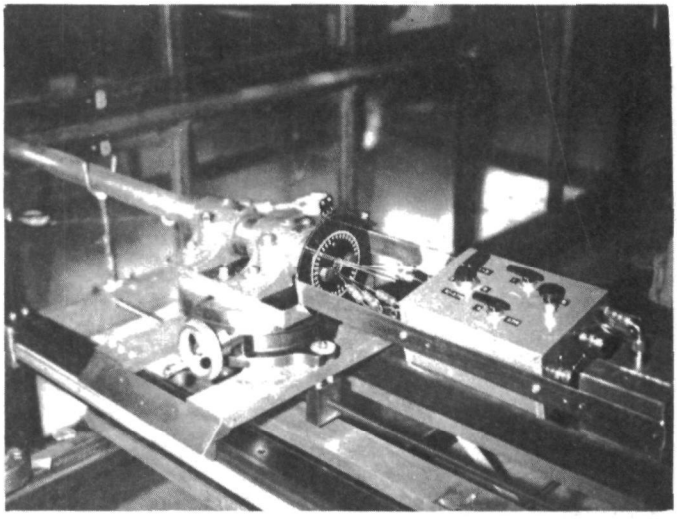

Figure II-47. MODIFIED PROBE POSITIONER FOR HOT-MODEL SAMPLING

The hot-probe hemispherical head, multidirectional impact tube (MDIT) was calibrated using the techniques outlined earlier in this report for the cold-model probe. Flow conditions of 17 ft/s and a Reynolds number, N_{Re}, of 25,000 were used for calibrating the hot hemispherical probe. The data were reduced by means of a computer program similar to one used by the International Flame Research Foundation. The following series of pressure differentials were used as data input to the calibration program:

$$\Delta P_{04} = p_0 - p_a \quad \text{(II-37)}$$

$$\Delta P_{13} = p_1 - p_3 \quad \text{(II-38)}$$

$$\Delta P_{24} = p_2 - p_4 \quad \text{(II-39)}$$

$$\Delta P_{03} = p_0 - p_3 \quad \text{(II-40)}$$

$$\Delta P_{04} = p_0 - p_4 \quad \text{(II-41)}$$

Then the following pressure differentials are calculated using the input values given above:

$$\Delta p_{01} = \Delta p_{03} - \Delta p_{13} \quad \text{(II-42)}$$

$$\Delta p_{02} = \Delta p_{04} - \Delta p_{24} \quad \text{(II-43)}$$

To simplify the equations for the pressure recovery factors, ΔP_n, the following identities are used:

$$P_T = \Delta p_{01} + \Delta p_{02} + \Delta p_{03} + \Delta p_{04} \quad \text{(II-44)}$$

$$P_R = \text{SQRT}\ [(\Delta p_{01})^2 + (\Delta p_{02})^2 + (\Delta p_{03})^2 + (\Delta p_{04})^2] \quad \text{(II-45)}$$

The MDIT is calibrated for the three recovery coefficients, K_Φ, K_v, and K_p. These coefficients are dependent on the conical angle, Φ, and are only slightly dependent on the magnitude of the velocity, V, and on the dihedral angle, δ. The angles, Φ and δ, are defined as spherical coordinates. (See Figure II-11.)

In the free jet used for the calibration —

$$P_S - P_A = 0$$

where —

P_S = static

P_A = atmospheric

Therefore at $\Phi = 0^0$

$$(\Delta P_{OA}) \text{ at } \Phi = 0^0 = P(\text{dynamic}) = 1/2\ PV^2 \quad \text{(II-46)}$$

For each pair of values of Φ and δ, P_R and P_T were calculated from the pressure differences with the aid of Equations II-44 and II-45; K_Φ, K_V, and K_p were calculated with the aid of Equations II-47, II-48, and II-49.

$$K_\Phi = \text{SQRT}\ (1 - P_T/2P_R) \tag{II-47}$$

$$K_V = \frac{(\Delta p_0 - A)_\Phi = 0}{P_{R_{\Phi, \delta}}} \tag{II-48}$$

$$K_p = \frac{(\Delta p_{0_A})_{\Phi, \delta}}{(\Delta p_{0_A})_{\Phi = 0}} \tag{II-49}$$

Using the method of least squares, the constants A_i, B_i, C, and D of the following equations were calculated:

$$\Phi = A_1 K_\Phi + A_3 K_\Phi^3 + A_5 K_\Phi^5 \tag{II-50}$$

$$K_V = B_o + B_2\ \Phi^2 + B_4\ \Phi^4 \tag{II-51}$$

$$K_p = 1 + C[\exp(-D\,\Phi^2) - 1] \tag{II-52}$$

The following equations represent the line of best fit for the calibration results of the hemispherical (8 mm, 40 degree) MDIT:

$$\Phi = 0.7706\ K_\Phi + 0.2724\ K_\Phi^3 - 0.0598\ K_\Phi^5 \tag{II-53}$$

$$K_V = 0.7377 - 0.1588\ \Phi^2 + 0.1292\ \Phi^4 \tag{II-54}$$

$$K_p = 1 + 4.37\ [\exp(-0.405\ \Phi^2) - 1] \tag{II-55}$$

Table II-5 shows the measured and the calculated (by the line of the best fit method) values of Φ, K_V, and K_p. The agreement is 1/2% for all values, which is considered very good for this type of system.

C. Hot-Modeling Furnace Instrumentation

Figure II-48 is an overall view of the hot-model instrumentation package. The instruments are mounted in two separate but interconnected dust-tight metal cabinets. The cabinet on the left contains the analyzer sections of four Beckman infrared units used to measure CO, CO_2, CH_4, and nitric oxide (NO). The three valves mounted at the top of the cabinet are used to direct the sample gas to the desired cell while providing a nitrogen-gas mixture to the unused cells.

Table II-5. EXPERIMENTAL VERSUS CALCULATED BEST FIT VALUES OF CALIBRATION DATA FOR THE FIVE-HOLE HEMISPHERICAL HEAD PITOT PROBE

Φ		K_V		K_p	
Measured	Calculated	Measured	Calculated	Measured	Calculated
0°05'	0°06'	0.74160	0.73722	1.00000	0.99999
10°00'	10°04'	0.73254	0.73300	0.95686	0.94643
20°00'	20°07'	0.71342	0.72028	0.80200	0.78961
30°00'	30°14'	0.70411	0.70389	0.55046	0.54080
35°00'	34°21'	0.69720	0.69645	0.39522	0.38710
40°00'	39°50'	0.69367	0.69101	0.19607	0.21724
45°00'	45°11'	0.69751	0.68893	0.01541	0.03399
50°00'	50°11'	0.68226	0.69172	−0.17142	−0.15976
55°00'	54°57'	0.69903	0.70111	−0.35147	−0.36112
60°00'	59°54'	0.72176	0.71898	−0.54699	−0.56721

The cabinet shown in the right side of Figure II-48 contains the amplifier and strip-chart recorder for each infrared analyzer, an oxygen analyzer, an NO_x ($NO + NO_2$) analyzer, and the sample flow-control system for all of the measuring equipment. The amplifiers and recorders for CO, CO_2, and CH_4 are mounted in the upper portion of the cabinet. Each recorder is mounted directly above its amplifier section (Figure II-49), thus allowing the operator to easily compare the meter reading with the strip-chart record while calibrating an instrument. The readings on the strip recorder and meter should both correspond on a 0-100 scale.

The sample calibration flow-control system is located in the lower portion of the control cabinet (Figure II-50) together with the NO amplifier and strip recorder. The flow controls for each gas being analyzed are grouped vertically and consist of a rotameter with an integral needle valve, a shutoff valve for the sample, a valve for each calibration gas, and a valve for the "zero" gas (pure nitrogen). The rotameters used for nitrogen oxides sampling are specially constructed: All of the surfaces that contact the sample are either made of Type-316 stainless steel or of Teflon.

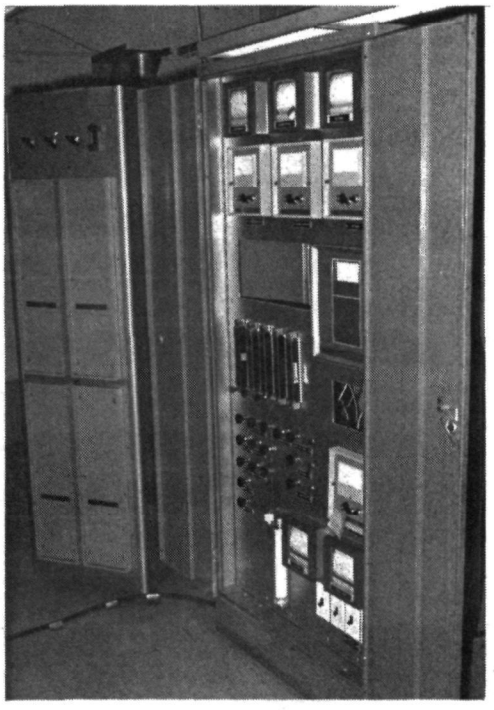

Figure II-48. OVERALL VIEW OF HOT-MODEL INSTRUMENTATION

In the lower center of the control panel, two filter chambers dry and remove particulate matter from the sample before it enters the analyzer. The sample for nitrogen oxides analysis is drawn separately, and the moisture is removed in a separate chamber (not shown) mounted on the side of the cabinet. The drying agent for the nitrogen oxides sample is a 3-angstrom molecular sieve which does not scrub the nitric oxide from the sample.

1. NO_x-NO Measurements

Nitric oxide and nitrogen dioxide (NO_2) concentrations were determined on a continuous basis using a nondispersive infrared analyzer for NO followed by an electrochemical cell instrument for NO_x. NO_2 was determined by difference in some cases. Evacuated flask grab samples were obtained periodically for wet-chemical spot-checks using the ASTM 1607-D (PDA) method for analysis.

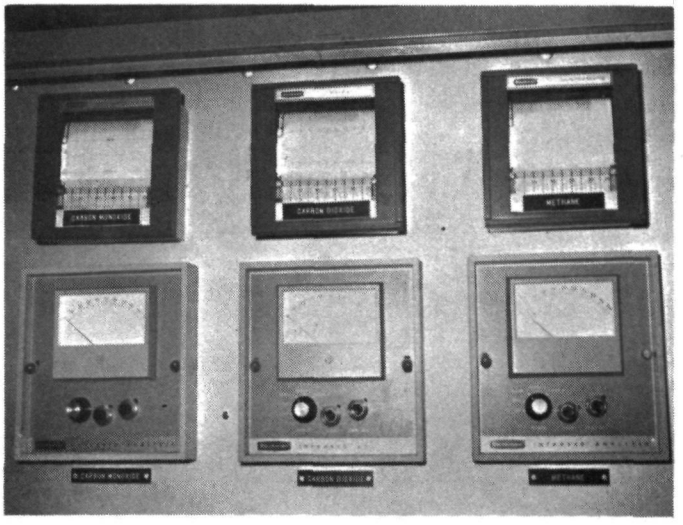

Figure II-49. CLOSE-UP VIEW OF INFRARED ANALYZER, AMPLIFIERS, AND STRIP CHARTS FOR CARBON MONOXIDE, CARBON DIOXIDE, AND METHANE

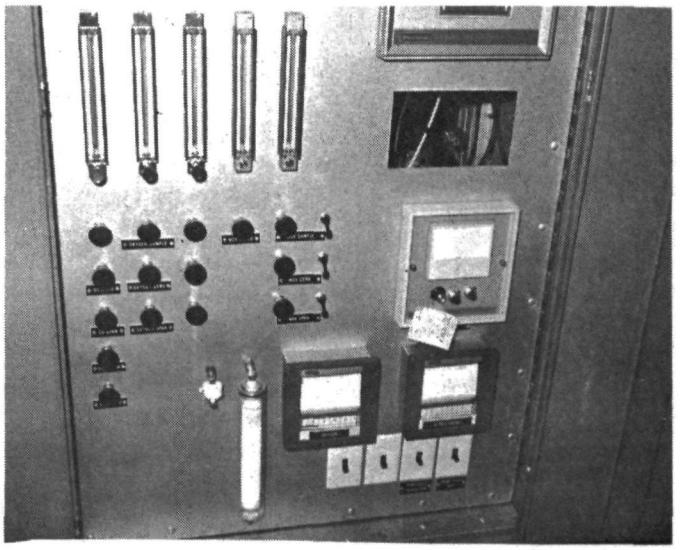

Figure II-50. SAMPLE TREATMENT AND FLOW-CONTROL SYSTEM

Instruments were calibrated using both a permeation tube having a controlled known release of NO_x and certified prepared cylinder gases containing known quantities of NO and NO_2. Figure II-51 shows the sample handling and conditioning system. All components of the sampling system were carefully designed to minimize loss of NO_x in the system through reaction or adsorption. NO_2 is extremely reactive with almost all materials. Below are the three basic criteria for designing a sampling system for NO_x (NO and NO_2):

- The sample system should be kept as short and compact as possible. This minimizes the amount of system wall area available for reaction with NO_2 and adsorption of NO.
- All materials of construction should be glass, Teflon, or Type-316 stainless steel only. These materials are least reactive with NO_2.
- Condensate traps with minimum gas-liquid contact should be used. NO_2 reacts readily with water to form nitric acid; therefore, the water vapor in the sample must not condense in an uncontrolled place such as the tubing.

The sample gas is drawn from the furnace through a special quartz probe (sections on sample probes) by a Dia-Pump Model 08-800-73 all stainless steel and Teflon pump delivering approximately 0.4 CF/min. (This sample delivery rate is dictated by the requirements of the measuring instruments.) The sample is immediately passed through a stainless steel large-particle filter. Both the pump and filter are kept above 50°C to prevent condensation of the water vapor inherent to combustion products.

Next the sample passes through a water trap (Figure II-52) to remove any water that otherwise might condense later in the sampling system. The sample then passes through a Whitney No. IGS4-A shutoff valve and No. IRS4-A flow control valve, both of stainless steel with Teflon seats and packing. An in-line flowmeter (rotameter) ensures an accurate measure of flow.

Once the sample has left the rotameter, it enters a Beckman Model 315A infrared NO analyzer. The electrical output of the analyzer is fed to a continuous strip recorder. The Beckman Model 315A uses a "nondestructive" method of analysis involving a simple optical system to measure the amount of infrared energy absorbed by the gas component of interest. Consequently, the sample leaves the analyzer in the same

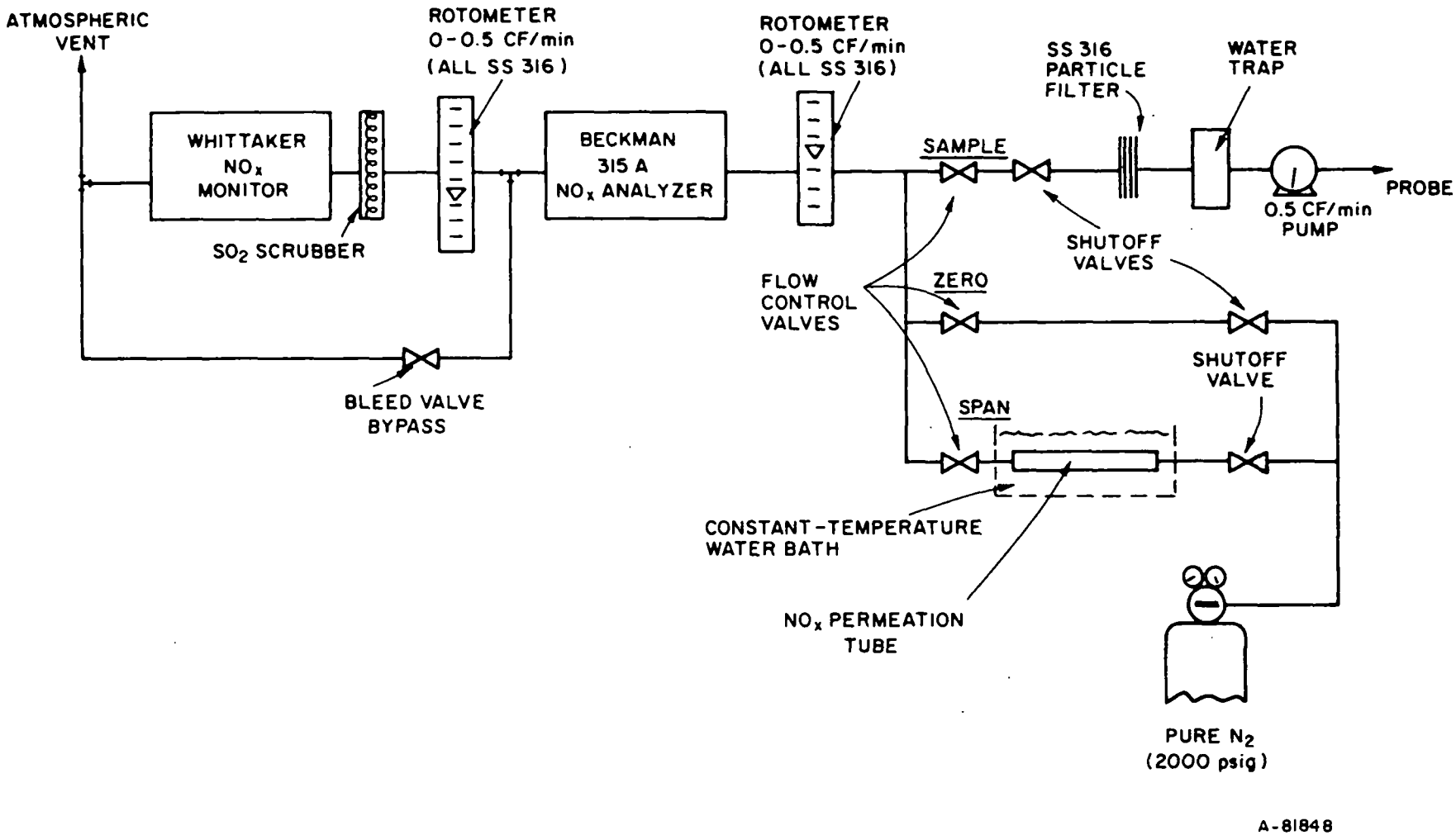

Figure II-51. NO_x-NO SAMPLING SYSTEM

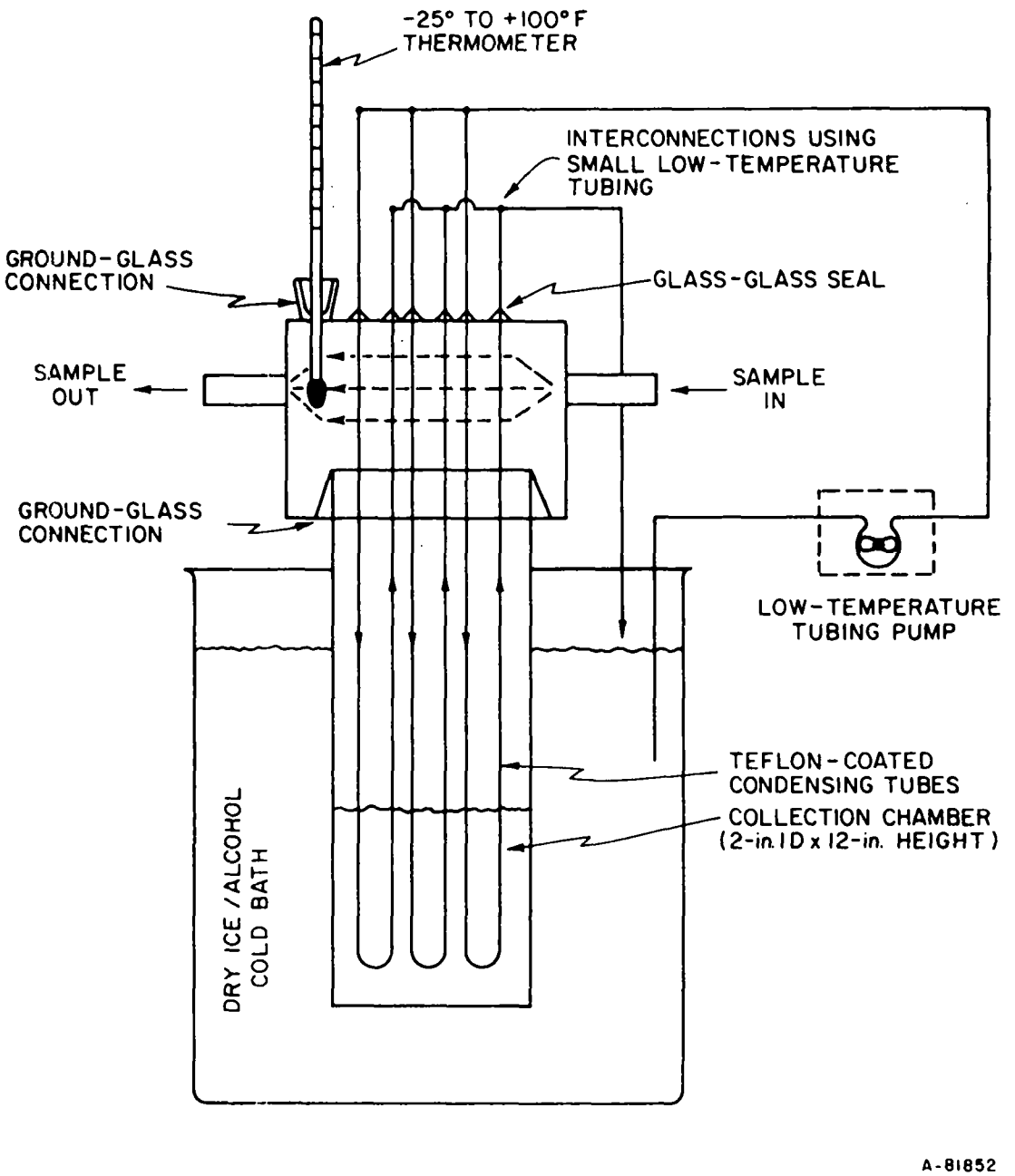

Figure II-52. DRYING SYSTEM FOR CONNECTION TO NO, NO_2, NO_x EQUIPMENT

condition as it entered. The sample can be passed on for further use because it is not altered by the NO analyzer. In our system the sample is then passed through another rotameter to regulate the flow necessary for the NO_x analyzer. In this case, flow is regulated by bleeding off part of the sample because the flow from the NO analyzer is larger than required by the NO_x analyzer. NO_x is determined by a Whittaker Model NX-110 cell, which is unaffected by nitrogen, oxygen, water vapor, hydrocarbons, carbon monoxide, and carbon dioxide. The analyzer operates on the principle of a fuel cell: NO_x is adsorbed in a special sensing electrode to form activated species capable of undergoing electroxidation. The resulting electrical current is directly proportional to the partial pressure of NO_x in the gas mixture. All interconnecting tubes in the system are Teflon with stainless steel end fittings.

Calibration of the NO_x-NO instruments is done with both compressed gas samples containing a known concentration of NO and NO_2 and a permeation tube. The permeation tube is filled with an appropriate material giving off NO_2. The NO_2 passes through the FEP Teflon walls of the tube at a known rate, which, when a flow of gas passes over the tube, produces a known concentration of NO_2 in the stream. The permeation rate is a function of tube temperature. Experience shows that the tube temperature must be constant to within ±2% accuracy. The permeation tube is used as the primary standard, with the compressed gas gauged against the tube.

2. Methane, CO, and CO_2 Measurements

Nondispersive infrared analyzers are used for CO, CO_2, and CH_4 measurements. These analyzers do not affect the sample gas and can be operated in series. They are calibrated by using certified gases with known concentrations of the species being determined. Figure II-53 is a schematic diagram of the system. The infrared analyzers require a completely dry sample. Therefore, the sample is first passed through a water trap and a calcium sulfate drying tube. A small in-line filter is placed immediately after the drying tube to trap particles of calcium sulfate that may be carried over by the gas stream.

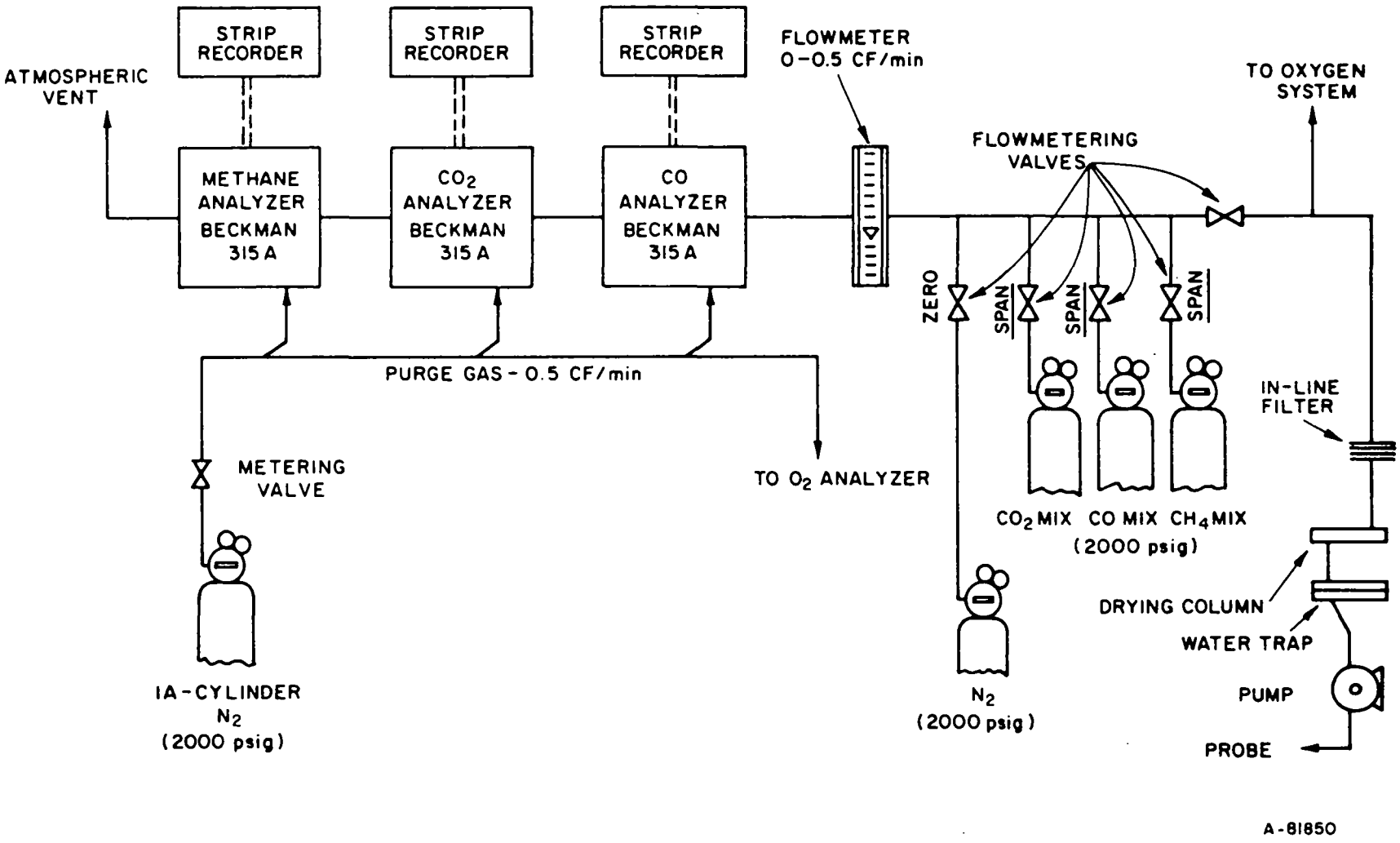

Figure II-53. CH_4, CO, AND CO_2 SAMPLING ANALYSIS SYSTEM

3. Oxygen Measurement

A portion of the "conditioned" sample gas is diverted from the infrared analyzers to a Beckman Model 742 oxygen analyzer, shown in Figure II-54.

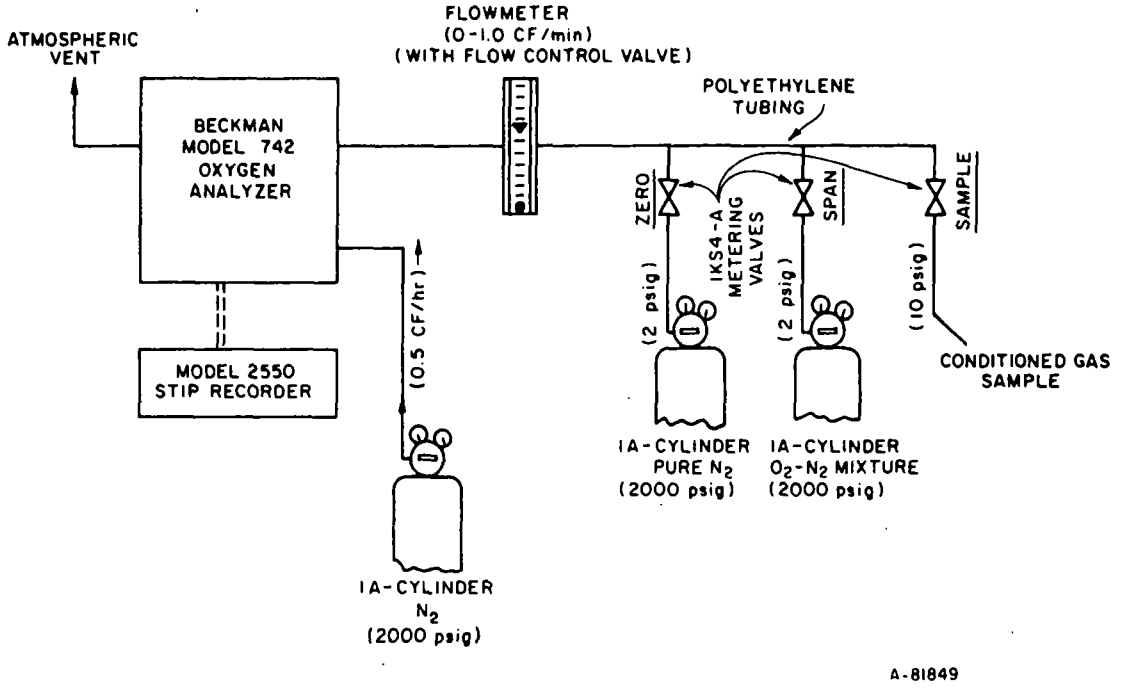

Figure II-54. SAMPLING/ANALYSIS SYSTEM FOR OXYGEN ANALYSIS

The analyzer consists of an amplifier unit coupled with a polarographic oxygen sensor. The sensor contains a silver anode and gold cathode that are protected from the gaseous sample by a thin membrane of Teflon. An aqueous KCl solution is retained in the sensor by the membrane and serves as an electrolytic agent. As Teflon is permeable to gases, oxygen will diffuse from the sample to the cathode with the following oxidation-reduction reactions:

$$\text{Cathode Reaction} \quad O_2 + 2H_2O + 4e \rightarrow 4OH$$

$$\text{Anode Reaction} \quad 4Ag + 4Cl \rightarrow 4AgCl + 4e$$

With an applied potential between the anode and cathode, oxygen is reduced at the cathode, causing a current to flow. The magnitude of the current is proportional to the partial pressure of oxygen present in the sample.

4. Hydrocarbon Measurements

Gas chromatography was used for a complete hydrocarbon analysis of C_1 to C_{10}. This chromatograph is equipped with a long capillary column internally coated with adsorbent, which gives the required resolution. As this chromatograph could not be moved to the test site, evacuated flask grab samples were used.

During flue gas sampling tests we found that the bulk water removal system was inadequate for a full day's run. After about 4 hours of sampling, the desiccant cylinder had absorbed its maximum capacity of water and had to be replaced. We designed and built a new bulk water removal system (Figure II-55) which operated together with our original unit.

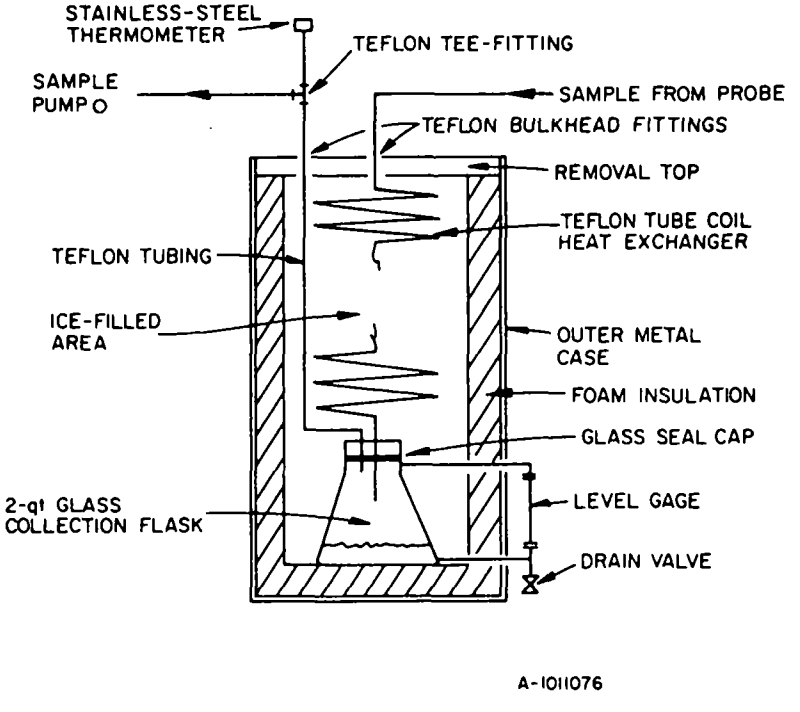

Figure II-55. MODIFIED BULK WATER REMOVAL COLD TRAP

A 25-foot coil of Teflon tubing with a 0.25-inch outer diameter was wound around a 10-inch-diameter plastic cylinder; a 1-liter removable flask was attached at the bottom end. The coil and flask are placed in an insulated container of ice where the gases are cooled to 40^0F. The condensed water flows down the Teflon coil and is trapped in the collection flask.

A data integration system was also installed.

The integrator receives a fluctuating signal from either the NDIR gas analyzers or the CGS electronic manometer measuring velocity. The integrator then computes a mean value of the concentration or velocity being measured and provides a digital display of this value. This integrator is coupled between the output of the Datametrics 1014A electric manometer and the Brush recorder. The d-c voltage output from the electric manometer is summed up by the voltage integrator and is displayed by the recorder as a voltage sum versus time. The manometer puts out a 10-volt signal for full-scale readings independent of the range switch setting. Thus to calibrate the integrator a 10-volt signal is applied and the time to reach sums between 0 and 80 volts is determined. To calculate the voltage of an unknown signal, the ratio is taken between the time intervals required for the unknown and the 10-volt signals to reach a given sum. This ratio is multiplied by 10 to give the voltage. The voltage can be transformed directly into a pressure differential by knowing the range switch setting of the electric manometer. Velocity measurements can be made with the experimental arrangement down to 1 ft/s, with preliminary measurements indicating a 2% error in reproducibility.

The results from the electronic integrator (Figure II-56) were compared with integrating the direct readout of the manometer by a graphical technique. The agreement between methods was within 1/2%.

For the case where the magnitude of fluctuations in the signal is about as large as that of the average signal, it may be impossible to get a constant time-averaged signal to the accuracy desired. If the time base operational amplifier No. 1 should approach saturation before sufficient stability has been reached by the time-averaged signal, a signal light tells the operator to close the switch to operational amplifier No. 3. This operational amplifier works in a sample-and-hold mode. Therefore, when the switch is closed, it takes the voltage at the output of the divider and holds that value on the digital voltmeter or recorder allowing the operator to record the value, reset the system, and start the next integration.

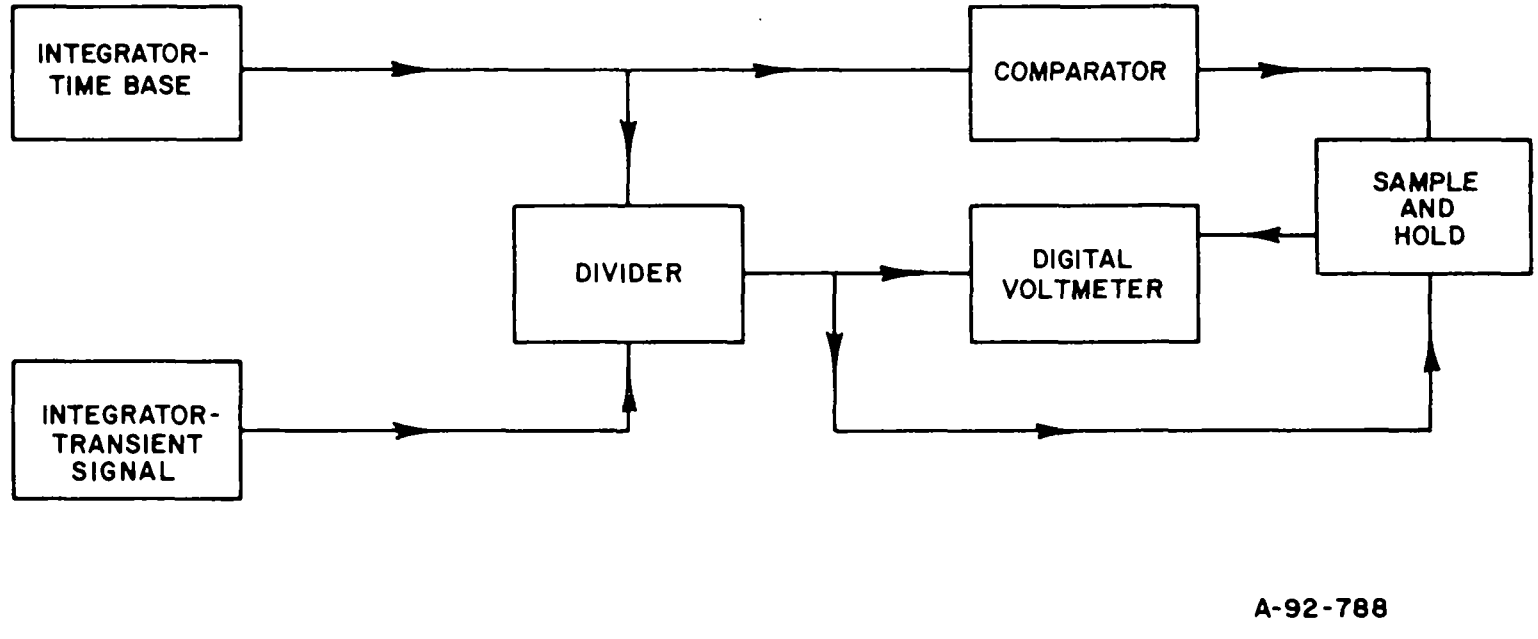

Figure II-56. BLOCK DIAGRAM OF AUTOMATIC DATA INTEGRATION SYSTEM

RAW AND REDUCED DATA AND DATA PLOTS

Five experimental burners were studied during this program. The raw data for each of these burners for both hot and cold tests are presented in the following sections. A complete description of each burner is also given. The analysis of these data together with recommendations for reducing NO_x emissions are presented in Volume I, a companion publication.

A. Intermediate-Flame-Length Ported Baffle Burner

1. Burner Design

The outside steel air housing used for the axial flow burner with the ported swirl baffle is identical to that used for the ASTM flow nozzle described later. However, the inside diameter was reduced to 11-1/4 in. by adding a 3.625-in.-thick insulating brick liner. The liner was coated with a thin layer of Babcock & Wilcox K-2800 castable insulating refractory to reduce the surface porosity of the brick liner and prevent air from bypassing the ported swirl baffle as shown in Figure II-57.

The length and shape of the flame is determined by the design of the baffle inserted into the burner housing. We have three baffle designs, generally described as producing a long, intermediate, and short flame available for study. The dimensions for each baffle are shown in Figure II-57. The baffle consists of a cylinder of refractory with a central gas nozzle and a number of air ports around the gas nozzle for the combustion air. The length of the flame is varied by changing the angle of the air holes to the burner axis and the thickness of the baffle. The shortest flame is produced by the baffle having a swirl intensity of about 0.4.

The burner block or entrance port geometry in the furnace wall differs for each baffle. The short flame diverges faster than the long flame and therefore requires a larger divergency of the burner block. The shape and dimensions of each burner block are shown in Figure II-57.

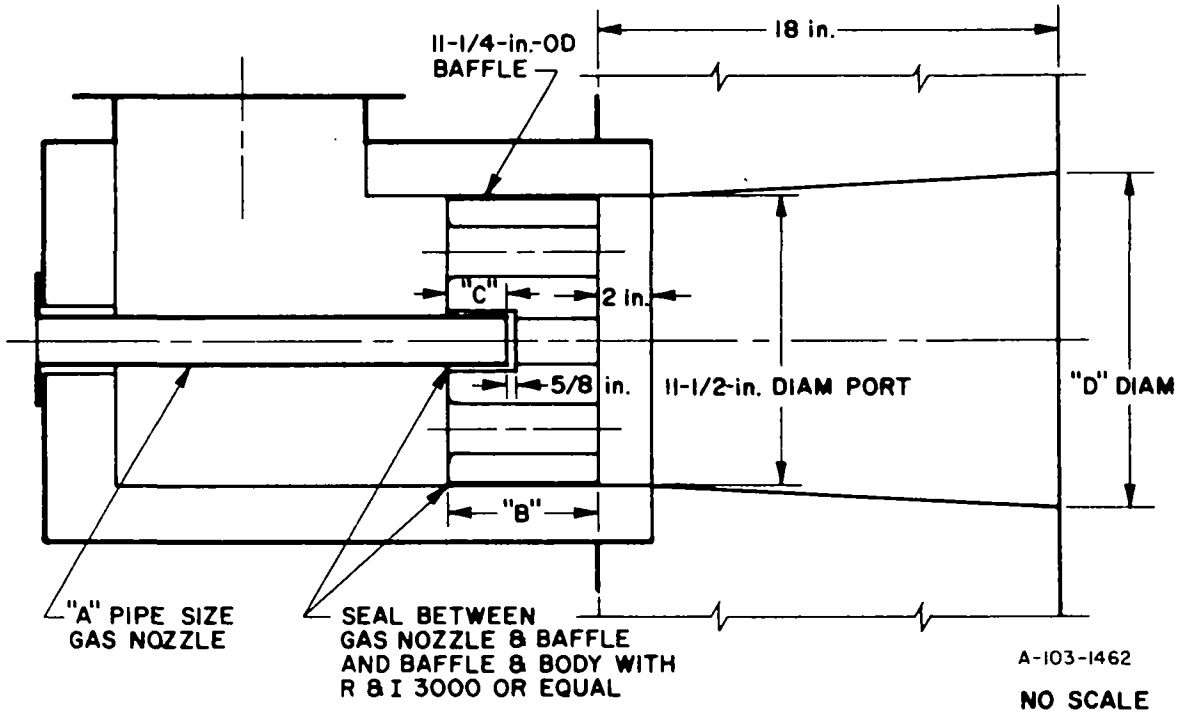

BAFFLE	AIR PRESSURE FOR 40,000 SCF/hr at 850°F	"A"	"B"	"C"	"D"
a. LONG FLAME	3.25 in. wc	1-1/4 in.	6 in.	2-3/8 in.	13 in.
b. SHORT FLAME	18 in. wc	3/4 in.	5 in.	2-3/8 in.	16-1/2 in.
c. INTER. FLAME	14 in. wc	1 in.	8 in.	3-7/8 in.	13 in.

Figure II-57. ASSEMBLY DRAWING OF AXIAL-FLOW BURNER WITH PORTED SWIRL BAFFLES

The central burner tube (Figure II-58) of the intermediate-flame ported swirl baffle was also tested in a modified form to provide radial rather than axial entrance of the natural gas. Radial entrance of the gas into the air stream is a common technique used to increase the mixing rate between gas and air; this shortens the flame. Shortening the flame was necessary because the original burner design did not provide complete combustion before the gases entered the furnace flue. Figure II-58 shows the details of how the burner tube was modified to provide radial gas entrance. The central nozzle was constructed of Type-316 stainless steel machined to an outside diameter of 1.125 in. with an inside diameter of 1 in. The end of the tube was capped, and six equally spaced holes were drilled in the sidewall 1/2 in. back from the tip. Each hole was drilled 7/32 in. in diameter without burrs; this provided a gas velocity of 530 ft/s at a 3000 CF/hr input. The gas nozzle was then pushed through the refractory baffle until the tip protruded 2 in. beyond the baffle.

During initial tests, we found that the rotational orientation of the nozzle noticeably changed the flame length. The nozzle was positioned for the shortest flame. This occurs when the gas nozzle holes approximately line up with the air holes in the baffle.

Table II-6 compares the flue gas analyses for the modified and unmodified burner nozzles while operating at 2 million Btu/hr with stoichiometric quantities of air. These data were collected using ambient air for combustion at 100^0F.

With the unmodified burner nozzle, we found both oxygen and methane in the flue. The oxygen concentration was very high for the fuel/air ratio. In addition, the concentrations of each of the flue components fluctuated with time between the concentrations shown in Table II-6.

When the burner was modified, fluctuations in concentration also disappeared and the CO_2 and O_2 concentrations more reasonably agreed with calculated amounts. In addition, no methane (unburned hydrocarbons) was detected.

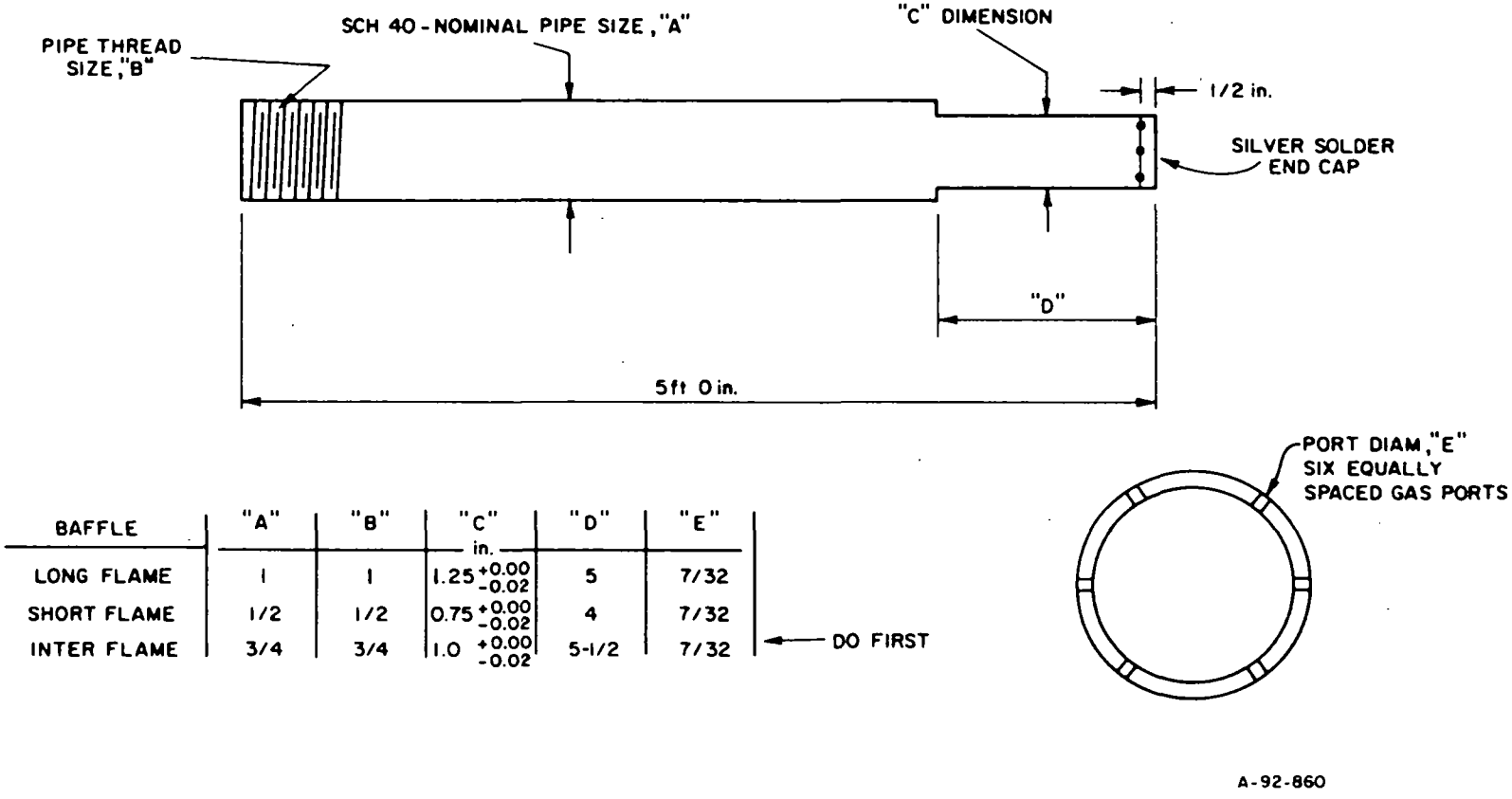

BAFFLE	"A"	"B"	"C" in.	"D"	"E"	
LONG FLAME	1	1	$1.25^{+0.00}_{-0.02}$	5	7/32	
SHORT FLAME	1/2	1/2	$0.75^{+0.00}_{-0.02}$	4	7/32	
INTER FLAME	3/4	3/4	$1.0^{+0.00}_{-0.02}$	5-1/2	7/32	← DO FIRST

Figure II-58. MODIFIED GAS NOZZLE CONSTRUCTION

Table II-6. FLUE GAS ANALYSIS COMPARISON FOR MODIFIED AND UNMODIFIED GAS BURNER NOZZLES

	Modified	Unmodified
Gas Input, 10^6 Btu/hr	2.0	2.0
Air/Fuel Ratio	10	10
Air Temperature, °F	100	100
Flue Analysis		
Carbon Monoxide, ppm	30	60-100
Carbon Dioxide, %	10.5	7-9.8
Methane, ppm	~0	1300-1800
Nitrogen Oxides, ppm*	--	330-410
Oxygen, %	1.0	3.5-7

2. Tracer-Gas Studies

The tracer-gas mixing study for the axial burner with the intermediate-flame ported swirl baffle is presented in Figure II-59.

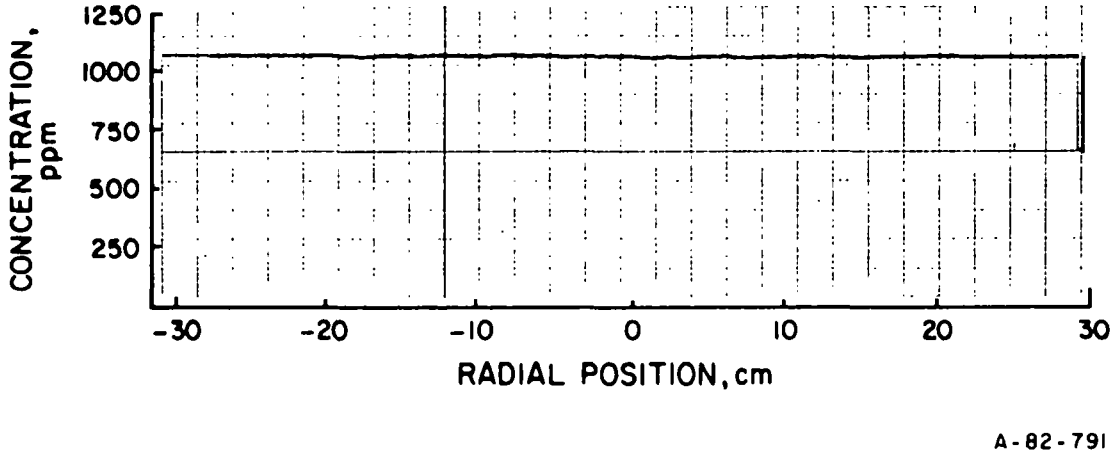

Figure II-59. TRACER-GAS (Carbon Monoxide) RADIAL SCAN 7.6 cm FROM BURNER BLOCK OF THE INTERMEDIATE-FLAME-LENGTH PORTED SWIRL BAFFLE BURNER

This scan, taken at an axial position of 7.6 cm from the burner block, shows the radial concentration readings are very near to ambient, thus indicating that mixing would be complete at this position. We conclude that the major mixing phenomena for the axial burner with ported swirl for an intermediate flame are occurring in the burner block, which is an area into which we cannot probe with our equipment. The scope of this project included only areas outside the burner block and in the "combustion chamber."

3. Cold-Model Velocity Data

Point-by-point velocity profile data were collected for the axial burner with the intermediate-flame ported swirl baffle by using a multidirectional impact tube (MDIT). The geometry used in data collection and reduction is shown in Figure II-60.

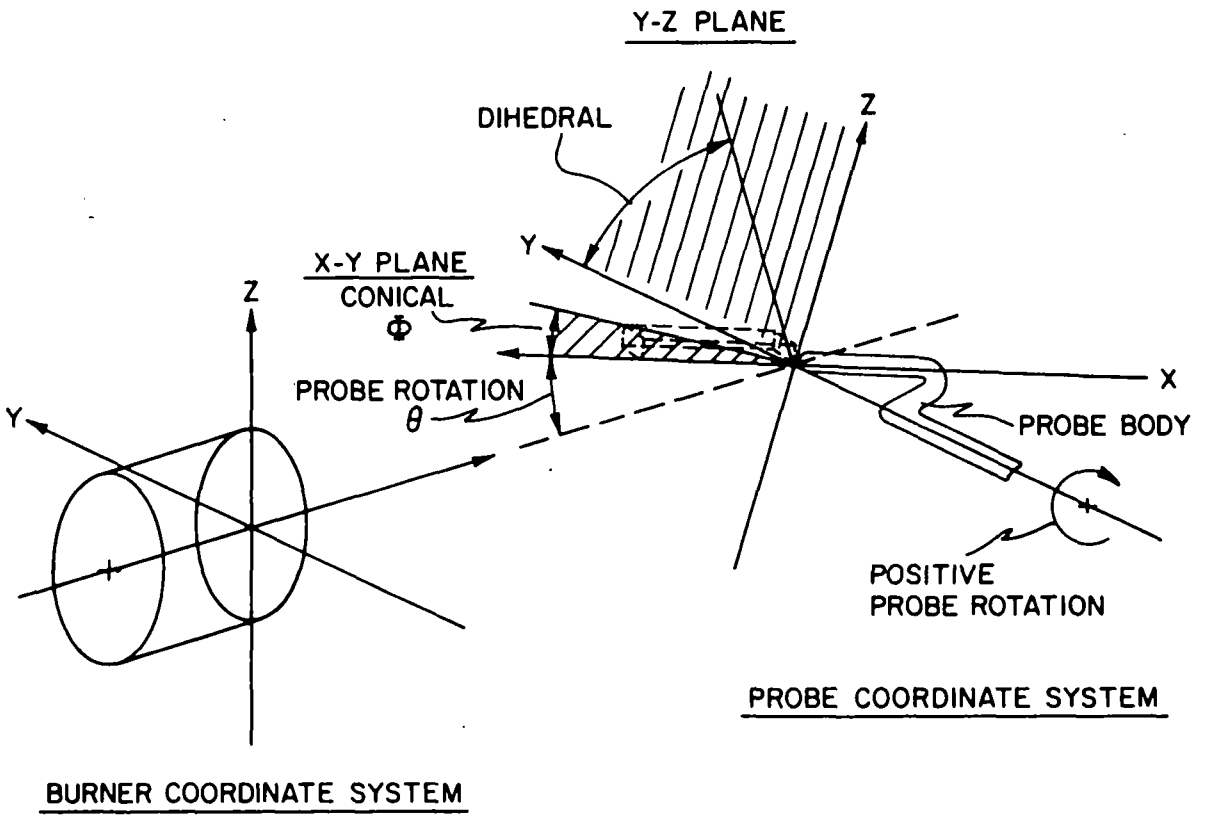

Figure II-60. SAMPLING PROBE AND BURNER COORDINATE SYSTEM

The raw data, obtained from the axial flow burner fitted with the ported swirl baffle, are shown in Table II-7. The rotation angle of the probe in the x-z plane is represented by θ. AP is the axial position of the probe in centimeters, and RP is its radial position in centimeters. PB is the atmospheric pressure in millimeters of mercury, and P_{xy} is the pressure differential between pressure holes, x and y, expressed in terms of time. The pressure differentials are expressed in terms of time because of the integration method used to collect the data. The pressure differentials we are measuring are constantly changing since we are dealing with a turbulent system.

We electronically sum the instantaneous values for a preset amount of time to determine the mean value of these transient pressure differentials. This total equals the product of the average instantaneous pressure differential and the time interval needed to reach it. Therefore, measuring the time interval needed to reach this sum by a transient pressure differential makes it possible to determine the mean value of the pressure differential. These experimentally determined mean pressure differentials yield the velocity (magnitude and direction) of the air stream by means of the techniques outlined earlier in this report. The raw pressure data are translated into velocities using a computer program written especially for this purpose, as shown in Appendix II-A.

The reduced velocity data for the intermediate-flame ported swirl burner are given in Table II-8. The direction of the velocity is defined by FI, the conical angle measured about the x-axis, and by Δ, the dihedral angle measured from the positive y-axis in the y-z plane. The magnitude of the velocity in ft/s is given by V, ρ is the density of the air in slugs/ft-sq in., and VX, VY, and VZ are the velocity components in ft/s. Both VT, the tangential velocity, and VR, the radial velocity, are expressed in ft/s. PST is the static pressure in psig.

The graphic representations of the axial velocity, VX, and of the tangential velocity, VT, as shown in Figures II-61 and II-62, respectively, are displayed by means of a computer plotting routine. These computer graphs allow a quick visual check on the quality of the data being collected and on whether more data are necessary to describe a profile.

Table II-7. RAW DATA OBTAINED FOR THE INTERMEDIATE-FLAME-LENGTH AXIAL FLOW BURNER FITTED WITH THE PORTED SWIRL BAFFLE

CALIBRATION COEFFICIENTS FOR FORWARD FLOW

A1 =	0.770590	A2 =	0.272353	A3 =	-0.059818
B0 =	0.737720	B2 =	-0.158821	B4 =	0.129246
C =	4.464660	D =	0.394812		

AXIAL BURNER WITH PORTED SWIRL FOR INTERMEDIATE FLAME - COLD MODEL

TOTAL DATA INPUT

THETA	AP	RP	P13	P03	P24	P04	POA	T	PB
0.	7.6	25.0	5960.00	3260.00	2680.00	3170.00	88.40	20.	760.
0.	7.6	20.0	5340.00	2720.00	1940.00	2590.00	69.00	20.	760.
0.	7.6	19.0	-10660.00	8330.00	1030.00	1760.00	72.10	20.	760.
0.	7.6	18.0	-552.00	-2890.00	295.00	530.00	72.00	20.	760.
0.	7.6	17.0	-347.00	-6440.00	152.00	277.00	74.00	20.	760.
0.	7.6	16.0	-332.00	695.00	86.00	162.00	69.40	20.	760.
0.	7.6	15.0	-411.00	650.00	107.00	172.00	77.40	20.	760.
0.	7.6	14.0	-621.00	591.00	116.00	195.00	80.60	20.	760.
0.	7.6	13.0	-1102.00	664.00	144.00	249.00	84.60	20.	760.
0.	7.6	12.0	-266.00	685.00	165.00	332.00	98.00	20.	760.
0.	7.6	12.0	-2640.00	626.00	136.00	273.00	81.70	20.	760.
0.	7.6	11.0	-6760.00	1060.00	233.00	410.00	103.00	20.	760.
0.	7.6	10.0	12370.00	1100.00	262.00	539.00	98.50	20.	760.
0.	7.6	9.0	4210.00	1370.00	366.00	733.00	104.00	20.	760.
0.	7.6	8.0	5230.00	1530.00	493.00	1070.00	103.00	20.	760.
0.	7.6	7.0	4430.00	2090.00	820.00	1540.00	115.00	20.	760.
0.	7.6	6.0	5440.00	2680.00	1330.00	2030.00	104.00	20.	760.
180.	7.6	5.0	-2150.00	2950.00	2850.00	2450.00	86.80	20.	760.
180.	7.6	4.0	-2400.00	2200.00	3010.00	1960.00	84.80	20.	760.
180.	7.6	3.0	-2410.00	1950.00	2560.00	1800.00	83.30	20.	760.
180.	7.6	2.0	-2560.00	1790.00	1830.00	1480.00	84.50	20.	760.
180.	7.6	1.0	-3270.00	1950.00	1880.00	1530.00	82.30	20.	760.
180.	7.6	0.0	-2900.00	1600.00	1610.00	1410.00	102.00	20.	760.
180.	7.6	-1.0	-4710.00	1380.00	1260.00	1200.00	95.00	20.	760.
180.	7.6	-2.0	-5530.00	1650.00	1280.00	1270.00	88.50	20.	760.
180.	7.6	-3.0	-5980.00	1580.00	1130.00	1360.00	87.20	20.	760.
180.	7.6	-4.0	-6380.00	1500.00	1160.00	1350.00	87.00	20.	760.
180.	7.6	-5.0	-8140.00	1750.00	1130.00	1420.00	90.00	20.	760.
0.	7.6	-6.0	-1003.00	-2510.00	-9170.00	11500.00	107.00	20.	760.
0.	7.6	-7.0	-735.00	-2330.00	-13400.00	34900.00	106.00	20.	760.
0.	7.6	-8.0	-600.00	-1540.00	1190.00	-6860.00	89.30	20.	760.
0.	7.6	-9.0	-492.00	-1670.00	-732.00	-2980.00	103.00	20.	760.
0.	7.6	-10.0	-434.00	-1910.00	-502.00	-2040.00	100.00	20.	760.
0.	7.6	-11.0	-406.00	-3340.00	-402.00	-1510.00	94.80	20.	760.
0.	7.6	-12.0	-436.00	14700.00	-298.00	-1116.00	107.00	20.	760.
0.	7.6	-13.0	-419.00	1890.00	-243.00	-898.00	82.50	20.	760.
0.	7.6	-14.0	-589.00	1480.00	-219.00	-756.00	67.30	20.	760.
0.	7.6	-15.0	-1160.00	681.00	-243.00	-766.00	74.80	20.	760.
0.	7.6	-16.0	79200.00	631.00	-317.00	-1330.00	71.40	20.	760.
0.	7.6	-17.0	1390.00	793.00	-469.00	-1500.00	71.30	20.	760.
0.	7.6	-18.0	2200.00	1660.00	-1004.00	-2270.00	74.50	20.	760.
0.	7.6	-19.0	6640.00	3370.00	-2920.00	-62400.00	75.30	20.	760.
0.	7.6	-20.0	-54500.00	4820.00	13000.00	5280.00	76.70	20.	760.
0.	7.6	-25.0	201600.00	4510.00	3400.00	3790.00	73.80	20.	760.

Table II-8. REDUCED VELOCITY DATA FOR THE INTERMEDIATE FLAME LENGTH OF THE AXIAL FLOW BURNER FITTED WITH THE PORTED SWIRL BAFFLE

AP	RP	FI	DELTA	RHO	V	VX	VY	VZ	VT	VR	PST	T	PB
7.6	25.0	23.5	114.2	0.0000159	6.39	5.86	-1.04	2.33	2.53	0.33	0.010854	20.	760.
7.6	20.0	26.7	109.9	0.0000159	7.10	6.34	-1.09	3.00	3.14	0.60	0.013949	20.	760.
7.6	19.0	43.0	84.4	0.0000159	7.91	5.78	0.52	5.38	5.06	1.89	0.013539	20.	760.
7.6	18.0	46.1	61.8	0.0000159	15.53	10.77	5.27	9.87	10.25	4.50	0.013626	20.	760.
7.6	17.0	44.8	66.3	0.0000159	21.43	15.21	6.06	13.83	13.80	6.13	0.013088	20.	760.
7.6	16.0	42.6	75.4	0.0000159	28.36	20.86	4.82	18.60	17.61	7.70	0.013337	20.	760.
7.6	15.0	36.7	75.4	0.0000159	26.20	20.98	3.95	15.18	14.67	5.55	0.010861	20.	760.
7.6	14.0	37.9	79.4	0.0000159	24.84	19.58	2.80	15.02	14.07	5.96	0.010738	20.	760.
7.6	13.0	38.8	82.5	0.0000159	22.09	17.19	1.79	13.75	12.55	5.92	0.010585	20.	760.
7.6	12.0	44.4	87.0	0.0000159	22.16	15.83	0.79	15.49	13.18	8.17	0.011771	20.	760.
7.6	11.0	41.0	88.0	0.0000159	16.97	12.79	0.38	11.13	9.54	5.74	0.009099	20.	760.
7.6	10.0	45.6	91.2	0.0000159	15.87	11.08	-0.24	11.35	8.96	6.97	0.009932	20.	760.
7.6	9.0	45.2	94.9	0.0000159	13.42	9.45	-0.82	9.49	7.25	6.17	0.009384	20.	760.
7.6	8.0	45.0	95.3	0.0000159	11.82	8.35	-0.78	8.33	6.06	5.77	0.009478	20.	760.
7.6	7.0	40.6	100.4	0.0000159	9.31	7.07	-1.10	5.96	4.43	4.13	0.008385	20.	760.
7.6	6.0	32.8	103.7	0.0000159	7.74	6.50	-0.99	4.08	3.25	2.66	0.009205	20.	760.
7.6	5.0	160.9	322.9	0.0000159	9.26	-8.75	2.41	-1.82	2.67	1.40	0.010737	20.	760.
7.6	4.0	165.3	321.4	0.0000159	10.03	-9.70	1.97	-1.57	2.26	1.12	0.010847	20.	760.
7.6	3.0	165.1	316.7	0.0000159	10.40	-10.05	1.94	-1.83	2.21	1.49	0.011004	20.	760.
7.6	2.0	164.8	305.5	0.0000159	10.78	-10.41	1.64	-2.29	1.96	2.02	0.010784	20.	760.
7.6	1.0	165.4	299.8	0.0000159	10.25	-9.92	1.28	-2.23	1.16	2.30	0.011165	20.	760.
7.6	0.0	164.1	299.0	0.0000159	11.02	-10.60	1.45	-2.62	0.00	3.00	0.008769	20.	760.
7.6	-1.0	163.7	284.9	0.0000159	11.38	-10.92	0.82	-3.08	-1.31	2.91	0.009430	20.	760.
7.6	-2.0	162.8	283.0	0.0000159	10.63	-10.16	0.70	-3.05	-2.03	2.38	0.010312	20.	760.
7.6	-3.0	158.7	280.7	0.0000159	10.58	-9.86	0.71	-3.77	-2.73	2.69	0.010557	20.	760.
7.6	-4.0	159.6	280.3	0.0000159	10.73	-10.06	0.66	-3.67	-3.04	2.14	0.010547	20.	760.
7.6	-5.0	157.3	277.9	0.0000159	10.10	-9.32	0.53	-3.84	-3.28	2.01	0.010293	20.	760.
7.6	-6.0	43.7	353.7	0.0000159	7.98	5.76	5.48	-0.60	-3.51	4.26	0.009117	20.	760.
7.6	-7.0	44.3	356.8	0.0000159	9.35	6.68	6.53	-0.35	-4.48	4.76	0.009204	20.	760.
7.6	-8.0	64.9	26.7	0.0000159	12.00	5.07	9.71	4.89	-4.79	9.76	0.011865	20.	760.
7.6	-9.0	40.3	326.0	0.0000159	12.69	9.68	6.82	-4.58	-6.67	4.78	0.009249	20.	760.
7.6	-10.0	37.6	319.1	0.0000159	14.42	11.42	6.67	-5.76	-7.60	4.46	0.009303	20.	760.
7.6	-11.0	35.3	314.7	0.0000159	15.83	12.91	6.44	-6.50	-8.22	4.02	0.009584	20.	760.
7.6	-12.0	33.1	304.3	0.0000159	17.42	14.59	5.37	-7.86	-8.80	3.63	0.008075	20.	760.
7.6	-13.0	30.9	300.1	0.0000159	19.43	16.65	5.01	-8.65	-9.43	3.31	0.010338	20.	760.
7.6	-14.0	32.4	290.3	0.0000159	19.22	16.22	3.59	-9.67	-9.75	3.37	0.013185	20.	760.
7.6	-15.0	29.6	281.8	0.0000159	18.97	16.49	1.92	-9.17	-9.00	2.59	0.011518	20.	760.
7.6	-16.0	25.8	269.7	0.0000159	17.16	15.45	-0.02	-7.47	-7.28	1.67	0.012188	20.	760.
7.6	-17.0	30.8	251.3	0.0000159	13.53	11.62	-2.21	-6.56	-6.69	1.78	0.012989	20.	760.
7.6	-18.0	37.9	245.4	0.0000159	8.96	7.07	-2.28	-5.01	-5.23	1.72	0.012968	20.	760.
7.6	-19.0	20.4	246.2	0.0000159	6.42	6.01	-0.90	-2.05	-2.22	0.33	0.012758	20.	760.
7.6	-20.0	7.2	76.5	0.0000159	5.84	5.80	0.17	0.71	-0.73	0.03	0.012512	20.	760.
7.6	-25.0	19.6	90.9	0.0000159	6.02	5.67	-0.03	2.02	-2.01	0.21	0.013049	20.	760.

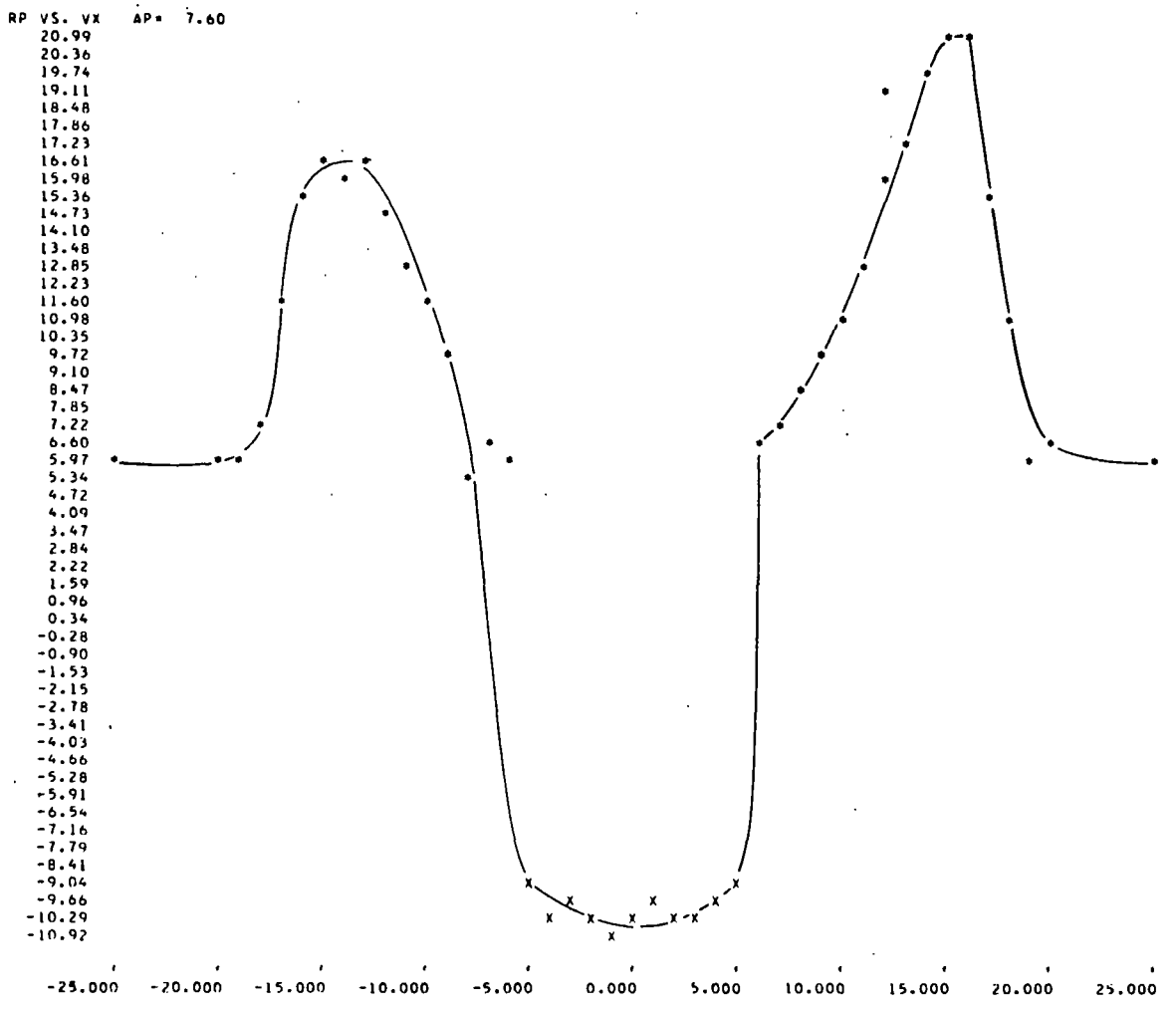

Figure II-61. AXIAL VELOCITY PROFILE FOR THE INTERMEDIATE FLAME AT THE AXIAL FLOW BURNER FITTED WITH THE PORTED SWIRL BAFFLE (7.6 cm From Burner Block Face)

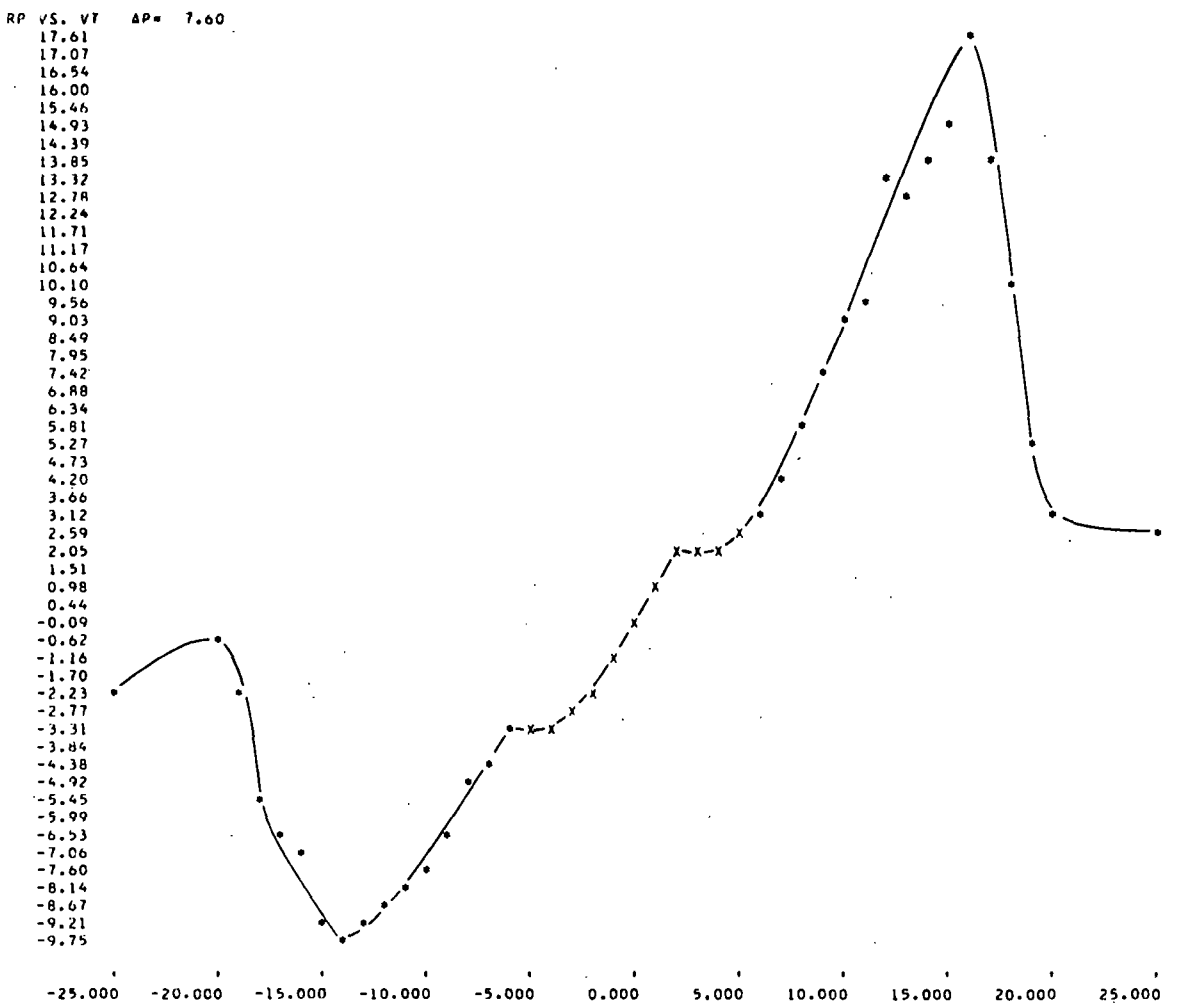

Figure II-62. TANGENTIAL VELOCITY PROFILE FOR THE INTERMEDIATE FLAME AT THE AXIAL FLOW BURNER FITTED WITH THE PORTED SWIRL BAFFLE (7.6 cm From Burner Block Face)

Figure II-61 shows the axial velocity at an axial position of 7.6 cm from the burner wall. Note that there is no central peak representing the output from the gas nozzle. In fact, the velocity data in the central region of the burner block at radial positions of ±5 cm show reverse flow. Forward velocity peaks do occur at radial positions of ±14 cm with magnitudes of 19.5 and 16.2 ft/s. Figure II-62 shows a tangential velocity of −9.75 ft/s at a radial position of −14 cm and 17.6 ft/s at 15 cm. We did not take velocity profiles beyond the 7.6-cm axial position because primary mixing is completed, as indicated by Figure II-59. A swirl number for the axial burner with the intermediate-flame ported swirl baffle was calculated using the data in Table II-8. The value of swirl intensity was 0.17.

4. Hot-Model Input-Output Data

The burner with a radial gas nozzle was operated at four gas inputs between 2335 CF/hr and 3160 CF/hr, with amounts of excess air between 5% and 20%, and at three different preheated air temperatures. Generally, we found that the amount of nitric oxide, NO, increased with increasing excess air between 5% and 12%, then decreased with additional excess air. Figure II-63 shows this expected effect at a gas input of 2335 CF/hr. The peak concentration of NO always occurred between about 1.25 and 2.25% oxygen in the flue. The peak NO formation increased significantly when preheated air was used, and the location of the peak shifted slightly. This same typical behavior was observed for gas inputs at 2626 CF/hr, 2900 CF/hr, and 3160 CF/hr, as shown by Figures II-64, II-65, and II-66.

Examination of the data in Figures II-63 through II-66 shows that our method of controlling the preheat temperature allowed variations from 450°F to 570°F as the gas input was changed. Therefore, a direct comparison of the NO emissions from these curves is not possible. We replotted the information for various excess oxygen levels as a function of the preheat temperature and reconstructed % O_2 vs. NO concentration curves by interpolation at preheat temperatures of 450°F and 245°F. Data for a 100°F preheat level were experimentally obtained at all gas inputs and are also plotted in these figures. In addition, we extrapolated our data and plotted a 700°F preheat temperature curve (also shown in the

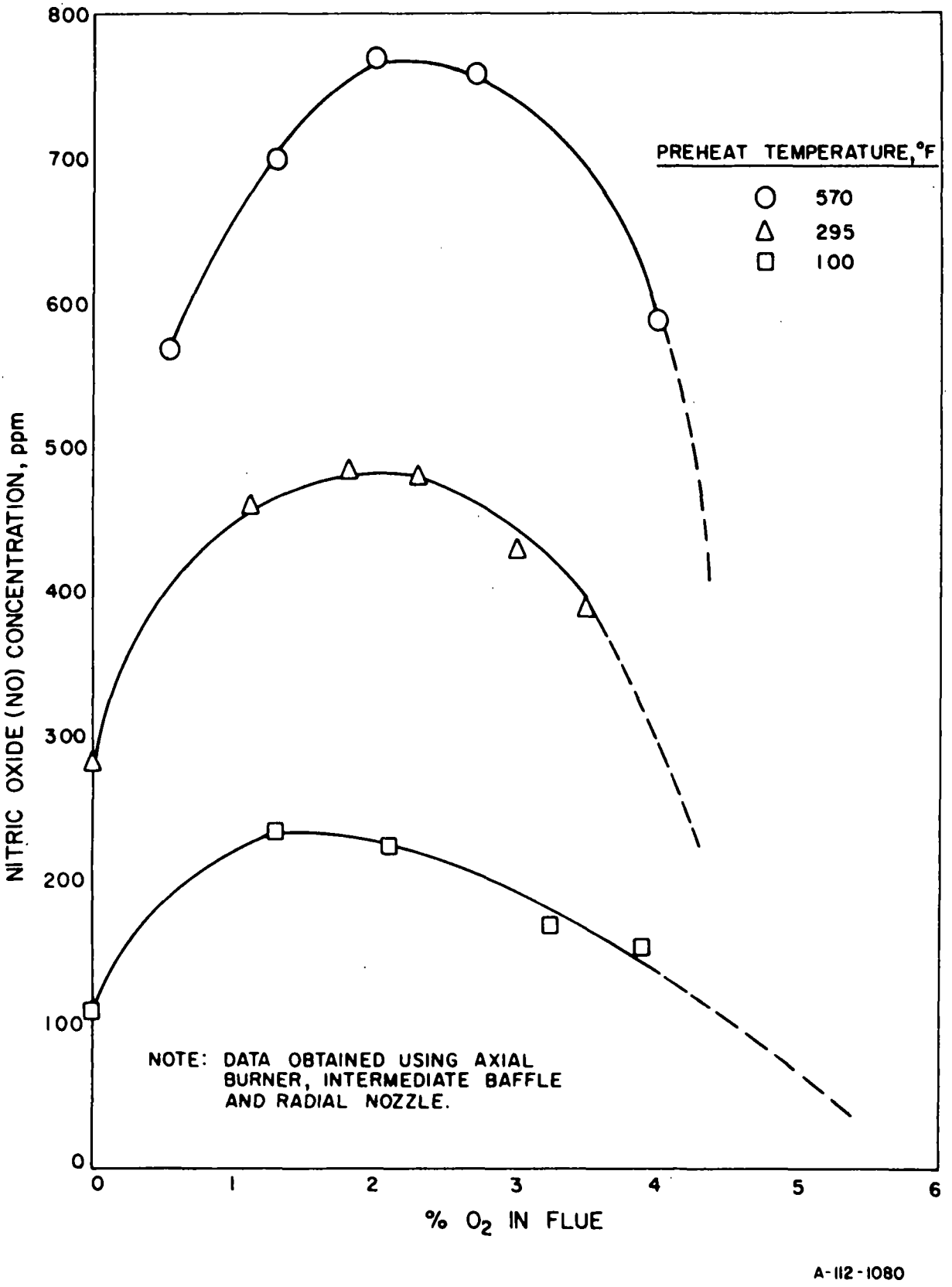

Figure II-63. NO CONCENTRATIONS WITH GAS INPUT OF 2335 CF/hr (Original Data)

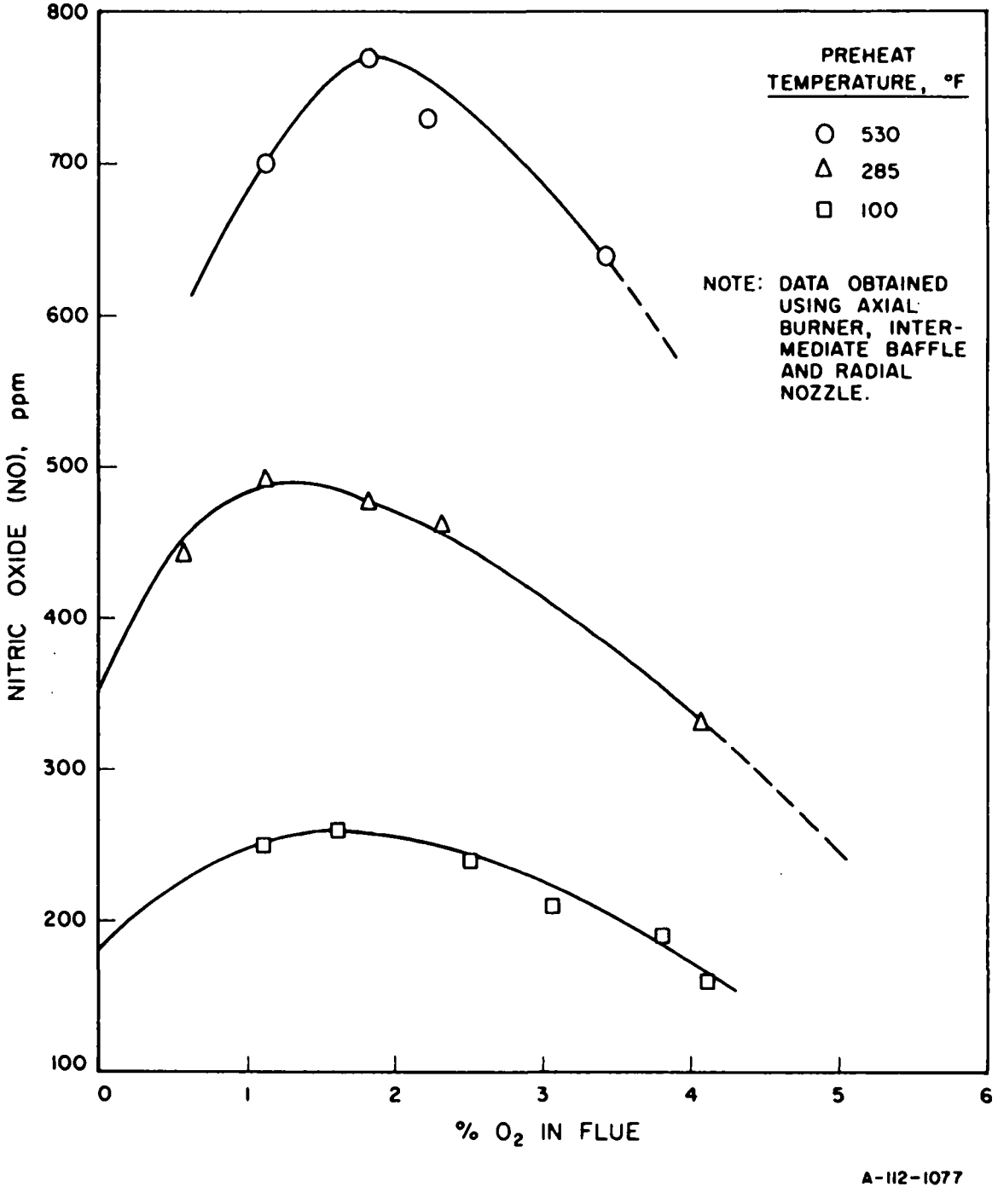

Figure II-64. NO CONCENTRATIONS WITH GAS INPUT OF 2626 CF/hr (Original Data)

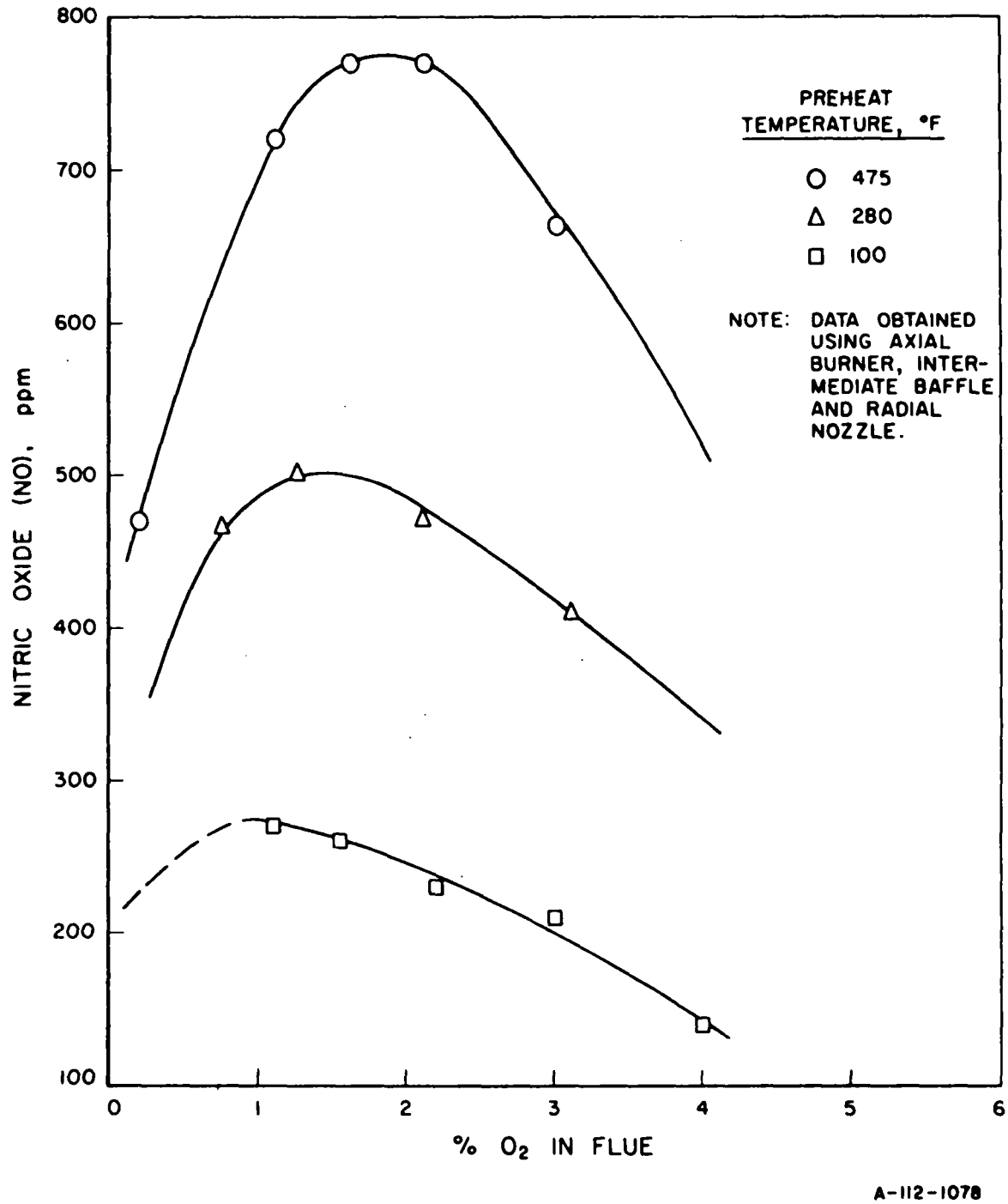

Figure II-65. NO CONCENTRATIONS WITH GAS INPUT OF 2900 CF/hr (Original Data)

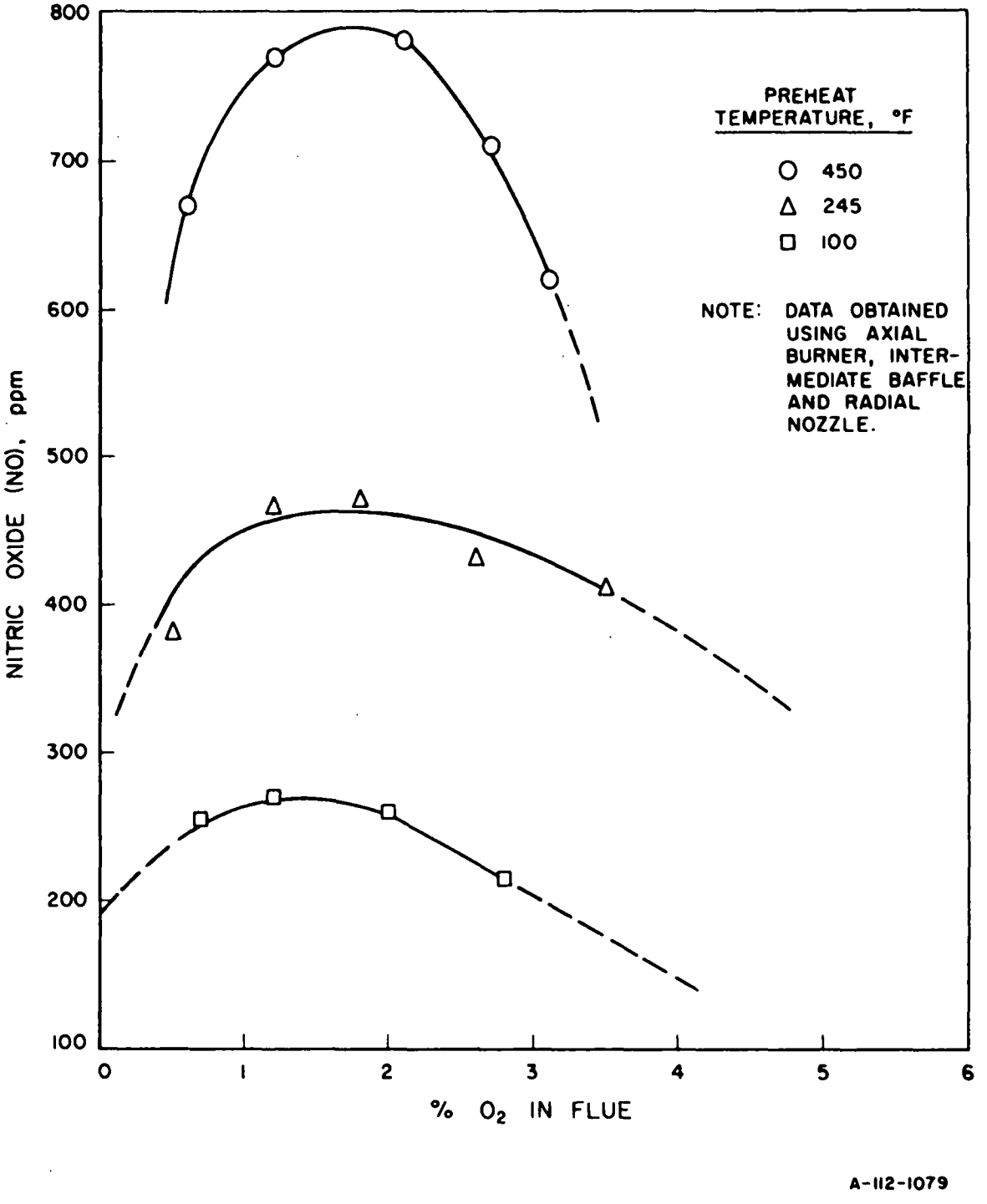

Figure II-66. NO CONCENTRATIONS WITH GAS INPUT OF 3160 CF/hr (Original Data)

figures). However, we have no experimental data to support the accuracy of this extrapolation. Figures II-66 through II-70 show these interpolated data, which are used for later analysis.

Working with the interpolated and actual NO_x curves, we found that the formation of NO (as measured in the flue) is nearly linear with gas input, as shown in Figure II-70, for two preheat temperatures. We also see from these data that the level of preheat temperature changes the magnitude of NO emissions but not the linear relationship with the gas input. Closer examination shows that the linearity of the curves improves with increasing amounts of excess oxygen (excess air for combustion). Figure II-71 shows these same data for a 450°F preheat temperature on an expended NO scale, where the change in linearity is more apparent. From these data, we determined that the average increase in NO emissions is 24% over the range of 2335-3100 CF/hr of natural gas input or 15.6 ppm per 1000 CF/hr change of gas input. We also found the rate at which NO emissions increase with increasing gas input is greater with higher preheat temperatures. At the 100°F preheat level, the rate of increase of NO emissions is only 4.0 ppm per 100 CF/hr change compared with 15.6 ppm per 100 CF/hr change at a 450°F preheat. The rate of increase of NO emission with increasing gas input at a 700°F preheat temperature should be compared with other preheat data with caution because of its extrapolated nature. Interestingly, the rate of increase is about 36 ppm per 100 CF/hr of gas input. Plotting the rate at which NO emissions change with changing gas input as a function of preheat temperature (Figure II-72) shows that the preheat temperature can change substantially between 70°F and 250°F without changing the NO rate as a function of gas input.

A limited amount of input-output testing was done for the intermediate-flame baffle with the axial gas nozzle. Gas inputs above 2147 CF/hr resulted in unburned gas in the flue; flue analysis was not possible under these conditions. However, using this maximum gas input resulted in the following comparison with radial gas nozzle operation.

a. The longer, less intense flame resulting from the burner with an axial gas nozzle produces substantially less nitric oxide.

b. Preheated air has a lesser effect of NO formation with the axial gas nozzle.

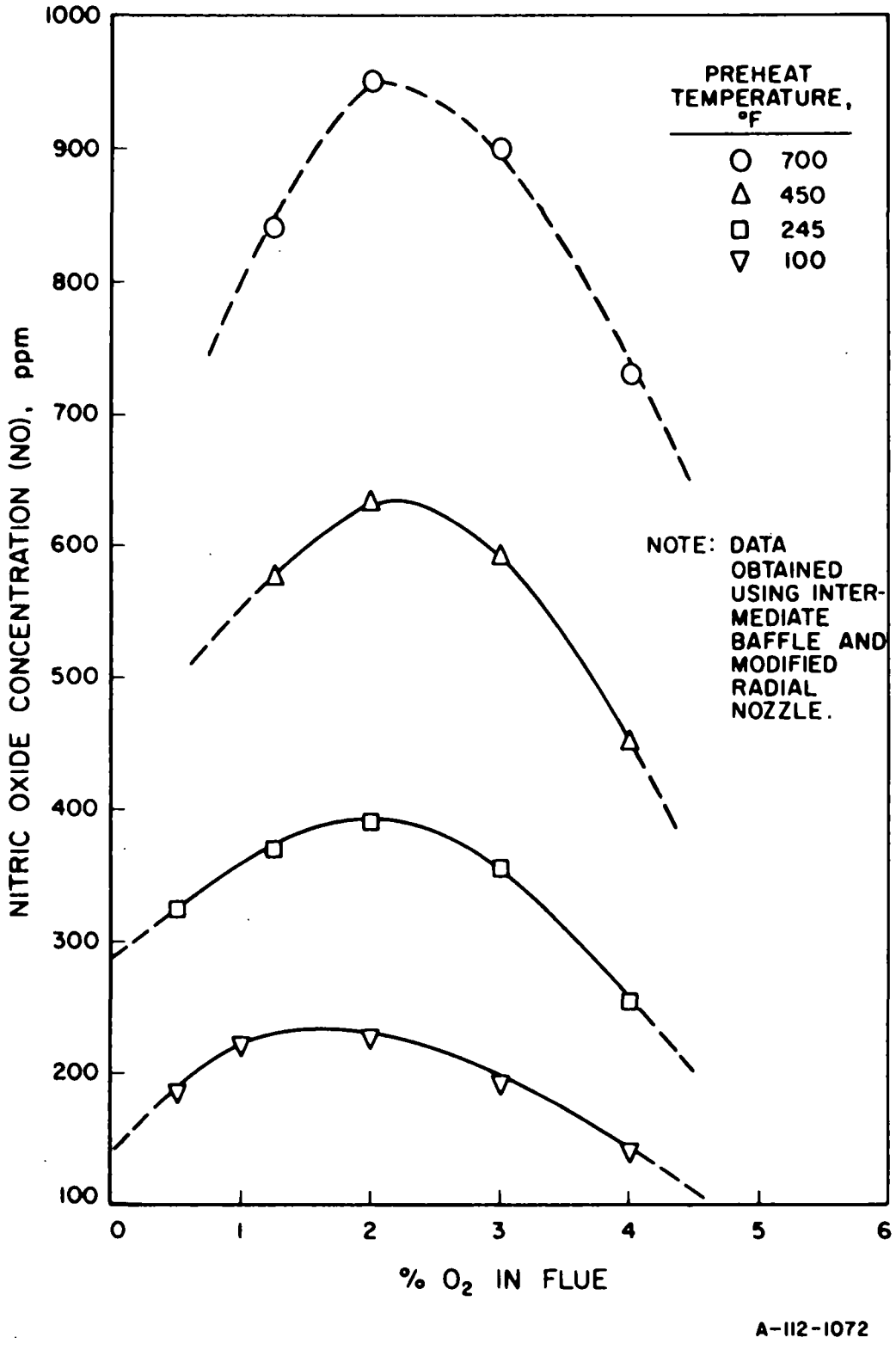

Figure II-67. NO CONCENTRATIONS WITH GAS INPUT OF 2335 CF/hr (Interpolated and Extrapolated Data)

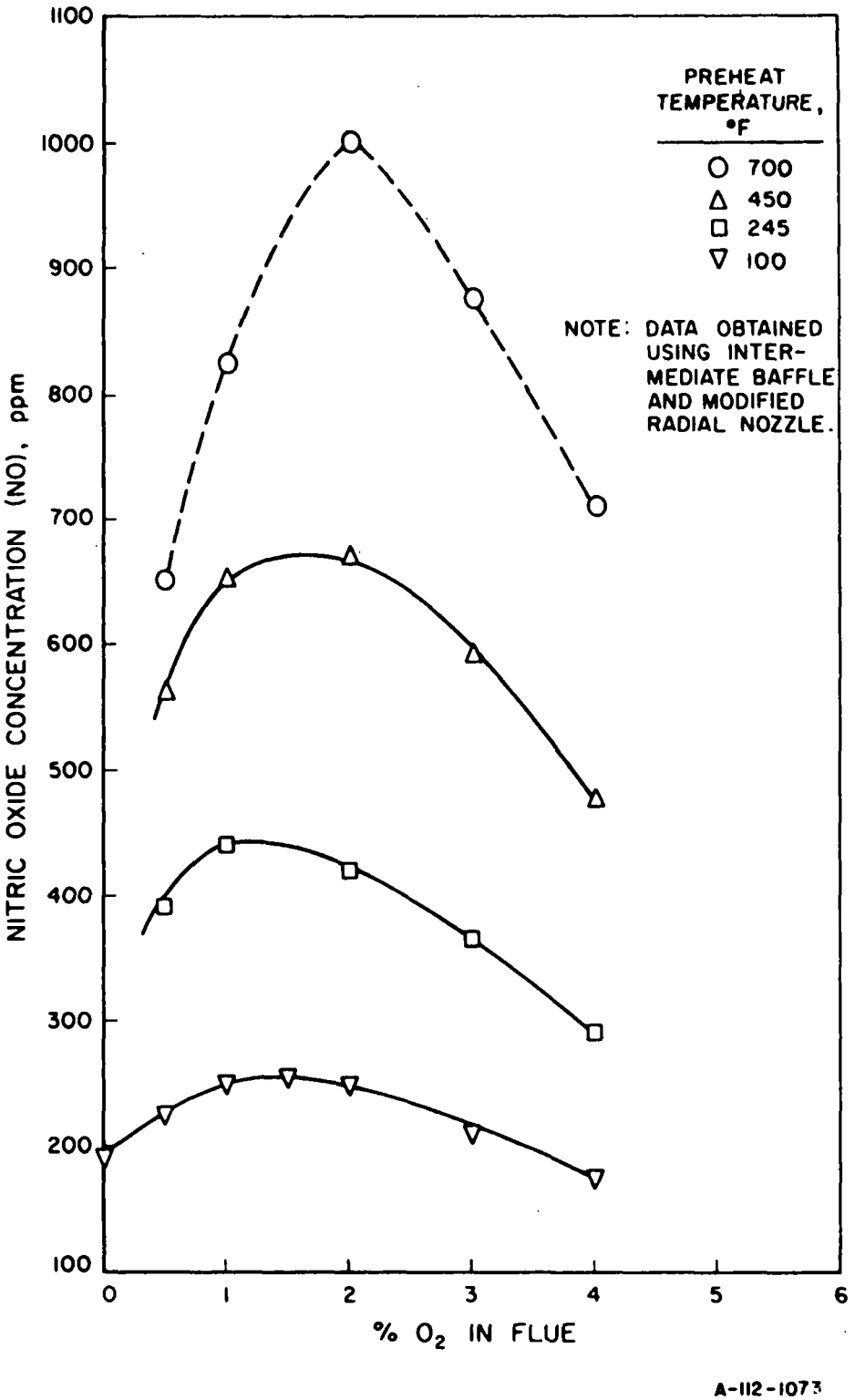

Figure II-68. NO CONCENTRATIONS WITH GAS INPUT OF 2626 CF/hr (Interpolated and Extrapolated Data)

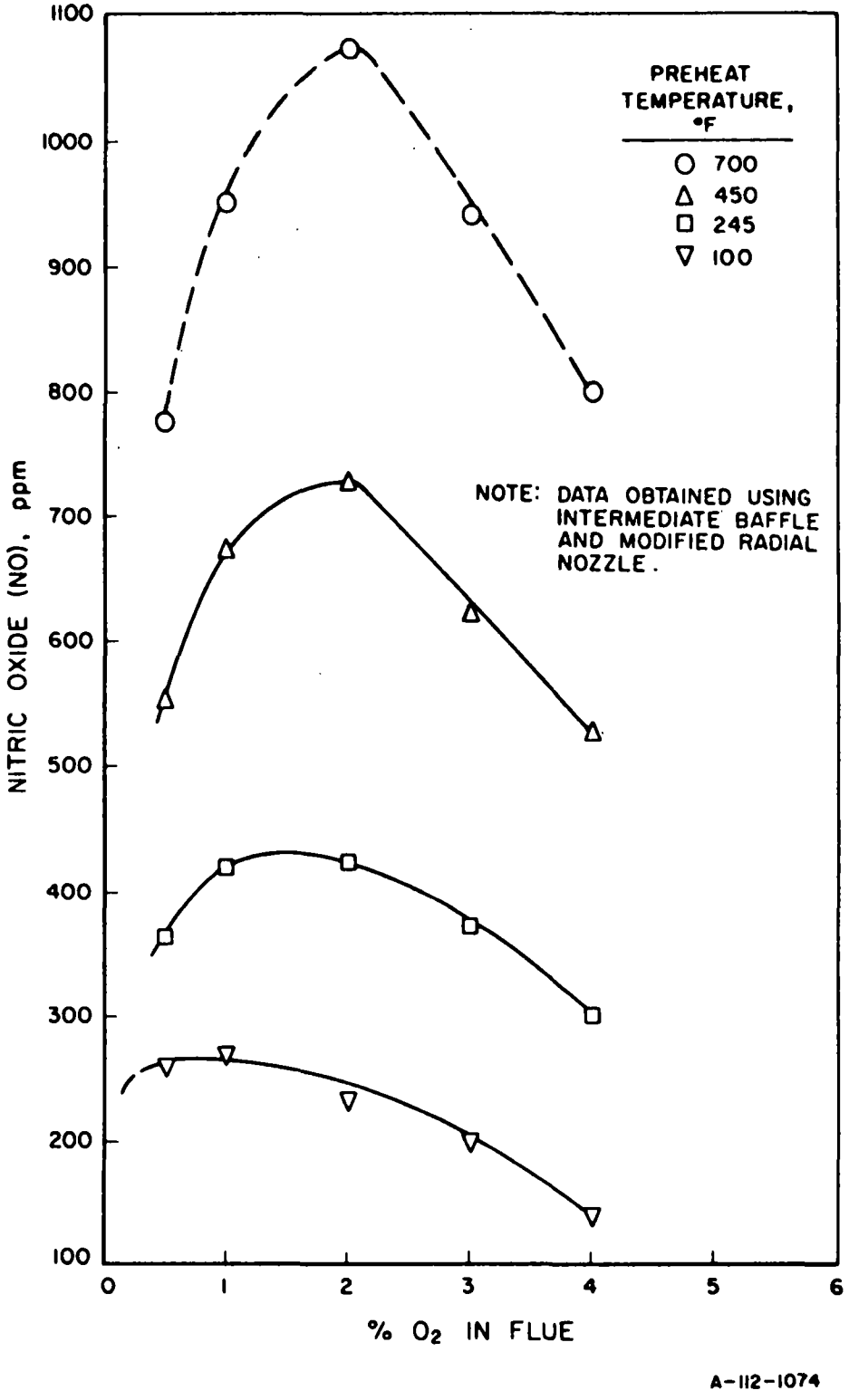

Figure II-69. NO CONCENTRATIONS WITH GAS INPUT OF 2900 CF/hr (Interpolated and Extrapolated Data)

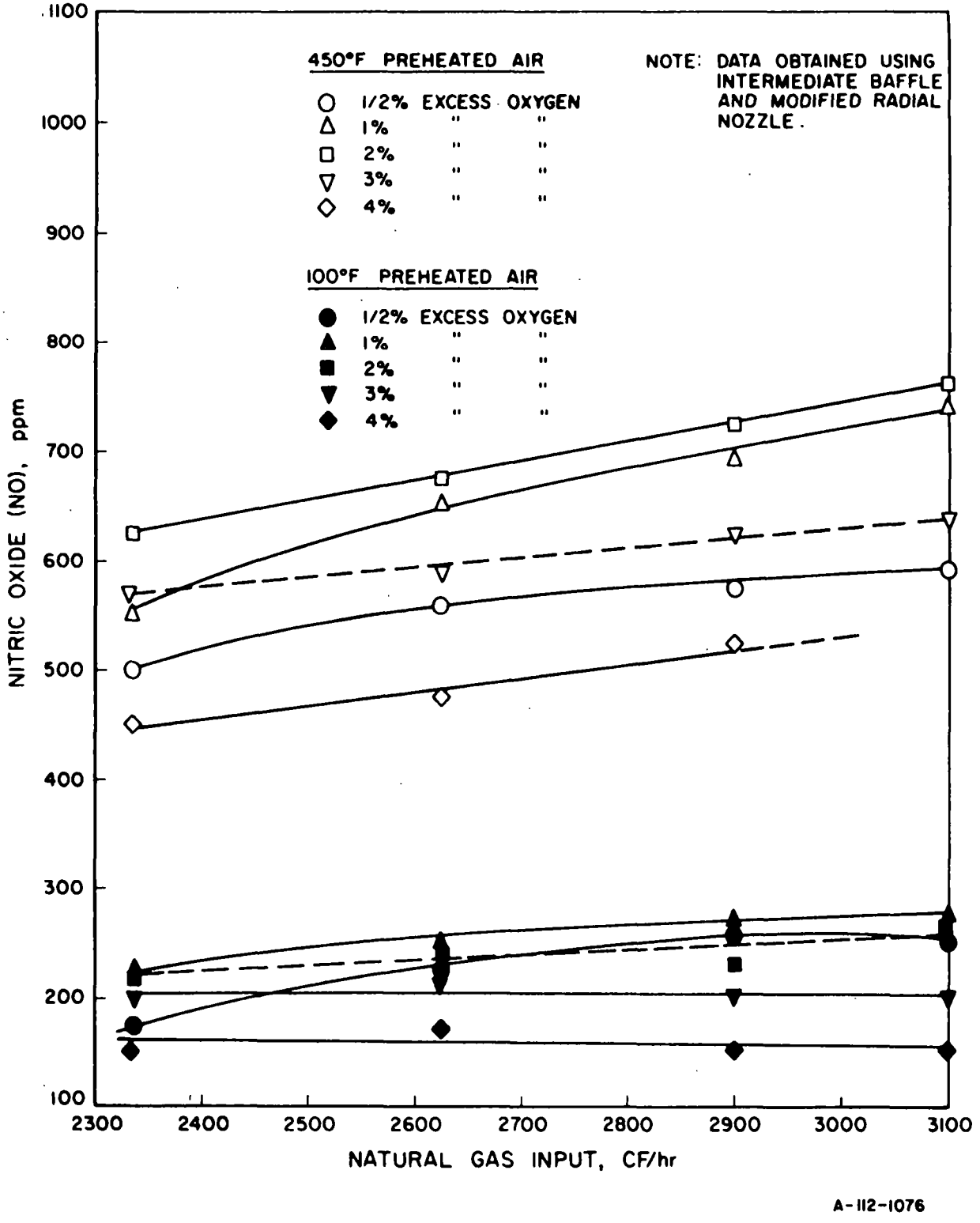

Figure II-70. NO CONCENTRATIONS WITH VARIOUS GAS INPUTS FOR TWO PREHEAT TEMPERATURES

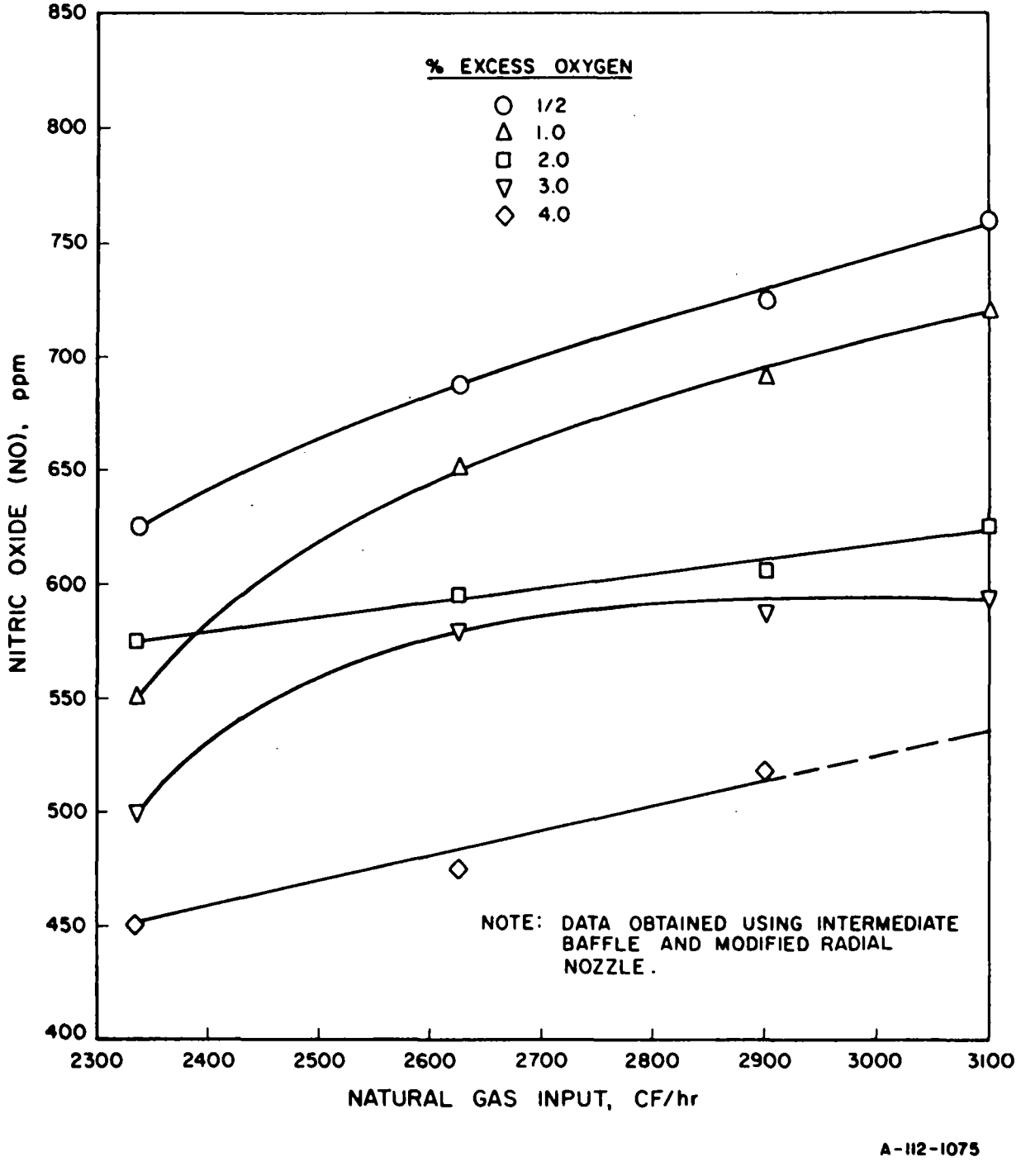

Figure II-71. NO CONCENTRATIONS WITH VARYING GAS INPUTS FOR 450°F PREHEAT TEMPERATURE (Expanded NO Scale)

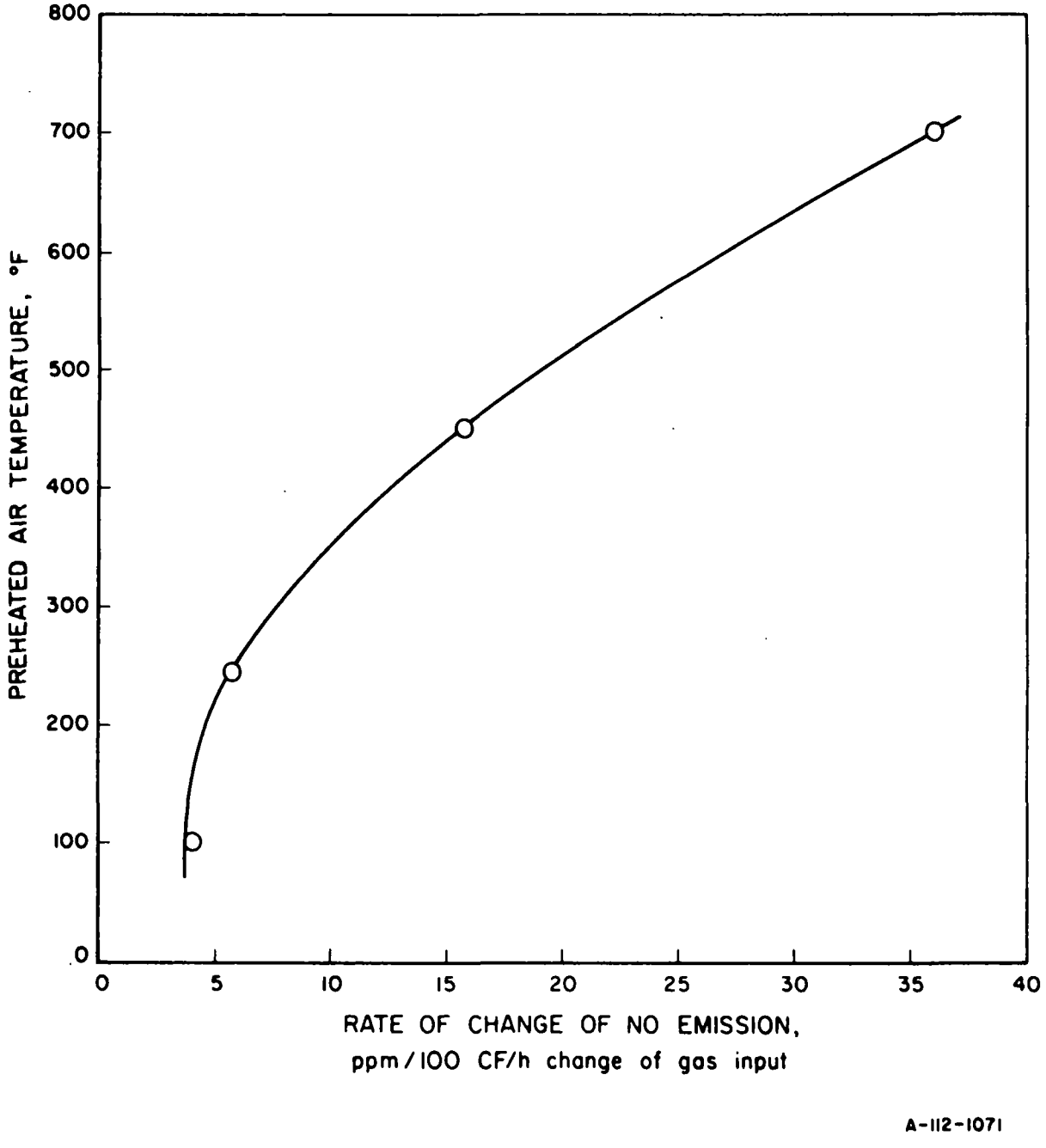

Figure II-72. RATE OF CHANGE OF NO EMISSIONS/100 CF/hr GAS INPUT AS A FUNCTION OF PREHEAT TEMPERATURE

c. The peak NO formation occurs at higher levels of excess air.

Figure II-73 shows the input-output test results for the intermediate baffle and axial gas nozzle. Inxreasing the preheated air temperature from 100^0 to 570^0F increased the NO emissions a maximum of 130 ppm. With the radial nozzle, the NO increased about 450 ppm for the same increase in preheat temperature of 470^0F. (The increase in NO for the radial nozzle was interpolated from the data of Figures II-67 and II-70.) In addition, the peak NO emissions occur with about 5.5% oxygen in the flue compared with 1.5-1.7% oxygen for the radial gas nozzle.

5. In-the-Flame Data Survey Results

As part of this program, we radially map the concentrations of CO, CO_2, CH_4, O_2, and NO, the temperature, and the gas velocity. This information is obtained to gain insight into the mechanism and location of NO formation for different flame conditions and as the input to an NO_x modeling program, also sponsored by EPA with Ultra Systems, Inc.

We completed gas species and temperature mapping for the intermediate-flame baffle burner with both the axial and radial gas nozzles. These maps were obtained while operating the burner at conditions producing the maximum amount of NO as determined from the input-output tests.

Profiles were first run on the burner using the radial gas nozzle. This nozzle was designed and installed to provide a shorter flame. The original axial gas nozzle produced a flame that was longer than the furnace with a gas input above 2175 CF/hr. The radial nozzle allows operation above 3100 CF/hr of gas. However, our initial survey of combustion species showed that combustion was essentially complete in the burner block. Figure II-74 shows a composite of the gas sampling profiles taken at an axial position 5 cm from the burner block face. (Five centimeters is the closest the probe can be positioned to the block.) The burner was operating at a 2547 CF/hr gas input, 10% excess air, and 510^0F preheated air. These data show (curve M) that methane concentration was only about 0.5%. The carbon monoxide (curve C) varied between 400 ppm at the center line to a peak of 2000 ppm at a 13.2-cm radial position. (The total width of the burner block opening is 42 cm.) Oxygen (curve O) varied from 1.52% at the center line to a minimum of 0.66% at a 8.8-

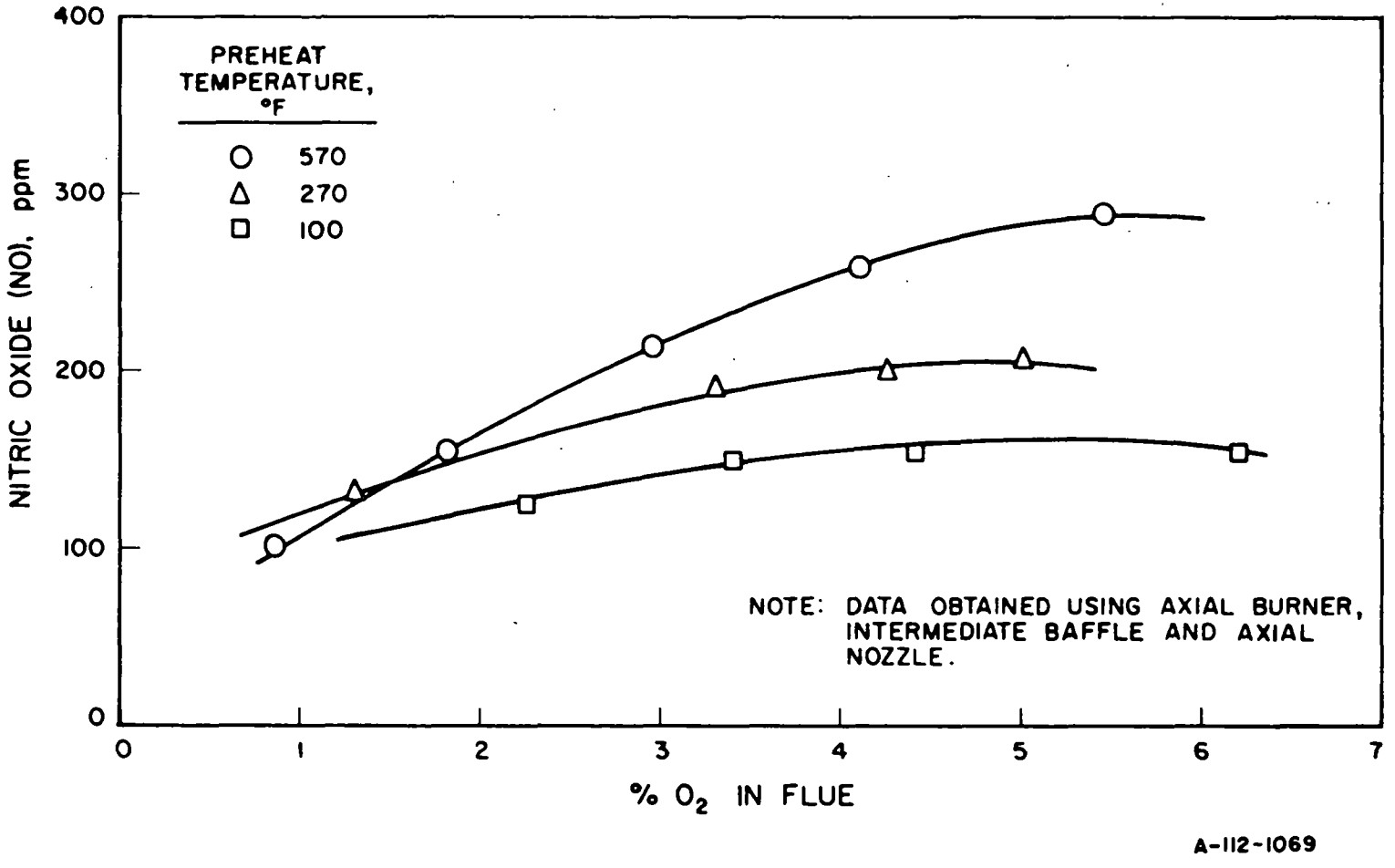

Figure II-73. NO CONCENTRATION AT GAS INPUT OF 2147 CF/hr (Excess O_2 Variable and Wall Temperature of 2570°F)

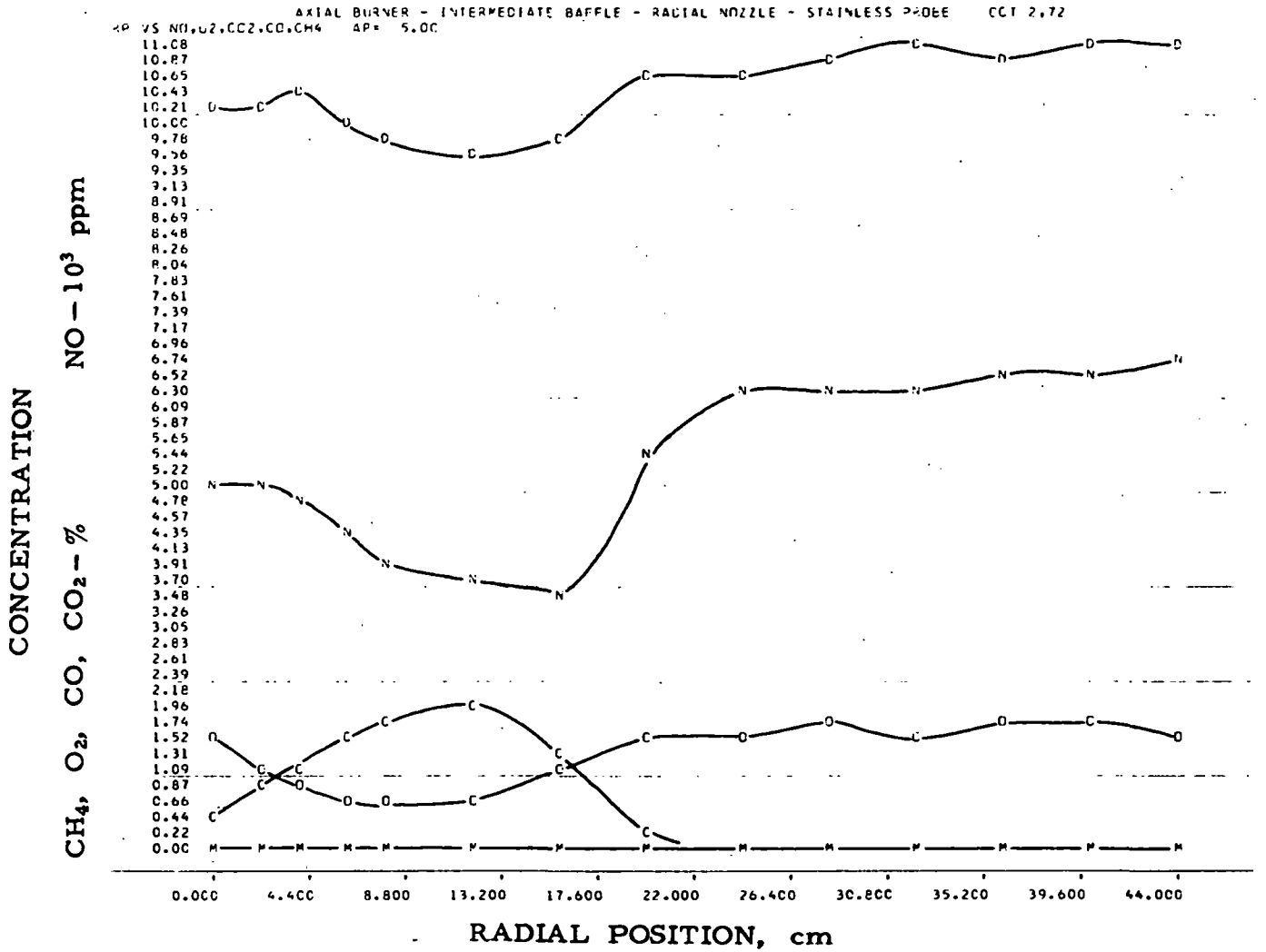

Figure II-74. COMPOSITE RADIAL PROFILES FOR NO, CO, CH_4, O_2, AND CO_2 WITH GAS INPUT OF 2547 CF/hr
(Intermediate Flame Baffle With Radial Gas Nozzle at an Axial Position of 5.0 cm, Preheat Temperature of 510°F, 10% Access Air, and Stainless-Steel Probe)

cm radial position. Nitric oxide (curve N) varied from 500 ppm at the center line to a minimum of 340 ppm at a 15-cm radial position. Carbon dioxide (curve D) varied from about 10% at the center line to 9.8% at a 13-cm radial position.

The increase in the concentrations of CO_2, NO, and O_2 beyond a 17.6-cm radial position is believed to be caused by recirculated combustion products moving back toward the burner along the walls. At a 44-cm radial position, the measured concentration of NO was 660 ppm, whereas the flue contained 742 ppm. However, 44 cm is only one-half the distance between the burner center line and furnace sidewall. We would expect the measured NO concentration to increase at positions beyond 44 cm, attaining approximately the NO concentration of the flue at the wall. The curves of Figure II-74 were plotted on a single 0-11% (approx) scale because of a computer limitation. The following legend applies to this figure and some of the others (computer print-outs) that follow:

AP – axial position

RP – radial position

The actual data were collected on a range of concentrations which provided greater resolution. The raw data are shown in Tables II-9 and II-10 and are shown plotted on the enlarged scale in Figures II-75 to II-79.

Figure II-80 shows the temperature profile across the furnace at the 5.0-cm axial probe position. The data support our conclusion of essentially complete combustion in the burner block. The temperature was essentially constant across the half width of the block (21 cm).

Considering that combustion was essentially complete in the burner block, further profiles at axial positions greater than 5 cm were considered unnecessary. Test work continued by reinstalling the axial flow gas nozzle and lowering the gas input until combustion was completed in the furnace. This occurred at a gas input of 2147 CF/hr, which was maintained for all remaining work with this particular gas nozzle. Data for radial profiles of gas species and temperature were again measured in the furnace.

Table II-9. DATA OBTAINED USING RADIAL GAS NOZZLE WITH 2547 CF/hr GAS INPUT
(Intermediate Baffle, Axial Burner, Radial Nozzle, and Stainless-Steel Probe)

TRACER GAS STUDIES OF COMBUSTION BURNERS PROGRAM 2
AXIAL BURNER - INTERMEDIATE BAFFLE - RADIAL NOZZLE - STAINLESS PROBE OCT 2,72

INPUT GAS 2547 WALL TEMPERATURE 2680 PREHEAT TEMPERATURE 510
OUTPUT ANALYSIS
NITROGEN OXIDE 77.20 PERCENT ON RANGE 1, 741.86 PPM OXYGEN 1.73 PERCENT
CARBON DIOXIDE 84.40 PERCENT ON RANGE 1, 11.06 PERCENT
CARBON MONOXIDE 13.10 PERCENT ON RANGE 3, 0.005 PERCENT
METHANE 0.00 PERCENT ON RANGE 3, 0.00 PERCENT

EXPERIMENTAL RESULTS

		NITROGEN OXIDE -NO			OXYGEN	CARBON DIOXIDE-CO2			CARBON MONOXIDE -CO			METHANE - CH4		
AP	RP	RANGE	X	Y	O2	RANGE	X	Y	RANGE	X	Y	RANGE	X	Y
5.00	0.00	1	54.50	502.1	1.52	1	80.20	10.15	1	17.20	0.481	3	0.00	0.00
5.00	2.00	1	53.90	496.0	1.19	1	80.10	10.13	1	26.30	0.796	3	0.00	0.00
5.00	4.00	1	51.60	472.7	0.89	1	81.60	10.45	1	34.70	1.126	3	0.00	0.00
5.00	6.00	1	47.90	435.8	0.68	1	79.20	9.94	1	44.10	1.541	3	0.00	0.00
5.00	8.00	1	44.20	399.3	0.67	1	78.30	9.75	1	49.50	1.801	3	0.00	0.00
5.00	12.00	1	40.90	367.2	0.63	1	77.80	9.65	1	50.90	1.870	3	0.00	0.00
5.00	16.00	1	38.50	344.1	1.04	1	78.30	9.75	1	38.00	1.266	3	0.00	0.00
5.00	20.00	1	57.50	532.7	1.42	1	82.60	10.66	2	19.00	0.317	3	0.00	0.00
5.00	24.00	1	66.00	621.2	1.60	1	83.00	10.75	3	44.20	0.019	3	0.00	0.00
5.00	28.00	1	67.40	636.1	1.64	1	83.50	10.86	3	30.90	0.013	3	0.00	0.00
5.00	32.00	1	67.50	637.1	1.59	1	84.50	11.08	3	29.70	0.012	3	0.00	0.00
5.00	36.00	1	68.20	644.6	1.73	1	83.50	10.86	3	28.50	0.012	3	0.00	0.00
5.00	40.00	1	68.70	649.9	1.66	1	84.30	11.03	3	27.30	0.011	3	0.00	0.00
5.00	44.00	1	70.20	665.9	1.58	1	84.30	11.03	3	27.10	0.011	3	0.00	0.00

Table II-10. COEFFICIENTS AND STANDARD DEVIATIONS OF THE MATHEMATICAL FIT FOR EACH GAS.

TRACER GAS STUDIES OF COMBUSTION BURNERS PROGRAM 2

NO-RANGE 1

X	OBSERVED Y	COMPUTED Y	STANDARD DEVIATION ON Y	COEFFICIENTS, Y=C(1)+C(2)*X+..+C(N+1)*X**N
0.000	0.000	1.192	7.04546	C(1)= 1.192C8C3
28.000	250.000	245.365		C(2)= 8.2232437
55.000	500.000	507.189		C(3)= 0.0177582
77.500	750.000	745.154		
100.000	1000.000	1001.099		

NO-RANGE 3

X	OBSERVED Y	COMPUTED Y	STANDARD DEVIATION ON Y	COEFFICIENTS, Y=C(1)+C(2)*X+..+C(N+1)*X**N
0.000	0.000	-0.038	0.34061	C(1)= -C.0388C39
26.000	50.000	50.192		C(2)= 1.9C82312
51.000	100.000	99.657		C(3)= 0.0005138
76.000	150.000	150.265		
100.000	200.000	199.922		

CO2 RANGE 1

X	OBSERVED Y	COMPUTED Y	STANDARD DEVIATION ON Y	COEFFICIENTS, Y=C(1)+C(2)*X+..+C(N+1)*X**N
0.000	0.000	0.060	0.33791	C(1)= 0.0607462
41.200	3.750	3.540		C(2)= 0.0406835
67.000	7.500	7.555		C(3)= 0.0010623
87.000	11.300	11.641		
100.000	15.000	14.752		

CO2 RANGE 2

X	OBSERVED Y	COMPUTED Y	STANDARD DEVIATION ON Y	COEFFICIENTS, Y=C(1)+C(2)*X+..+C(N+1)*X**N
0.000	0.000	0.008	0.04551	C(1)= 0.0088310
33.000	1.250	1.232		C(2)= 0.0308988
59.000	2.500	2.484		C(3)= 0.0001873
82.000	3.750	3.802		
100.000	5.000	4.972		

CO2 RANGE 3

X	OBSERVED Y	COMPUTED Y	STANDARD DEVIATION ON Y	COEFFICIENTS, Y=C(1)+C(2)*X+..+C(N+1)*X**N
0.000	0.000	0.000	0.00285	C(1)= 0.0005971
32.000	0.125	0.123		C(2)= 0.0033220
58.000	0.250	0.248		C(3)= 0.0000165
81.000	0.375	0.378		
100.000	0.500	0.498		

CO RANGE 1

X	OBSERVED Y	COMPUTED Y	STANDARD DEVIATION ON Y	COEFFICIENTS, Y=C(1)+C(2)*X+..+C(N+1)*X**N
0.000	0.000	0.007	0.02630	C(1)= 0.0074353
37.000	1.250	1.223		C(2)= 0.0229367
63.000	2.500	2.518		C(3)= 0.0002686
83.000	3.750	3.762		
100.000	5.000	4.987		

CO RANGE 2

X	OBSERVED Y	COMPUTED Y	STANDARD DEVIATION ON Y	COEFFICIENTS, Y=C(1)+C(2)*X+..+C(N+1)*X**N
0.000	0.000	0.001	0.00766	C(1)= 0.0017783
29.100	0.500	0.497		C(2)= 0.0158220
55.000	1.000	0.996		C(3)= 0.0000411
79.000	1.500	1.508		
100.000	2.000	1.995		

CO RANGE 3

X	OBSERVED Y	COMPUTED Y	STANDARD DEVIATION ON Y	COEFFICIENTS, Y=C(1)+C(2)*X+..+C(N+1)*X**N
0.000	0.000	0.000	0.00019	C(1)= 0.0000444
29.100	0.012	0.012		C(2)= 0.0003955
55.000	0.025	0.024		C(3)= 0.0000010
79.000	0.037	0.037		
100.000	0.050	0.049		

Table II-10, Cont. COEFFICIENTS AND STANDARD DEVIATIONS OF THE MATHEMATICAL FIT FOR EACH GAS

TRACER GAS STUDIES OF COMBUSTION BURNERS PROGRAM 2

CH4 RANGE 1

X	OBSERVED Y	COMPUTED Y	STANDARD DEVIATION ON Y	COEFFICIENTS, Y=C(1)+C(2)*X+..+C(N+1)*X**N
0.000	0.000	0.084	0.33885	C(1)= 0.0843171
39.100	5.000	4.701		C(2)= 0.0673895
66.000	10.000	10.181		C(3)= 0.0012968
85.200	15.000	15.240		
100.000	20.000	19.792		

CH4 RANGE 2

X	OBSERVED Y	COMPUTED Y	STANDARD DEVIATION ON Y	COEFFICIENTS, Y=C(1)+C(2)*X+..+C(N+1)*X**N
0.000	0.000	0.012	0.03837	C(1)= 0.0122515
32.500	2.500	2.467		C(2)= 0.0639469
58.800	5.000	5.007		C(3)= 0.0003571
81.000	7.500	7.534		
100.000	10.000	9.978		

CH4 RANGE 3

X	OBSERVED Y	COMPUTED Y	STANDARD DEVIATION ON Y	COEFFICIENTS, Y=C(1)+C(2)*X+..+C(N+1)*X**N
0.000	0.000	0.004	0.01073	C(1)= 0.0041916
28.000	1.250	1.240		C(2)= 0.0419261
54.000	2.500	2.500		C(3)= 0.0000797
78.000	3.750	3.759		
100.000	5.000	4.994		

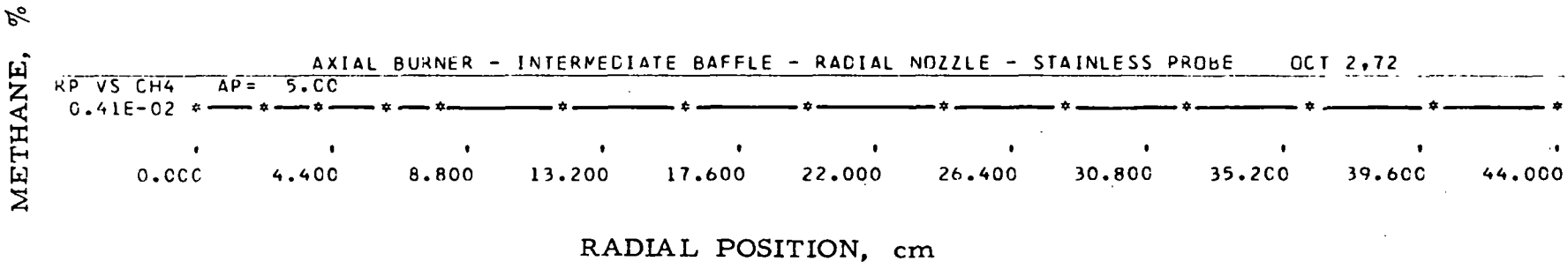

Figure II-75. RADIAL PROFILE FOR CH_4 WITH GAS INPUT OF 2547 CF/hr (Intermediate-Flame Baffle With Radial Gas Nozzle at an Axial Position of 5.0 cm, Preheat Temperature of 510°F, 10% Excess Air, and Stainless-Steel Probe)

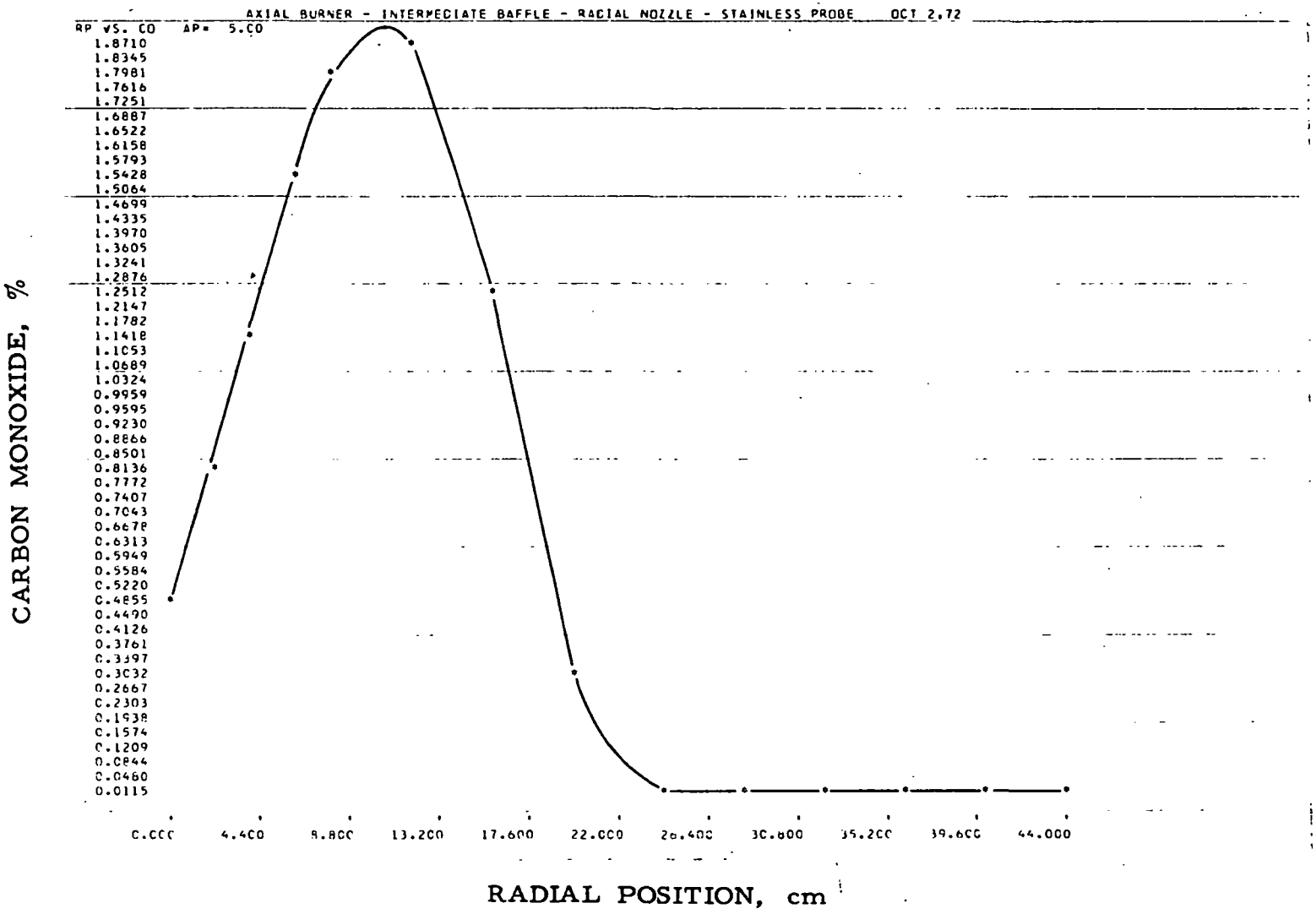

Figure II-76. RADIAL PROFILE FOR CO WITH GAS INPUT OF 2547 CF/hr (Intermediate-Flame Baffle With Radial Gas Nozzle at an Axial Position of 5.0 cm, Preheat Temperature of 510^{0}F, 10% Excess Air, and Stainless-Steel Probe)

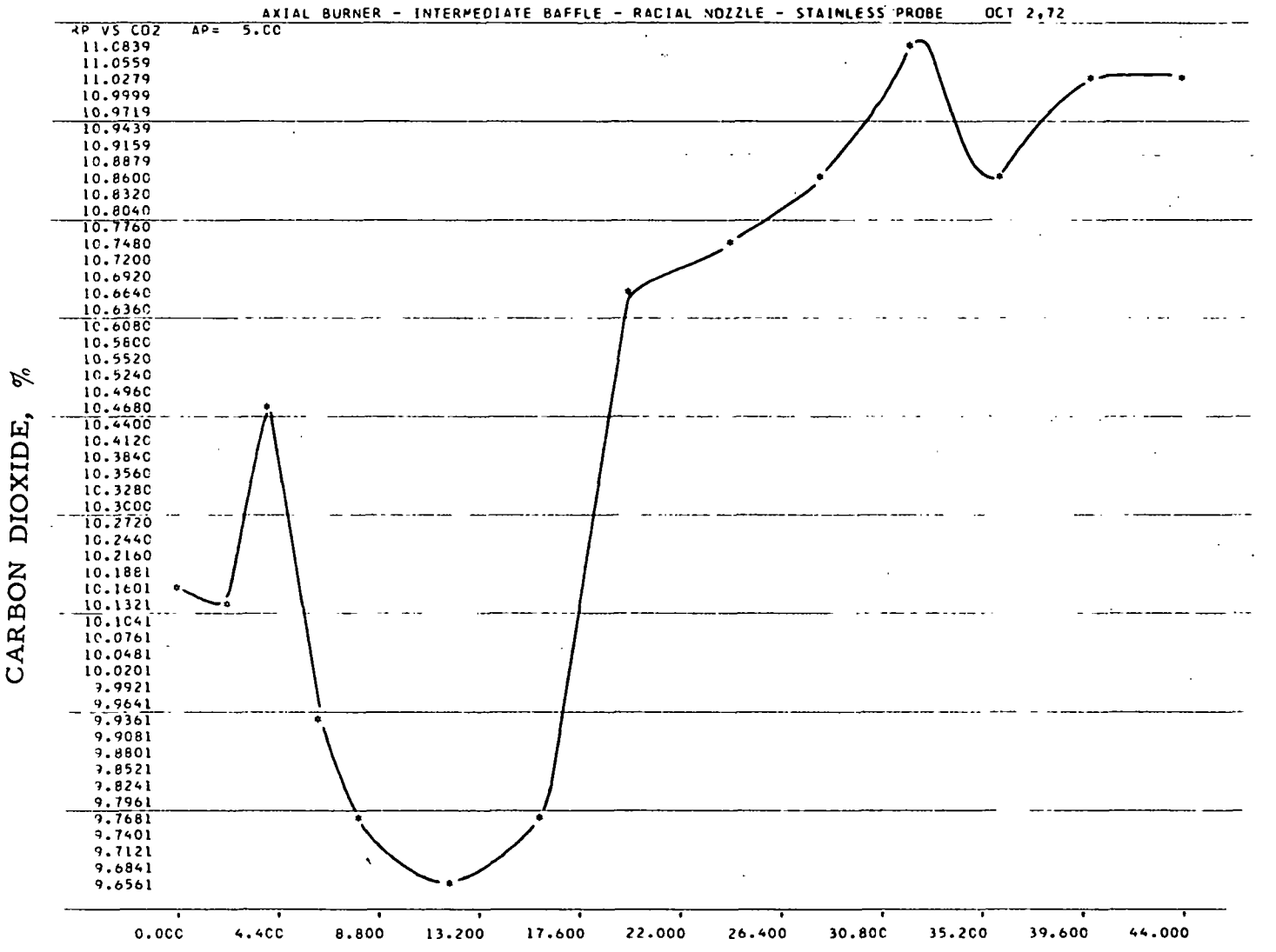

Figure II-77. RADIAL PROFILE FOR CO_2 WITH GAS INPUT OF 2547 CF/hr (Intermediate-Flame Baffle With Radial Gas Nozzle at an Axial Position of 5.0 cm, Preheat Temperature of 510°F, 10% Excess Air, and Stainless-Steel Probe)

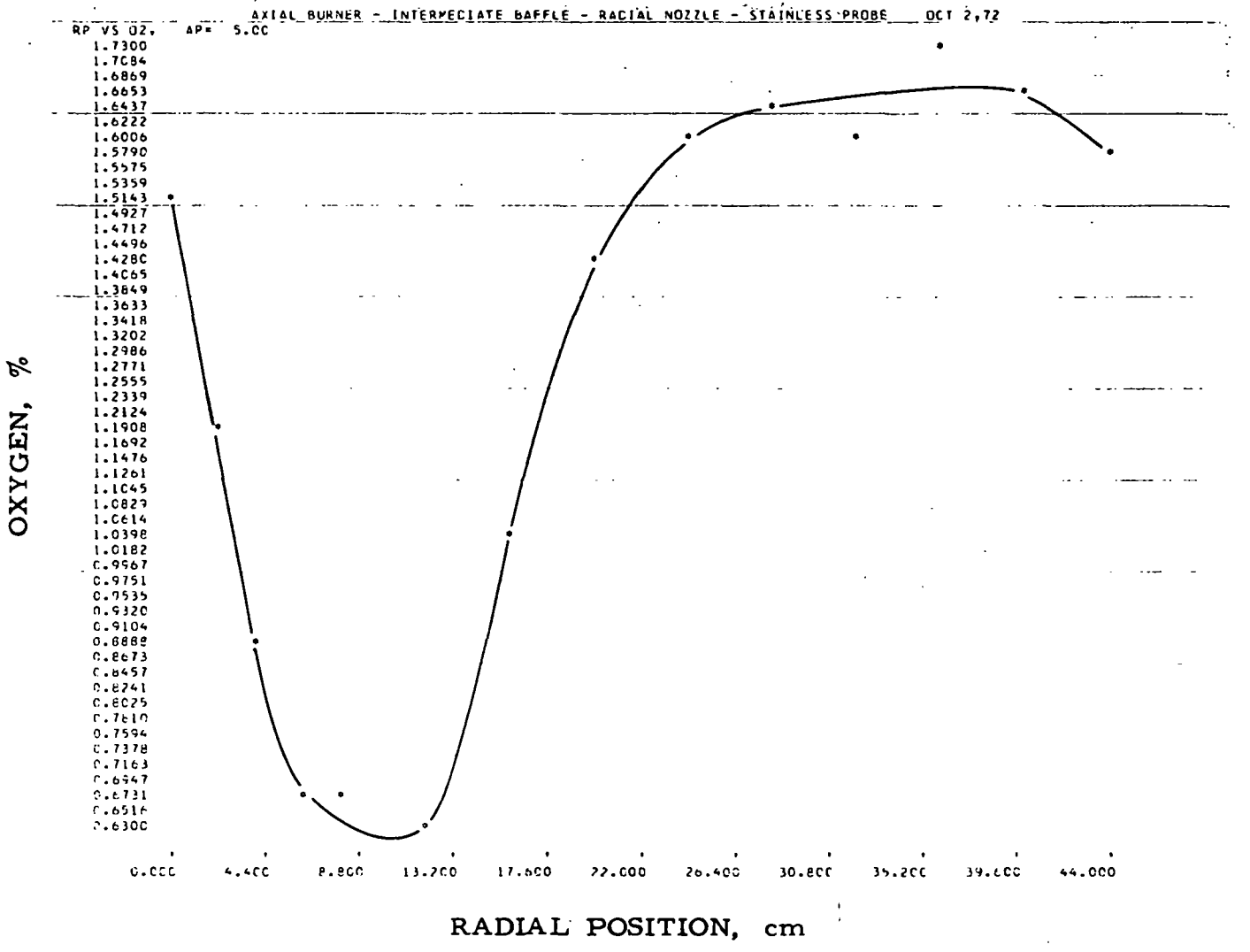

Figure II-78. RADIAL PROFILE FOR O_2 WITH GAS INPUT OF 2547 CF/hr (Intermediate Flame Baffle With Radial Gas Nozzle at an Axial Position of 5.0 cm, Preheat Temperature of 510°F, 10% Excess Air, and Stainless-Steel Probe)

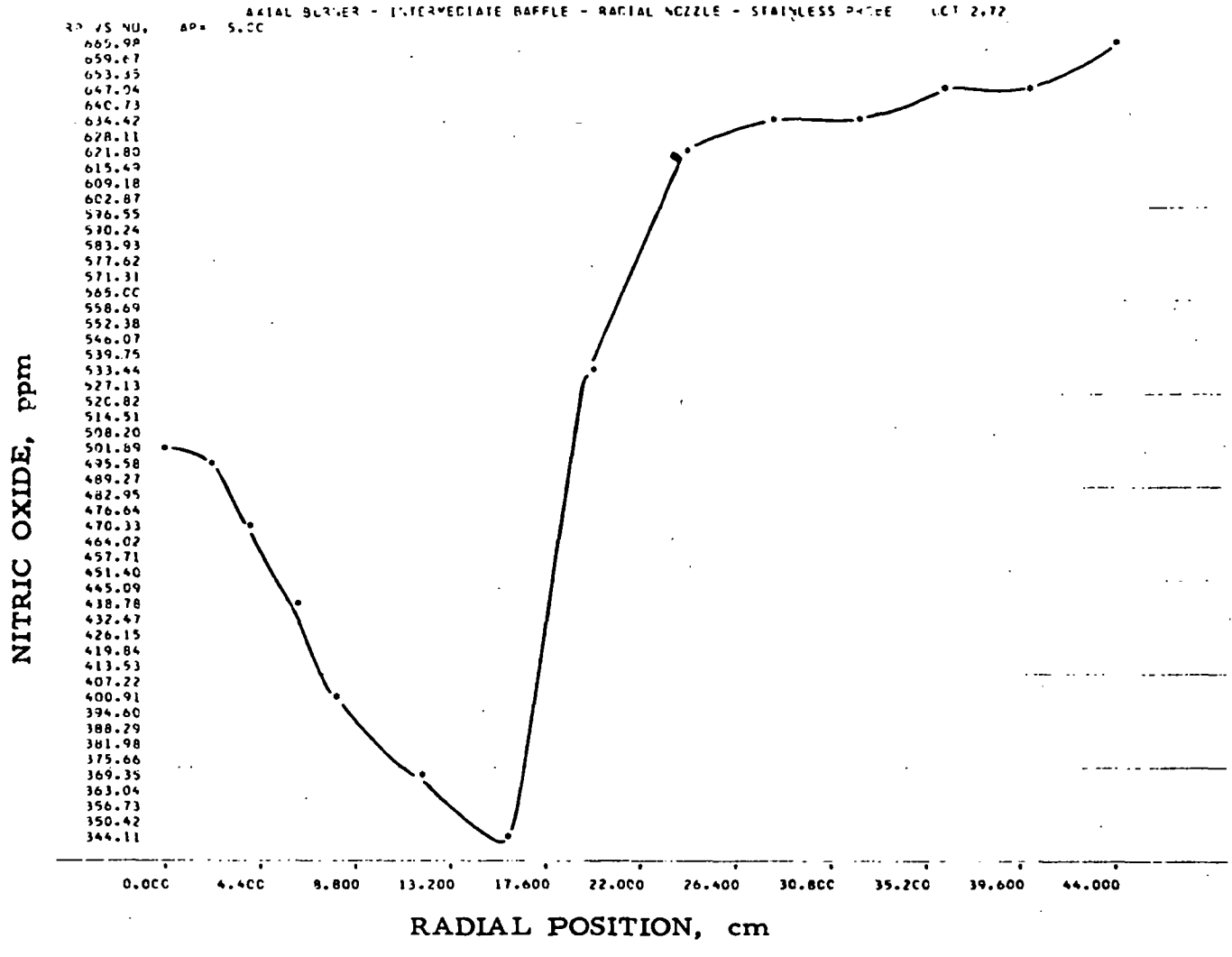

Figure II-79. RADIAL PROFILE FOR NO WITH GAS INPUT OF 2547 CF/hr (Intermediate-Flame Baffle With Radial Gas Nozzle at an Axial Position of 5.0 cm, Preheat Temperature of 510°F, 10% Excess Air, and Stainless-Steel Probe)

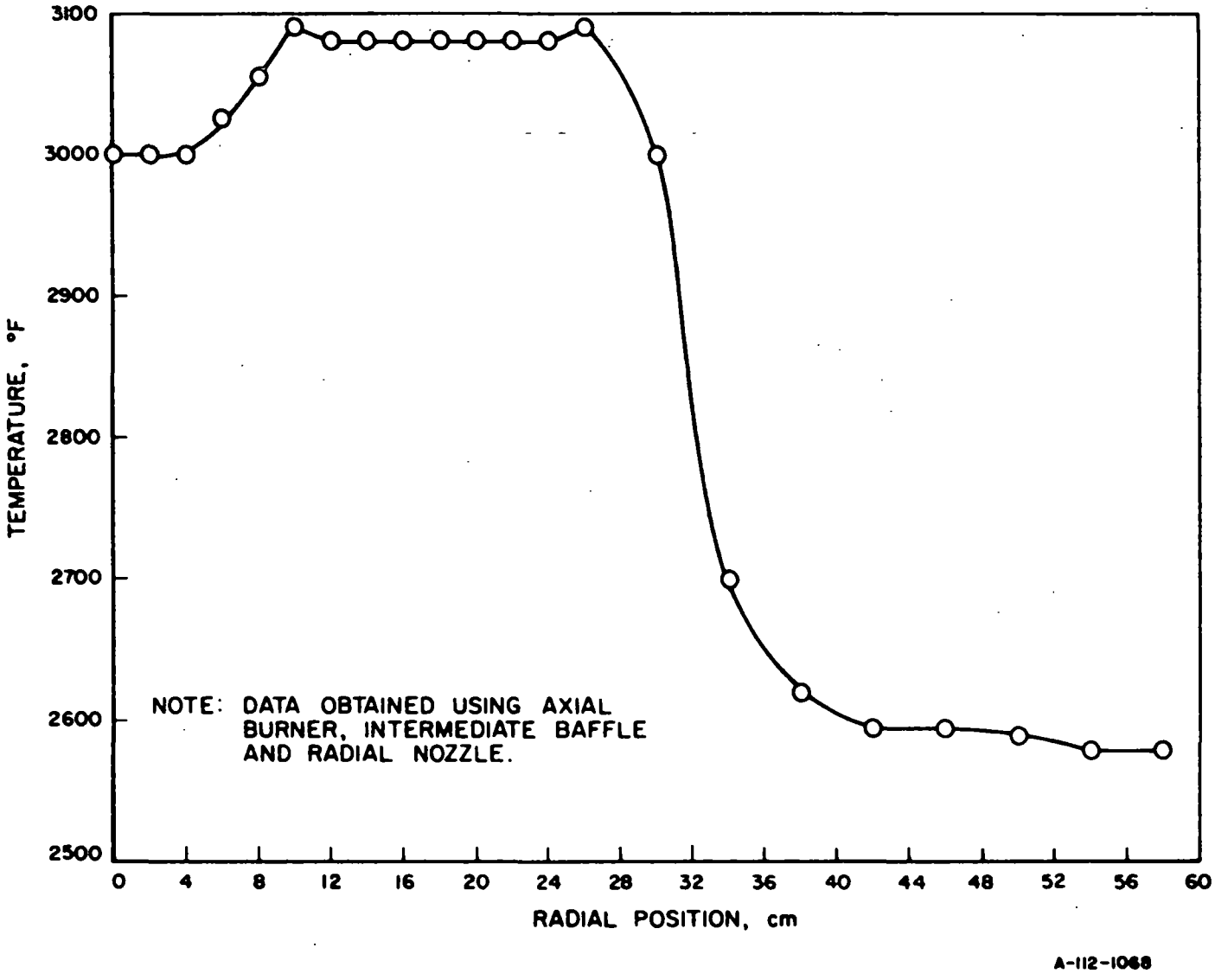

Figure II-80. TEMPERATURE PROFILE ACROSS FURNACE WITH GAS INPUT OF 2546 CF/hr AND 5.0-cm AXIAL PROBE POSITION

Figure II-81 shows a composite plot of CO, CO_2, CH_4, NO, and O_2. The methane concentration (curve M) was 10.63% at the burner center line, decreasing to about 0.25% at a 19-cm radial position. A very approximate integration under the methane curve showed that the average concentration was about 6%. Consequently, about 35% of the combustion can be assumed complete. Significant concentrations of O_2, CO_2, NO, and CO at the center line of the burner where the methane reading indicates essentially no combustion is occurring are probably caused by diffusion. The nitric oxide concentration (curve N) was 133 ppm at the center line, decreasing to 30 ppm at a 13-cm radial position and again increasing in a probable recirculation zone beyond 19 cm. Oxygen (curve O) was 3.46% at the center line, increasing to 13.55% near the perimeter of the burner-block opening. Nitric oxide (curve N) increased to only 77% of the 255 ppm of NO measured in the flue. However, measurements again were not taken out to the furnace wall. Data plots with greater resolution are given in Figures II-82 to II-86 and the raw data in Table II-11.

Data were taken at three axial positions for the axial gas nozzle. Figure II-87 shows composite chemical species profiles at a 77.5-cm axial position; Figure II-88 shows these same profiles for a 152.5-cm axial position. We found that essentially all the CH_4 (curve M) is consumed at 77.5 cm, leaving only CO (curve C) for further combustion. Nitric oxide (curve N) was essentially constant across the width of the burner; oxygen (curve O) was 4.76% at the center line, decreasing to about 3.9% at the 12.6-cm radial position. The oxygen at the center line increased from 4.76 to 5.10% between the 77.5-cm and 152.5-cm axial positions while lower amounts were measured at all radial positions other than the center line. Concurrently, CO and CH_4 decreased as expected while NO increased slightly in the postflame region. In addition, recirculation was barely evident at the outer radial positions.

Figure II-89 shows the temperature profile across the furnace at axial positions of 5.0, 77.5, and 152.5 cm for the axial gas nozzle, 12.5% of 570°F preheated excess air. The rapid rise in temperature between 0 and 3 cm for the 5-cm axial position confirms the high methane concentration found at the center line (Figure II-86). The rapid decrease

Figure II-81 shows a composite plot of CO, CO_2, CH_4, NO, and O_2. The methane concentration (curve M) was 10.63% at the burner center line, decreasing to about 0.25% at a 19-cm radial position. A very approximate integration under the methane curve showed that the average concentration was about 6%. Consequently, about 35% of the combustion can be assumed complete. Significant concentrations of O_2, CO_2, NO, and CO at the center line of the burner where the methane reading indicates essentially no combustion is occurring are probably caused by diffusion. The nitric oxide concentration (curve N) was 133 ppm at the center line, decreasing to 30 ppm at a 13-cm radial position and again increasing in a probable recirculation zone beyond 19 cm. Oxygen (curve O) was 3.46% at the center line, increasing to 13.55% near the perimeter of the burner-block opening. Nitric oxide (curve N) increased to only 77% of the 255 ppm of NO measured in the flue. However, measurements again were not taken out to the furnace wall. Data plots with greater resolution are given in Figures II-82 to II-86 and the raw data in Table II-11.

Data were taken at three axial positions for the axial gas nozzle. Figure II-87 shows composite chemical species profiles at a 77.5-cm axial position; Figure II-88 shows these same profiles for a 152.5-cm axial position. We found that essentially all the CH_4 (curve M) is consumed at 77.5 cm, leaving only CO (curve C) for further combustion. Nitric oxide (curve N) was essentially constant across the width of the burner; oxygen (curve O) was 4.76% at the center line, decreasing to about 3.9% at the 12.6-cm radial position. The oxygen at the center line increased from 4.76 to 5.10% between the 77.5-cm and 152.5-cm axial positions while lower amounts were measured at all radial positions other than the center line. Concurrently, CO and CH_4 decreased as expected while NO increased slightly in the postflame region. In addition, recirculation was barely evident at the outer radial positions.

Figure II-89 shows the temperature profile across the furnace at axial positions of 5.0, 77.5, and 152.5 cm for the axial gas nozzle, 12.5% of 570°F preheated excess air. The rapid rise in temperature between 0 and 3 cm for the 5-cm axial position confirms the high methane concentration found at the center line (Figure II-86). The rapid decrease

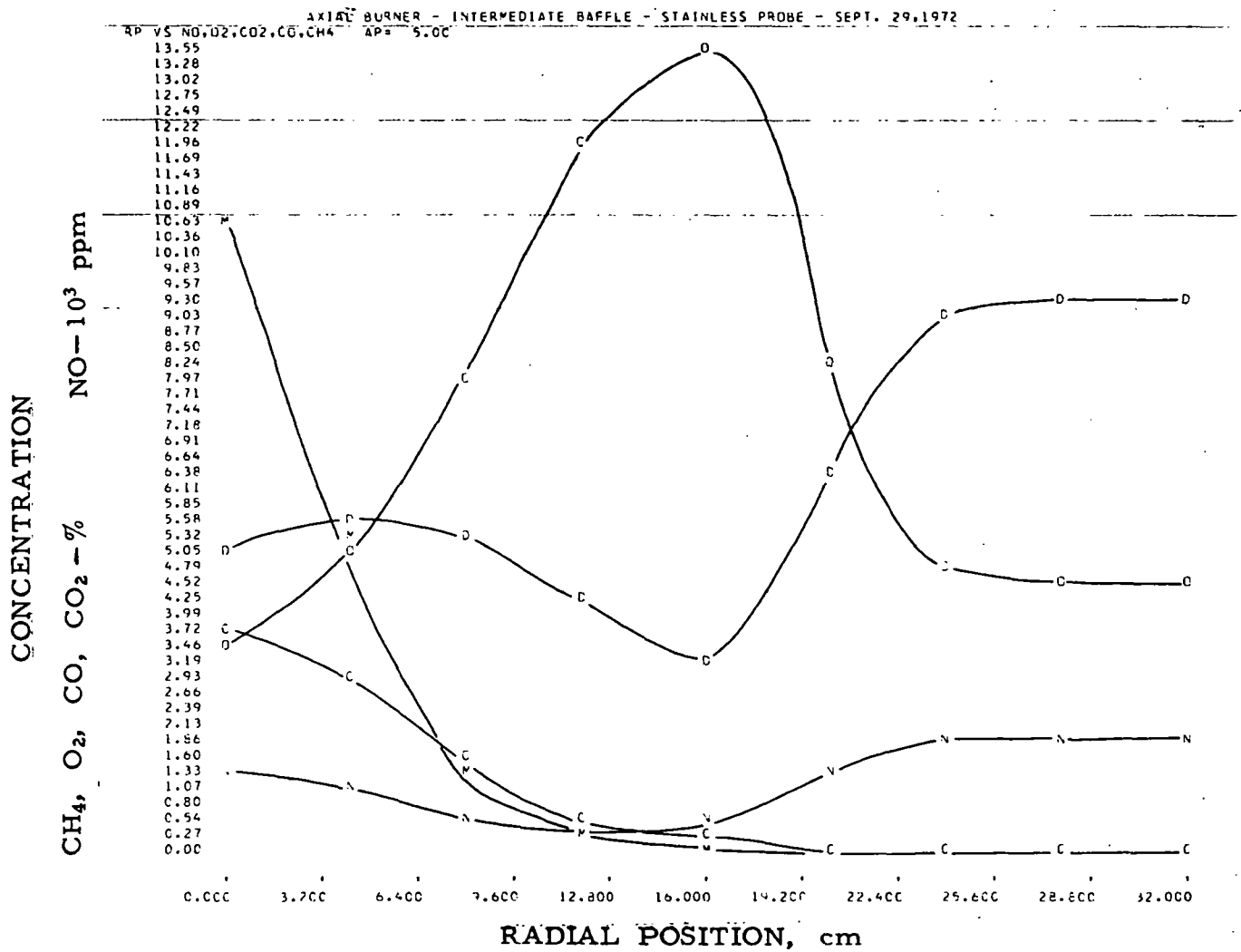

Figure II-81. COMPOSITE RADIAL PROFILES FOR NO, CO, CH_4, O_2, AND CO_2 WITH GAS INPUT OF 2147 CF/hr
(Intermediate-Flame Baffle With Radial Gas Nozzle at an Axial Position of 5.0 cm, Preheat Temperature of 570°F, 10% Excess Air, and Stainless-Steel Probe)

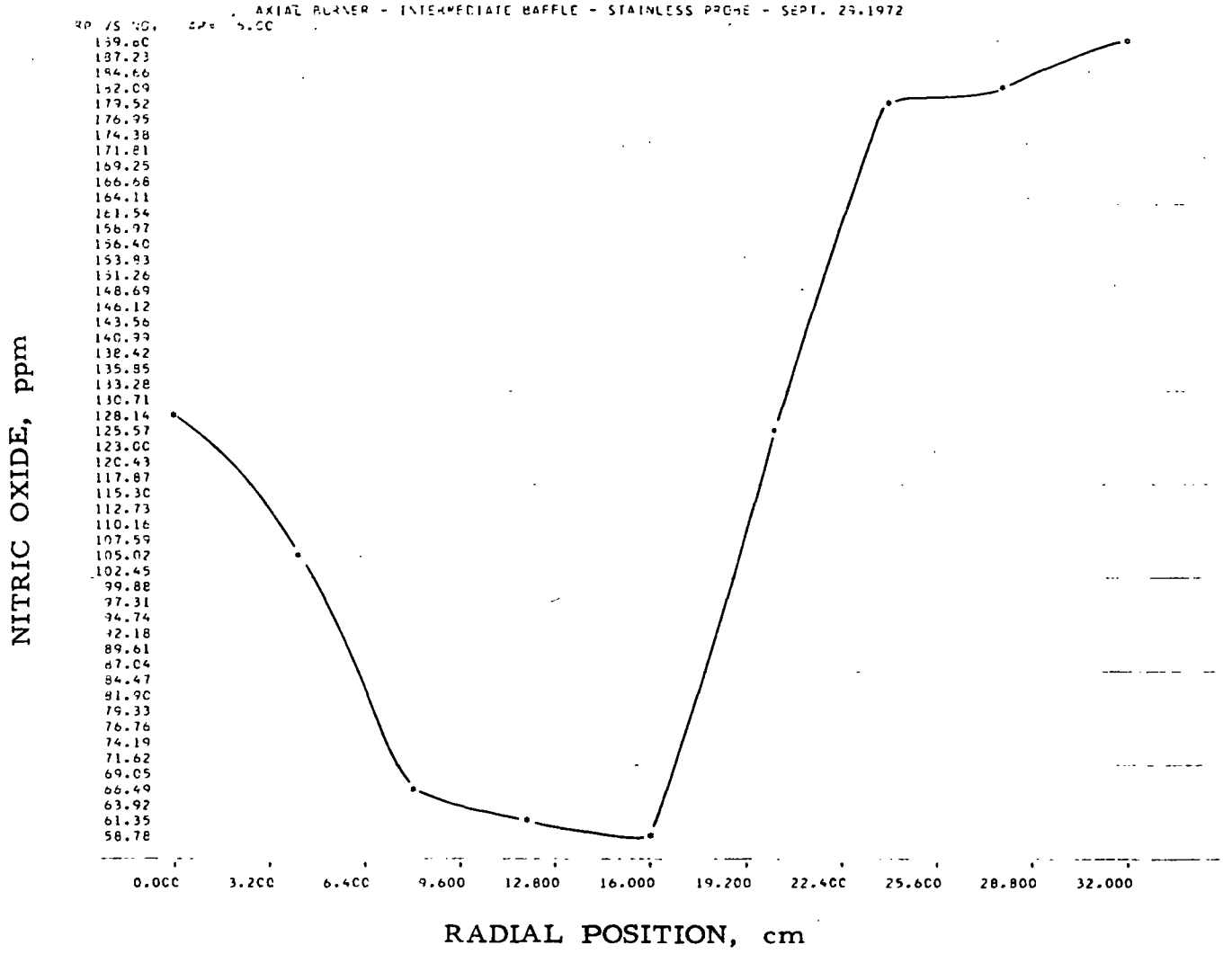

Figure II-82. RADIAL PROFILE FOR NO WITH GAS INPUT OF 2147 CF/hr (Intermediate-Flame Baffle With Axial Gas Nozzle at an Axial Position of 5.0 cm, Preheat Temperature of 570°F, 10% Excess Air, and Stainless-Steel Probe)

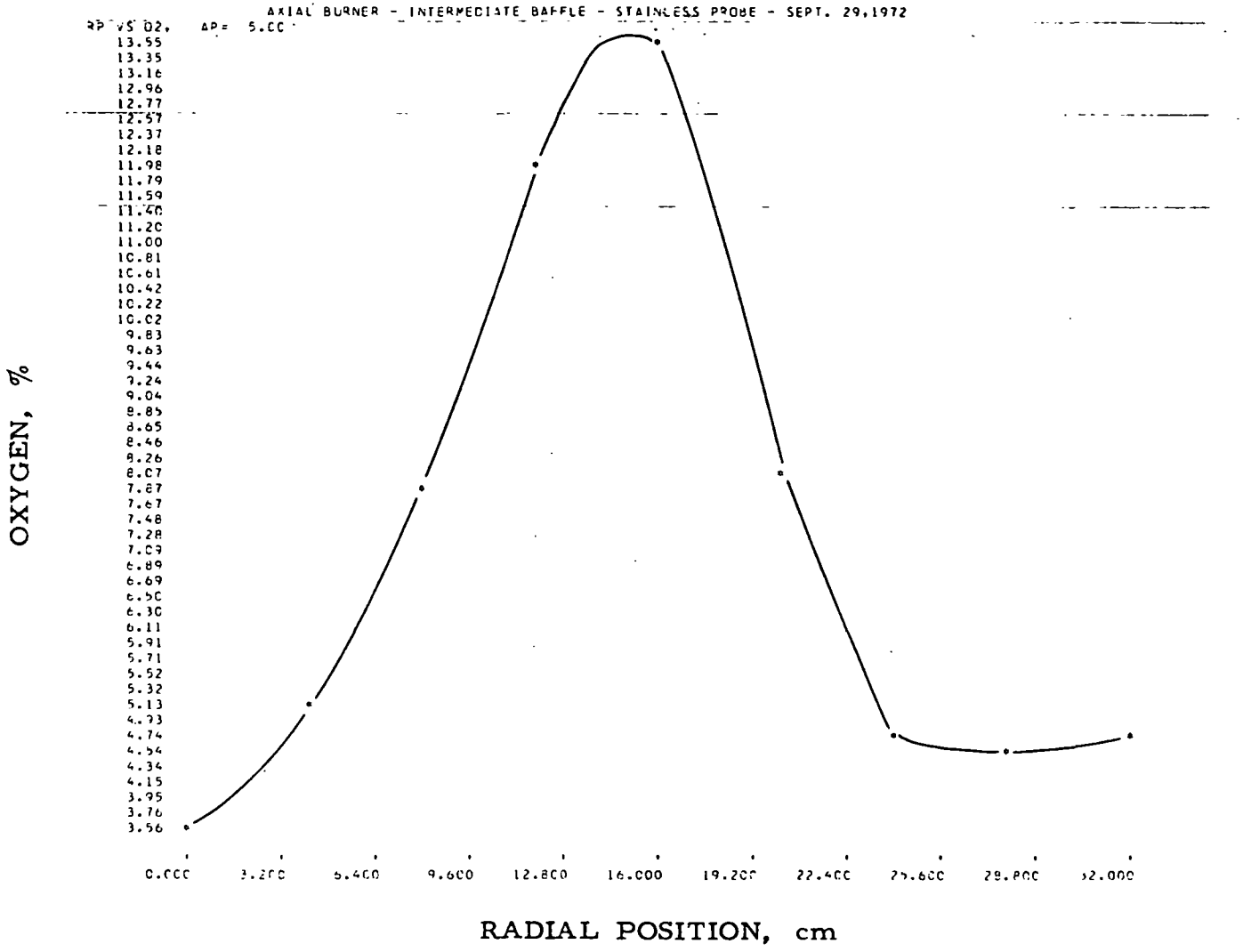

Figure II-83. RADIAL PROFILE FOR O_2 WITH GAS INPUT OF 2147 CF/hr (Intermediate-Flame Baffle With Axial Gas Nozzle at an Axial Position of 5.0 cm, Preheat Temperature of 570°F, 10% Excess Air, and Stainless-Steel Probe)

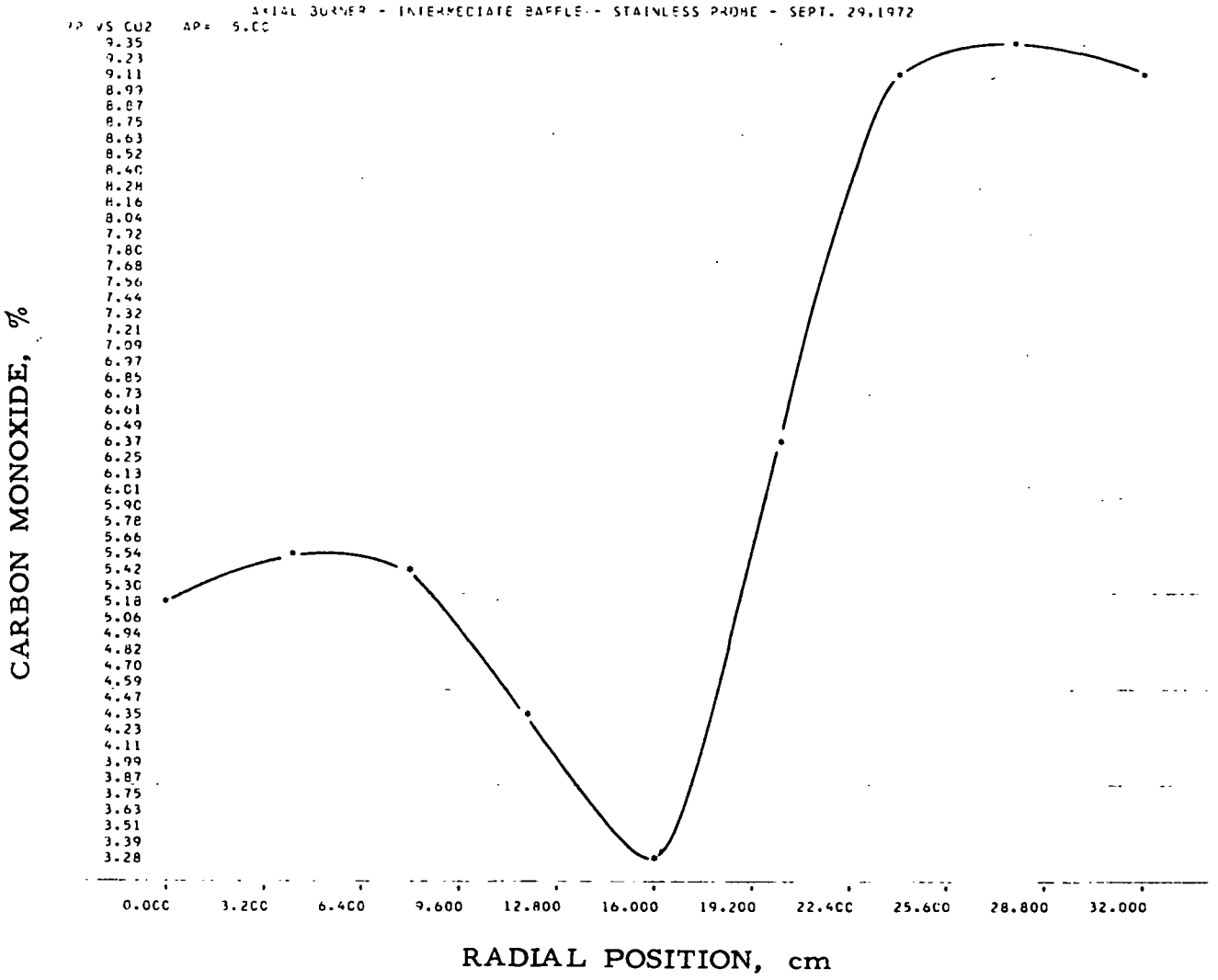

Figure II-84. RADIAL PROFILE FOR CO_2 WITH GAS INPUT OF 2147 CF/hr (Intermediate-Flame Baffle With Axial Gas Nozzle at an Axial Position of 5.0 cm, Preheat Temperature of 570°F, 10% Excess Air, and Stainless-Steel Probe)

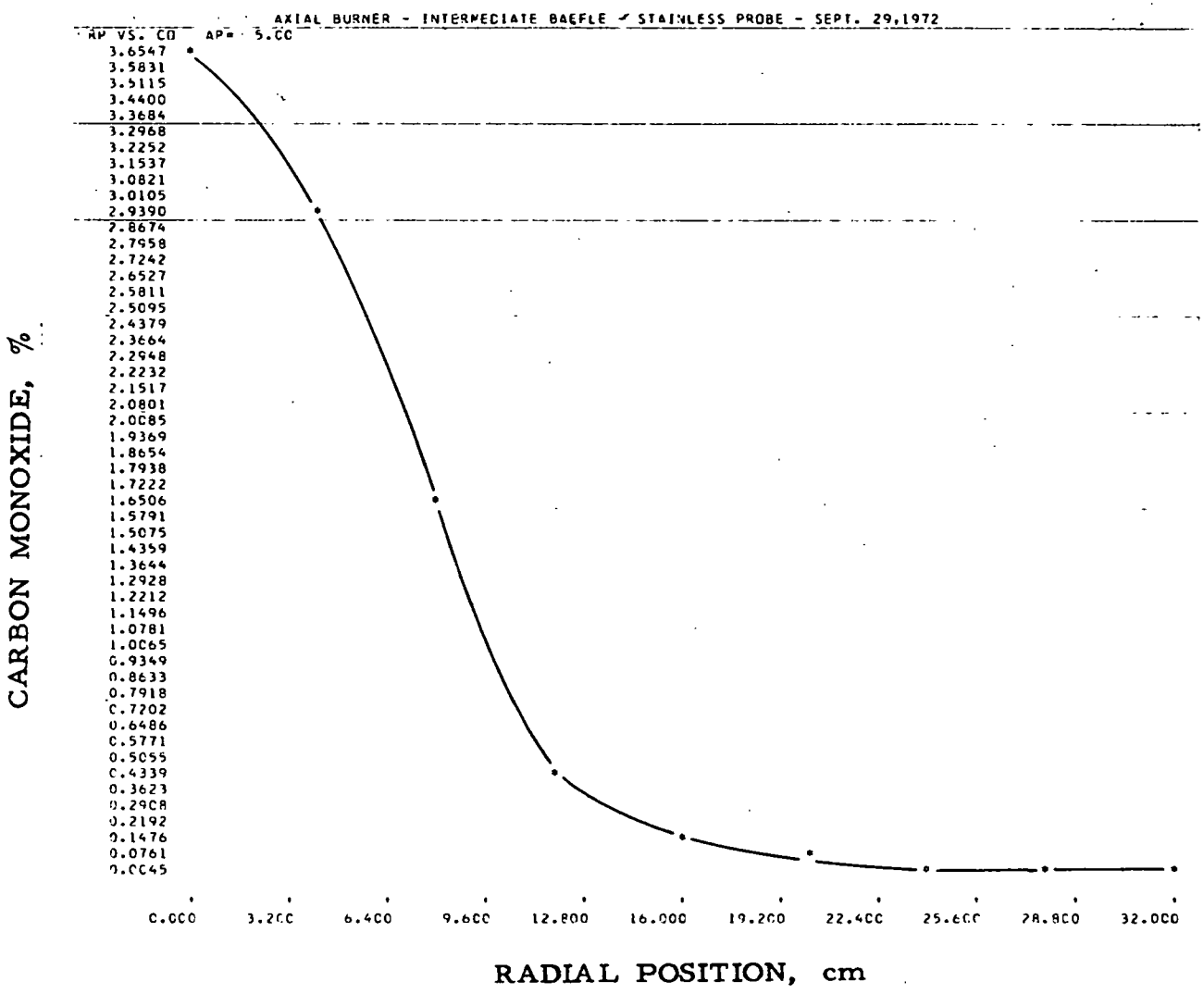

Figure II-85. RADIAL PROFILE FOR CO WITH GAS INPUT OF 2147 CF/hr (Intermediate-Flame Baffle With Axial Gas Nozzle at an Axial Position of 5.0 cm, Preheat Temperature of 570^{0}F, 10% Excess Air, and Stainless-Steel Probe)

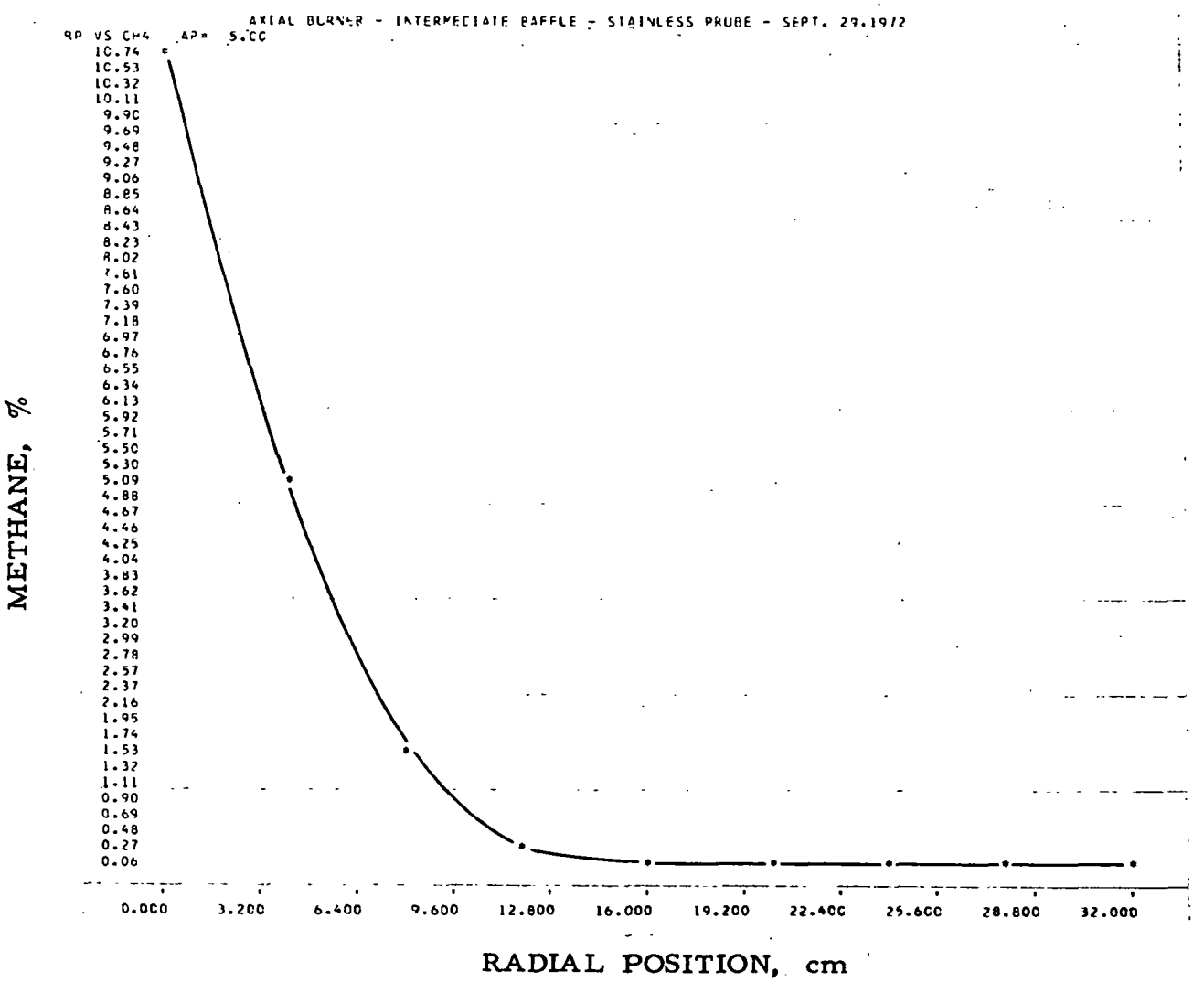

Figure II-86. RADIAL PROFILE FOR CH_4 WITH GAS INPUT OF 2147 CF/hr (Intermediate-Flame Baffle With Axial Gas Nozzle at an Axial Position of 5.0 cm Preheat Temperature of 570°F, 10% Excess Air, and Stainless-Steel Probe)

Table II-11. DATA OBTAINED WITH STAINLESS-STEEL PROBE USING AXIAL GAS NOZZLE AND AXIAL POSITION OF 5.0 cm

TRACER GAS STUDIES OF COMBUSTION BURNERS PROGRAM 2
AXIAL BURNER - INTERMEDIATE BAFFLE - STAINLESS PROBE - SEPT. 29,1972

INPUT GAS 2147 WALL TEMPERATURE 2570 PREHEAT TEMPERATURE 570
OUTPUT ANALYSIS
NITROGEN OXIDE 29.10 PERCENT ON RANGE 1, 255.52 PPM OXYGEN 2.63 PERCENT
CARBON DIOXIDE 82.50 PERCENT ON RANGE 1, 10.64 PERCENT
CARBON MONOXIDE 11.60 PERCENT ON RANGE 3, 0.004 PERCENT
METHANE C.CO PERCENT ON RANGE 3, 0.00 PERCENT

EXPERIMENTAL RESULTS

		NITROGEN OXIDE -NO			OXYGEN	CARBON DIOXIDE-CO2			CARBON MONOXIDE -CO			METHANE - CH4		
ΔP	RP	RANGE	X	Y	O2	RANGE	X	Y	RANGE	X	Y	RANGE	X	Y
5.0C	0.00	1	15.00	128.5	3.56	1	52.80	5.17	1	81.4C	3.654	1	68.30	10.73
5.0C	4.00	1	12.20	104.1	5.15	1	55.50	5.59	1	69.6C	2.9C5	1	41.90	5.18
5.0C	8.00	1	7.80	66.4	7.91	1	54.10	5.37	1	47.1C	1.683	1	15.5C	1.44
5.0C	12.00	1	7.10	60.4	11.92	1	47.00	4.31	1	16.0C	C.443	3	5.30	0.22
5.0C	16.00	1	6.90	58.7	13.55	1	39.10	3.27	2	9.00	C.147	3	1.40	0.06
5.0C	20.0C	1	14.60	125.0	8.16	1	60.50	6.41	2	3.80	C.C62	3	1.50	0.06
5.0C	24.00	1	20.70	179.0	4.7C	1	75.00	9.08	3	12.10	C.CC4	3	1.60	0.07
5.0C	28.00	1	21.10	182.6	4.48	1	76.30	9.34	3	10.9C	C.004	3	2.0C	0.08
5.0C	32.00	1	21.90	189.7	4.65	1	75.40	9.16	3	11.6C	C.C04	3	1.80	C.07

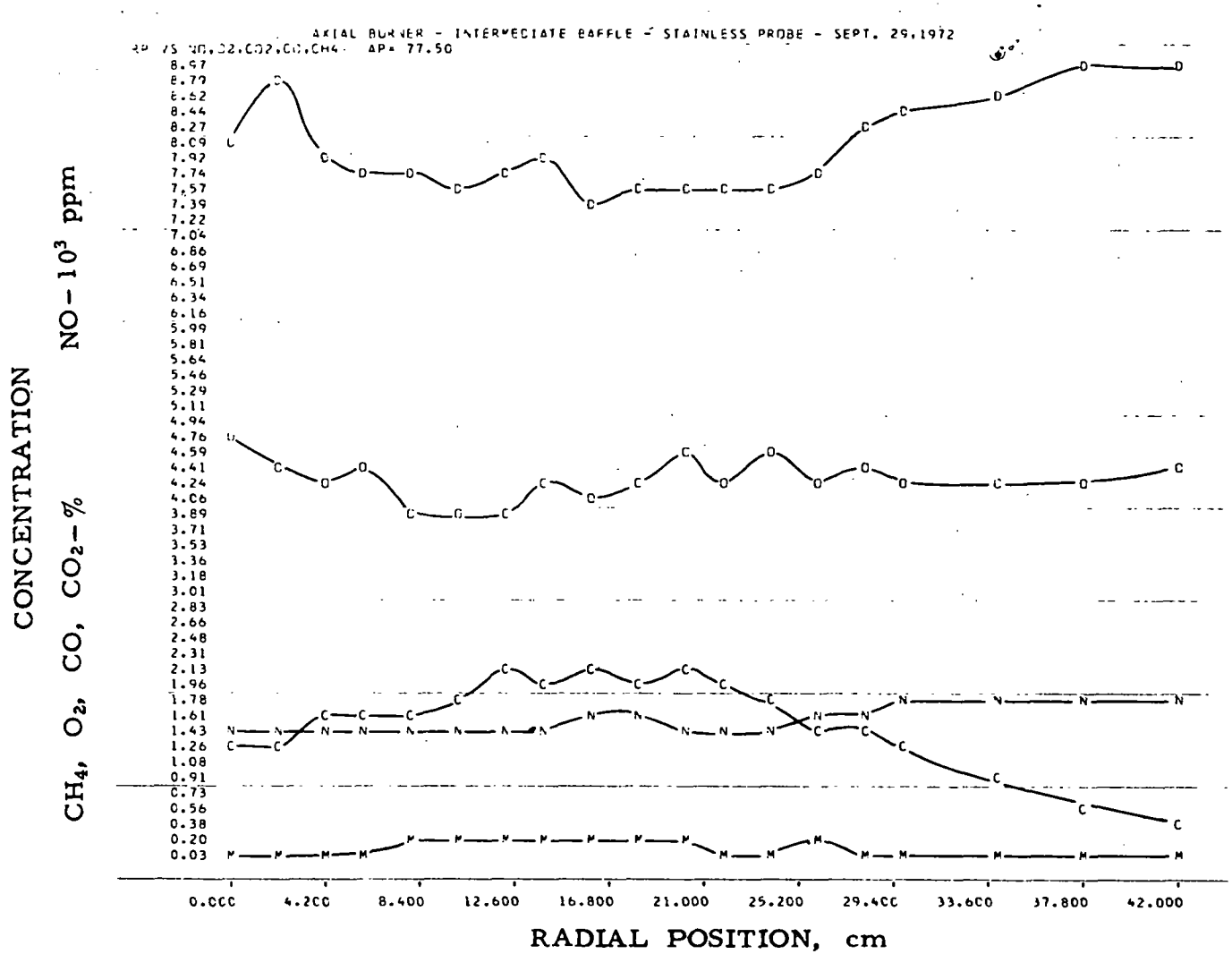

Figure II-87. COMPOSITE RADIAL PROFILES FOR NO, CO, CH_4, O_2 AND CO_2 WITH GAS INPUT OF 2147 CF/hr
(Intermediate-Flame Baffle With Axial Gas Nozzle at an Axial Position of 77.5 cm, Preheat Temperature of 570°F, 10% Excess Air, and Stainless-Steel Probe)

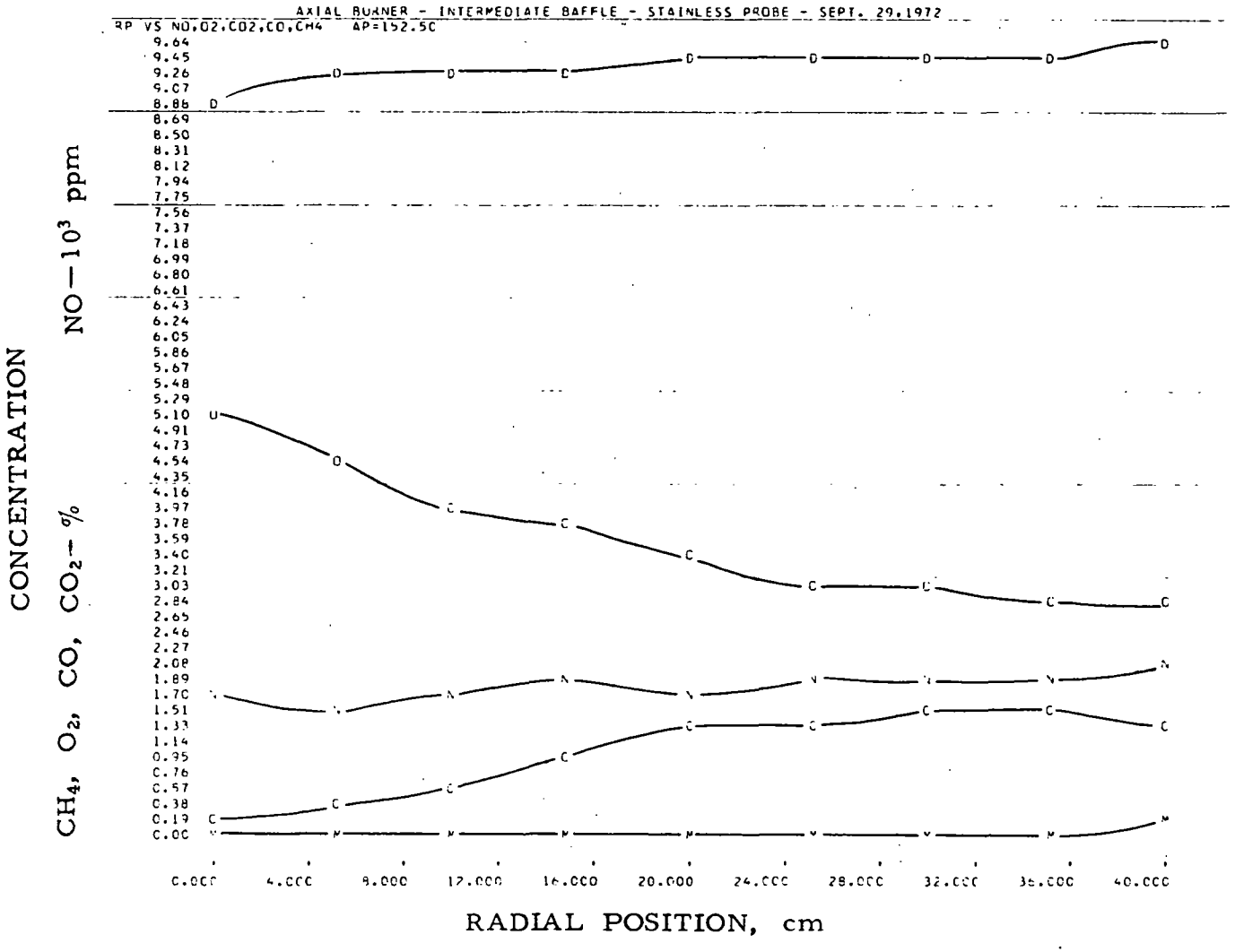

Figure II-88. COMPOSITE RADIAL PROFILES FOR NO, CO, CH_4, O_2 AND CO_2 WITH GAS INPUT OF 2147 CF/hr
(Intermediate Flame Baffle With Axial Gas Nozzle at an Axial Position of 152 cm, Preheat Temperature of 570°F, 10% Excess Air, and Stainless-Steel Probe)

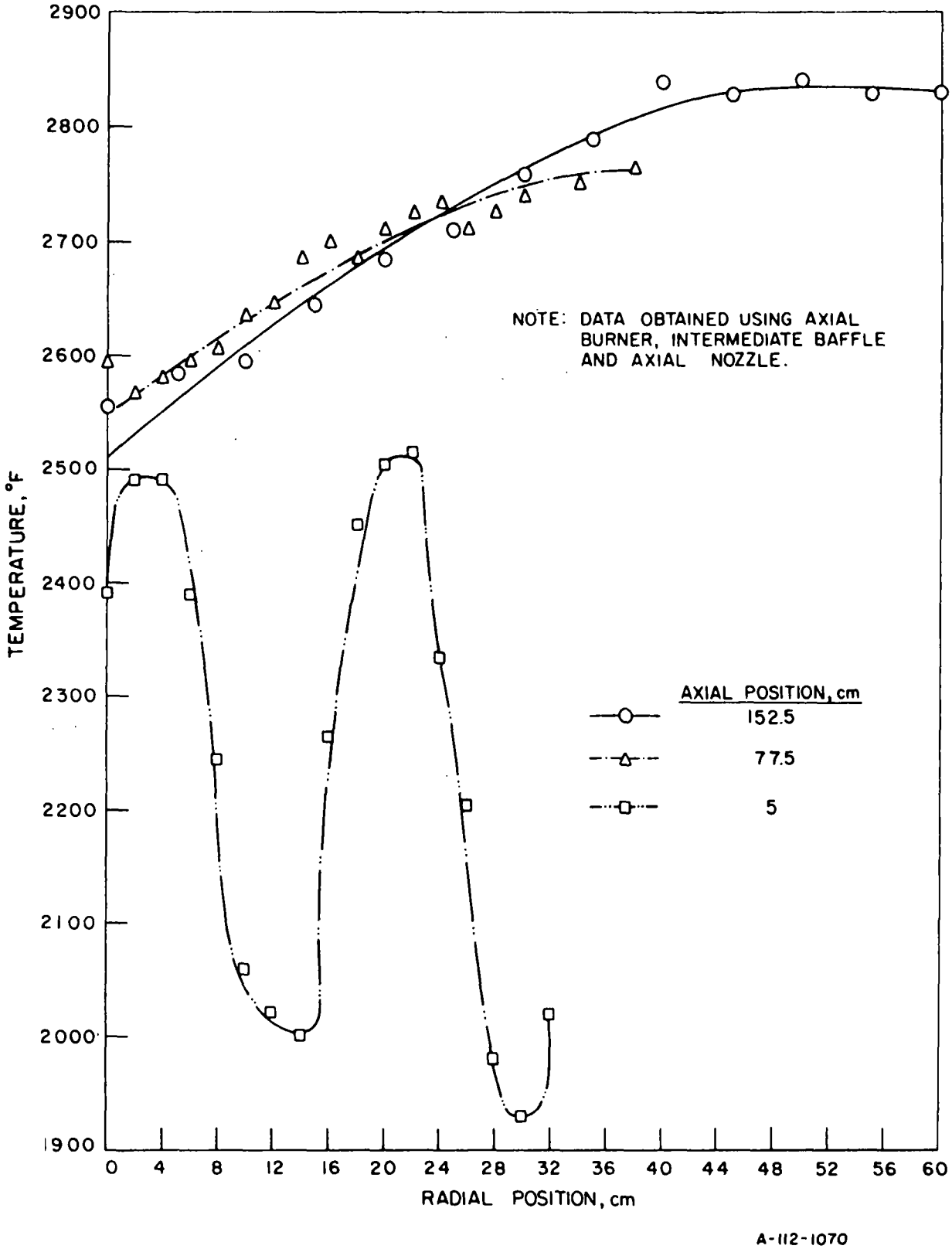

Figure II-89. TEMPERATURE PROFILE ACROSS FURNACE WITH GAS INPUT OF 2147 CF/hr AND AXIAL POSITIONS OF 5, 77.5, AND 152.5 cm (Excess O_2 of 2.9%, Wall Temperature of 2570°F, and Preheat of 570°F)

in temperature between 3 and 14 cm reflects the completeness of combustion toward the perimeter of the burner block. The second temperature peak at 21 cm (the outer edge of the burner-block opening) and the gas concentration profiles of Figure II-86 suggest the presence of hot recirculated flue products.

Data plots with greater resolution are given in Figures II-90 to II-99 and the raw data appear in Tables II-12 and II-13.

In-the-flame measurements of gas species were made using both stainless-steel and quartz-lined fast-quench sampling probes. We concluded from a comparison of the data that either probe was suitable for measuring NO. However, we found an unexplainable change in oxygen concentration with sampling time using the quartz probe. Therefore, further measurements were made using the stainless-steel type.

Figures II-100 and II-101 show the gas sampling data collected with the quartz probe from the intermediate-flame baffle burner (axial gas nozzle) at axial positions of 5.0 cm and 77.5 cm, respectively. In Figure II-102, these data for nitric oxide are compared with the data taken with a stainless-steel probe (Figures II-81 and II-87). The two sets of data agree to within 17 ppm or about 10%. A portion of this difference is caused by an error in resetting the furnace, which was shut down between runs. The data also show that neither of the probes measured consistently higher or lower than the other. Figures II-103 to II-112 show the data of Figures II-100 and II-101 with greater resolution. Tables II-14 and II-15 show the raw data.

B. Short-Flame-Length Ported Baffle Burner

1. Burner Design

The test burner used for this study was identical to that used for the intermediate-flame-length one except for the angle of the ports in the baffle. (See Figure II-57.) This burner was also studied with both the axial and radial gas nozzles. (See Figure II-58.)

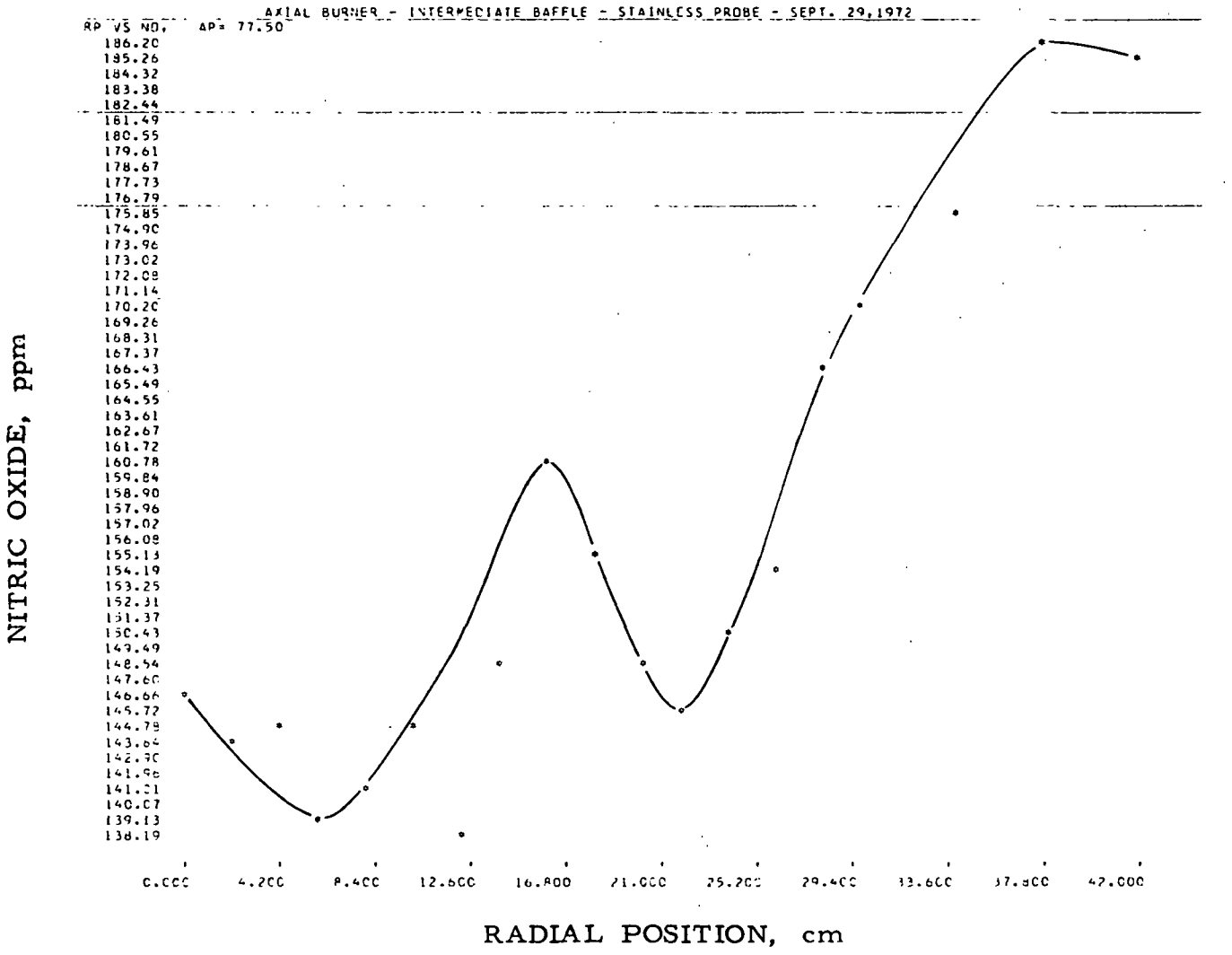

Figure II-90. RADIAL PROFILE FOR NO WITH GAS INPUT OF 2147 CF/hr (Intermediate Flame Baffle With Axial Gas Nozzle at an Axial Position of 77.5 cm, Preheat Temperature of 570^{0}F, 10% Excess Air, and Stainless-Steel Probe)

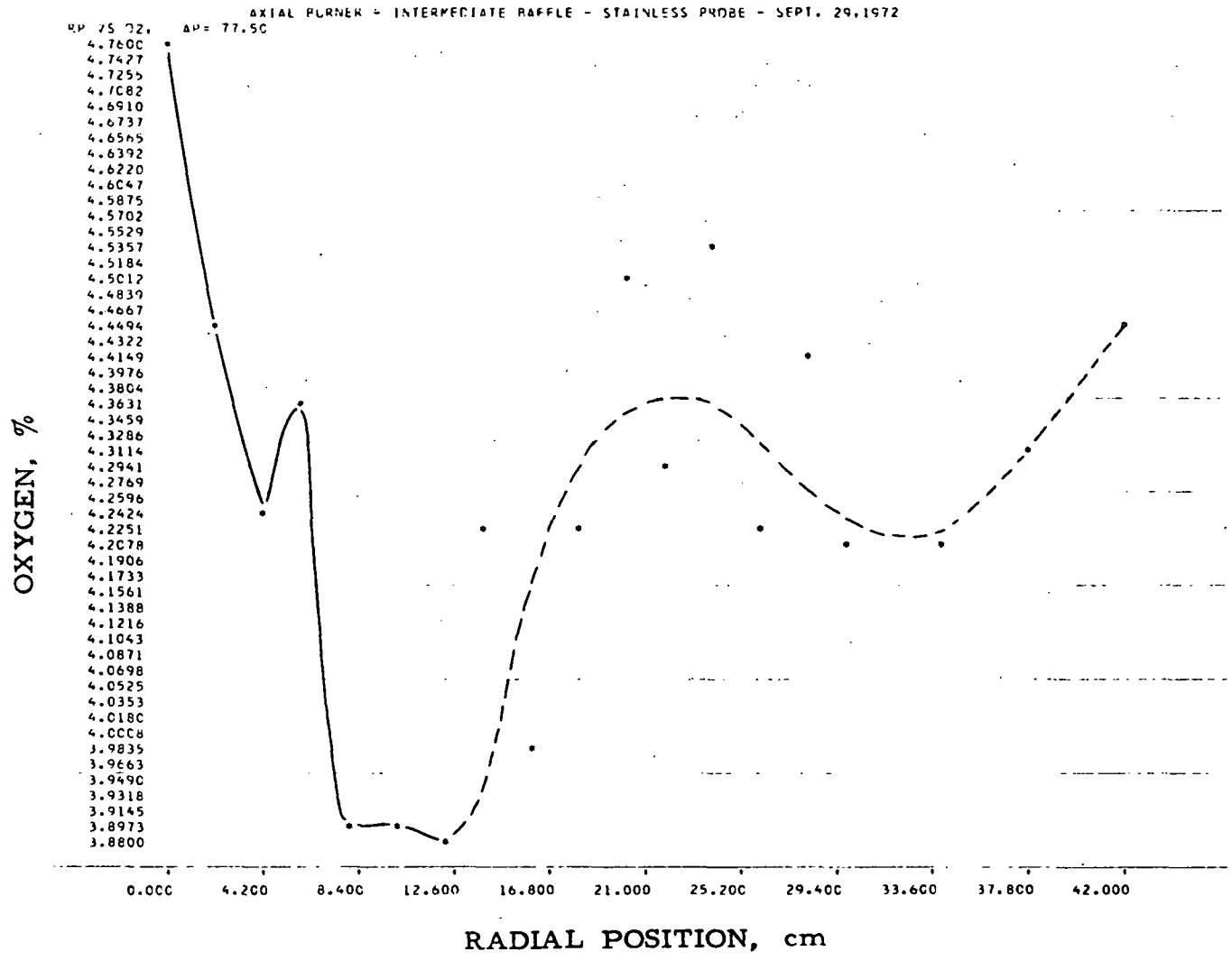

Figure II-91. RADIAL PROFILE FOR O_2 WITH GAS INPUT OF 2147 CF/hr (Intermediate-Flame Baffle With Axial Gas Nozzle at an Axial Position of 77.5 cm, Preheat Temperature of 570°F, 10% Excess Air, and Stainless-Steel Probe)

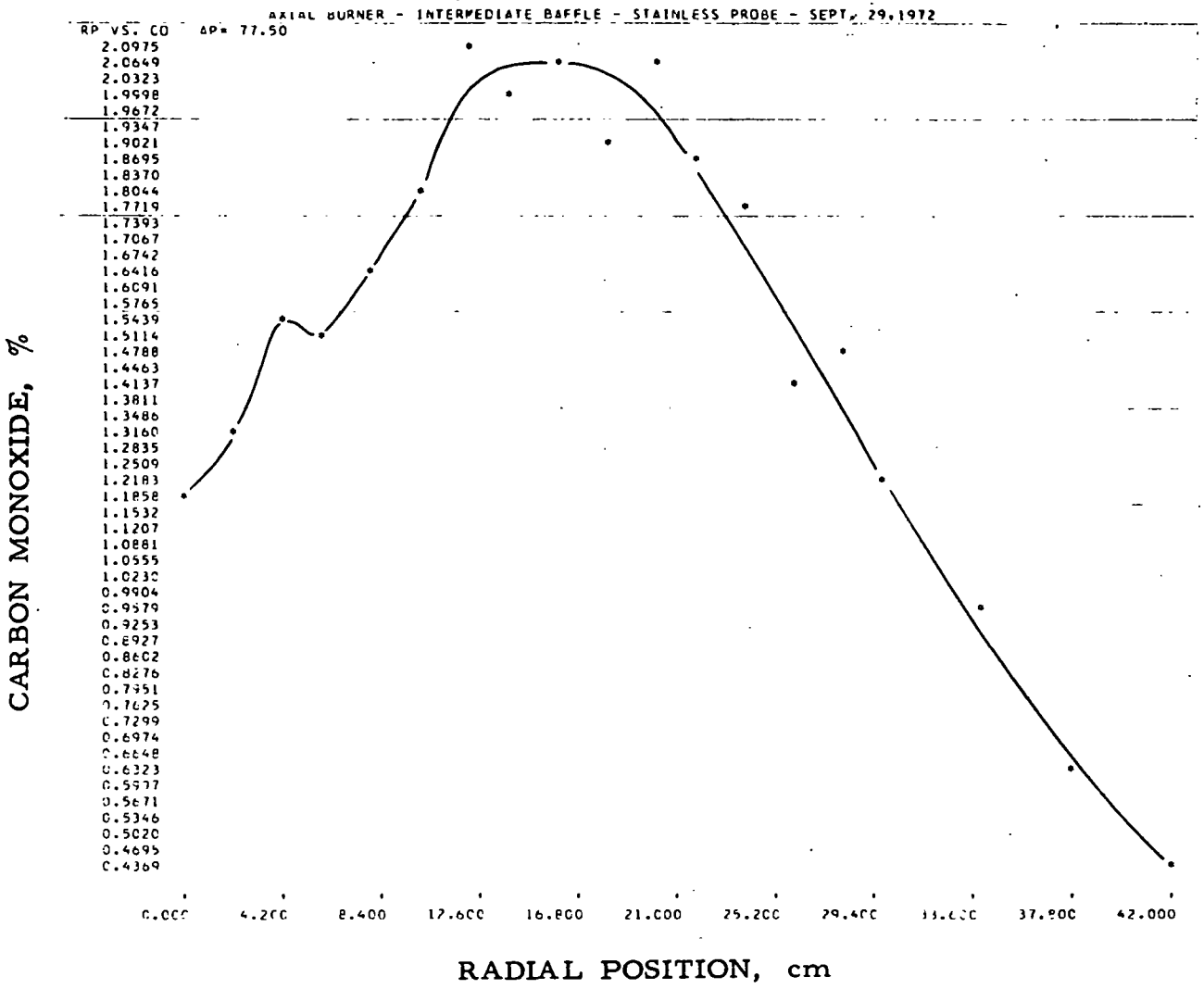

Figure II-92. RADIAL PROFILE FOR CO WITH GAS INPUT OF 2147 CF/hr (Intermediate-Flame Baffle With Axial Gas Nozzle at an Axial Position of 77.5 cm, Preheat Temperature of 570°F, 10% Excess Air, and Stainless-Steel Probe)

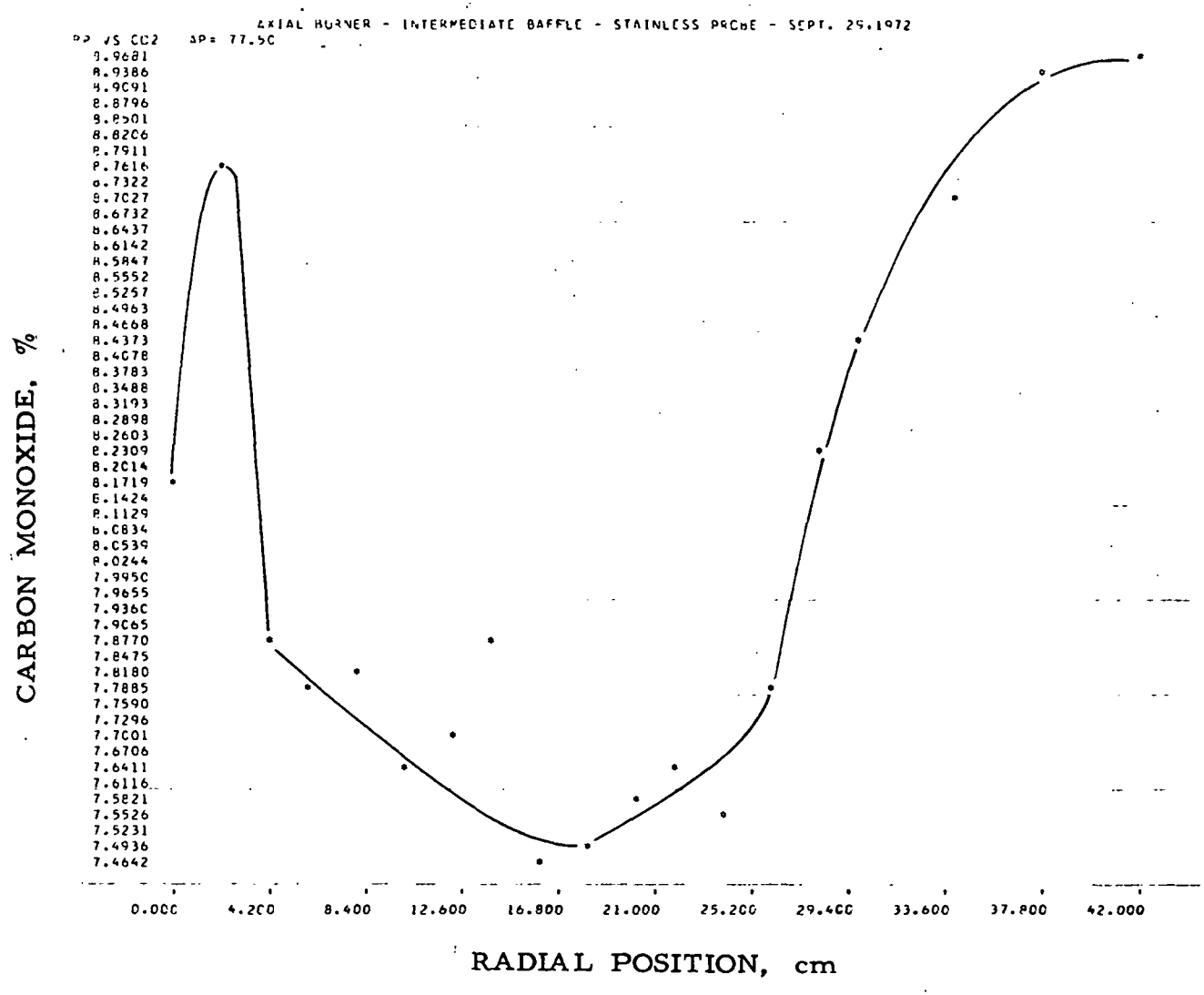

Figure II-93. RADIAL PROFILE FOR CO_2 WITH GAS INPUT OF 2147 CF/hr (Intermediate-Flame Baffle With Axial Gas Nozzle at an Axial Position of 77.5 cm, Preheat Temperature of 570°F, 10% Excess Air, and Stainless-Steel Probe)

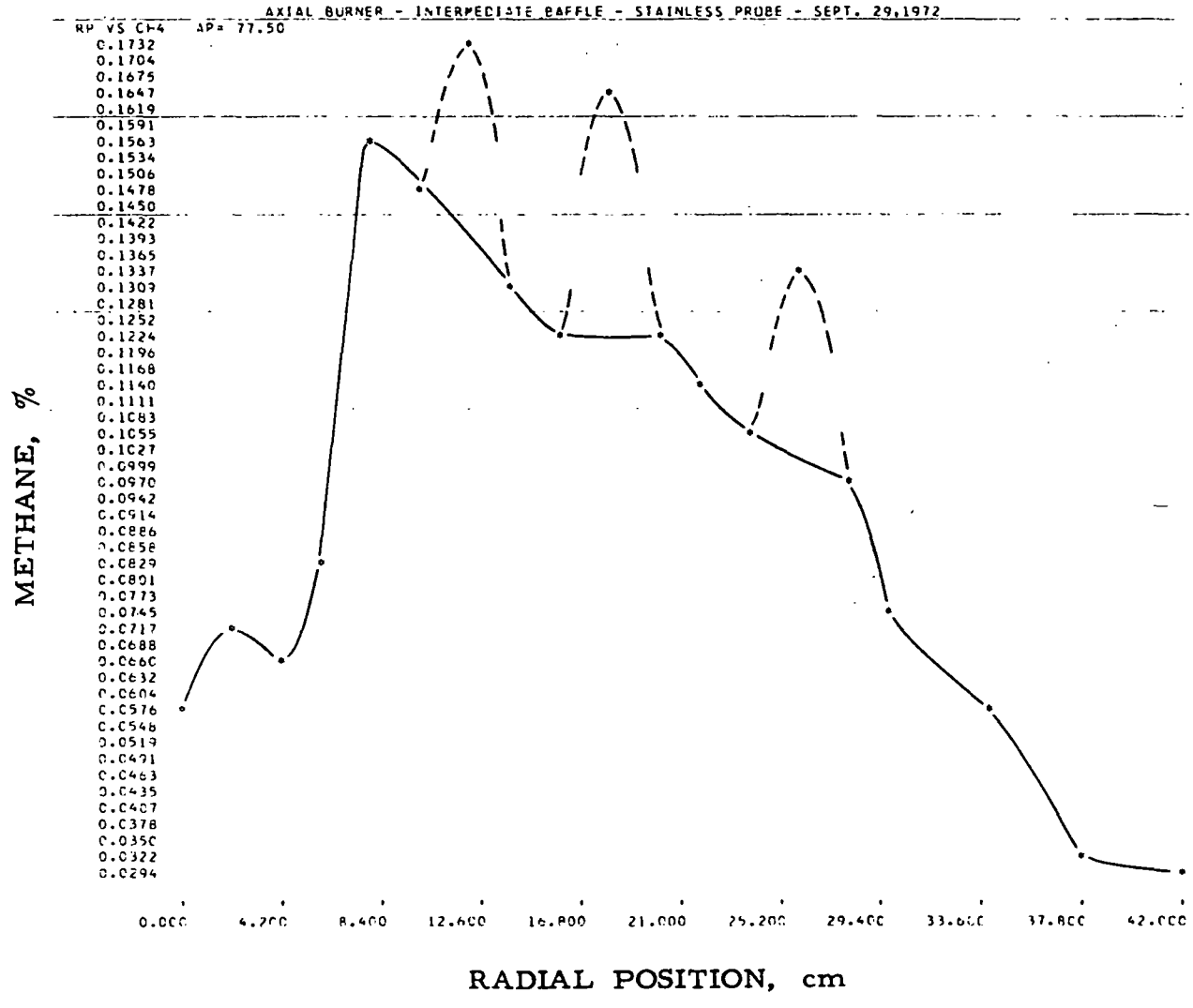

Figure II-94. RADIAL PROFILE FOR CH_4 WITH GAS INPUT OF 2147 CF/hr (Intermediate-Flame Baffle With Axial Gas Nozzle at an Axial Position of 77.5 cm, Preheat Temperature of 570°F, 10% Excess Air, and Stainless-Steel Probe)

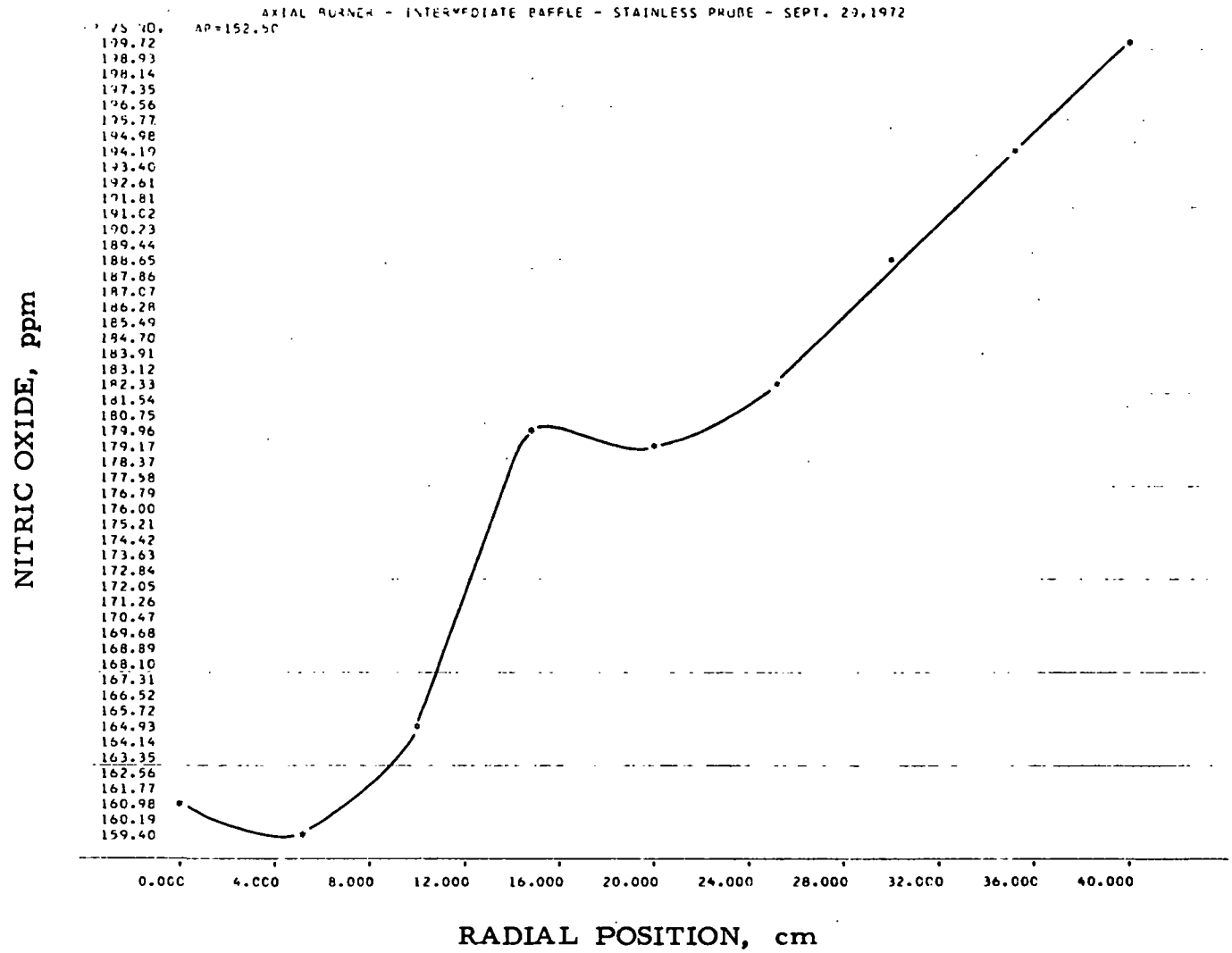

Figure II-95. RADIAL PROFILE FOR NO WITH GAS INPUT OF 2147 CF/hr (Intermediate-Flame Baffle With Axial Gas Nozzle at an Axial Position of 152 cm, Preheat Temperature of 570°F, 10% Excess Air, and Stainless-Steel Probe)

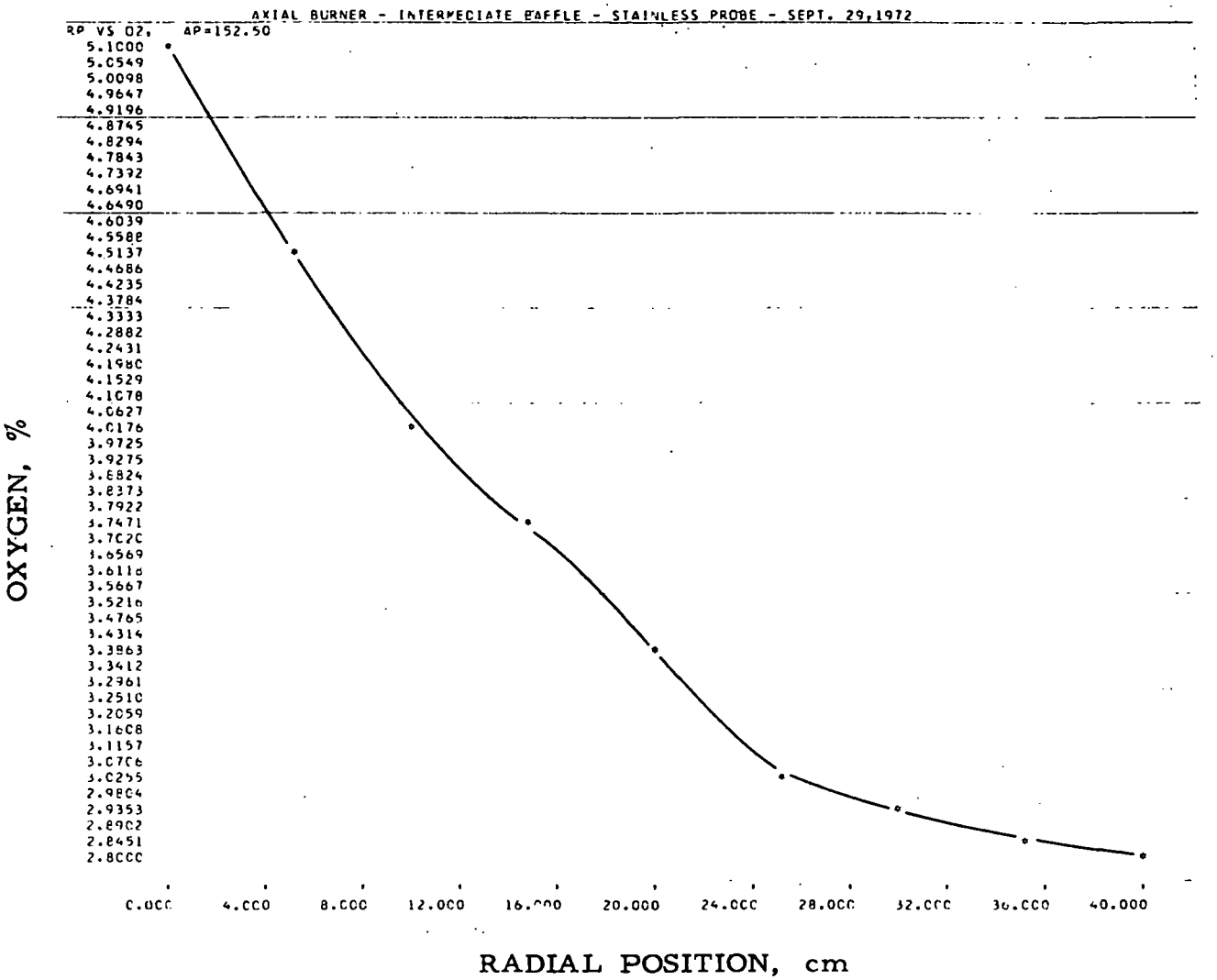

Figure II-96. RADIAL PROFILE FOR O_2 WITH GAS INPUT OF 2147 CF/hr (Intermediate-Flame Baffle With Axial Gas Nozzle at an Axial Position of 152 cm, Preheat Temperature of 570^{0}F, 10% Excess Air, and Stainless-Steel Probe)

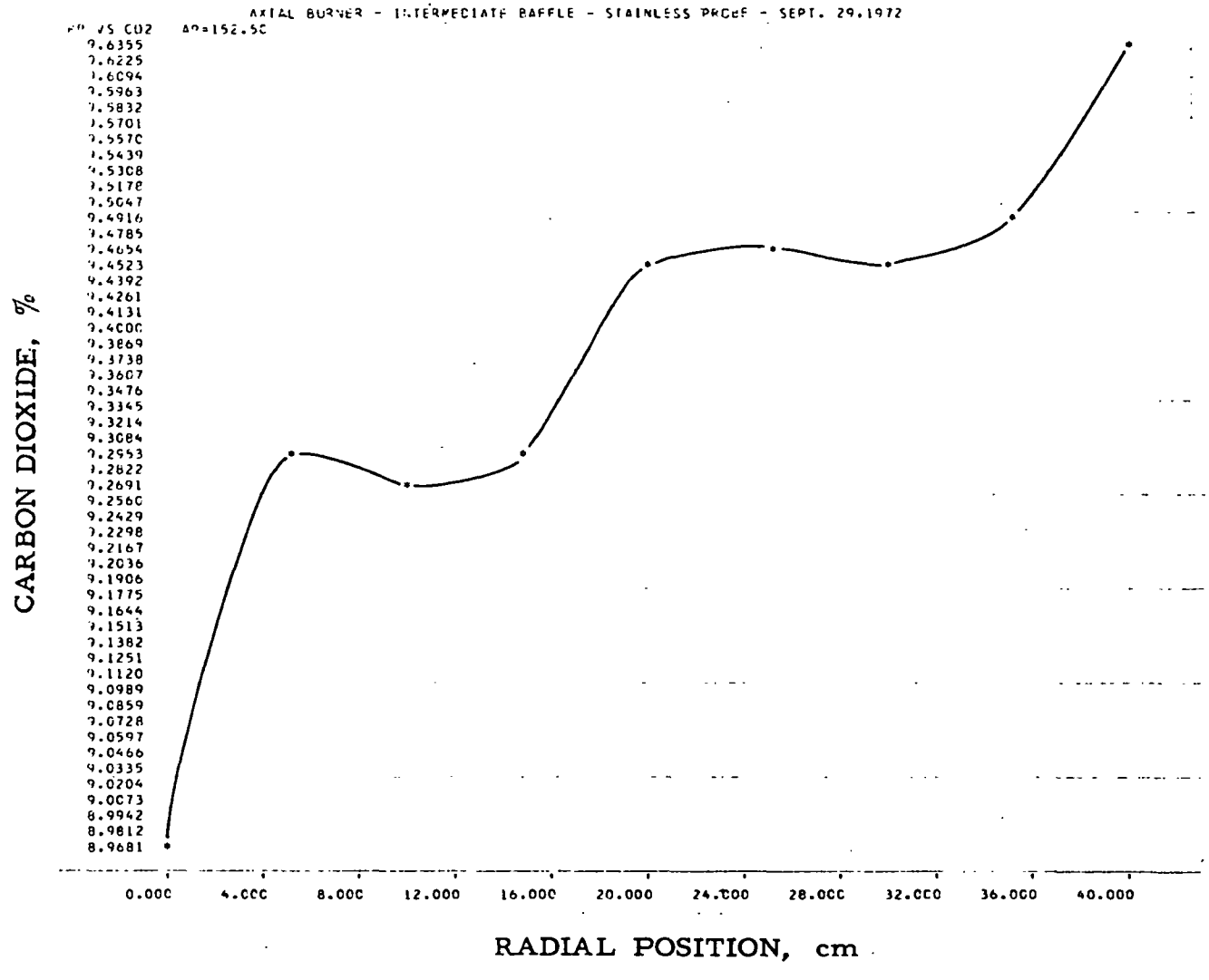

Figure II-97. RADIAL PROFILE FOR CO_2 WITH GAS INPUT OF 2147 CF/hr (Intermediate-Flame Baffle With Axial Gas Nozzle at an Axial Position of 152 cm, Preheat Temperature of 570°F, 10% Excess Air, and Stainless-Steel Probe)

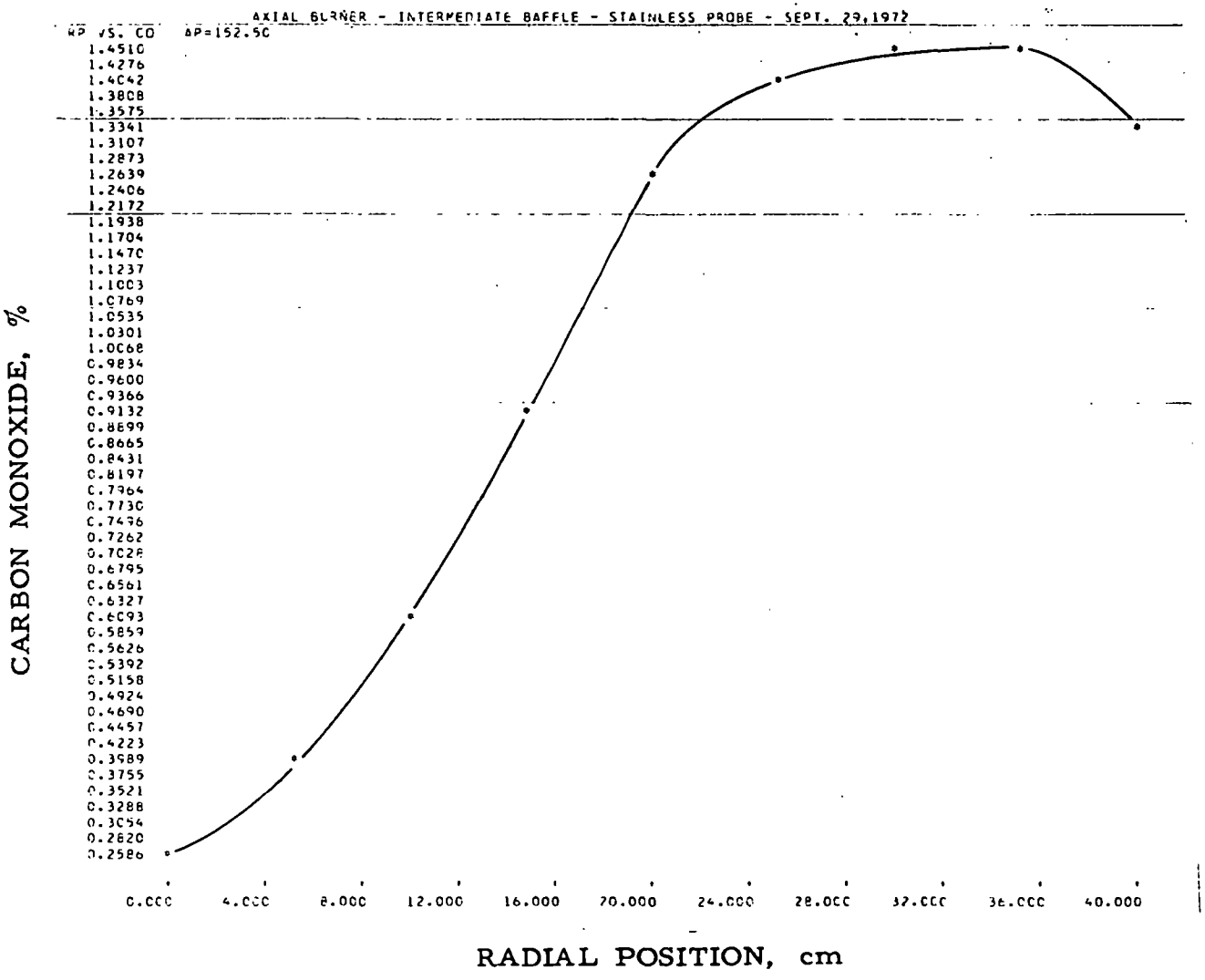

Figure II-98. RADIAL PROFILE FOR CO WITH GAS INPUT OF 2147 CF/hr (Intermediate-Flame Baffle With Axial Gas Nozzle at an Axial Position of 152 cm, Preheat Temperature of 570°F, 10% Excess Air, and Stainless-Steel Probe)

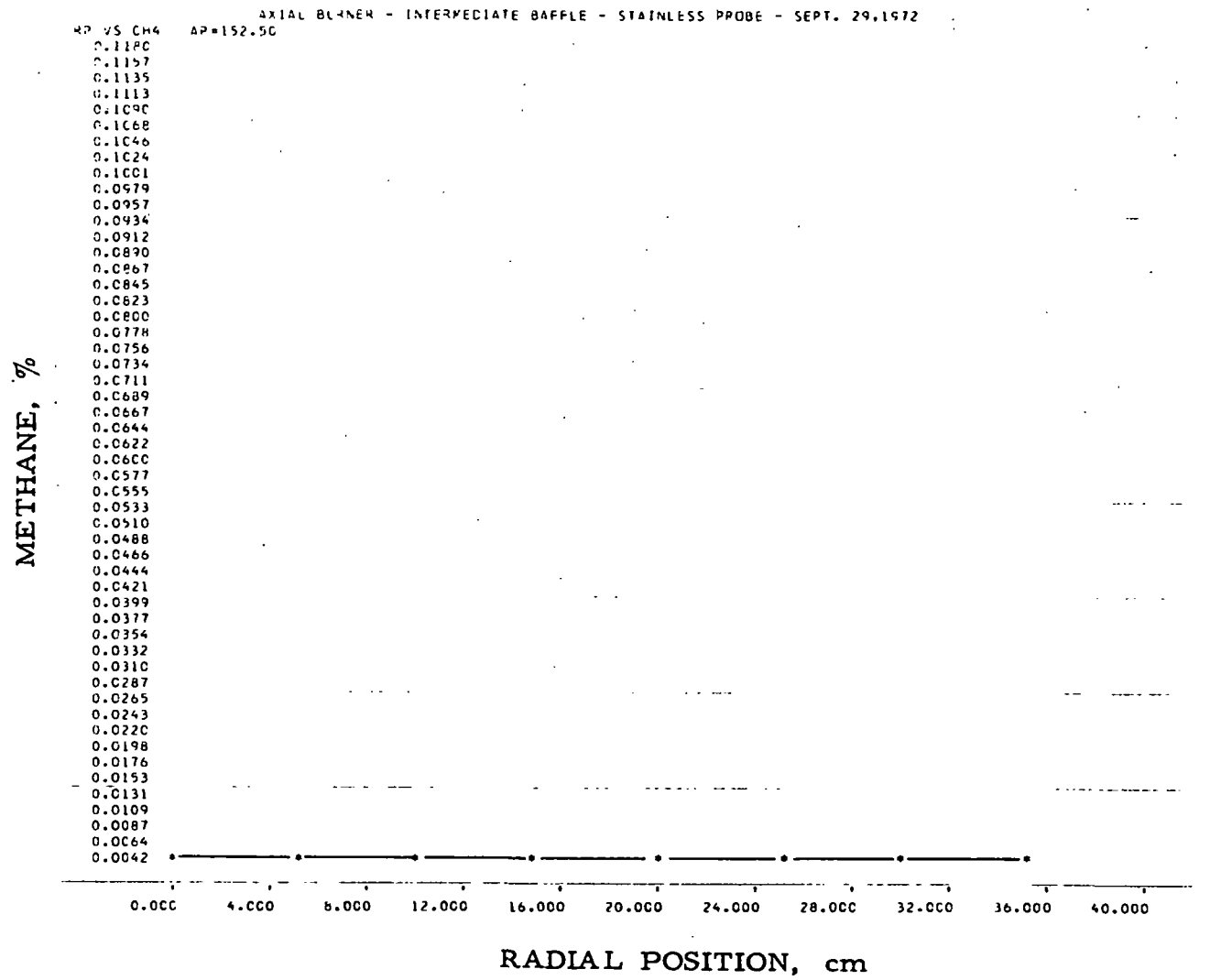

Figure II-99. RADIAL PROFILE FOR CH_4 WITH GAS INPUT OF 2147 CF/hr (Intermediate-Flame Baffle With Axial Gas Nozzle at an Axial Position of 152 cm, Preheat Temperature of 570°F, 10% Excess Air, and Stainless-Steel Probe)

Table II-12. DATA OBTAINED WITH STAINLESS-STEEL PROBE USING AXIAL GAS NOZZLE AND AXIAL POSITION OF 77.5 cm

TRACER GAS STUDIES OF COMBUSTION BURNERS PROGRAM 2
AXIAL BURNER - INTERMEDIATE BAFFLE - STAINLESS PROBE - SEPT. 29,1972

INPUT GAS 2147 WALL TEMPERATURE 2570 PREHEAT TEMPERATURE 57C
OUTPUT ANALYSIS
NITROGEN OXIDE 29.10 PERCENT ON RANGE 1, 255.52 PPM OXYGEN 2.63 PERCENT
CARBON DIOXIDE 82.50 PERCENT ON RANGE 1, 10.64 PERCENT
CARBON MONOXIDE 11.60 PERCENT ON RANGE 3, 0.004 PERCENT
METHANE 0.00 PERCENT ON RANGE 3, 0.00 PERCENT

EXPERIMENTAL RESULTS

		NITROGEN OXIDE -NO			OXYGEN	CARBON DIOXIDE-CO2			CARBON MONOXIDE -CO			METHANE - CH4		
AP	RP	RANGE	X	Y	O2	RANGE	X	Y	RANGE	X	Y	RANGE	X	Y
77.50	0.00	1	17.10	147.0	4.76	1	70.30	8.17	2	63.60	1.174	3	1.30	0.05
77.50	2.00	1	16.70	143.4	4.45	1	73.30	8.75	2	70.10	1.313	3	1.60	0.07
77.50	4.00	1	16.90	145.2	4.24	1	68.80	7.88	2	80.80	1.549	3	1.50	0.06
77.50	6.00	1	16.20	139.0	4.36	1	68.30	7.79	1	43.70	1.522	3	1.90	0.08
77.50	8.00	1	16.40	140.8	3.89	1	68.40	7.81	1	46.10	1.635	3	3.60	0.15
77.50	10.00	1	16.80	144.3	3.90	1	67.40	7.62	1	49.40	1.796	3	3.40	0.14
77.50	12.00	1	16.10	138.1	3.88	1	67.80	7.70	1	55.30	2.097	3	4.00	0.17
77.50	14.00	1	17.30	148.7	4.22	1	68.70	7.86	1	53.30	1.993	3	3.00	0.13
77.50	16.00	1	18.70	161.1	3.99	1	66.50	7.46	1	54.50	2.055	3	2.80	0.12
77.50	18.00	1	18.00	154.9	4.22	1	66.70	7.50	1	51.80	1.916	3	3.60	0.16
77.50	20.00	1	17.30	148.7	4.50	1	67.10	7.57	1	54.90	2.076	3	2.80	0.12
77.50	22.00	1	17.00	146.1	4.29	1	67.40	7.62	1	51.10	1.881	3	2.60	0.11
77.50	24.00	1	17.50	150.5	4.53	1	67.00	7.55	1	49.10	1.781	3	2.40	0.10
77.50	26.00	1	17.90	154.0	4.23	1	68.30	7.79	1	41.20	1.408	3	3.10	0.13
77.50	28.00	1	19.30	166.5	4.42	1	70.60	8.22	1	43.00	1.490	3	2.20	0.09
77.50	30.00	1	19.70	170.0	4.21	1	71.70	8.43	1	36.90	1.219	3	1.70	0.07
77.50	34.00	1	20.30	175.4	4.21	1	73.00	8.69	1	30.50	0.956	3	1.30	0.05
77.50	38.00	1	21.50	186.2	4.32	1	74.20	8.92	1	21.40	0.621	3	0.70	0.03
77.50	42.00	1	21.40	185.3	4.45	1	74.40	8.96	1	15.80	0.436	3	0.60	0.02

Table II-13. DATA OBTAINED WITH STAINLESS STEEL PROBE USING AXIAL GAS NOZZLE AND AXIAL POSITION OF 152.5 cm

TRACER GAS STUDIES OF COMBUSTION BURNERS PROGRAM 2
AXIAL BURNER - INTERMEDIATE BAFFLE - STAINLESS PROBE - SEPT. 29,1972

INPUT GAS 2147 WALL TEMPERATURE 2570 PREHEAT TEMPERATURE 570

OUTPUT ANALYSIS

NITROGEN OXIDE	29.10 PERCENT	ON RANGE 1,	255.52 PPM	OXYGEN	2.63 PERCENT
CARBON DIOXIDE	82.50 PERCENT	ON RANGE 1,	10.64 PERCENT		
CARBON MONOXIDE	11.60 PERCENT	ON RANGE 3,	0.004 PERCENT		
METHANE	C.CO PERCENT	ON RANGE 3,	0.00 PERCENT		

EXPERIMENTAL RESULTS

		NITROGEN OXIDE -NO			OXYGEN	CARBON DIOXIDE-CO2			CARBON MONOXICE -CO			METHANE - CH4		
ΔP	RP	RANGE	X	Y	C2	RANGE	X	Y	RANGE	X	Y	RANGE	X	Y
152.50	0.00	1	18.70	161.1	5.10	1	74.40	8.96	2	15.60	C.258	3	C.00	0.00
152.50	5.00	1	18.50	159.3	4.53	1	76.00	9.28	2	23.20	C.391	3	C.00	0.00
152.50	10.00	1	19.10	164.7	4.02	1	75.90	9.26	2	34.90	C.604	3	C.00	0.00
152.50	15.00	1	20.80	179.9	3.75	1	76.00	9.28	2	50.60	0.907	3	C.00	0.00
152.50	20.00	1	20.70	179.0	3.37	1	76.80	9.45	2	67.30	1.253	3	C.00	0.00
152.50	25.00	1	21.10	182.6	3.03	1	76.90	9.47	2	74.20	1.402	3	C.00	0.00
152.50	30.00	1	21.80	188.8	2.95	1	76.80	9.45	2	76.00	1.442	3	0.00	0.00
152.50	35.00	1	22.40	194.3	2.84	1	77.00	9.49	2	76.40	1.450	3	C.00	0.00
152.50	40.00	1	23.00	199.7	2.80	1	77.70	9.63	2	70.70	1.326	3	2.70	0.11

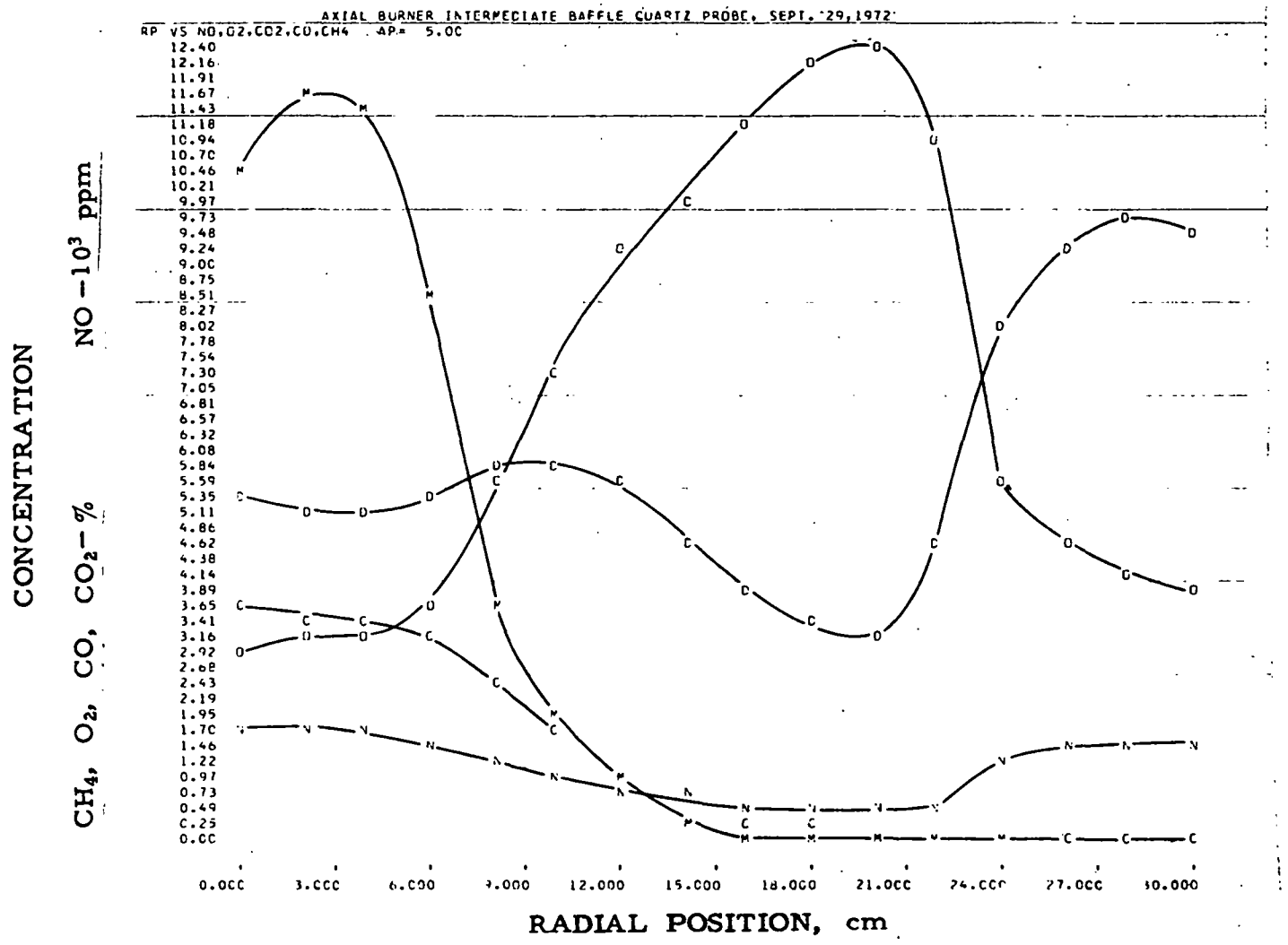

Figure II-100. COMPOSITE RADIAL PROFILES FOR NO, CO, CH_4, O_2, AND CO_2 WITH GAS INPUT OF 2147 CF/hr (Intermediate-Flame Baffle With Axial Gas Nozzle at an Axial Position of 5.0 cm, Preheat Temperature of 570°F, 10% Excess Air, and Quartz Probe)

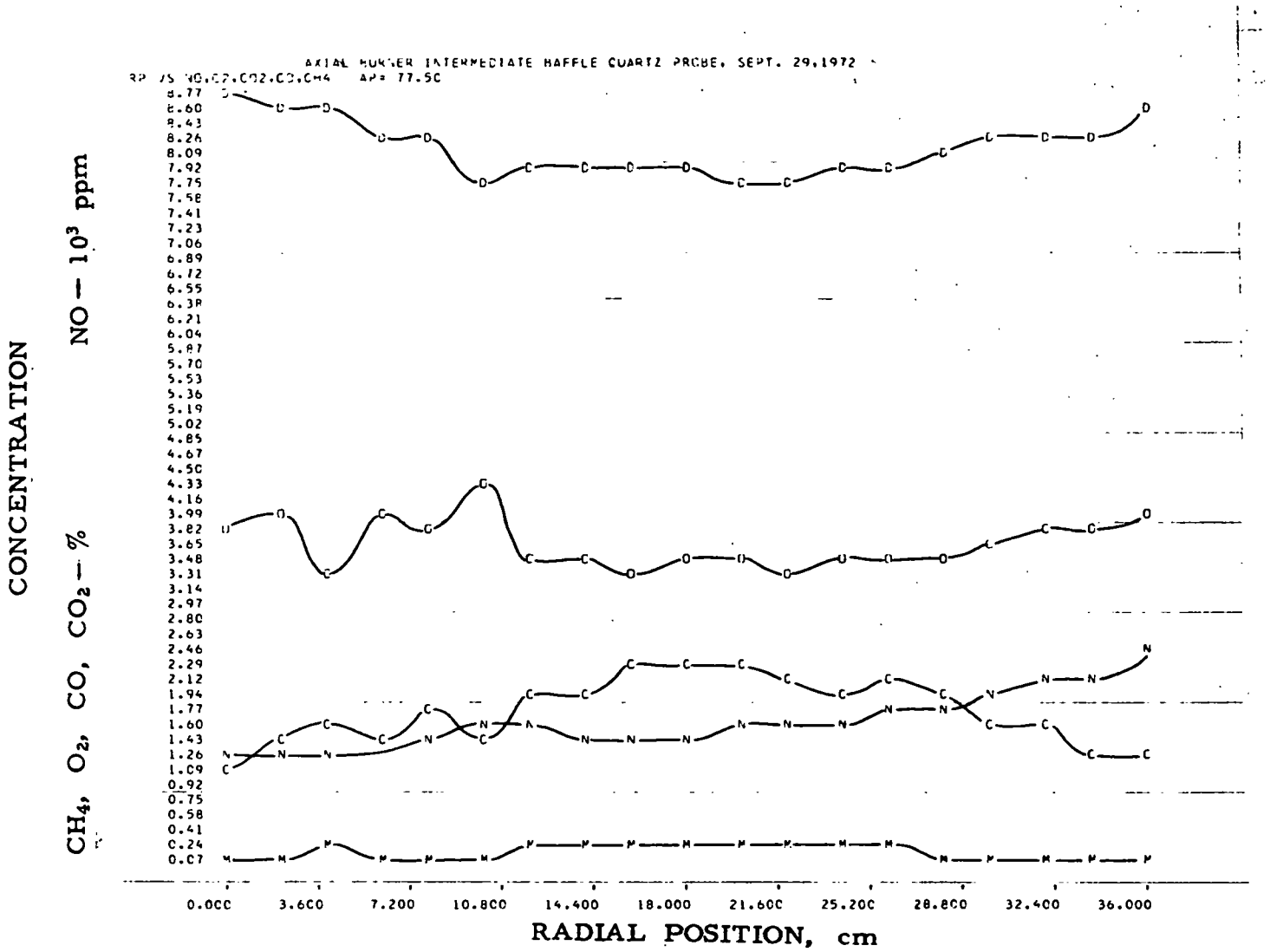

Figure II-101. COMPOSITE RADIAL PROFILES FOR NO, CO, CH_4, O_2, AND CO_2 WITH GAS INPUT OF 2147 CF/hr (Intermediate-Flame Baffle With Axial Gas Nozzle at an Axial Position of 77.5 cm, Preheat Temperature of 570°F, 10% Excess Air, and Quartz Probe)

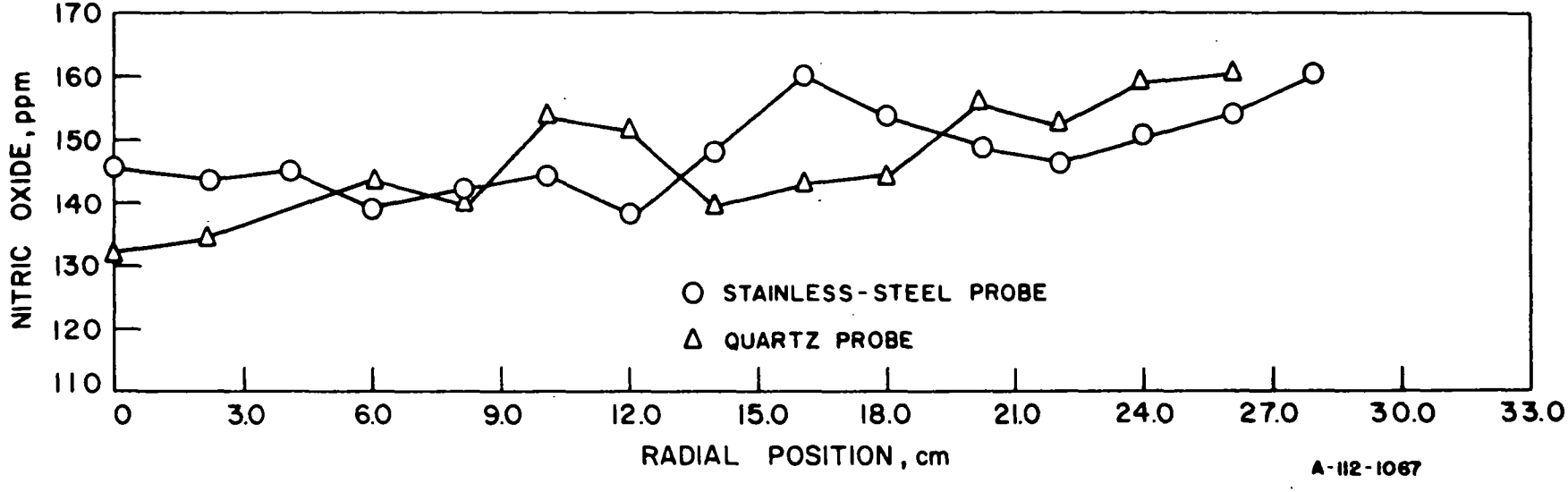

Figure II-102. COMPARISON OF NO PROFILES TAKEN WITH STAINLESS-STEEL AND QUARTZ PROBES USING SAME BURNER OPERATING CONDITIONS AND WITH SAMPLE LOCATED 77.5 cm FROM BURNER BLOCK

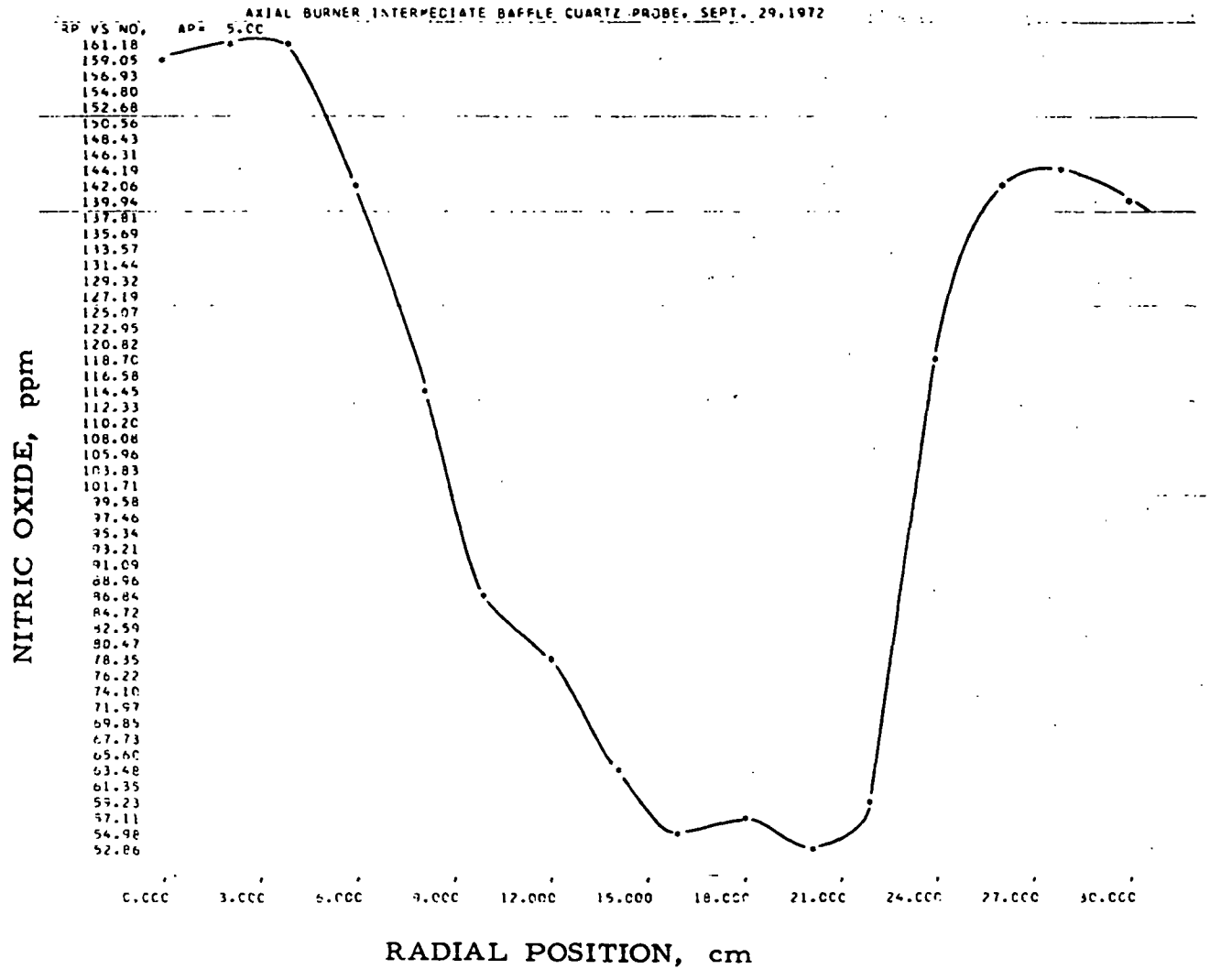

Figure II-103. RADIAL PROFILE FOR NO WITH GAS INPUT OF 2147 CF/hr (Intermediate-Flame Baffle With Axial Gas Nozzle at an Axial Position of 5.0 cm, Preheat Temperature of 570°F, 10% Excess Air, and Quartz Probe)

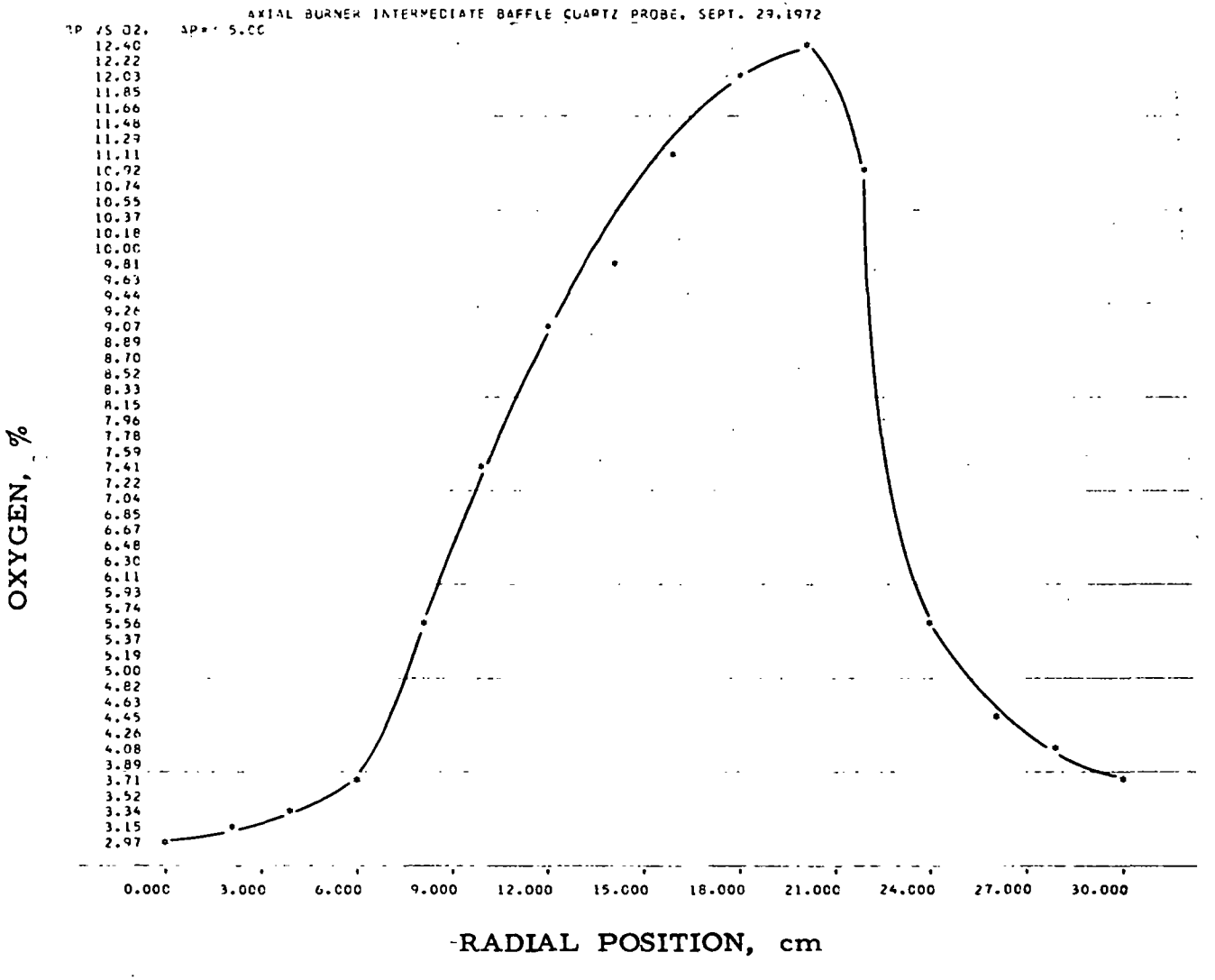

Figure II-104. RADIAL PROFILE FOR O_2 WITH GAS INPUT OF 2147 CF/hr (Intermediate-Flame Baffle With Axial Gas Nozzle at an Axial Position of 5.0 cm, Preheat Temperature of 570°F, 10% Excess Air, and Quartz Probe)

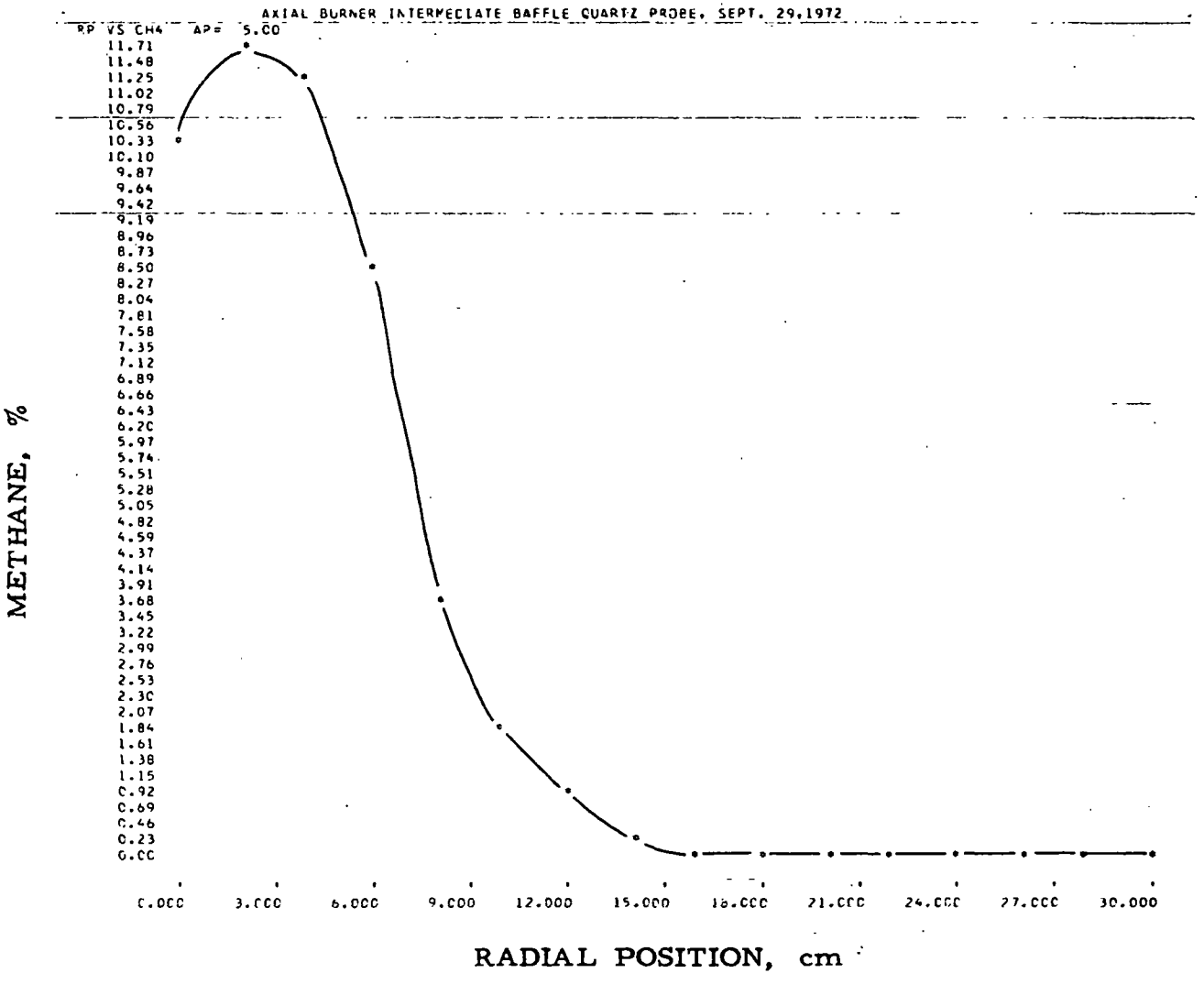

Figure II-105. RADIAL PROFILE FOR CH_4 WITH GAS INPUT OF 2147 CF/hr (Intermediate-Flame Baffle With Axial Gas Nozzle at an Axial Position of 5.0 cm, Preheat Temperature of 570°F, 10% Excess Air, and Quartz Probe)

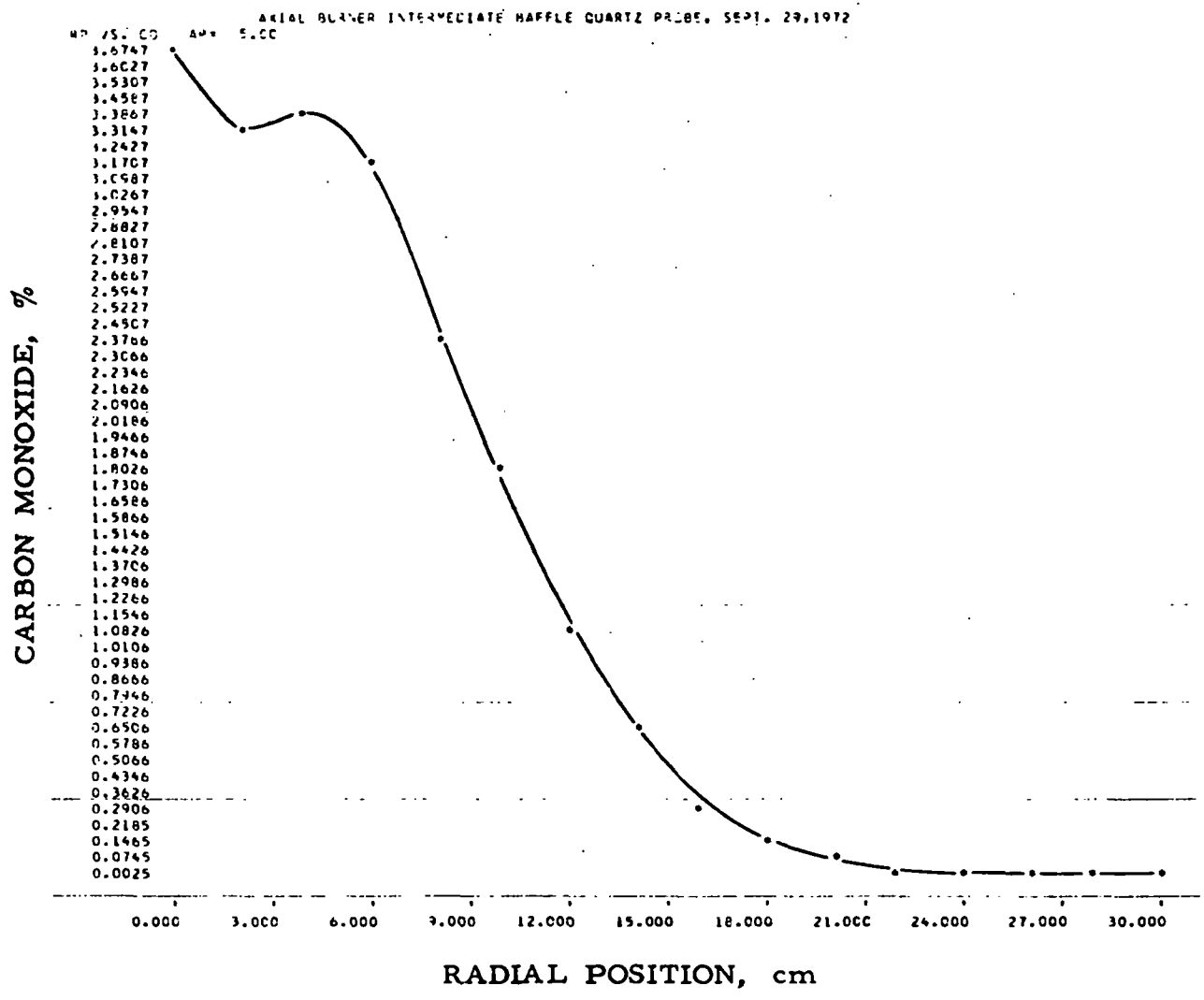

Figure II-106. RADIAL PROFILE FOR CO WITH GAS INPUT OF 2147 CF/hr (Intermediate-Flame Baffle With Axial Gas Nozzle at an Axial Position of 5.0 cm, Preheat Temperature of 570°F, 10% Excess Air, and Quartz Probe)

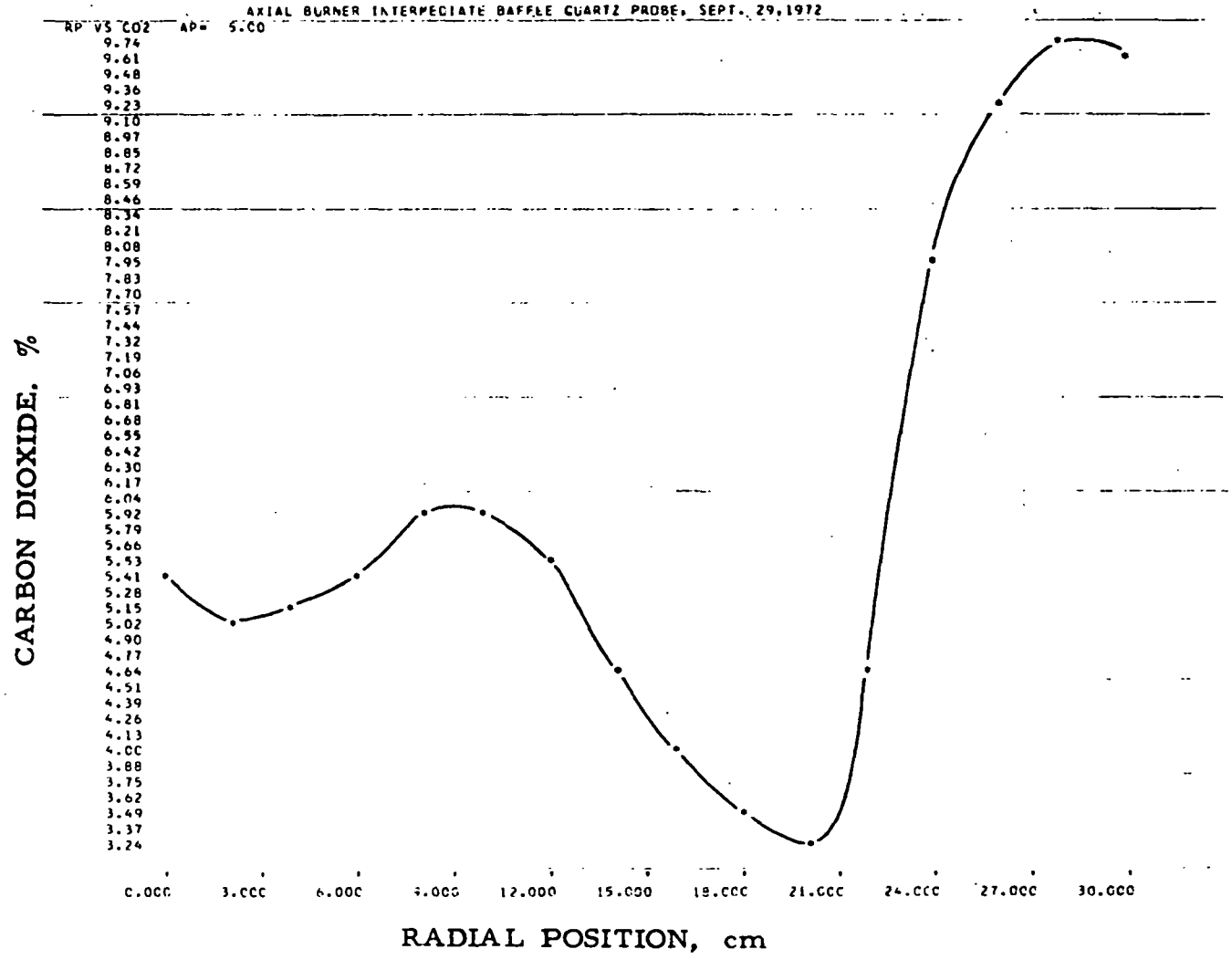

Figure II-107. RADIAL PROFILE FOR CO_2 WITH GAS INPUT OF 2147 CF/hr (Intermediate-Flame Baffle With Axial Gas Nozzle at an Axial Position of 5.0 cm, Preheat Temperature of 570°F, 10% Excess Air, and Quartz Probe)

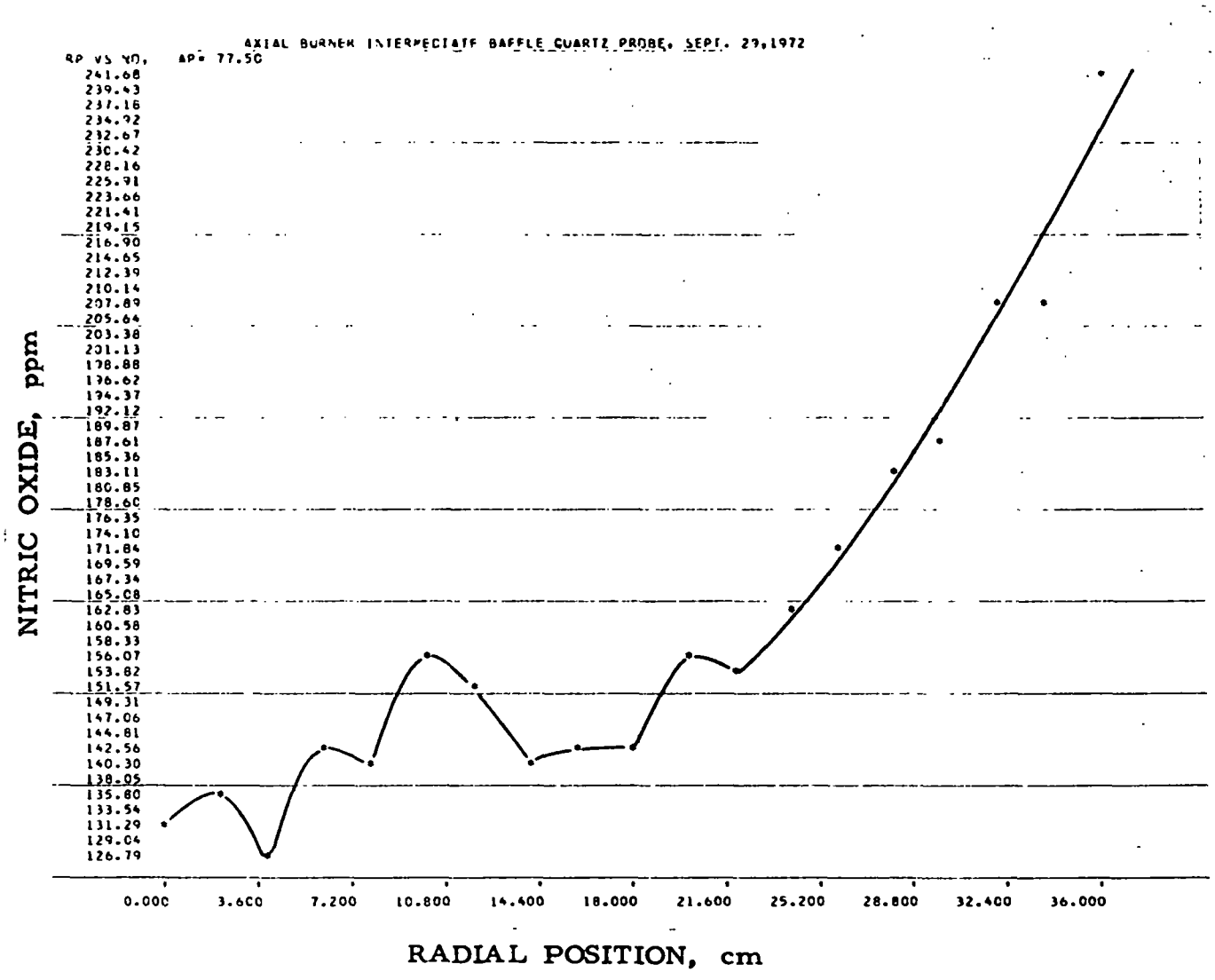

Figure II-108. RADIAL PROFILE FOR NO WITH GAS INPUT OF 2147 CF/hr (Intermediate-Flame Baffle With Axial Gas Nozzle at an Axial Position of 77.5 cm, Preheat Temperature of 570°F, 10% Excess Air, and Quartz Probe)

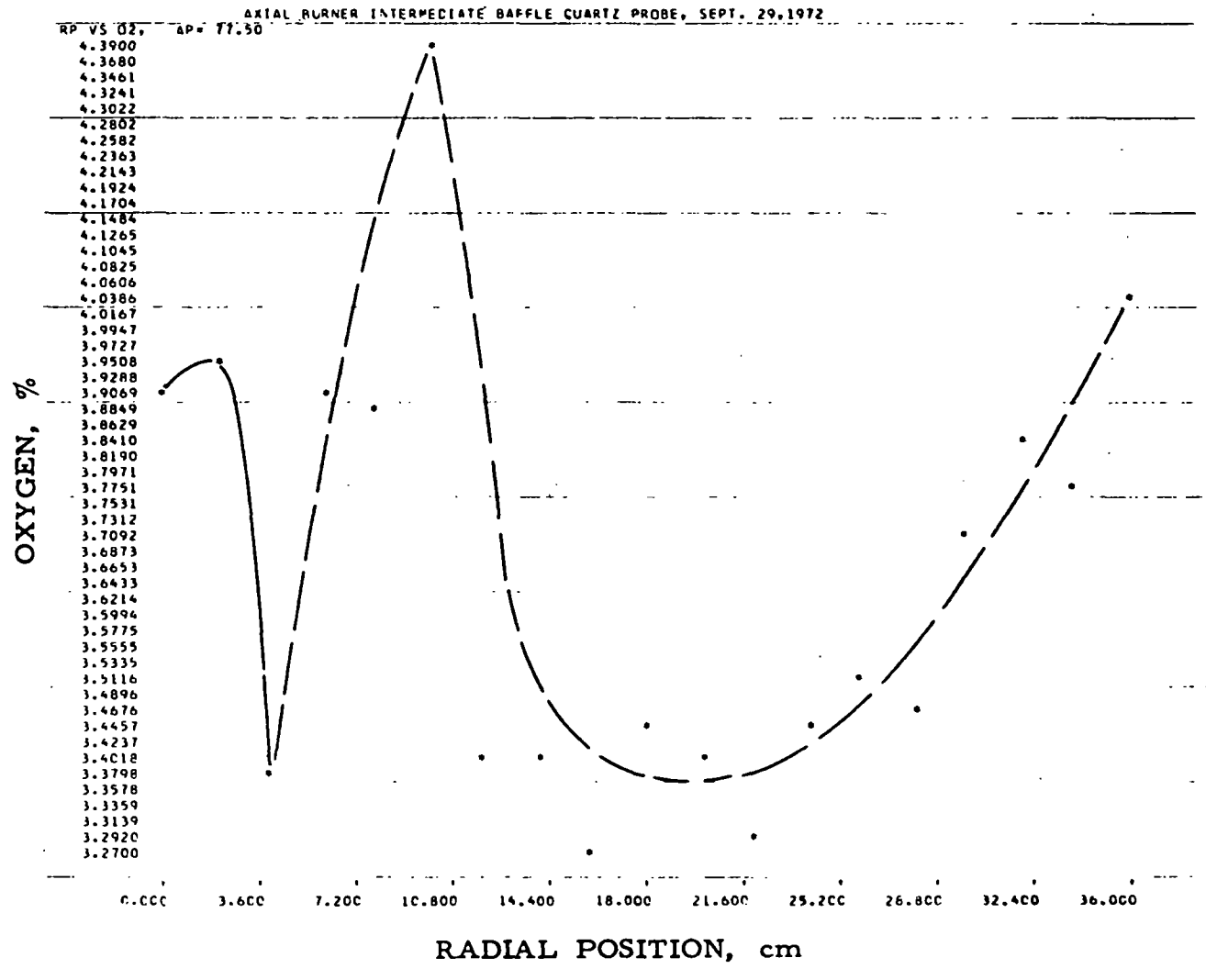

Figure II-109. RADIAL PROFILE FOR O_2 WITH GAS INPUT OF 2147 CF/hr (Intermediate-Flame Baffle With Axial Gas Nozzle at an Axial Position of 77.5 cm, Preheat Temperature of 570°F, 10% Excess Air, and Quartz Probe)

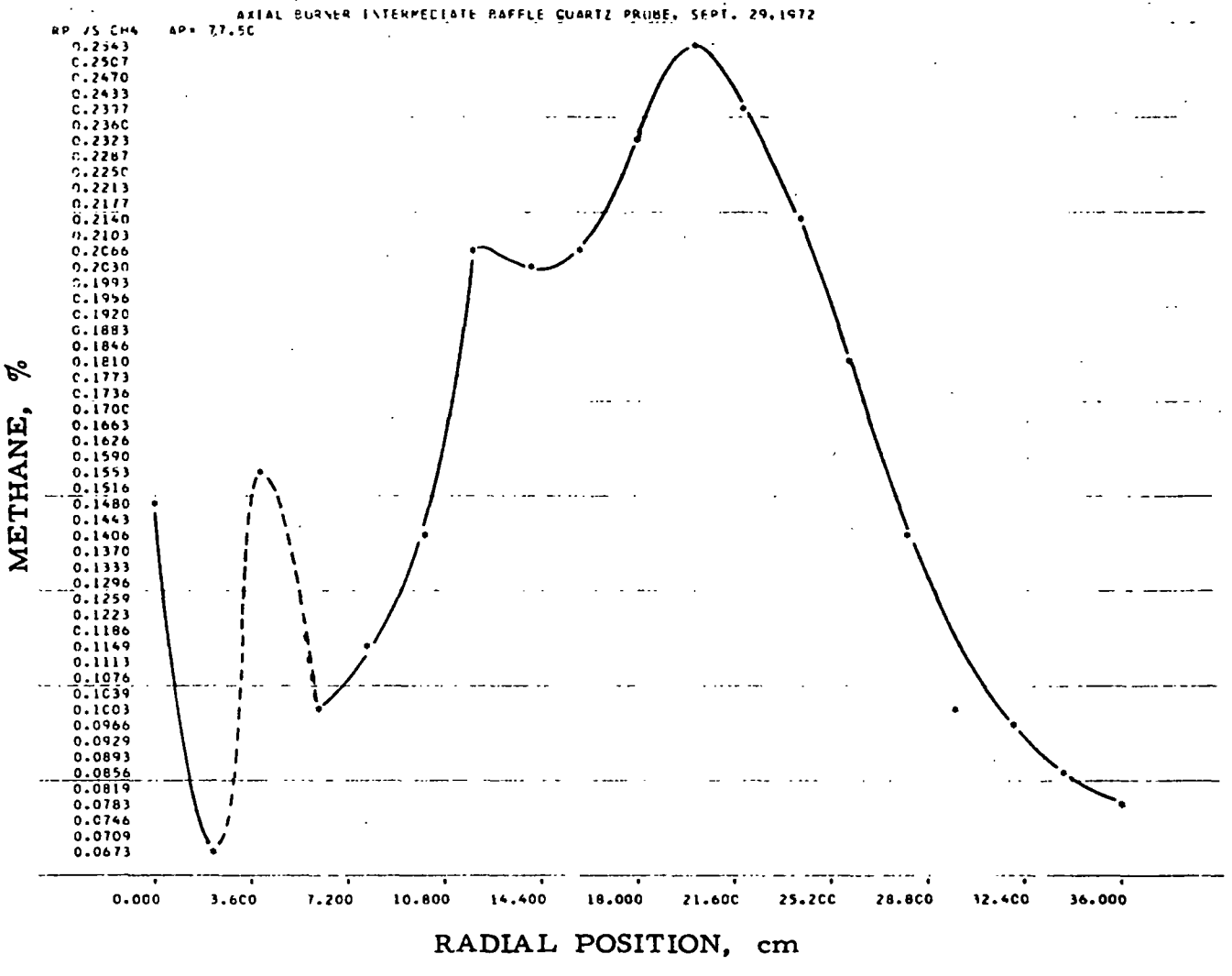

Figure II-110. RADIAL PROFILE FOR CH_4 WITH GAS INPUT OF 2147 CF/hr (Intermediate-Flame Baffle With Axial Gas Nozzle at an Axial Position of 77.5 cm, Preheat Temperature of 570°F, 10% Excess Air, and Quartz Probe)

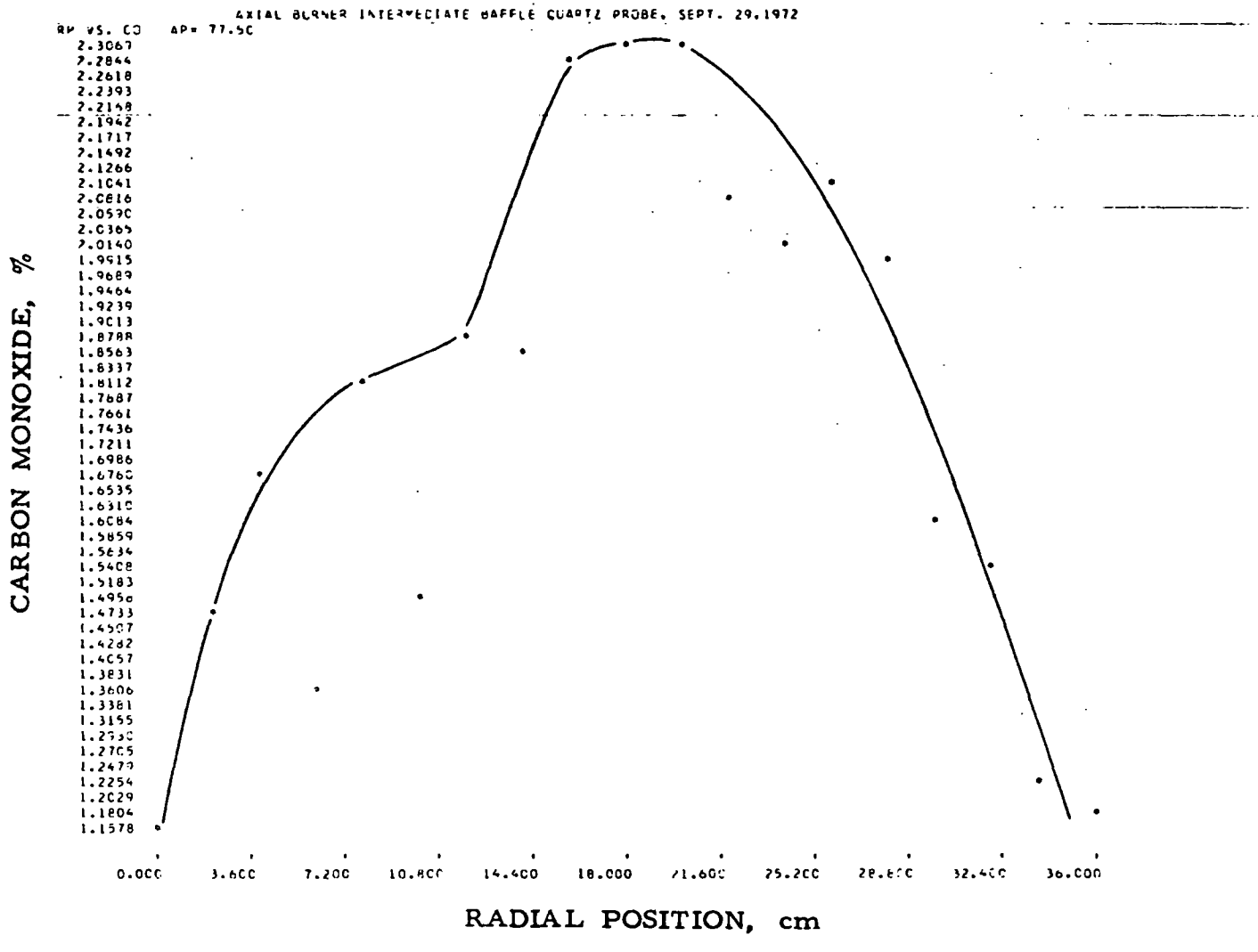

Figure II-111. RADIAL PROFILE FOR CO WITH GAS INPUT OF 2147 CF/hr (Intermediate-Flame Baffle With Axial Gas Nozzle at an Axial Position of 77.5 cm, Preheat Temperature of 570°F, 10% Excess Air, and Quartz Probe)

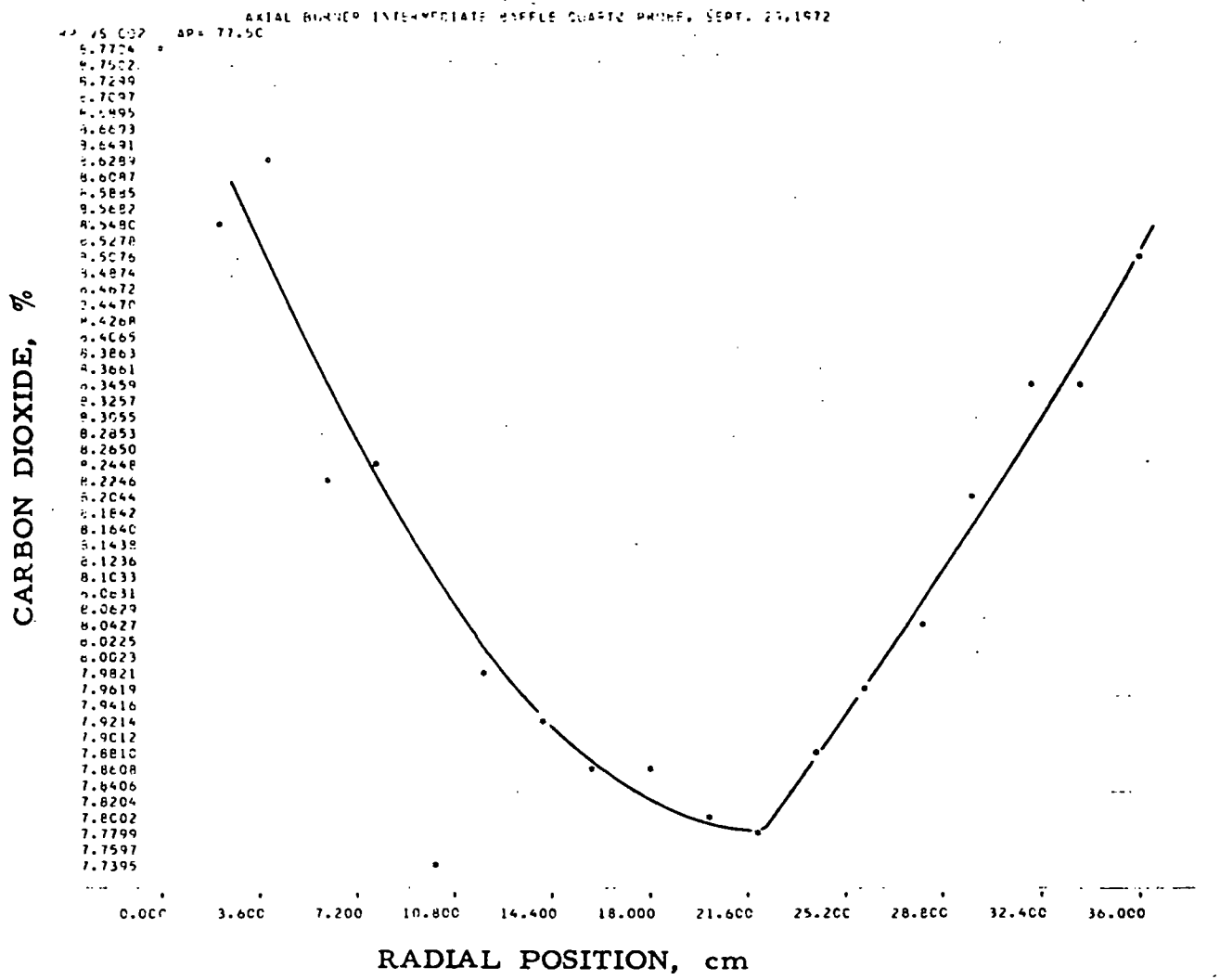

Figure II-112. RADIAL PROFILE FOR CO_2 WITH GAS INPUT OF 2147 CF/hr (Intermediate-Flame Baffle With Axial Gas Nozzle at an Axial Position of 77.5 cm, Preheat Temperature of 570°F, 10% Excess Air, and Quartz Probe)

Table II-14. DATA OBTAINED WITH QUARTZ PROBE USING AXIAL GAS NOZZLE AND AXIAL POSITION OF 5.0 cm

TRACER GAS STUDIES OF COMBUSTION BURNERS PROGRAM 2
AXIAL BURNER INTERMEDIATE BAFFLE QUARTZ PROBE, SEPT. 29,1972

INPUT GAS 2147 WALL TEMPERATURE 2560 PREHEAT TEMPERATURE 570
OUTPUT ANALYSIS
NITROGEN OXIDE 27.80 PERCENT ON RANGE 1, 243.52 PPM OXYGEN 2.98 PERCENT
CARBON DIOXIDE 8C.9C PERCENT ON RANGE 1, 10.30 PERCENT
CARBON MONOXIDE 19.30 PERCENT ON RANGE 3, 0.008 PERCENT
METHANE C.CO PERCENT ON RANGE 0, 0.00 PERCENT

EXPERIMENTAL RESULTS

		NITROGEN OXIDE -NO			OXYGEN	CARBON DIOXIDE-CO2			CARBON MONOXIDE -CO			METHANE - CH4		
AP	RP	RANGE	X	Y	C2	RANGE	X	Y	RANGE	X	Y	RANGE	X	Y
5.00	C.00	1	18.50	159.3	2.97	1	54.30	5.40	1	81.70	3.674	1	66.8C	1C.37
5.0C	2.0C	1	18.60	160.2	3.15	1	51.90	5.03	1	76.60	3.340	1	72.20	11.71
5.0C	4.00	1	18.70	161.1	3.27	1	52.90	5.18	1	76.80	3.353	1	7C.80	11.35
5.0C	6.0C	1	16.50	141.7	3.75	1	54.70	5.46	1	73.40	3.138	1	59.10	8.59
5.0C	8.00	1	13.40	114.5	5.51	1	57.40	5.89	1	60.60	2.384	1	32.2C	3.59
5.0C	1C.00	1	1C.10	86.0	7.41	1	57.60	5.92	1	48.90	1.771	1	19.7C	1.91
5.0C	12.00	1	9.20	78.3	9.16	1	55.10	5.52	1	33.0C	1.C56	3	22.00	0.96
5.00	14.00	1	7.40	63.0	9.90	1	49.60	4.69	2	37.0C	C.643	3	4.30	0.18
5.00	16.C0	1	6.40	54.5	11.15	1	44.40	3.96	2	16.6C	C.275	3	1.00	0.04
5.0C	18.CC	1	6.60	56.2	12.1C	1	40.80	3.48	2	8.9C	C.145	3	1.00	0.04
5.00	2C.00	1	6.20	52.8	12.40	1	38.80	3.23	2	5.9C	C.096	3	1.00	0.04
5.0C	22.00	1	6.90	58.7	10.90	1	49.00	4.60	3	61.3C	C.028	3	C.CO	0.00
5.00	24.00	1	13.80	118.0	5.51	1	68.90	7.90	3	12.7C	C.CC5	3	0.00	0.00
5.00	26.00	1	16.60	142.5	4.50	1	76.00	9.28	3	6.90	C.002	3	0.C0	0.00
5.00	28.0C	1	16.80	144.3	4.10	1	78.20	9.73	3	6.20	C.C02	3	C.00	0.00
5.00	30.00	1	16.40	140.8	3.80	1	77.30	9.55	3	6.50	C.002	3	C.00	0.00

Table II-15. DATA OBTAINED WITH QUARTZ PROBE USING AXIAL GAS NOZZLE AND AXIAL POSITION OF 77.5 cm

TRACER GAS STUDIES OF COMBUSTION BURNERS PROGRAM 2
AXIAL BURNER INTERMEDIATE BAFFLE QUARTZ PROBE, SEPT. 29,1972

INPUT GAS 2147 WALL TEMPERATURE 2560 PREHEAT TEMPERATURE 570

OUTPUT ANALYSIS

NITROGEN OXIDE	27.80 PERCENT	ON RANGE 1,	243.52 PPM	OXYGEN	2.98 PERCENT
CARBON DIOXIDE	80.90 PERCENT	ON RANGE 1,	10.30 PERCENT		
CARBON MONOXIDE	19.30 PERCENT	ON RANGE 3,	0.008 PERCENT		
METHANE	C.00 PERCENT	ON RANGE 0,	0.00 PERCENT		

EXPERIMENTAL RESULTS

		NITROGEN OXIDE -NO			OXYGEN	CARBON DIOXIDE-CO2			CARBON MONOXICE -CO			METHANE - CH4		
AP	RP	RANGE	X	Y	O2	RANGE	X	Y	RANGE	X	Y	RANGE	X	Y
77.50	0.00	1	15.40	132.0	3.90	1	73.40	8.77	2	62.8C	1.157	3	3.4C	C.14
77.50	2.00	1	15.7C	134.6	3.96	1	72.30	8.55	2	77.2C	1.468	3	1.50	C.06
77.50	4.0C	1	14.80	126.7	3.39	1	72.70	8.63	2	86.0C	1.667	3	3.6C	C.15
77.50	6.00	1	16.7C	143.4	3.91	1	70.60	8.22	2	72.4C	1.363	3	2.3C	C.1C
77.50	8.00	1	16.3C	139.9	3.88	1	70.70	8.24	2	92.30	1.813	3	2.6C	C.11
77.50	1C.00	1	18.00	154.9	4.39	1	68.00	7.73	1	42.9C	1.485	3	3.2C	C.13
77.50	12.00	1	17.7C	152.3	3.40	1	69.30	7.98	1	51.20	1.886	3	4.80	0.2C
77.5C	14.00	1	16.30	139.9	3.40	1	69.00	7.92	1	50.7C	1.860	3	4.7C	0.20
77.5C	16.0C	1	16.50	141.7	3.27	1	68.60	7.85	1	58.8C	2.285	3	4.80	0.20
77.5C	18.00	1	16.60	142.5	3.44	1	68.60	7.85	1	59.2C	2.306	3	5.4C	0.23
77.50	2C.0C	1	18.20	156.7	3.41	1	68.30	7.79	1	59.1C	2.301	3	5.9C	0.25
77.50	22.0C	1	17.8C	153.1	3.29	1	68.20	7.77	1	55.2C	2.C92	3	5.6C	0.24
77.50	24.00	1	19.00	163.8	3.44	1	68.80	7.88	1	53.9C	2.C24	3	5.0C	0.21
77.50	26.00	1	19.80	17C.9	3.51	1	69.20	7.96	1	55.40	2.102	3	4.2C	C.18
77.50	28.0C	1	21.20	183.5	3.47	1	69.60	8.03	1	53.3C	1.993	3	3.20	0.13
77.50	30.00	1	21.70	187.9	3.70	1	70.50	8.20	1	45.3C	1.597	3	2.3C	C.1C
77.50	32.00	1	23.90	207.8	3.84	1	71.20	8.34	1	44.3C	1.550	3	2.20	0.09
77.50	34.00	1	24.0C	208.7	3.78	1	71.20	8.34	1	36.9C	1.219	3	1.9C	0.08
77.50	36.00	1	27.60	241.6	4.04	1	72.10	8.51	1	35.9C	1.177	3	1.8C	0.07

2. Tracer-Gas Studies

The tracer-gas mixing study for the axial burner with the short-flame ported swirl baffle is presented in Figure II-113. This scan, taken at an axial position of 5.1 cm, shows that the radial concentration readings are very near to ambient, thus indicating that mixing would be complete at this position. We conclude that the major mixing phenomena are occurring in the burner block, which is an area into which we cannot probe with our equipment. The scope of the project included only areas outside the burner block and in the "combustion chamber."

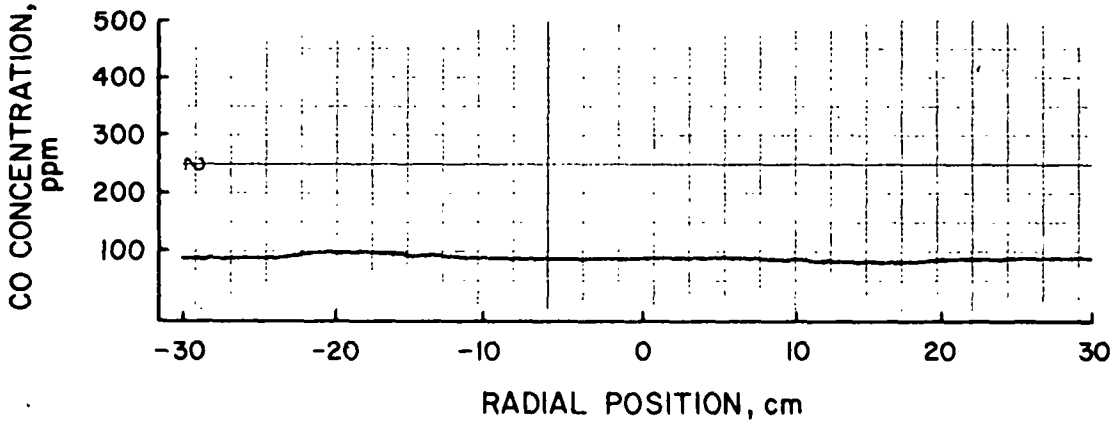

Figure II-113. RADIAL CONCENTRATION PROFILE OF CARBON MONOXIDE FROM THE AXIAL BURNER FITTED WITH THE SHORT-FLAME PORTED SWIRL BAFFLE [Air Velocity, 55 ft/s; Gas Velocity (air), 270 ft/s; 1000:1 Air/CO Ratio in Gas Stream]

3. Cold-Model Velocity Data

The raw pressure data for the axial burner, fitted with the short-flame ported swirl baffle, are given in Table II-16; the reduced profile data are listed in Table II-17. Figure II-114 shows the axial velocity at an axial position 5.1 cm from the burner wall. Note that there is no central peak representing the output from the gas nozzle. In fact, the velocity data in the central region of the burner block at radial positions of ±12 cm show reverse flow. Forward velocity peaks do occur at radial positions of ±18 cm with magnitudes of 32.7 and 21.7 ft/s. Figure II-115

Table II-16. RAW VELOCITY DATA FOR THE AXIAL BURNER WITH THE SHORT-FLAME PORTED SWIRL BAFFLE AT THE 5.1-cm AXIAL POSITION

AERODYNAMIC MODELING OF COMBUSTION BURNERS

CALIBRATION COEFFICIENTS FOR FORWARD FLOW

A1 =	0.770590	A2 =	0.272353	A3 =	-0.059818
B0 =	0.737720	B2 =	-0.158821	B4 =	0.129246
C =	4.464660	D =	0.394812		

AXIAL BURNER WITH BLOOM BAFFLE FOR SHORT FLAME - COLD MODEL

TOTAL DATA INPUT

THETA	AP	RP	P13	P03	P24	P04	POA	T	PB
0.	5.1	-30.0	21200.00	5500.00	5280.00	4490.00	79.00	20.	760.
0.	5.1	-25.0	-4430.00	23000.00	19200.00	7380.00	79.00	20.	760.
0.	5.1	-23.0	848.00	2440.00	-535.00	-2030.00	88.00	20.	760.
0.	5.1	-21.0	107.00	88.10	-44.20	-95.00	56.80	20.	760.
0.	5.1	-18.0	1340.00	141.00	-32.30	-69.80	77.80	20.	760.
0.	5.1	-15.0	-1300.00	613.00	-104.00	-151.00	144.00	20.	760.
180.	5.1	-12.0	1840.00	1140.00	574.00	602.00	156.00	20.	760.
180.	5.1	-9.0	644.00	807.00	363.00	365.00	138.00	20.	760.
180.	5.1	-6.0	1400.00	388.00	230.00	295.00	114.00	20.	760.
180.	5.1	-3.0	1860.00	336.00	322.00	284.00	117.00	20.	760.
180.	5.1	0.0	24700.00	318.00	1280.00	313.00	104.00	20.	760.
180.	5.1	3.0	15600.00	363.00	7160.00	470.00	106.00	20.	760.
180.	5.1	6.0	-5120.00	578.00	-402.00	5300.00	136.00	20.	760.
180.	5.1	9.0	-1290.00	1310.00	-297.00	-709.00	172.00	20.	760.
180.	5.1	12.0	-1700.00	3100.00	-468.00	-760.00	175.00	20.	760.
0.	5.1	15.0	456.00	518.00	153.00	387.00	140.00	20.	760.
0.	5.1	18.0	1080.00	272.00	72.80	142.00	104.00	20.	760.
0.	5.1	21.0	328.00	686.00	88.40	172.00	74.00	20.	760.
0.	5.1	23.0	3980.00	12300.00	551.00	1390.00	85.00	20.	760.
0.	5.1	25.0	3280.00	3100.00	1530.00	3200.00	79.00	20.	760.
0.	5.1	30.0	5120.00	3500.00	2440.00	3900.00	77.00	20.	760.

Table II-17. COMPUTER REDUCED DATA FOR THE AXIAL BURNER WITH THE SHORT-FLAME PORTED SWIRL BAFFLE AT THE 5.1-cm AXIAL POSITION

AXIAL BURNER WITH BLOOM BAFFLE FOR SHORT FLAME - COLD MODEL

RESULTS

AP	RP	FI	DELTA	RHO	V	VX	VY	VZ	VT	VR	PST	T	PB
5.1	-30.0	14.6	103.9	0.0000159	5.35	5.17	-0.32	1.31	-1.35	0.06	0.012203	20.	760.
5.1	-25.0	18.5	12.9	0.0000159	5.30	5.02	1.63	0.37	-1.67	0.11	0.012221	20.	760.
5.1	-23.0	50.4	237.7	0.0000159	12.05	7.66	-4.96	-7.86	-8.97	2.41	0.011343	20.	760.
5.1	-21.0	41.4	247.5	0.0000159	40.98	30.72	-10.35	-25.06	-26.51	5.68	0.015021	20.	760.
5.1	-18.0	43.4	268.6	0.0000159	45.07	32.70	-0.74	-31.00	-29.95	8.04	0.011108	20.	760.
5.1	-15.0	55.3	274.5	0.0000159	26.02	14.78	1.70	-21.34	-19.21	9.45	0.008835	20.	760.
5.1	-12.0	155.0	252.6	0.0000159	12.94	-11.73	-1.62	-5.21	-5.35	1.06	0.005378	20.	760.
5.1	-9.0	148.6	240.5	0.0000159	16.16	-13.80	-4.13	-7.32	-7.95	2.74	0.006057	20.	760.
5.1	-6.0	154.6	260.6	0.0000159	20.40	-18.44	-1.41	-8.60	-8.09	3.25	0.006383	20.	760.
5.1	-3.0	165.0	260.1	0.0000159	21.65	-20.92	-0.95	-5.49	-5.08	2.30	0.005086	20.	760.
5.1	0.0	176.6	266.9	0.0000159	23.27	-23.23	-0.07	-1.36	0.00	1.36	0.005141	20.	760.
5.1	3.0	175.6	245.3	0.0000159	20.93	-20.87	-0.66	-1.45	1.58	0.20	0.005795	20.	760.
5.1	6.0	163.6	85.5	0.0000159	18.25	-17.52	0.40	5.11	4.97	1.23	0.004927	20.	760.
5.1	9.0	143.0	77.0	0.0000159	15.91	-12.71	2.14	9.32	8.80	3.75	0.005047	20.	760.
5.1	12.0	131.3	74.6	0.0000159	12.46	-8.24	2.48	9.01	8.42	4.06	0.005729	20.	760.
5.1	15.0	55.2	108.5	0.0000159	21.01	11.98	-5.49	16.37	15.50	7.59	0.008304	20.	760.
5.1	18.0	44.0	93.8	0.0000159	30.20	21.71	-1.41	20.95	20.25	5.55	0.008909	20.	760.
5.1	21.0	55.9	105.0	0.0000159	26.80	15.02	-5.77	21.44	20.89	7.50	0.015526	20.	760.
5.1	23.0	62.6	97.8	0.0000159	10.93	5.02	-1.33	9.61	8.92	3.82	0.012174	20.	760.
5.1	25.0	45.6	115.0	0.0000159	6.92	4.83	-2.09	4.48	4.84	1.01	0.012401	20.	760.
5.1	30.0	33.1	115.4	0.0000159	6.03	5.05	-1.41	2.97	3.27	0.36	0.012597	20.	760.

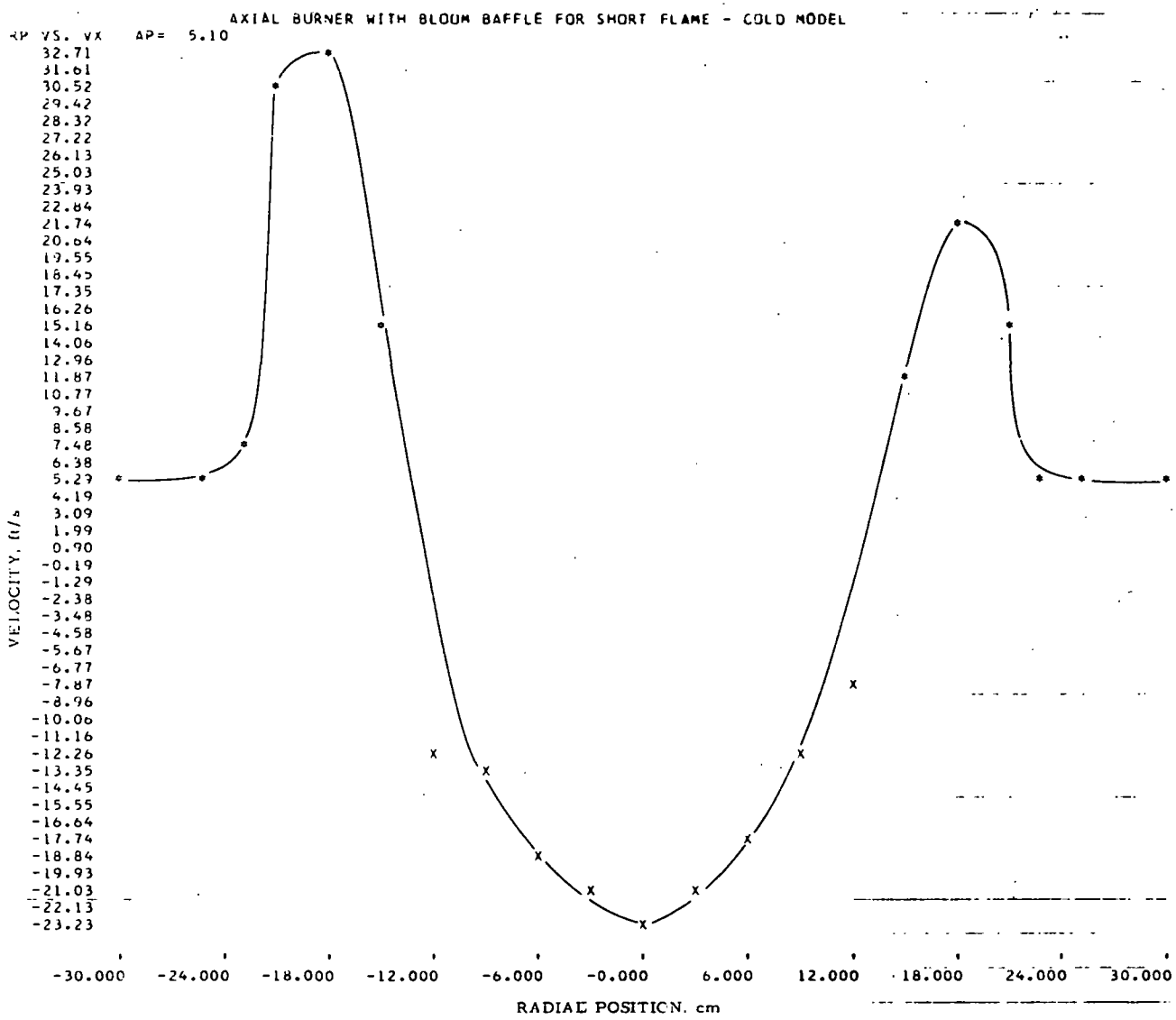

Figure II-114. AXIAL VELOCITY PROFILE FOR THE AXIAL BURNER WITH THE SHORT-FLAME PORTED SWIRL BAFFLE AT THE 5.1-cm AXIAL POSITION

shows a tangential velocity of 29.9 ft/s radially at −18 cm and 20.9 ft/s and +18 cm. The reason for the antisymmetrical velocity arises because the baffle is rotated in such a way that more output is directed into the negative y-region of the probing plane than into the positive y-region. We did not take velocity profiles beyond the 5.1-cm axial position because primary mixing is completed, as indicated by Figure II-112 and by our earlier discussion. A swirl number for the axial burner with the short-flame ported swirl baffle was calculated using the data in Table II-17. The value of swirl intensity was 0.43.

4. Hot-Model Input-Output Data

The burner with a radial gas nozzle (short flame) was operated at a gas input of 2593 CF/hr, with amounts of excess air between 5 and 20% and at three different preheated air temperatures. Figure II-116 shows the input-output data for the radial gas nozzle at a 2593 CF/hr gas input as a function of excess air and preheat temperature. The peak concentration of NO can be seen to shift toward higher excess air levels as the preheated air temperature increases.

Input-output tests were conducted for the short-flame baffle with the axial gas nozzle (long flame) at three gas inputs between 1769 CF/hr and 2415 CF/hr, with amounts of excess air between 5% and 20% and at three different preheats. Figures II-117, II-118, and II-119 show these input-output test results. Increasing the preheated air temperature from 100° to 550°F results in a nonlinear increase in the amount of NO emissions at a given level of excess air. The nature of these emission curves is in sharp contrast to the "bell-shaped" characteristics displayed by the radial gas nozzle. Note also that the emission curves taken at ambient conditions suggest that the amount of NO formed is relatively independent of the excess air level above 2.5% oxygen in the flue.

5. In-the-Flame Data Survey Results

As part of this program, we again radially mapped the concentrations of CO, CO_2, CH_4, O_2, and NO; the temperature; and the gas velocity. This information is obtained to gain insight into the mechanism and location of NO formation for different flame conditions.

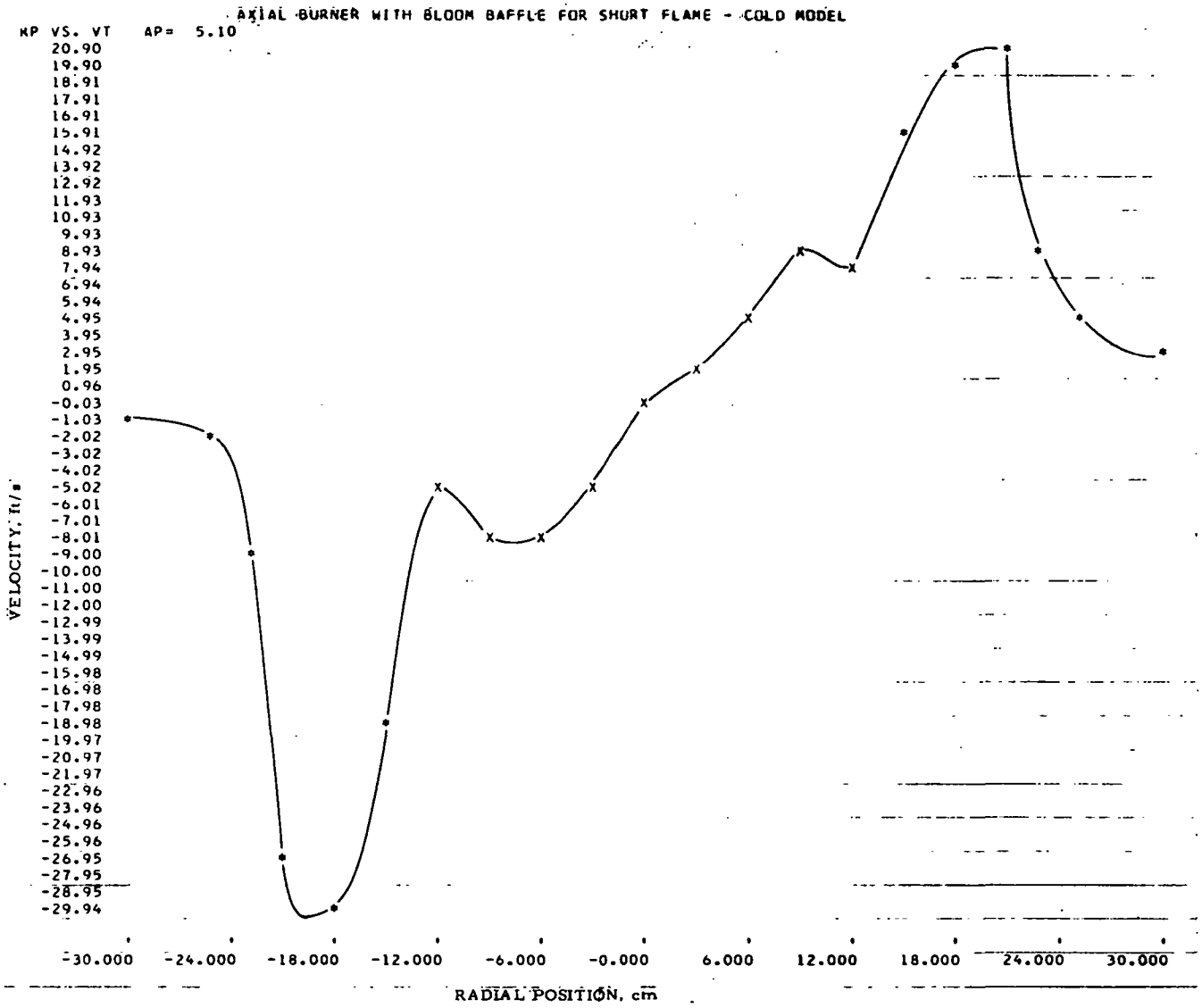

Figure II-115. TANGENTIAL VELOCITY PROFILE FOR THE AXIAL BURNER WITH THE SHORT-FLAME PORTED SWIRL BAFFLE AT THE 5.1-cm AXIAL POSITION

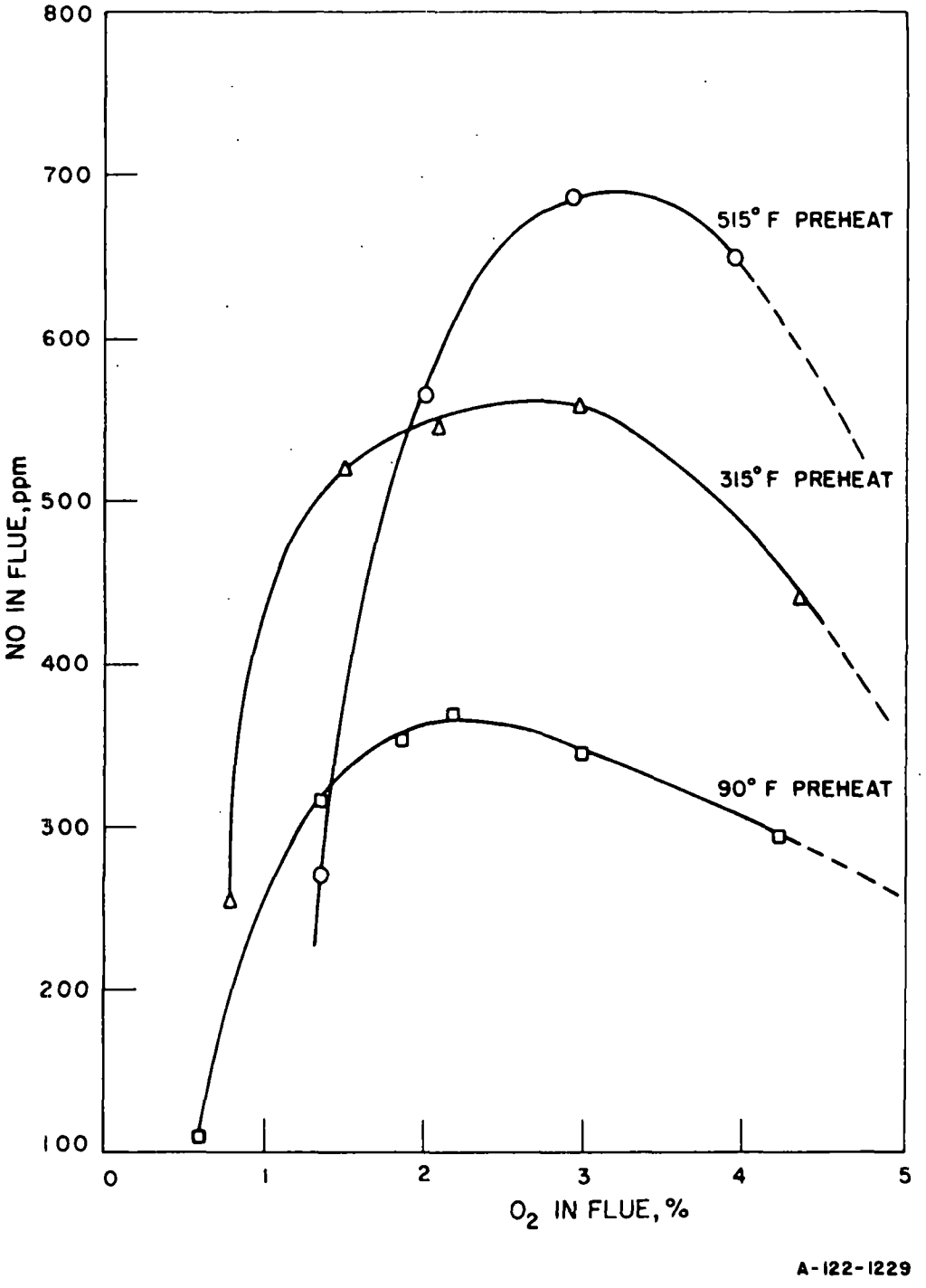

Figure II-116. NO CONCENTRATION IN THE FLUE AS A FUNCTION OF EXCESS AIR (Short-Flame Baffle – Radial Nozzle) AND PREHEATED AIR TEMPERATURE; GAS INPUT, 2593 CF/hr

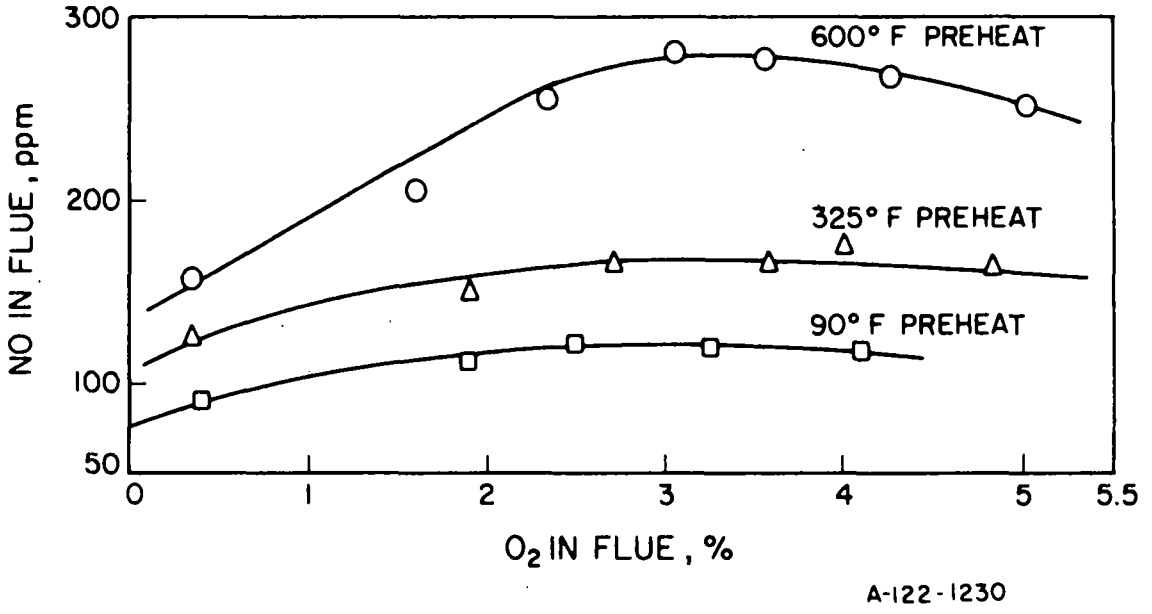

Figure II-117. NO CONCENTRATION IN THE FLUE AS A FUNCTION OF EXCESS AIR (Short-Flame Baffle – Axial Gas Nozzle) AND PREHEATED AIR TEMPERATURE; GAS INPUT, 1769 CF/hr

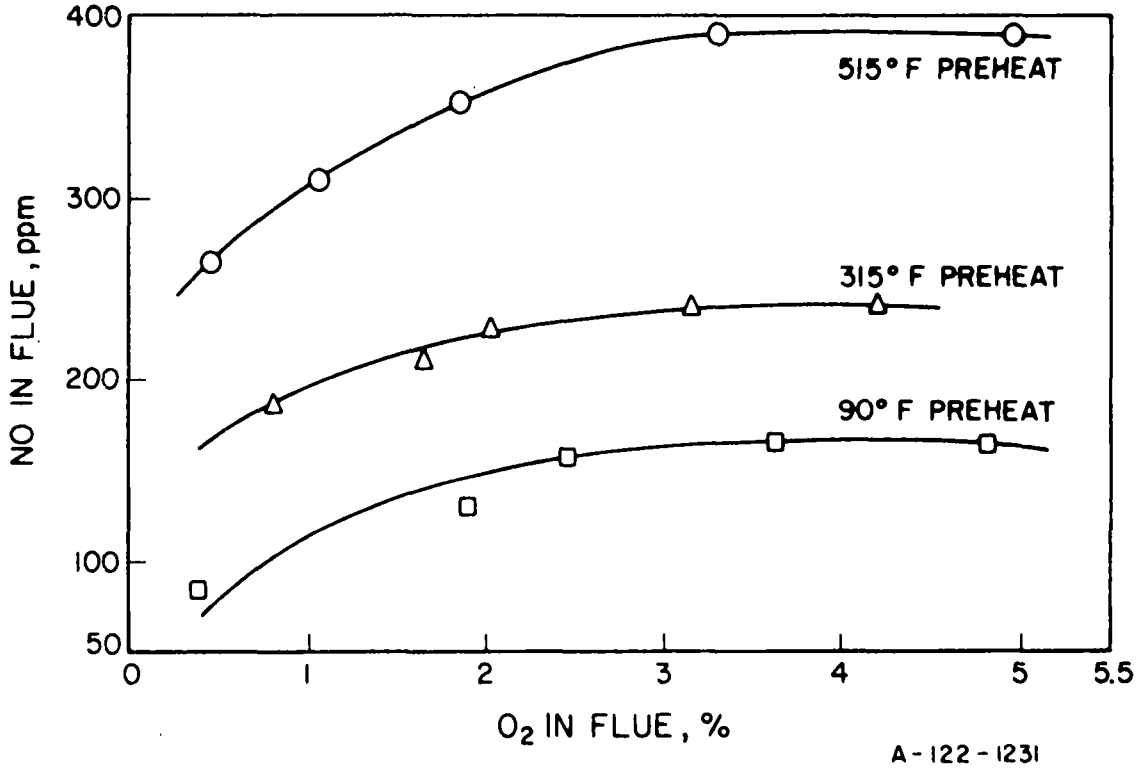

Figure II-118. NO CONCENTRATIONS IN THE FLUE GAS AS A FUNCTION OF EXCESS AIR (Short-Flame Baffle – Axial Gas Nozzle) AND PREHEATED AIR TEMPERATURE; GAS INPUT, 2109 CF/hr

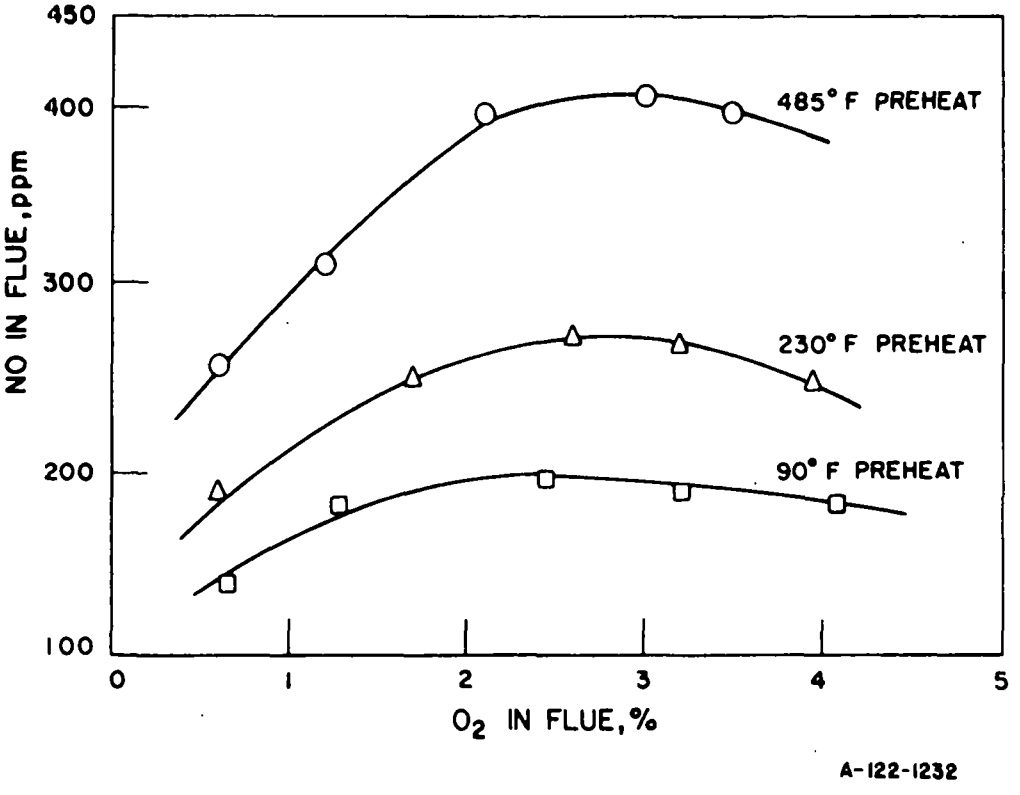

Figure II-119. NO CONCENTRATION IN THE FLUE GAS AS A FUNCTION OF EXCESS AIR (Short-Flame Baffle – Axial Gas Nozzle) AND PREHEATED AIR TEMPERATURE; GAS INPUT, 2415 CF/hr

We first completed gas species, temperature, and velocity mapping for the short-flame baffle burner with the axial gas nozzle. The maps were obtained while operating the burner at conditions of intermediate-level NO production as determined from the input-output data tests. Additional gas species mapping was performed while operating the burner at conditions producing the maximum amount of NO.

Profiles were first run by scanning the radial axis with the gas-sampling probe moving at a constant velocity (approximately 1.5 cm/s), with the gas species concentrations being displayed by a high-speed record. These scanning traverses were made at 30-cm intervals from the burner wall. These data were then inspected from the degree of primary and secondary combustion as well as the NO concentration and its variation with radial position. From these analyses, we determined that a point-by-point time-averaged measurement of the gas species, temperature, and velocity would be taken at axial positions of 7.6 cm, 45.7 cm, and 90 cm.

The profiles were first run on the axial burner with the short-flame ported baffle with the input conditions set at 2190 CF/hr gas input, with a 315°F preheat temperature and 3% excess oxygen. Figure II-120 shows a composite of the gas-sampling profiles taken at an axial position of 7.6 cm from the burner block face. These curves show (curve M) that methane concentration was in excess of 20% on the axis of the burner (0.0 cm). The carbon monoxide (curve C) varied between 4 and 6% in the region of the burner block (from +21 cm to −21 cm) to a minimum of 300 ppm near the sidewalls of the furnace. Oxygen (curve O) varied from 1.2% on the center line to a maximum of 13.1% at a 24-cm radial position to a recirculation value of 4.1%. Nitric oxide (curve N) had a maximum of 215 ppm at the center line and a minimum of 69 ppm at a radial position of 21 cm. Carbon dioxide (curve D) varied from about 3% at the center line to 10% in the recirculation zone.

The curves of Figure II-120 were plotted on a single 0-24% scale because of computer limitations. The following legend applies to this figure and some of the others (computer print-outs) that follow:

AP = axial position
RP = radial position

The actual data were collected on a range of concentrations which provided greater resolution of the measuring equipment as shown in Figures II-121 to II-125. The raw data are given in Table II-18.

Figure II-126 shows the temperature profile across the furnace at the 7.6-cm axial probe position. These data support the gas concentration analysis in that the "cold" region (temperatures below the 2475°F ambient) of the flame front corresponds to positions of high oxygen (21 cm and −21 cm) and methane (3 cm) concentrations, with the hot regions (temperatures above 2475°F ambient) (15 cm and −15 cm) appearing on the shear (high-mixing) area between these high oxygen and methane concentrations.

Figure II-127 displays the axial component of velocity as a function of radial position at a 7.6-cm axial probe position. There are peaks in the forward velocity at −18 cm, 6 cm, and 21 cm. By comparing these peaks with the temperature and gas concentration analysis, we can conclude that very good agreement exists about the position of the high

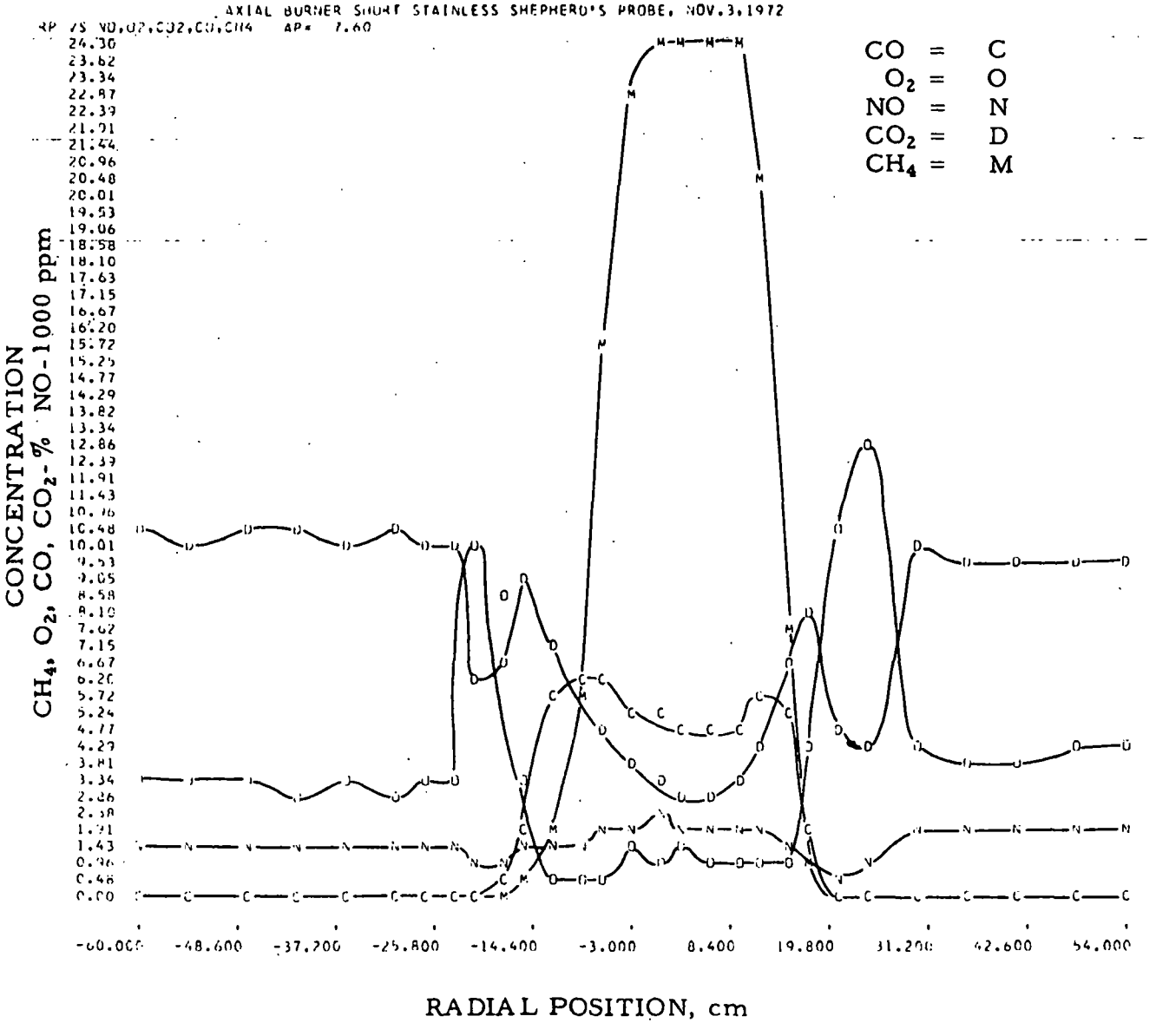

Figure II-120. COMPOSITE PLOT OF GAS SAMPLING PROFILES FOR CO, CO_2, CH_4, NO, AND O_2 FOR THE SHORT-FLAME BAFFLE USING THE AXIAL NOZZLE AT AN AXIAL POSITION OF 7.6 cm. GAS INPUT, 2190 CF/hr; EXCESS OXYGEN, 3.0%; PREHEATED AIR, 315°F

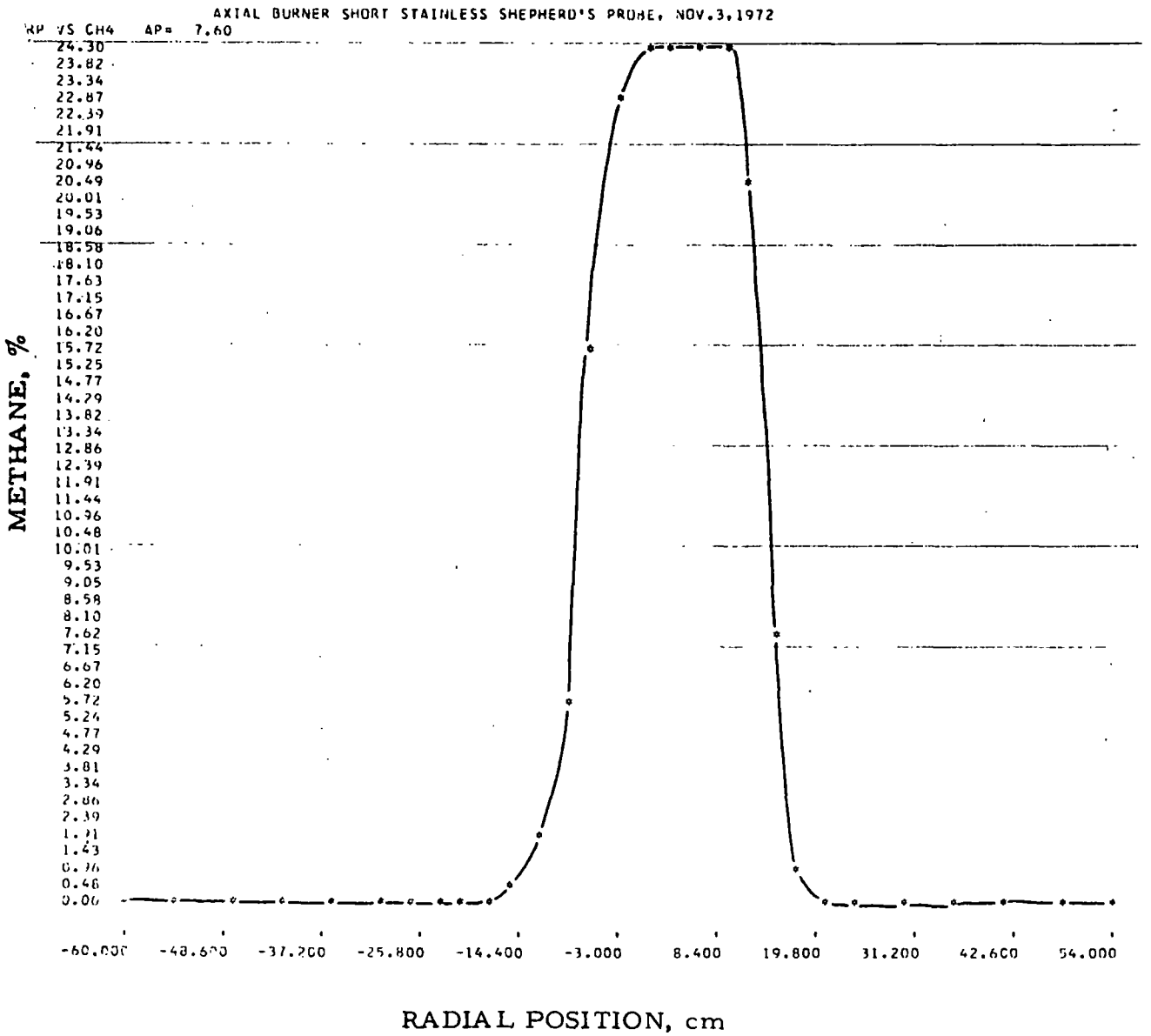

Figure II-121. RADIAL COMPOSITION PROFILE FOR METHANE (CH_4) FOR THE SHORT-FLAME BAFFLE USING THE AXIAL NOZZLE AT AN AXIAL POSITION OF 7.6 cm. GAS INPUT, 2190 CF/hr; EXCESS OXYGEN, 3.0%; PREHEATED AIR, 315^{0}F

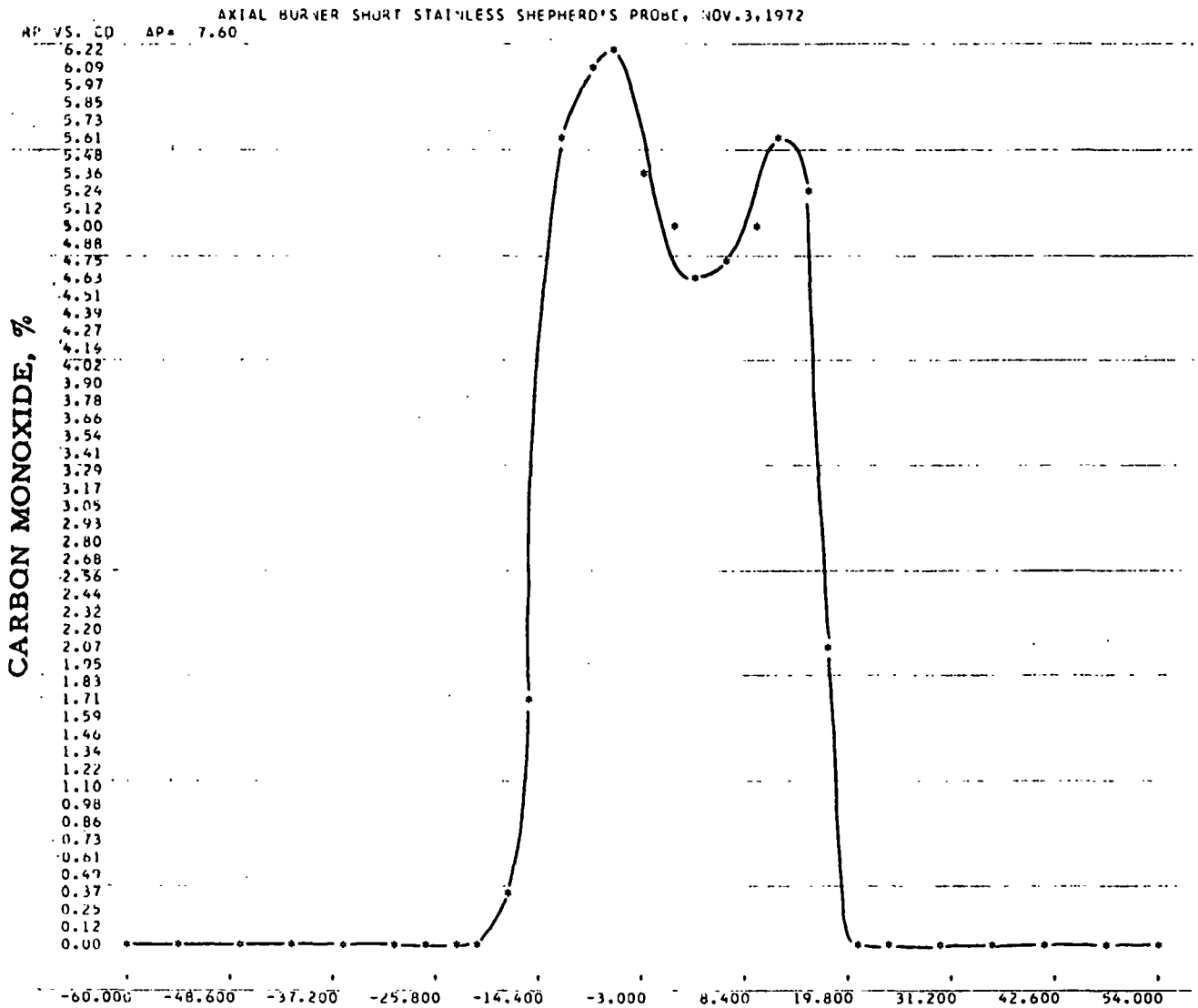

Figure II-122. RADIAL COMPOSITION PROFILE FOR CARBON MONOXIDE (CO) FOR THE SHORT-FLAME BAFFLE USING THE AXIAL NOZZLE AT AN AXIAL POSITION OF 7.6 cm. GAS INPUT, 2190 CF/hr; EXCESS OXYGEN, 3.0%; PREHEATED AIR, 315°F

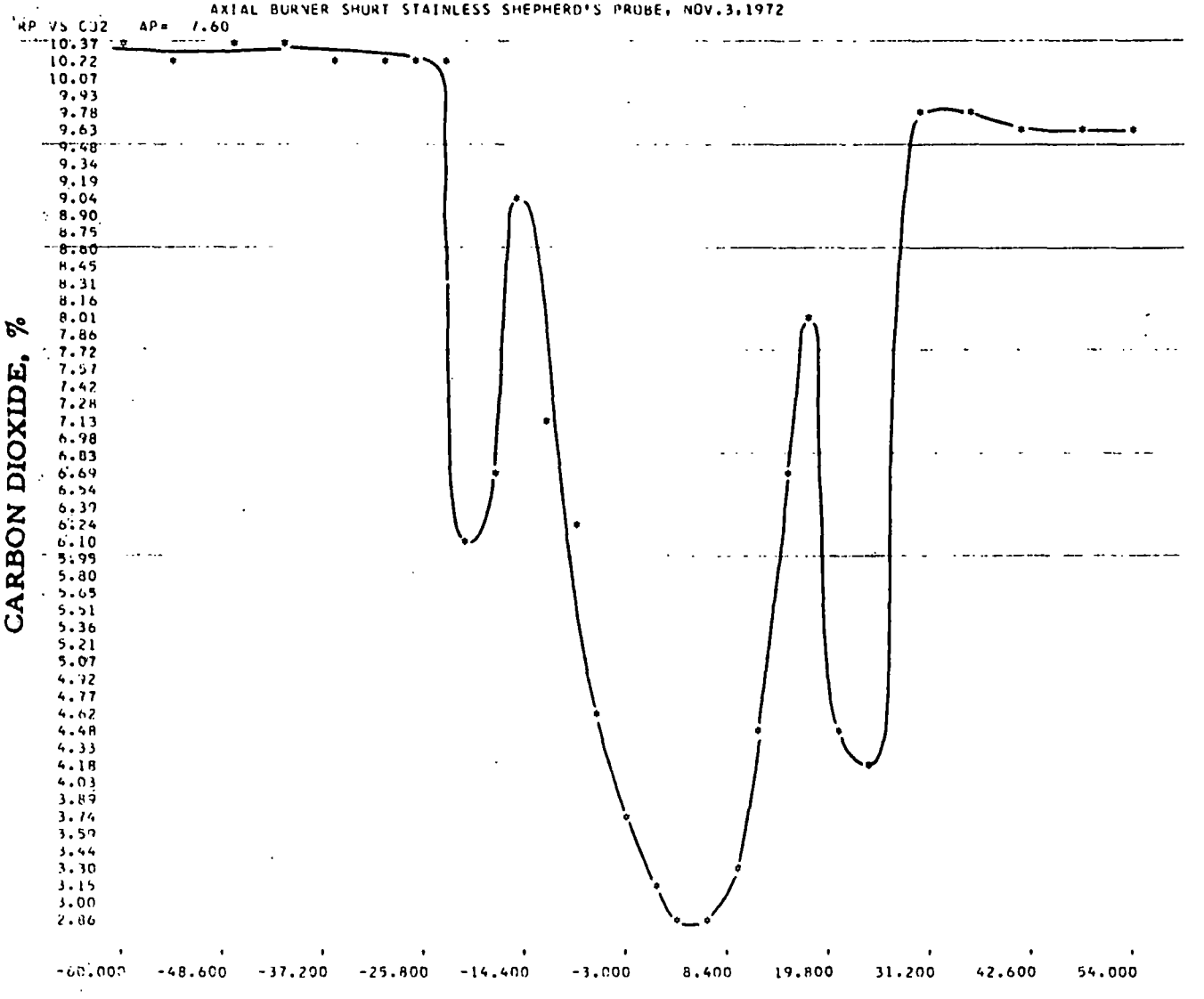

Figure II-123. RADIAL COMPOSITION PROFILE FOR CARBON DIOXIDE (CO_2) FOR THE SHORT-FLAME BAFFLE USING THE AXIAL NOZZLE AT AN AXIAL POSITION OF 7.6 cm. GAS INPUT, 2190 CF/hr; EXCESS OXYGEN, 3.0%; PREHEATED AIR, 315°F

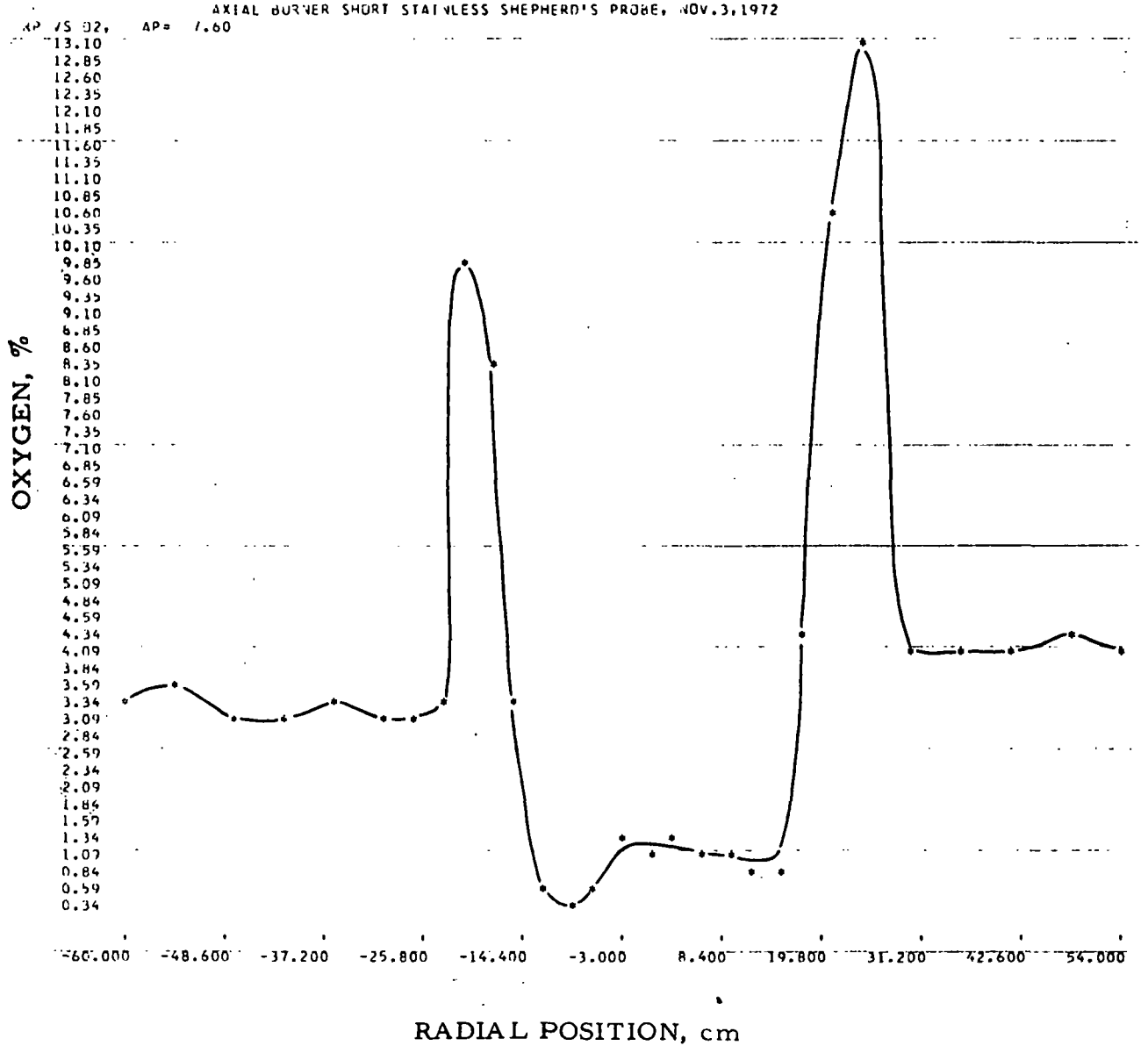

Figure II-124. RADIAL COMPOSITION PROFILE FOR OXYGEN (O_2) FOR THE SHORT-FLAME BAFFLE USING THE AXIAL NOZZLE AT AN AXIAL POSITION OF 7.6 cm. GAS INPUT, 2190 CF/hr; EXCESS OXYGEN, 3.0%; PREHEATED AIR, 315^{0}F

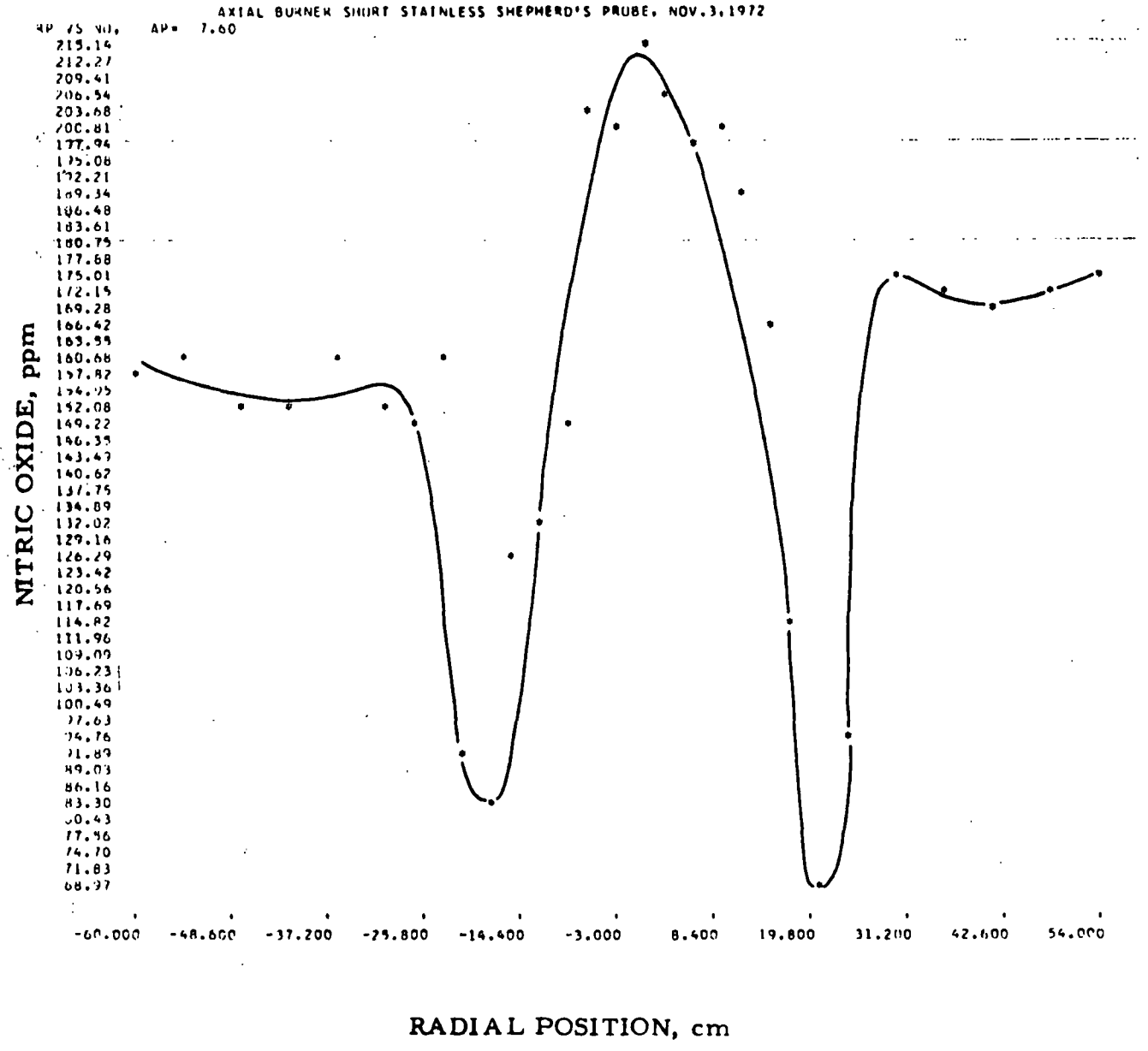

Figure II-125. RADIAL COMPOSITION PROFILE FOR NITRIC OXIDE (NO) FOR THE SHORT-FLAME BAFFLE USING THE AXIAL NOZZLE AT AN AXIAL POSITION OF 7.6 cm. GAS INPUT, 2190 CF/hr; EXCESS OXYGEN, 3.0%; PREHEATED AIR, 315°F

Table II-18. RAW (Gas Analysis) DATA FOR SHORT-FLAME BAFFLE BURNER

TRACER GAS STUDIES OF COMBUSTION BURNERS PROGRAM 2
AXIAL BURNER SHORT STAINLESS SHEPHERD'S PROBE, NOV.3,1972

INPUT GAS 2190 WALL TEMPERATURE 2524 PREHEAT TEMPERATURE 315

OUTPUT ANALYSIS

NITROGEN OXIDE	21.80 PERCENT ON RANGE 1,	188.89 PPM	OXYGEN	2.97 PERCENT	
CARBON DIOXIDE	81.00 PERCENT ON RANGE 1,	10.32 PERCENT			
CARBON MONOXIDE	6.40 PERCENT ON RANGE 3,	0.002 PERCENT			
METHANE	0.00 PERCENT ON RANGE 0,	0.00 PERCENT			

EXPERIMENTAL RESULTS

		NITROGEN OXIDE -NO			OXYGEN	CARBON DIOXIDE-CO2			CARBON MONOXIDE -CO			METHANE - CH4		
AP	RP	RANGE	X	Y	O2	RANGE	X	Y	RANGE	X	Y	RANGE	X	Y
7.60	-60.00	1	18.30	157.6	3.42	1	80.90	10.30	3	10.00	0.004	3	0.00	0.00
7.60	-54.00	1	18.60	160.2	3.56	1	80.50	10.22	3	9.40	0.003	3	1.20	0.05
7.60	-48.00	1	17.70	152.3	3.10	1	81.20	10.36	3	10.30	0.004	3	1.20	0.05
7.60	-42.00	1	17.70	152.3	3.01	1	81.00	10.32	3	10.90	0.004	3	2.80	0.12
7.60	-36.00	1	18.50	159.3	3.37	1	80.20	10.15	3	10.50	0.004	3	3.00	0.13
7.60	-30.00	1	17.70	152.3	3.09	1	80.70	10.26	3	11.40	0.004	3	3.50	0.15
7.60	-27.00	1	17.50	150.5	3.18	1	80.60	10.24	3	11.70	0.004	3	3.00	0.13
7.60	-24.00	1	18.60	160.2	3.23	1	80.50	10.22	3	13.00	0.005	3	3.20	0.13
7.60	-21.00	1	10.70	91.2	9.92	1	58.70	6.10	3	25.10	0.010	3	3.60	0.15
7.60	-18.00	1	9.90	84.3	8.34	1	62.40	6.73	2	18.70	0.312	3	4.30	0.18
7.60	-15.00	1	14.80	126.7	3.25	1	74.60	9.00	1	48.00	1.727	3	8.70	0.37
7.60	-12.00	1	15.50	132.9	0.64	1	65.00	7.19	1	107.20	5.553	3	46.80	2.14
7.60	-9.00	1	17.50	150.5	0.34	1	59.10	6.17	1	114.40	6.147	2	65.00	5.67
7.60	-6.00	1	23.40	203.3	0.49	1	49.10	4.61	1	115.20	6.215	1	87.40	15.88
7.60	-3.00	1	23.00	199.7	1.44	1	42.70	3.73	1	105.10	5.385	1	108.80	22.76
7.60	0.00	1	24.70	215.1	1.17	1	38.50	3.20	1	100.60	5.033	1	113.00	24.25
7.60	3.00	1	23.60	205.1	1.33	1	35.60	2.85	1	95.30	4.633	1	112.60	24.11
7.60	6.00	1	22.80	197.9	1.11	1	36.00	2.90	1	96.70	4.737	1	112.60	24.11
7.60	9.00	1	23.10	200.6	1.03	1	39.20	3.28	1	99.70	4.964	1	113.10	24.29
7.60	12.00	1	22.00	190.6	0.76	1	48.10	4.47	1	108.00	5.618	1	101.40	20.25
7.60	15.00	1	19.30	166.5	0.81	1	62.50	6.75	1	103.60	5.267	1	53.90	7.48
7.60	18.00	1	13.40	114.5	4.37	1	69.50	8.01	1	55.60	2.113	3	22.90	1.00
7.60	21.00	1	8.10	68.9	10.58	1	48.50	4.53	3	7.40	0.003	3	1.40	0.06
7.60	24.00	1	11.20	95.5	13.10	1	46.50	4.24	3	10.10	0.004	3	1.20	0.05
7.60	30.00	1	20.20	174.5	4.06	1	78.40	9.78	3	9.40	0.003	3	1.20	0.05
7.60	36.00	1	19.90	171.8	4.04	1	78.10	9.71	3	8.60	0.003	3	0.00	0.00
7.60	42.00	1	19.50	168.2	4.05	1	77.70	9.63	3	10.10	0.004	3	0.50	0.02
7.60	48.00	1	19.90	171.8	4.27	1	77.40	9.57	3	9.40	0.003	3	0.00	0.00
7.60	54.00	1	20.10	173.6	4.06	1	78.00	9.69	3	9.70	0.003	3	0.00	0.00

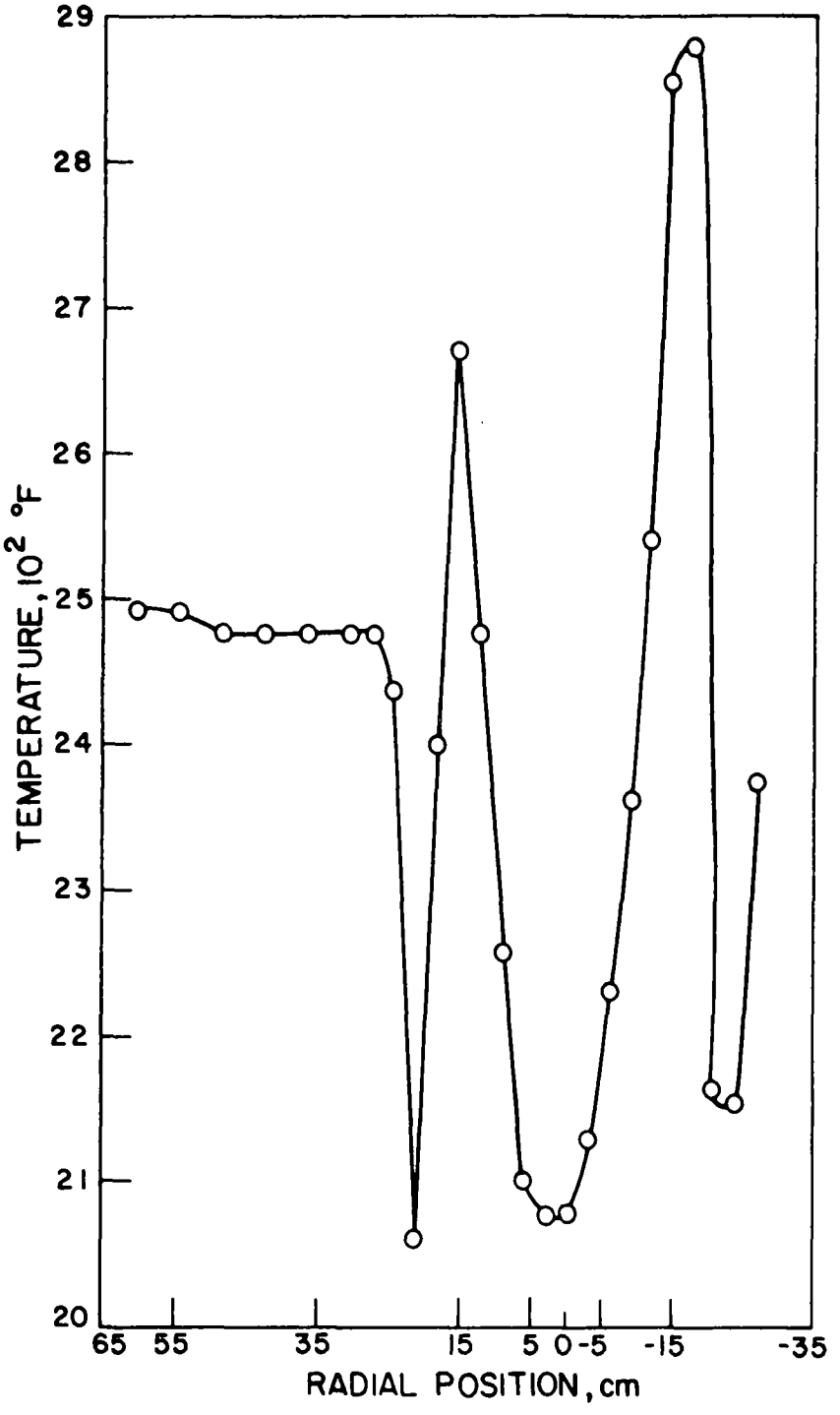

Figure II-126. AXIAL TEMPERATURE PROFILE FROM SHORT-FLAME AXIAL NOZZLE BAFFLE BURNER AT A 7.6-cm AXIAL POSITION. GAS INPUT, 2190 CF/hr; EXCESS OXYGEN, 3.3%; PREHEAT TEMPERATURE, 310°F

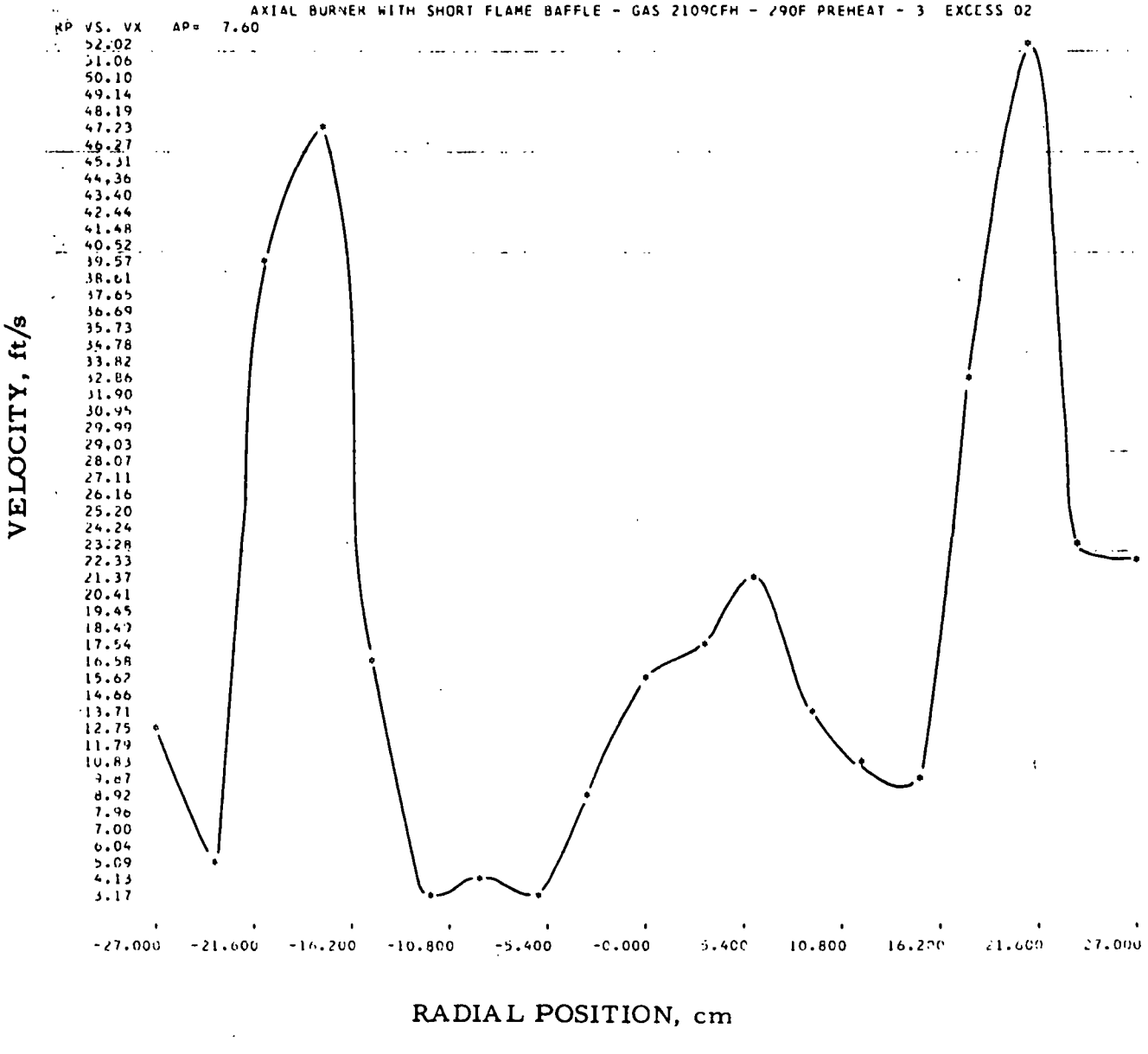

Figure II-127. RADIAL VELOCITY PROFILE (Axial Component) AT AN AXIAL POSITION OF 7.6 cm FOR THE SHORT-FLAME BAFFLE USING THE AXIAL NOZZLE. GAS INPUT, 2190 CF/hr; EXCESS OXYGEN, 3.3%; PREHEATED AIR, 310^{0}F

concentrations of oxygen and methane. Figure II-128 shows the tangential velocity component. The raw data are shown in Table II-19.

Figure II-129 shows a composite plot of CO, CO_2, CH_4, NO, and O_2 at an axial position of 48.3 cm. The methane concentration has decreased from above 23 to 2% on the burner center. In contrast, the CO is still maintaining readings of 6% in the region of the burner block. The CO_2 concentration (curve D) maintains a relatively constant value of 10% except in the burner block region. The nitric oxide concentration (curve N) was 116 ppm at the center line and increases to 170 ppm near the sidewall as the radial position is charged in a positive direction. Oxygen (curve O) was 0.26% at the center line and increases to about 4.5% near the perimeter of the burner block opening. Data plots with greater resolution are given in Figures II-130 to II-134 and the raw data in Table II-20.

Figure II-135 shows the temperature profile at the axial position 48.3 cm. The "cold" spots have disappeared and the high-temperature regions have shifted their peaks to radial positions of 9 cm and −21 cm.

Figure II-136 displays the axial component of velocity as a function of radial position at 48.3 cm. It is interesting that the shapes of the axial velocity curve and the temperature profile curve are very similar. The peak velocities occur at radial positions of 21 cm and −12 cm in sharp contrast to the position of the temperature peaks. The tangential velocity, shown in Figure II-137, has decreased 60% from its value at the 7.6-cm axial positions. It is also showing a large scattering of data points on the negative side of the burner center line. The raw data are presented in Table II-21.

The composite plot of the gas species concentrations for an axial position of 91 cm is displayed in Figure II-138. There is only a trace of methane present at this axial position. The oxygen (O curve) still shows a higher concentration on the left of the burner center line (positive radial position) than the right, with a 50% decrease in average value in the region of the burner block. The carbon dioxide (curve D) and the nitric oxide (curve N) have reached relatively constant values of 10% and 150 ppm, respectively. The carbon monoxide (curve C) has a peak value of 1.9% on the axis of the burner and drops to 400 ppm near the sidewalls.

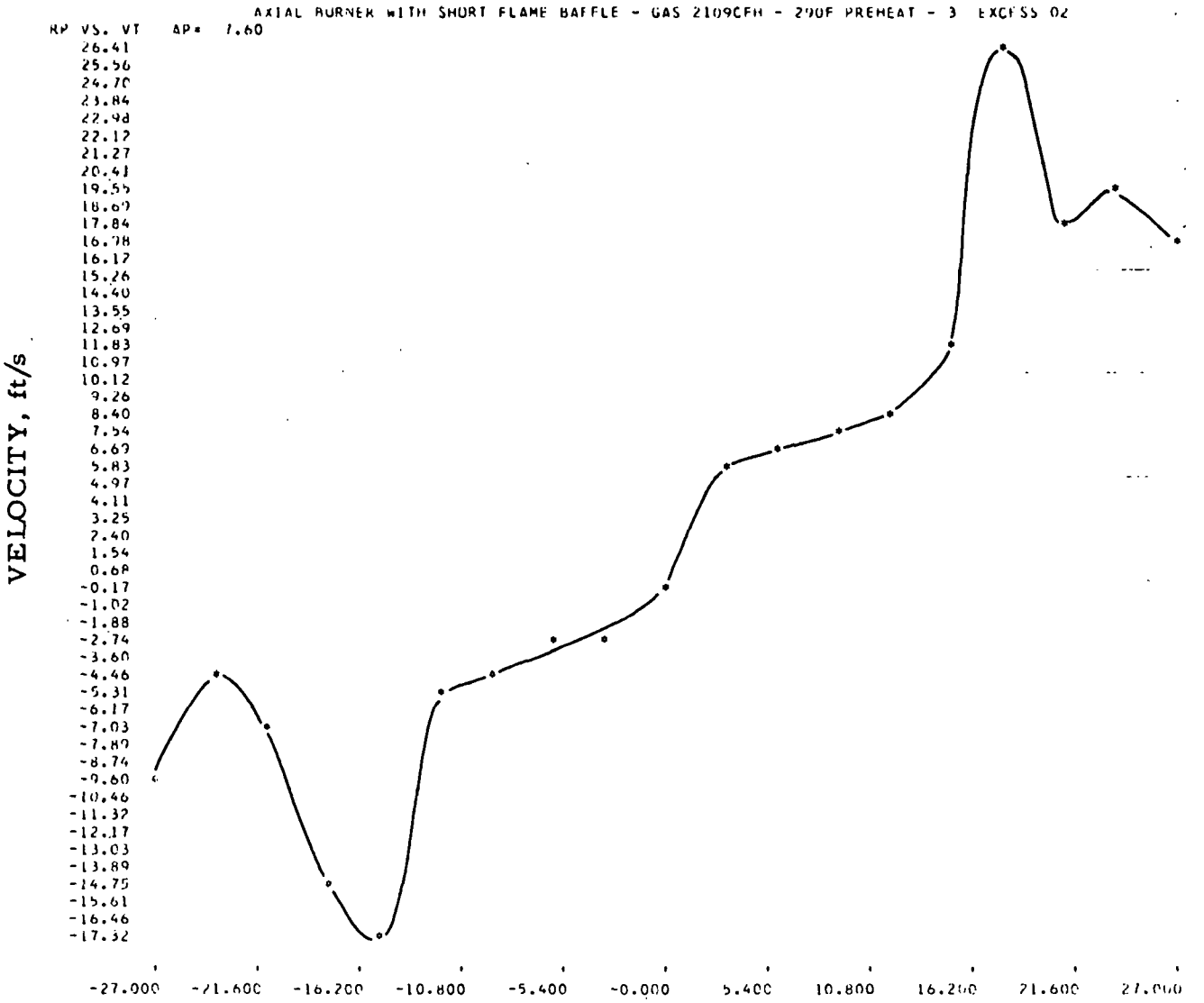

Figure II-128. RADIAL VELOCITY PROFILE (Tangential Component) AT AN AXIAL POSITION OF 7.6 cm FOR THE SHORT-FLAME BAFFLE USING THE AXIAL NOZZLE. GAS INPUT, 2190 CF/hr; EXCESS OXYGEN, 3.3%; PREHEATED AIR, 310°F

Table II-19. RAW (Velocity) DATA FOR SHORT-FLAME BAFFLE BURNER

AERODYNAMIC MODELING OF COMBUSTION BURNERS

CALIBRATION COEFFICIENTS FOR FORWARD FLOW

A1 =	0.770590	A2 =	0.272353	A3 =	-0.059818
B0 =	0.737720	B2 =	-0.158821	B4 =	0.129246
C =	4.464660	D =	0.394812		

AXIAL BURNER WITH SHORT FLAME BAFFLE - GAS 2109CFH - 290F PREHEAT - 3 EXCESS 02

TOTAL DATA INPUT

THETA	AP	RP	P13	P03	P24	P04	P0A	T	PB
0.	7.6	-27.0	-6.04	-0.24	0.07	-0.15	-1.34	2375.	760.
0.	7.6	-24.0	-1.24	-0.14	-0.47	-0.37	-0.06	2154.	760.
0.	7.6	-21.0	-2.84	16.45	14.72	23.46	22.20	2167.	760.
0.	7.6	-18.0	11.53	24.07	-27.72	3.61	18.02	2882.	760.
0.	7.6	-15.0	5.47	5.64	-15.67	-9.13	-10.82	2856.	760.
0.	7.6	-12.0	3.54	-1.14	-6.11	-6.32	-17.14	2543.	760.
0.	7.6	-9.0	-4.00	-2.09	-0.96	-2.01	-17.85	2361.	760.
0.	7.6	-6.0	-1.48	-0.82	0.44	0.04	-15.89	2232.	760.
0.	7.6	-3.0	-2.48	0.28	1.69	0.66	-14.60	2128.	760.
0.	7.6	0.0	-5.74	0.67	6.19	4.31	-11.66	2076.	760.
0.	7.6	3.0	-11.34	0.64	4.52	0.88	-5.23	2076.	760.
0.	7.6	6.0	-8.03	0.51	-2.16	4.07	-5.44	2102.	760.
0.	7.6	9.0	-5.72	-0.80	-3.28	-0.14	-8.48	2258.	760.
0.	7.6	12.0	-4.81	-0.64	-1.24	-0.78	-10.21	2478.	760.
0.	7.6	15.0	-7.45	-2.69	2.23	-0.16	-10.85	2673.	760.
0.	7.6	18.0	-42.06	-9.42	27.52	17.90	-2.90	2400.	760.
0.	7.6	21.0	-49.38	4.25	24.24	41.29	31.76	2062.	760.
0.	7.6	24.0	-20.02	-0.23	2.39	-0.81	-0.41	2439.	760.
0.	7.6	27.0	-16.25	-0.32	-0.39	-0.59	-0.40	2478.	760.

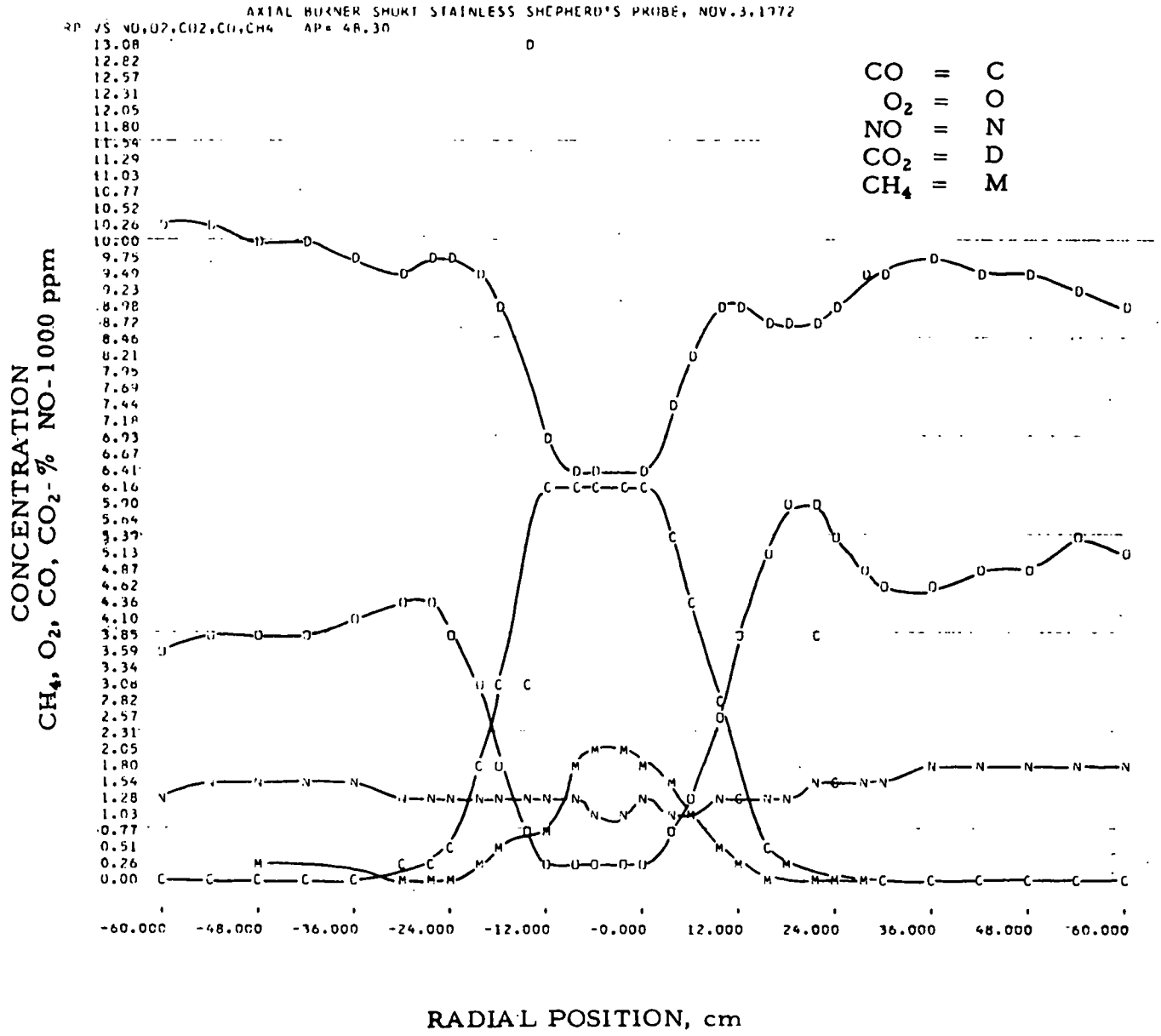

Figure II-129. COMPOSITE PLOT OF GAS SAMPLING PROFILES FOR CO, CO_2, CH_4, NO, AND O_2 FOR THE SHORT-FLAME BAFFLE USING THE AXIAL NOZZLE AT AN AXIAL POSITION OF 48.3 cm. GAS INPUT, 2190 CF/hr; EXCESS OXYGEN, 3.0%; PREHEATED AIR, 315^{0}F

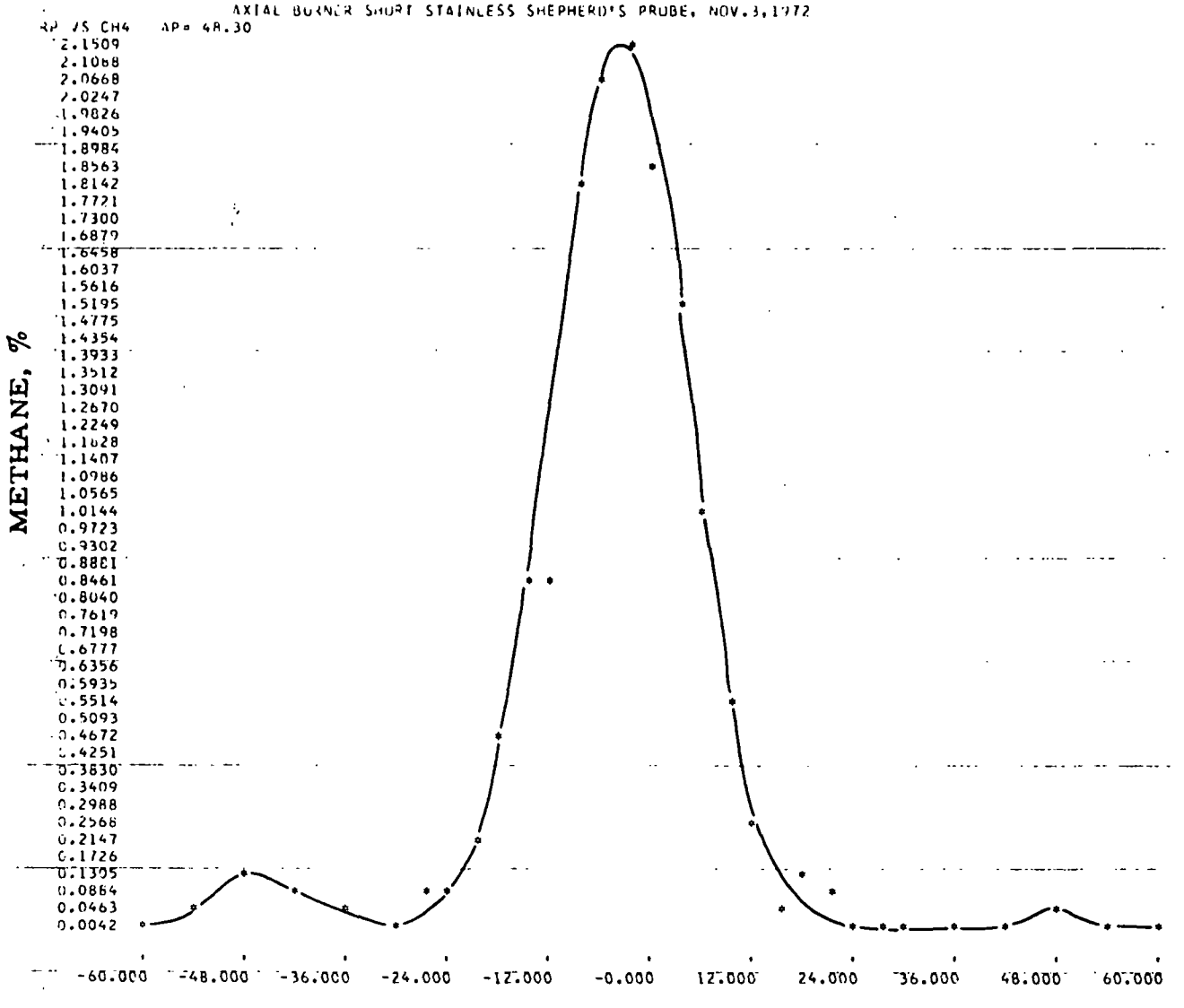

Figure II-130. RADIAL COMPOSITION PROFILE FOR METHANE (CH_4) FOR THE SHORT-FLAME BAFFLE USING THE AXIAL NOZZLE AT AN AXIAL POSITION OF 48.3 cm. GAS INPUT, 2190 CF/hr; EXCESS OXYGEN, 3.0%; PREHEATED AIR, 315^{0}F

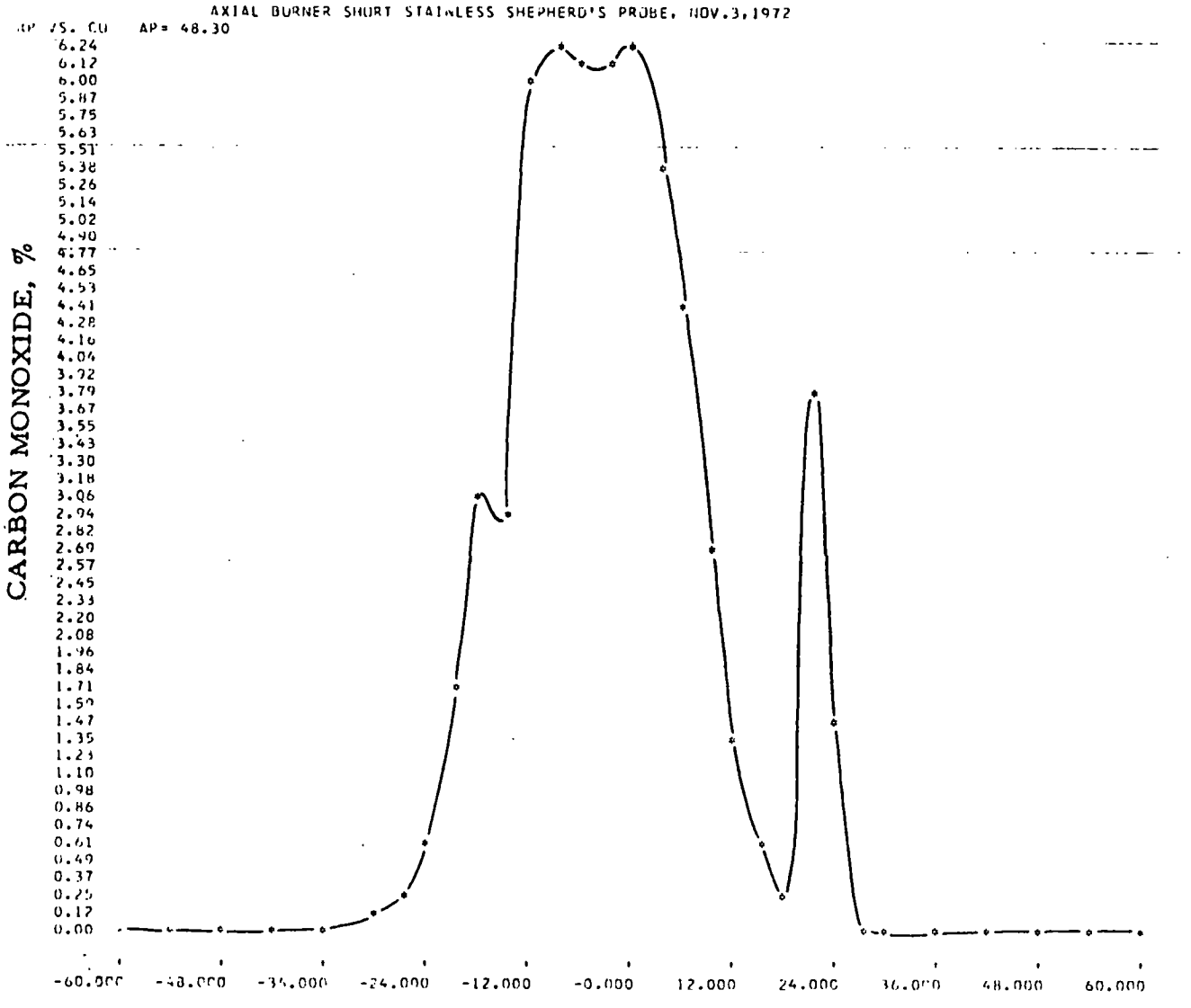

Figure II-131. RADIAL COMPOSITION PROFILE FOR CARBON MONOXIDE (CO) FOR THE SHORT-FLAME BAFFLE USING THE AXIAL NOZZLE AT AN AXIAL POSITION OF 48.3 cm. GAS INPUT, 2190 CF/hr; EXCESS OXYGEN, 3.0%; PREHEATED AIR, 315^{0}F

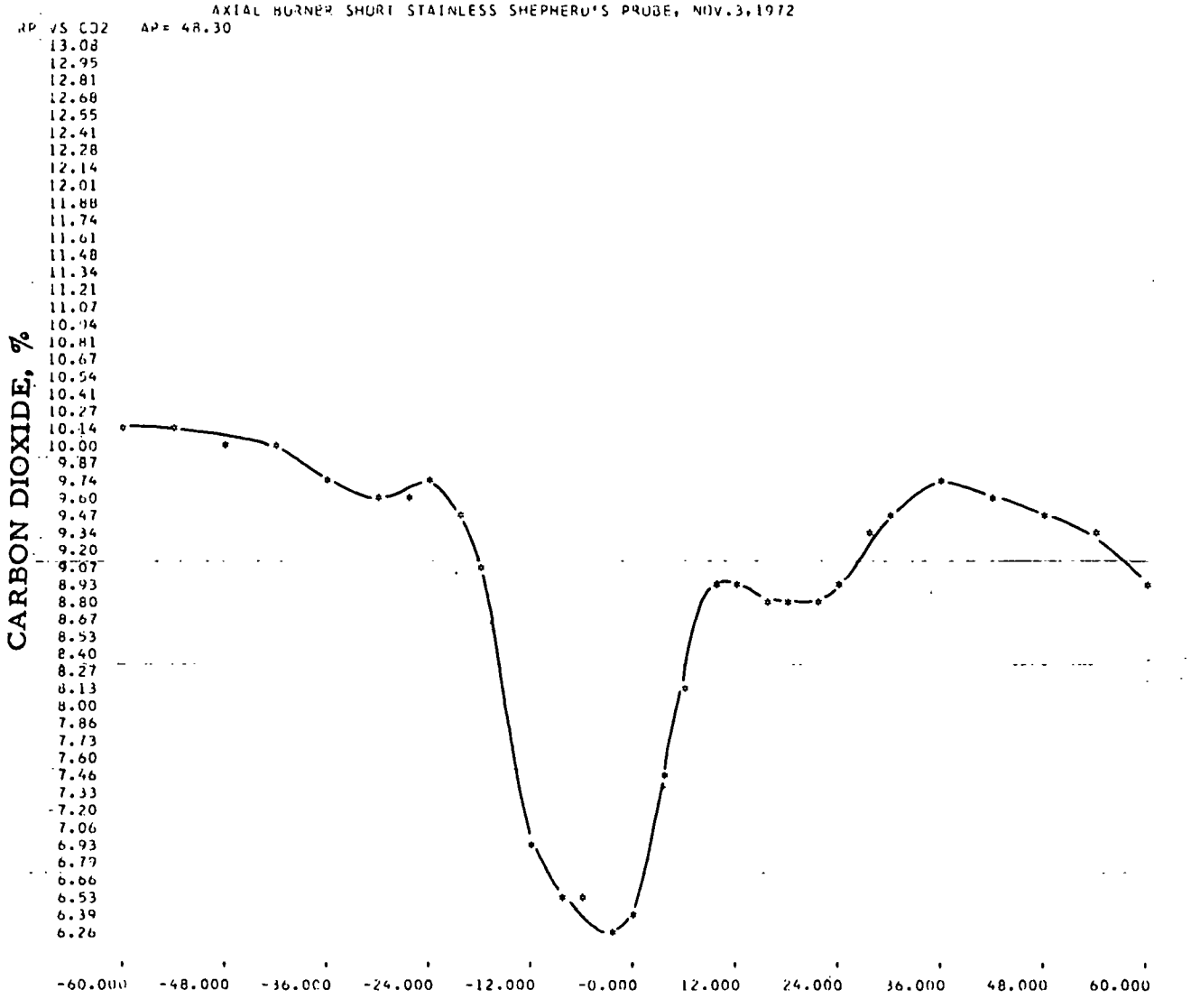

Figure II-132. RADIAL COMPOSITION PROFILE FOR CARBON DIOXIDE (CO_2) FOR THE SHORT-FLAME BAFFLE USING THE AXIAL NOZZLE AT AN AXIAL POSITION OF 48.3 cm. GAS INPUT, 2190 CF/hr; EXCESS OXYGEN, 3.0%; PREHEATED AIR, 315°F

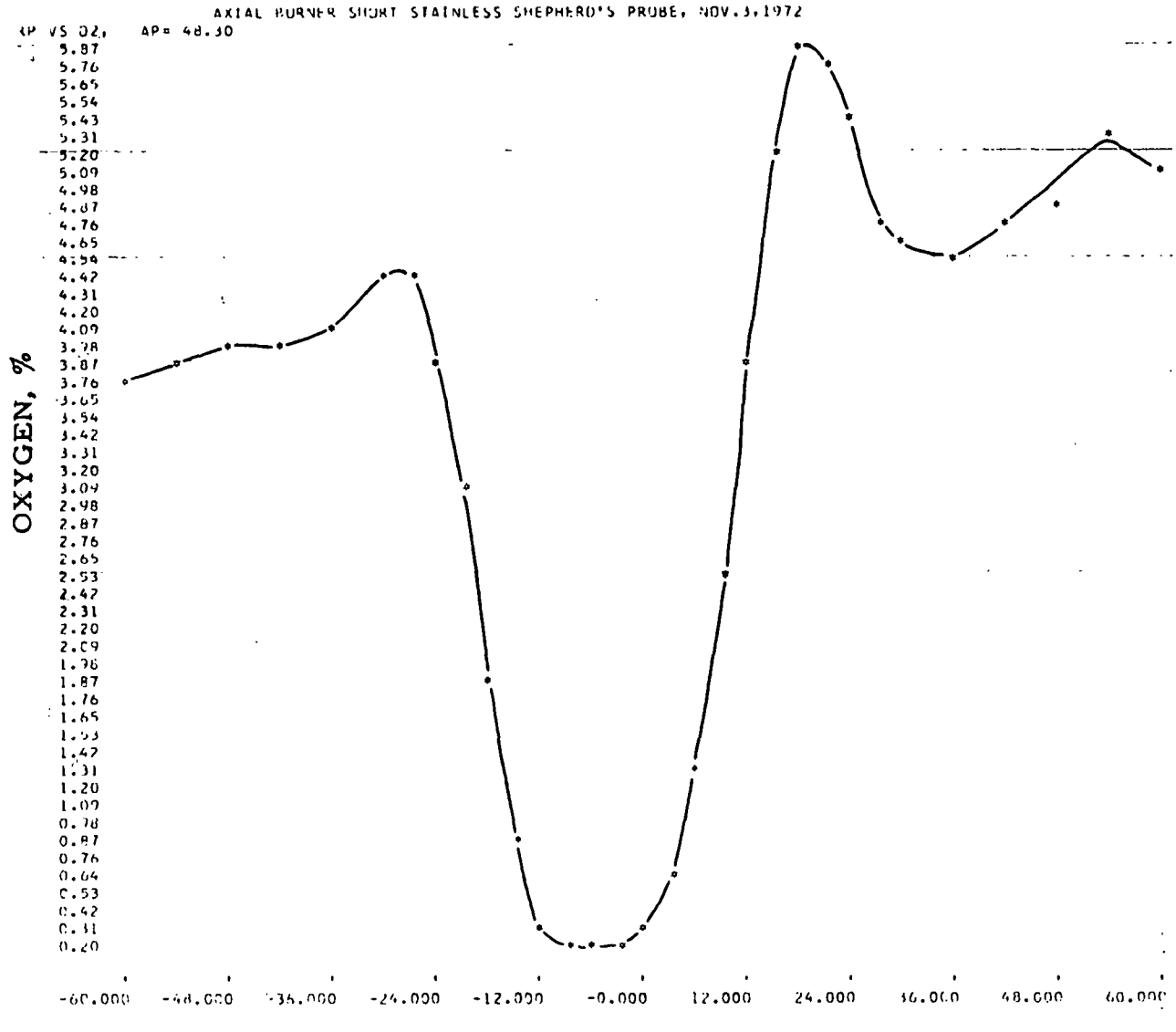

Figure II-133. RADIAL COMPOSITION PROFILE FOR OXYGEN (O_2) FOR THE SHORT-FLAME BAFFLE USING THE AXIAL NOZZLE AT AN AXIAL POSITION OF 48.3 cm. GAS INPUT, 2190 CF/hr; EXCESS OXYGEN, 3.0%; PREHEATED AIR, 315^{0}F

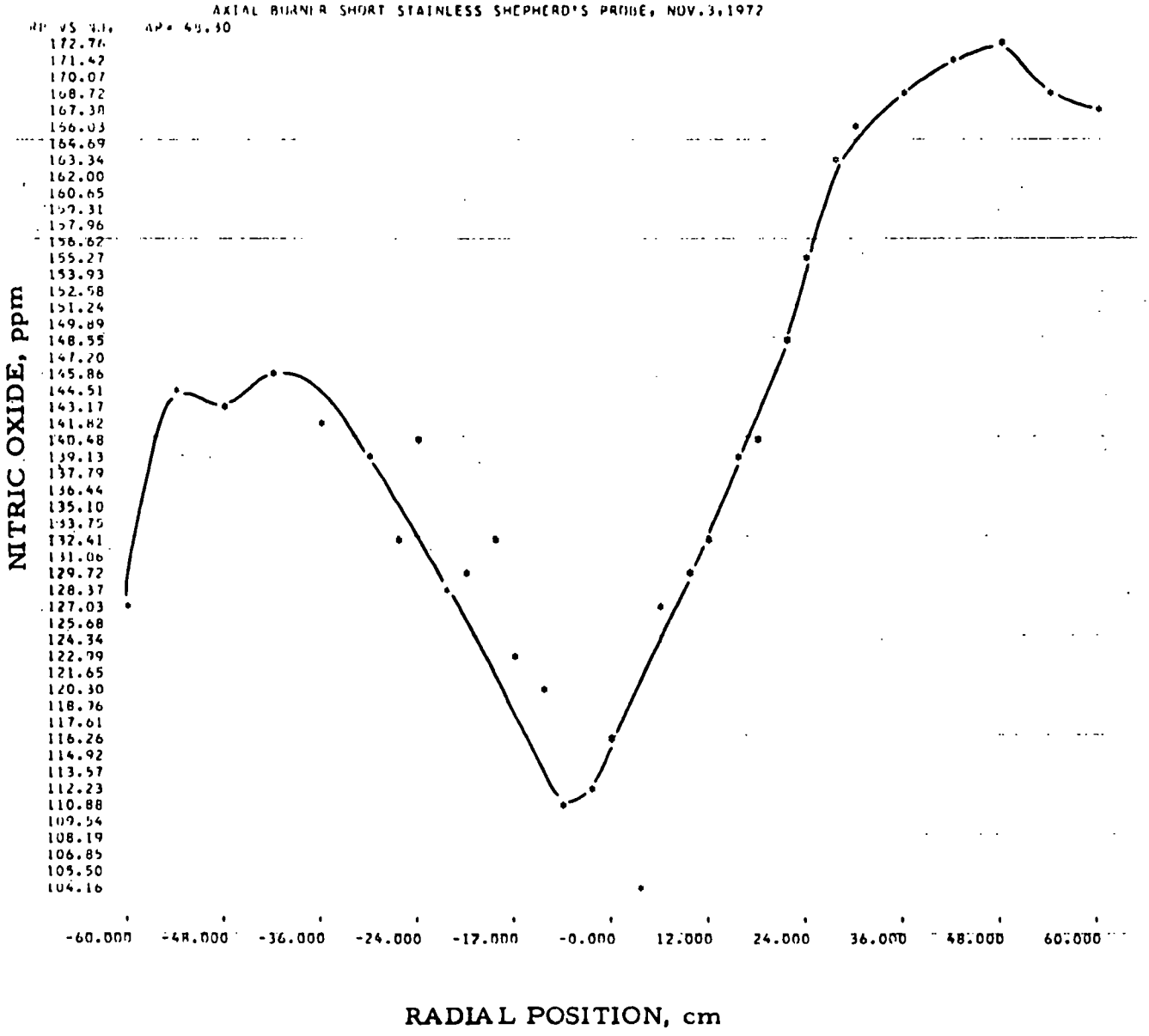

Figure II-134. RADIAL COMPOSITION PROFILE FOR NITRIC OXIDE (NO) FOR THE SHORT-FLAME BAFFLE USING THE AXIAL NOZZLE AT AN AXIAL POSITION OF 48.3 cm. GAS INPUT, 2190 CF/hr; EXCESS OXYGEN, 3.0%; PREHEATED AIR, 315^{0}F

Table II-20. RAW (Gas Analysis) DATA FOR SHORT-FLAME BAFFLE BURNER

TRACER GAS STUDIES OF COMBUSTION BURNERS PROGRAM 2
AXIAL BURNER SHORT STAINLESS SHEPHERD'S PROBE, NOV.3,1972

INPUT GAS 2190 WALL TEMPERATURE 2572 PREHEAT TEMPERATURE 310
OUTPUT ANALYSIS
NITROGEN OXIDE 21.20 PERCENT ON RANGE 1, 183.50 PPM OXYGEN 3.12 PERCENT
CARBON DIOXIDE 81.90 PERCENT ON RANGE 1, 10.51 PERCENT
CARBON MONOXIDE 4.80 PERCENT ON RANGE 3, 0.001 PERCENT
METHANE 0.00 PERCENT ON RANGE 0, 0.00 PERCENT

EXPERIMENTAL RESULTS

		NITROGEN OXIDE -NO			OXYGEN	CARBON DIOXIDE-CO2			CARBON MONOXIDE -CO			METHANE - CH4		
AP	RP	RANGE	X	Y	O2	RANGE	X	Y	RANGE	X	Y	RANGE	X	Y
48.30	-60.00	1	14.80	126.7	3.72	1	80.30	10.17	3	4.90	0.002	3	0.00	0.00
48.30	-54.00	1	16.80	144.3	3.88	1	80.30	10.17	3	4.20	0.001	3	1.20	0.05
48.30	-48.00	1	16.70	143.4	3.93	1	79.60	10.03	3	6.70	0.002	3	3.30	0.14
48.30	-42.00	1	17.00	146.1	3.97	1	79.50	10.00	3	7.40	0.003	3	1.60	0.07
48.30	-36.00	1	16.50	141.7	4.12	1	78.40	9.78	3	20.90	0.008	3	0.80	0.03
48.30	-30.00	1	16.20	139.0	4.42	1	77.50	9.59	2	9.00	0.147	3	0.00	0.00
48.30	-27.00	1	15.50	132.9	4.42	1	77.80	9.65	2	17.20	0.286	3	2.20	0.09
48.30	-24.00	1	16.40	140.8	3.87	1	78.00	9.69	2	34.30	0.592	3	2.10	0.09
48.30	-21.00	1	15.00	128.5	3.06	1	76.60	9.41	1	47.40	1.698	3	4.60	0.19
48.30	-18.00	1	15.20	130.2	1.85	1	75.00	9.08	1	72.20	3.064	3	11.10	0.47
48.30	-15.00	1	15.40	132.0	0.84	1	93.20	13.08	1	71.10	2.996	3	19.30	0.84
48.30	-12.00	1	14.40	123.2	0.30	1	63.60	6.94	1	113.10	6.038	3	18.90	0.82
48.30	-9.00	1	14.00	119.7	0.23	1	61.10	6.51	1	115.50	6.240	3	40.00	1.80
48.30	-6.00	1	13.00	111.0	0.21	1	61.20	6.52	1	114.70	6.172	3	45.50	2.07
48.30	-3.00	1	13.10	111.9	0.20	1	59.60	6.25	1	114.10	6.122	3	47.00	2.15
48.30	0.00	1	13.60	116.3	0.33	1	60.70	6.44	1	114.80	6.181	3	41.10	1.86
48.30	3.00	1	12.20	104.1	0.69	1	66.70	7.50	1	105.50	5.417	3	33.80	1.51
48.30	6.00	1	14.80	126.7	1.26	1	70.40	8.19	1	91.50	4.355	3	22.80	1.00
48.30	9.00	1	15.10	129.4	2.48	1	74.00	8.88	1	66.10	2.697	3	12.30	0.53
48.30	12.00	1	15.50	132.9	3.88	1	74.50	8.98	1	38.80	1.301	3	6.10	0.26
48.30	15.00	1	16.20	139.0	5.24	1	73.70	8.82	2	33.30	0.574	3	1.40	0.06
48.30	18.00	1	16.30	139.9	5.87	1	73.30	8.75	2	14.00	0.231	3	3.00	0.13
48.30	21.00	1	17.20	147.8	5.81	1	73.70	8.82	1	83.90	3.823	3	2.30	0.10
48.30	24.00	1	18.10	155.8	5.38	1	73.90	8.86	1	42.40	1.462	3	0.30	0.01
48.30	27.00	1	19.00	163.8	4.81	1	76.40	9.36	3	17.90	0.007	3	0.00	0.00
48.30	30.00	1	19.30	166.5	4.68	1	76.80	9.45	3	6.70	0.002	3	0.00	0.00
48.30	36.00	1	19.50	168.2	4.56	1	78.10	9.71	3	4.90	0.002	3	0.00	0.00
48.30	42.00	1	19.80	170.9	4.80	1	77.50	9.59	3	5.00	0.002	3	0.00	0.00
48.30	48.00	1	20.00	172.7	4.86	1	76.60	9.41	3	4.50	0.001	3	1.30	0.05
48.30	54.00	1	19.60	169.1	5.26	1	75.90	9.26	3	5.10	0.002	3	0.00	0.00
48.30	60.00	1	19.40	167.4	5.06	1	74.40	8.96	3	4.20	0.001	3	0.00	0.00

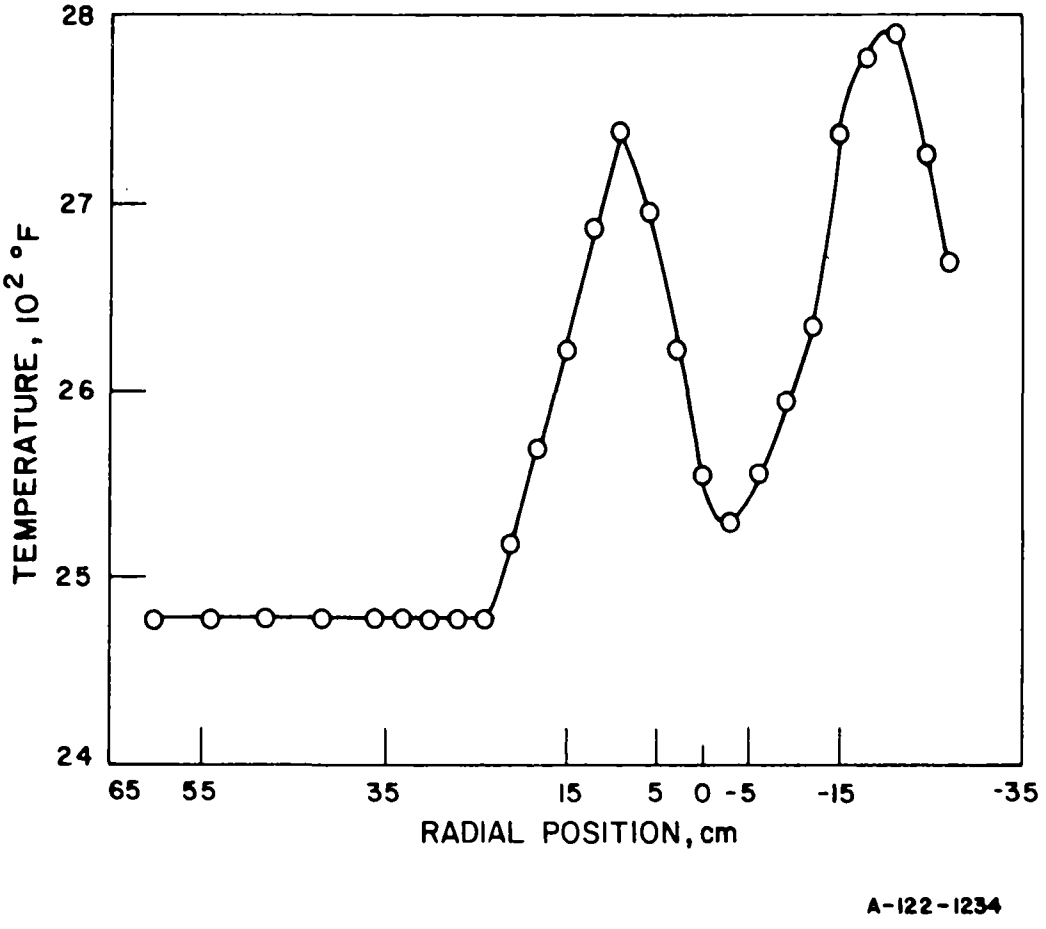

Figure II-135. AXIAL TEMPERATURE PROFILE FROM SHORT-FLAME AXIAL NOZZLE BAFFLE BURNER AT A 48.3-cm AXIAL POSITION. GAS INPUT, 2190 CF/hr; EXCESS OXYGEN, 3.3%; PREHEAT TEMPERATURE, 310°F

Data plots of gas composition for an axial position of 91 cm are given in Figures II-139 to II-143 with greater resolution. The raw data are shown in Table II-22.

The temperature profile for a 91-cm axial position is shown in Figure II-144. The flame front is still fairly well defined, with a peak temperature of 2800°F at the burner center line decreasing to 2500°F out near the walls.

The axial component of velocity data is shown in Figure II-145 for an axial position of 97.4 cm. Unlike the temperature profile, the axial velocity profile has maintained the same quantitative shape that it displayed at the 48.3-cm axial position. The velocity peaks occur at −9

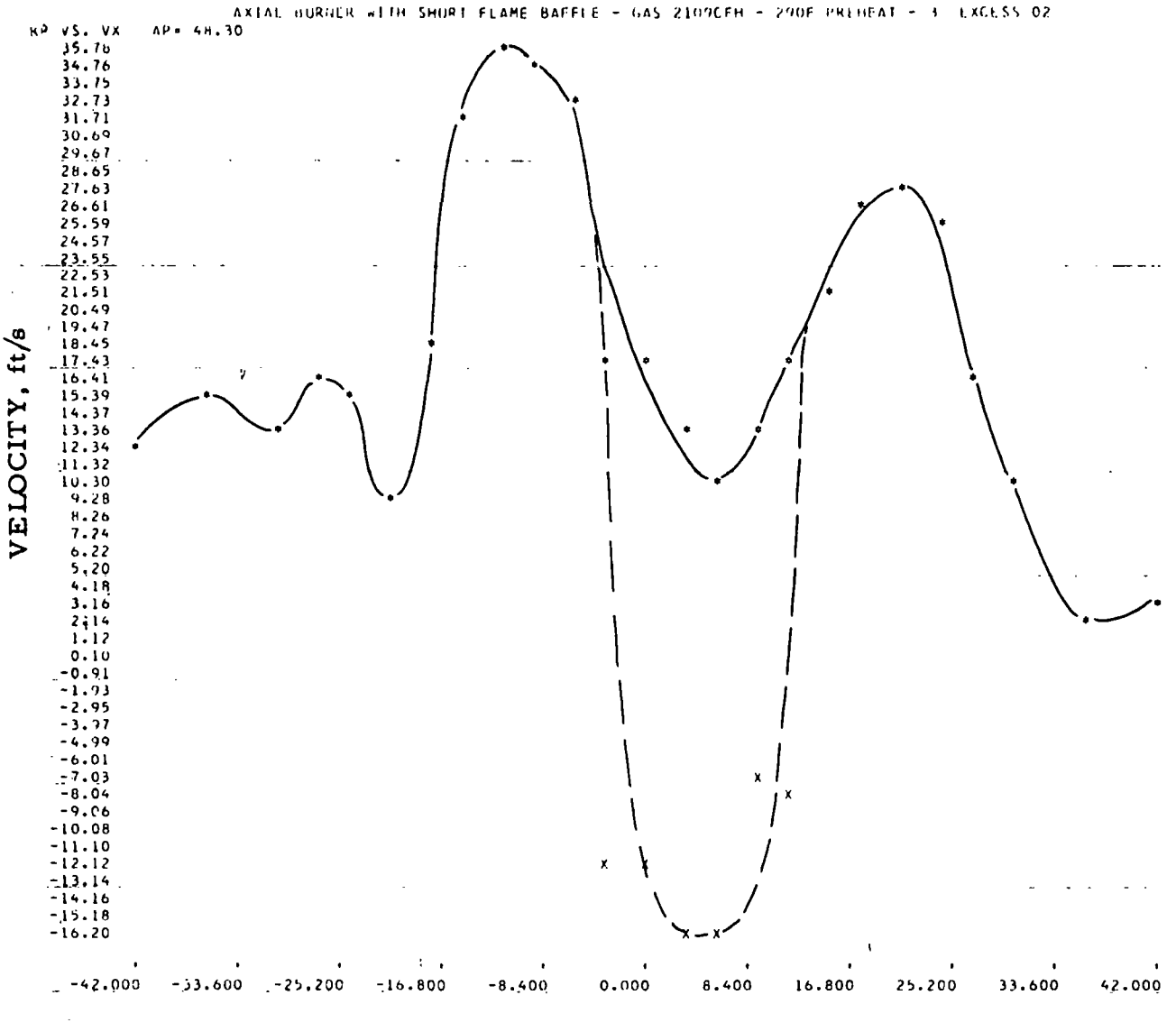

Figure II-136. RADIAL VELOCITY PROFILE (Axial Component) AT AN AXIAL POSITION OF 48.3 cm FOR THE SHORT-FLAME BAFFLE USING THE AXIAL NOZZLE. GAS INPUT, 2190 CF/hr; EXCESS OXYGEN, 3.0%; PREHEATED AIR, 310°F

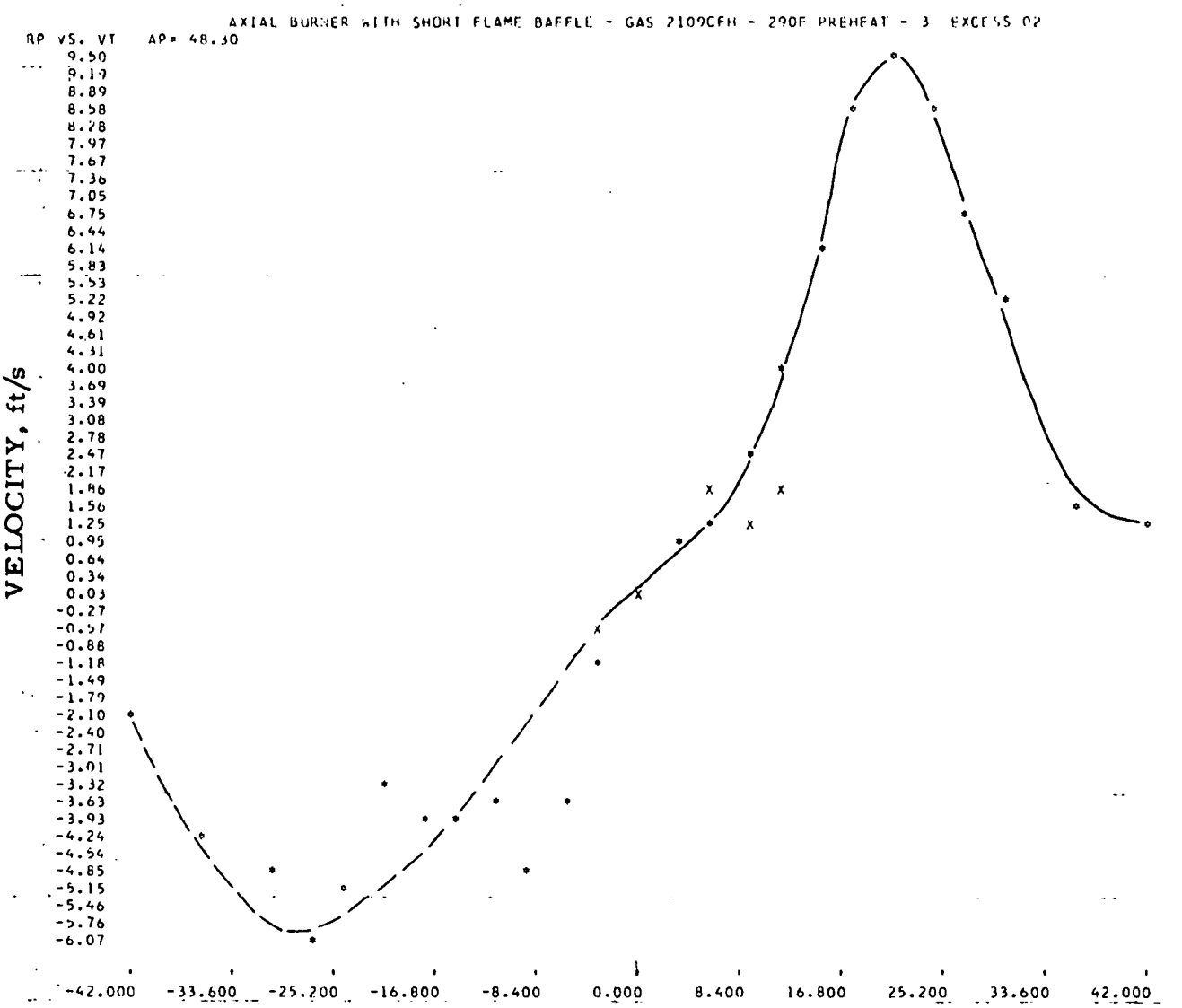

Figure II-137. RADIAL VELOCITY PROFILE (Tangential Component) AT AN AXIAL POSITION OF 48.3 cm FOR THE SHORT-FLAME BAFFLE USING THE AXIAL NOZZLE. GAS INPUT, 2190 CF/hr; EXCESS OXYGEN, 3.0%; PREHEATED AIR, 290^{0}F

Table II-21. RAW (Velocity) DATA FOR SHORT-FLAME BAFFLE BURNER

AERODYNAMIC MODELING OF COMBUSTION BURNERS

CALIBRATION COEFFICIENTS FOR FORWARD FLOW

A1 =	0.770590	A2 =	0.272353	A3 =	-0.059818
B0 =	0.737720	B2 =	-0.158821	B4 =	0.129246
C =	4.464660	D =	0.394812		

AXIAL BURNER WITH SHORT FLAME BAFFLE - GAS 2109CFH - 290F PREHEAT - 3 EXCESS 02

TOTAL DATA INPUT

THETA	AP	RP	P13	P03	P24	P04	P0A	T	PB
0.	48.3	-42.0	-1.35	0.82	-0.29	1.48	1.19	2478.	760.
0.	48.3	-36.0	-3.00	1.27	0.28	1.79	2.28	2480.	760.
0.	48.3	-30.0	-3.64	-0.05	-1.30	0.62	-0.01	2600.	760.
0.	48.3	-27.0	-5.24	0.79	-0.31	0.76	-0.16	2673.	760.
0.	48.3	-24.0	-4.47	0.73	-0.33	1.02	-0.42	2725.	760.
0.	48.3	-21.0	1.16	1.69	1.66	1.21	-0.02	2790.	760.
0.	48.3	-18.0	3.47	4.56	2.37	4.36	2.13	2777.	760.
0.	48.3	-15.0	5.72	11.56	2.90	10.96	11.35	2738.	760.
0.	48.3	-12.0	5.78	15.38	-1.86	9.99	9.98	2634.	760.
0.	48.3	-9.0	3.16	15.93	-6.68	4.74	7.06	2595.	760.
0.	48.3	-6.0	0.59	13.67	-10.02	1.24	2.36	2556.	760.
0.	48.3	-3.0	-1.01	4.96	-6.60	-4.38	-8.16	2530.	760.
0.	48.3	0.0	-1.37	1.04	-4.96	1.42	-8.53	2556.	760.
0.	48.3	3.0	-3.73	-0.48	-5.37	-1.65	-8.11	2621.	760.
0.	48.3	6.0	-6.39	-2.98	-4.21	-1.54	-8.31	2699.	760.
0.	48.3	9.0	-12.03	-6.85	-3.77	-0.08	-7.07	2738.	760.
0.	48.3	12.0	-16.06	-9.34	-2.52	2.66	-3.59	2686.	760.
0.	48.3	15.0	-17.69	-9.66	-0.93	6.25	1.90	2621.	760.
0.	48.3	18.0	-20.13	-8.79	-1.06	9.35	7.57	2569.	760.
0.	48.3	21.0	-18.47	-6.03	-3.41	8.67	11.23	2517.	760.
0.	48.3	24.0	-13.96	-2.99	-4.50	5.25	7.35	2478.	760.
0.	48.3	27.0	-7.44	-2.20	-3.30	1.60	2.79	2478.	760.
0.	48.3	30.0	-4.17	-1.55	-1.74	0.30	-0.62	2478.	760.
0.	48.3	36.0	-0.55	-0.33	-0.12	-0.06	-1.27	2478.	760.
0.	48.3	42.0	-0.17	0.07	0.04	0.07	-0.82	2478.	760.
180.	48.3	-3.0	-1.82	1.02	1.08	1.11	-7.78	2530.	760.
180.	48.3	0.0	-2.57	0.54	0.73	1.14	-9.00	2556.	760.
180.	48.3	3.0	-6.41	0.83	0.57	0.36	-9.01	2621.	760.
180.	48.3	6.0	-4.82	0.26	-0.46	1.42	-8.21	2699.	760.
180.	48.3	9.0	7.88	-0.33	-0.01	0.78	-6.27	2738.	760.
180.	48.3	12.0	5.37	0.03	-0.36	1.21	-4.15	2686.	760.

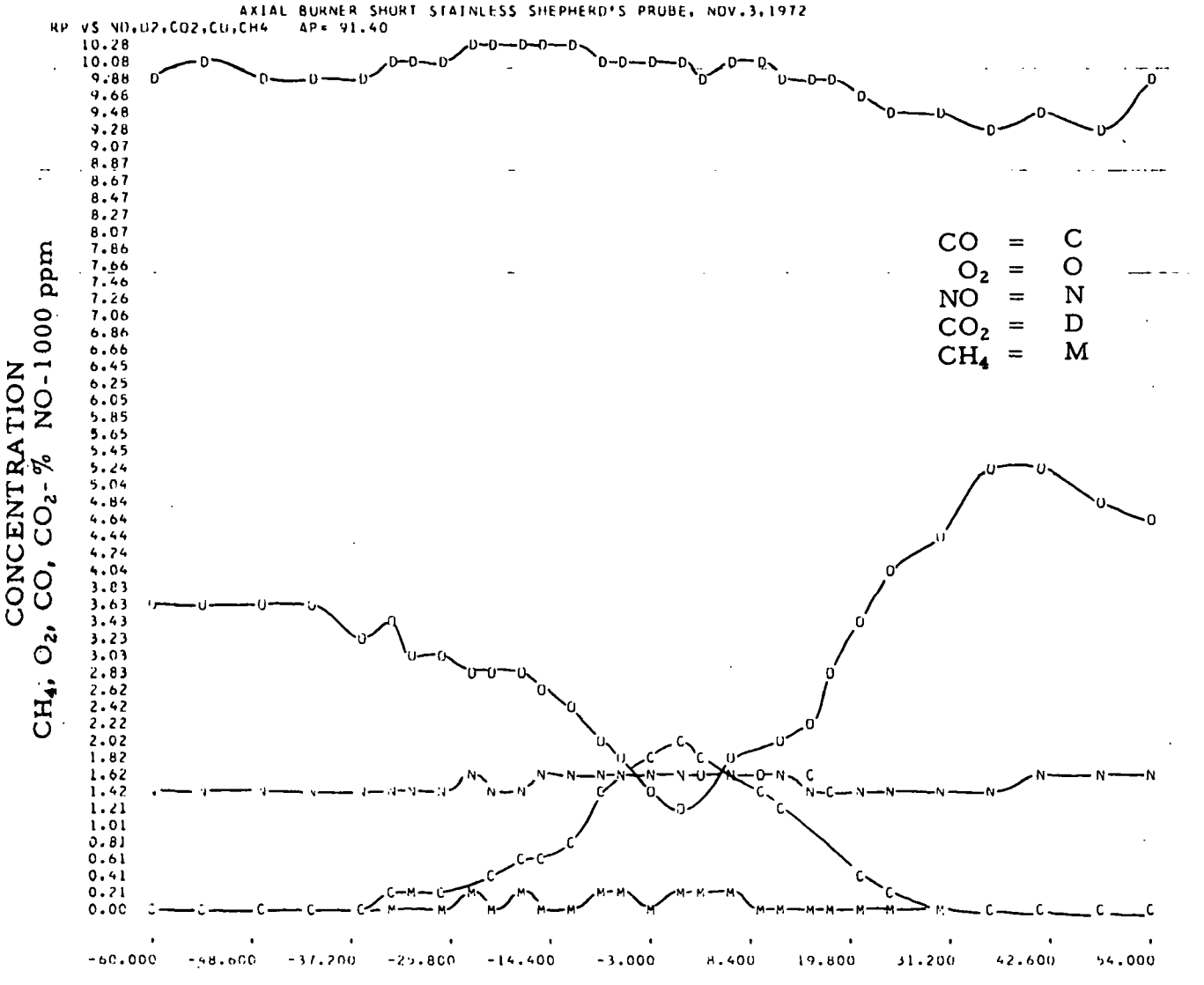

Figure II-138. COMPOSITE PLOT OF GAS SAMPLING PROFILES FOR CO, CO_2, CH_4, NO, AND O_2 FOR THE SHORT-FLAME BAFFLE USING THE AXIAL NOZZLE AT AN AXIAL POSITION OF 91.4 cm. GAS INPUT, 2190 CF/hr; EXCESS OXYGEN, 3.0%; PREHEATED AIR, 290°F

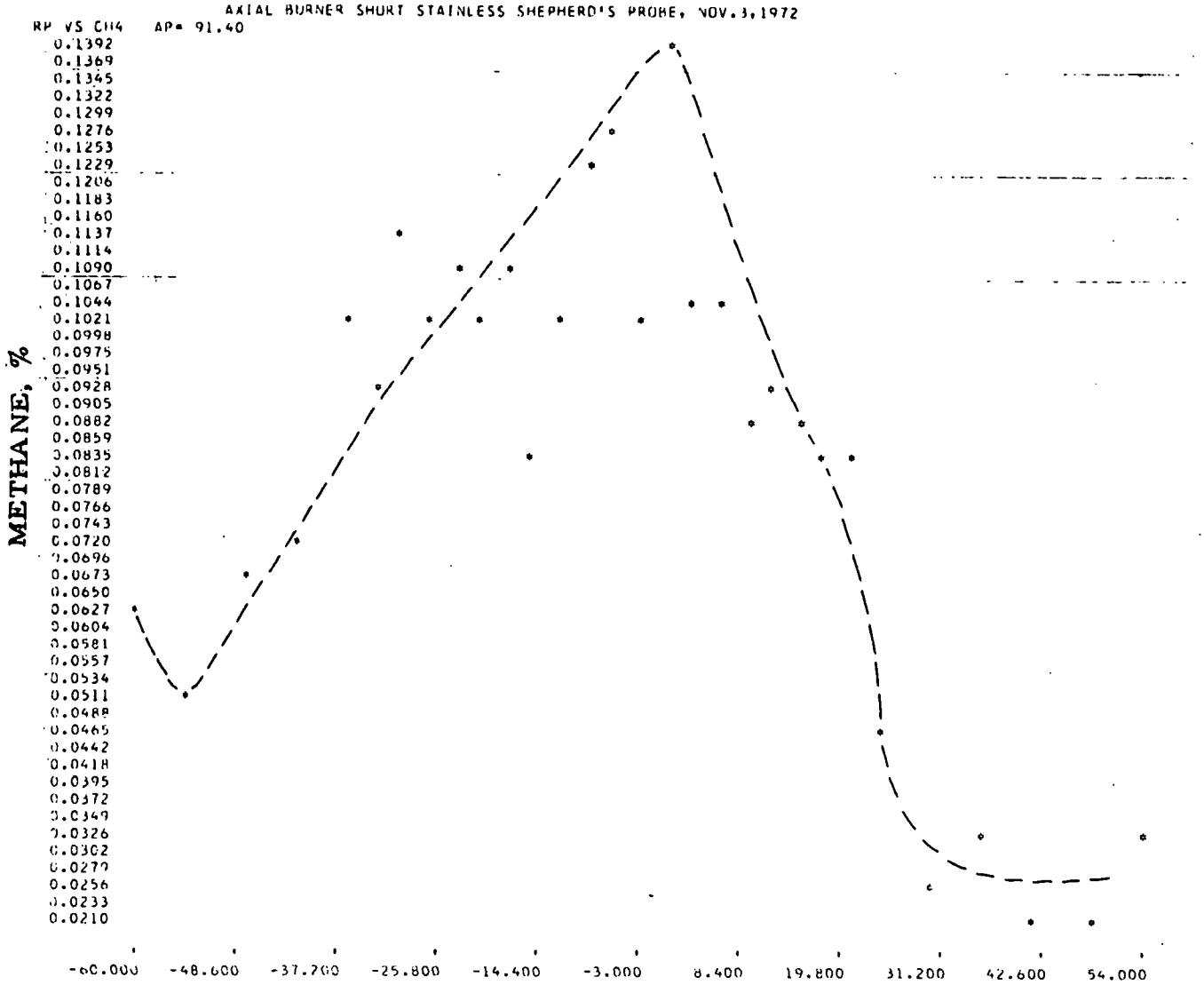

Figure II-139. RADIAL COMPOSITION PROFILE FOR METHANE (CH_4) FOR THE SHORT-FLAME BAFFLE USING THE AXIAL NOZZLE AT AN AXIAL POSITION OF 91.4 cm. GAS INPUT, 2190 CF/hr; EXCESS OXYGEN, 3.0%; PREHEATED AIR, 315^{0}F

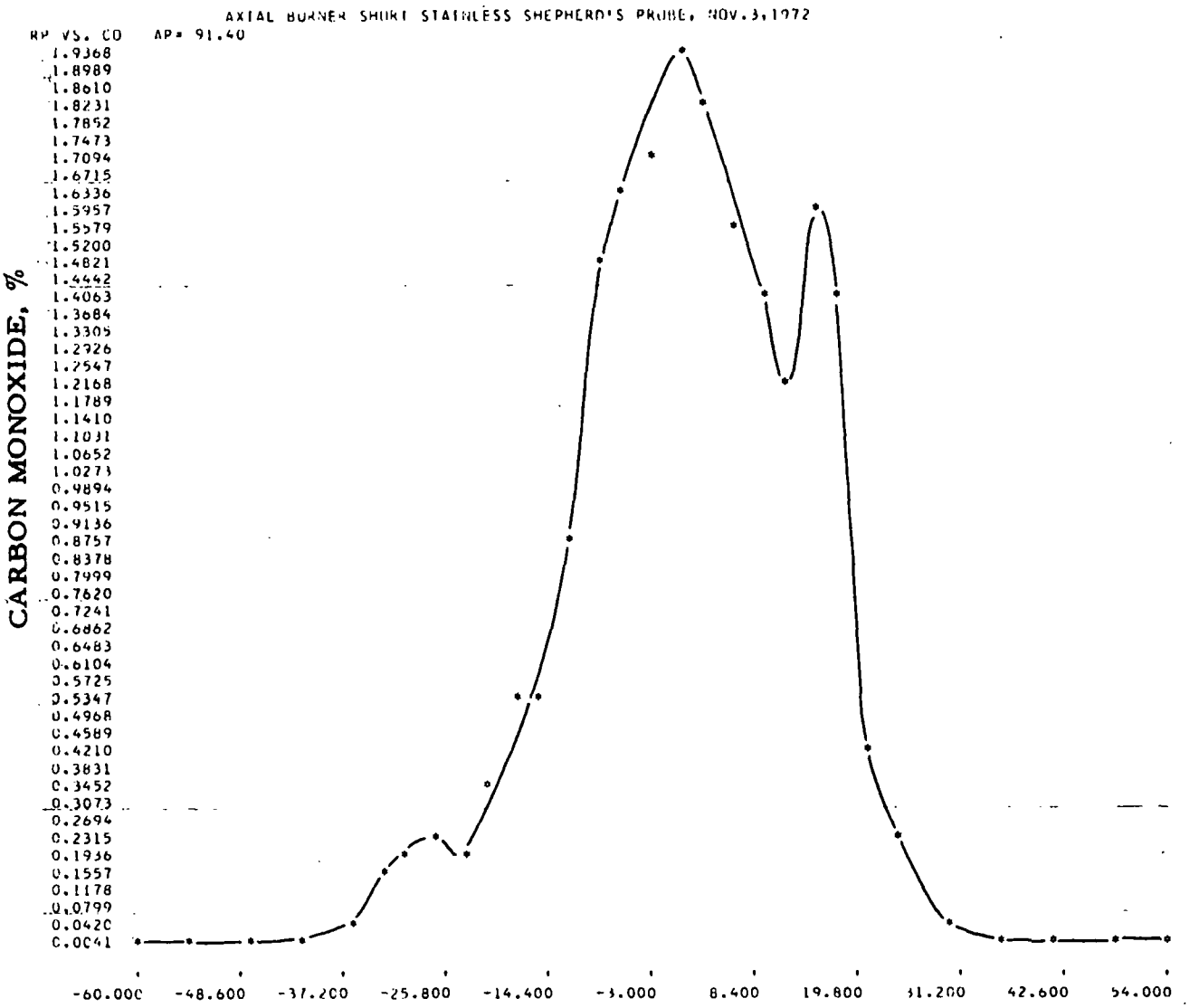

Figure II-140. RADIAL COMPOSITION PROFILE FOR CARBON MONOXIDE (CO) FOR THE SHORT-FLAME BAFFLE USING THE AXIAL NOXXLE AT AN AXIAL POSITION OF 91.4 cm. GAS INPUT, 2190 CF/hr; EXCESS OXYGEN, 3.0%; PREHEATED AIR, 315°F

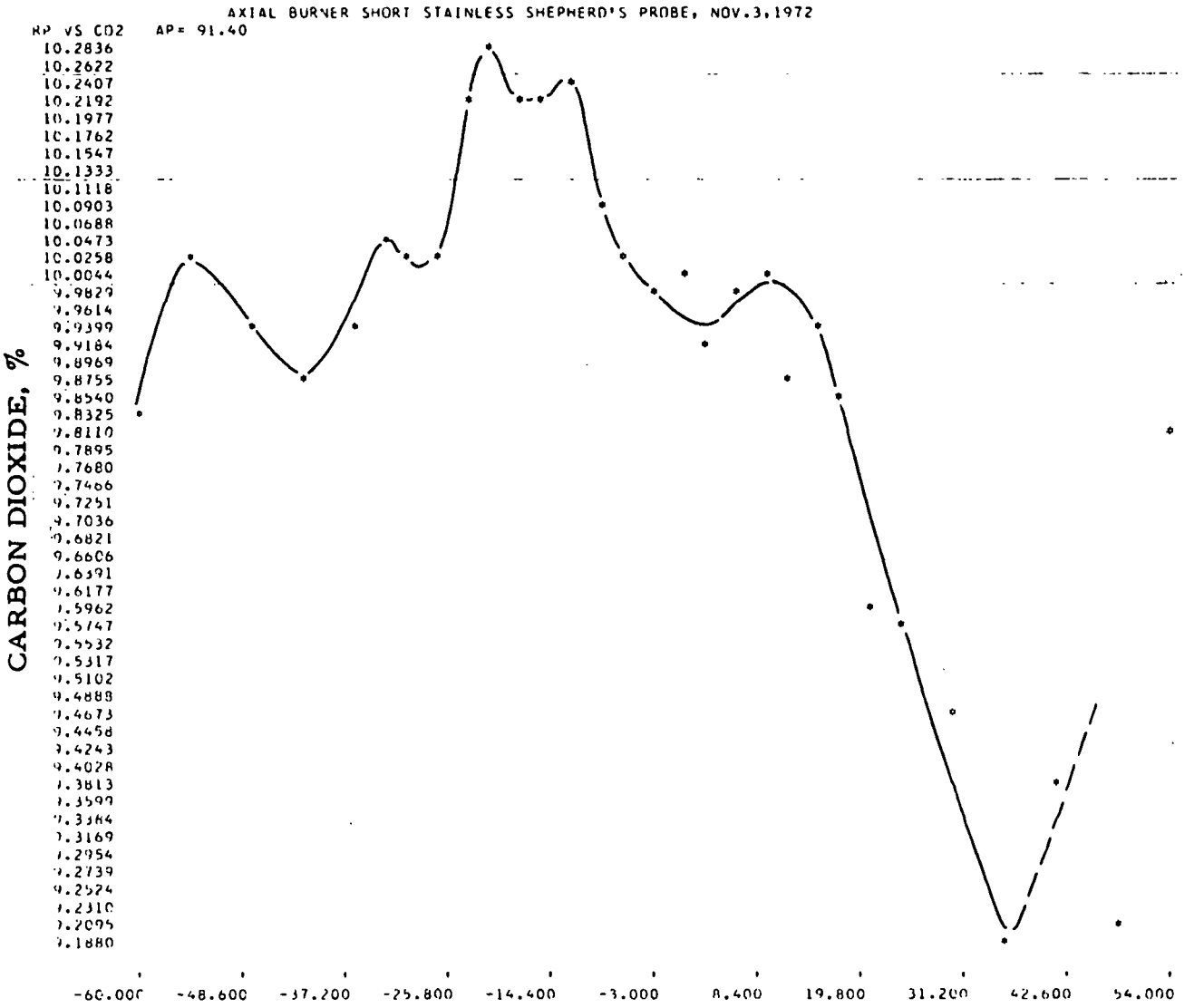

Figure II-141. RADIAL COMPOSITION PROFILE FOR CARBON DIOXIDE (CO_2) FOR THE SHORT-FLAME BAFFLE USING THE AXIAL NOZZLE AT AN AXIAL POSITION OF 91.4 cm. GAS INPUT, 2190 CF/hr; EXCESS OXYGEN, 3.0%; PREHEATED AIR, 315°F

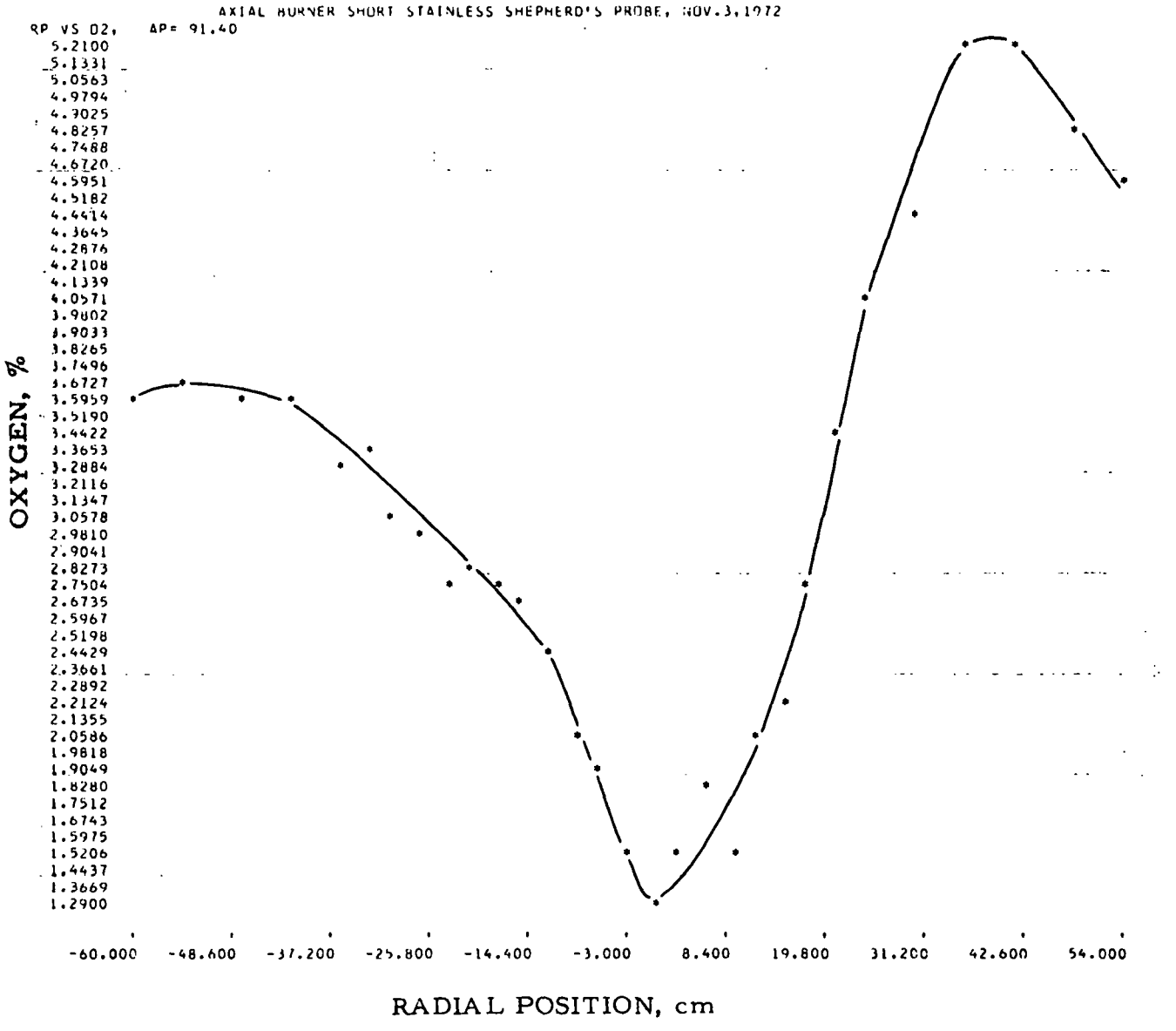

Figure II-142. RADIAL COMPOSITION PROFILE FOR OXYGEN (O_2) FOR THE SHORT-FLAME BAFFLE USING THE AXIAL NOZZLE AT AN AXIAL POSITION OF 91.4 cm. GAS INPUT, 2190 CF/hr; EXCESS OXYGEN, 3.0%; PREHEATED AIR, 315^{0}F

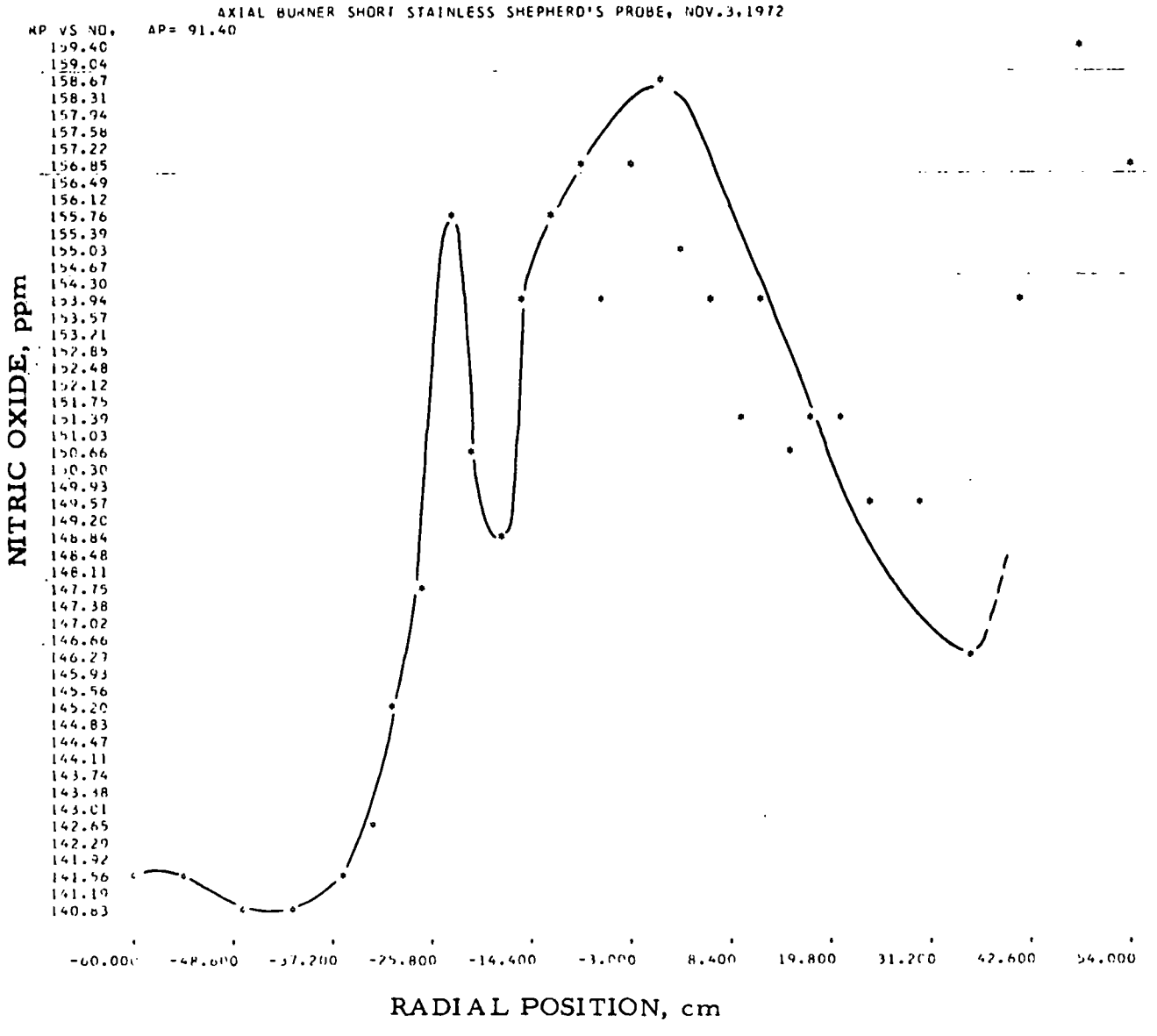

Figure II-143. RADIAL COMPOSITION PROFILE FOR NITRIC OXIDE (NO) FOR THE SHORT-FLAME BAFFLE USING THE AXIAL NOZZLE AT AN AXIAL POSITION OF 91.4 cm. GAS INPUT, 2190 CF/hr; EXCESS OXYGEN, 3.0%; PREHEATED AIR, 315^{0}F

Table II-22. RAW (Gas Analysis) DATA FOR SHORT-FLAME BAFFLE BURNER

TRACER GAS STUDIES OF COMBUSTION BURNERS PROGRAM 2
AXIAL BURNER SHORT STAINLESS SHEPHERD'S PROBE, NOV.3,1972

INPUT GAS 2190 WALL TEMPERATURE 2483 PREHEAT TEMPERATURE 315

OUTPUT ANALYSIS

NITROGEN OXIDE 22.20 PERCENT ON RANGE 1, 192.50 PPM OXYGEN 3.38 PERCENT
CARBON DIOXIDE 79.30 PERCENT ON RANGE 1, 9.96 PERCENT
CARBON MONOXIDE 8.70 PERCENT ON RANGE 3, 0.003 PERCENT
METHANE 0.00 PERCENT ON RANGE 0, 0.00 PERCENT

EXPERIMENTAL RESULTS

		NITROGEN OXIDE -NO			OXYGEN	CARBON DIOXIDE-CO2			CARBON MONOXIDE -CO			METHANE - CH4		
AP	RP	RANGE	X	Y	O2	RANGE	X	Y	RANGE	X	Y	RANGE	X	Y
91.40	-60.00	1	16.50	141.7	3.58	1	78.70	9.84	3	11.50	0.004	3	1.40	0.06
91.40	-54.00	1	16.50	141.7	3.69	1	79.60	10.03	3	12.70	0.005	3	1.10	0.05
91.40	-48.00	1	16.40	140.8	3.58	1	79.20	9.94	3	19.70	0.008	3	1.50	0.06
91.40	-42.00	1	16.40	140.8	3.57	1	78.90	9.88	3	31.60	0.013	3	1.60	0.07
91.40	-36.00	1	16.50	141.7	3.28	1	79.20	9.94	3	74.30	0.035	3	2.30	0.10
91.40	-33.00	1	16.60	142.5	3.34	1	79.70	10.05	2	8.50	0.139	3	2.10	0.09
91.40	-30.00	1	16.90	145.2	3.05	1	79.60	10.03	2	12.10	0.199	3	2.60	0.11
91.40	-27.00	1	17.20	147.8	3.01	1	79.60	10.03	2	13.70	0.226	3	2.30	0.10
91.40	-24.00	1	18.10	155.8	2.78	1	80.50	10.22	2	11.10	0.182	3	2.50	0.10
91.40	-21.00	1	17.50	150.5	2.81	1	80.80	10.28	2	19.70	0.329	3	2.30	0.10
91.40	-18.00	1	17.30	148.7	2.78	1	80.50	10.22	2	30.90	0.530	3	2.50	0.10
91.40	-15.00	1	17.90	154.0	2.65	1	80.50	10.22	2	30.20	0.517	3	1.90	0.08
91.40	-12.00	1	18.10	155.8	2.46	1	80.60	10.24	2	48.50	0.866	3	2.30	0.10
91.40	-9.00	1	18.20	156.7	2.07	1	79.90	10.09	2	77.20	1.468	3	2.80	0.12
91.40	-6.00	1	17.90	154.0	1.89	1	79.60	10.03	2	84.30	1.628	3	2.90	0.12
91.40	-3.00	1	18.20	156.7	1.50	1	79.40	9.98	1	47.80	1.717	3	2.30	0.10
91.40	0.00	1	18.40	158.5	1.29	1	79.50	10.00	1	52.20	1.936	3	3.20	0.13
91.40	3.00	1	18.00	154.9	1.54	1	79.10	9.92	1	49.60	1.806	3	2.40	0.10
91.40	6.00	1	17.90	154.0	1.84	1	79.40	9.98	1	44.30	1.550	3	2.40	0.10
91.40	9.00	1	17.60	151.4	1.55	1	79.50	10.00	1	41.20	1.408	3	2.00	0.08
91.40	12.00	1	17.90	154.0	2.05	1	78.90	9.88	1	36.70	1.211	3	2.10	0.09
91.40	15.00	1	17.50	150.5	2.18	1	79.20	9.94	2	82.70	1.591	3	2.00	0.08
91.40	18.00	1	17.60	151.4	2.75	1	78.80	9.86	2	74.50	1.409	3	1.90	0.08
91.40	21.00	1	17.60	151.4	3.41	1	77.50	9.59	2	24.20	0.408	3	1.90	0.08
91.40	24.00	1	17.40	149.6	4.02	1	77.40	9.57	2	14.90	0.246	3	1.00	0.04
91.40	30.00	1	17.40	149.6	4.45	1	76.90	9.47	2	3.20	0.052	3	0.50	0.02
91.40	36.00	1	17.00	146.1	5.19	1	75.50	9.18	3	34.50	0.014	3	0.70	0.03
91.40	42.00	1	17.90	154.0	5.21	1	76.50	9.39	3	20.80	0.008	3	0.40	0.02
91.40	48.00	1	18.50	159.3	4.85	1	75.60	9.20	3	12.60	0.005	3	0.40	0.02
91.40	54.00	1	18.20	156.7	4.59	1	78.60	9.82	3	10.00	0.004	3	0.70	0.03

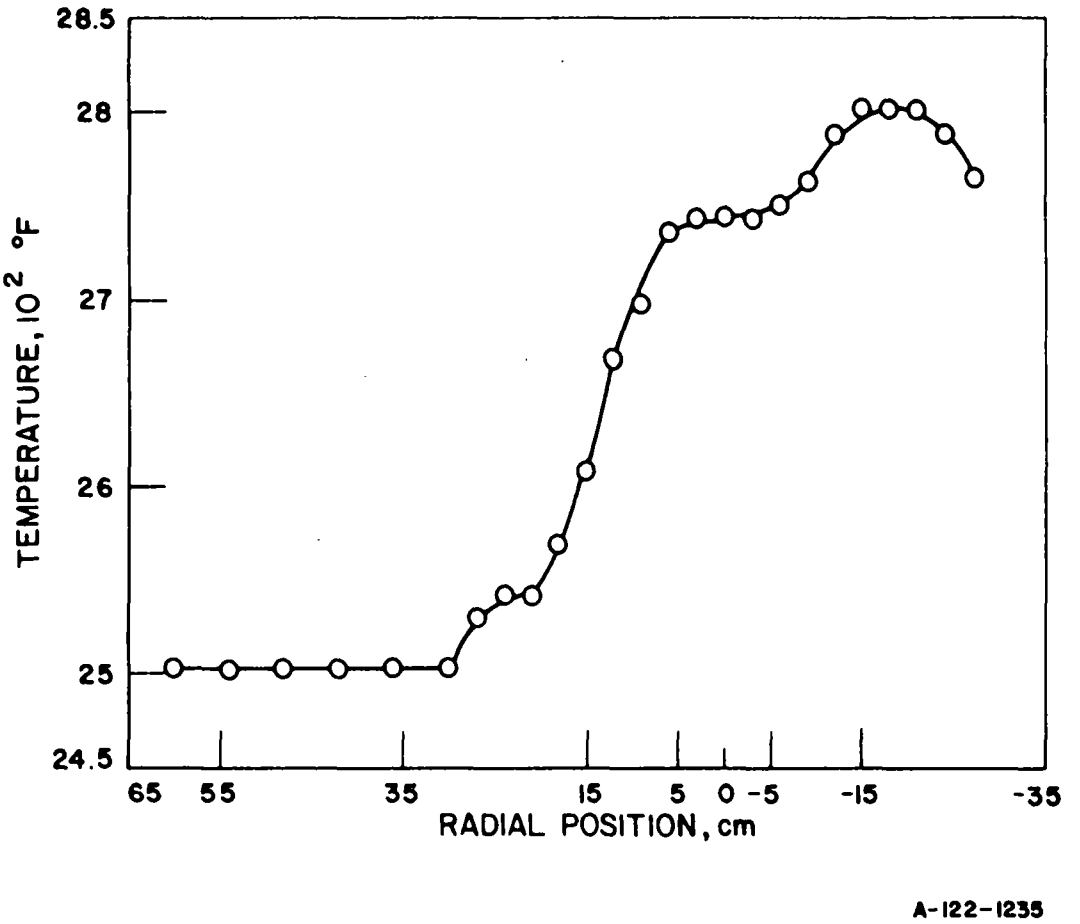

Figure II-144. AXIAL TEMPERATURE PROFILE FROM THE SHORT-FLAME AXIAL NOZZLE BAFFLE BURNER AT AN AXIAL POSITION OF 91.4 cm. GAS INPUT, 2190 CF/hr; EXCESS OXYGEN, 3.3%; PREHEAT TEMPERATURE, 310°F

cm and 18 cm as compared with −12 cm and +20 cm at the 48.3-cm axial position. Figure II-146 shows the tangential velocity at the 97.4-cm axial position. The raw numerical velocity data are given in Table II-23.

An examination of a gas sample from the center line of the burner at a 7.6-cm axial position was made to determine if higher hydrocarbons were being formed during the combustion process. Table II-24 lists the chemical components of the natural gas being used in the burner. Table II-25 lists the gas species analysis on the burner center line as determined by the mass spectrograph. We conclude that the only hydrocarbons which were formed in the combustion process were 0.4% ethylene and 0.5% acetylene.

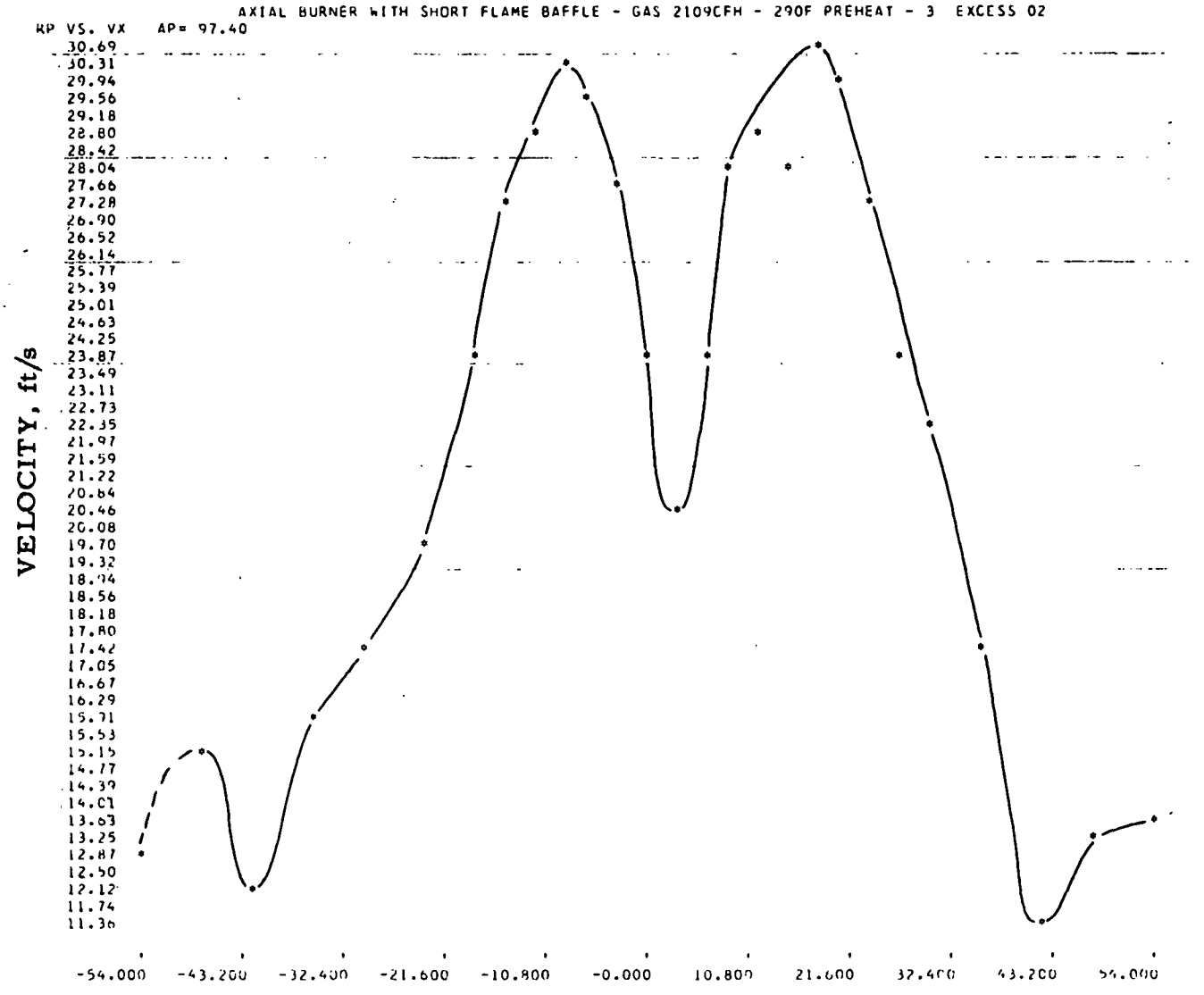

Figure II-145. RADIAL VELOCITY PROFILE (Axial Component) AT AN AXIAL POSITION OF 97.4 cm FOR THE SHORT-FLAME BAFFLE USING THE AXIAL NOZZLE. GAS INPUT, 2190 CF/hr; EXCESS OXYGEN, 3.0%; PREHEATED AIR, 290^{0}F

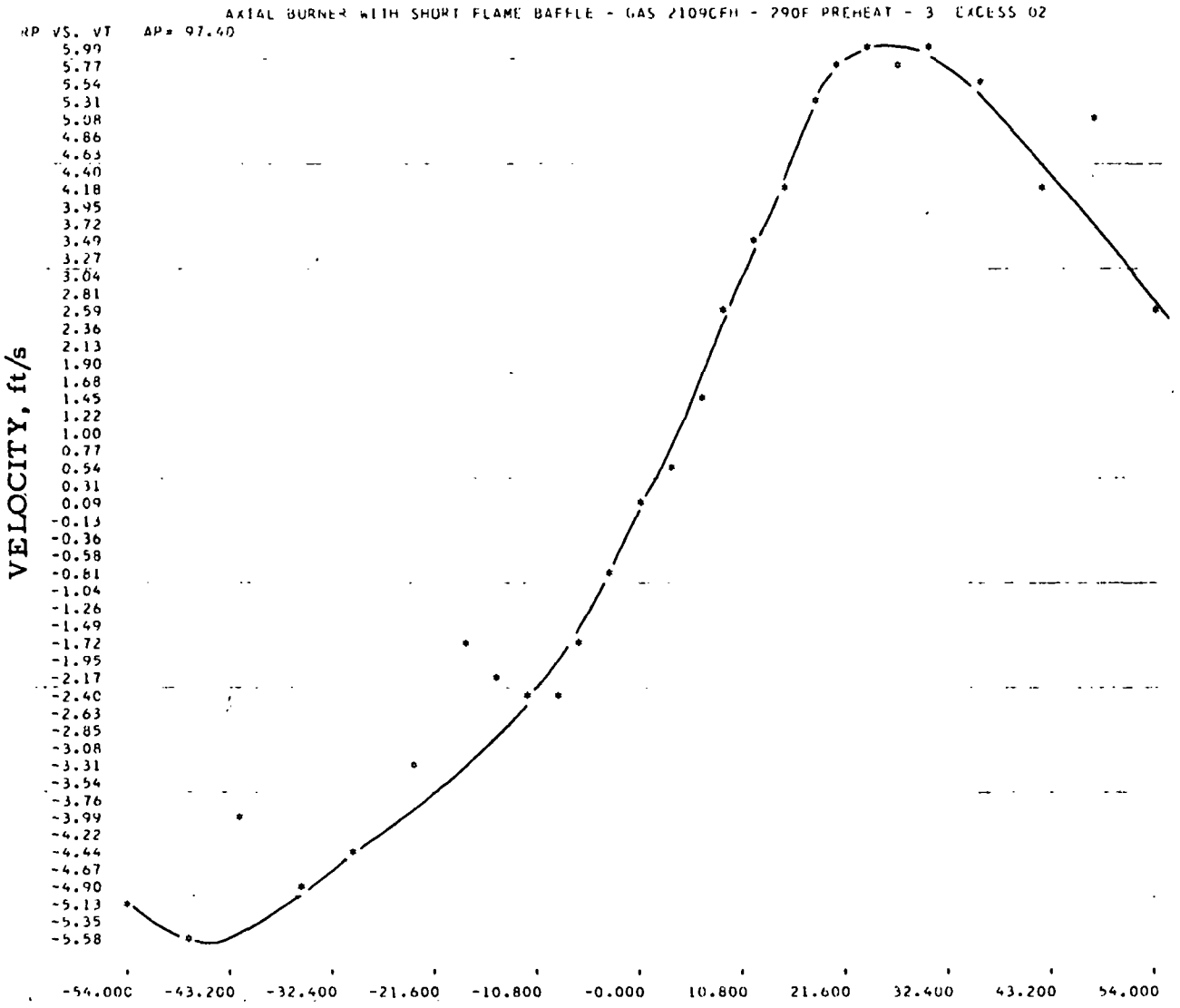

Figure II-146. RADIAL VELOCITY PROFILE (Tangential Component) AT AN AXIAL POSITION OF 97.4 cm FOR THE SHORT-FLAME BAFFLE USING THE AXIAL NOZZLE. GAS INPUT, 2190 CF/hr; EXCESS OXYGEN, 3.0%; PREHEATED AIR, 290^{0}F

Table II-23. RAW (Velocity) DATA FOR SHORT-FLAME BAFFLE BURNER

AERODYNAMIC MODELING OF COMBUSTION BURNERS

CALIBRATION COEFFICIENTS FOR FORWARD FLOW

A1 = 0.770590 A2 = 0.272353 A3 = -0.059818

B0 = 0.737720 B2 = -0.158821 B4 = 0.129246

C = 4.464660 D = 0.394812

AXIAL BURNER WITH SHORT FLAME BAFFLE - GAS 2109CFH - 290F PREHEAT - 3 EXCESS 02

TOTAL DATA INPUT

THETA	AP	RP	P13	P03	P24	P04	P0A	T	PB
0.	97.4	42.0	-4.57	-0.62	-1.27	-0.31	-1.84	2504.	760.
0.	97.4	48.0	-5.07	-0.67	-1.89	0.05	-1.35	2504.	760.
0.	97.4	54.0	-1.41	1.49	-0.15	1.22	0.77	2504.	760.
0.	97.4	-54.0	-4.23	0.22	0.05	0.59	0.12	2500.	760.
0.	97.4	-48.0	-5.53	0.30	0.02	0.71	0.12	2530.	760.
0.	97.4	-42.0	-2.90	0.47	0.07	0.59	0.10	2600.	760.
0.	97.4	-36.0	-5.91	0.52	0.25	0.70	-0.07	2655.	760.
0.	97.4	-30.0	-5.62	1.02	0.60	1.39	0.22	2730.	760.
0.	97.4	-24.0	-2.42	3.04	1.42	3.01	1.30	2790.	760.
0.	97.4	-18.0	-0.60	5.11	0.94	4.80	4.21	2803.	760.
0.	97.4	-15.0	0.81	7.04	-2.79	4.71	4.53	2803.	760.
0.	97.4	-12.0	3.00	8.52	-2.52	6.08	6.14	2790.	760.
0.	97.4	-9.0	1.77	9.38	-5.27	5.02	5.77	2764.	760.
0.	97.4	-6.0	-2.69	8.00	-5.71	3.13	4.32	2751.	760.
0.	97.4	-3.0	-5.49	5.91	-8.58	-0.04	1.60	2745.	760.
0.	97.4	0.0	-4.00	4.00	-9.00	-1.12	1.39	2745.	760.
0.	97.4	3.0	-6.68	0.87	-10.29	-3.03	0.98	2745.	760.
0.	97.4	6.0	-12.74	-0.29	-8.83	-1.61	0.12	2738.	760.
0.	97.4	9.0	-19.77	-0.89	-7.78	-0.38	1.25	2699.	760.
0.	97.4	12.0	-21.66	-1.99	-6.43	0.99	2.81	2673.	760.
0.	97.4	15.0	-20.20	-2.09	-5.66	2.30	3.81	2608.	760.
0.	97.4	18.0	-20.81	-0.09	-4.24	3.78	5.49	2569.	760.
0.	97.4	21.0	-18.02	-0.32	-5.06	4.40	6.10	2543.	760.
0.	97.4	24.0	-17.27	-0.75	-4.06	2.75	3.71	2543.	760.
0.	97.4	27.0	-13.72	-1.38	-4.97	1.74	3.02	2530.	760.
0.	97.4	30.0	-11.74	-0.63	-4.23	1.45	2.15	2504.	760.
0.	97.4	36.0	-8.61	-1.13	-3.10	0.47	0.03	2504.	760.

Table II-24. MASS SPECTROMETER LABORATORY ANALYTICAL REPORT

Material 8933 Natural Gas from Pilot Plant Date 11/8/72

Requested by _____ M. S. Run No. 3238

	Mol %		Mol %
Nitrogen	2.40	Ethylene	
Carbon Monoxide		Propylene	
Nitrogen+CO		Butenes	
Oxygen		Pentenes	
Carbon Dioxide	0.56	Hexenes	
Hydrogen			
Argon		1,3-Butadiene	
Water Vapor		Pentadienes	
Helium	0.08	Cyclopentadiene	
Methane	91.74	Acetylene	
Ethane	3.93	Diacetylene	
Propane	0.95	Methyl Acetylene	
n-Butane	0.16	+Propadiene	
Isobutane	0.07	Vinyl Acetylene	
Pentanes	0.06	Benzene	
Hexanes	0.03	Toluene	
Heptanes	0.02	Xylenes	
Octanes		Ethyl Benzene	
		Styrene	
		Indene	
		Napthalene	
		TOTAL	100.0

Calc. H. V., Btu SCF _____ Air Content _____

Calc. sp gr.(Air 1.000) _____ Approved by _____

Table II-25. MASS SPECTROMETER LABORATORY ANALYTICAL REPORT

Material 8933 Sample # 2 11/16/72 Date 11/17/72

Requested by _____ M. S. Run No. 3289

	Mol %		Mol %
Nitrogen	42.6	Ethylene	0.4
Carbon Monoxide	4.0	Propylene	
Nitrogen+CO		Butenes	
Oxygen	2.4	Pentenes	
Carbon Dioxide	2.7	Hexenes	
Hydrogen	5.8		
Argon	0.5	1,3-Butadiene	
Water Vapor		Pentadienes	
Helium		Cyclopentadiene	
Methane	39.6	Acetylene	0.5
Ethane	1.2	Diacetylene	
Propane	0.0	Methyl Acetylene	
n-Butane	0.1	+Propadiene	
Isobutane		Vinyl Acetylene	
Pentanes		Benzene	
Hexanes		Toluene	
Heptanes		Xylenes	
Octanes		Ethyl Benzene	
		Styrene	
		Indene	
		Napthalene	
		TOTAL	100.0

Calc. H. V., Btu/SCF _____ Air Content _____

Calc. sp gr (Air 1.000) _____ Approved by _____

We decided to do an in-depth profile of the gas concentrations along the center line of the burners because of the interesting variation of the nitric oxide concentration along the center line of the burner. (It had a maximum value near the burner block, dipped sharply at a 48.3-cm axial position, and recovered its initial value at a 91-cm axial position.) The profile is presented in Figure II-147. The decrease in NO concentration corresponds to an increase in oxygen which leads one to believe that a dilution process takes place which could be caused by interval recirculation.

To investigate this theory, further velocity data were taken at the axial position of 48.3 cm measuring reverse flow. These data are plotted in Figure II-136 as X. It can be seen that they are the same magnitude as the forward velocity and thus cannot in our opinion be neglected from a velocity magnitude argument.

Figure II-147 was used to make an estimate of the flame length by assuming a symmetrical flame (which as a result of the gas concentration, temperature, and velocity profile data is a very questionable assumption for this burner). However, we are defining flame length as that axial position where the concentration of methane, averaged across the furnace width, is less than 1.0%. For this profile, the end of the flame occurs at an axial position of approximately 70 cm.

Additional gas concentration profiles were taken with the same combustion conditions except the preheated air temperature was increased to 515^{0}F. Figures II-148, II-149, and II-150 show the composite of chemical species profiles at axial positions of 7.6, 37.7, and 91.4 cm, respectively.

These data show that increased preheated air temperature increased both NO_x formation and mixing at the outer edges of the visible flame envelope. NO_x increased approximately 40 ppm at the burner center line while the oxygen concentration at the flame edges decreased about 1.0% as air temperature was increased from 290^0 to 515^{0}F. Data plots with greater resolution are given in Figures II-151 to II-175 and the raw data appear in Tables II-26, II-27, and II-28.

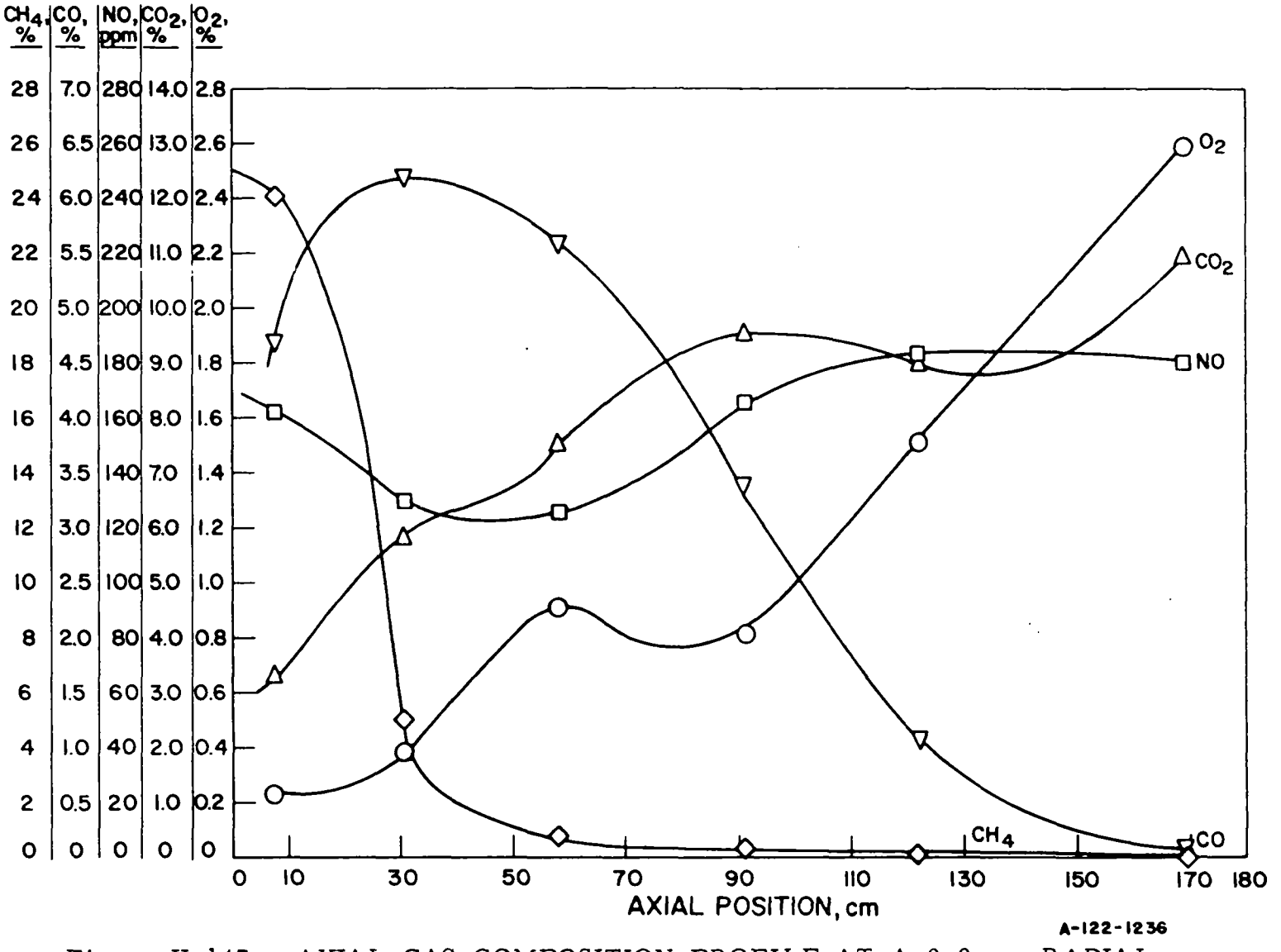

Figure II-147. AXIAL GAS COMPOSITION PROFILE AT A 0.0-cm RADIAL POSITION FOR THE SHORT-FLAME BAFFLE USING THE AXIAL NOZZLE. GAS INPUT, 2190 CF/hr; EXCESS OXYGEN, 3%; PREHEATED AIR, 290°F

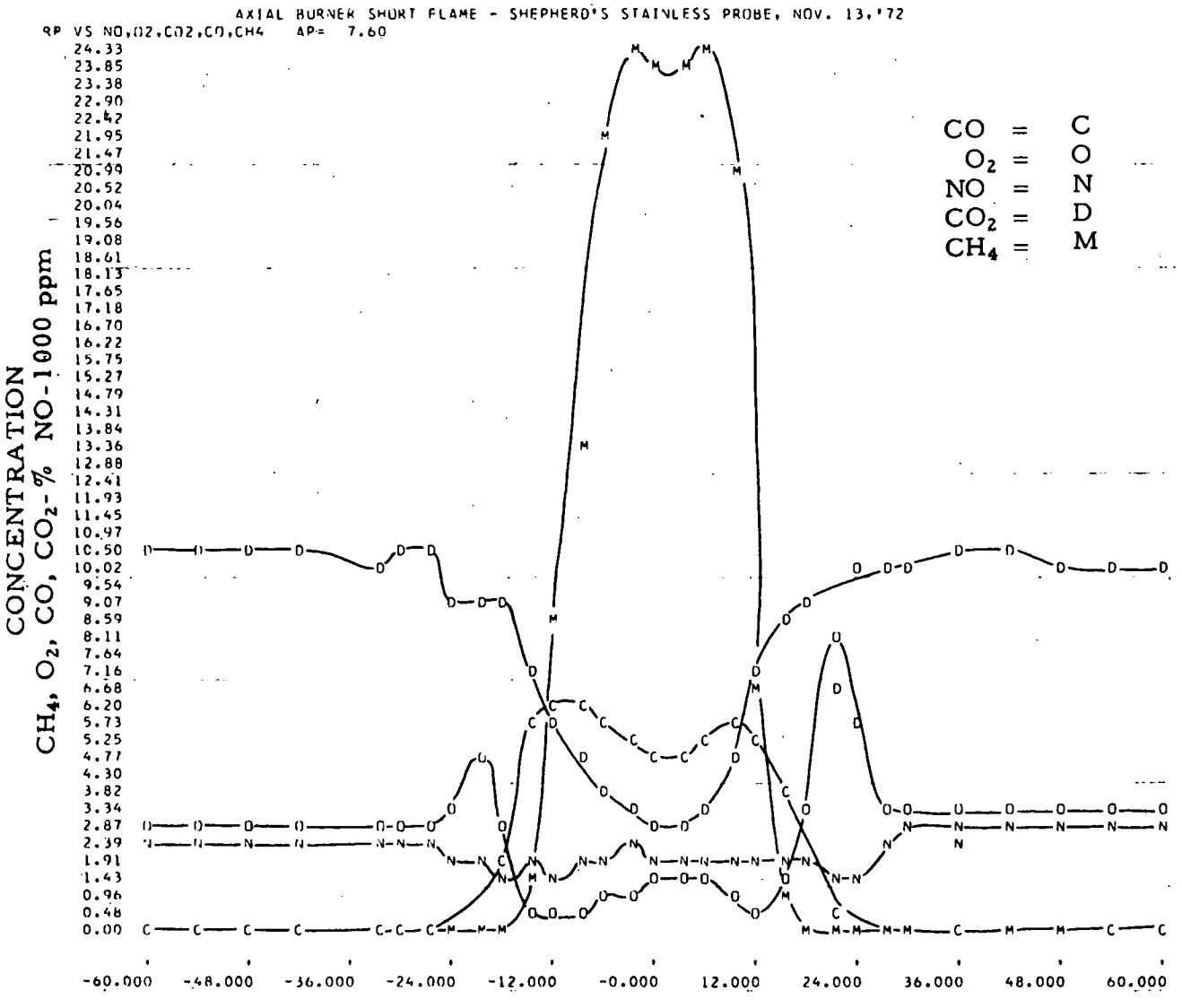

Figure II-148. COMPOSITE PLOT OF GAS SAMPLING PROFILES FOR CO, CO_2, CH_4, NO, AND O_2 FOR THE SHORT-FLAME BAFFLE USING THE AXIAL NOZZLE AT AN AXIAL POSITION OF 7.6 cm. GAS INPUT, 2190 CF/hr; EXCESS OXYGEN, 3.0%; PREHEATED AIR, 515°F

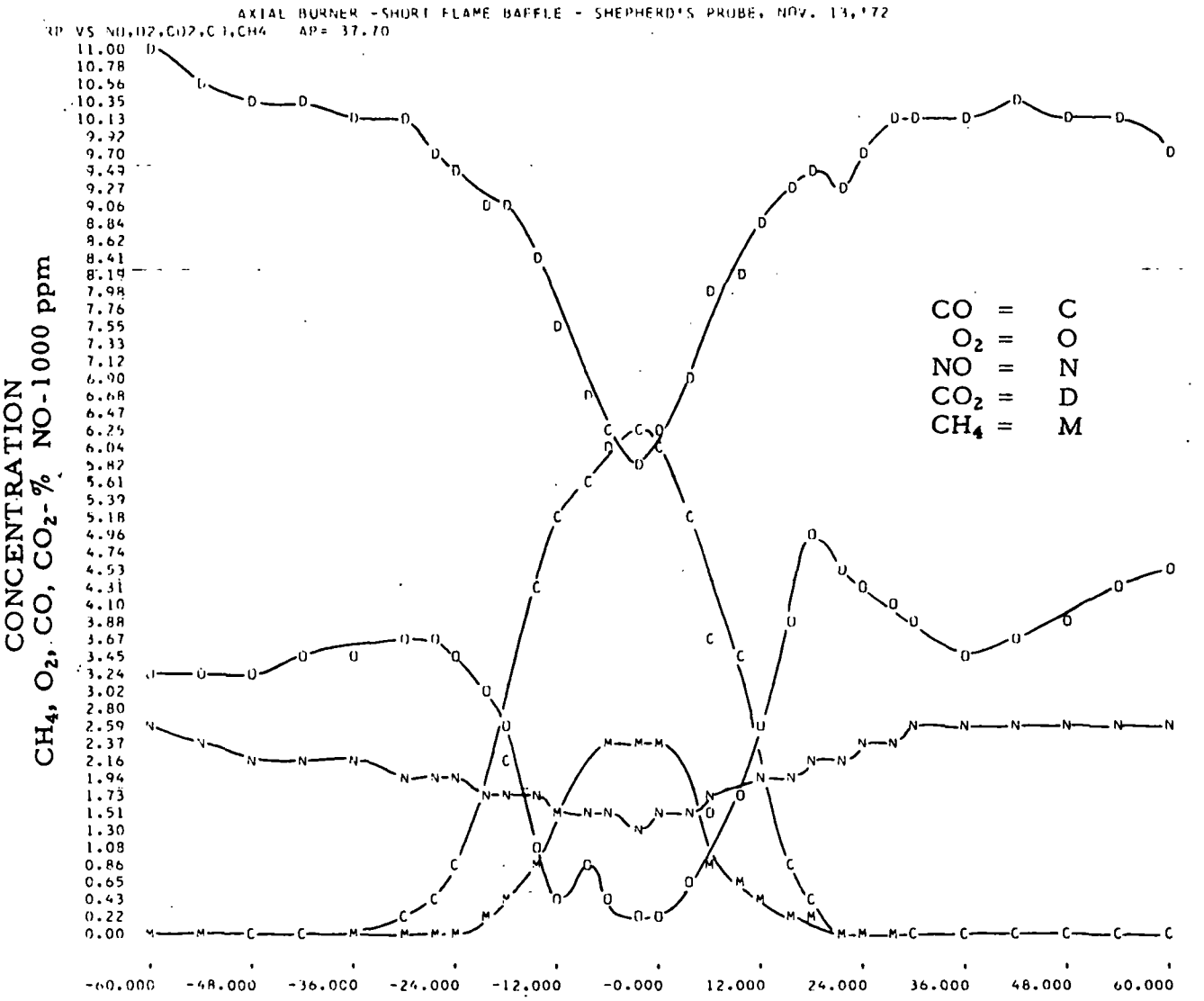

Figure II-149. COMPOSITE PLOT OF GAS SAMPLING PROFILES FOR CO, CO_2, CH_4, NO, AND O_2 FOR THE SHORT-FLAME BAFFLE USING THE AXIAL NOZZLE AT AN AXIAL POSITION OF 37.7 cm. GAS INPUT, 2190 CF/hr; EXCESS OXYGEN, 3.0%; PREHEATED AIR, 515°F

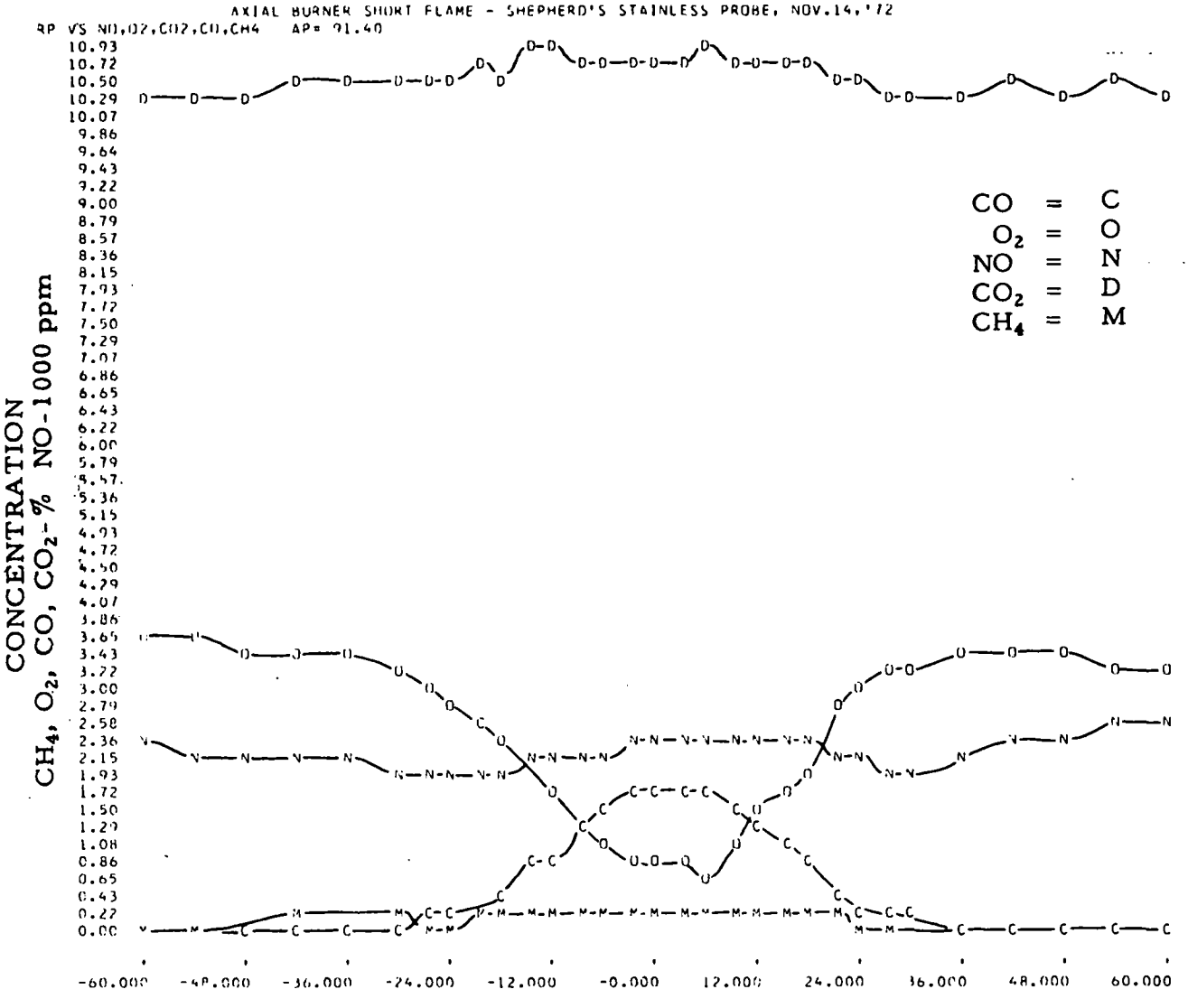

Figure II-150. COMPOSITE PLOT OF GAS SAMPLING PROFILES FOR CO, CO_2, CH_4, NO, AND O_2 FOR THE SHORT-FLAME BAFFLE USING THE AXIAL NOZZLE AT AN AXIAL POSITION OF 91.4 cm. GAS INPUT, 2190 CF/hr; EXCESS OXYGEN, 3.0%; PREHEATED AIR, 515°F

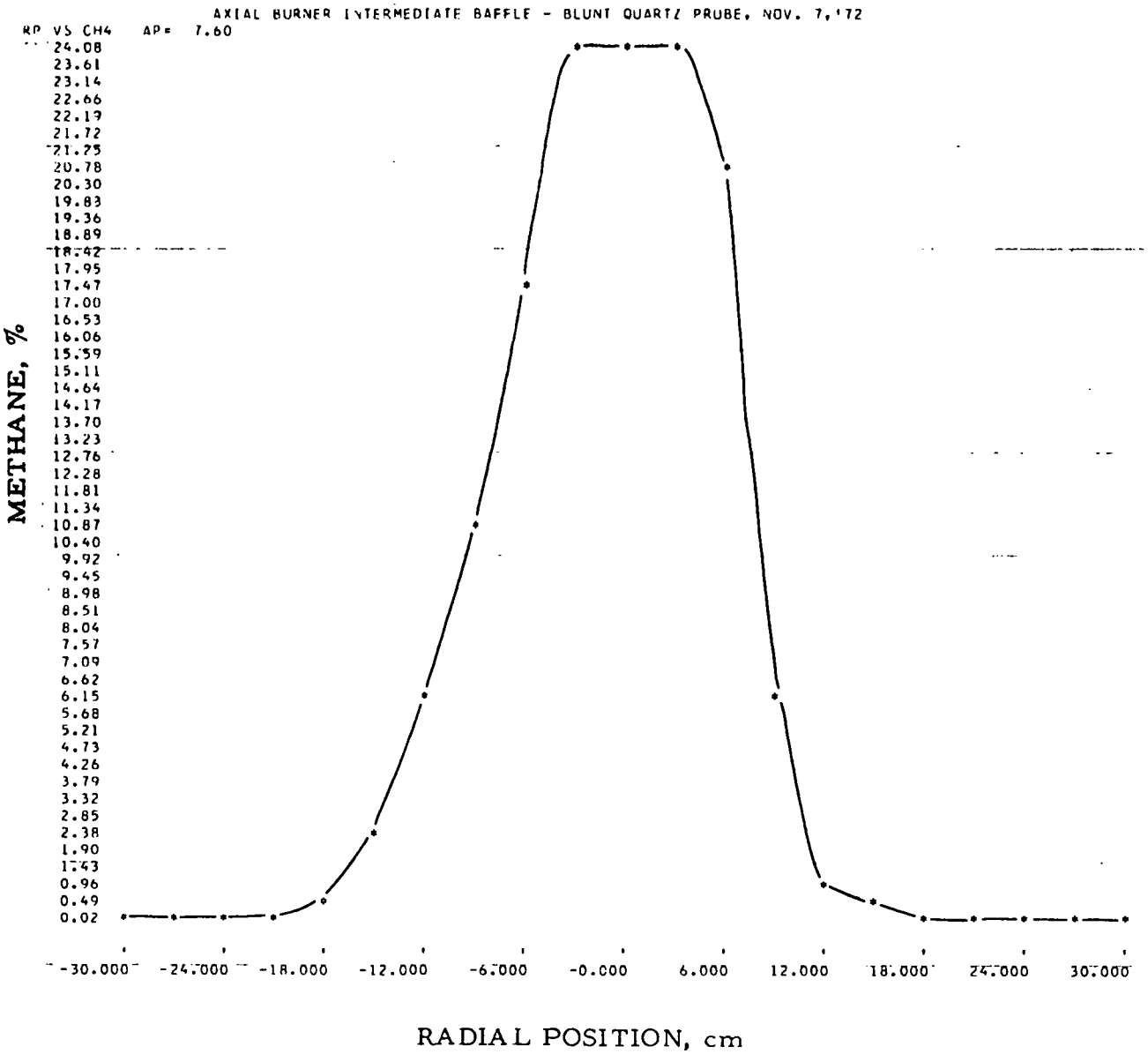

Figure II-151. RADIAL COMPOSITION PROFILE FOR METHANE (CH_4) FOR THE SHORT-FLAME BAFFLE USING THE AXIAL NOZZLE AT AN AXIAL POSITION OF 7.6 cm. GAS INPUT, 2190 CF/hr; EXCESS OXYGEN, 3.0%; PREHEATED AIR, 315^{0}F

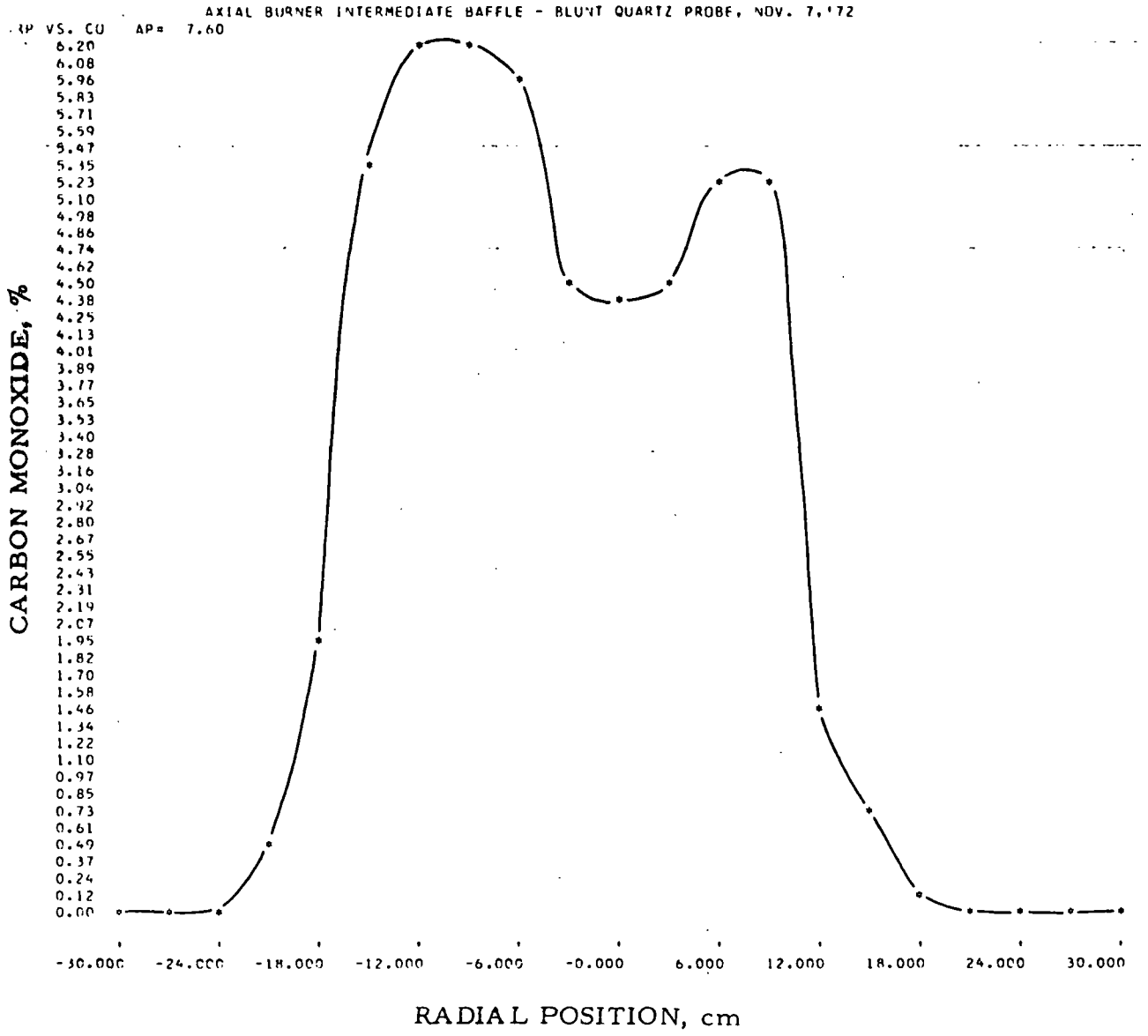

Figure II-152. RADIAL COMPOSITION PROFILE FOR CARBON MONOXIDE (CO) FOR THE SHORT-FLAME BAFFLE USING THE AXIAL NOZZLE AT AN AXIAL POSITION OF 7.6 cm. GAS INPUT, 2190 CF/hr; EXCESS OXYGEN, 3.0%; PREHEATED AIR, 315^{0}F

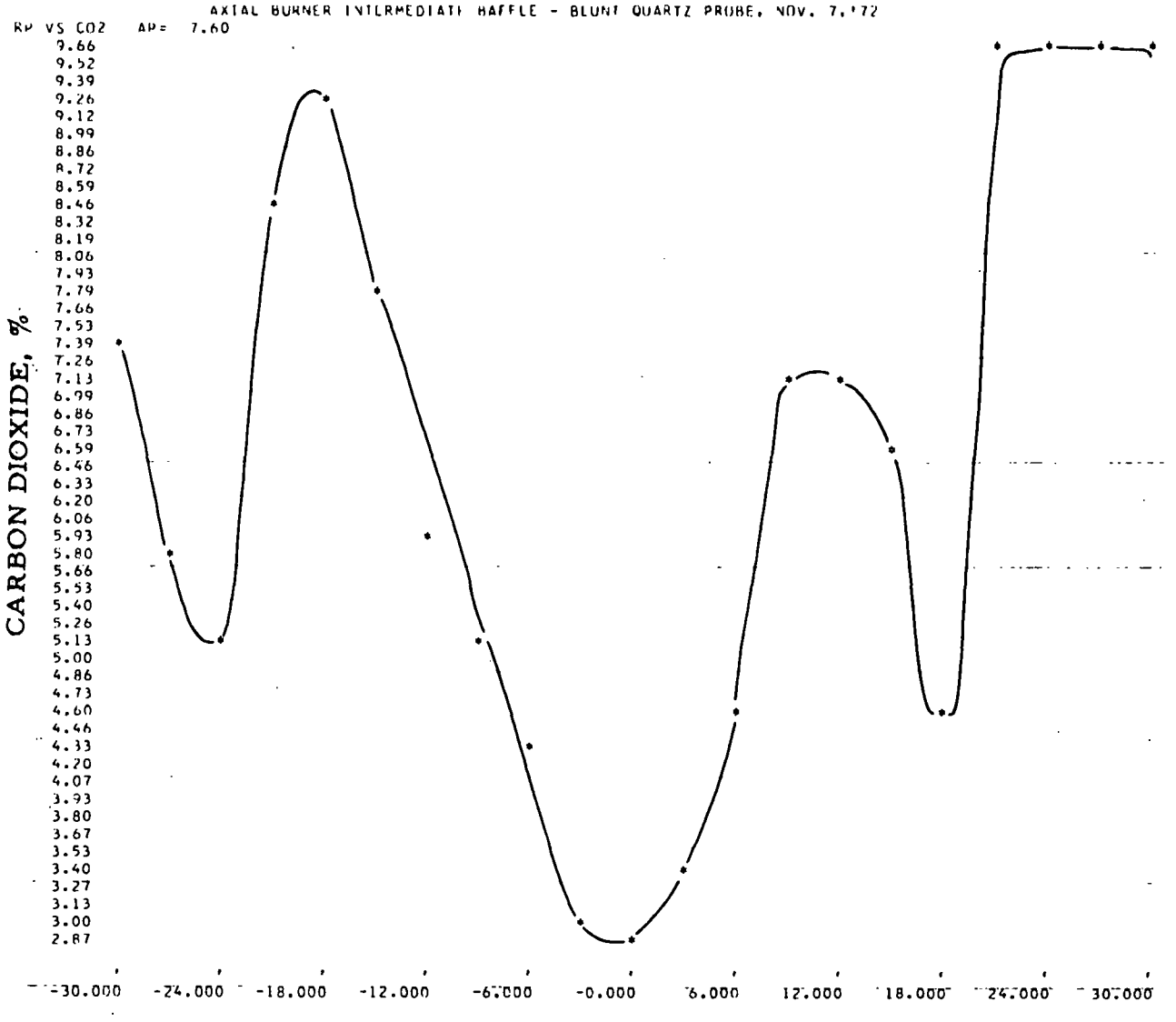

Figure II-153. RADIAL COMPOSITION PROFILE FOR CARBON DIOXIDE (CO_2) FOR THE SHORT-FLAME BAFFLE USING THE AXIAL NOZZLE AT AN AXIAL POSITION OF 7.6 cm. GAS INPUT, 2190 CF/hr; EXCESS OXYGEN, 3.0%; PREHEATED AIR, 315^{0}F

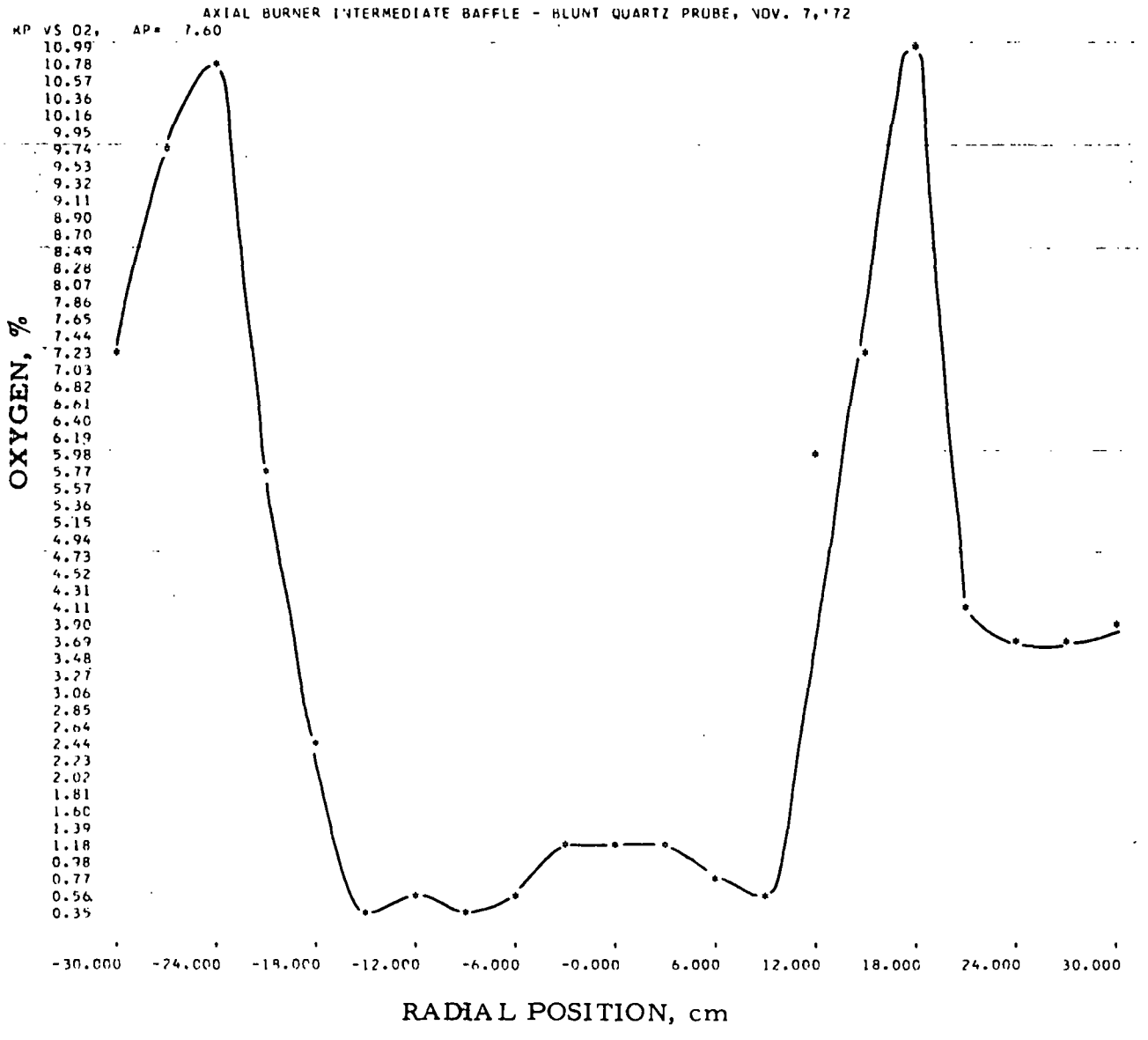

Figure II-154. RADIAL COMPOSITION PROFILE FOR OXYGEN (O_2) FOR THE SHORT-FLAME BAFFLE USING THE AXIAL NOZZLE AT AN AXIAL POSITION OF 7.6 cm. GAS INPUT, 2190 CF/hr; EXCESS OXYGEN, 3.0%; PREHEATED AIR, 315°F

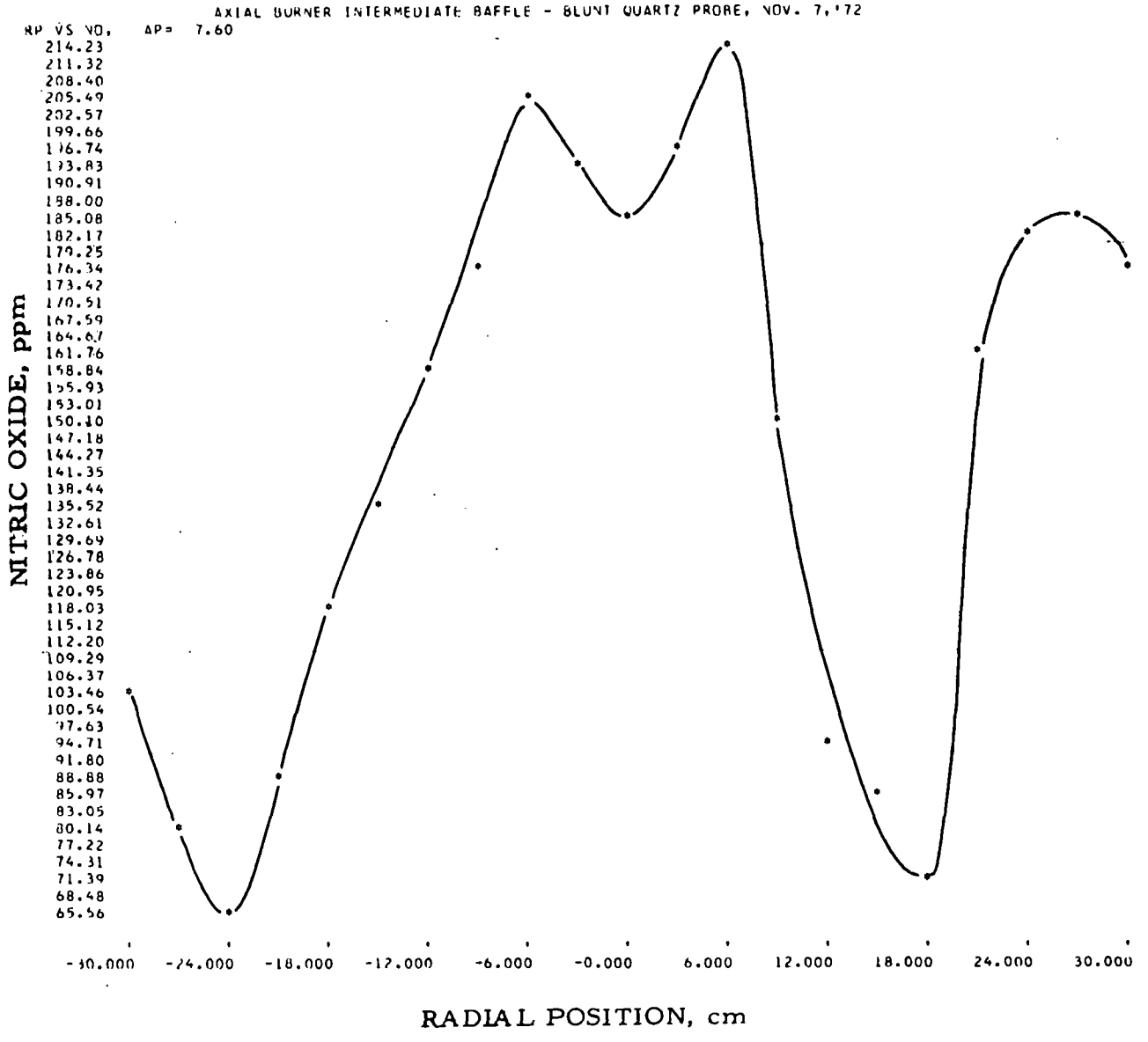

Figure II-155. RADIAL COMPOSITION PROFILE FOR NITRIC OXIDE (NO) FOR THE SHORT-FLAME BAFFLE USING THE AXIAL NOZZLE AT AN AXIAL POSITION OF 7.6 cm. GAS INPUT, 2190 CF/hr; EXCESS OXYGEN, 3.0%; PREHEATED AIR, 315°F

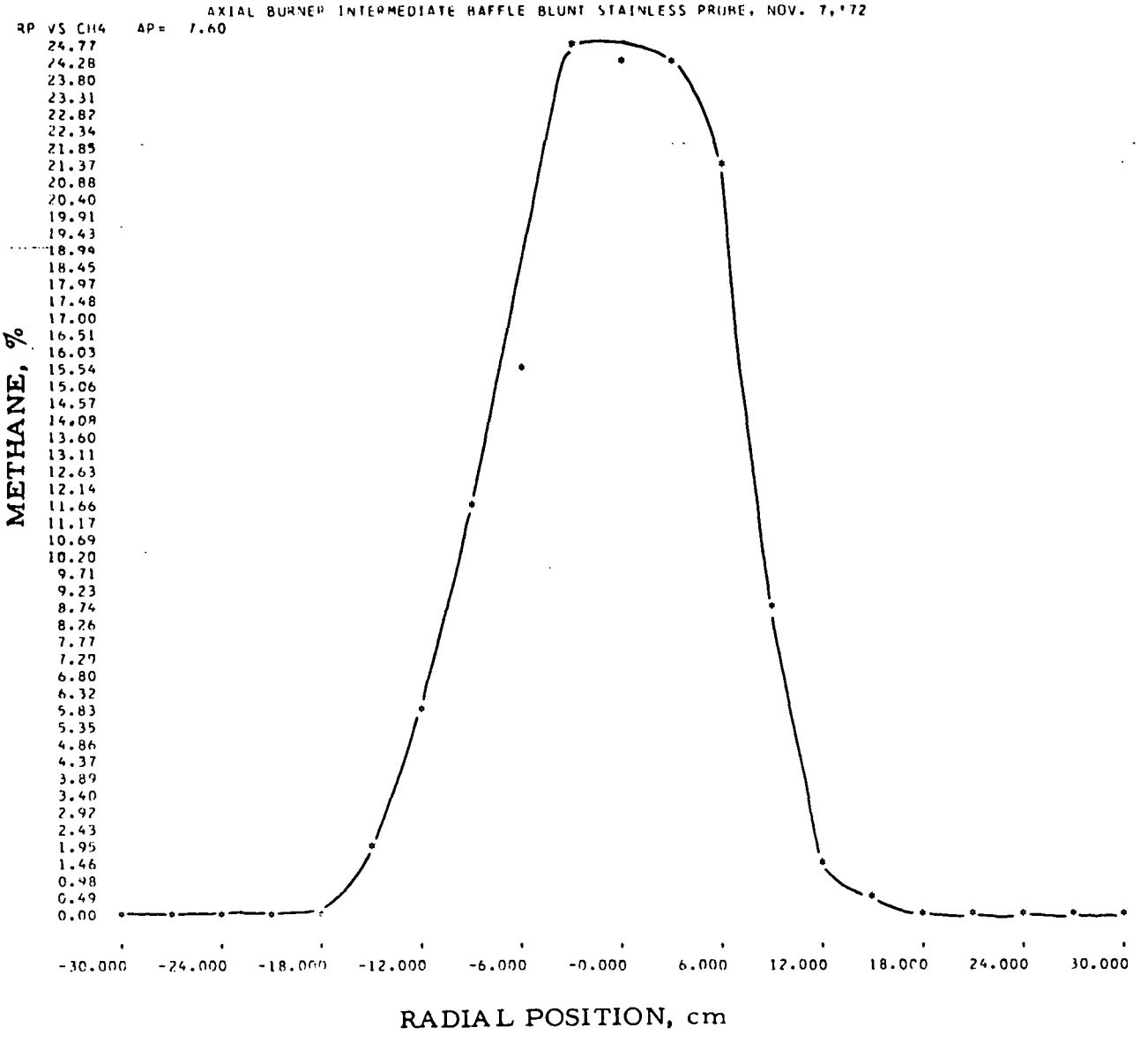

Figure II-156. RADIAL COMPOSITION PROFILE FOR METHANE (CH_4) FOR THE SHORT-FLAME BAFFLE USING AN AXIAL POSITION OF 7.6 cm. GAS INPUT, 2190 CF/hr; EXCESS OXYGEN, 3.0%; PREHEATED AIR, 315°F

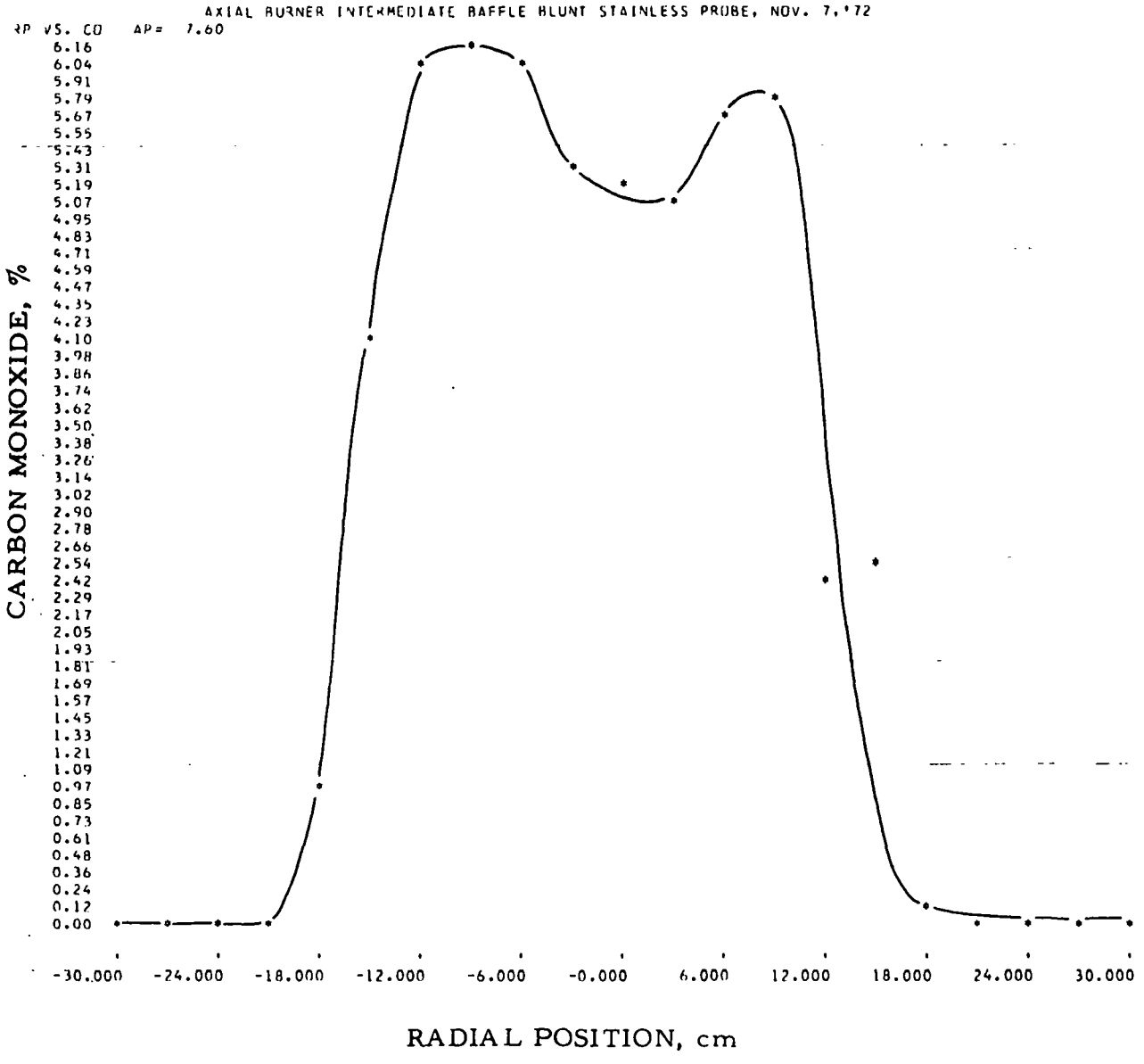

Figure II-157. RADIAL COMPOSITION PROFILE FOR CARBON MONOXIDE (CO) FOR THE SHORT-FLAME BAFFLE USING THE AXIAL NOZZLE AT AN AXIAL POSITION OF 7.6 cm. GAS INPUT, 2190 CF/hr; EXCESS OXYGEN, 3.0%; PREHEATED AIR, 315^{0}F

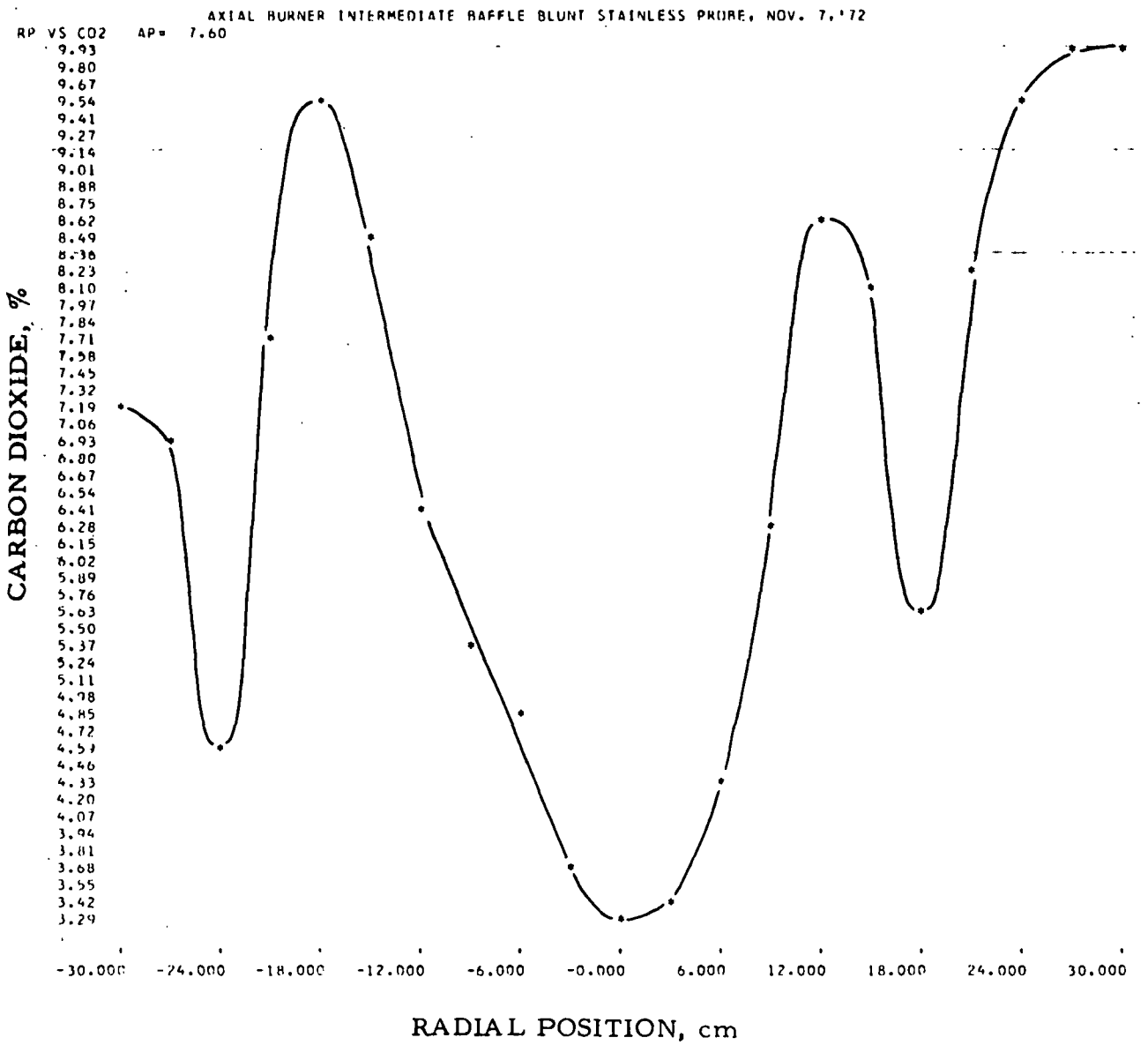

Figure II-158. RADIAL COMPOSITION PROFILE FOR CARBON DIOXIDE (CO_2) FOR THE SHORT-FLAME BAFFLE USING THE AXIAL NOZZLE AT AN AXIAL POSITION OF 7.6 cm. GAS INPUT, 2190 CF/hr; EXCESS OXYGEN, 3.0%; PREHEATED AIR, 315^{0}F

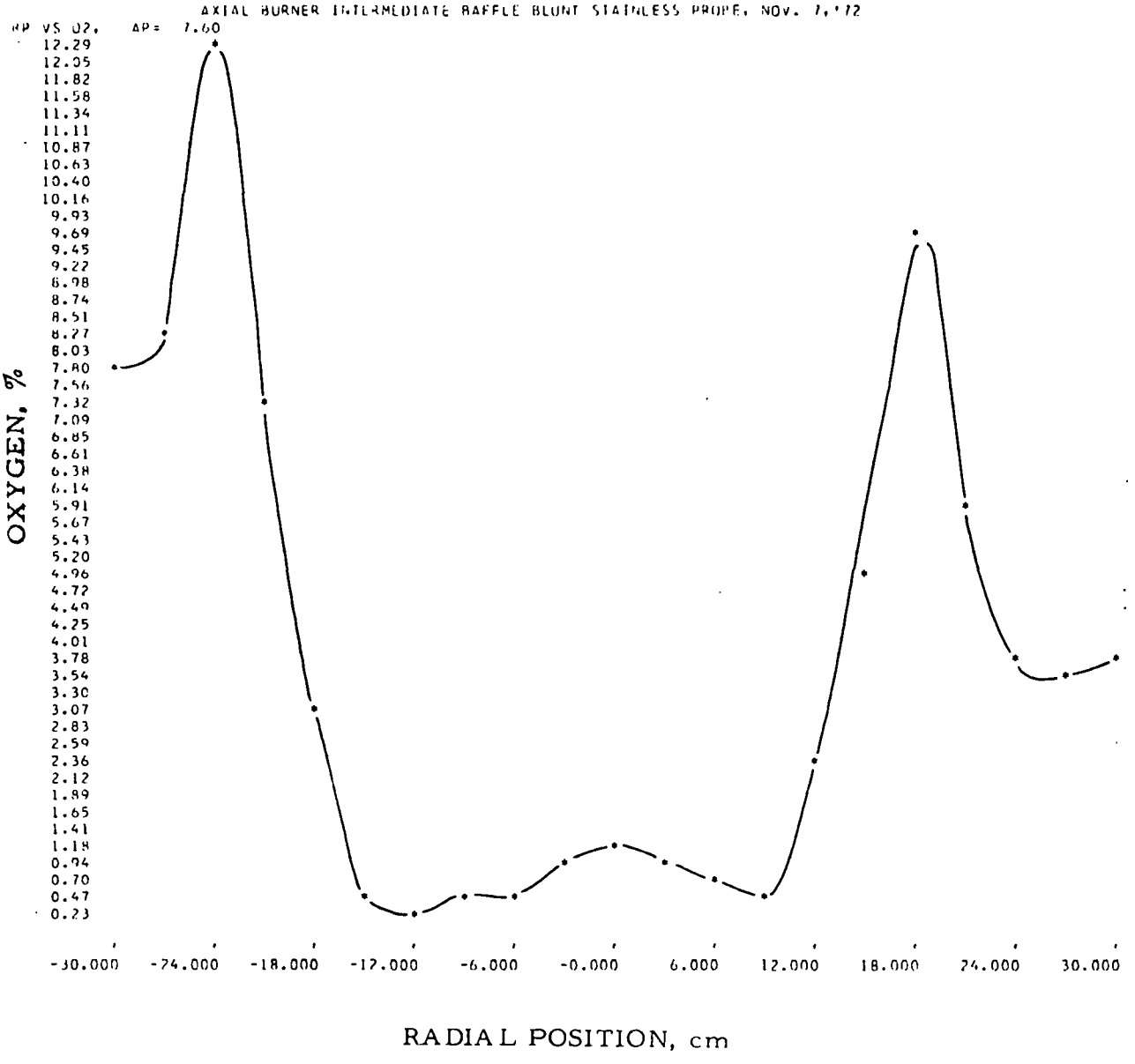

Figure II-159. RADIAL COMPOSITION PROFILE FOR OXYGEN (O_2) FOR THE SHORT-FLAME BAFFLE USING THE AXIAL NOZZLE AT AN AXIAL POSITION OF 7.6 cm. GAS INPUT, 2190 CF/hr; EXCESS OXYGEN, 3.0%; PREHEATED AIR, 315^{0}F

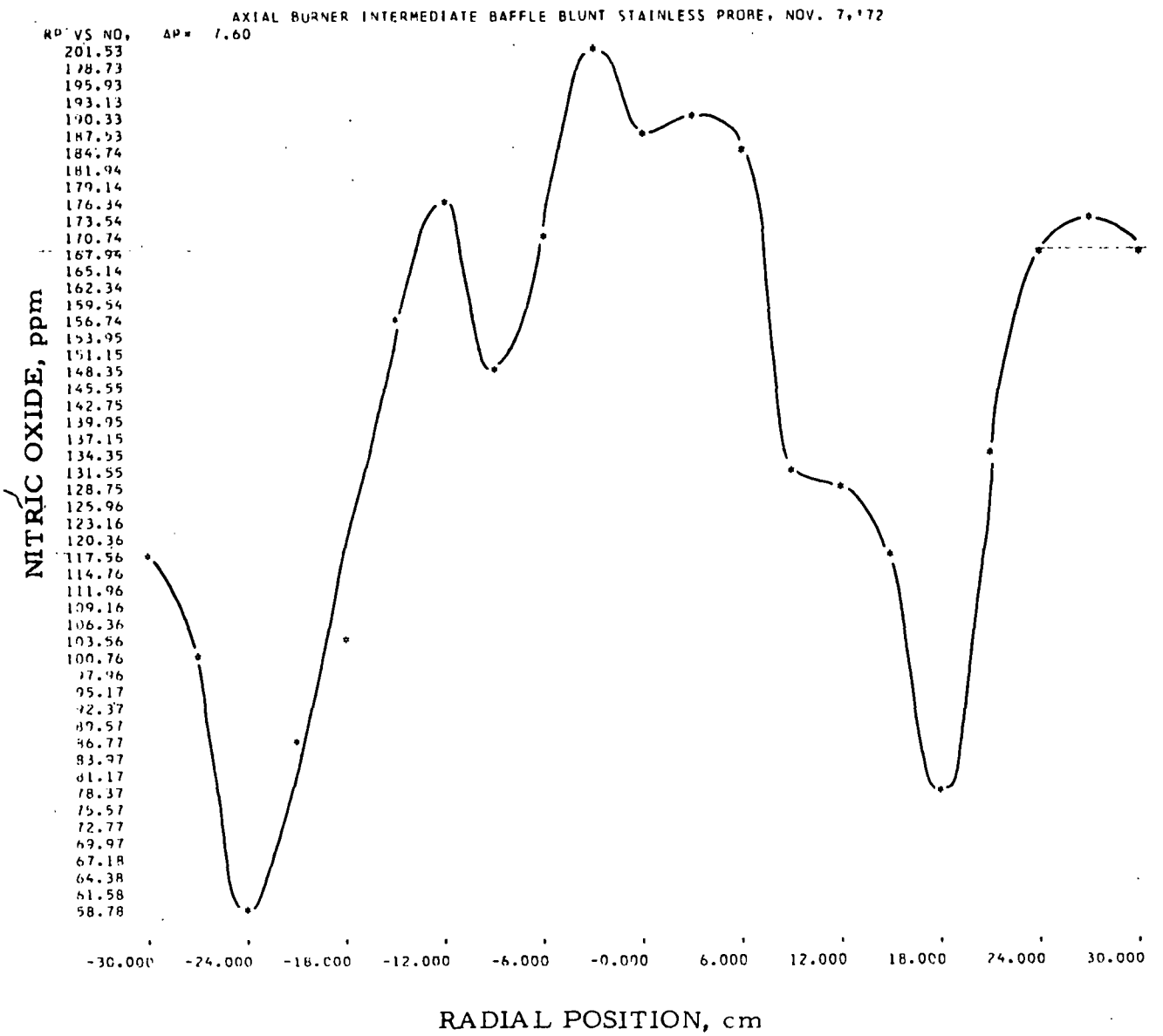

Figure II-160. RADIAL COMPOSITION PROFILE FOR NITRIC OXIDE (NO) FOR THE SHORT-FLAME BAFFLE USING THE AXIAL NOZZLE AT AN AXIAL POSITION OF 7.6 cm. GAS INPUT, 2190 CF/hr; EXCESS OXYGEN, 3.0%; PREHEATED AIR, 315^{0}F

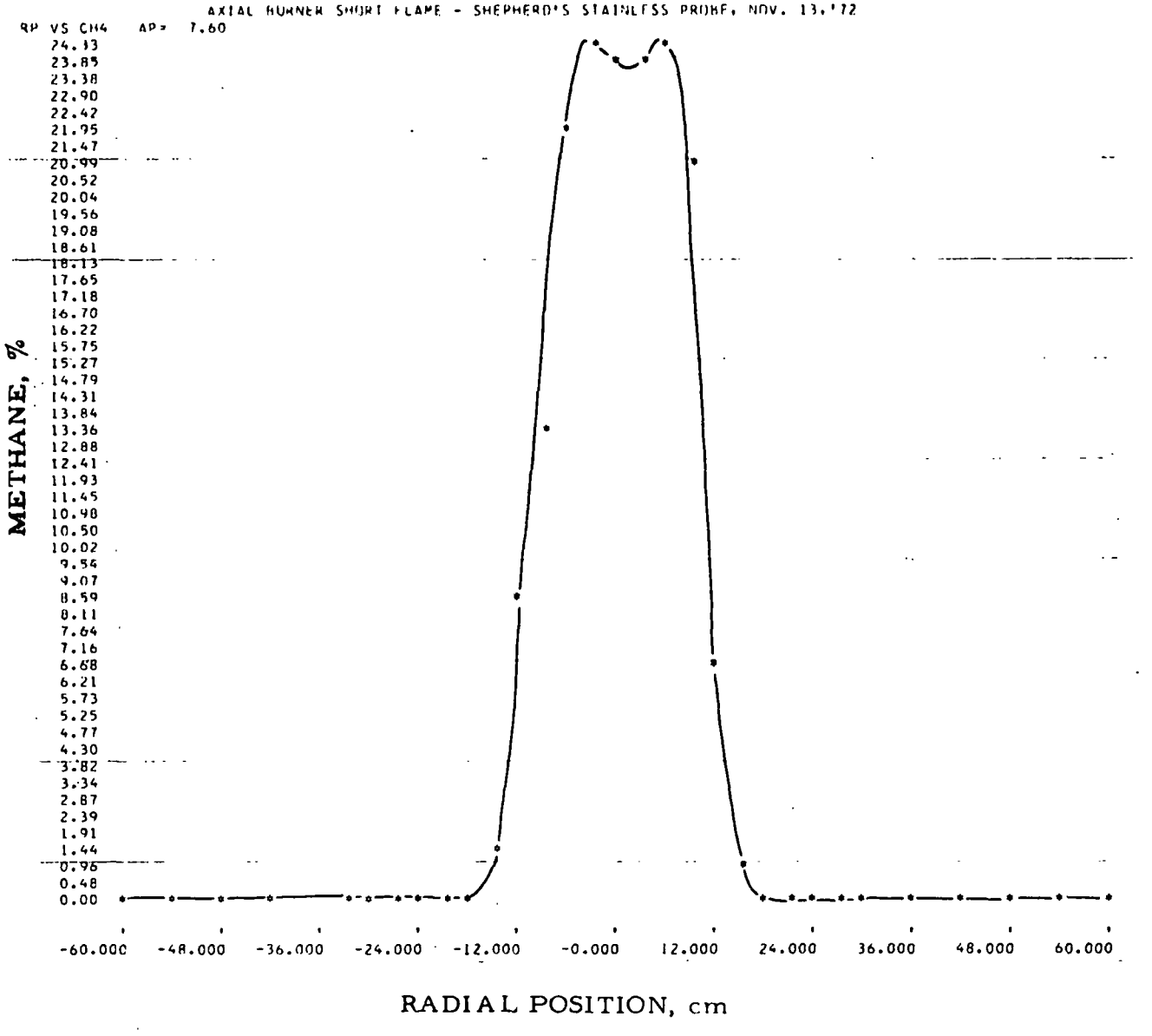

Figure II-161. RADIAL COMPOSITION PROFILE FOR METHANE (CH_4) FOR THE SHORT-FLAME BAFFLE USING THE AXIAL NOZZLE AT AN AXIAL POSITION OF 7.6 cm. GAS INPUT, 2190 CF/hr; EXCESS OXYGEN, 3.0%; PREHEATED AIR, 515^{0}F

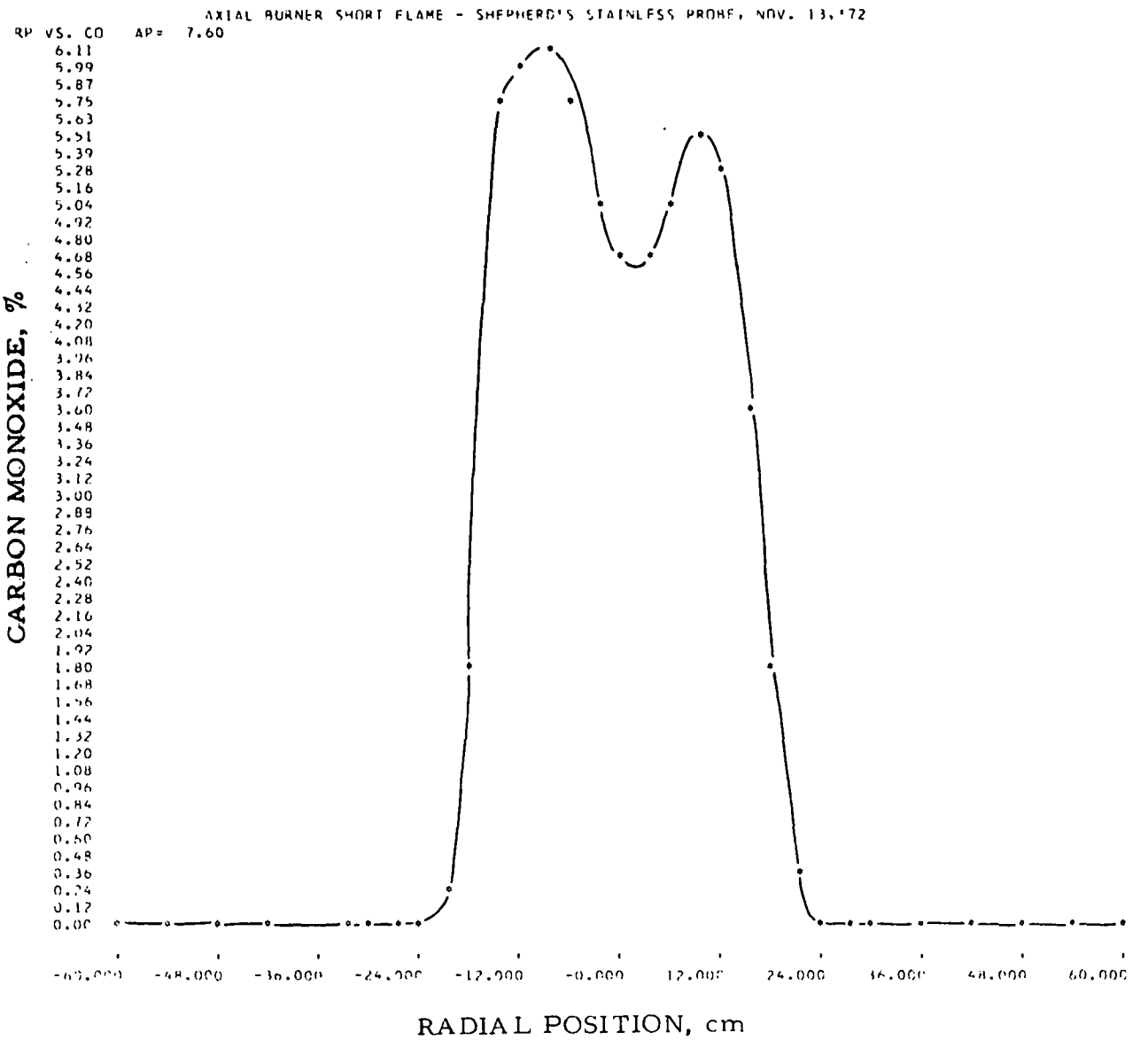

Figure II-162. RADIAL COMPOSITION PROFILE FOR CARBON MONOXIDE (CO) FOR THE SHORT-FLAME BAFFLE USING THE AXIAL NOZZLE AT AN AXIAL POSITION OF 7.6 cm. GAS INPUT, 2190 CF/hr; EXCESS OXYGEN, 3.0%; PREHEATED AIR, 515°F

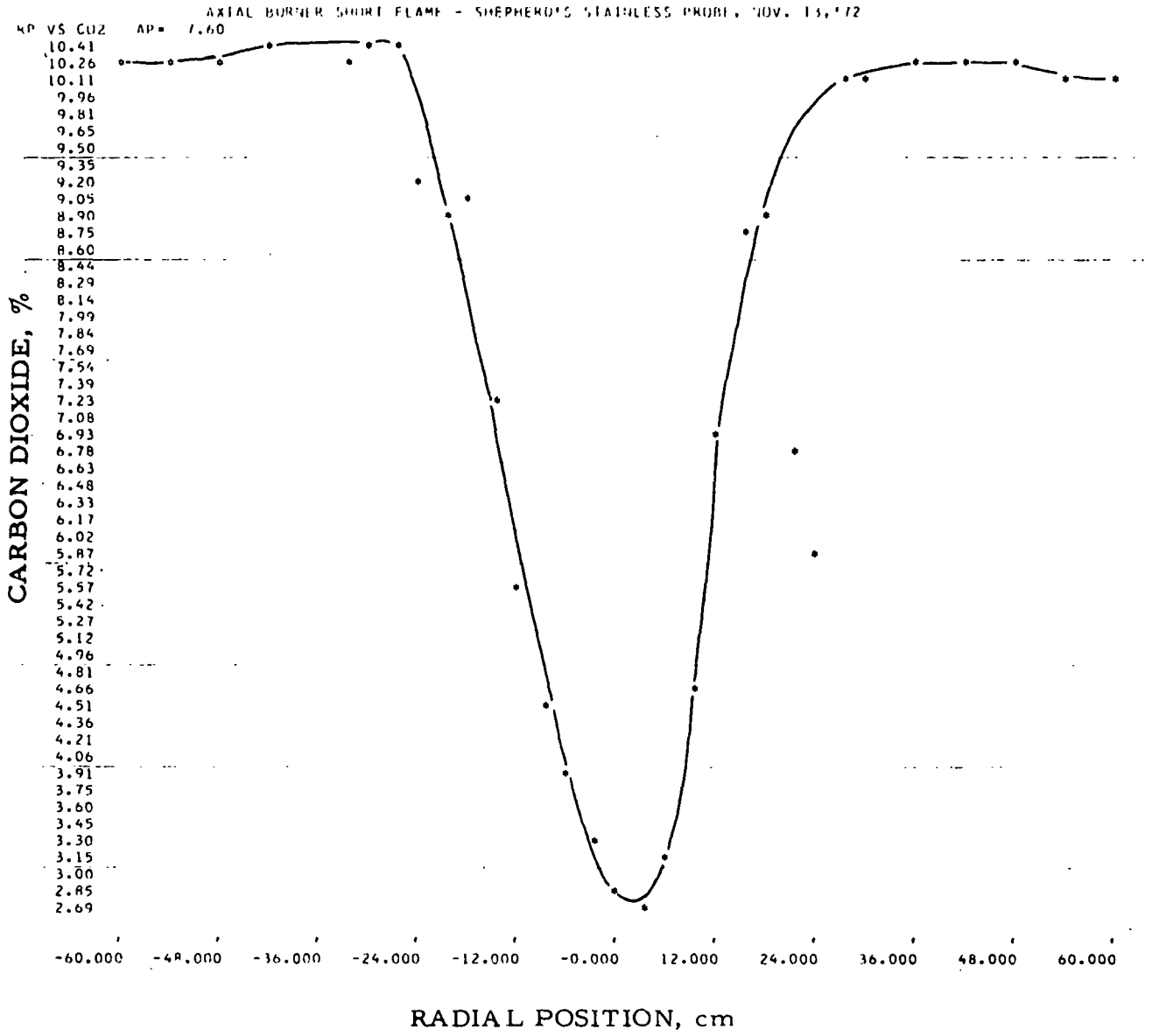

Figure II-163. RADIAL COMPOSITION PROFILE FOR CARBON DIOXIDE (CO_2) FOR THE SHORT-FLAME BAFFLE USING THE AXIAL NOZZLE AT AN AXIAL POSITION OF 7.6 cm. GAS INPUT, 2190 CF/hr; EXCESS OXYGEN, 3.0%; PREHEATED AIR, 515^{0}F

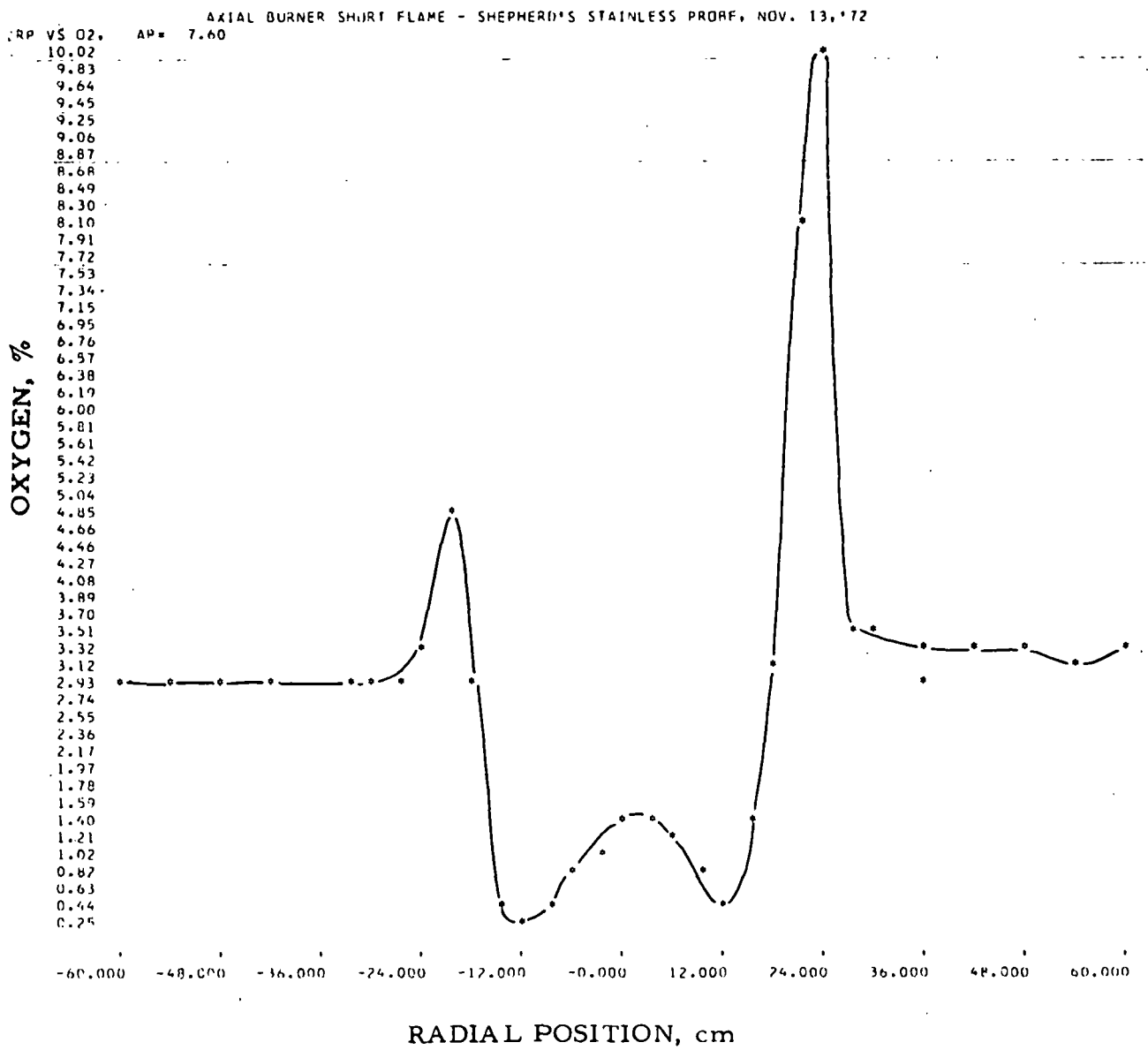

Figure II-164. RADIAL COMPOSITION PROFILE FOR OXYGEN (O_2) FOR THE SHORT-FLAME BAFFLE USING THE AXIAL NOZZLE AT AN AXIAL POSITION OF 7.6 cm. GAS INPUT, 2190 CF/hr; EXCESS OXYGEN, 3.0%; PREHEATED AIR, 515^{0}F

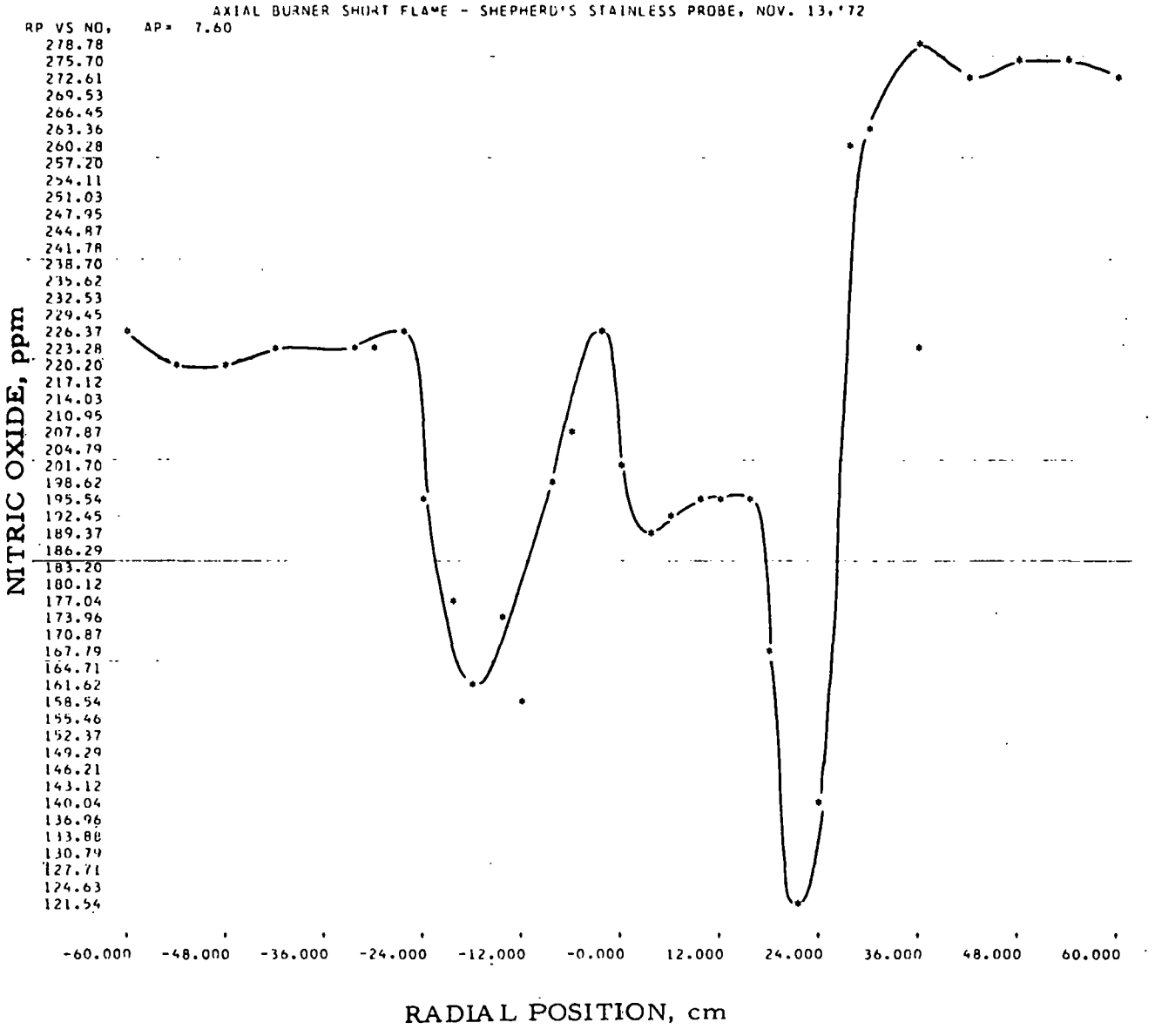

Figure II-165. RADIAL COMPOSITION PROFILE FOR NITRIC OXIDE (NO) FOR THE SHORT-FLAME BAFFLE USING THE AXIAL NOZZLE AT AN AXIAL POSITION OF 7.6 cm. GAS INPUT, 2190 CF/hr; EXCESS OXYGEN, 3.0%; PREHEATED AIR, 515^{0}F

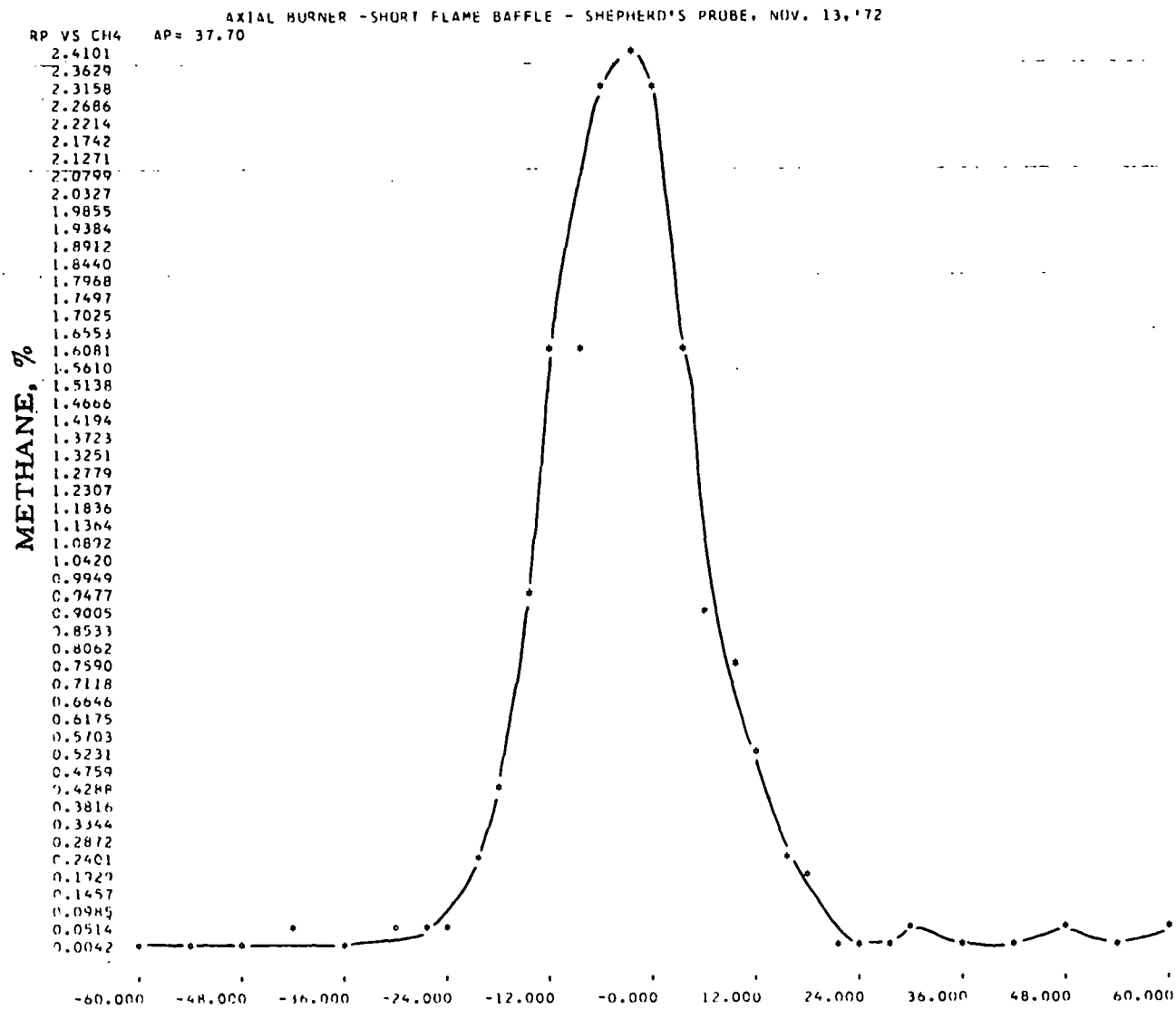

Figure II-166. RADIAL COMPOSITION PROFILE FOR METHANE (CH_4) FOR THE SHORT-FLAME BAFFLE USING THE AXIAL NOZZLE AT AN AXIAL POSITION OF 37.7 cm. GAS INPUT, 2190 CF/hr; EXCESS OXYGEN, 3.0% ; PREHEATED AIR, 502^{0}F

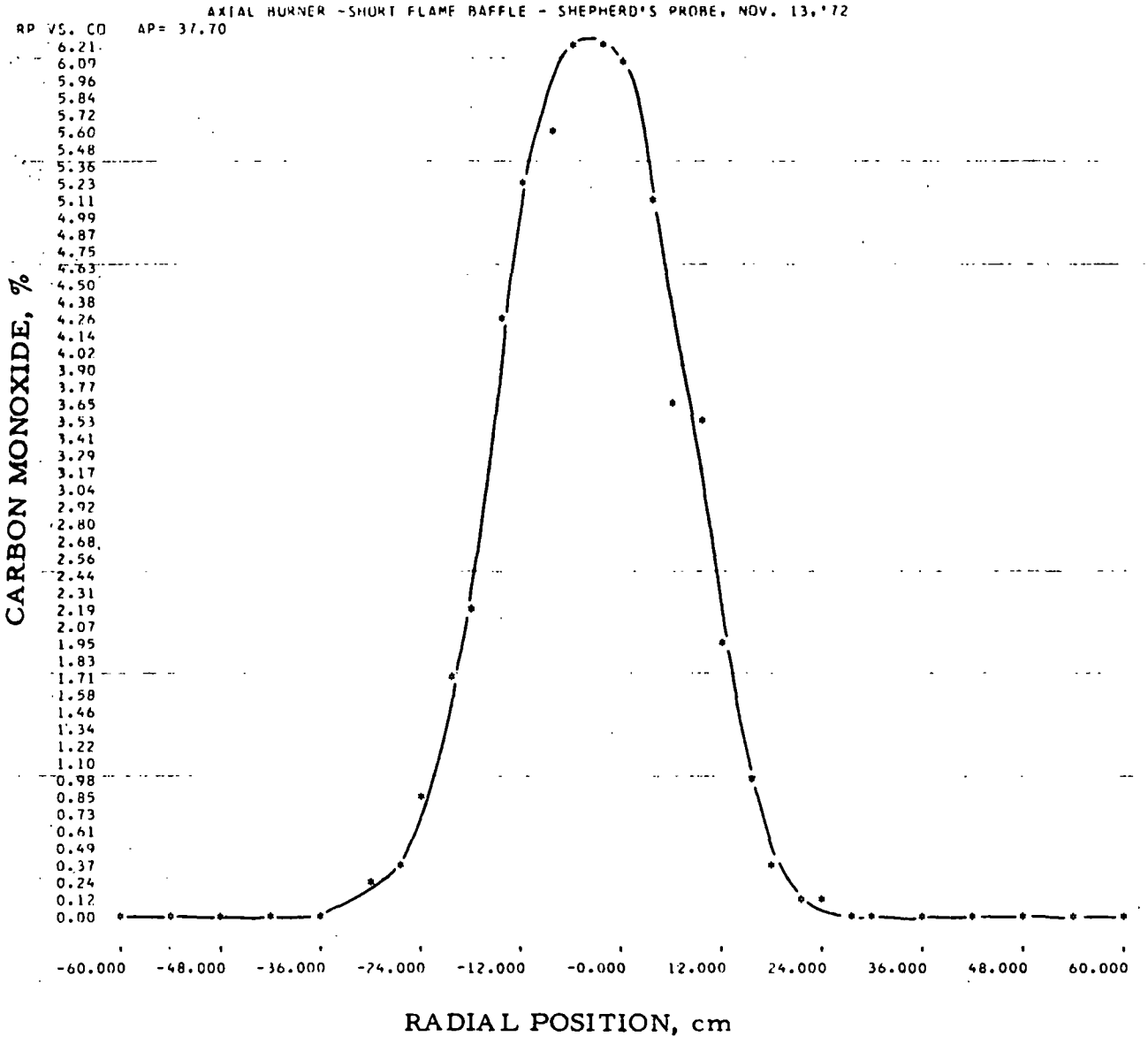

Figure II-167. RADIAL COMPOSITION PROFILE FOR CARBON MONOXIDE (CO) FOR THE SHORT-FLAME BAFFLE USING THE AXIAL NOZZLE AT AN AXIAL POSITION OF 37.7 cm. GAS INPUT, 2190 CF/hr; EXCESS OXYGEN, 3.0%; PREHEATED AIR, 502°F

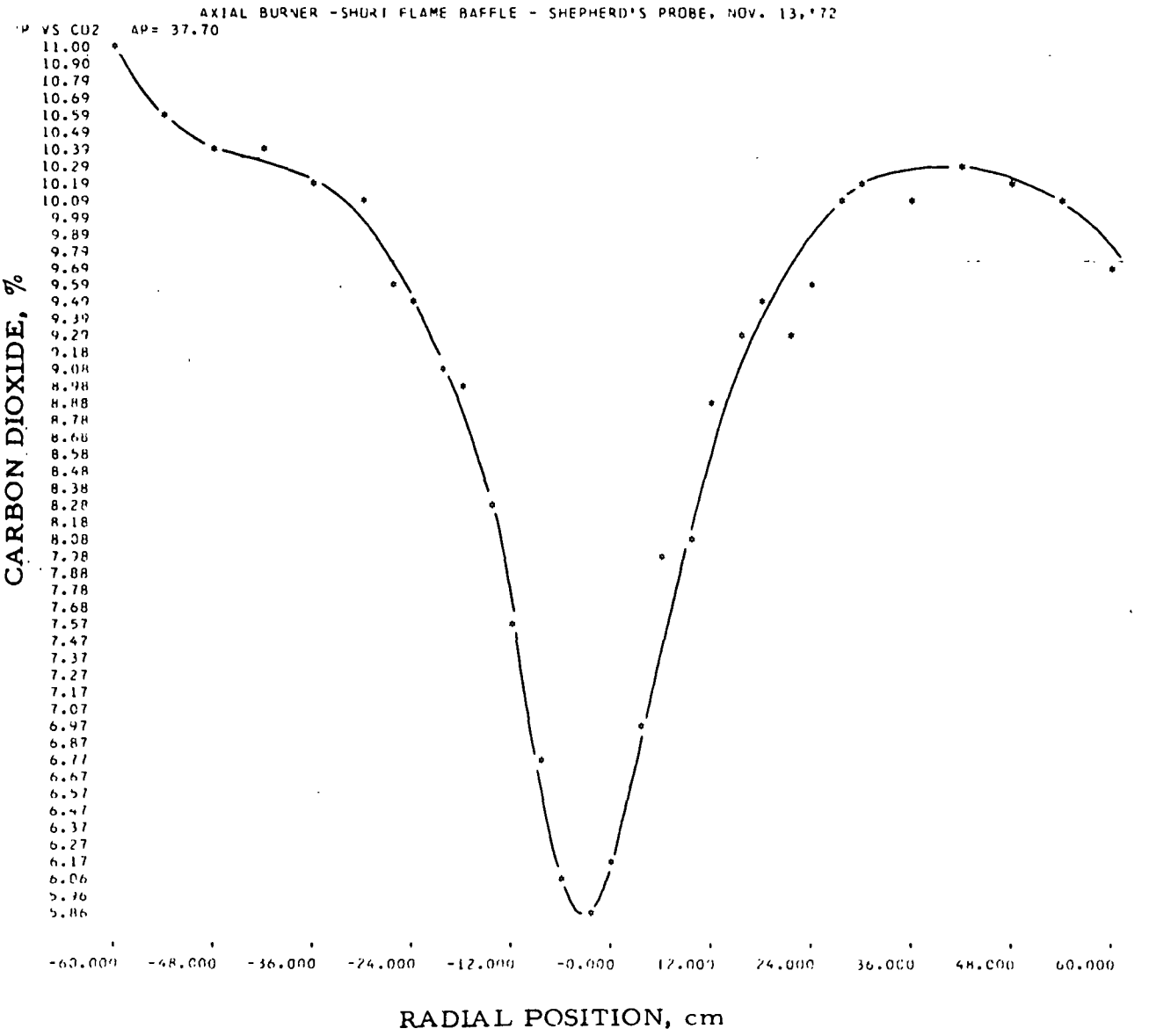

Figure II-168. RADIAL COMPOSITION PROFILE FOR CARBON DIOXIDE (CO_2) FOR THE SHORT-FLAME BAFFLE USING THE AXIAL NOZZLE AT AN AXIAL POSITION OF 37.7 cm. GAS INPUT, 2190 CF/hr; EXCESS OXYGEN, 3.0%; PREHEATED AIR, 502°F

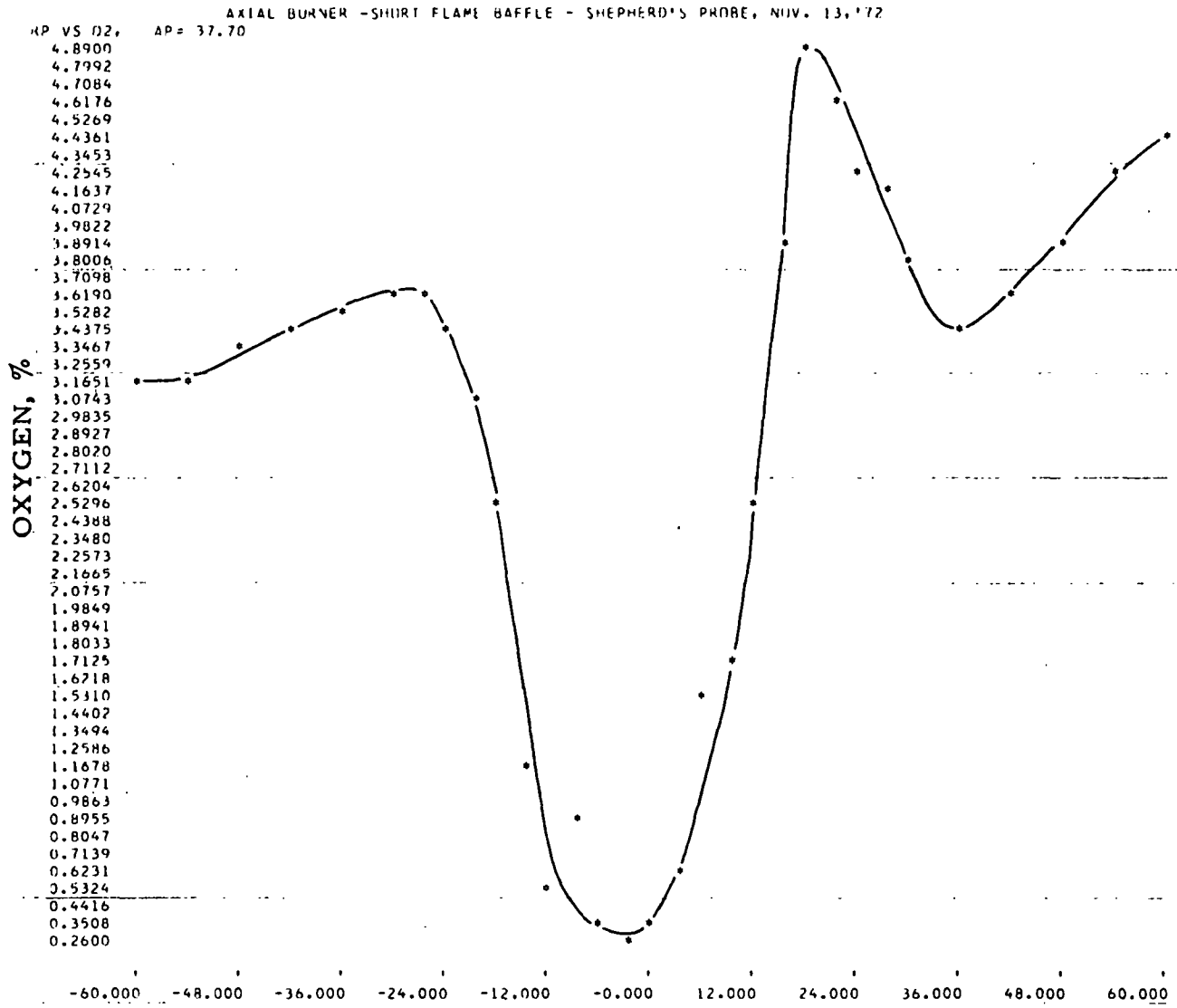

Figure II-169. RADIAL COMPOSITION PROFILE FOR OXYGEN (O_2) FOR THE SHORT-FLAME BAFFLE USING THE AXIAL NOZZLE AT AN AXIAL POSITION OF 37.7 cm. GAS INPUT, 2190 CF/hr; EXCESS OXYGEN, 3.0%; PREHEATED AIR, 502^{0}F

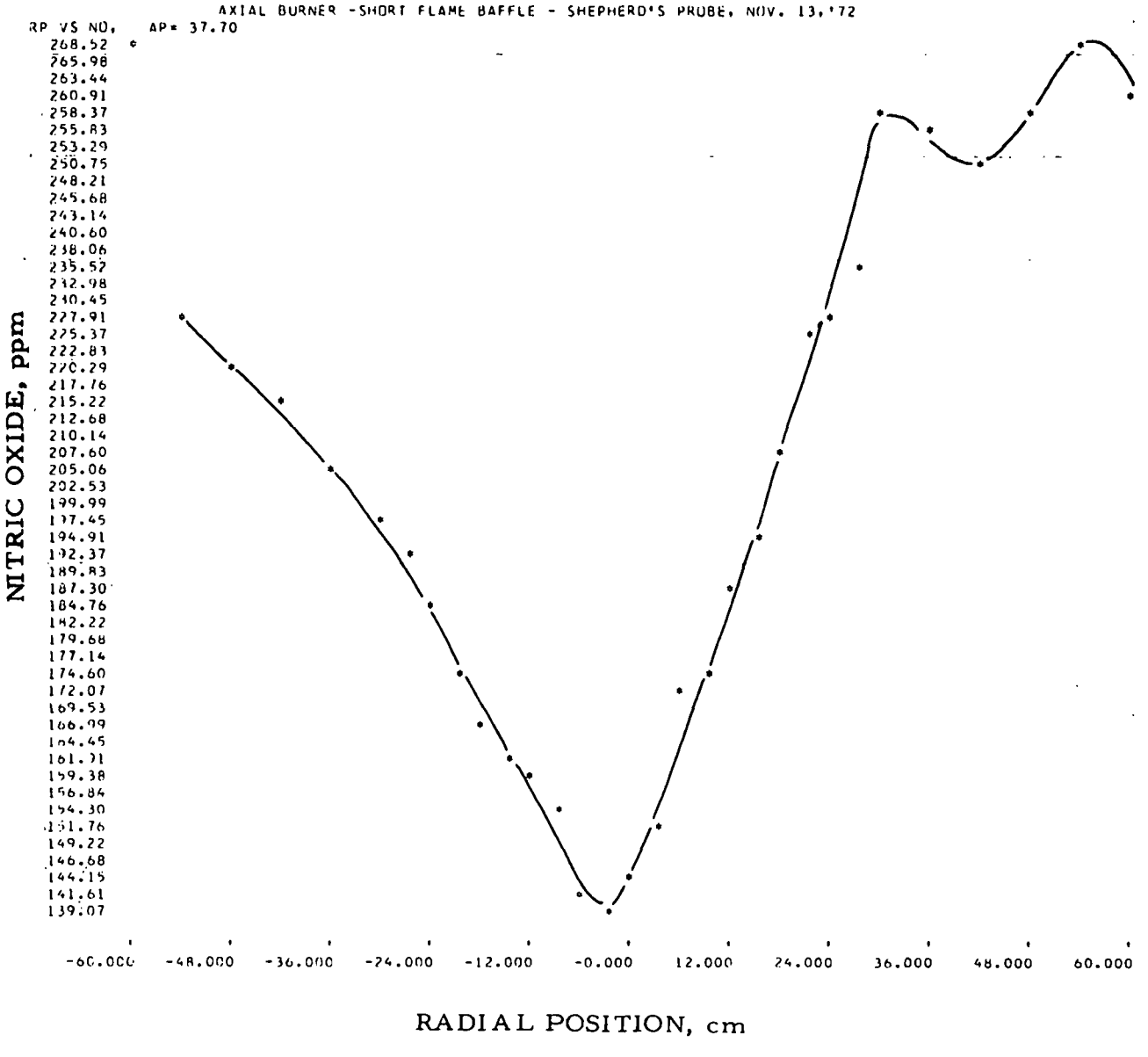

Figure II-170. RADIAL COMPOSITION PROFILE FOR NITRIC OXIDE (NO) FOR THE SHORT-FLAME BAFFLE USING THE AXIAL NOZZLE AT AN AXIAL POSITION OF 37.7 cm. GAS INPUT, 2190 CF/hr; EXCESS OXYGEN, 3.0%; PREHEATED AIR, 502°F

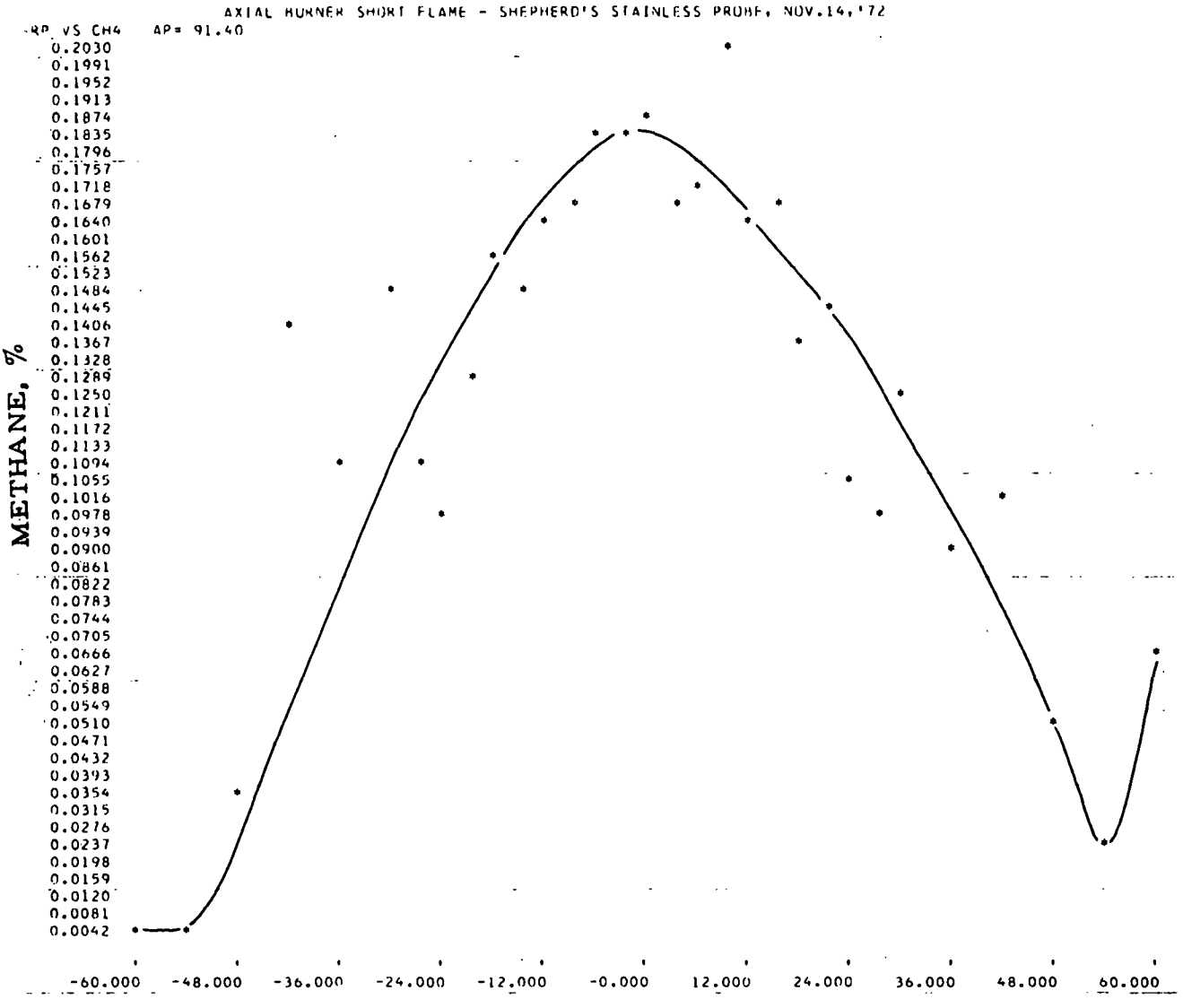

Figure II-171. RADIAL COMPOSITION PROFILE FOR METHANE (CH_4) FOR THE SHORT-FLAME BAFFLE USING THE AXIAL NOZZLE AT AN AXIAL POSITION OF 91.4 cm. GAS INPUT, 2190 CF/hr; EXCESS OXYGEN, 3.0%; PREHEATED AIR, 502^{0}F

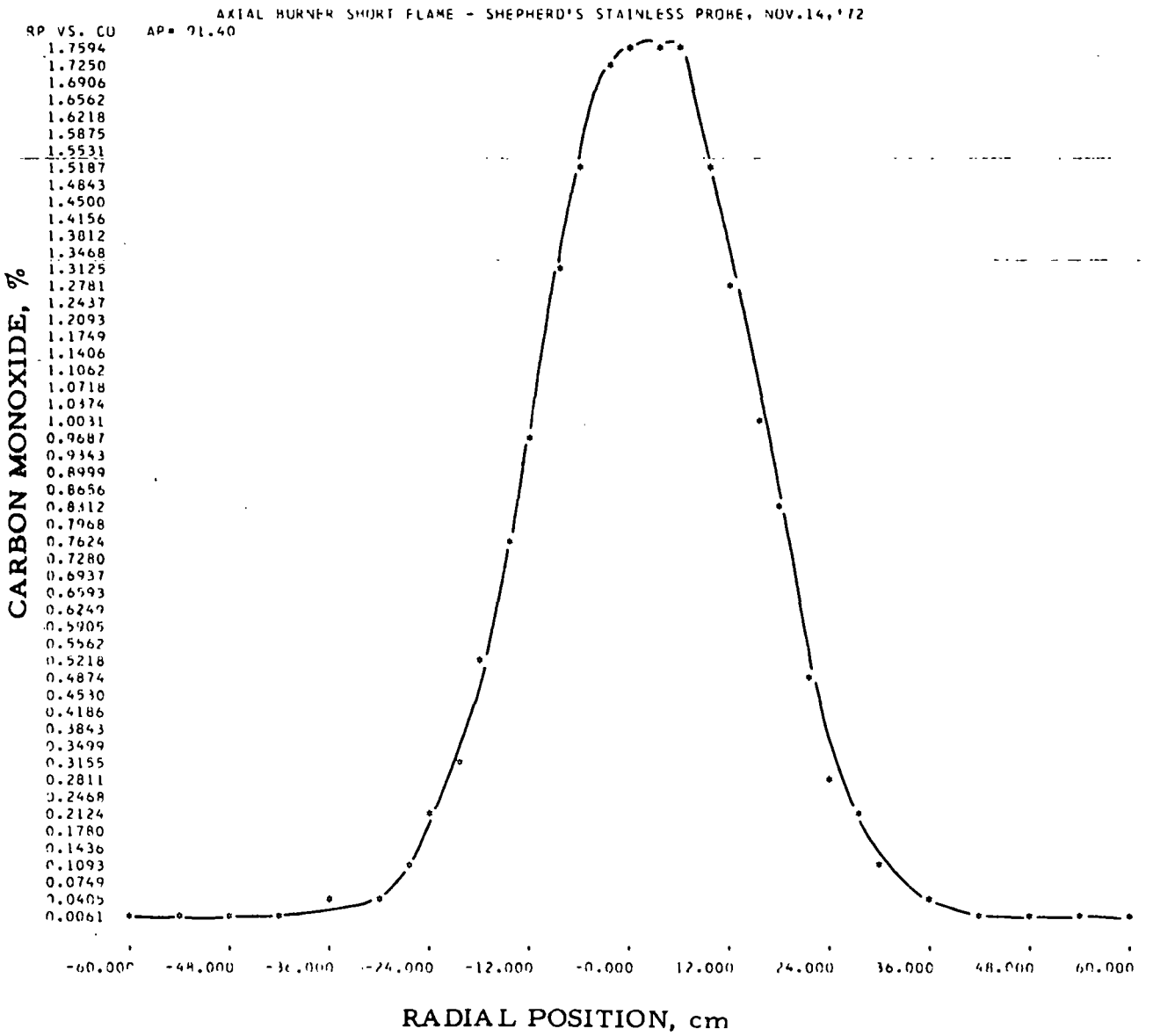

Figure II-172. RADIAL COMPOSITION PROFILE FOR CARBON MONOXIDE (CO) FOR THE SHORT-FLAME BAFFLE USING THE AXIAL NOZZLE AT AN AXIAL POSITION OF 91.4 cm. GAS INPUT, 2190 CF/hr; EXCESS OXYGEN, 3.0%; PREHEATED AIR, 502°F

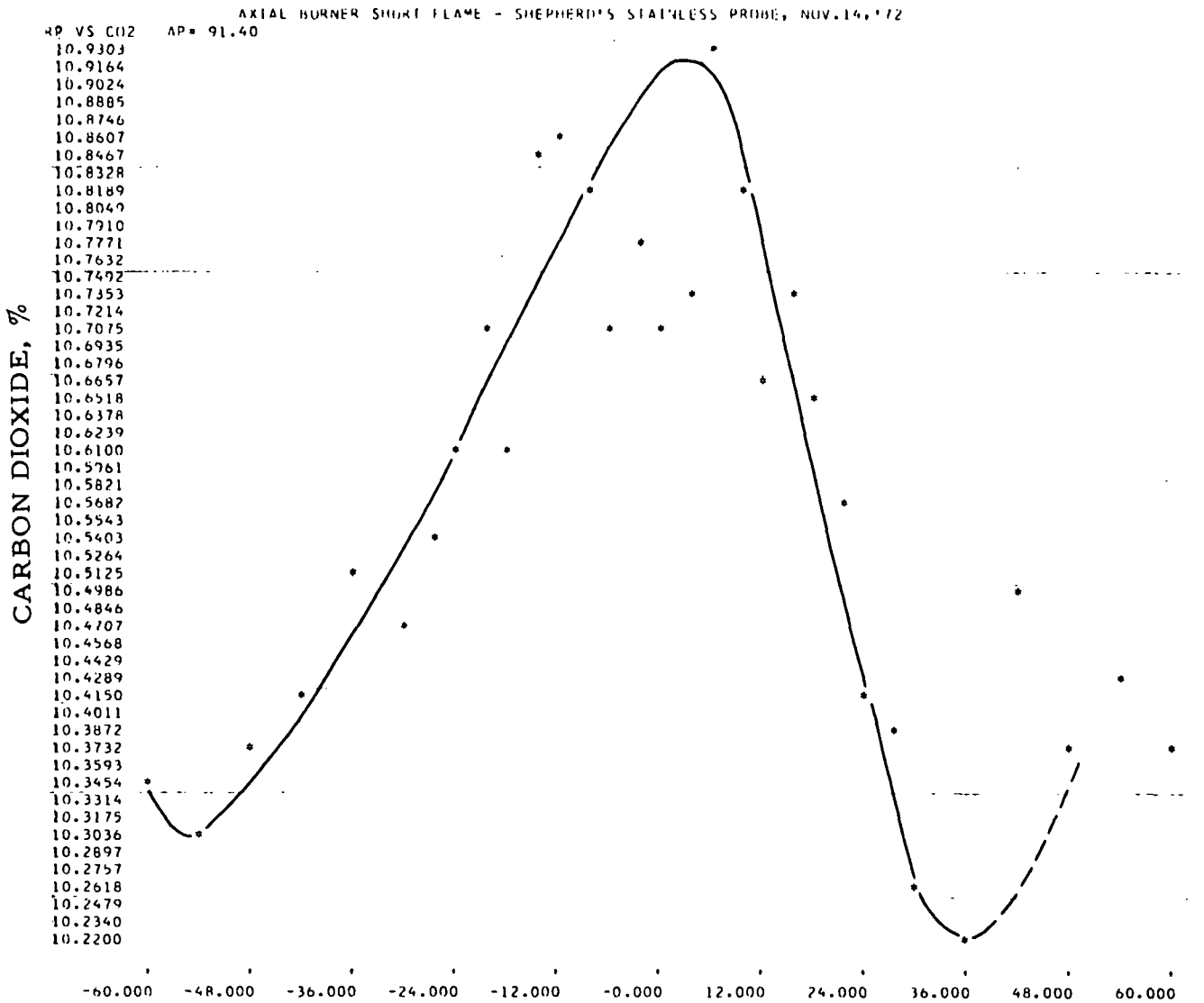

Figure II-173. RADIAL COMPOSITION PROFILE FOR CARBON DIOXIDE (CO_2) FOR THE SHORT-FLAME BAFFLE USING THE AXIAL NOZZLE AT AN AXIAL POSITION OF 91.4 cm. GAS INPUT, 2190 CF/hr; EXCESS OXYGEN, 3.0%; PREHEATED AIR, 485^{0}F

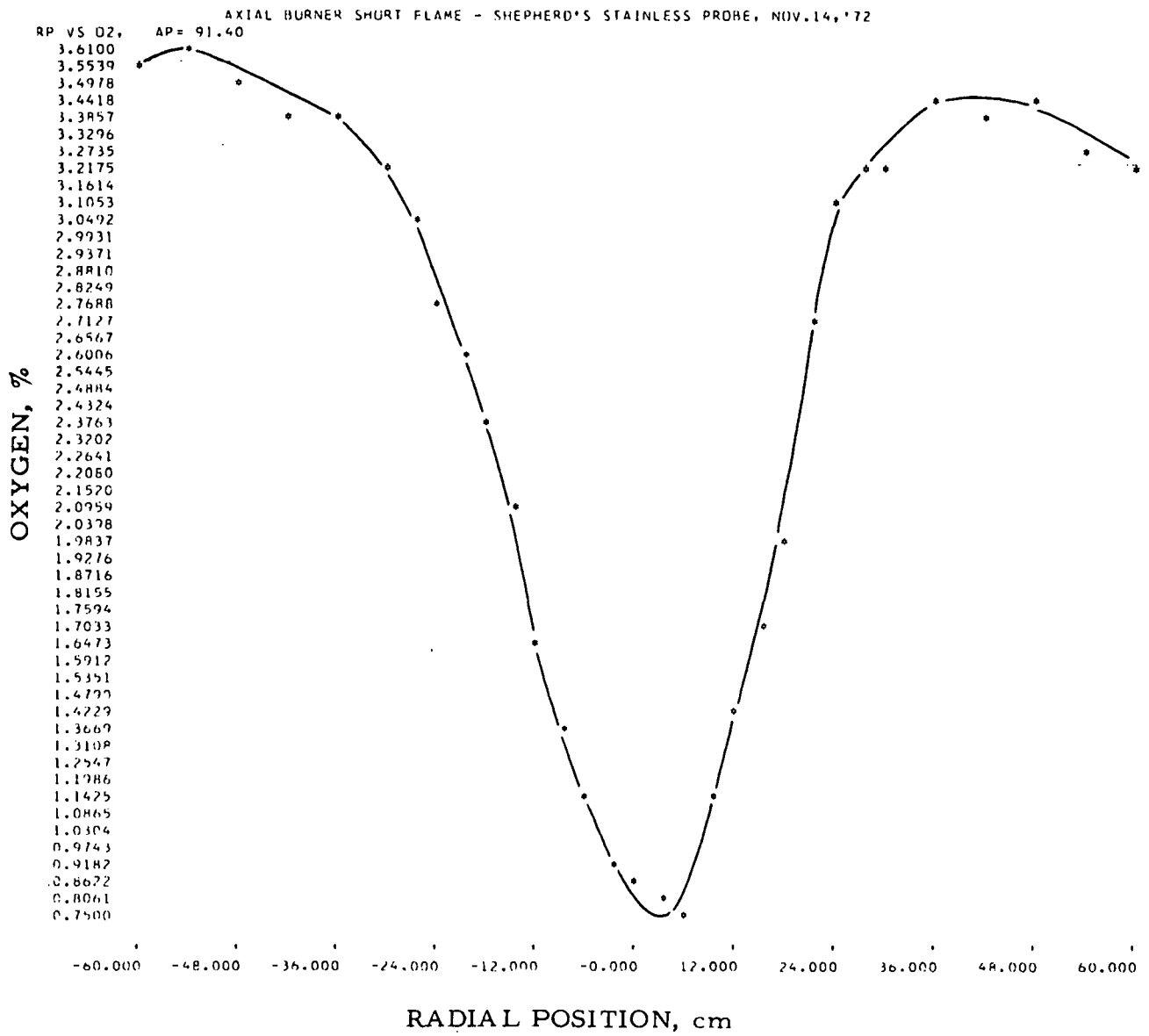

Figure II-174. RADIAL COMPOSITION PROFILE FOR OXYGEN (O_2) FOR THE SHORT-FLAME BAFFLE USING THE AXIAL NOZZLE AT AN AXIAL POSITION OF 91.4 cm. GAS INPUT, 2190 CF/hr; EXCESS OXYGEN, 3.0%; PREHEATED AIR, 485^{0}F

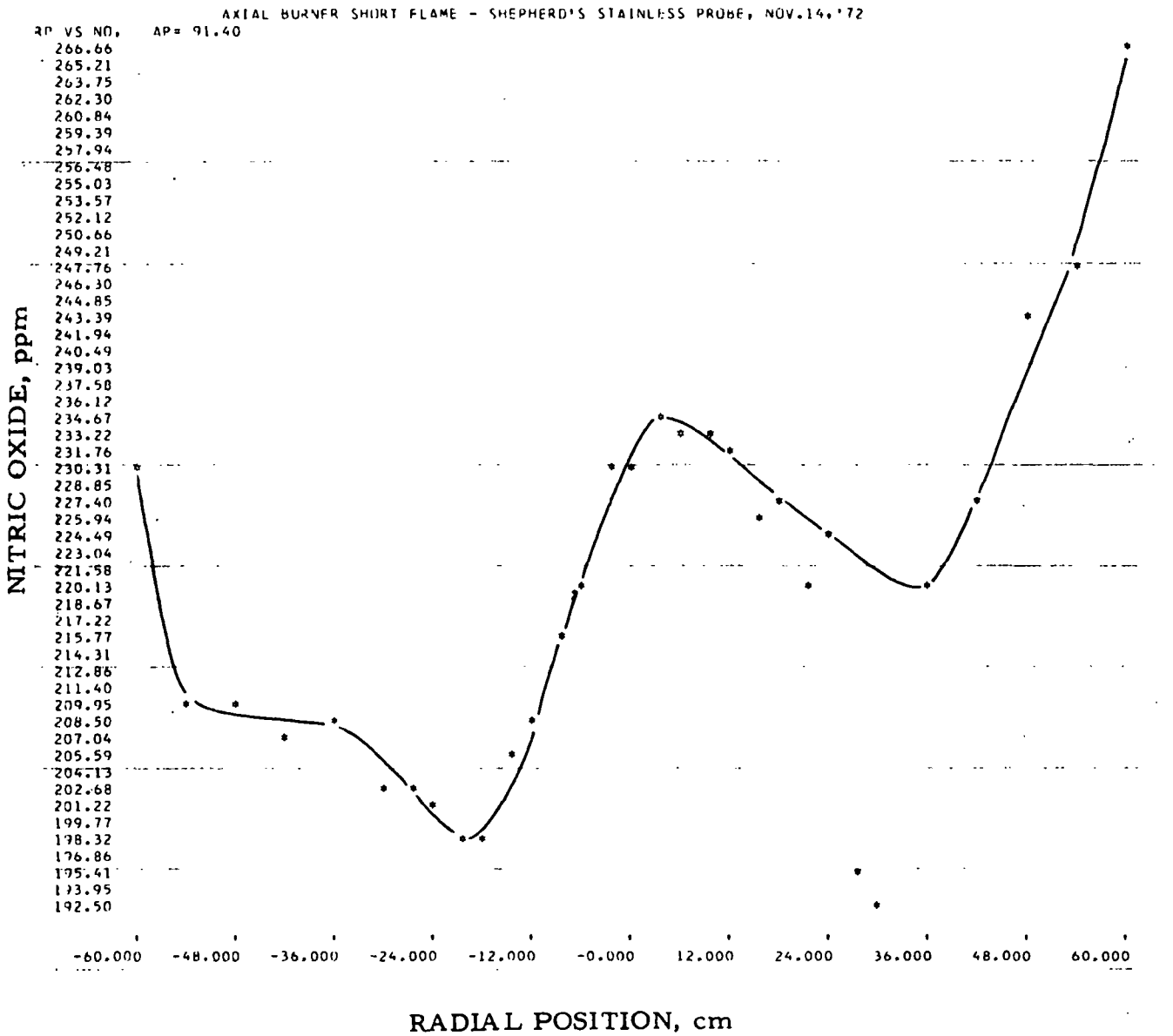

Figure II-175. RADIAL COMPOSITION PROFILE FOR NITRIC OXIDE (NO) FOR THE SHORT-FLAME BAFFLE USING THE AXIAL NOZZLE AT AN AXIAL POSITION OF 91.4 cm. GAS INPUT, 2190 CF/hr; EXCESS OXYGEN, 3.0%; PREHEATED AIR, 485^{0}F

Table II-26. RAW (Gas Analysis) DATA FOR SHORT-FLAME BAFFLE BURNER

TRACER GAS STUDIES OF COMBUSTION BURNERS PROGRAM 2
AXIAL BURNER SHORT FLAME - SHEPHERD'S STAINLESS PROBE, NOV. 13,'72

INPUT GAS 2190 WALL TEMPERATURE 2570 PREHEAT TEMPERATURE 515

OUTPUT ANALYSIS

NITROGEN OXIDE	36.50	PERCENT ON RANGE 1,	324.99	PPM	OXYGEN	2.87 PERCENT
CARBON DIOXIDE	81.20	PERCENT ON RANGE 1,	10.36	PERCENT		
CARBON MONOXIDE	5.30	PERCENT ON RANGE 3,	0.002	PERCENT		
METHANE	0.00	PERCENT ON RANGE 0,	0.00	PERCENT		

EXPERIMENTAL RESULTS

		NITROGEN OXIDE -NO			OXYGEN	CARBON DIOXIDE-CO2			CARBON MONOXIDE -CO			METHANE - CH4		
AP	RP	RANGE	X	Y	O2	RANGE	X	Y	RANGE	X	Y	RANGE	X	Y
7.60	-60.00	1	25.80	225.1	2.90	1	80.80	10.28	3	10.00	0.004	3	0.00	0.00
7.60	-54.00	1	25.10	218.7	2.88	1	80.90	10.30	3	8.90	0.003	3	0.00	0.00
7.60	-48.00	1	25.30	220.6	2.84	1	81.00	10.32	3	7.80	0.003	3	0.00	0.00
7.60	-42.00	1	25.50	222.4	2.91	1	81.20	10.36	3	8.40	0.003	3	0.00	0.00
7.60	36.00	1	25.50	222.4	2.95	1	81.00	10.32	3	8.10	0.003	3	0.00	0.00
7.60	-33.00	1	25.60	223.3	2.88	1	80.50	10.22	3	8.20	0.003	3	0.00	0.00
7.60	-30.00	1	25.70	224.2	2.95	1	81.30	10.39	3	8.20	0.003	3	0.00	0.00
7.60	-27.00	1	25.80	225.1	2.99	1	81.40	10.41	3	8.90	0.003	3	0.00	0.00
7.60	-24.00	1	22.70	197.0	3.37	1	75.40	9.16	3	92.30	0.045	3	0.00	0.00
7.60	-21.00	1	20.60	178.1	4.92	1	74.00	8.88	2	13.20	0.217	3	0.40	0.02
7.60	-18.00	1	18.60	160.2	3.00	1	74.50	8.98	1	49.30	1.791	3	1.70	0.07
7.60	-15.00	1	20.20	174.5	0.43	1	65.30	7.24	1	110.00	5.781	1	14.50	1.33
7.60	-12.00	1	18.30	157.6	0.25	1	55.10	5.52	1	112.60	5.996	1	59.10	8.59
7.60	-9.00	1	22.80	197.9	0.46	1	48.70	4.56	1	114.00	6.113	1	78.80	13.44
7.60	-6.00	1	23.90	207.8	0.75	1	43.70	3.86	1	109.80	5.764	1	106.10	21.83
7.60	-3.00	1	25.80	225.1	1.08	1	38.70	3.22	1	101.30	5.087	1	112.70	24.15
7.60	0.00	1	23.30	202.4	1.31	1	35.00	2.78	1	96.60	4.730	1	112.40	24.04
7.60	3.00	1	22.00	190.6	1.39	1	34.20	2.69	1	95.20	4.625	1	112.40	24.04
7.60	6.00	1	22.20	192.5	1.20	1	38.10	3.15	1	100.50	5.026	1	113.20	24.33
7.60	9.00	1	22.70	197.0	0.89	1	49.30	4.64	1	106.90	5.529	1	103.70	21.01
7.60	12.00	1	22.70	197.0	0.48	1	63.70	6.96	1	104.40	5.330	1	49.50	6.59
7.60	15.00	1	22.60	196.1	1.35	1	73.30	8.75	1	80.50	3.594	3	18.00	0.78
7.60	18.00	1	19.50	168.2	3.13	1	74.30	8.94	1	49.70	1.811	3	2.00	0.08
7.60	21.00	1	14.20	121.5	8.02	1	62.90	6.82	2	20.70	0.346	3	0.90	0.04
7.60	24.00	1	16.40	140.8	10.02	1	56.80	5.79	3	18.00	0.007	3	0.00	0.00
7.60	27.00	1	29.50	259.2	3.49	1	80.10	10.13	3	10.40	0.004	3	0.00	0.00
7.60	30.00	1	30.00	263.8	3.43	1	79.90	10.09	3	11.10	0.004	3	0.00	0.00
7.60	36.00	1	31.60	278.7	3.36	1	80.80	10.28	3	11.10	0.004	3	0.00	0.00
7.60	42.00	1	31.10	274.1	3.40	1	81.00	10.32	3	10.50	0.004	3	0.00	0.00
7.60	48.00	1	31.40	276.9	3.41	1	80.40	10.19	3	10.80	0.004	3	0.00	0.00
7.60	54.00	1	31.40	276.9	3.20	1	79.80	10.07	3	9.90	0.004	3	0.00	0.00
7.60	60.00	1	30.80	271.3	3.33	1	80.20	10.15	3	10.20	0.004	3	0.00	0.00

Table II-27. RAW (Gas Analysis) DATA FOR SHORT-FLAME BAFFLE BURNER

TRACER GAS STUDIES OF COMBUSTION BURNERS PROGRAM 2
AXIAL BURNER -SHORT FLAME BAFFLE - SHEPHERD'S PROBE, NOV. 13,'72

INPUT GAS 2190 WALL TEMPERATURE 2584 PREHEAT TEMPERATURE 502

OUTPUT ANALYSIS

NITROGEN OXIDE	35.20 PERCENT ON RANGE 1,	312.65 PPM	OXYGEN	2.90 PERCENT	
CARBON DIOXIDE	82.40 PERCENT ON RANGE 1,	10.62 PERCENT			
CARBON MONOXIDE	5.50 PERCENT ON RANGE 3,	0.002 PERCENT			
METHANE	0.00 PERCENT ON RANGE 0,	0.00 PERCENT			

EXPERIMENTAL RESULTS

		NITROGEN OXIDE -NO			OXYGEN	CARBON DIOXIDE-CO2			CARBON MONOXIDE -CO			METHANE - CH4		
AP	RP	RANGE	X	Y	O2	RANGE	X	Y	RANGE	X	Y	RANGE	X	Y
37.70	-60.00	1	30.40	267.5	3.17	1	84.10	10.99	3	15.40	0.006	3	0.00	0.00
37.70	-54.00	1	26.00	227.0	3.19	1	82.10	10.56	3	13.70	0.005	3	0.00	0.00
37.70	-48.00	1	25.40	221.5	3.34	1	81.40	10.41	3	14.20	0.005	3	0.20	0.01
37.70	-42.00	1	24.60	214.2	3.41	1	81.30	10.39	3	20.00	0.008	3	0.70	0.03
37.70	-36.00	1	23.70	206.0	3.49	1	80.60	10.24	3	59.30	0.027	3	0.40	0.02
37.70	-30.00	1	22.70	197.0	3.58	1	79.80	10.07	2	12.20	0.200	3	0.80	0.03
37.70	-27.00	1	22.10	191.5	3.58	1	77.60	9.61	2	22.10	0.371	3	1.10	0.05
37.70	-24.00	1	21.30	184.4	3.48	1	76.80	9.45	2	46.30	0.822	3	1.50	0.06
37.70	-21.00	1	20.20	174.5	3.04	1	75.20	9.12	2	90.20	1.764	3	6.00	0.25
37.70	-18.00	1	19.30	166.5	2.49	1	74.60	9.00	1	57.20	2.198	3	9.80	0.42
37.70	-15.00	1	18.90	162.9	1.13	1	71.10	8.32	1	89.80	4.233	3	21.40	0.93
37.70	-12.00	1	18.60	160.2	0.51	1	66.90	7.53	1	103.60	5.267	3	35.40	1.58
37.70	-9.00	1	18.00	154.9	0.92	1	62.50	6.75	1	108.50	5.658	3	36.00	1.61
37.70	-6.00	1	16.60	142.5	0.38	1	58.20	6.02	1	115.10	6.206	3	50.00	2.29
37.70	-3.00	1	16.20	139.0	0.26	1	57.20	5.86	1	114.50	6.156	3	52.20	2.41
37.70	0.00	1	16.80	144.3	0.32	1	59.10	6.17	1	113.00	6.029	3	50.40	2.31
37.70	3.00	1	17.50	150.5	0.60	1	63.80	6.98	1	101.80	5.126	3	35.50	1.59
37.70	6.00	1	19.90	171.8	1.49	1	69.10	7.94	1	81.60	3.668	3	20.50	0.89
37.70	9.00	1	20.30	175.4	1.68	1	70.00	8.11	1	79.50	3.528	3	17.30	0.75
37.70	12.00	1	21.70	187.9	2.51	1	74.20	8.92	1	51.80	1.916	3	11.80	0.51
37.70	15.00	1	22.40	194.3	3.87	1	76.20	9.32	1	30.10	0.941	3	5.20	0.22
37.70	18.00	1	23.80	206.9	4.89	1	76.80	9.45	1	14.10	0.384	3	4.30	0.18
37.70	21.00	1	25.70	224.2	4.60	1	76.00	9.28	1	3.00	0.078	3	0.00	0.00
37.70	24.00	1	26.10	227.9	4.27	1	77.60	9.61	1	3.30	0.086	3	0.00	0.00
37.70	27.00	1	27.00	236.1	4.18	1	80.00	10.11	3	17.10	0.007	3	0.00	0.00
37.70	30.00	1	29.30	257.3	3.84	1	80.20	10.15	3	8.00	0.003	3	0.80	0.03
37.70	36.00	1	29.00	254.6	3.40	1	80.00	10.11	3	4.00	0.001	3	0.00	0.00
37.70	42.00	1	28.60	250.9	3.63	1	80.80	10.28	3	5.20	0.002	3	0.00	0.00
37.70	48.00	1	29.30	257.3	3.90	1	80.50	10.22	3	5.10	0.002	3	0.80	0.03
37.70	54.00	1	30.50	268.5	4.24	1	79.70	10.05	3	5.20	0.002	3	0.50	0.02
37.70	60.00	1	29.80	262.0	4.43	1	78.00	9.69	3	5.10	0.002	3	0.70	0.03

Table II-28. RAW (Gas Analysis) DATA FOR SHORT-FLAME BAFFLE BURNER

TRACER GAS STUDIES OF COMBUSTION BURNERS PROGRAM 2
AXIAL BURNER SHORT FLAME - SHEPHERD'S STAINLESS PROBE, NOV.14,'72

INPUT GAS 2190 WALL TEMPERATURE 2619 PREHEAT TEMPERATURE 485

OUTPUT ANALYSIS

NITROGEN OXIDE	35.00 PERCENT ON RANGE 1,	310.75 PPM	OXYGEN	2.92 PERCENT
CARBON DIOXIDE	81.90 PERCENT ON RANGE 1,	10.51 PERCENT		
CARBON MONOXIDE	7.60 PERCENT ON RANGE 3,	0.003 PERCENT		
METHANE	0.00 PERCENT ON RANGE 0,	0.00 PERCENT		

EXPERIMENTAL RESULTS

		NITROGEN OXIDE -NO			OXYGEN	CARBON DIOXIDE-CO2			CARBON MONOXIDE -CO			METHANE - CH4		
AP	RP	RANGE	X	Y	O2	RANGE	X	Y	RANGE	X	Y	RANGE	X	Y
91.40	-60.00	1	26.40	230.6	3.55	1	81.10	10.34	3	19.10	0.007	3	0.00	0.00
91.40	-54.00	1	24.20	210.5	3.61	1	80.90	10.30	3	20.00	0.008	3	0.00	0.00
91.40	-48.00	1	24.20	210.5	3.49	1	81.20	10.36	3	21.20	0.008	3	0.70	0.03
91.40	-42.00	1	23.80	206.9	3.37	1	81.40	10.41	3	32.00	0.013	3	3.20	0.13
91.40	-36.00	1	24.00	208.7	3.36	1	81.90	10.51	3	54.20	0.024	3	2.50	0.10
91.40	-30.00	1	23.30	202.4	3.20	1	81.70	10.47	3	96.70	0.047	3	3.40	0.14
91.40	-27.00	1	23.30	202.4	3.05	1	82.00	10.54	2	7.30	0.119	3	2.50	0.10
91.40	-24.00	1	23.20	201.5	2.78	1	82.30	10.60	2	12.20	0.200	3	2.20	0.09
91.40	-21.00	1	22.80	197.9	2.60	1	82.80	10.71	2	19.10	0.319	3	3.00	0.13
91.40	-18.00	1	22.90	198.8	2.35	1	82.30	10.60	2	29.90	0.511	3	3.60	0.15
91.40	-15.00	1	23.60	205.1	2.07	1	83.40	10.84	2	43.80	0.773	3	3.40	0.14
91.40	-12.00	1	24.00	208.7	1.67	1	83.50	10.86	2	53.10	0.958	3	3.80	0.16
91.40	-9.00	1	24.80	216.0	1.34	1	83.30	10.82	2	70.00	1.311	3	3.90	0.16
91.40	-6.00	1	25.30	220.6	1.12	1	82.80	10.71	2	78.80	1.504	3	4.20	0.18
91.40	-3.00	1	26.30	229.7	0.91	1	83.10	10.77	2	88.50	1.724	3	4.20	0.18
91.40	0.00	1	26.40	230.6	0.88	1	82.80	10.71	2	89.40	1.745	3	4.30	0.18
91.40	3.00	1	26.80	234.3	0.78	1	82.90	10.73	2	90.00	1.759	3	3.90	0.16
91.40	6.00	1	26.70	233.4	0.75	1	83.80	10.93	2	89.90	1.757	3	4.00	0.17
91.40	9.00	1	26.60	232.4	1.14	1	83.30	10.82	2	80.00	1.531	3	4.70	0.20
91.40	12.00	1	26.50	231.5	1.44	1	82.60	10.66	2	69.10	1.291	3	3.80	0.16
91.40	15.00	1	25.90	226.0	1.71	1	82.90	10.73	2	55.50	1.006	3	3.90	0.16
91.40	18.00	1	26.00	227.0	1.97	1	82.50	10.64	2	46.40	0.824	3	3.10	0.13
91.40	21.00	1	25.20	219.6	2.73	1	82.10	10.56	2	29.20	0.498	3	3.30	0.14
91.40	24.00	1	25.80	225.1	3.11	1	81.40	10.41	2	17.10	0.284	3	2.40	0.10
91.40	27.00	1	22.60	196.1	3.22	1	81.30	10.39	2	13.10	0.216	3	2.20	0.09
91.40	30.00	1	22.20	192.5	3.19	1	80.70	10.26	2	7.50	0.122	3	2.90	0.12
91.40	36.00	1	25.20	219.6	3.45	1	80.50	10.22	3	71.50	0.033	3	2.00	0.08
91.40	42.00	1	26.00	227.0	3.41	1	81.80	10.49	3	46.50	0.020	3	2.30	0.10
91.40	48.00	1	27.80	243.5	3.44	1	81.20	10.36	3	15.20	0.006	3	1.10	0.05
91.40	54.00	1	28.30	248.1	3.28	1	81.50	10.43	3	14.80	0.006	3	0.50	0.02
91.40	60.00	1	30.30	266.6	3.22	1	81.20	10.36	3	15.10	0.006	3	1.50	0.06

C. Movable Block Swirl Burner

1. Burner Design

The movable block burner is constructed so that the ratio of the axial and radial velocities can be varied. (See a cross-sectional view in Figure II-176.) The outlet of the burner was designed so that divergent sections of different angles could be interchanged (Figure II-177).

Swirl vanes, located in the rear air chamber (Figure II-178), will produce varying degrees of swirl intensity of the air stream by adjusting the vane positions. The movable vanes are attached to a circular rotating ring. The fuel nozzle is located down the center of the burner and is retractable to allow for variation of the port mixing. The diameter of the gas nozzle is easily varied by substituting a new center pipe and swirl-guide section. This provides an easy means for changing the air/fuel velocity ratio. Figure II-179 shows an approximate measure of swirl intensity as a function of vane setting E.

2. Tracer-Gas Studies

We made radial scans of tracer-gas concentration to determine the exact areas where point-by-point sampling should be undertaken. Figure II-180 shows the coordinate system used to define the probe position in the cold-model unit.

Data were gathered by moving the tracer-gas sampling probe radially across the chamber at a constant velocity, at several fixed axial positions, which corresponds to the axis of the burner. These scans were limited to distances on the Y-axis of +30 cm from the X-axis.

Figures II-181, II-182, II-183, and II-184 show gas concentration profiles for the intermediate swirl intensity on the burner axis at 2.5, 6.12, 12.7, and 16.8 cm from the burner. Comparing Figure II-181 with later velocity data, we found that the width of the central concentration peak increased significantly with increasing swirl intensity. Figure II-183 shows that at 16.78 cm from the burner wall the tracer gas is completely mixed and its concentration uniform across the chamber width; however, for the case of minimum swirl, the tracer gas was not completely mixed until it reached a point 101.62 cm from the burner wall.

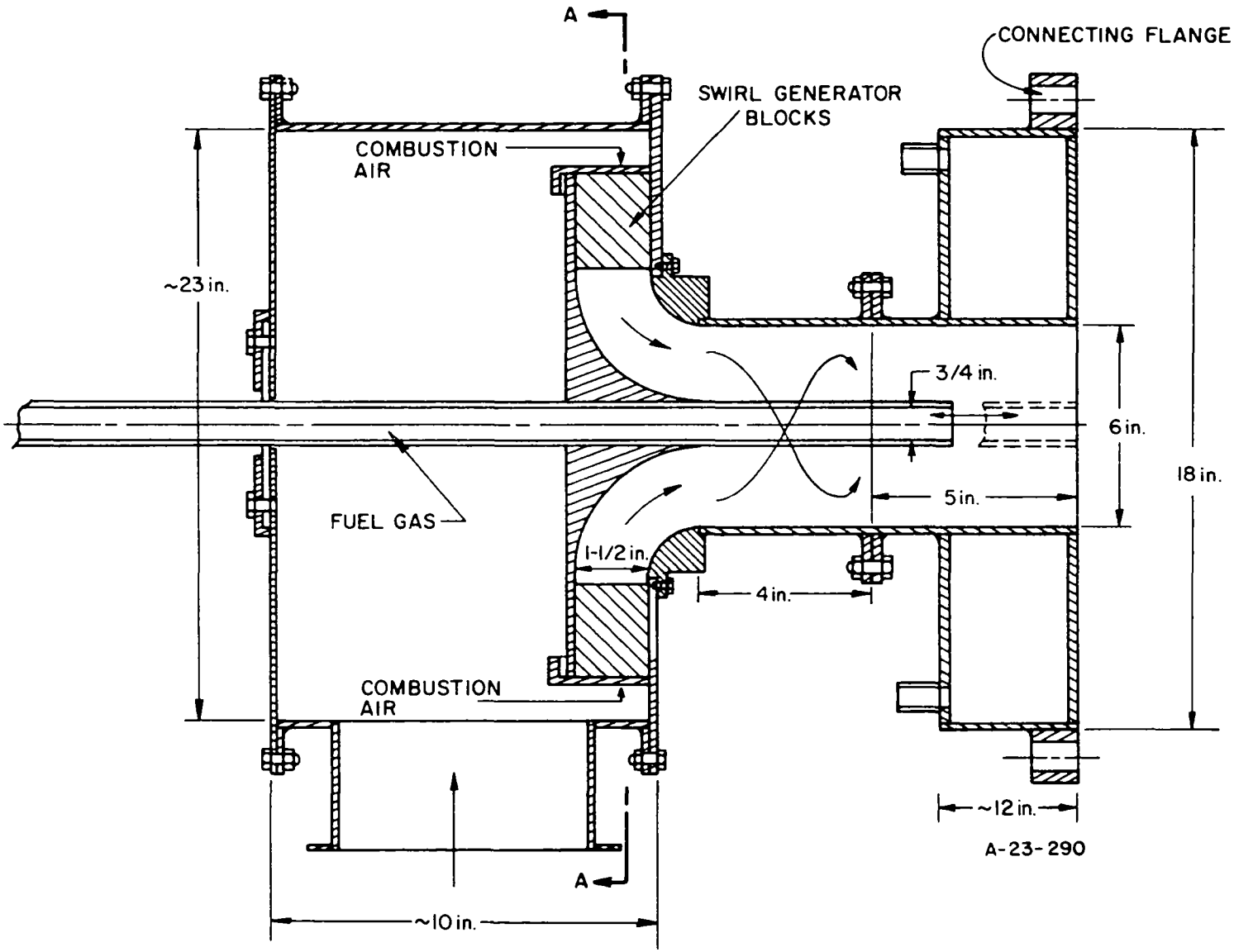

Figure II-176. CROSS SECTION OF HOT-MODEL BURNER

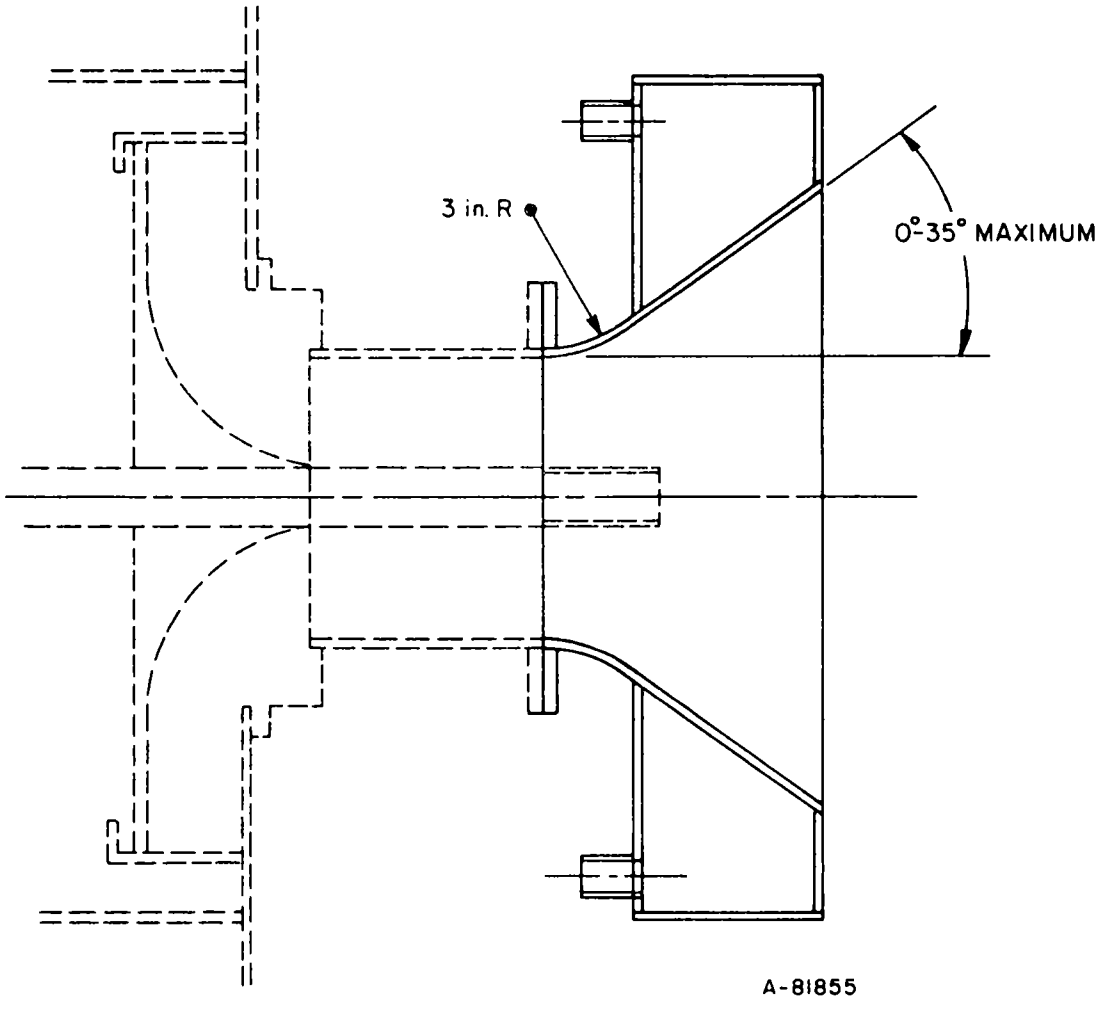

Figure II-177. DIVERGENT FLOW ADAPTER OF HOT-MODEL BURNER

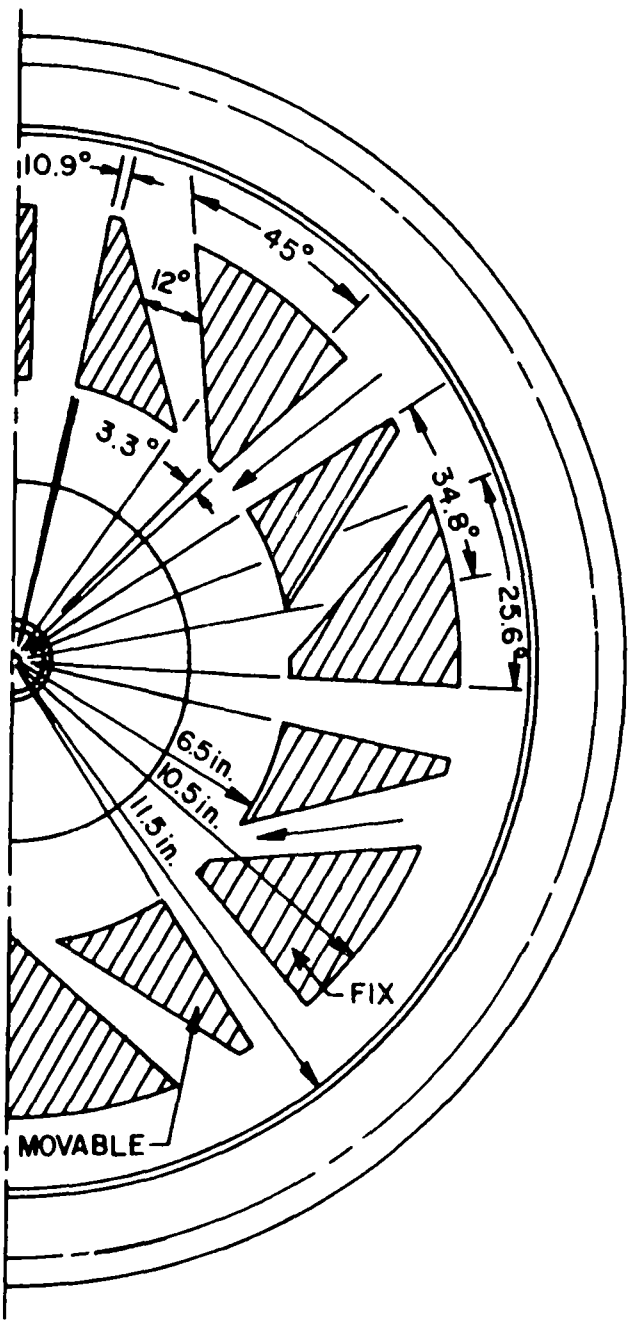

A-23-291

Figure II-178. SWIRL VANES OF HOT-MODEL BURNER

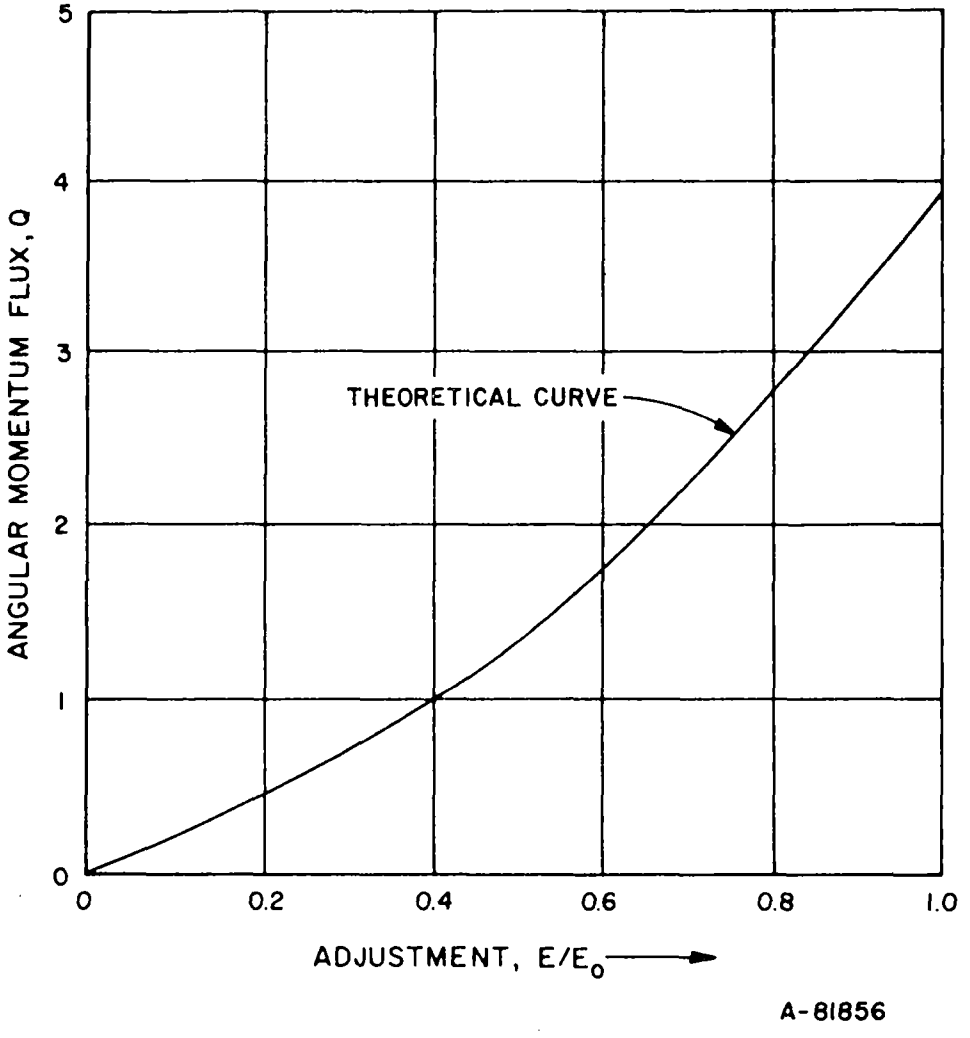

Figure II-179. SWIRL CURVE OF HOT-MODEL BURNER

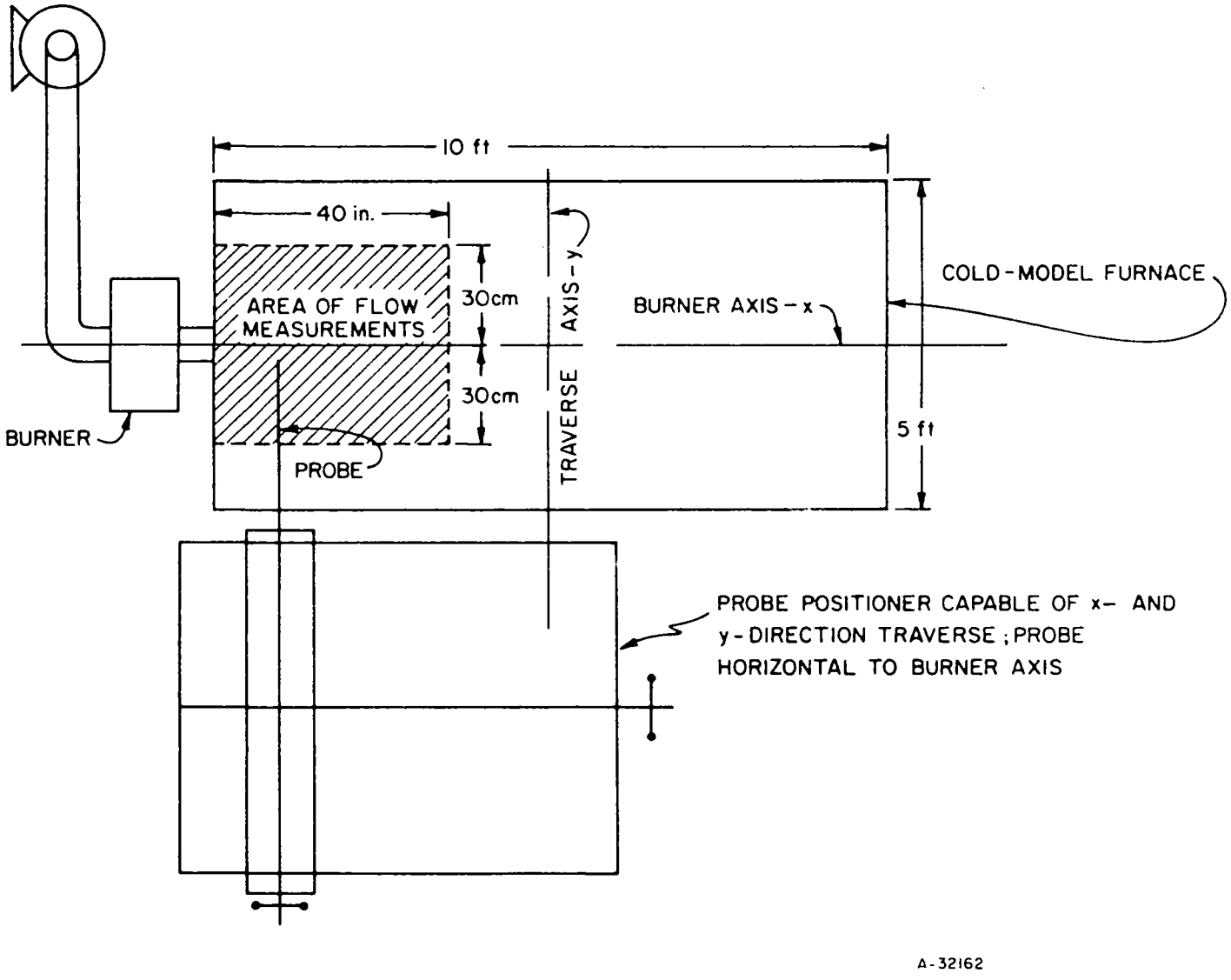

Figure II-180. COLD-MODEL PROBE-POSITIONING COORDINATE SYSTEM

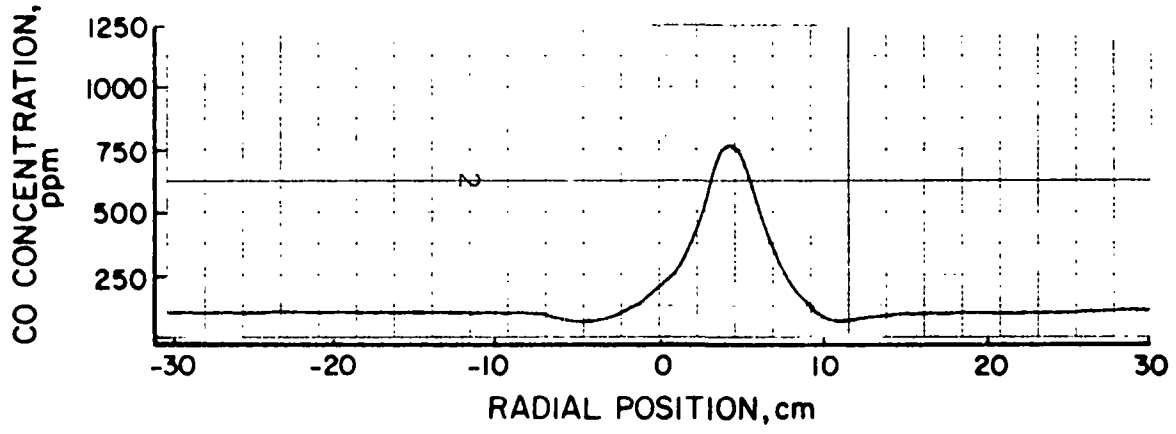

Figure II-181. RADIAL CONCENTRATION PROFILE OF CARBON MONOXIDE FROM THE MOVABLE-BLOCK BURNER 2.59 cm OUT FROM BURNER TIP [Air Velocity 28 ft/s; Gas Velocity (Air) 110 ft/s; 1000:1 Air/CO Ratio in Gas Stream]. INTERMEDIATE SWIRL

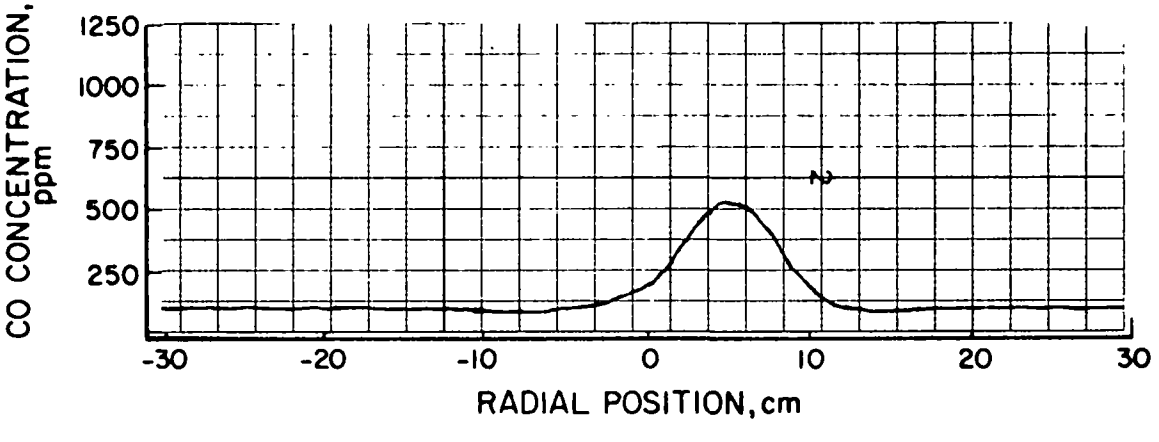

Figure II-182. RADIAL CONCENTRATION PROFILE OF CARBON MONOXIDE FROM THE MOVABLE-BLOCK BURNER 6.12 cm OUT FROM THE BURNER TIP [Air Velocity 28 ft/s; Gas Velocity (Air) 110 ft/s; 1000:1 Air/CO Ratio in Gas Stream]. INTERMEDIATE SWIRL

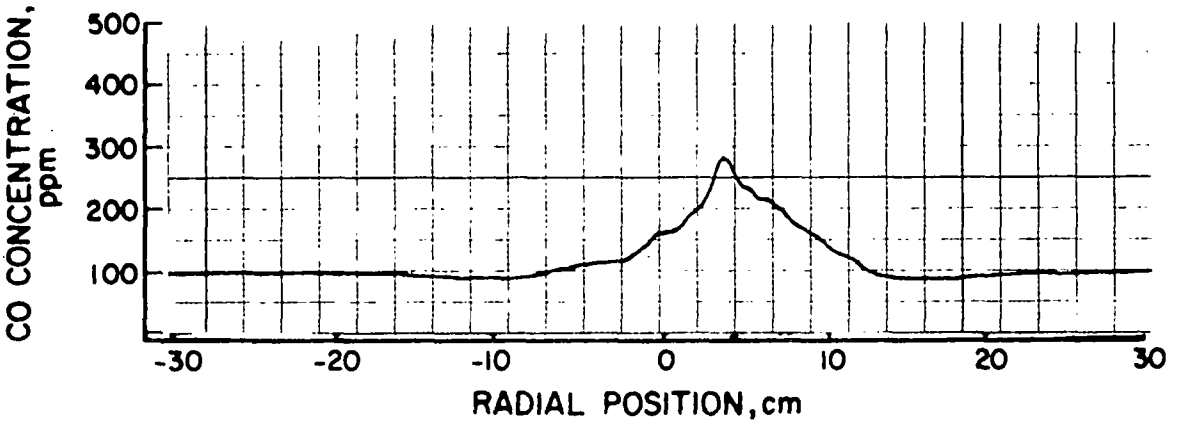

A-32208

Figure II-183. RADIAL CONCENTRATION PROFILE OF CARBON MONOXIDE FROM MOVABLE-BLOCK BURNER 12.70 cm OUT FROM BURNER TIP [Air Velocity 28 ft/s; Gas Velocity (Air) 110 ft/s; 1000:1 Air/CO Ratio]. INTERMEDIATE SWIRL

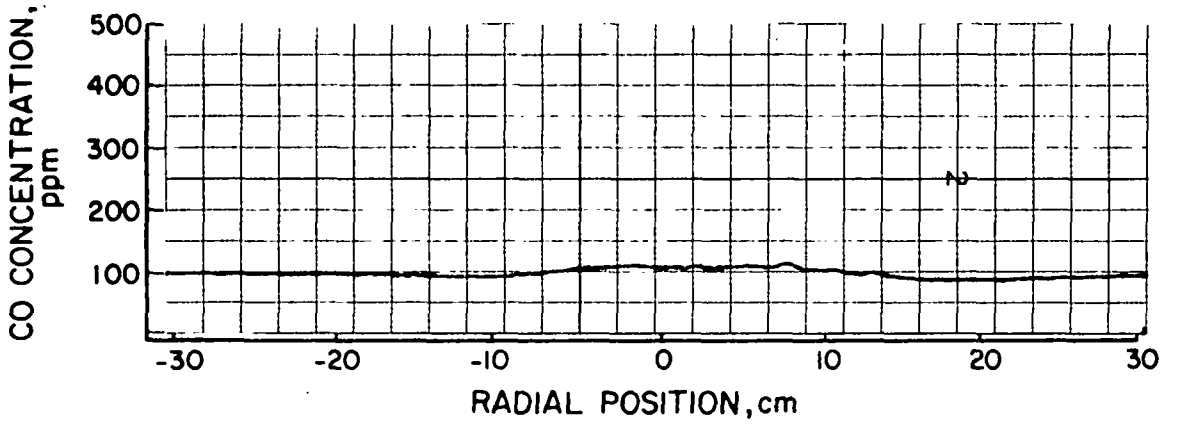

A-32209

Figure II-184. RADIAL CONCENTRATION PROFILE OF CARBON MONOXIDE FROM THE MOVABLE-BLOCK BURNER SET FOR INTERMEDIATE SWIRL 16.78 cm FROM THE BURNER TIP [Air Velocity 28 ft/s; Gas Velocity (Air) 110 ft/s; 1000:1 Air/CO Ratio]

The tracer-gas profiles for the swirl burner set at minimum swirl are shown in Figures II-185, II-186, II-187, and II-188 at axial positions of 5.08, 50.8, 76.2, and 101.6 cm, respectively.

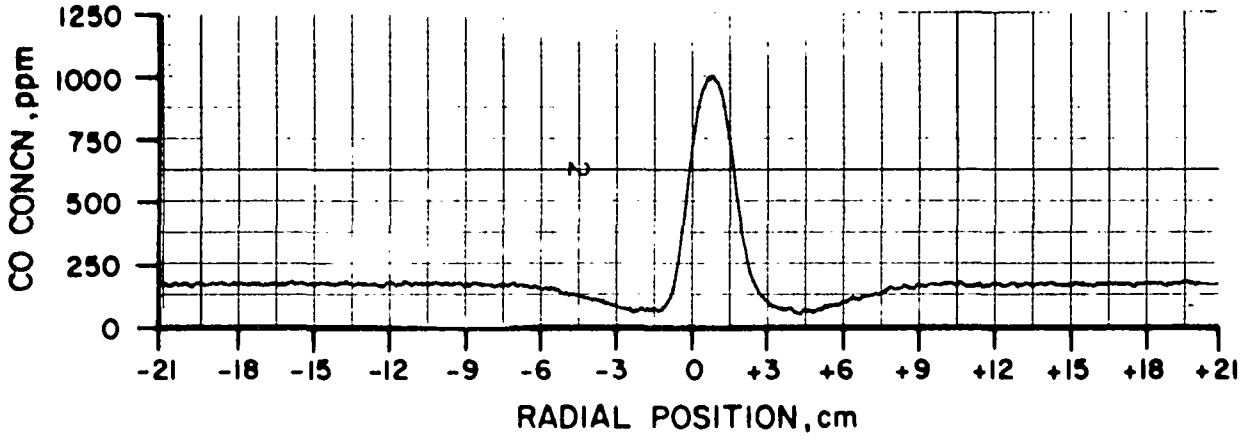

Figure II-185. RADIAL CONCENTRATION PROFILE OF CARBON MONOXIDE FROM THE SWIRL BURNER 5.08 cm FROM BURNER TIP [Air Velocity 28 ft/s; Gas Velocity (Air) 110 ft/s; 1000:1 Air/CO Ratio in Gas Stream]

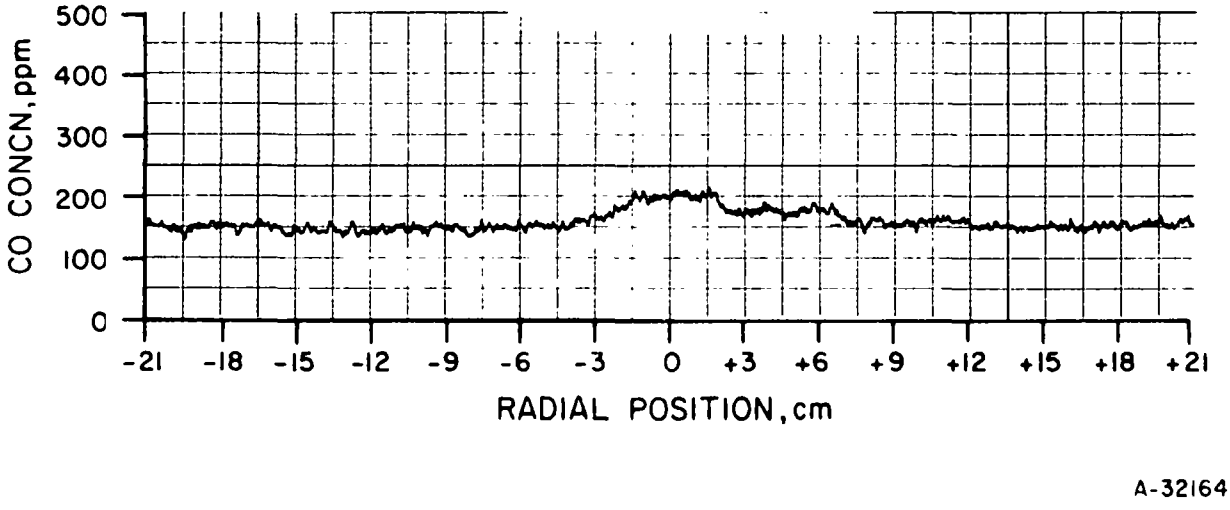

Figure II-186. RADIAL CARBON MONOXIDE CONCENTRATION PROFILE OF SWIRL BURNER 50.8 cm FROM BURNER TIP [Air Velocity 28 ft/s; Gas Velocity (Air) 110 ft/s; 1000:1 Air/CO Ratio in Gas Stream]

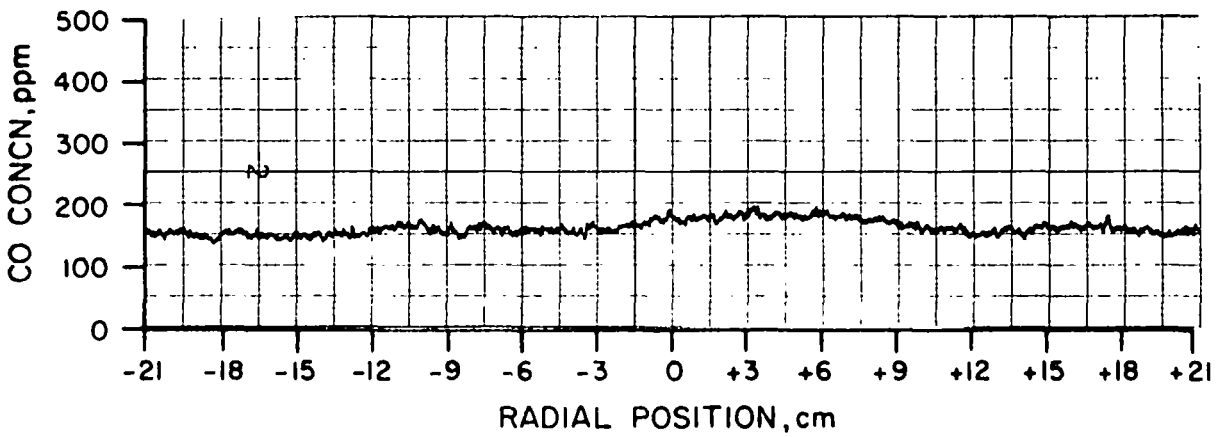

A-32165

Figure II-187. RADIAL CARBON MONOXIDE CONCENTRATION PROFILE OF SWIRL BURNER 76.2 cm FROM BURNER TIP [Air Velocity 28 ft/s; Gas Velocity (Air) 110 ft/s]. SET FOR MINIMUM SWIRL.

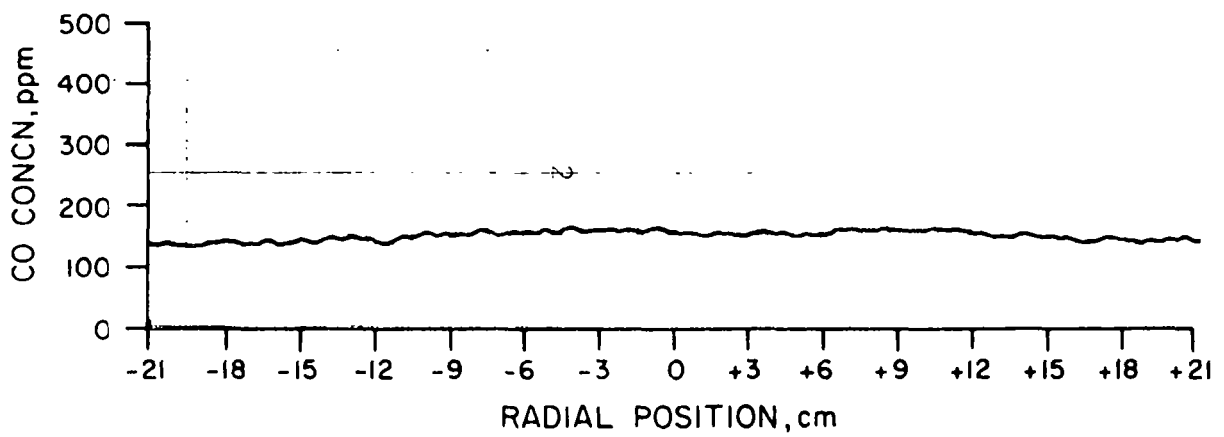

A-32166

Figure II-188. RADIAL CARBON MONOXIDE CONCENTRATION PROFILE OF SWIRL BURNER 101.6 cm FROM BURNER TIP [Air Velocity 28 ft/s; Gas Velocity (Air) 110 ft/s]. SET FOR MINIMUM SWIRL.

Figures II-189, II-190, II-191, and II-192 show gas concentration profiles at maximum swirl. Again we found that, as a function of swirl intensity, the central peak of the tracer gas concentration in the burner region decreases its amplitude and increases its width as the swirl increases and the turbulence of the air stream increases, accompanied by a stronger recirculation in the burner region as the swirl increases.

As a result of the continuous tracer-gas scans, we undertook point-by-point tracer-gas samples. Radial profiles were mapped at 3.8, 7.6, 17.8, 30.5, and 63.5 cm for both the minimum swirl and intermediate swirl (swirl intensity = 0.8). The data plots are shown in Figures II-193 to II-199. The raw numerical data are given in Tables II-29 to II-34. Table II-35 shows the column heading code.

3. Cold-Model Velocity Data

Velocity scans were taken in the cold model much like the tracer-gas scans. A continuous radial scan was made at several axial positions for minimum, intermediate, and maximum swirl. These scans for minimum swirl are shown in Figures II-200 to II-203.

Figure II-204 shows the radial velocity profile for the swirl burner set for an intermediate swirl intensity with the probe tip positioned toward the burner, 7.62 cm from the burner tip. Comparing Figures II-200 and II-204, note the large difference in the structure of the velocity profile between the minimum and intermediate swirl intensities. The continuous-scan data obtained in Figure II-204 are sufficient to determine the radial areas of interest for planning the point-by-point survey. However, they are insufficient for determining the general direction of flow, which is also needed for the detailed survey. We discussed earlier that the rotational orientation of the probe must be such that the direction of the flow vector is within ±60 degrees of the axis of the probe (Figure II-205) so that accurate data can be obtained. Where negative velocities are observed in Figure II-204, the direction of the flow cannot be determined from the radial scan alone. It is necessary to obtain the radial scan with four different rotational orientations, each exactly 90 degrees apart. The proper direction (rotational orientation) of the probe for the point-by-point measurements is the direction of the probe during the continuous scan for which the velocity is found to be the highest.

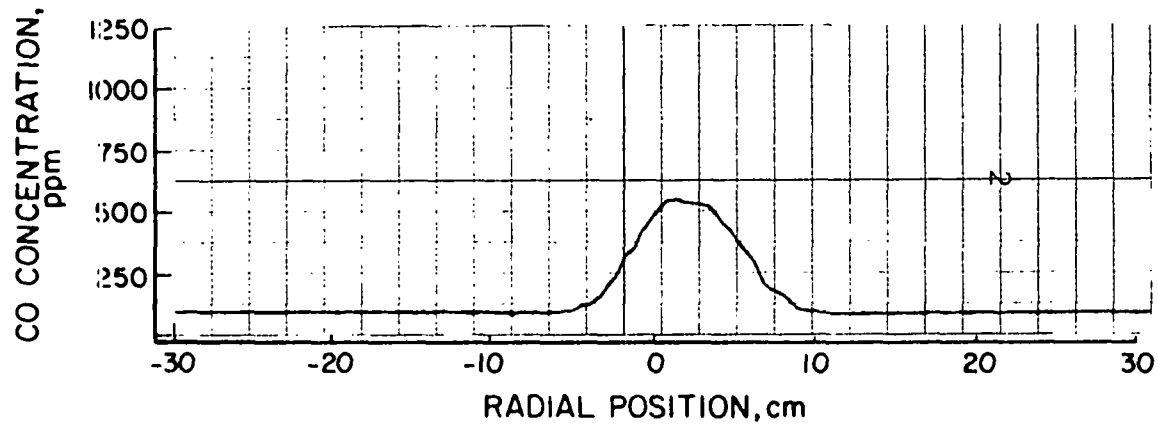

Figure II-189. RADIAL CONCENTRATION PROFILE OF CARBON MONOXIDE FROM THE MOVABLE-BLOCK BURNER SET FOR MAXIMUM SWIRL 2.54 cm OUT FROM THE BURNER TIP [Air Velocity 28 ft/s; Gas Velocity (Air) 110 ft/s; 1000:1 Air/CO Ratio in Gas Stream]

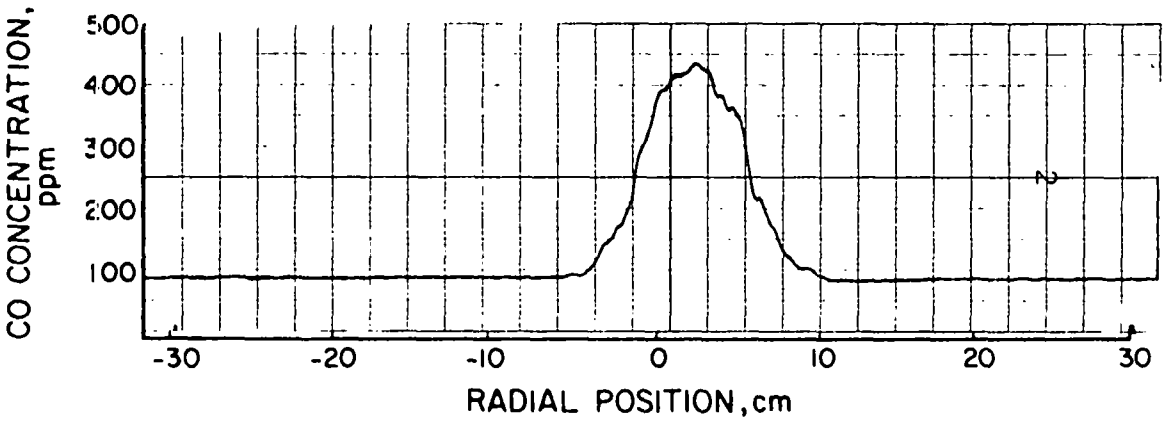

Figure II-190. RADIAL CONCENTRATION PROFILE OF CARBON MONOXIDE FROM THE MOVABLE-BLOCK BURNER SET FOR MAXIMUM SWIRL 5.08 cm OUT FROM BURNER TIP [Air Velocity 28 ft/s; Gas Velocity (Air) 110 ft/s; 1000:1 Air/CO Ratio in Gas Stream]

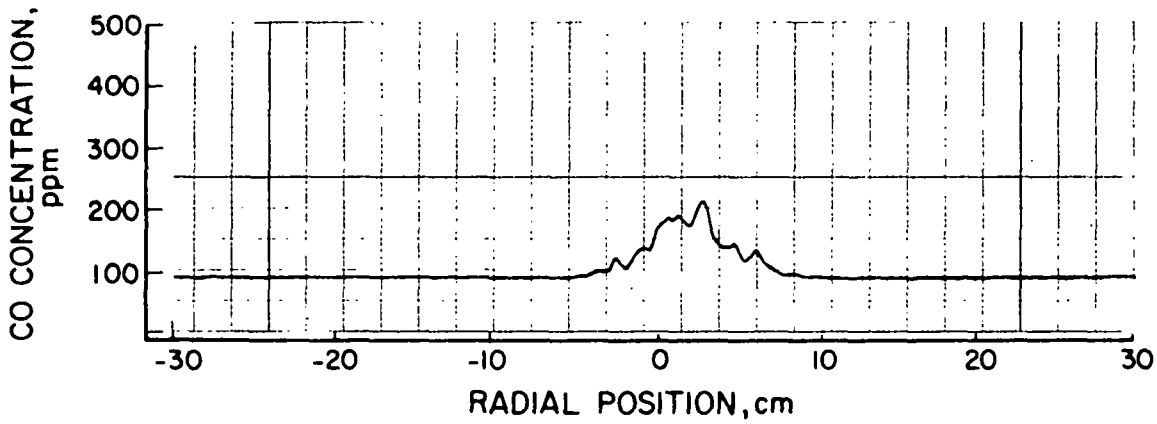

A-32216

Figure II-191. RADIAL CONCENTRATION PROFILE OF CARBON MONOXIDE FROM THE MOVABLE-BLOCK BURNER SET FOR MAXIMUM SWIRL 7.62 cm OUT FROM THE BURNER TIP [Air Velocity 28 ft/s; Gas Velocity (Air) 110 ft/s; 1000:2 Air/CO Ratio in Gas Stream]

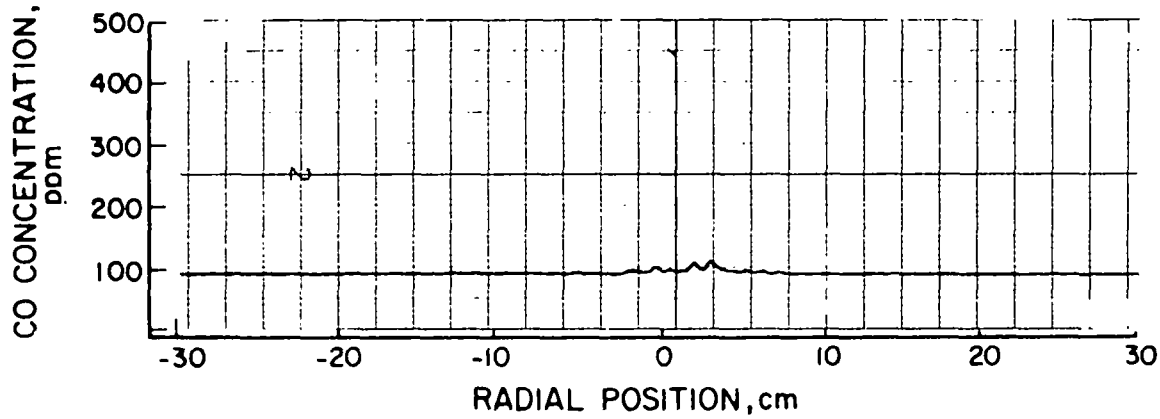

A-32217

Figure II-192. RADIAL CONCENTRATION PROFILE OF CARBON MONOXIDE FROM THE MOVABLE-BLOCK BURNER SET FOR MAXIMUM SWIRL 10.16 cm OUT FROM THE BURNER TIP [Air Velocity 28 ft/s; Gas Velocity (Air) 110 ft/s; 1000:1 Air/CO Ratio in Gas Stream]

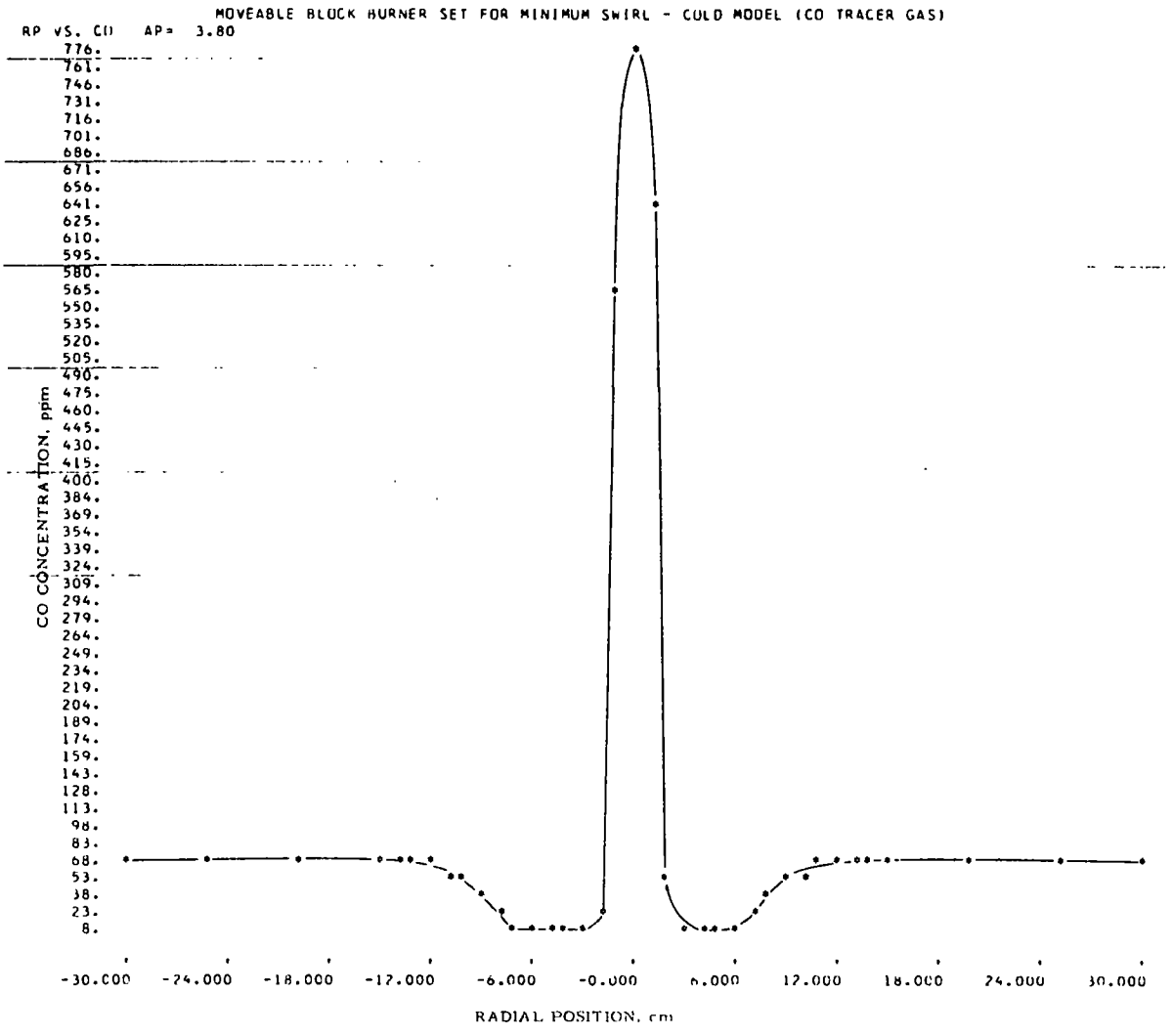

Figure II-193. TRACER-GAS MIXING PROFILES FOR THE SWIRL BURNER SET FOR MINIMUM SWIRL AT THE 3.8-cm AXIAL POSITION

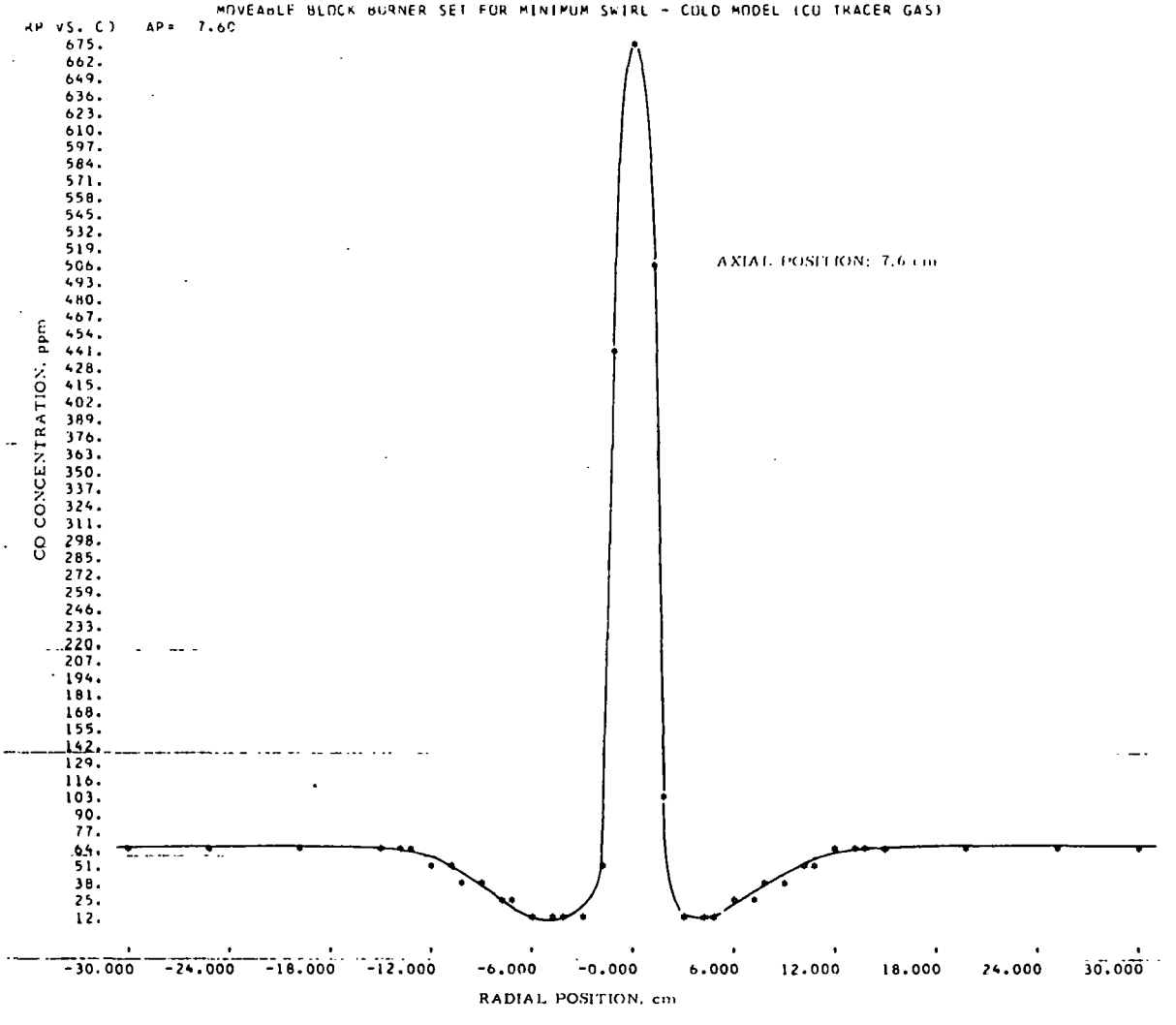

Figure II-194. TRACER-GAS MIXING PROFILE SET FOR MINIMUM SWIRL AT THE 7.6-cm AXIAL POSITION

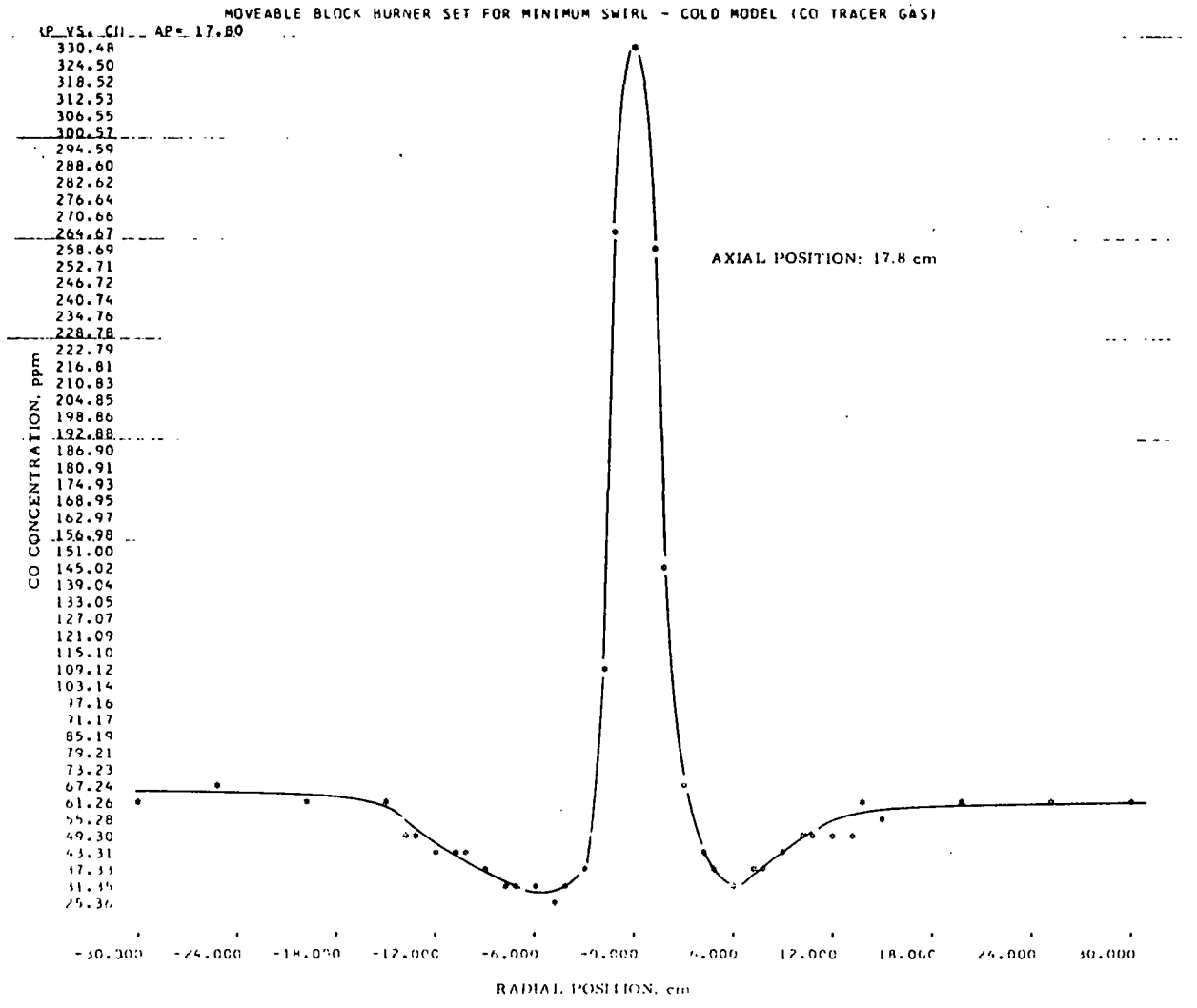

Figure II-195. TRACER-GAS MIXING PROFILE FOR THE SWIRL BURNER SET FOR MINIMUM SWIRL AT THE 17.8-cm AXIAL POSITION

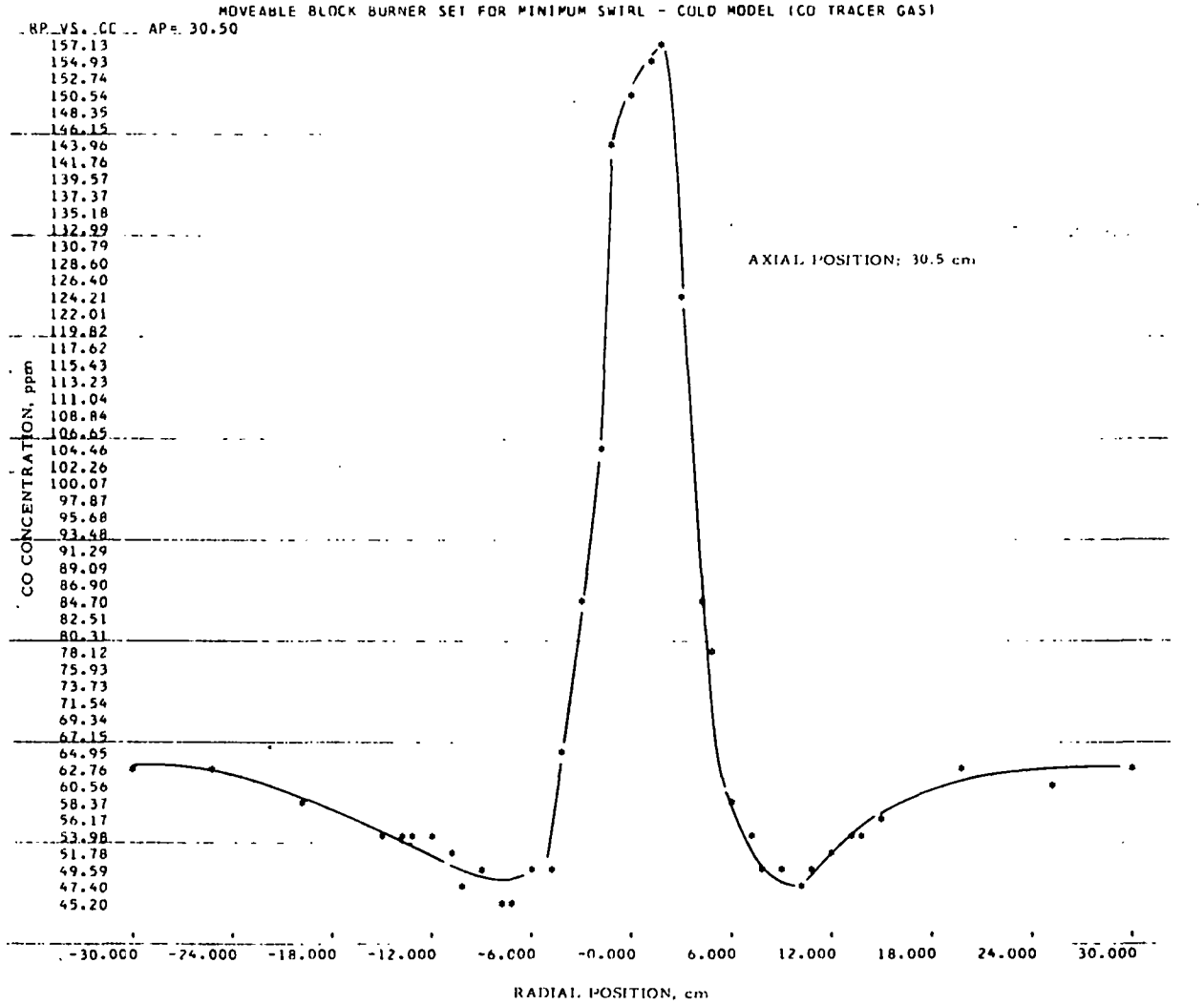

Figure II-196. TRACER-GAS MIXING FOR THE SWIRL BURNER SET FOR MINIMUM SWIRL AT THE 30.5-cm AXIAL POSITION

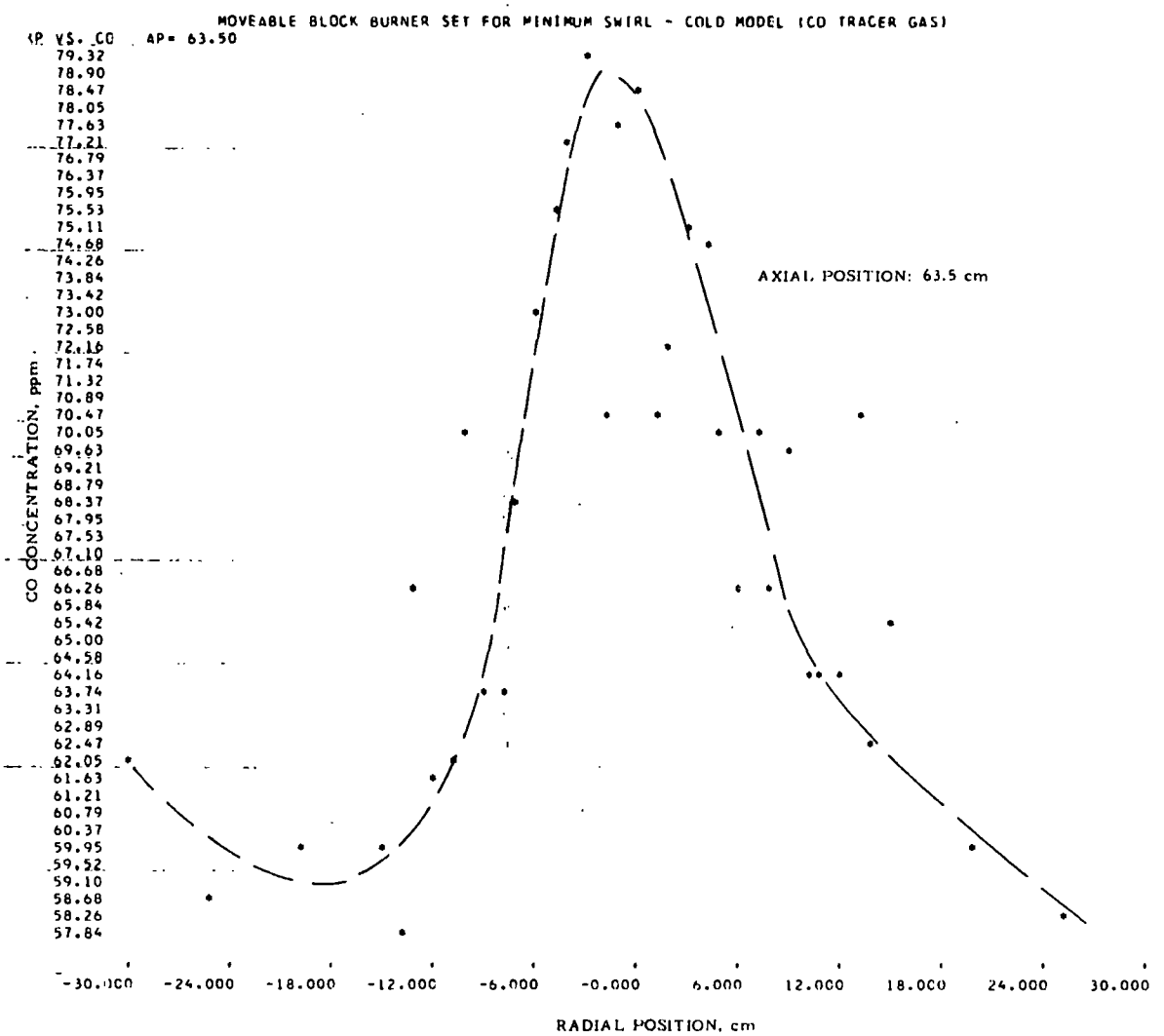

Figure II-197. TRACER-GAS MIXING PROFILE FOR THE SWIRL BURNER SET FOR MINIMUM SWIRL AT THE 63.5-cm AXIAL POSITION

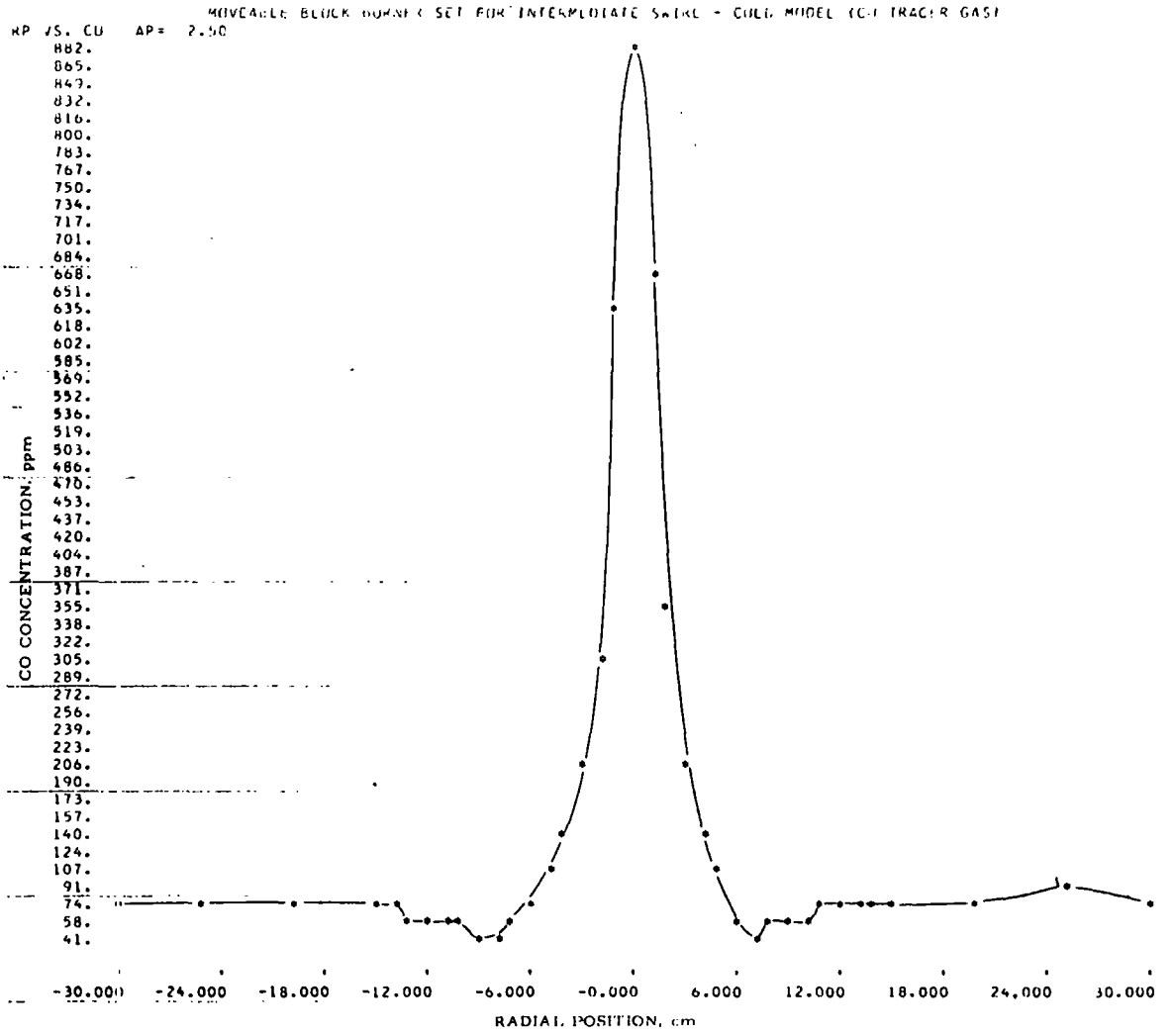

Figure II-198. TRACER-GAS MIXING PROFILE FOR THE SWIRL BURNER (Swirl Number, S = 0.8) AT THE 2.5-cm AXIAL POSITION

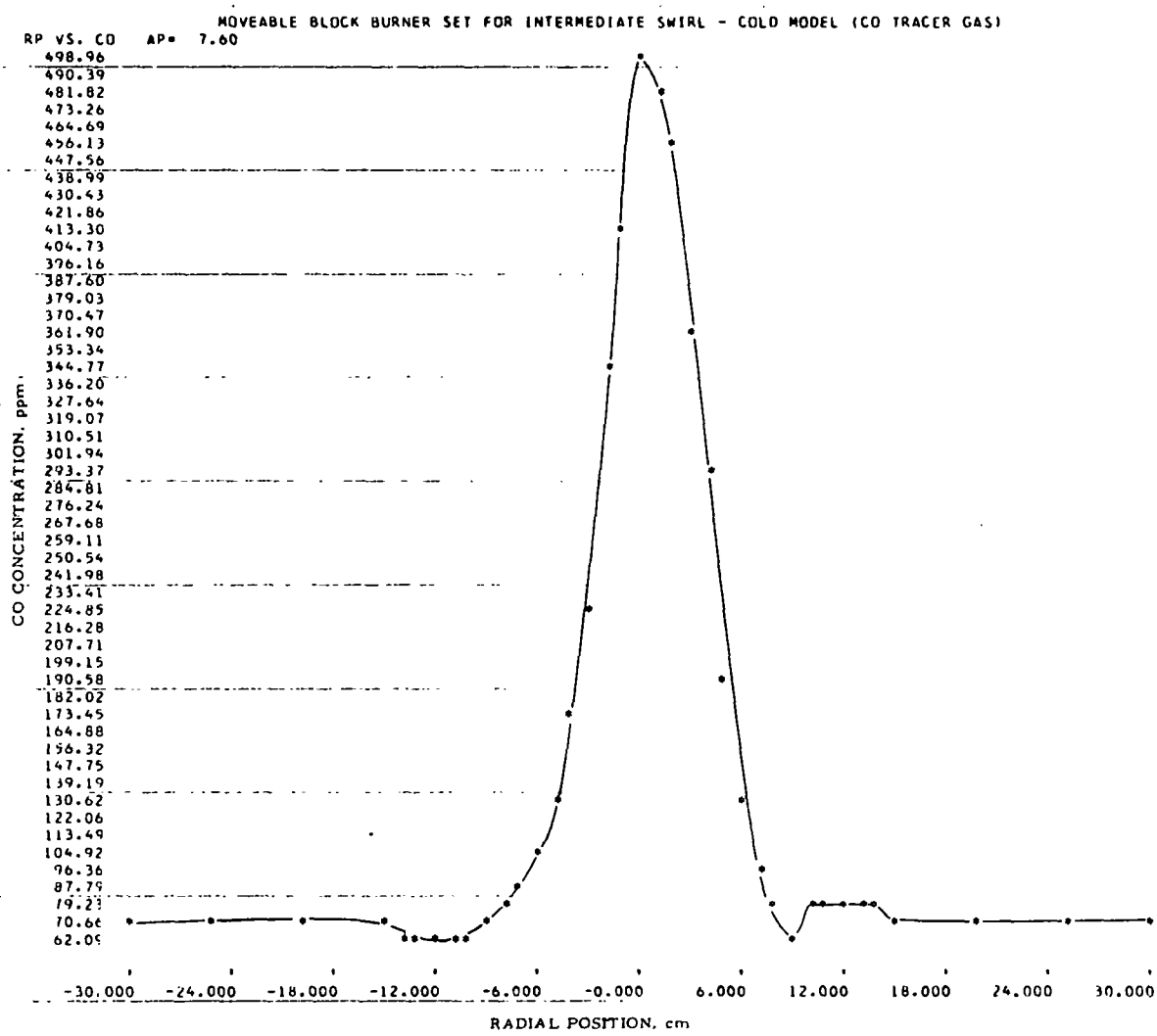

Figure II-199. TRACER-GAS MIXING PROFILE FOR THE SWIRL BURNER (Swirl Number, S = 0.8) AT THE 7.6-cm AXIAL POSITION

Table II-29. RAW AND COMPUTED TRACER-GAS MIXING DATA FOR THE SWIRL BURNER SET FOR MINIMUM SWIRL AT THE 3.8-cm AXIAL POSITION

TRACER GAS STUDIES OF COMBUSTION BURNERS
MOVEABLE BLOCK BURNER SET FOR MINIMUM SWIRL - COLD MODEL (CO TRACER GAS)

Y OBSERVED	Y COMPUTED	DIFFERENCE
0.00	0.44	0.44457
125.00	124.26	-0.73118
250.00	249.14	-0.85674
375.00	377.18	2.18748
500.00	498.95	-1.04412

SD Y= 0.19159E 01

COEFFICIENTS FOR Y= C(1)+C(2)*X+...+C(N+1)*X**N
C(1)= 0.4445
C(2)= 395.5515
C(3)= 102.9597

EXPERIMENTAL RESULTS

AP	RP	X(V)	CO
3.80	30.00	0.162	67.22
3.80	25.00	0.160	66.36
3.80	20.00	0.158	65.51
3.80	15.00	0.158	65.51
3.80	14.00	0.157	65.08
3.80	13.00	0.155	64.22
3.80	12.00	0.155	64.22
3.80	11.00	0.151	62.52
3.80	10.00	0.144	59.53
3.80	9.00	0.117	48.13
3.80	8.00	0.087	35.63
3.80	7.00	0.047	19.26
3.80	6.00	0.022	9.19
3.80	5.00	0.020	8.39
3.80	4.00	0.021	8.79
3.80	3.00	0.025	10.39
3.80	2.00	0.126	51.91
3.80	1.00	1.220	636.26
3.80	0.00	1.430	776.62
3.80	-1.00	1.110	566.36
3.80	-2.00	0.052	21.29
3.80	-3.00	0.023	9.59
3.80	-4.00	0.024	9.99
3.80	-5.00	0.024	9.99
3.80	-6.00	0.027	11.19
3.80	-7.00	0.033	13.60
3.80	-8.00	0.063	25.77
3.80	-9.00	0.098	40.19
3.80	-10.00	0.128	52.76
3.80	-11.00	0.144	59.53
3.80	-12.00	0.156	64.65
3.80	-13.00	0.157	65.08
3.80	-14.00	0.156	64.65
3.80	-15.00	0.157	65.08
3.80	-20.00	0.157	65.08
3.80	-25.00	0.155	64.22
3.80	-30.00	0.155	64.22

Table II-30. RAW AND COMPUTED TRACER-GAS MIXING DATA FOR THE SWIRL BURNER (Minimum Swirl) AT THE 17.8-cm AXIAL POSITION

TRACER GAS STUDIES OF COMBUSTION BURNERS
MOVEABLE BLOCK BURNER SET FOR MINIMUM SWIRL - COLD MODEL (CO TRACER GAS)

Y OBSERVED	Y COMPUTED	DIFFERENCE
0.00	0.44	0.44457
125.00	124.26	-0.73118
250.00	249.14	-0.85674
375.00	377.18	2.18748
500.00	498.95	-1.04412

SD Y= 0.19159E 01

COEFFICIENTS FOR Y= C(1)+C(2)*X+...+C(N+1)*X**N
C(1)= 0.4445
C(2)= 395.5515
C(3)= 102.9597

EXPERIMENTAL RESULTS

AP	RP	X(V)	CO
17.80	30.00	0.153	63.37
17.80	25.00	0.153	63.37
17.80	20.00	0.153	63.37
17.80	15.00	0.141	58.26
17.80	14.00	0.147	60.81
17.80	13.00	0.121	49.81
17.80	12.00	0.122	50.23
17.80	11.00	0.119	48.97
17.80	10.00	0.115	47.29
17.80	9.00	0.105	43.11
17.80	8.00	0.093	38.12
17.80	7.00	0.089	36.46
17.80	6.00	0.083	33.98
17.80	5.00	0.090	36.87
17.80	4.00	0.105	43.11
17.80	3.00	0.160	66.36
17.80	2.00	0.333	143.58
17.80	1.00	0.570	259.36
17.80	0.00	0.705	330.48
17.80	-1.00	0.585	267.07
17.80	-2.00	0.256	108.45
17.80	-3.00	0.092	37.70
17.80	-4.00	0.082	33.57
17.80	-5.00	0.062	25.36
17.80	-6.00	0.070	28.63
17.80	-7.00	0.080	32.74
17.80	-8.00	0.080	32.74
17.80	-9.00	0.092	37.70
17.80	-10.00	0.109	44.78
17.80	-11.00	0.110	45.20
17.80	-12.00	0.112	46.03
17.80	-13.00	0.125	51.49
17.80	-14.00	0.122	50.23
17.80	-15.00	0.145	59.96
17.80	-20.00	0.152	62.94
17.80	-25.00	0.156	64.65
17.80	-30.00	0.154	63.80

Table II-31. RAW AND COMPUTED TRACER-GAS MIXING DATA FOR THE SWIRL BURNER (Minimum Swirl) AT THE 30.5-cm AXIAL POSITION

TRACER GAS STUDIES OF COMBUSTION BURNERS
MOVEABLE BLOCK BURNER SET FOR MINIMUM SWIRL - COLD MODEL (CO TRACER GAS)

Y OBSERVED	Y COMPUTED	DIFFERENCE
0.00	0.44	0.44457
125.00	124.26	-0.73118
250.00	249.14	-0.85674
375.00	377.18	2.18748
500.00	498.95	-1.04412

SD Y= 0.19159E 01

COEFFICIENTS FOR Y= C(1)+C(2)*X+...+C(N+1)*X**N
C(1)= 0.4445
C(2)= 395.5515
C(3)= 102.9597

EXPERIMENTAL RESULTS

AP	RP	X(V)	CO
30.50	30.00	0.150	62.09
30.50	25.00	0.148	61.24
30.50	20.00	0.152	62.94
30.50	15.00	0.138	56.99
30.50	14.00	0.129	53.18
30.50	13.00	0.132	54.45
30.50	12.00	0.125	51.49
30.50	11.00	0.121	49.81
30.50	10.00	0.117	48.13
30.50	9.00	0.120	49.39
30.50	8.00	0.122	50.23
30.50	7.00	0.130	53.60
30.50	6.00	0.141	58.26
30.50	5.00	0.185	77.14
30.50	4.00	0.204	85.42
30.50	3.00	0.290	123.81
30.50	2.00	0.362	157.12
30.50	1.00	0.357	154.77
30.50	0.00	0.350	151.50
30.50	-1.00	0.335	144.50
30.50	-2.00	0.247	104.42
30.50	-3.00	0.204	85.42
30.50	-4.00	0.158	65.51
30.50	-5.00	0.118	48.55
30.50	-6.00	0.119	48.97
30.50	-7.00	0.111	45.61
30.50	-8.00	0.110	45.20
30.50	-9.00	0.118	48.55
30.50	-10.00	0.116	47.71
30.50	-11.00	0.124	51.07
30.50	-12.00	0.129	53.18
30.50	-13.00	0.130	53.60
30.50	-14.00	0.132	54.45
30.50	-15.00	0.130	53.60
30.50	-20.00	0.140	57.83
30.50	-25.00	0.150	62.09
30.50	-30.00	0.154	63.80

Table II-32. RAW AND COMPUTED TRACER-GAS MIXING DATA FOR THE SWIRL BURNER (Minimum Swirl) AT THE 63.5-cm AXIAL POSITION

TRACER GAS STUDIES OF COMBUSTION BURNERS
MOVEABLE BLOCK BURNER SET FOR MINIMUM SWIRL - COLD MODEL (CO TRACER GAS)

Y OBSERVED	Y COMPUTED	DIFFERENCE
0.00	0.44	0.44457
125.00	124.26	-0.73118
250.00	249.14	-0.85674
375.00	377.18	2.18748
500.00	498.95	-1.04412

SD Y= 0.19159E 01

COEFFICIENTS FOR Y= C(1)+C(2)*X+...+C(N+1)*X**N
C(1)= 0.4445
C(2)= 395.5515
C(3)= 102.9597

EXPERIMENTAL RESULTS

AP	RP	X(V)	CO
63.50	30.00	0.150	62.09
63.50	25.00	0.141	58.26
63.50	20.00	0.145	59.96
63.50	15.00	0.158	65.51
63.50	14.00	0.151	62.52
63.50	13.00	0.170	70.66
63.50	12.00	0.155	64.22
63.50	11.00	0.155	64.22
63.50	10.00	0.155	64.22
63.50	9.00	0.168	69.80
63.50	8.00	0.160	66.36
63.50	7.00	0.169	70.23
63.50	6.00	0.160	66.36
63.50	5.00	0.169	70.23
63.50	4.00	0.179	74.54
63.50	3.00	0.180	74.97
63.50	2.00	0.173	71.95
63.50	1.00	0.170	70.66
63.50	0.00	0.188	78.44
63.50	-1.00	0.186	77.57
63.50	-2.00	0.170	70.66
63.50	-3.00	0.190	79.31
63.50	-4.00	0.185	77.14
63.50	-5.00	0.181	75.41
63.50	-6.00	0.175	72.81
63.50	-7.00	0.165	68.51
63.50	-8.00	0.154	63.80
63.50	-9.00	0.154	63.80
63.50	-10.00	0.169	70.23
63.50	-11.00	0.150	62.09
63.50	-12.00	0.149	61.66
63.50	-13.00	0.160	66.36
63.50	-14.00	0.140	57.83
63.50	-15.00	0.145	59.96
63.50	-20.00	0.145	59.96
63.50	-25.00	0.142	58.68
63.50	-30.00	0.150	62.09

Table II-33. RAW AND COMPUTED TRACER-GAS MIXING DATA FOR THE SWIRL BURNER (Maximum Swirl) AT THE 2.5-cm AXIAL POSITION

TRACER GAS STUDIES OF COMBUSTION BURNERS
MOVEABLE BLOCK BURNER SET FOR MAXIMUM SWIRL - COLD MODEL (CO TRACER GAS)

Y OBSERVED	Y COMPUTED	DIFFERENCE
0.00	C.44	0.44457
125.00	124.26	-0.73118
250.00	249.14	-0.85674
375.00	377.18	2.18748
500.00	498.95	-1.04412

SD Y= 0.19159E 01

COEFFICIENTS FOR Y= C(1)+C(2)*X+...+C(N+1)*X**N

C(1)= 0.4445
C(2)= 395.5515
C(3)= 102.9597

EXPERIMENTAL RESULTS

AP	RP	X(V)	CO
2.50	-30.00	0.181	75.41
2.50	-25.00	0.180	74.97
2.50	-20.00	0.176	73.25
2.50	-15.00	0.174	72.38
2.50	-14.00	0.168	69.80
2.50	-13.00	0.160	66.36
2.50	-12.00	0.153	63.37
2.50	-11.00	0.155	64.22
2.50	-10.00	0.130	53.60
2.50	-9.00	0.106	43.52
2.50	-8.00	0.102	41.86
2.50	-7.00	0.124	51.07
2.50	-6.00	0.177	73.68
2.50	-5.00	0.242	102.19
2.50	-4.00	0.320	137.56
2.50	-3.00	0.450	199.29
2.50	-2.00	0.650	301.05
2.50	-1.00	1.230	642.74
2.50	0.00	1.580	882.44
2.50	1.00	1.260	662.29
2.50	2.00	0.750	355.02
2.50	3.00	0.480	214.03
2.50	4.00	0.344	148.69
2.50	5.00	0.240	101.30
2.50	6.00	0.157	65.08
2.50	7.00	0.116	47.71
2.50	8.00	0.130	53.60
2.50	9.00	0.155	64.22
2.50	10.00	0.160	66.36
2.50	11.00	0.170	70.66
2.50	12.00	0.171	71.09
2.50	13.00	0.173	71.95
2.50	14.00	0.173	71.95
2.50	15.00	0.177	73.68
2.50	20.00	0.180	74.97
2.50	25.00	0.199	83.23
2.50	30.00	0.195	81.49

Table II-34. RAW AND COMPUTED TRACER-GAS MIXING DATA FOR THE SWIRL BURNER (Maximum Swirl) AT THE 7.6-cm AXIAL POSITION

TRACER GAS STUDIES OF COMBUSTION BURNERS
MOVEABLE BLOCK BURNER SET FOR MAXIMUM SWIRL - COLD MODEL (CO TRACER GAS)

Y OBSERVED	Y COMPUTED	DIFFERENCE
0.00	0.44	0.44457
125.00	124.26	-0.73118
250.00	249.14	-0.85674
375.00	377.18	2.18748
500.00	498.95	-1.04412

SD Y= 0.19159E 01

COEFFICIENTS FOR Y= C(1)+C(2)*X+...+C(N+1)*X**N
C(1)= 0.4445
C(2)= 395.5515
C(3)= 102.9597

EXPERIMENTAL RESULTS

AP	RP	X(V)	CO
7.60	-30.00	0.174	72.38
7.60	-25.00	0.173	71.95
7.60	-20.00	0.172	71.52
7.60	-15.00	0.165	68.51
7.60	-14.00	0.160	66.36
7.60	-13.00	0.150	62.09
7.60	-12.00	0.150	62.09
7.60	-11.00	0.150	62.09
7.60	-10.00	0.160	66.36
7.60	-9.00	0.163	67.65
7.60	-8.00	0.185	77.14
7.60	-7.00	0.200	83.67
7.60	-6.00	0.250	105.76
7.60	-5.00	0.310	132.95
7.60	-4.00	0.400	175.13
7.60	-3.00	0.510	228.95
7.60	-2.00	0.730	344.06
7.60	-1.00	0.860	416.76
7.60	0.00	1.000	498.95
7.60	1.00	0.970	481.00
7.60	2.00	0.925	454.42
7.60	3.00	0.760	360.53
7.60	4.00	0.630	290.50
7.60	5.00	0.435	191.99
7.60	6.00	0.309	132.50
7.60	7.00	0.220	92.44
7.60	8.00	0.180	74.97
7.60	9.00	0.160	66.36
7.60	10.00	0.180	74.97
7.60	11.00	0.197	82.36
7.60	12.00	0.186	77.57
7.60	13.00	0.180	74.97
7.60	14.00	0.180	74.97
7.60	15.00	0.168	69.80
7.60	20.00	0.170	70.66
7.60	25.00	0.165	68.51
7.60	30.00	0.170	70.66

Table II-35. COLUMN HEADING CODE

AP = axial probe position, cm

CO = carbon monoxide concentration, ppm

C(1), C(2), etc. = coefficients of fitted calibration

Difference = $Y_{observed} - Y_{calculated}$, ppm

RP = radial probe position, cm

SD = standard deviation of Y-computed

X(V) = experimentally measured time-averaged voltage, V

Y-computed = carbon monoxide concentration from fitted calibration, ppm

Y-observed = carbon monoxide concentration from calibration curve, ppm

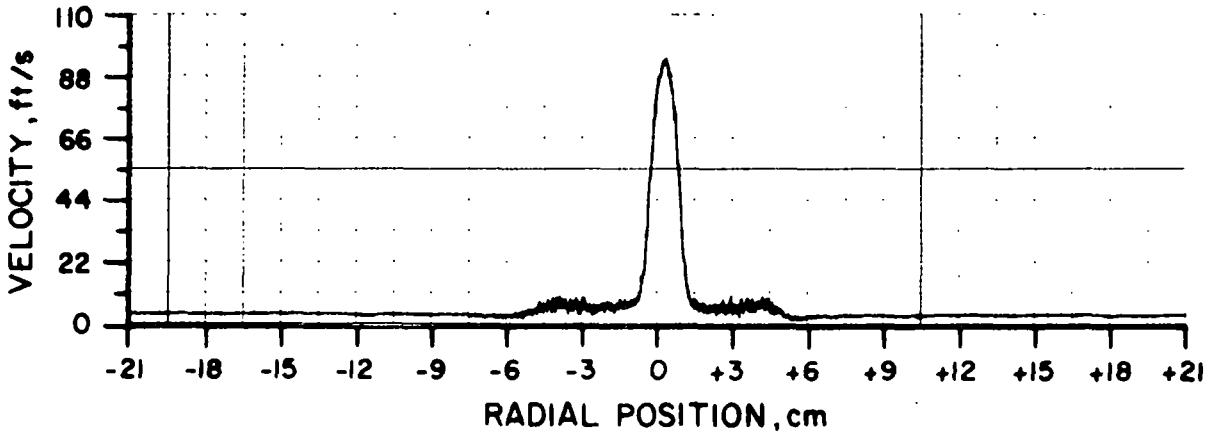

Figure II-200. RADIAL VELOCITY PROFILE OF SWIRL BURNER 5.08 cm FROM BURNER TIP [Air Velocity 28 ft/s; Gas Velocity (Air) 110 ft/s]

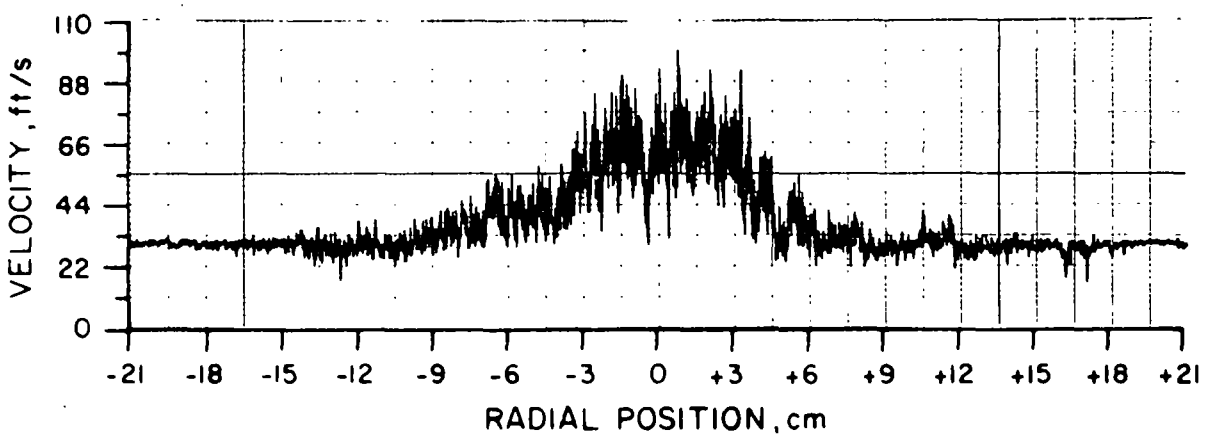

Figure II-201. RADIAL VELOCITY PROFILE OF SWIRL BURNER 50.8 cm FROM BURNER TIP [Air Velocity 28 ft/s; Gas Velocity (Air) 110 ft/s]

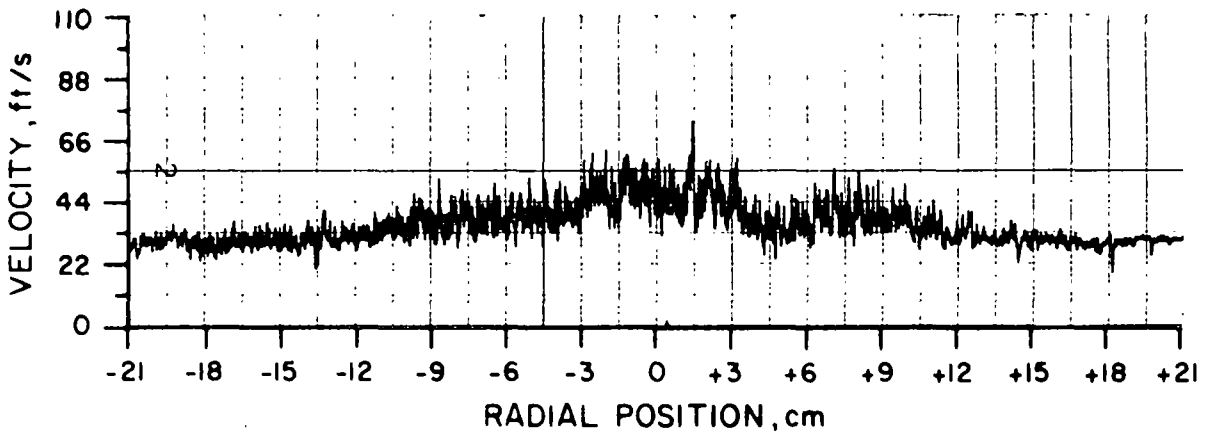

Figure II-202. RADIAL VELOCITY PROFILE OF SWIRL BURNER 76.2 cm FROM BURNER TIP [Air Velocity 28 ft/s; Gas Velocity (Air) 110 ft/s]. SET FOR MINIMUM SWIRL.

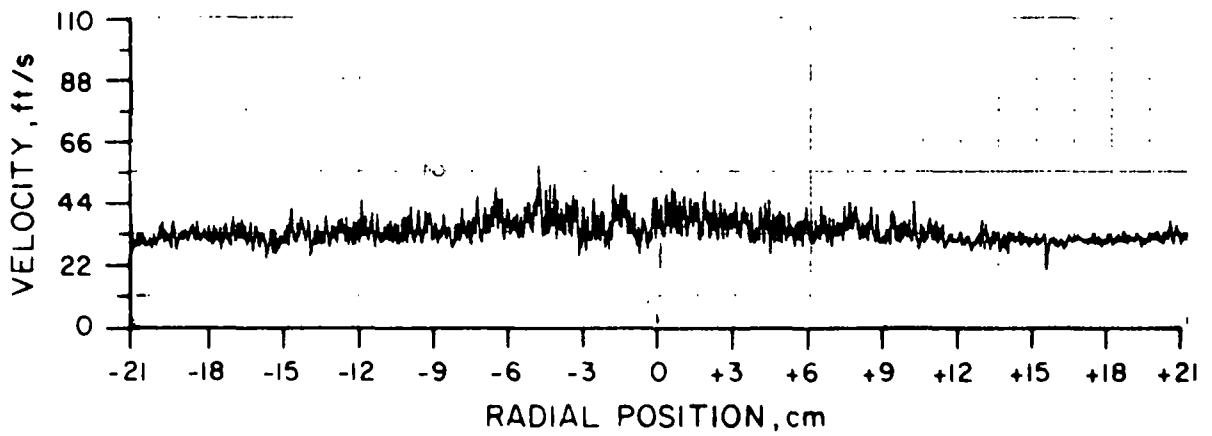

Figure II-203. RADIAL VELOCITY PROFILE OF SWIRL BURNER 101.6 cm FROM BURNER TIP [Air Velocity 28 ft/s; Gas Velocity (Air) 110 ft/s]. SET FOR MINIMUM SWIRL.

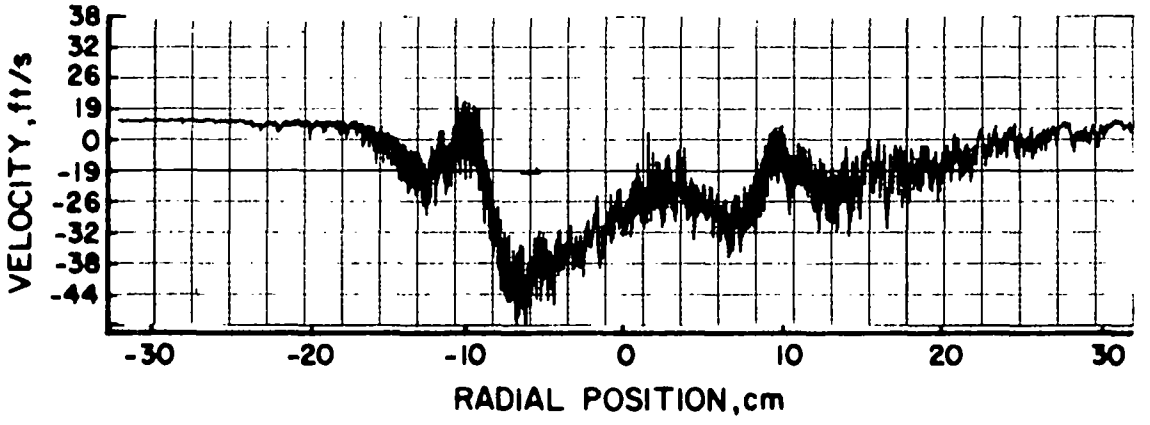

Figure II-204. RADIAL VELOCITY PROFILE OF MOVABLE-BLOCK BURNER SET FOR INTERMEDIATE SWIRL 7.62 cm OUT FROM BURNER TIP. PROBE ROTATED AT AN ANGLE OF 0^0
[Air Velocity 28 ft/s; Gas Velocity (Air) 110 ft/s]

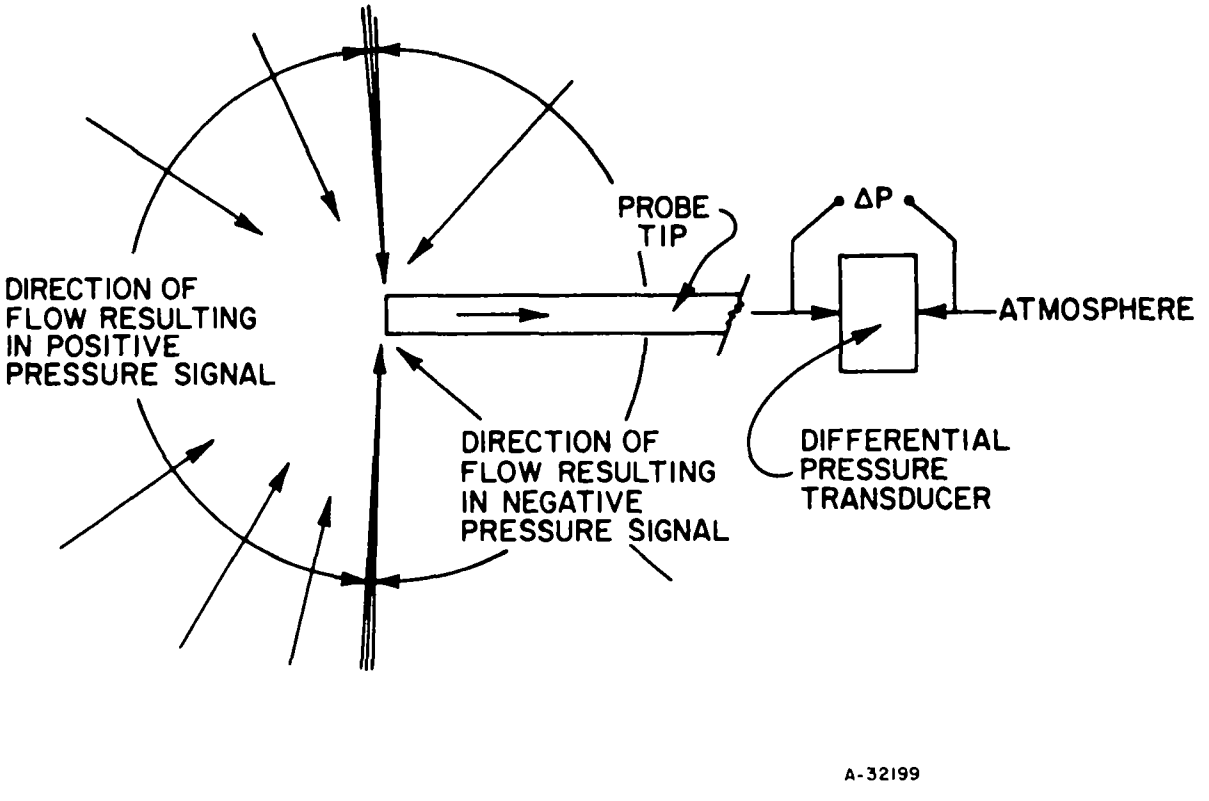

Figure II-205. PRESSURE SIGNAL RESPONSE FOR VARIOUS FLOW DIRECTIONS

Figures II-204, II-206, II-207, and II-208 show the radial velocity profiles for the swirl burner set for the intermediate swirl intensity at 7.62 cm from the burner tip for the four rotational orientations. (Zero degrees corresponds to the probe pointed toward the burner.) Similar profiles were run at various distances from the burner from 1.0 to 30 inches.

Figures II-209, II-210, II-211, and II-212 show velocity profiles for the maximum swirl intensity obtainable with our burner.

Considering all of the velocity- and tracer-gas-concentration scans as a function of both axial position and level of swirl intensity, the following point-by-point survey was undertaken as shown in Table II-36.

We collected the point-by-point profile data for the swirl burner by using a multidirectional impact pitot tube (MDIT). The coordinate system used in data collection and reduction is shown in Figure II-213.

A typical set of raw data obtained from the MDIT is shown in Table II-37 for the burner set at minimum swirl and at a 3.8-cm axial position. The probe is rotated through angle θ in the x-z plane; AP is the axial position of the probe in centimeters and RP is its radial position in centimeters. The temperature, T, is measured in degrees centigrade at the points where the data are collected. PB is the atmospheric pressure in millimeters of mercury, and P_{xy} is the pressure differential between pressure holes x and y expressed in terms of time because of the integration method used in collecting the data. The pressure differentials we measured were constantly changing, since we were dealing with a turbulent system. To determine the mean value of these transient pressure differentials, the instantaneous values are electronically summed up for a preset amount of time. This total equals the product of the average instantaneous pressure differential and the time interval needed to reach it. Therefore, by measuring the time interval needed to reach this sum by a transient pressure differential, it is possible to experimentally determine the mean value of the pressure differential. These yield the velocity (magnitude and direction) of the air stream, using the techniques outlined earlier in this report. The computer program which performs this calculation is shown in Appendix A.

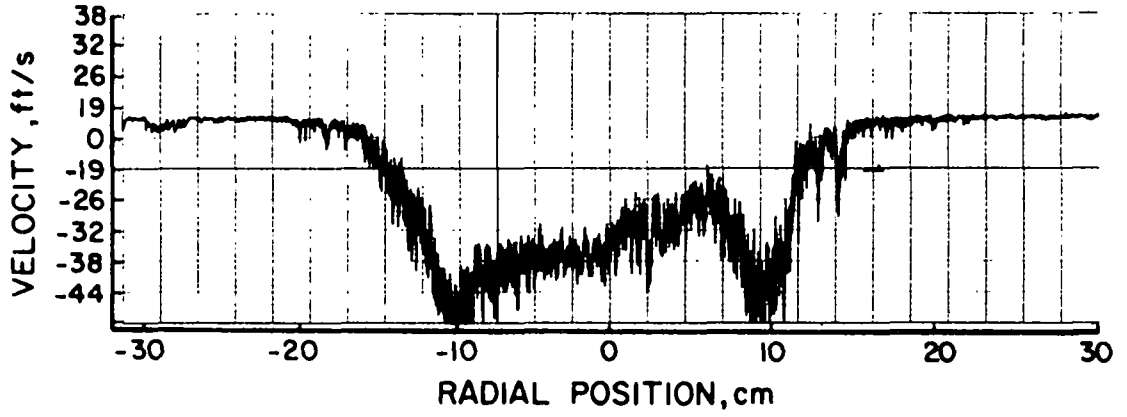

A-32203

Figure II-206. RADIAL VELOCITY PROFILE OF MOVABLE-BLOCK BURNER SET FOR INTERMEDIATE SWIRL 7.62 cm OUT FROM BURNER TIP. PROBE ROTATED 270° ABOUT y-AXIS [Air Velocity 28 ft/s; Gas Velocity (Air) 110 ft/s]

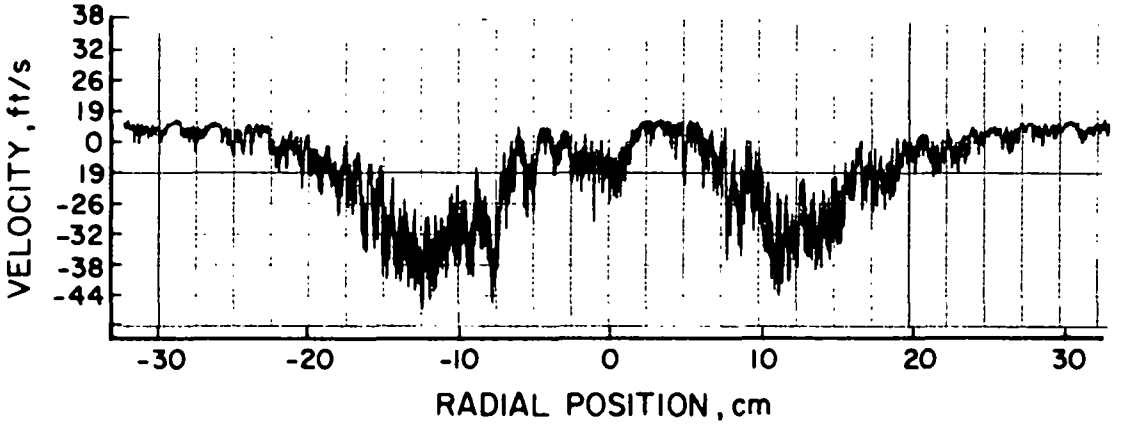

A-32204

Figure II-207. RADIAL VELOCITY PROFILE OF MOVABLE-BLOCK BURNER SET FOR INTERMEDIATE SWIRL 7.62 cm OUT FROM BURNER TIP. PROBE ROTATED 180° ABOUT y-AXIS [Air Velocity 28 ft/s; Gas Velocity (Air) 110 ft/s]

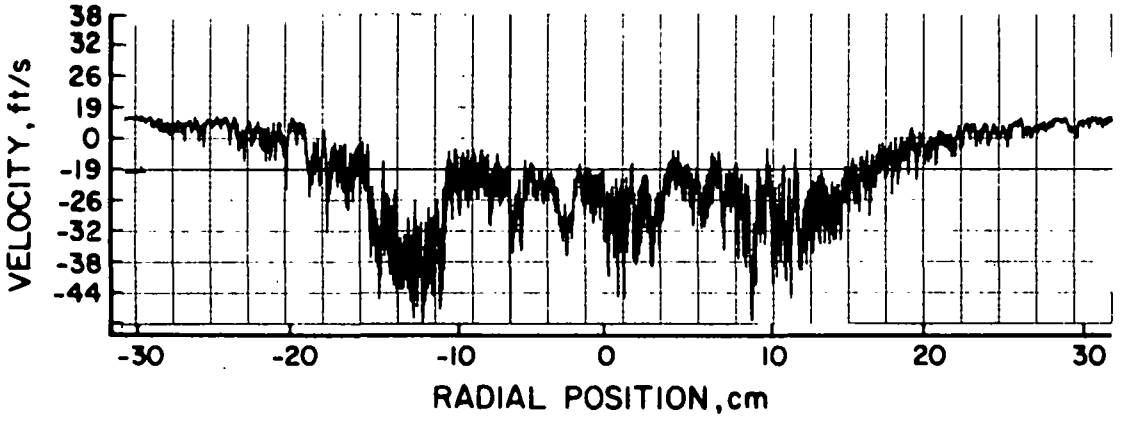

Figure II-208. RADIAL VELOCITY PROFILE OF MOVABLE-BLOCK BURNER SET FOR INTERMEDIATE SWIRL 7.62 cm OUT FROM BURNER TIP. PROBE ROTATED 90° ABOUT y-AXIS [Air Velocity 28 ft/s; Gas Velocity (Air) 110 ft/s]

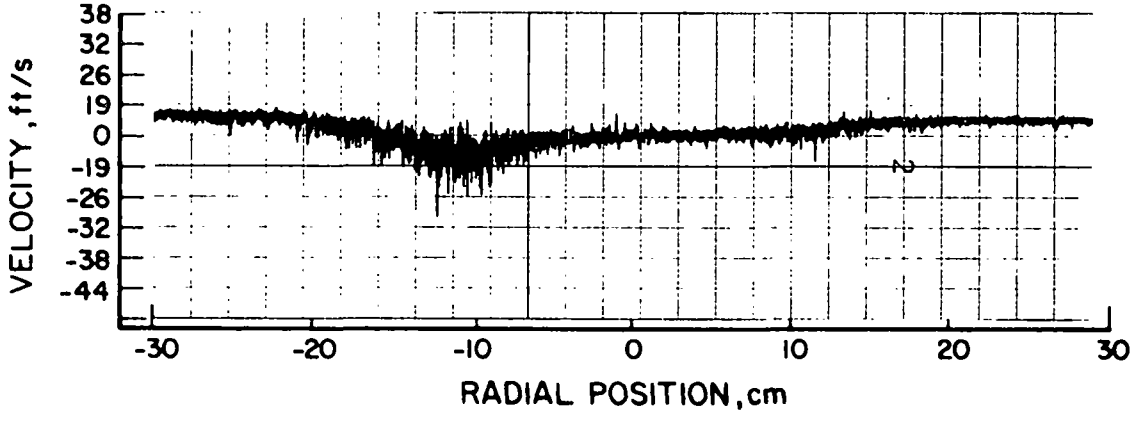

Figure II-209. RADIAL VELOCITY PROFILE OF MOVABLE-BLOCK BURNER SET FOR MAXIMUM SWIRL 7.62 cm OUT FROM BURNER TIP. PROBE ROTATED 0° ABOUT THE y-AXIS [Air Velocity 28 ft/s; Gas Velocity (Air) 110 ft/s]

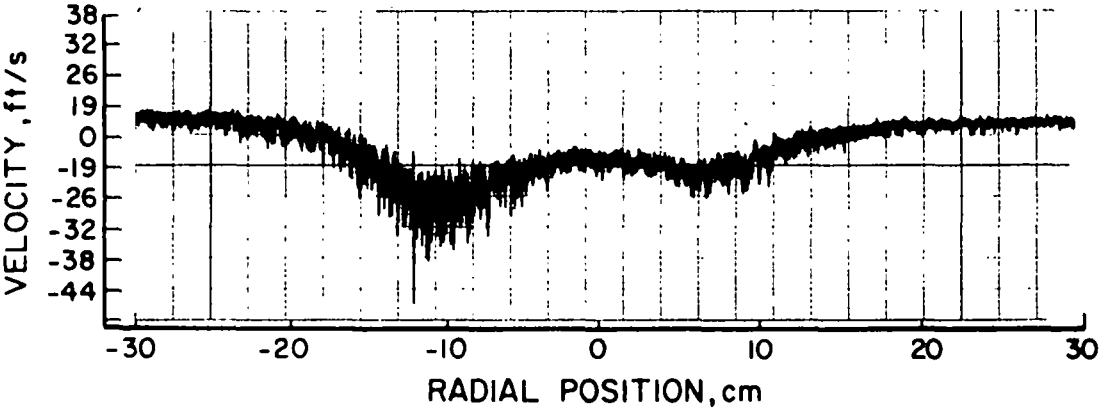

Figure II-210. RADIAL VELOCITY PROFILE OF MOVABLE-BLOCK BURNER SET FOR MAXIMUM SWIRL 7.62 cm OUT FROM BURNER TIP. PROBE ROTATED 270° ABOUT THE y-AXIS [Air Velocity 28 ft/s; Gas Velocity (Air) 110 ft/s]

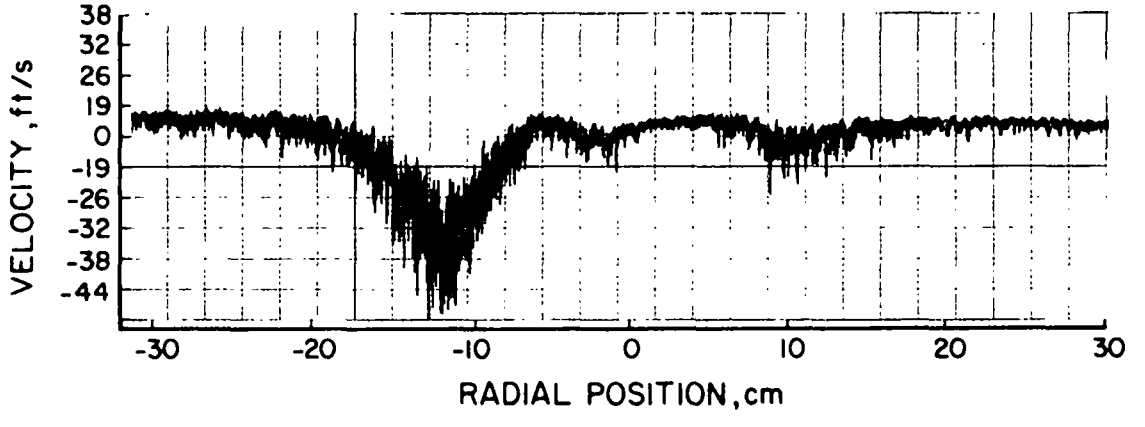

Figure II-211. RADIAL VELOCITY PROFILE OF MOVABLE-BLOCK BURNER SET FOR MAXIMUM SWIRL 7.62 cm FROM BURNER TIP. PROBE ROTATED 90° ABOUT THE y-AXIS [Air Velocity 28 ft/s; Gas Velocity (Air) 110 ft/s]

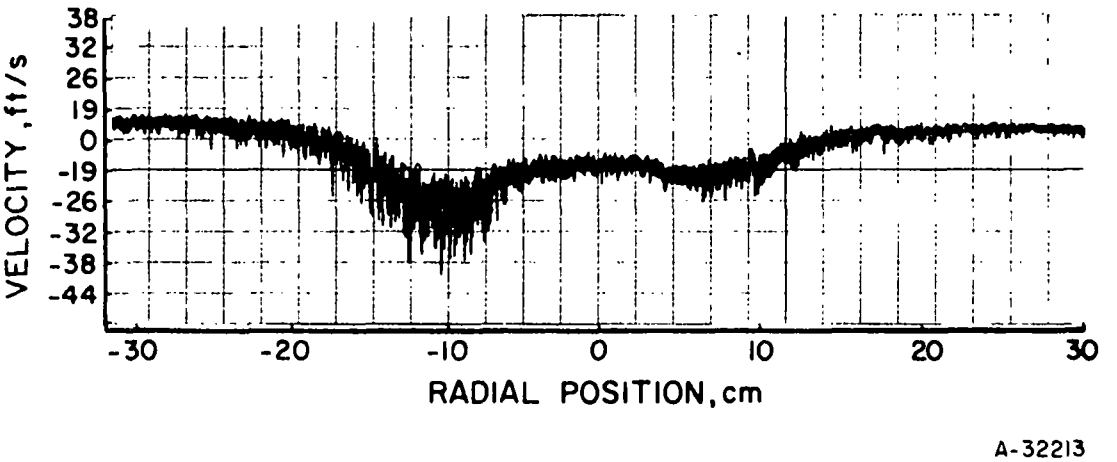

Figure II-212. RADIAL VELOCITY PROFILE OF MOVABLE-BLOCK BURNER SET FOR MAXIMUM SWIRL 7.62 cm OUT FROM BURNER TIP. PROBE ROTATED 90° ABOUT y-AXIS [Air Velocity 28 ft/s; Gas Velocity (Air) 110 ft/s]

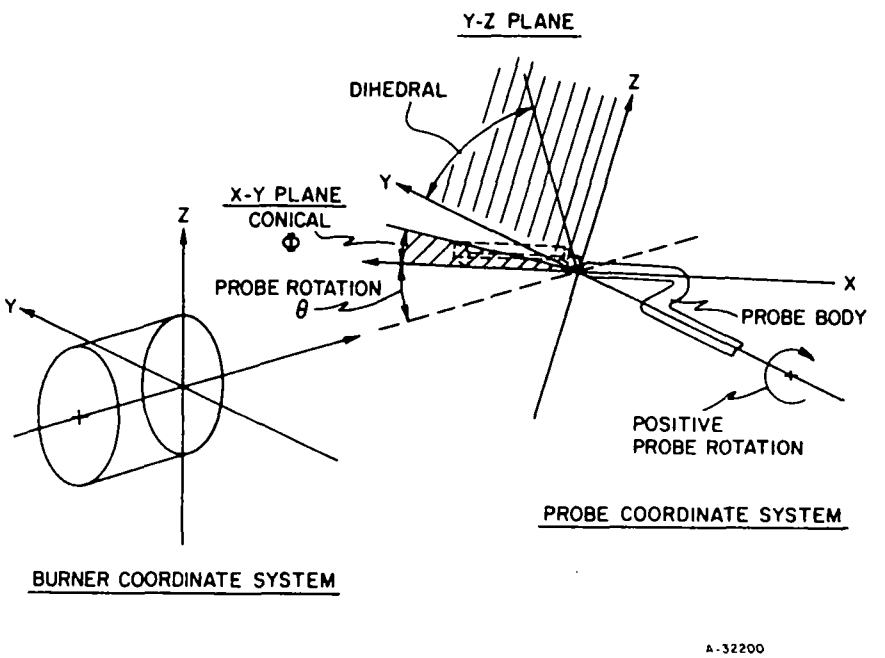

Figure II-213. BURNER AND PROBE COORDINATE SYSTEMS

Table II-36. VELOCITY SAMPLING LOCATIONS PLANNED FOR SWIRL BURNER

Swirl Intensity	Radial Positions, cm	Axial Position, cm
Minimum ($s \cong 0$)	+1.5 to −1.5 in 0.5-cm intervals +1.5 to +6.0 in 1.0-cm intervals −1.5 to −6.0 in 1.0-cm intervals +6.0 to +30.0 in 10.0-cm intervals −6.0 to −30.0 in 10.0-cm intervals	5.08
	+6.0 to −6.0 in 1.0-cm intervals +6.0 to +30.0 in 10.0-cm intervals −6.0 to −30.0 in 10.0-cm intervals	50.8
	+10.0 to −6.0 in 1.0-cm intervals +10.0 to +30.0 in 10.0-cm intervals −6.0 to −30.0 in 10.0-cm intervals	76.2
	−30.0 to +30.0 in 10.0-cm intervals	101.6
Intermediate ($s \cong 0.8$)	+10.0 to −10.0 in 1.0-cm intervals +10.0 to +30.0 in 5.0-cm intervals −10.0 to −30.0 in 5.0-cm intervals	2.54
	+10.0 to −10.0 in 0.5-cm intervals +10.0 to +30.0 in 1.0-cm intervals −10.0 to −30.0 in 1.0-cm intervals	7.62
	+10.0 to −10.0 in 1.0-cm intervals +10.0 to +30.0 in 10.0-cm intervals −10.0 to −30.0 in 10.0-cm intervals	16.78
	Plans for run based on results at 16.78-cm axial position	30.48
Maximum	+5.0 to −5.0 in 1.0-cm intervals +5.0 to +15.0 in 0.5-cm intervals −5.0 to −15.0 in 0.5-cm intervals +15.0 to +30.0 in 5.0-cm intervals −15.0 to −30.0 in 5.0-cm intervals	2.54
	Same as for 2.54-cm axial position	7.62
	+10.0 to −10.0 in 1.0-cm intervals +10.0 to +30.0 in 5.0-cm intervals −10.0 to −30.0 in 5.0-cm intervals	10.16

Table II-37. EXAMPLE OF RAW DATA OBTAINED FROM MDIT VELOCITY PROBE FOR THE SWIRL BURNER SET FOR MINIMUM SWIRL AT THE 3.80-cm AXIAL POSITION

AERODYNAMIC MODELING OF COMBUSTION BURNERS

CALIBRATION COEFFICIENTS FOR FORWARD FLOW

A1 =	0.770590	A2 =	0.272353	A3 =	-0.059818
B0 =	0.737720	B2 =	-0.158821	B4 =	0.129246
C =	4.464660	D =	0.394812		

MOVEABLE BLOCK BURNER SET FOR MINIMUM SWIRL - COLD MODEL

TOTAL DATA INPUT

THETA	AP	RP	P13	P03	P24	P04	P0A	T	Pb
0.	3.8	-30.0	3830.00	-3930.00	-3600.00	-3850.00	410.00	20.	760.
0.	3.8	-25.0	3090.00	-3980.00	-4400.00	-3800.00	427.00	20.	760.
0.	3.8	-20.0	3120.00	-3680.00	-3820.00	-3590.00	450.00	20.	760.
0.	3.8	-15.0	3370.00	-4120.00	-3680.00	-4120.00	433.00	20.	760.
0.	3.8	-14.0	3130.00	-3380.00	-3830.00	-3670.00	463.00	20.	760.
0.	3.8	-13.0	3800.00	-3930.00	-4030.00	-3660.00	500.00	20.	760.
0.	3.8	-12.0	4260.00	-3830.00	-3710.00	-2520.00	726.00	20.	760.
0.	3.8	-11.0	4900.00	-3620.00	-3100.00	-2470.00	698.00	20.	760.
0.	3.8	-10.0	8860.00	-2910.00	-1760.00	-1850.00	1180.00	20.	760.
0.	3.8	-9.0	5110.00	-2900.00	-857.00	-1620.00	1106.00	20.	760.
0.	3.8	-8.0	398.00	1005.00	-240.00	-428.00	880.00	20.	760.
0.	3.8	-7.0	252.00	126.00	-66.10	-202.00	195.00	20.	760.
0.	3.8	-6.0	920.00	134.00	-71.40	-204.00	154.00	20.	760.
0.	3.8	-5.0	13000.00	207.00	-66.30	-227.00	236.00	20.	760.
0.	3.8	-4.0	-930.00	196.00	-80.80	-550.00	177.00	20.	760.
0.	3.8	-3.0	-773.00	196.00	-100.00	-1860.00	177.00	20.	760.
0.	3.8	-2.0	-2130.00	207.00	-138.00	1064.00	184.00	20.	760.
0.	3.8	-1.0	32.70	19.20	-51.60	37.50	20.80	20.	760.
0.	3.8	0.0	-222.00	16.50	-1188.00	16.00	11.90	20.	760.
0.	3.8	1.0	-30.80	187.00	-92.60	37.90	30.80	20.	760.
0.	3.8	2.0	-3960.00	215.00	419.00	163.00	180.00	20.	760.
0.	3.8	3.0	7960.00	199.00	199.00	140.00	183.00	20.	760.
0.	3.8	4.0	15180.00	201.00	127.00	114.00	190.00	20.	760.
0.	3.8	5.0	-2260.00	198.00	84.80	99.60	203.00	20.	760.
0.	3.8	6.0	-1844.00	189.00	68.60	88.60	178.00	20.	760.
0.	3.8	7.0	-652.00	185.00	62.60	79.00	163.00	20.	760.
0.	3.8	8.0	-239.00	420.00	70.10	100.00	202.00	20.	760.
0.	3.8	9.0	-343.00	-1240.00	195.00	390.00	545.00	20.	760.
0.	3.8	10.0	-5020.00	-4570.00	1300.00	4160.00	553.00	20.	760.
0.	3.8	11.0	3700.00	6700.00	4600.00	19400.00	422.00	20.	760.
0.	3.8	12.0	5620.00	10920.00	23500.00	-17000.00	410.00	20.	760.
0.	3.8	13.0	12660.00	13700.00	9000.00	79900.00	400.00	20.	760.
0.	3.8	14.0	15400.00	24900.00	19700.00	75900.00	403.00	20.	760.
0.	3.8	15.0	31900.00	19000.00	26000.00	100800.00	370.00	20.	760.
0.	3.8	20.0	46500.00	29200.00	23500.00	31300.00	365.00	20.	760.
0.	3.8	25.0	57000.00	23800.00	17400.00	21000.00	355.00	20.	760.
0.	3.8	30.0	28700.00	24200.00	18100.00	19100.00	360.00	20.	760.

A typical set of reduced velocity data calculated from Table II-37 is given in Table II-38. The direction of the velocity is defined by FI, the conical angle measured about the x-axis, and by delta, the dihedral angle measured from the positive y-axis in the y-z plane. The magnitude of the velocity is given by V in ft/s. ρ is the density of the air in slugs/ft-sq in. The components of the velocity, VX, VY, and VZ, are given in ft/s. The tangential velocity, VT, and the radial velocity, VR, are both expressed in ft/s. PST is the static pressure in psig.

A computer plotting subroutine is used to graphically represent the axial velocity, VX, and the tangential velocity, VT, shown in Figures II-214 and II-215.

Data were collected for the swirl burner with the probe facing both toward and away from the burner for all radial positions between ±15 cm of the burner axis. We found that in some sampling locations, velocities were measured for both forward and reverse positions of the probe. Since during a given time interval the velocity vector cannot point in two directions simultaneously, a procedure had to be developed to determine which of the measured velocities was real and which was fictitious. The most quantitative method for doing this would be to calibrate the multidirectional impact tube for reverse flow (probe pointed in the same direction as on jet). This would allow a comparison of the velocities measured with the probe going into and away from the air stream. The major shortcoming of this technique was that all velocities which were calculated using the recovery coefficients determined by the reverse flow calibration procedure were imaginary. However, the following general qualitative results concerning the velocity vector arise from the attempted reverse flow calibration: Using the forward flow calibration coefficients on the data collected with the probe pointed in the same direction as the air jet, we determined real-valued velocities whose magnitudes were 4-5 times less than the actual velocity and in a direction opposite to that of the uniform air jet. Additional qualitative information concerning the direction of flow was also obtained with wool tufts. Using these qualitative types of information, we found that for the movable-block burner, the minimum swirl setting showed no reverse flow, while the intermediate swirl setting showed reverse flow in the center of the burner region.

Table II-38. TYPICAL COMPUTER OUTPUT OF REDUCED VELOCITY DATA

MOVEABLE BLOCK BURNER SET FOR MINIMUM SWIRL - COLD MODEL

RESULTS

AP	RP	FI	DELTA	RHO	V	VX	VY	VZ	VT	VR	PST	T	P
3.8	-30.0	82.0	226.7	0.0000159	8.62	1.19	-5.84	-6.22	-6.32	5.74	0.003264	20.	760.
3.8	-25.0	82.7	215.0	0.0000159	9.01	1.14	-7.31	-5.13	-5.75	6.84	0.003267	20.	760.
3.8	-20.0	82.5	219.2	0.0000159	9.17	1.19	-7.04	-5.75	-5.18	7.47	0.003179	20.	760.
3.8	-15.0	81.4	222.4	0.0000159	8.62	1.28	-6.29	-5.76	-4.36	7.33	0.003092	20.	760.
3.8	-14.0	82.3	219.2	0.0000159	9.33	1.23	-7.16	-5.85	-4.09	8.29	0.003149	20.	760.
3.8	-13.0	83.0	223.3	0.0000159	8.75	1.06	-6.32	-5.96	-3.34	8.02	0.002885	20.	760.
3.8	-12.0	85.1	228.9	0.0000159	9.35	0.79	-6.12	-7.02	-2.42	8.91	0.002460	20.	760.
3.8	-11.0	84.6	237.6	0.0000159	9.26	0.86	-4.93	-7.79	-2.40	8.90	0.002431	20.	760.
3.8	-10.0	82.9	258.7	0.0000159	9.71	1.19	-1.87	-9.45	-2.98	9.16	0.001965	20.	760.
3.8	-9.0	71.9	260.4	0.0000159	10.20	3.16	-1.60	-9.56	-5.93	7.67	0.001770	20.	760.
3.8	-8.0	61.6	238.9	0.0000159	17.65	8.38	-8.02	-13.30	-11.66	10.26	0.002695	20.	760.
3.8	-7.0	31.7	255.3	0.0000159	35.25	29.98	-4.70	-17.93	-17.57	5.90	0.000175	20.	760.
3.8	-6.0	29.9	265.5	0.0000159	35.16	30.47	-1.35	-17.50	-16.49	6.01	0.001019	20.	760.
3.8	-5.0	31.9	269.7	0.0000159	34.01	28.87	-0.09	-17.97	-16.24	7.68	-0.000314	20.	760.
3.8	-4.0	24.0	274.9	0.0000159	34.30	31.33	1.20	-13.90	-12.85	5.44	-0.001021	20.	760.
3.8	-3.0	20.1	277.3	0.0000159	33.33	31.29	1.47	-11.38	-10.41	4.83	-0.001419	20.	760.
3.8	-2.0	15.8	273.7	0.0000159	31.27	30.08	0.55	-8.50	-7.50	4.04	-0.001420	20.	760.
3.8	-1.0	10.6	212.3	0.0000159	83.63	82.19	-13.07	-8.28	-12.58	9.01	-0.005133	20.	760.
3.8	0.0	0.8	349.4	0.0000159	106.95	106.94	1.47	-0.27	0.00	1.50	-0.000575	20.	760.
3.8	1.0	14.6	341.6	0.0000159	73.03	70.65	17.53	-5.81	13.10	13.02	-0.005770	20.	760.
3.8	2.0	5.4	83.9	0.0000159	29.92	29.78	0.29	2.82	2.79	0.50	-0.001562	20.	760.
3.8	3.0	11.3	91.4	0.0000159	30.38	29.79	-0.14	5.95	5.77	1.46	-0.001464	20.	760.
3.8	4.0	16.7	90.4	0.0000159	31.71	30.37	-0.07	9.11	8.76	2.49	-0.001660	20.	760.
3.8	5.0	24.1	87.8	0.0000159	33.32	30.40	0.51	13.63	12.91	4.40	-0.001329	20.	760.
3.8	6.0	27.8	87.8	0.0000159	35.12	31.06	0.60	16.38	15.54	5.19	-0.000410	20.	760.
3.8	7.0	27.2	84.5	0.0000159	37.10	32.99	1.62	16.88	16.34	4.56	-0.000771	20.	760.
3.8	8.0	33.0	73.6	0.0000159	33.36	27.97	5.11	17.45	17.37	5.36	0.000857	20.	760.
3.8	9.0	50.5	60.3	0.0000159	19.09	12.12	7.26	12.81	13.11	6.73	0.002324	20.	760.
3.8	10.0	70.9	75.4	0.0000159	7.81	2.55	1.85	7.14	4.97	5.46	0.002270	20.	760.
3.8	11.0	62.2	141.1	0.0000159	4.82	2.24	-3.33	2.67	3.57	2.34	0.002445	20.	760.
3.8	12.0	71.7	166.5	0.0000159	4.13	1.29	-3.81	0.91	2.83	2.72	0.002534	20.	760.
3.8	13.0	59.1	125.4	0.0000159	3.29	1.69	-1.64	2.30	2.54	1.24	0.002496	20.	760.
3.8	14.0	58.9	141.9	0.0000159	2.33	1.20	-1.57	1.23	1.82	0.82	0.002454	20.	760.
3.8	15.0	52.4	129.1	0.0000159	2.53	1.54	-1.27	1.56	1.91	0.62	0.002661	20.	760.
3.8	20.0	27.2	116.8	0.0000159	2.08	1.85	-0.42	0.84	0.94	0.09	0.002663	20.	760.
3.8	25.0	23.4	106.9	0.0000159	2.46	2.25	-0.28	0.93	0.97	0.06	0.002726	20.	760.
3.8	30.0	25.2	122.2	0.0000159	2.42	2.19	-0.55	0.87	1.03	0.06	0.002590	20.	760.

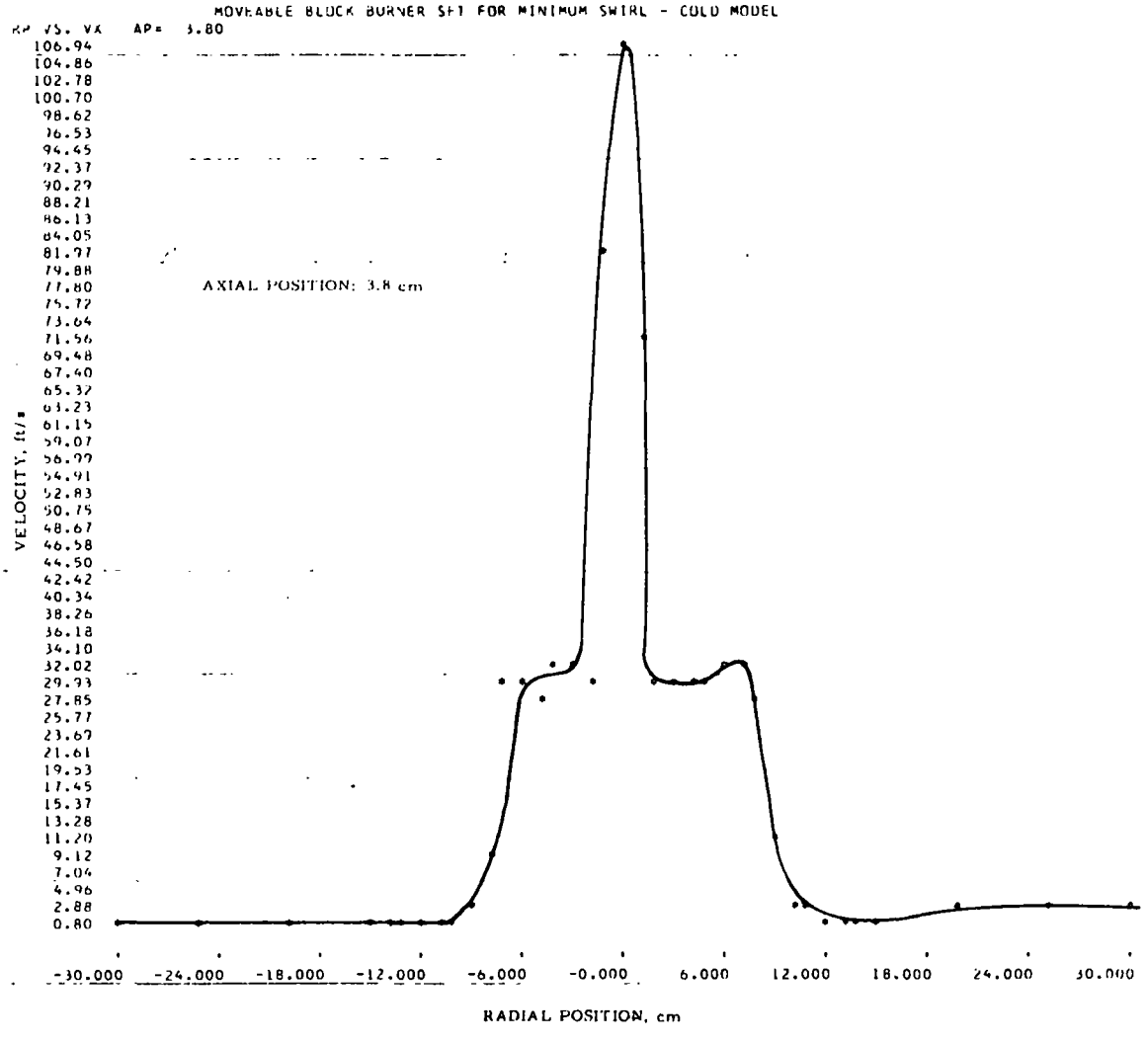

Figure II-214. AXIAL VELOCITY PROFILE FOR SWIRL BURNER SET FOR MINIMUM SWIRL AT THE 3.8-cm AXIAL POSITION

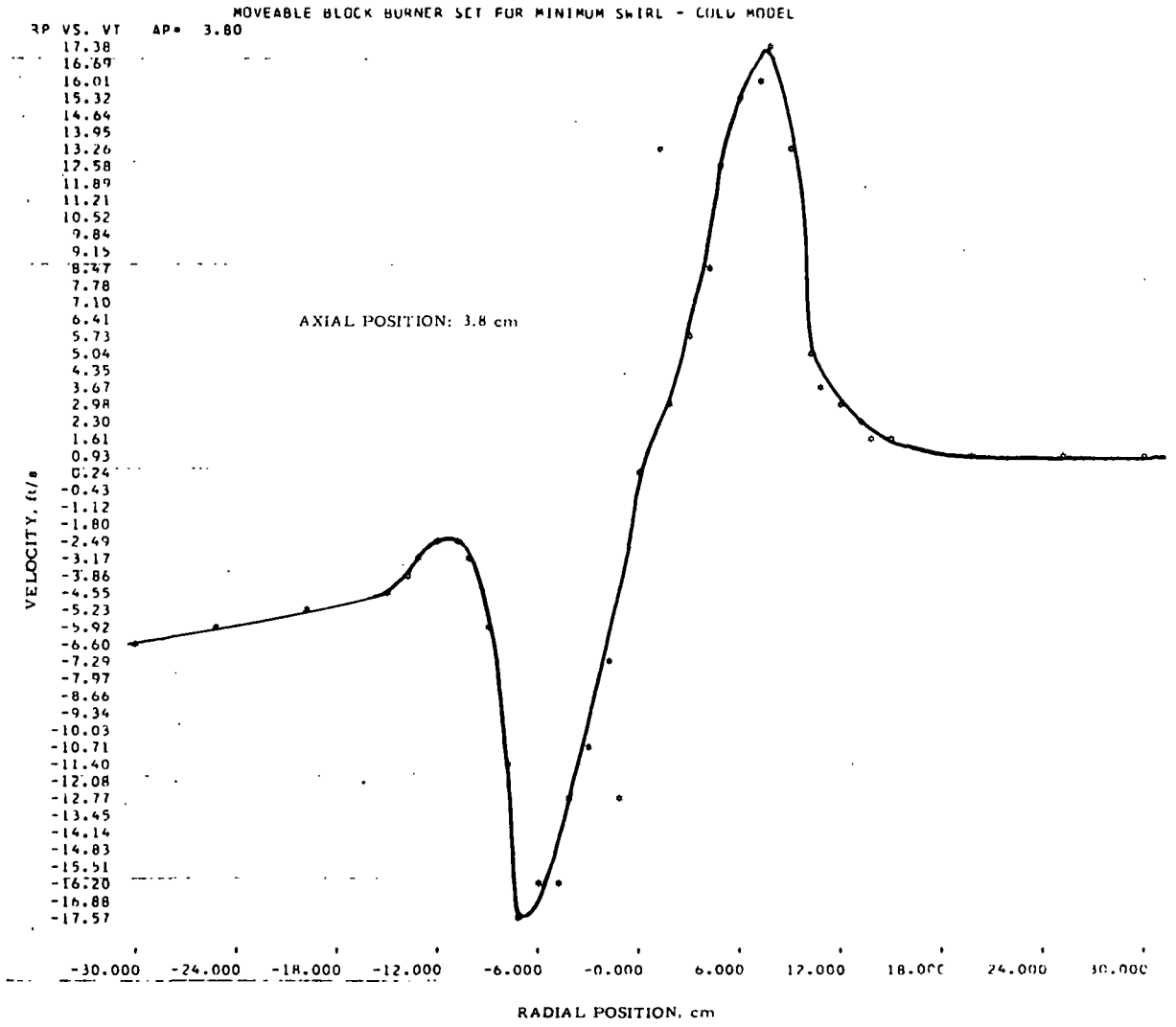

Figure II-215. TANGENTIAL VELOCITY PROFILE FOR SWIRL BURNER SET FOR MINIMUM SWIRL AT THE 3.8-cm AXIAL POSITION

For the case of minimum swirl, the raw pressure input data are given in Table II-37 and Tables II-39 to II-42. The reduced profile data are listed in Table II-38 and Tables II-43 to II-46. Table II-47 shows the column heading symbols for these tables. Figure II-214 shows the axial velocity for minimum swirl at an axial position of 3.8 cm. The central peak occurs in the region of the gas nozzle, while the velocities reach a plateau at 30 ft/s in the region of the throat of the burner. Figure II-216 shows the tangential velocity as a function of the burner's radial position. The maximum magnitude of the tangential velocity is approximately 18 ft/s, while preliminary work on the axial burner with the variable mixing rate axial flow burner nozzle indicates a maximum tangential velocity of only 5 ft/s. Figures II-216 and II-217 show the axial and tangential velocity profiles at an axial position of 7.6 cm: There is little change in the structure of the curves from those at 3.8 cm. The axial velocity profile at 17.8 cm is illustrated in Figure II-218. The constant axial velocity plateau no longer appears the region of the burner, and the velocities decrease as a function of radial position. Figure II-219 shows that the peaks of the tangential velocity profile are opening toward the outside walls of the cold model and that the magnitude of the velocity has decreased by a factor of 2 from its value at the 7.8-cm axial position. The axial velocity in Figure II-220 lost the identity of the gas nozzle, and there is a systematic decrease in the velocity from the axis of the burner. Figure II-221 shows that the peaks of the tangential velocity are continuing to open and that its magnitude is still decreasing. In Figures II-222 and II-223 at an axial position of 63.5 cm, the tangential velocity component has disappeared and the axial velocity is about one-sixth its initial magnitude at the burner.

The numerical raw data for the movable-block burner, set for intermediate swirl (swirl number, $S = 0.8$), are included in Tables II-48 to II-51. The computer reduced form of the data, giving both the magnitude and direction of the velocity as functions of the axial and radial positions, is presented in Tables II-52 to II-55. The graphical representations of these data, Figures II-224 to II-231, are discussed below.

Table II-39. RAW DATA FOR THE SWIRL BURNER (Minimum Swirl) AT THE 7.6-cm AXIAL POSITION

AERODYNAMIC MODELING OF COMBUSTION BURNERS

CALIBRATION COEFFICIENTS FOR FORWARD FLOW

A1 =	0.770590	A2 =	0.272353	A3 =	-0.059818
B0 =	0.737720	B2 =	-0.158821	B4 =	0.129246
C =	4.464660	D =	0.394812		

MOVEABLE BLOCK BURNER SET FOR MINIMUM SWIRL - COLD MODEL

TOTAL DATA INPUT

THETA	AP	RP	P13	P03	P24	P04	PCA	T	Pb
0.	7.6	30.0	62800.00	18700.00	19100.00	20900.00	339.00	20.	760.
0.	7.6	25.0	68800.00	24000.00	11700.00	20500.00	356.00	20.	760.
0.	7.6	20.0	34800.00	23500.00	10500.00	28300.00	354.00	20.	760.
0.	7.6	15.0	16600.00	15600.00	22900.00	30800.00	383.00	20.	760.
0.	7.6	14.0	11560.00	12300.00	14150.00	19000.00	375.00	20.	760.
0.	7.6	13.0	8220.00	18000.00	20500.00	51000.00	418.00	20.	760.
0.	7.6	12.0	7700.00	33600.00	2950.00	31000.00	444.00	20.	760.
0.	7.6	11.0	-2590.00	-8530.00	1010.00	2750.00	583.00	20.	760.
0.	7.6	10.0	-765.00	-2380.00	299.00	698.00	503.00	20.	760.
0.	7.6	9.0	-390.00	13900.00	203.00	245.00	344.00	20.	760.
0.	7.6	8.0	-301.00	530.00	107.00	147.00	220.00	20.	760.
0.	7.6	7.0	-514.00	243.00	79.50	100.00	195.00	20.	760.
0.	7.6	6.0	-2900.00	204.00	77.20	99.00	184.00	20.	760.
0.	7.6	5.0	2590.00	204.00	100.00	113.60	201.00	20.	760.
0.	7.6	4.0	1339.00	201.00	139.00	129.00	188.00	20.	760.
0.	7.6	3.0	1656.00	221.00	217.00	148.00	196.00	20.	760.
0.	7.6	2.0	-652.00	260.00	910.00	166.00	162.00	20.	760.
0.	7.6	0.0	-113.60	17.80	2700.00	16.10	12.40	20.	760.
0.	7.6	-2.0	309.00	135.00	-131.00	437.00	142.00	20.	760.
0.	7.6	-3.0	-896.00	237.00	-106.00	-720.00	225.00	20.	760.
0.	7.6	-4.0	-880.00	216.00	-88.50	-490.00	210.00	20.	760.
0.	7.6	-5.0	-7450.00	188.00	-77.00	-303.00	191.00	20.	760.
0.	7.6	-6.0	930.00	163.00	-75.50	-282.00	195.00	20.	760.
0.	7.6	-7.0	309.00	182.00	-77.00	-308.00	250.00	20.	760.
0.	7.6	-8.0	340.00	280.00	-127.00	-341.00	445.00	20.	760.
0.	7.6	-9.0	956.00	1870.00	-375.00	-628.00	1010.00	20.	760.
0.	7.6	-10.0	10600.00	-17000.00	-880.00	-1220.00	780.00	20.	760.
0.	7.6	-11.0	-11980.00	-12800.00	-4920.00	-3050.00	539.00	20.	760.
0.	7.6	-12.0	-9540.00	-19300.00	-12960.00	-5820.00	510.00	20.	760.
0.	7.6	-13.0	-31400.00	-26000.00	-16100.00	39700.00	473.00	20.	760.
0.	7.6	-14.0	155000.00	-125400.00	25200.00	73400.00	433.00	20.	760.
0.	7.6	-15.0	79600.00	214800.00	23000.00	-89600.00	448.00	20.	760.
0.	7.6	-20.0	32600.00	27000.00	19700.00	25700.00	415.00	20.	760.
0.	7.6	-25.0	35900.00	27000.00	21700.00	55000.00	400.00	20.	760.
0.	7.6	-30.0	39800.00	23500.00	19000.00	34300.00	390.00	20.	760.

Table II-40. RAW DATA FOR THE SWIRL BURNER (Minimum Swirl) AT THE 17.8-cm AXIAL POSITION

AERODYNAMIC MODELING OF COMBUSTION BURNERS

CALIBRATION COEFFICIENTS FOR FORWARD FLOW

A1 =	0.770590	A2 =	0.272353	A3 =	-0.059818
B0 =	0.737720	B2 =	-0.158821	B4 =	0.129246
C =	4.464660	D =	0.394812		

MOVEABLE BLOCK BURNER SET FOR MINIMUM SWIRL - COLD MODEL

TOTAL DATA INPUT

THETA	AP	RP	P13	P03	P24	P04	P0A	T	PB
0.	17.8	-30.0	-60500.00	8900.00	9640.00	9450.00	399.00	20.	760.
0.	17.8	-25.0	-56500.00	36600.00	34600.00	29960.00	405.00	20.	760.
0.	17.8	-20.0	63600.00	52300.00	-97400.00	37400.00	401.00	20.	760.
0.	17.8	-15.0	111400.00	-27400.00	-94400.00	-3410.00	450.00	20.	760.
0.	17.8	-14.0	-34800.00	48600.00	-4910.00	-48800.00	483.00	20.	760.
0.	17.8	-13.0	-54800.00	19800.00	-3300.00	-5800.00	558.00	20.	760.
0.	17.8	-12.0	2490.00	-5650.00	-1120.00	-1830.00	1850.00	20.	760.
0.	17.8	-11.0	11020.00	6710.00	-1240.00	-3720.00	570.00	20.	760.
0.	17.8	-10.0	4420.00	2800.00	-895.00	-1570.00	488.00	20.	760.
0.	17.8	-9.0	3140.00	2090.00	-497.00	-1040.00	468.00	20.	760.
0.	17.8	-8.0	1470.00	788.00	-312.00	-2000.00	483.00	20.	760.
0.	17.8	-7.0	1140.00	888.00	-213.00	-1026.00	423.00	20.	760.
0.	17.8	-6.0	7800.00	652.00	-193.00	-868.00	312.00	20.	760.
0.	17.8	-5.0	3670.00	517.00	-220.00	-855.00	315.00	20.	760.
0.	17.8	-4.0	2520.00	368.00	-176.00	-1150.00	251.00	20.	760.
0.	17.8	-3.0	587.00	283.00	-162.00	2310.00	183.00	20.	760.
0.	17.8	-2.0	281.00	97.00	-189.00	141.00	129.00	20.	760.
0.	17.8	-1.0	101.00	41.30	-1160.00	54.80	37.00	20.	760.
0.	17.8	0.0	-287.00	37.20	399.00	35.00	26.00	20.	760.
0.	17.8	1.0	129.40	39.70	3680.00	42.80	38.00	20.	760.
0.	17.8	2.0	-433.00	239.00	1104.00	174.00	133.00	20.	760.
0.	17.8	3.0	543.00	260.00	-169.00	698.00	195.00	20.	760.
0.	17.8	4.0	2300.00	348.00	-181.00	-2390.00	269.00	20.	760.
0.	17.8	5.0	2940.00	414.00	-200.00	-1220.00	295.00	20.	760.
0.	17.8	6.0	2170.00	540.00	-171.00	-956.00	346.00	20.	760.
0.	17.8	7.0	1800.00	700.00	-312.00	-1115.00	418.00	20.	760.
0.	17.8	8.0	1100.00	824.00	-504.00	-1270.00	439.00	20.	760.
0.	17.8	9.0	-1820.00	1620.00	540.00	563.00	381.00	20.	760.
0.	17.8	10.0	2640.00	2650.00	-690.00	-1650.00	544.00	20.	760.
0.	17.8	11.0	-2560.00	-10520.00	848.00	1540.00	511.00	20.	760.
0.	17.8	12.0	12300.00	11000.00	-3740.00	-4680.00	520.00	20.	760.
0.	17.8	13.0	5240.00	-5600.00	11090.00	10900.00	553.00	20.	760.
0.	17.8	14.0	999999999.50	98400.00	-8400.00	-6000.00	440.00	20.	760.
0.	17.8	15.0	999999999.50	-188000.00	-30600.00	-6000.00	505.00	20.	760.
0.	17.8	20.0	32800.00	32000.00	22900.00	45000.00	410.00	20.	760.
0.	17.8	25.0	20000.00	33000.00	22700.00	72600.00	402.00	20.	760.
0.	17.8	30.0	31500.00	20800.00	24000.00	18000.00	395.00	20.	760.

Table II-41. RAW DATA FOR THE SWIRL BURNER (Minimum Swirl) AT THE 30.5-cm AXIAL POSITION

AERODYNAMIC MODELING OF COMBUSTION BURNERS

CALIBRATION COEFFICIENTS FOR FORWARD FLOW

A1 =	0.770590	A2 =	0.272353	A3 =	-0.059818
B0 =	0.737720	B2 =	-0.158821	B4 =	0.129246
C =	4.464660	D =	0.394812		

MOVEABLE BLOCK BURNER SET FOR MINIMUM SWIRL - COLD MODEL

TOTAL DATA INPUT

THETA	AP	RP	P13	P03	P24	P04	P0A	T	Pb
0.	30.5	-30.0	3420.00	-4180.00	-4420.00	-4200.00	480.00	20.	760.
0.	30.5	-25.0	3340.00	-4420.00	-4060.00	-3900.00	440.00	20.	760.
0.	30.5	-20.0	3280.00	-4680.00	-3480.00	-2260.00	512.00	20.	760.
0.	30.5	-15.0	2790.00	-4910.00	-2340.00	-2390.00	490.00	20.	760.
0.	30.5	-14.0	2450.00	-11310.00	-2120.00	-2250.00	674.00	20.	760.
0.	30.5	-13.0	2340.00	-7420.00	-1160.00	-2220.00	521.00	20.	760.
0.	30.5	-12.0	2040.00	-9000.00	-726.00	-1780.00	536.00	20.	760.
0.	30.5	-10.0	1820.00	4240.00	-694.00	-2380.00	490.00	20.	760.
0.	30.5	-9.0	832.00	3480.00	-552.00	-1970.00	535.00	20.	760.
0.	30.5	-8.0	1304.00	1482.00	-352.00	-2940.00	430.00	20.	760.
0.	30.5	-7.0	1000.00	1057.00	-351.00	-6920.00	381.00	20.	760.
0.	30.5	-6.0	732.00	290.00	-326.00	1980.00	281.00	20.	760.
0.	30.5	-5.0	491.00	252.00	-403.00	858.00	245.00	20.	760.
0.	30.5	-4.0	376.00	214.00	-274.00	880.00	140.00	20.	760.
0.	30.5	-3.0	402.00	192.00	-271.00	296.00	118.00	20.	760.
0.	30.5	-2.0	244.00	134.00	-526.00	192.00	99.60	20.	760.
0.	30.5	-1.0	556.00	141.00	-528.00	152.00	78.20	20.	760.
0.	30.5	0.0	-3180.00	129.00	-2396.00	123.00	99.00	20.	760.
0.	30.5	1.0	-362.00	194.00	-278.00	184.00	88.60	20.	760.
0.	30.5	2.0	-3000.00	285.00	-110.00	225.00	146.20	20.	760.
0.	30.5	3.0	-468.00	404.00	3220.00	338.00	206.00	20.	760.
0.	30.5	4.0	-860.00	434.00	930.00	342.00	229.00	20.	760.
0.	30.5	5.0	-920.00	394.00	730.00	179.00	332.00	20.	760.
0.	30.5	6.0	1620.00	615.00	700.00	466.00	460.00	20.	760.
0.	30.5	7.0	1270.00	1010.00	717.00	648.00	351.00	20.	760.
0.	30.5	8.0	4660.00	1400.00	740.00	820.00	395.00	20.	760.
0.	30.5	9.0	2500.00	1850.00	950.00	1188.00	380.00	20.	760.
0.	30.5	10.0	999999999.50	3660.00	2040.00	1570.00	364.00	20.	760.
0.	30.5	11.0	999999999.50	6400.00	1960.00	4310.00	422.00	20.	760.
0.	30.5	12.0	5040.00	53000.00	2630.00	4300.00	436.00	20.	760.
0.	30.5	13.0	4620.00	-18840.00	3720.00	5800.00	512.00	20.	760.
0.	30.5	14.0	4790.00	-9980.00	2520.00	7710.00	497.00	20.	760.
0.	30.5	15.0	4720.00	-8640.00	2220.00	-10440.00	484.00	20.	760.
0.	30.5	20.0	3240.00	-6080.00	-5680.00	-3870.00	452.00	20.	760.
0.	30.5	25.0	3240.00	-4420.00	-5040.00	-4720.00	427.00	20.	760.
0.	30.5	30.0	3470.00	-5480.00	-5000.00	-4920.00	430.00	20.	760.

Table II-42. RAW DATA FOR THE SWIRL BURNER (Minimum Swirl) AT 63.5-cm AXIAL POSITION

AERODYNAMIC MODELING OF COMBUSTION BURNERS

CALIBRATION COEFFICIENTS FOR FORWARD FLOW

A1 =	0.770590	A2 =	0.272353	A3 =	-0.059818
B0 =	0.737720	B2 =	-0.158821	B4 =	0.129246
C =	4.464660	D =	0.394812		

MOVEABLE BLOCK BURNER SET FOR MINIMUM SWIRL - COLD MODEL

TOTAL DATA INPUT

THETA	AP	RP	P13	P03	P24	P04	P0A	T	PB
0.	63.5	-30.0	4370.00	10960.00	-7520.00	-36000.00	460.00	20.	760.
0.	63.5	-25.0	2450.00	5720.00	-4060.00	-15200.00	437.00	20.	760.
0.	63.5	-20.0	3400.00	2450.00	-3980.00	-19760.00	428.00	20.	760.
0.	63.5	-15.0	1680.00	980.00	-2120.00	12640.00	365.00	20.	760.
0.	63.5	-14.0	1586.00	905.00	-1870.00	4700.00	374.00	20.	760.
0.	63.5	-13.0	980.00	1020.00	-2330.00	5390.00	348.00	20.	760.
0.	63.5	-12.0	1054.00	630.00	-1570.00	2440.00	295.00	20.	760.
0.	63.5	-11.0	880.00	500.00	-1180.00	2640.00	260.00	20.	760.
0.	63.5	-10.0	1204.00	465.00	-1500.00	1890.00	329.00	20.	760.
0.	63.5	-9.0	950.00	730.00	-1590.00	1500.00	302.00	20.	760.
0.	63.5	-8.0	1280.00	738.00	-1720.00	1536.00	282.00	20.	760.
0.	63.5	-7.0	1020.00	383.00	-1790.00	1840.00	299.00	20.	760.
0.	63.5	-6.0	1280.00	478.00	-3720.00	900.00	235.00	20.	760.
0.	63.5	-5.0	1580.00	542.00	-1880.00	780.00	249.00	20.	760.
0.	63.5	-4.0	1200.00	560.00	-2040.00	620.00	248.00	20.	760.
0.	63.5	-3.0	1220.00	430.00	-2060.00	710.00	218.00	20.	760.
0.	63.5	-2.0	3940.00	670.00	-6040.00	650.00	213.00	20.	760.
0.	63.5	-1.0	19550.00	530.00	-3650.00	560.00	247.00	20.	760.
0.	63.5	0.0	19550.00	530.00	-6070.00	738.00	232.00	20.	760.
0.	63.5	1.0	-4500.00	632.00	-2600.00	552.00	248.00	20.	760.
0.	63.5	2.0	-2900.00	1000.00	-3040.00	690.00	216.00	20.	760.
0.	63.5	3.0	-2280.00	905.00	-2880.00	790.00	277.00	20.	760.
0.	63.5	4.0	-4580.00	880.00	5200.00	660.00	255.00	20.	760.
0.	63.5	5.0	-2560.00	950.00	15600.00	820.00	277.00	20.	760.
0.	63.5	6.0	-1600.00	1170.00	999999999.50	766.00	270.00	20.	760.
0.	63.5	7.0	-2050.00	800.00	9160.00	1630.00	305.00	20.	760.
0.	63.5	8.0	-1350.00	1740.00	9470.00	980.00	274.00	20.	760.
0.	63.5	9.0	-2280.00	3940.00	-4330.00	1414.00	403.00	20.	760.
0.	63.5	10.0	-920.00	2100.00	11060.00	1040.00	355.00	20.	760.
0.	63.5	11.0	-4500.00	3370.00	4030.00	1480.00	290.00	20.	760.
0.	63.5	12.0	-1070.00	3840.00	3580.00	1120.00	364.00	20.	760.
0.	63.5	13.0	-980.00	4880.00	10400.00	3340.00	345.00	20.	760.
0.	63.5	14.0	-1740.00	5200.00	5350.00	2420.00	362.00	20.	760.
0.	63.5	15.0	-2470.00	4820.00	3750.00	3150.00	374.00	20.	760.
0.	63.5	20.0	-4100.00	11300.00	2140.00	4480.00	388.00	20.	760.
0.	63.5	25.0	-7180.00	18800.00	4020.00	4530.00	404.00	20.	760.
0.	63.5	30.0	-20200.00	21000.00	5940.00	3980.00	403.00	20.	760.

Table II-43. COMPUTER-REDUCED DATA FOR SWIRL BURNER (Minimum Swirl) AT THE 7.6-cm AXIAL POSITION

MOVEABLE BLOCK BURNER SET FOR MINIMUM SWIRL - COLD MODEL

RESULTS

AP	RP	FI	DELTA	RHO	V	VX	VY	VZ	VT	VR	PST	T	PB
7.6	30.0	19.3	106.9	0.0000159	2.68	2.53	-0.25	0.85	0.88	0.07	0.002844	20.	760.
7.6	25.0	35.5	99.6	0.0000159	2.59	2.11	-0.25	1.48	1.47	0.32	0.002732	20.	760.
7.6	20.0	48.9	106.7	0.0000159	2.65	1.74	-0.57	1.91	1.83	0.80	0.002775	20.	760.
7.6	15.0	30.9	144.0	0.0000159	2.51	2.15	-1.04	0.75	1.23	0.37	0.002532	20.	760.
7.6	14.0	33.3	140.7	0.0000159	2.91	2.43	-1.24	1.01	1.50	0.53	0.002583	20.	760.
7.6	13.0	60.2	158.1	0.0000159	2.87	1.42	-2.31	0.92	1.74	1.78	0.002382	20.	760.
7.6	12.0	74.2	110.9	0.0000159	5.78	1.57	-1.99	5.20	2.27	5.08	0.002516	20.	760.
7.6	11.0	58.9	68.6	0.0000159	8.29	4.28	2.58	6.61	4.66	5.35	0.001967	20.	760.
7.6	10.0	56.4	68.6	0.0000159	14.98	8.28	4.54	11.62	8.21	9.39	0.002697	20.	760.
7.6	9.0	31.3	62.5	0.0000159	20.65	17.62	4.96	9.54	9.56	4.92	0.001150	20.	760.
7.6	8.0	30.4	70.4	0.0000159	28.13	24.24	4.78	13.45	12.45	6.96	0.001014	20.	760.
7.6	7.0	26.8	81.2	0.0000159	33.26	29.67	2.29	14.84	13.16	7.23	-0.000512	20.	760.
7.6	6.0	27.3	88.4	0.0000159	33.31	29.57	0.40	15.32	12.81	8.41	-0.000098	20.	760.
7.6	5.0	23.0	92.2	0.0000159	31.29	28.80	-0.47	12.22	10.27	6.63	-0.000766	20.	760.
7.6	4.0	17.1	95.9	0.0000159	30.10	28.76	-0.91	8.82	7.65	4.48	-0.000878	20.	760.
7.6	3.0	11.5	97.4	0.0000159	28.92	28.34	-0.75	5.72	5.13	2.65	-0.001182	20.	760.
7.6	2.0	4.8	35.6	0.0000159	30.44	30.33	2.11	1.51	2.46	0.80	-0.001227	20.	760.
7.6	0.0	1.6	2.4	0.0000159	105.59	105.55	2.98	0.12	0.00	2.99	-0.009515	20.	760.
7.6	-2.0	14.6	247.0	0.0000159	34.49	33.36	-3.41	-8.05	-6.19	6.17	-0.001476	20.	760.
7.6	-3.0	23.2	276.7	0.0000159	30.60	28.12	1.41	-11.97	-8.16	8.87	-0.001005	20.	760.
7.6	-4.0	24.8	275.7	0.0000159	32.48	29.47	1.36	-13.59	-10.25	9.03	-0.001040	20.	760.
7.6	-5.0	27.9	270.5	0.0000159	33.34	29.44	0.16	-15.64	-12.17	9.62	-0.000163	20.	760.
7.6	-6.0	28.3	265.3	0.0000159	33.68	29.65	-1.29	-15.93	-13.20	9.01	-0.000291	20.	760.
7.6	-7.0	31.5	256.0	0.0000159	32.02	27.30	-4.04	-16.23	-13.93	9.26	-0.000139	20.	760.
7.6	-8.0	38.0	249.5	0.0000159	24.08	18.97	-5.19	-13.90	-11.91	8.65	0.000877	20.	760.
7.6	-9.0	60.6	248.5	0.0000159	13.53	6.62	-4.30	-10.98	-6.53	9.82	0.001840	20.	760.
7.6	-10.0	70.1	265.2	0.0000159	9.32	3.16	-0.72	-8.74	-3.76	7.92	0.001944	20.	760.
7.6	-11.0	80.1	292.3	0.0000159	6.38	1.09	2.39	-5.82	-1.53	6.10	0.002272	20.	760.
7.6	-12.0	77.2	323.6	0.0000159	4.75	1.04	3.73	-2.75	-1.55	4.37	0.002153	20.	760.
7.6	-13.0	42.9	297.1	0.0000159	2.89	2.12	0.90	-1.75	-1.73	0.94	0.002064	20.	760.
7.6	-14.0	73.8	99.2	0.0000159	1.85	0.51	-0.28	1.76	-0.84	1.57	0.002294	20.	760.
7.6	-15.0	76.6	106.1	0.0000159	2.45	0.56	-0.66	2.29	-1.01	2.16	0.002248	20.	760.
7.6	-20.0	29.7	121.1	0.0000159	2.19	1.90	-0.56	0.93	-1.06	0.23	0.002340	20.	760.
7.6	-25.0	42.1	121.1	0.0000159	2.07	1.53	-0.72	1.19	-1.34	0.36	0.002445	20.	760.
7.6	-30.0	33.6	115.5	0.0000159	2.25	1.87	-0.53	1.13	-1.23	0.20	0.002495	20.	760.

Table II-44. COMPUTER-REDUCED DATA FOR SWIRL BURNER (Minimum Swirl) AT THE 17.8-cm AXIAL POSITION

MOVEABLE BLOCK BURNER SET FOR MINIMUM SWIRL - COLD MODEL

RESULTS

AP	RP	FI	DELTA	RHO	V	VX	VY	VZ	VT	VR	PST	T	PB
17.8	-30.0	16.7	80.9	0.0000159	4.23	4.05	0.19	1.20	-1.20	0.21	0.002334	20.	760.
17.8	-25.0	15.8	58.5	0.0000159	2.36	2.27	0.33	0.55	-0.63	0.42	0.002381	20.	760.
17.8	-20.0	16.6	213.1	0.0000159	2.10	2.01	-0.50	-0.33	-0.58	0.15	0.002413	20.	760.
17.8	-15.0	82.0	229.7	0.0000159	6.95	0.96	-4.45	-5.25	-0.80	6.84	0.002746	20.	760.
17.8	-14.0	31.2	278.0	0.0000159	4.07	3.48	0.29	-2.09	-1.67	1.29	0.001962	20.	760.
17.8	-13.0	50.0	273.4	0.0000159	4.45	2.86	0.20	-3.40	-1.78	2.90	0.001781	20.	760.
17.8	-12.0	74.5	245.7	0.0000159	9.56	2.55	-3.78	-8.40	-1.69	9.06	0.001385	20.	760.
17.8	-11.0	41.2	263.5	0.0000159	7.27	5.47	-0.53	-4.76	-2.76	3.91	0.001645	20.	760.
17.8	-10.0	49.1	258.5	0.0000159	8.67	5.66	-1.30	-6.43	-2.86	5.90	0.002084	20.	760.
17.8	-9.0	47.0	261.0	0.0000159	11.32	7.71	-1.29	-8.19	-3.53	7.50	0.002139	20.	760.
17.8	-8.0	28.6	258.0	0.0000159	16.38	14.37	-1.63	-7.69	-4.99	6.08	0.000792	20.	760.
17.8	-7.0	35.5	259.4	0.0000159	18.55	15.09	-1.98	-10.60	-5.20	9.44	0.001301	20.	760.
17.8	-6.0	30.4	268.5	0.0000159	20.13	17.35	-0.25	-10.21	-5.07	8.86	0.001439	20.	760.
17.8	-5.0	28.5	266.5	0.0000159	19.54	17.16	-0.55	-9.32	-4.28	8.30	0.001340	20.	760.
17.8	-4.0	24.3	266.0	0.0000159	23.07	21.01	-0.66	-9.50	-4.23	8.53	0.000975	20.	760.
17.8	-3.0	20.9	254.5	0.0000159	26.15	24.43	-2.48	-8.99	-3.76	8.54	0.001158	20.	760.
17.8	-2.0	7.8	236.0	0.0000159	41.31	40.92	-3.15	-4.69	-3.56	4.39	-0.005529	20.	760.
17.8	-1.0	5.7	184.9	0.0000159	59.16	58.86	-5.91	-0.51	-2.88	5.19	-0.000858	20.	760.
17.8	0.0	1.8	35.7	0.0000159	71.37	71.33	1.86	1.33	0.00	2.29	-0.002739	20.	760.
17.8	1.0	4.0	177.9	0.0000159	63.87	63.71	-4.50	0.15	2.80	3.52	-0.006372	20.	760.
17.8	2.0	5.1	21.4	0.0000159	31.27	31.14	2.60	1.01	2.18	1.74	-0.000300	20.	760.
17.8	3.0	18.2	252.7	0.0000159	27.76	26.36	-2.58	-8.31	3.95	7.75	-0.000027	20.	760.
17.8	4.0	21.8	265.5	0.0000159	23.71	22.00	-0.69	-8.81	4.31	7.71	0.000289	20.	760.
17.8	5.0	24.5	266.1	0.0000159	21.61	19.65	-0.60	-8.96	4.70	7.65	0.000767	20.	760.
17.8	6.0	29.3	265.4	0.0000159	21.72	18.92	-0.83	-10.62	5.47	9.14	0.000733	20.	760.
17.8	7.0	30.5	260.1	0.0000159	16.09	13.86	-1.39	-8.05	4.53	6.79	0.001259	20.	760.
17.8	8.0	35.8	245.3	0.0000159	12.76	10.35	-3.11	-6.79	3.94	6.34	0.001764	20.	760.
17.8	9.0	21.8	73.4	0.0000159	13.99	12.96	1.48	4.99	4.07	3.23	0.001403	20.	760.
17.8	10.0	45.5	255.3	0.0000159	9.68	6.77	-1.74	-6.69	3.33	6.06	0.001792	20.	760.
17.8	11.0	49.5	71.6	0.0000159	8.72	5.66	2.08	6.30	3.09	5.87	0.002002	20.	760.
17.8	12.0	60.8	253.0	0.0000159	4.60	2.24	-1.17	-3.85	1.41	3.76	0.001986	20.	760.
17.8	13.0	74.5	154.7	0.0000159	6.59	1.75	-5.74	2.71	1.25	6.23	0.002178	20.	760.
17.8	14.0	75.0	269.9	0.0000159	4.25	1.09	-0.00	-4.11	0.84	4.02	0.002399	20.	760.
17.8	15.0	80.0	269.9	0.0000159	4.92	0.85	-0.00	-4.84	0.71	4.79	0.002210	20.	760.
17.8	20.0	41.6	124.9	0.0000159	1.93	1.44	-0.73	1.05	1.00	0.79	0.002385	20.	760.
17.8	25.0	58.5	138.6	0.0000159	2.07	1.08	-1.32	1.17	1.15	1.34	0.002455	20.	760.
17.8	30.0	16.3	127.3	0.0000159	2.61	2.51	-0.44	0.58	0.72	0.12	0.002434	20.	760.

Table II-45. COMPUTER-REDUCED DATA FOR SWIRL BURNER (Minimum Swirl) AT THE 30.5-cm AXIAL POSITION

MOVEABLE BLOCK BURNER SET FOR MINIMUM SWIRL - COLD MODEL

RESULTS

AP	RP	FI	DELTA	RHO	V	VX	VY	VZ	VT	VR	PST	T	PB
30.5	-30.0	82.3	217.7	0.0000159	8.63	1.15	-6.76	-5.23	-1.12	8.48	0.002923	20.	760.
30.5	-25.0	82.3	219.4	0.0000159	8.61	1.14	-6.59	-5.42	-0.93	8.49	0.003107	20.	760.
30.5	-20.0	84.9	223.3	0.0000159	9.55	0.84	-6.92	-6.52	-0.55	9.49	0.003066	20.	760.
30.5	-15.0	82.1	230.0	0.0000159	9.28	1.26	-5.90	-7.04	-0.62	9.17	0.003015	20.	760.
30.5	-14.0	80.5	229.1	0.0000159	8.77	1.44	-5.66	-6.54	-0.66	8.62	0.002320	20.	760.
30.5	-13.0	71.3	243.6	0.0000159	9.11	2.91	-3.83	-7.73	-1.23	8.54	0.002570	20.	760.
30.5	-12.0	63.3	250.4	0.0000159	10.28	4.60	-3.08	-8.65	-1.77	9.01	0.002425	20.	760.
30.5	-10.0	47.7	249.1	0.0000159	9.97	6.70	-2.63	-6.90	-2.10	7.08	0.002024	20.	760.
30.5	-9.0	54.4	236.4	0.0000159	12.09	7.02	-5.44	-8.20	-2.02	9.63	0.002227	20.	760.
30.5	-8.0	35.0	254.8	0.0000159	14.97	12.26	-2.23	-8.29	-3.01	8.04	0.001587	20.	760.
30.5	-7.0	31.4	250.6	0.0000159	15.75	13.43	-2.72	-7.75	-2.88	7.69	0.001587	20.	760.
30.5	-6.0	15.3	245.9	0.0000159	22.01	21.22	-2.36	-5.31	-3.39	4.72	0.000113	20.	760.
30.5	-5.0	13.1	230.6	0.0000159	22.92	22.32	-3.29	-4.01	-2.99	4.25	0.000203	20.	760.
30.5	-4.0	15.1	233.9	0.0000159	25.18	24.31	-3.87	-5.31	-2.86	5.91	0.002568	20.	760.
30.5	-3.0	11.2	236.0	0.0000159	29.71	29.15	-3.23	-4.79	-2.56	5.17	0.001752	20.	760.
30.5	-2.0	8.7	204.8	0.0000159	32.98	32.60	-4.53	-2.10	-1.96	4.59	0.001536	20.	760.
30.5	-1.0	5.1	226.4	0.0000159	35.52	35.38	-2.19	-2.31	-1.09	3.00	0.002638	20.	760.
30.5	0.0	1.0	306.9	0.0000159	38.44	38.43	0.43	-0.58	0.00	0.73	-0.001846	20.	760.
30.5	1.0	7.3	307.5	0.0000159	35.81	35.51	2.79	-3.63	1.12	4.44	0.001158	20.	760.
30.5	2.0	18.9	272.0	0.0000159	36.73	34.74	0.43	-11.91	2.23	11.70	-0.002004	20.	760.
30.5	3.0	8.2	8.2	0.0000159	24.38	24.13	3.45	0.50	1.96	2.88	0.000199	20.	760.
30.5	4.0	7.1	42.7	0.0000159	22.14	21.97	2.03	1.88	1.99	1.91	0.000487	20.	760.
30.5	5.0	8.4	51.5	0.0000159	27.37	27.07	2.50	3.16	2.98	2.71	-0.002778	20.	760.
30.5	6.0	12.1	113.3	0.0000159	16.33	15.96	-1.36	3.16	2.32	2.54	0.000175	20.	760.
30.5	7.0	22.2	119.4	0.0000159	12.78	11.83	-2.38	4.22	2.36	4.22	0.001828	20.	760.
30.5	8.0	23.1	99.0	0.0000159	11.51	10.59	-0.70	4.46	2.36	3.84	0.001718	20.	760.
30.5	9.0	29.8	110.8	0.0000159	9.46	8.21	-1.67	4.39	2.15	4.18	0.002169	20.	760.
30.5	10.0	16.2	89.9	0.0000159	8.24	7.91	0.00	2.30	1.72	1.52	0.002227	20.	760.
30.5	11.0	44.1	89.9	0.0000159	6.00	4.31	0.00	4.17	1.45	3.91	0.002302	20.	760.
30.5	12.0	60.4	117.5	0.0000159	5.41	2.66	-2.17	4.17	1.02	4.59	0.002374	20.	760.
30.5	13.0	68.9	128.8	0.0000159	5.69	2.04	-3.33	4.14	0.85	5.25	0.002158	20.	760.
30.5	14.0	76.9	117.7	0.0000159	6.87	1.55	-3.11	5.92	0.70	6.66	0.002450	20.	760.
30.5	15.0	82.8	115.1	0.0000159	8.84	1.10	-3.73	7.94	0.54	8.75	0.002962	20.	760.
30.5	20.0	83.5	209.7	0.0000159	8.31	0.92	-7.17	-4.09	0.60	8.24	0.003014	20.	760.
30.5	25.0	81.9	212.7	0.0000159	8.52	1.19	-7.10	-4.56	0.97	8.38	0.003147	20.	760.
30.5	30.0	81.7	214.7	0.0000159	7.98	1.14	-6.48	-4.50	1.11	7.81	0.003021	20.	760.

Table II-46. COMPUTER-REDUCED DATA FOR SWIRL BURNER (Minimum Swirl) AT THE 63.5-cm AXIAL POSITION

MOVEABLE BLOCK BURNER SET FOR MINIMUM SWIRL - COLD MODEL

RESULTS

AP	RP	FI	DELTA	RHO	V	VX	VY	VZ	VT	VR	PST	T	PB
63.5	-30.0	53.3	210.1	0.0000159	4.12	2.45	-2.86	-1.66	-1.09	3.12	0.002170	20.	760.
63.5	-25.0	53.3	211.1	0.0000159	5.47	3.27	-3.76	-2.26	-1.23	4.21	0.002312	20.	760.
63.5	-20.0	25.9	220.5	0.0000159	6.42	5.78	-2.13	-1.82	-1.52	2.35	0.002075	20.	760.
63.5	-15.0	18.7	218.3	0.0000159	10.49	9.94	-2.63	-2.09	-1.92	2.76	0.001970	20.	760.
63.5	-14.0	15.4	220.3	0.0000159	11.32	10.91	-2.29	-1.94	-1.88	2.35	0.001728	20.	760.
63.5	-13.0	24.3	202.8	0.0000159	10.15	9.24	-3.85	-1.62	-1.72	3.81	0.002248	20.	760.
63.5	-12.0	14.4	213.8	0.0000159	13.55	13.12	-2.81	-1.89	-2.00	2.73	0.002023	20.	760.
63.5	-11.0	15.6	216.7	0.0000159	15.04	14.48	-3.25	-2.42	-2.13	3.45	0.002202	20.	760.
63.5	-10.0	13.3	218.7	0.0000159	15.98	15.55	-2.87	-2.30	-2.03	3.06	0.001138	20.	760.
63.5	-9.0	14.3	210.8	0.0000159	13.48	13.05	-2.86	-1.71	-1.61	2.92	0.001957	20.	760.
63.5	-8.0	10.9	216.6	0.0000159	13.52	13.27	-2.06	-1.54	-1.40	2.16	0.002114	20.	760.
63.5	-7.0	15.3	209.6	0.0000159	17.23	16.61	-3.96	-2.25	-1.69	4.23	0.001210	20.	760.
63.5	-6.0	7.7	198.9	0.0000159	16.58	16.43	-2.11	-0.72	-1.27	1.83	0.002052	20.	760.
63.5	-5.0	5.8	220.0	0.0000159	16.85	16.76	-1.32	-1.11	-1.04	1.37	0.001718	20.	760.
63.5	-4.0	8.0	210.4	0.0000159	17.37	17.20	-2.09	-1.22	-0.98	2.21	0.001633	20.	760.
63.5	-3.0	6.2	210.6	0.0000159	18.16	18.05	-1.71	-1.01	-0.78	1.82	0.001926	20.	760.
63.5	-2.0	3.4	213.1	0.0000159	16.52	16.49	-0.83	-0.54	-0.46	0.88	0.002443	20.	760.
63.5	-1.0	1.7	259.4	0.0000159	18.55	18.55	-0.10	-0.54	-0.25	0.48	0.001232	20.	760.
63.5	0.0	4.1	252.7	0.0000159	17.38	17.33	-0.37	-1.20	0.00	1.26	0.001843	20.	760.
63.5	1.0	3.7	300.0	0.0000159	18.39	18.35	0.59	-1.03	0.28	1.15	0.001281	20.	760.
63.5	2.0	6.1	316.3	0.0000159	16.05	15.95	1.24	-1.19	0.48	1.65	0.002530	20.	760.
63.5	3.0	4.6	321.6	0.0000159	15.92	15.87	1.00	-0.79	0.64	1.11	0.001543	20.	760.
63.5	4.0	3.1	41.3	0.0000159	15.59	15.57	0.64	0.56	0.64	0.56	0.001918	20.	760.
63.5	5.0	3.6	9.3	0.0000159	14.92	14.89	0.94	0.15	0.73	0.60	0.001779	20.	760.
63.5	6.0	5.8	0.0	0.0000159	15.10	15.02	1.52	0.00	1.04	1.11	0.001847	20.	760.
63.5	7.0	14.5	12.6	0.0000159	14.31	13.85	3.50	0.78	1.40	3.30	0.001766	20.	760.
63.5	8.0	8.5	8.1	0.0000159	13.40	13.25	1.96	0.27	1.27	1.51	0.002203	20.	760.
63.5	9.0	11.5	332.2	0.0000159	11.18	10.95	1.98	-1.04	1.27	1.84	0.001508	20.	760.
63.5	10.0	12.1	4.7	0.0000159	13.70	13.40	2.87	0.23	1.70	2.33	0.001383	20.	760.
63.5	11.0	8.8	48.1	0.0000159	9.50	9.39	0.97	1.08	1.08	0.97	0.002691	20.	760.
63.5	12.0	13.9	16.6	0.0000159	12.11	11.75	2.79	0.83	1.76	2.32	0.001645	20.	760.
63.5	13.0	24.0	5.3	0.0000159	10.66	9.73	4.33	0.40	1.81	3.95	0.002207	20.	760.
63.5	14.0	16.7	18.0	0.0000159	9.06	8.68	2.48	0.80	1.54	2.10	0.002149	20.	760.
63.5	15.0	19.7	33.3	0.0000159	8.00	7.53	2.25	1.48	1.48	2.25	0.002214	20.	760.
63.5	20.0	39.6	62.4	0.0000159	6.37	4.90	1.88	3.60	1.44	3.80	0.002451	20.	760.
63.5	25.0	24.8	60.7	0.0000159	5.12	4.64	1.05	1.87	1.39	1.63	0.002263	20.	760.
63.5	30.0	18.7	73.6	0.0000159	5.04	4.77	0.45	1.55	1.31	0.94	0.002266	20.	760.

Table II-47. COLUMN HEADING SYMBOLS FOR TABLES II-37 TO II-46.

AP = axial probe position, cm

delta = dihedral angle, deg

FI = conical angle, deg

P_{ab} = differential pressure across probe holes a and b, psig

PB = atmospheric pressure, mmHg

PST = static pressure, psig

rho = density of flowing gases

RP = radial probe position, cm

T = temperature of flowing gases, °C

theta = probe rotation, deg

V = absolute velocity, ft/s

VR = radial velocity, ft/s

VT = tangential velocity, ft/s

VX = velocity in x-direction, ft/s

VY = velocity in y-direction, ft/s

VZ = velocity in z-direction, ft/s

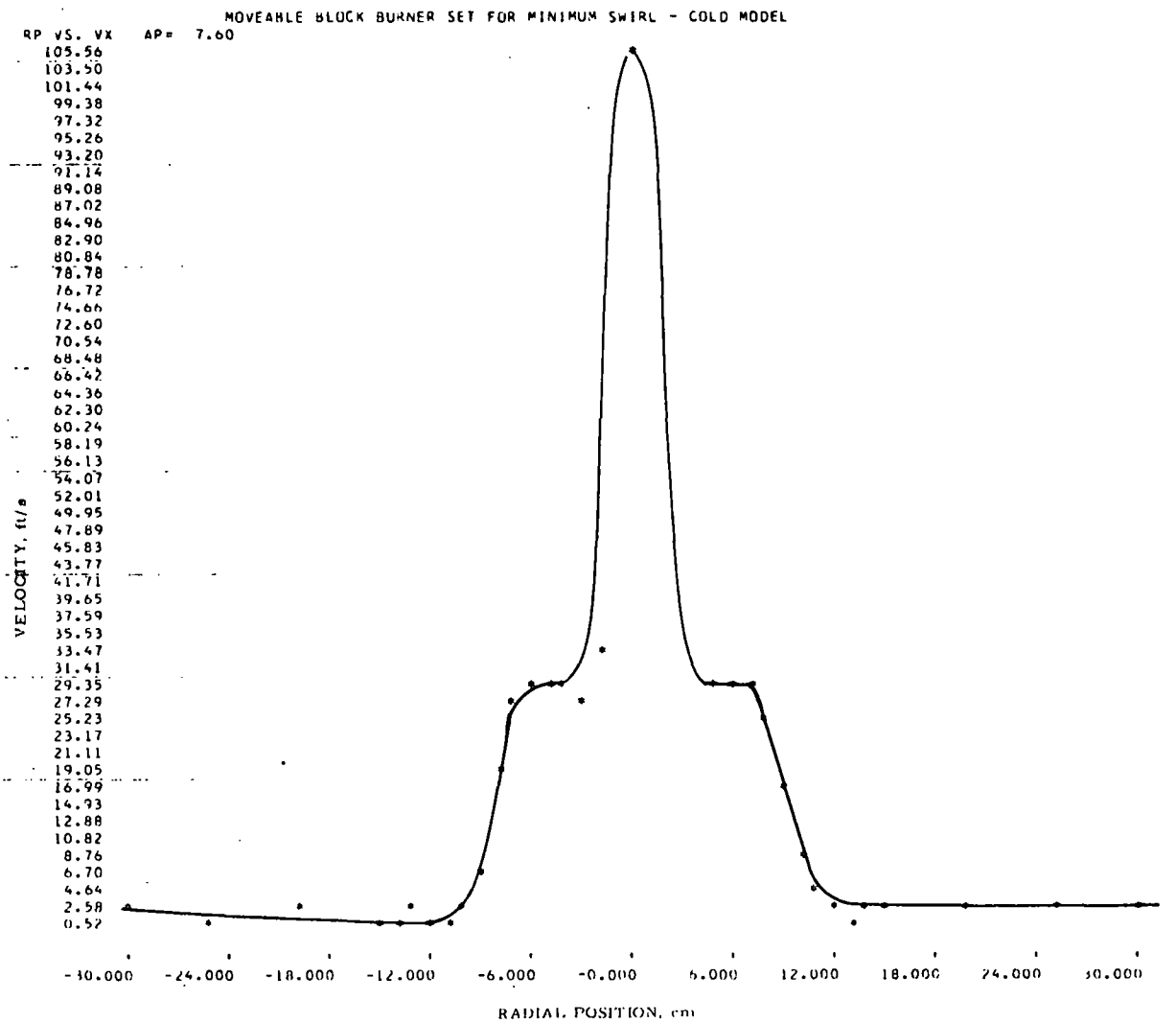

Figure II-216. AXIAL VELOCITY PROFILE FOR SWIRL BURNER SET FOR MINIMUM SWIRL AT THE 7.6-cm AXIAL POSITION

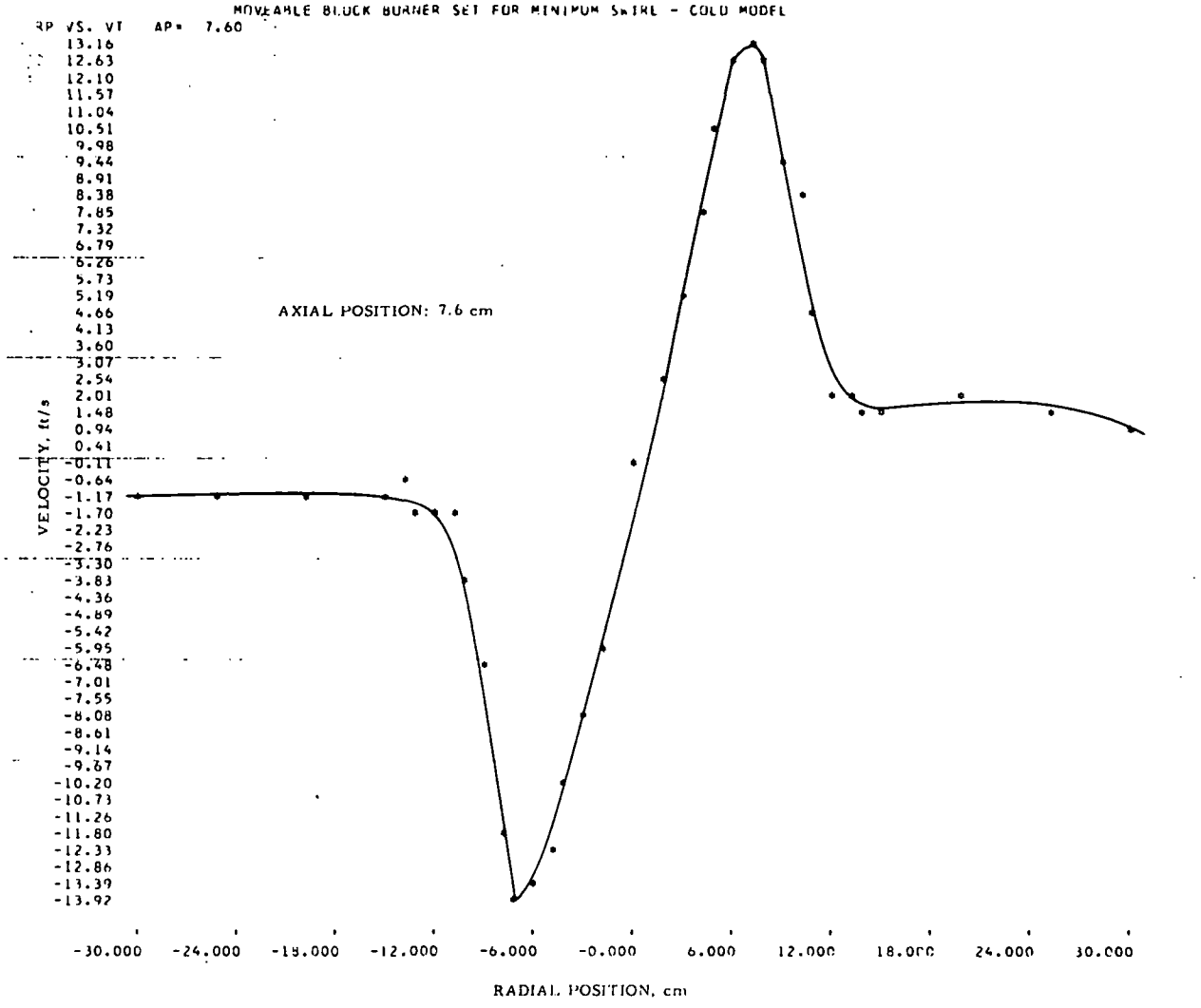

Figure II-217. TANGENTIAL VELOCITY PROFILE FOR SWIRL BURNER SET FOR MINIMUM SWIRL AT THE 7.6-cm AXIAL POSITION

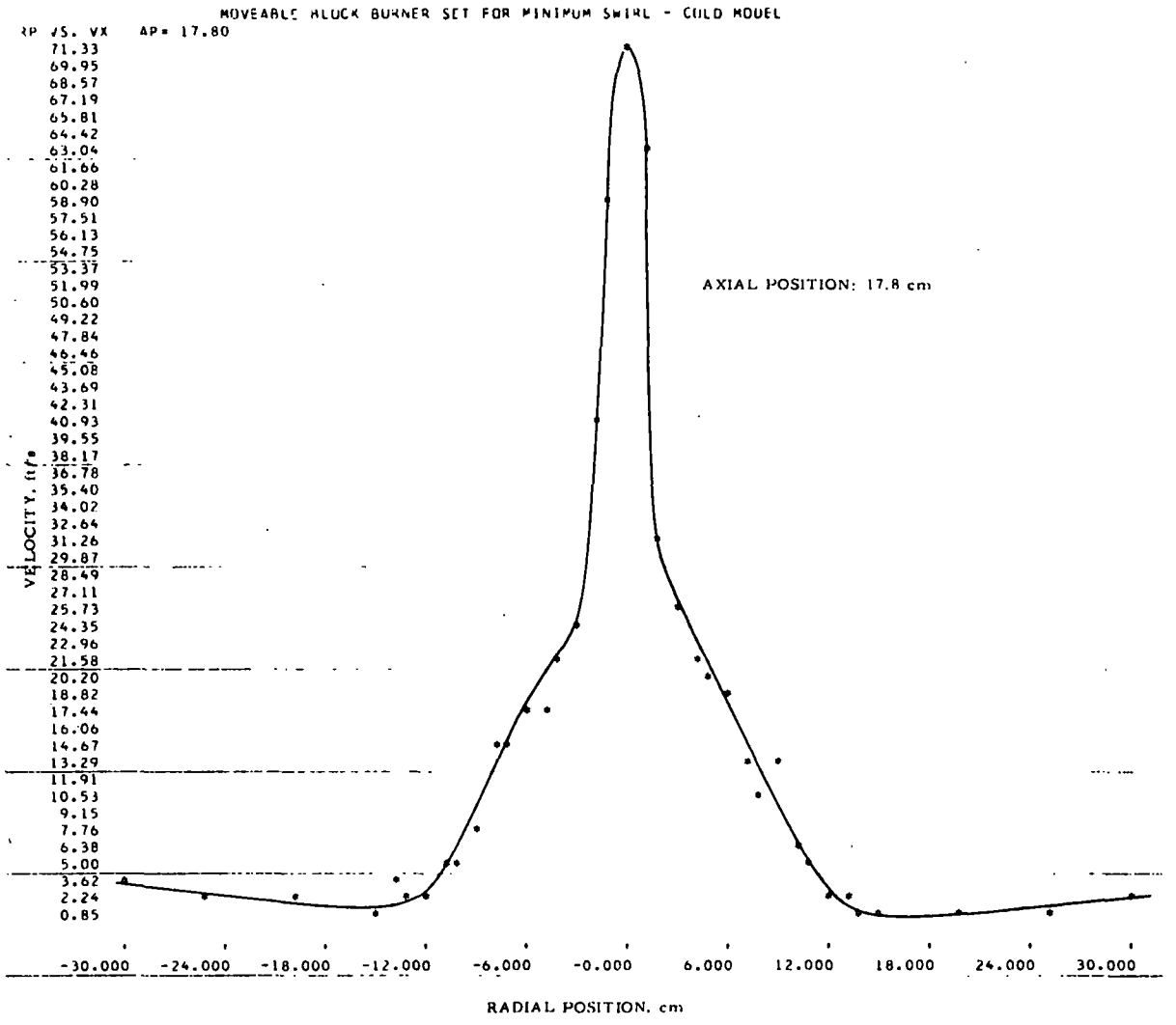

Figure II-218. AXIAL VELOCITY PROFILE FOR THE SWIRL BURNER SET FOR MINIMUM SWIRL AT THE 17.8-cm AXIAL POSITION

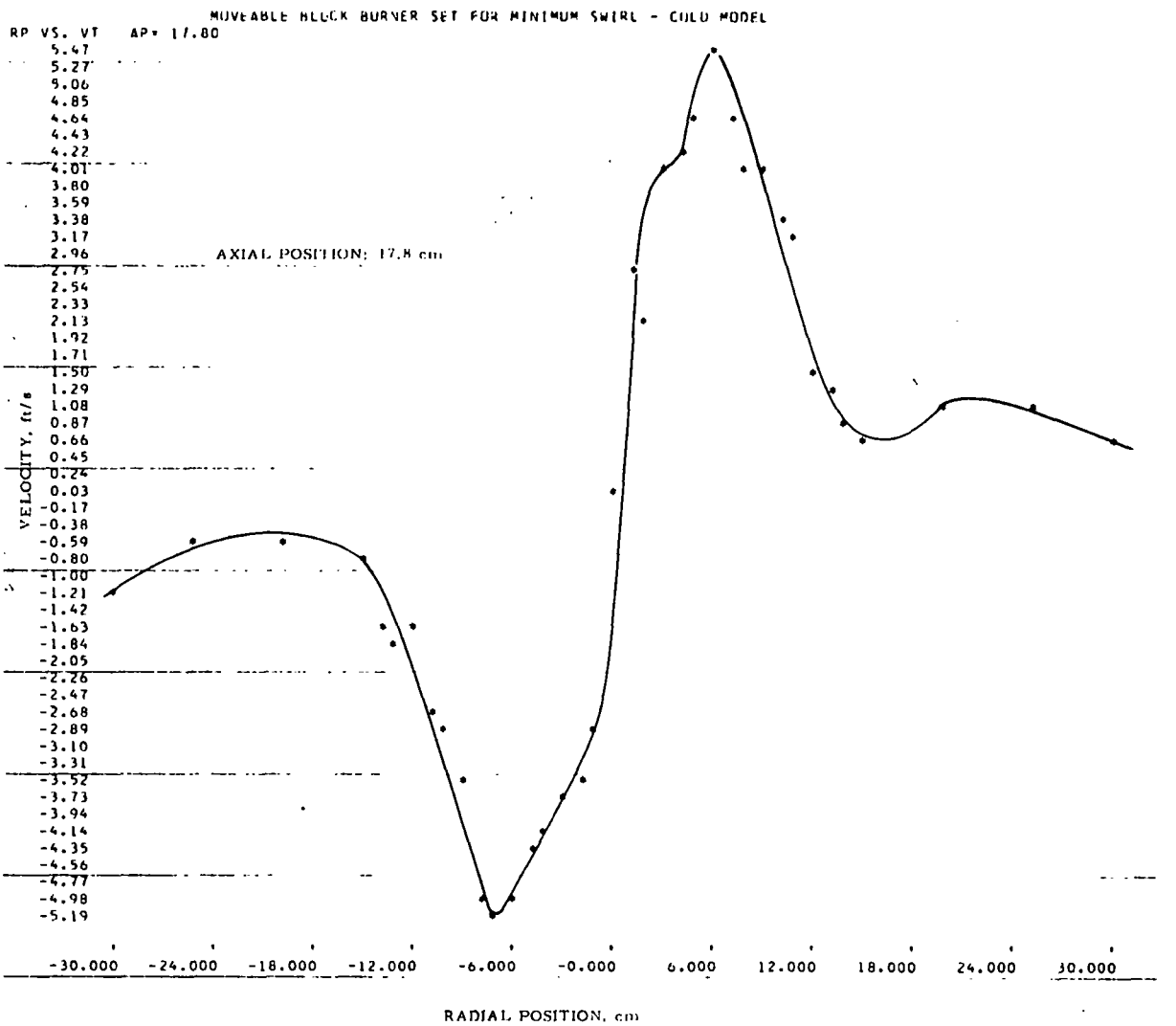

Figure II-219. TANGENTIAL VELOCITY PROFILE FOR THE SWIRL BURNER SET FOR MINIMUM SWIRL AT THE 17.8-cm AXIAL POSITION

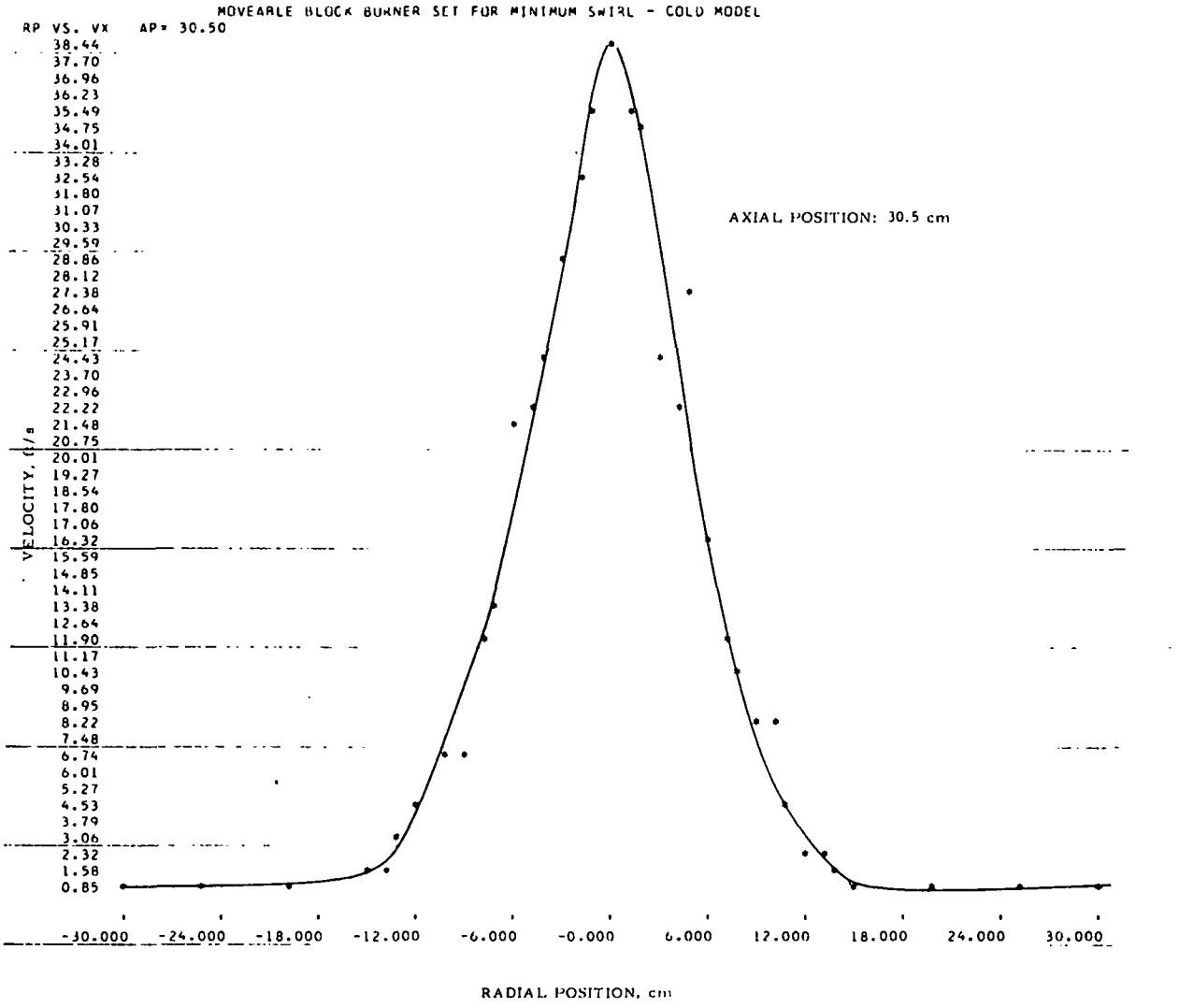

Figure II-220. AXIAL VELOCITY PROFILE FOR THE SWIRL BURNER SET FOR MINIMUM SWIRL AT THE 30.5-cm AXIAL POSITION

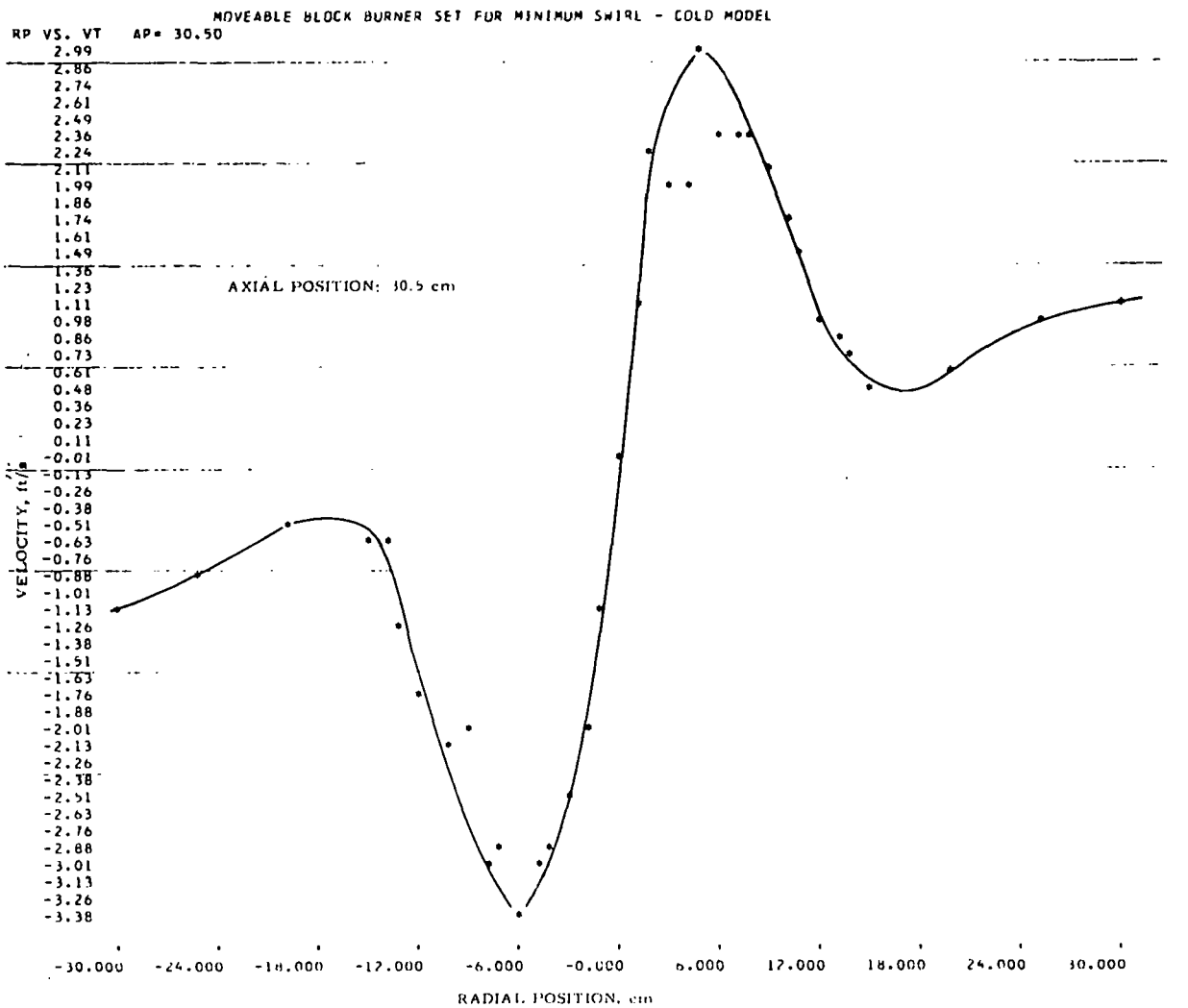

Figure II-221. TANGENTIAL VELOCITY PROFILE FOR THE SWIRL BURNER SET FOR MINIMUM SWIRL AT THE 30.5-cm AXIAL POSITION

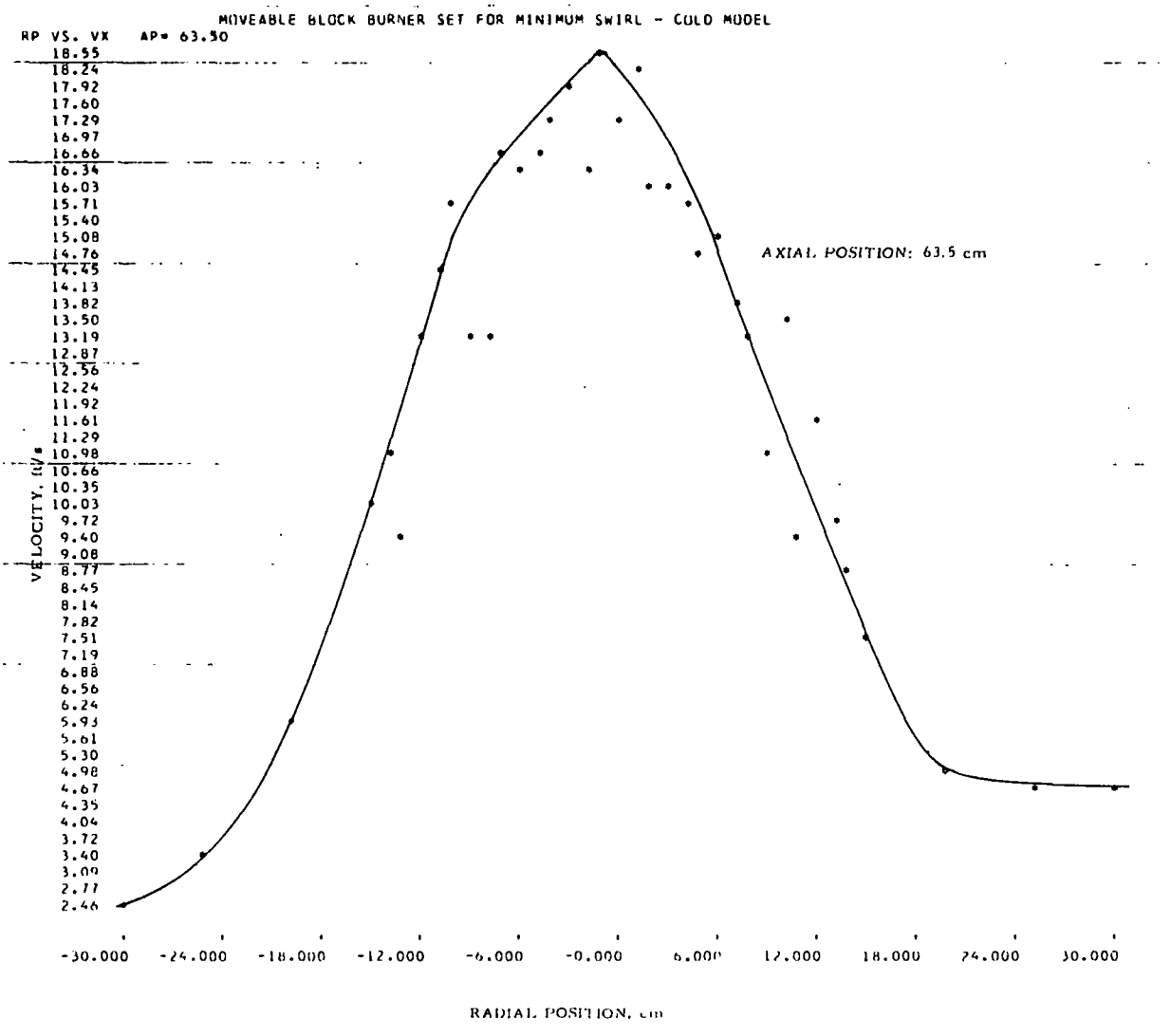

Figure II-222. AXIAL VELOCITY PROFILE FOR THE SWIRL BURNER SET FOR MINIMUM SWIRL AT THE 63.5-cm AXIAL POSITION

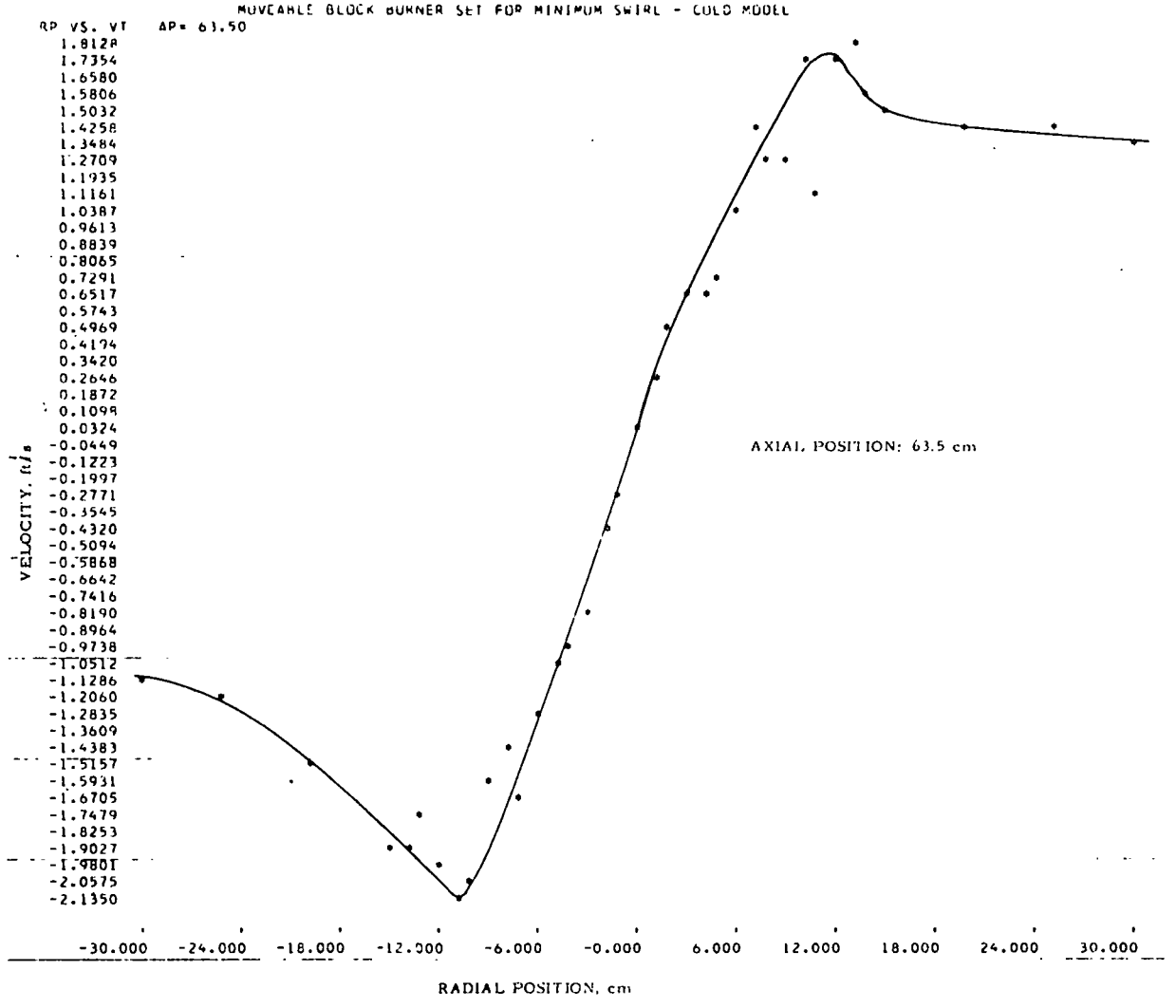

Figure II-223. TANGENTIAL VELOCITY PROFILE FOR THE SWIRL BURNER SET FOR MINIMUM SWIRL AT THE 63.5-cm AXIAL POSITION

Table II-48. RAW DATA FOR THE SWIRL BURNER (Swirl Number, S = 0.8) AT THE 2.5-cm AXIAL POSITION

AERODYNAMIC MODELING OF COMBUSTION BURNERS

CALIBRATION COEFFICIENTS FOR FORWARD FLOW

A1 =	0.770590	A2 =	0.272353	A3 =	-0.059818
B0 =	0.737720	B2 =	-0.158821	B4 =	0.129246
C =	4.464660	D =	0.394812		

MOVEABLE BLOCK BURNER SET FOR INTERMEDIATE SWIRL - COLD MODEL

TOTAL DATA INPUT

THETA	AP	RP	P13	P03	P24	P04	POA	T	PB
45.	2.5	-30.0	744.00	8300.00	-3340.00	-6880.00	805.00	20.	760.
45.	2.5	-25.0	750.00	-71500.00	-1730.00	-2400.00	965.00	20.	760.
45.	2.5	-20.0	1140.00	16600.00	-1055.00	-1450.00	15700.00	20.	760.
45.	2.5	-15.0	736.00	999999999.50	-504.00	-712.00	-238.00	20.	760.
45.	2.5	-14.0	724.00	-89600.00	-476.00	-636.00	-130.80	20.	760.
45.	2.5	-13.0	648.00	11750.00	-355.00	-698.00	-127.00	20.	760.
45.	2.5	-12.0	440.00	-64000.00	-501.00	-950.00	-92.20	20.	760.
45.	2.5	-11.0	705.00	6600.00	-612.00	7800.00	-105.20	20.	760.
45.	2.5	-10.0	112.00	445.00	-1080.00	672.00	-59.20	20.	760.
0.	2.5	-9.0	1039.00	-846.00	-200.00	-372.00	-180.00	20.	760.
0.	2.5	-8.0	52.40	140.20	-42.10	-99.00	-267.00	20.	760.
46.	2.5	-7.0	30.60	18.00	293.00	31.50	30.70	20.	760.
44.	2.5	-6.0	422.00	60.00	-82.80	126.00	120.00	20.	760.
58.	2.5	-5.0	-4960.00	146.00	1820.00	188.00	-214.00	20.	760.
43.	2.5	-4.0	-1170.00	1500.00	-380.00	-2280.00	-85.20	20.	760.
44.	2.5	-3.0	-3330.00	3330.00	-209.00	-1080.00	-60.00	20.	760.
16.	2.5	-2.0	85.00	504.00	-192.00	-2000.00	-65.60	20.	760.
0.	2.5	-1.0	19.20	18.30	-197.00	29.30	34.50	20.	760.
0.	2.5	0.0	503.00	21.00	376.00	20.40	20.50	20.	760.
0.	2.5	1.0	-41.00	-210.00	208.00	72.80	370.00	20.	760.
315.	2.5	2.0	-560.00	-500.00	193.00	344.00	-98.00	20.	760.
315.	2.5	3.0	1380.00	3480.00	357.00	712.00	-96.40	20.	760.
315.	2.5	4.0	860.00	1620.00	850.00	1500.00	-79.80	20.	760.
315.	2.5	5.0	910.00	1040.00	1730.00	2100.00	-78.00	20.	760.
315.	2.5	6.0	1020.00	520.00	1230.00	926.00	-79.20	20.	760.
315.	2.5	7.0	-4000.00	160.00	161.00	126.00	-132.00	20.	760.
315.	2.5	8.0	-87.00	68.50	81.00	39.10	64.40	20.	760.
315.	2.5	9.0	-18.30	246.00	-199.00	33.80	29.00	20.	760.
315.	2.5	10.0	-20.00	-40.80	-132.00	100.80	287.00	20.	760.
315.	2.5	11.0	-80.60	-118.00	-268.00	675.00	-1376.00	20.	760.
315.	2.5	13.0	580.00	1750.00	-7350.00	8900.00	-2780.00	20.	760.
315.	2.5	14.0	805.00	3650.00	-34000.00	77000.00	1520.00	20.	760.
315.	2.5	15.0	725.00	5090.00	91500.00	20200.00	804.00	20.	760.
315.	2.5	20.0	2690.00	41600.00	22600.00	22000.00	432.00	20.	760.
315.	2.5	25.0	3750.00	86200.00	23400.00	37500.00	410.00	20.	760.
315.	2.5	30.0	3470.00	-30600.00	34500.00	94500.00	407.00	20.	760.

Table II-49. RAW DATA FOR THE SWIRL BURNER (Swirl Number, S = 0.8) AT THE 7.6-cm AXIAL POSITION

AERODYNAMIC MODELING OF COMBUSTION BURNERS

CALIBRATION COEFFICIENTS FOR FORWARD FLOW

A1 =	0.770590	A2 =	0.272353	A3 =	-0.059818
B0 =	0.737720	B2 =	-0.158821	B4 =	0.129246
C =	4.464660	D =	0.394812		

MOVEABLE BLOCK BURNER SET FOR INTERMEDIATE SWIRL - COLD MODEL

TOTAL DATA INPUT

THETA	AP	RP	P13	P03	P24	P04	P0A	T	PS
45.	7.6	-30.0	999999999.50	999999999.50	-2780.00	-7920.00	460.00	20.	760.
45.	7.6	-25.0	700.00	3530.00	-1460.00	-3720.00	750.00	20.	760.
0.	7.6	-20.0	2240.00	-2402.00	-1046.00	-1092.00	-810.00	20.	760.
0.	7.6	-15.0	620.00	-252.00	-404.00	-508.00	-188.00	20.	760.
0.	7.6	-14.0	341.00	-11220.00	-306.00	-423.00	-149.00	20.	760.
65.	7.6	-13.0	-84700.00	250.00	575.00	446.00	-315.00	20.	760.
40.	7.6	-12.0	66200.00	187.00	-599.00	419.00	-493.00	20.	760.
30.	7.6	-11.0	77.30	-2360.00	-229.00	550.00	-1730.00	20.	760.
33.	7.6	-10.0	83.50	97.70	-364.00	250.00	680.00	20.	760.
40.	7.6	-9.0	186.00	130.00	1843.00	230.00	982.00	20.	760.
35.	7.6	-8.0	87.00	226.00	-457.00	323.00	1480.00	20.	760.
180.	7.6	-7.0	840.00	835.00	26920.00	1220.00	-540.00	20.	760.
180.	7.6	-6.0	1600.00	636.00	770.00	576.00	92500.00	20.	760.
180.	7.6	-5.0	11200.00	665.00	937.00	562.00	693.00	20.	760.
180.	7.6	-4.0	999999999.50	960.00	1700.00	680.00	601.00	20.	760.
0.	7.6	-3.0	290.00	517.00	-1380.00	1600.00	-790.00	20.	760.
0.	7.6	-2.0	258.00	261.00	-1176.00	458.00	2132.00	20.	760.
0.	7.6	-1.0	380.00	140.00	2830.00	160.00	350.00	20.	760.
0.	7.6	0.0	-470.00	208.00	790.00	165.00	320.00	20.	760.
0.	7.6	1.0	-244.00	2790.00	495.00	388.00	1287.00	20.	760.
0.	7.6	2.0	-395.00	-438.00	2410.00	455.00	-427.00	20.	760.
180.	7.6	3.0	-1000.00	1096.00	-1200.00	1370.00	-726.00	20.	760.
180.	7.6	4.0	-418.00	773.00	-432.00	740.00	-677.00	20.	760.
180.	7.6	5.0	-244.00	3380.00	-256.00	-8990.00	-598.00	20.	760.
180.	7.6	6.0	-310.00	-4800.00	-190.00	-512.00	-106.00	20.	760.
0.	7.6	7.0	1830.00	-3000.00	-4630.00	-2990.00	-752.00	20.	760.
315.	7.6	8.0	615.00	1010.00	635.00	617.00	-204.00	20.	760.
315.	7.6	9.0	2228.00	322.00	772.00	353.00	-470.00	20.	760.
315.	7.6	10.0	-198.00	325.00	-448.00	290.00	900.00	20.	760.
315.	7.6	11.0	-74.70	-1314.00	-201.00	372.00	484.00	20.	760.
315.	7.6	12.0	-128.00	-186.00	-132.00	503.00	-3916.00	20.	760.
315.	7.6	13.0	-58.90	-122.00	-232.00	554.00	-347.00	20.	760.
315.	7.6	14.0	-77.30	-134.00	-421.00	720.00	-267.00	20.	760.
315.	7.6	15.0	-123.00	-174.00	-2048.00	810.00	-287.00	20.	760.
315.	7.6	20.0	-870.00	-835.00	1160.00	1560.00	-1600.00	20.	760.
315.	7.6	25.0	-3800.00	-3990.00	1420.00	2740.00	772.00	20.	760.
315.	7.6	30.0	-11260.00	-6570.00	2420.00	4780.00	523.00	20.	760.

Table II-50. RAW DATA FOR THE SWIRL BURNER (Swirl Number, S = 0.8) AT THE 17.8-cm AXIAL POSITION

AERODYNAMIC MODELING OF COMBUSTION BURNERS

CALIBRATION COEFFICIENTS FOR FORWARD FLOW

A1 =	0.770590	A2 =	0.272353	A3 =	-0.059818
B0 =	0.737720	B2 =	-0.158821	B4 =	0.129246
C =	4.464660	D =	0.394812		

MOVEABLE BLOCK BURNER SET FOR INTERMEDIATE SWIRL - COLD MODEL

TOTAL DATA INPUT

THETA	AP	RP	P13	P03	P24	P04	P0A	T	PB
0.	17.8	-30.0	68400.00	-19600.00	-15300.00	-17500.00	453.00	20.	760.
0.	17.8	-25.0	-141600.00	-13700.00	-4260.00	-5450.00	462.00	20.	760.
0.	17.8	-20.0	4720.00	-25000.00	-1440.00	-2250.00	642.00	20.	760.
0.	17.8	-15.0	975.00	5900.00	-601.00	-1395.00	800.00	20.	760.
0.	17.8	-14.0	1255.00	3838.00	-759.00	-1738.00	759.00	20.	760.
0.	17.8	-13.0	218.00	340.00	-164.00	-485.00	764.00	20.	760.
0.	17.8	-12.0	324.00	334.00	-139.00	-400.00	700.00	20.	760.
0.	17.8	-11.0	431.00	272.00	-127.00	-384.00	687.00	20.	760.
0.	17.8	-10.0	638.00	330.00	-117.00	-340.00	830.00	20.	760.
0.	17.8	-9.0	5060.00	441.00	-115.00	-332.00	1640.00	20.	760.
0.	17.8	-8.0	-950.00	795.00	-150.00	-257.00	-3700.00	20.	760.
0.	17.8	-7.0	-1000.00	2000.00	-176.00	-363.00	-1100.00	20.	760.
180.	17.8	-6.0	69700.00	2130.00	3000.00	2140.00	-439.00	20.	760.
180.	17.8	-5.0	4080.00	2000.00	1180.00	2810.00	-566.00	20.	760.
180.	17.8	-4.0	2820.00	1450.00	960.00	1670.00	-840.00	20.	760.
180.	17.8	-3.0	2650.00	1300.00	708.00	1210.00	-642.00	20.	760.
180.	17.8	-2.0	3580.00	1135.00	638.00	910.00	-1025.00	20.	760.
180.	17.8	-1.0	7260.00	980.00	832.00	735.00	-2080.00	20.	760.
180.	17.8	0.0	9300.00	898.00	1030.00	817.00	-12840.00	20.	760.
180.	17.8	1.0	9660.00	840.00	1800.00	810.00	12880.00	20.	760.
180.	17.8	2.0	999999999.50	830.00	14000.00	994.00	6760.00	20.	760.
180.	17.8	3.0	-9600.00	477.00	-1680.00	1510.00	-5020.00	20.	760.
180.	17.8	4.0	-8570.00	570.00	-1260.00	2280.00	-4990.00	20.	760.
180.	17.8	5.0	-39600.00	2530.00	-3190.00	4000.00	470.00	20.	760.
180.	17.8	6.0	58800.00	2480.00	-656.00	4410.00	574.00	20.	760.
180.	17.8	7.0	-1830.00	2300.00	-1570.00	6570.00	553.00	20.	760.
180.	17.8	8.0	-1510.00	31400.00	-1120.00	13110.00	514.00	20.	760.
180.	17.8	9.0	-7440.00	3060.00	-2630.00	17660.00	577.00	20.	760.
315.	17.8	10.0	5920.00	314.00	7200.00	9400.00	835.00	20.	760.
315.	17.8	11.0	5590.00	330.00	-828.00	500.00	346.00	20.	760.
315.	17.8	12.0	-600.00	303.00	-438.00	432.00	265.00	20.	760.
315.	17.8	13.0	-283.00	452.00	-296.00	434.00	243.00	20.	760.
315.	17.8	14.0	-205.00	850.00	-312.00	537.00	240.00	20.	760.
315.	17.8	15.0	-193.00	4320.00	-237.00	581.00	260.00	20.	760.
315.	17.8	20.0	-574.00	-3090.00	7370.00	1050.00	480.00	20.	760.
315.	17.8	25.0	11500.00	8640.00	3830.00	4570.00	424.00	20.	760.
315.	17.8	30.0	5280.00	11400.00	7990.00	11180.00	456.00	20.	760.

Table II-51. RAW DATA FOR THE SWIRL BURNER (Swirl Number, S = 0.8) AT THE 30.5-cm AXIAL POSITION

AERODYNAMIC MODELING OF COMBUSTION BURNERS

CALIBRATION COEFFICIENTS FOR FORWARD FLOW

A1 =	0.770590	A2 =	0.272353	A3 =	-0.059818
B0 =	0.737720	B2 =	-0.158821	B4 =	0.129246
C =	4.464660	D =	0.394812		

MOVEABLE BLOCK BURNER SET FOR INTERMEDIATE SWIRL - COLD MODEL

TOTAL DATA INPUT

THETA	AP	RP	P13	P03	P24	P04	P0A	T	PB
0.	30.5	-30.0	29000.00	2800.00	-2960.00	-8850.00	752.00	20.	760.
0.	30.5	-25.0	21500.00	105300.00	-8240.00	17400.00	482.00	20.	760.
0.	30.6	-20.0	2890.00	-5220.00	-3420.00	-4190.00	482.00	20.	760.
0.	30.5	-18.0	470.00	516.00	-336.00	-609.00	469.00	20.	760.
0.	30.5	-16.0	403.00	640.00	-286.00	-729.00	479.00	20.	760.
0.	30.5	-14.0	555.00	-4200.00	-305.00	-4300.00	497.00	20.	760.
0.	30.5	-12.0	576.00	1432.00	-218.00	-368.00	485.00	20.	760.
180.	30.5	12.0	-3550.00	2650.00	20200.00	4120.00	373.00	20.	760.
180.	30.5	10.0	-3400.00	2450.00	12400.00	3200.00	365.00	20.	760.
180.	30.5	8.0	-4670.00	2680.00	7420.00	5570.00	575.00	20.	760.
180.	30.5	6.0	-3580.00	2104.00	22400.00	2720.00	564.00	20.	760.
180.	30.5	4.0	-5060.00	1875.00	9150.00	2050.00	500.00	20.	760.
180.	30.5	2.0	-10150.00	1830.00	3280.00	2090.00	515.00	20.	760.
180.	30.5	0.0	-11780.00	1680.00	2430.00	1940.00	467.00	20.	760.
180.	30.5	-2.0	-14320.00	1930.00	2140.00	1920.00	545.00	20.	760.
180.	30.5	-4.0	-14080.00	2030.00	1970.00	2090.00	625.00	20.	760.
180.	30.5	-6.0	-34500.00	2370.00	2300.00	2650.00	676.00	20.	760.
180.	30.5	-8.0	-10950.00	2320.00	2350.00	2580.00	756.00	20.	760.
180.	30.5	-10.0	-7260.00	5500.00	4160.00	4000.00	8000.00	20.	760.
0.	30.5	14.0	33700.00	1870.00	610.00	1230.00	648.00	20.	760.
0.	30.5	16.0	-1820.00	2410.00	390.00	540.00	622.00	20.	760.
3.	30.5	18.0	-630.00	8900.00	268.00	445.00	530.00	20.	760.
0.	30.5	20.0	-485.00	-5080.00	283.00	441.00	530.00	20.	760.
0.	30.5	22.0	-487.00	-2030.00	342.00	528.00	562.00	20.	760.
0.	30.5	24.0	-592.00	-2040.00	453.00	720.00	596.00	20.	760.
0.	30.5	25.0	-950.00	-1675.00	526.00	824.00	542.00	20.	760.
0.	30.5	30.0	-1510.00	-3630.00	1650.00	3000.00	520.00	20.	760.

Table II-52. COMPUTER REDUCED DATA FOR THE SWIRL BURNER (Swirl Number, S = 0.8) AT THE 2.5-cm AXIAL POSITION

MOVEABLE BLOCK BURNER SET FOR INTERMEDIATE SWIRL - COLD MODEL

RESULTS

AP	RP	FI	DELTA	RHO	V	VX	VY	VZ	VT	VR	PST	T	PA
2.5	-30.0	68.1	175.0	0.0000159	11.10	4.12	-10.27	0.89	-10.09	2.10	0.002242	20.	76
2.5	-25.0	63.2	186.0	0.0000159	12.19	5.49	-10.83	-1.14	-10.68	2.11	0.002449	20.	76
2.5	-20.0	46.4	205.4	0.0000159	10.67	7.35	-6.98	-3.32	-7.66	1.00	0.001125	20.	76
2.5	-15.0	41.2	214.3	0.0000159	14.50	10.90	-7.89	-5.39	-9.45	1.3[illegible]	-0.002160	20.	76
2.5	-14.0	41.3	216.4	0.0000159	15.05	11.30	-7.99	-5.89	-9.81	1.54	-0.005318	20.	76
2.5	-13.0	31.6	213.0	0.0000159	15.19	12.92	-6.69	-4.34	-7.92	0.94	-0.006175	20.	76
2.5	-12.0	48.3	197.2	0.0000159	16.34	10.87	-11.65	-3.60	-11.88	2.77	-0.006360	20.	76
2.5	-11.0	30.1	174.0	0.0000159	13.62	11.78	-6.79	0.71	-6.77	0.89	-0.009105	20.	76
2.5	-10.0	63.8	159.3	0.0000159	25.77	11.34	-21.64	8.17	-20.61	10.50	-0.014074	20.	76
2.5	-9.0	71.0	259.1	0.0000159	20.60	6.67	-3.68	-19.14	-15.14	12.27	-0.001955	20.	76
2.5	-8.0	57.3	231.2	0.0000159	43.78	23.59	-23.10	-28.75	-33.14	16.18	0.003345	20.	76
2.5	-7.0	48.1	104.7	0.0000159	81.49	54.41	-15.43	58.67	-56.36	22.44	-0.017504	20.	76
2.5	-6.0	35.0	93.0	0.0000159	52.73	43.18	-1.62	30.21	-29.04	8.47	-0.012946	20.	76
2.5	-5.0	62.7	88.0	0.0000159	33.21	15.20	1.00	29.50	-21.18	20.56	-0.013230	20.	76
2.5	-4.0	19.5	65.9	0.0000159	15.61	14.71	2.12	4.76	-5.09	1.12	-0.012756	20.	76
2.5	-3.0	7.2	72.4	0.0000159	18.54	18.40	0.70	2.21	-2.31	0.24	-0.017197	20.	76
2.5	-2.0	56.8	194.9	0.0000159	31.52	17.25	-25.48	-6.78	-12.23	23.36	-0.009727	20.	76
2.5	-1.0	16.9	185.5	0.0000159	82.09	78.52	-23.85	-2.32	-19.05	14.54	-0.017040	20.	76
2.5	0.0	0.8	126.7	0.0000159	92.61	92.60	-0.82	1.10	0.00	1.37	-0.020377	20.	76
2.5	1.0	25.4	11.1	0.0000159	47.75	43.11	20.13	3.96	13.20	15.70	-0.009416	20.	76
2.5	2.0	23.6	43.4	0.0000159	19.51	17.87	5.66	5.37	6.85	3.74	-0.007688	20.	76
2.5	3.0	16.8	136.7	0.0000159	13.38	12.80	-2.82	2.66	3.76	0.95	-0.009498	20.	76
2.5	4.0	34.0	182.9	0.0000159	10.04	8.32	-5.61	-0.28	5.17	2.16	-0.012086	20.	76
2.5	5.0	39.5	217.4	0.0000159	9.66	7.45	-4.75	-3.91	5.69	2.35	-0.012861	20.	76
2.5	6.0	36.2	248.4	0.0000159	14.68	11.83	-3.19	-8.08	8.31	2.54	-0.013844	20.	76
2.5	7.0	32.4	270.9	0.0000159	33.05	27.88	0.28	-17.73	17.30	3.93	-0.015363	20.	76
2.5	8.0	38.6	280.0	0.0000159	61.26	47.84	6.69	-37.67	37.12	9.27	-0.013270	20.	76
2.5	9.0	49.1	293.6	0.0000159	81.46	53.24	24.75	-56.46	58.68	18.87	-0.010200	20.	76
2.5	10.0	63.3	318.5	0.0000159	58.79	26.35	39.38	-34.79	47.03	23.44	0.000038	20.	76
2.5	11.0	74.4	322.1	0.0000159	30.42	8.14	23.14	-17.99	22.69	18.55	0.001226	20.	76
2.5	13.0	71.8	205.4	0.0000159	10.77	3.36	-9.24	-4.39	8.63	5.16	0.000148	20.	76
2.5	14.0	75.1	197.2	0.0000159	9.74	2.49	-9.00	-2.79	7.81	5.27	0.001310	20.	76
2.5	15.0	75.2	194.6	0.0000159	10.75	2.74	-10.06	-2.63	8.79	5.55	0.002131	20.	76
2.5	20.0	71.2	189.9	0.0000159	5.84	1.87	-5.45	-0.95	5.19	1.91	0.002536	20.	76
2.5	25.0	70.9	186.9	0.0000159	5.05	1.65	-4.74	-0.57	4.53	1.32	0.002606	20.	76
2.5	30.0	75.5	186.7	0.0000159	5.80	1.45	-5.58	-0.65	5.35	1.72	0.002729	20.	76

Table II-53. COMPUTER-REDUCED DATA FOR THE SWIRL BURNER (Swirl Number, S = 0.8) AT THE 7.6-cm AXIAL POSITION

MOVEABLE BLOCK BURNER SET FOR INTERMEDIATE SWIRL - COLD MODEL

RESULTS

AP	RP	FI	DELTA	RHO	V	VX	VY	VZ	VT	VR	PST	T	PS
7.6	-30.0	3.6	269.9	0.0000159	4.75	4.74	-0.00	-0.29	-0.29	0.00	0.002149	20.	760.
7.6	-25.0	55.5	179.5	0.0000159	10.91	6.17	-9.00	0.06	-8.23	3.65	0.002091	20.	760.
7.6	-20.0	82.3	244.9	0.0000159	12.53	1.66	-5.25	-11.25	-4.13	11.71	0.000651	20.	760.
7.6	-15.0	81.2	236.9	0.0000159	28.77	4.39	-15.52	-23.82	-8.29	27.20	0.004302	20.	760.
7.6	-14.0	75.7	228.0	0.0000159	20.37	5.02	-13.18	-14.69	-8.38	17.88	-0.002533	20.	760.
7.6	-13.0	80.9	89.8	0.0000159	23.39	3.68	0.04	23.09	-6.07	22.28	-0.006877	20.	760.
7.6	-12.0	31.2	90.1	0.0000159	28.37	24.24	-0.03	14.73	-13.75	5.29	-0.008130	20.	760.
7.6	-11.0	57.8	181.5	0.0000159	36.69	19.52	-31.06	-0.83	-20.90	22.98	0.007003	20.	760.
7.6	-10.0	35.5	134.0	0.0000159	33.81	27.51	-13.66	14.12	-17.27	9.37	-0.004824	20.	760.
7.6	-9.0	42.9	109.2	0.0000159	29.83	21.83	-6.69	19.20	-15.98	12.57	-0.005440	20.	760.
7.6	-8.0	49.4	157.4	0.0000159	29.64	19.25	-20.80	8.64	-15.07	16.75	0.000578	20.	760.
7.6	-7.0	162.1	181.7	0.0000159	12.12	-11.53	-3.72	-0.11	-3.51	1.23	-0.002786	20.	760.
7.6	-6.0	166.7	244.2	0.0000159	15.18	-14.78	-1.50	-3.13	-3.33	0.99	-0.001652	20.	760.
7.6	-5.0	171.0	265.2	0.0000159	15.96	-15.76	-0.20	-2.46	-2.41	0.57	-0.000842	20.	760.
7.6	-4.0	173.8	270.4	0.0000159	14.31	-14.23	0.00	-1.52	-1.49	0.30	0.000042	20.	760.
7.6	-3.0	39.7	191.8	0.0000159	15.63	12.02	-9.79	-2.05	-4.28	9.03	-0.001681	20.	760.
7.6	-2.0	18.5	192.3	0.0000159	21.83	20.69	-6.78	-1.48	-4.28	5.46	-0.002643	20.	760.
7.6	-1.0	4.9	172.3	0.0000159	33.07	32.94	-2.82	0.37	-2.38	1.56	-0.005763	20.	760.
7.6	0.0	4.9	30.7	0.0000159	32.22	32.10	2.39	1.42	0.00	2.78	-0.005067	20.	760.
7.6	1.0	23.0	26.2	0.0000159	21.39	19.68	7.51	3.70	2.47	8.00	-0.001972	20.	760.
7.6	2.0	46.0	9.3	0.0000159	17.59	12.21	12.49	2.04	3.11	12.26	-0.002285	20.	760.
7.6	3.0	168.6	39.8	0.0000159	15.69	-15.38	2.37	1.98	2.75	1.40	-0.003170	20.	760.
7.6	4.0	165.9	44.0	0.0000159	22.27	-21.60	3.89	3.76	4.89	2.33	-0.004977	20.	760.
7.6	5.0	154.4	43.6	0.0000159	22.57	-20.37	7.04	6.71	7.87	5.71	-0.004327	20.	760.
7.6	6.0	140.6	58.4	0.0000159	20.41	-15.77	6.76	11.04	8.97	9.33	-0.010041	20.	760.
7.6	7.0	82.7	201.5	0.0000159	10.96	1.37	-10.11	-3.99	1.25	10.80	-0.002449	20.	760.
7.6	8.0	30.5	213.9	0.0000159	13.10	11.28	-5.52	-3.71	5.80	3.25	-0.005292	20.	760.
7.6	9.0	38.1	266.1	0.0000159	21.71	17.06	-0.90	-13.39	11.18	7.42	-0.005729	20.	760.
7.6	10.0	50.8	284.2	0.0000159	31.39	19.84	5.98	-23.58	17.79	16.56	-0.006144	20.	760.
7.6	11.0	57.2	297.5	0.0000159	36.34	19.66	14.13	-27.09	20.82	22.36	-0.005207	20.	760.
7.6	12.0	78.2	299.0	0.0000159	31.15	6.35	14.80	-26.66	9.53	28.96	-0.001542	20.	760.
7.6	13.0	67.2	317.0	0.0000159	33.98	13.12	22.74	-21.35	18.24	25.48	-0.003458	20.	760.
7.6	14.0	69.3	324.0	0.0000159	29.33	10.33	22.22	-16.11	15.64	22.55	-0.002474	20.	760.
7.6	15.0	69.8	333.6	0.0000159	23.95	8.25	20.16	-9.96	13.19	18.21	-0.001299	20.	760.
7.6	20.0	48.0	8.6	0.0000159	11.36	7.59	8.36	1.27	7.78	3.29	0.000767	20.	760.
7.6	25.0	24.4	40.9	0.0000159	7.11	6.47	2.22	1.92	2.91	0.40	0.001951	20.	760.
7.6	30.0	24.4	62.0	0.0000159	5.62	5.12	1.09	2.05	2.30	0.26	0.002094	20.	760.

Table II-54. COMPUTER-REDUCED DATA FOR THE SWIRL BURNER (Swirl Number, S = 0.8) AT THE 17.8-cm AXIAL POSITION

MOVEABLE BLOCK BURNER SET FOR INTERMEDIATE SWIRL - COLD MODEL

RESULTS

AP	RP	FI	DELTA	RHO	V	VX	VY	VZ	VT	VR	PST	T	P0
17.8	-30.0	82.5	257.3	0.0000159	3.46	0.45	-0.75	-3.35	-0.74	3.35	0.002406	20.	760.
17.8	-25.0	77.2	271.7	0.0000159	4.81	1.05	0.14	-4.69	-1.41	4.47	0.002358	20.	760.
17.8	-20.0	70.9	253.0	0.0000159	7.49	2.43	-2.06	-6.77	-2.55	6.60	0.001765	20.	760.
17.8	-15.0	61.9	238.3	0.0000159	11.50	5.41	-5.32	-8.63	-4.16	9.25	0.001907	20.	760.
17.8	-14.0	58.1	238.8	0.0000159	9.87	5.21	-4.33	-7.17	-3.68	7.53	0.001971	20.	760.
17.8	-13.0	45.1	233.0	0.0000159	21.89	15.45	-9.32	-12.39	-9.12	12.54	0.001164	20.	760.
17.8	-12.0	39.7	246.7	0.0000159	22.80	17.53	-5.74	-13.39	-9.18	11.32	0.000460	20.	760.
17.8	-11.0	34.0	253.5	0.0000159	24.64	20.40	-3.90	-13.25	-9.31	10.20	-0.000589	20.	760.
17.8	-10.0	36.1	259.6	0.0000159	24.77	20.00	-2.63	-14.38	-8.91	11.59	-0.000526	20.	760.
17.8	-9.0	36.5	268.6	0.0000159	24.69	19.85	-0.33	-14.68	-8.28	12.13	-0.001046	20.	760.
17.8	-8.0	47.7	278.9	0.0000159	21.53	14.49	2.48	-15.73	-6.02	14.74	-0.000709	20.	760.
17.8	-7.0	46.6	279.9	0.0000159	19.15	13.14	2.41	-13.71	-4.84	13.05	-0.000309	20.	760.
17.8	-6.0	168.6	267.5	0.0000159	8.57	-8.40	-0.07	-1.69	-1.45	0.86	-0.002776	20.	760.
17.8	-5.0	138.4	253.8	0.0000159	8.38	-6.27	-1.54	-5.34	-1.67	5.39	-0.001915	20.	760.
17.8	-4.0	146.2	251.1	0.0000159	9.59	-7.97	-1.71	-5.04	-1.69	5.05	-0.001479	20.	760.
17.8	-3.0	145.0	255.0	0.0000159	10.68	-8.76	-1.58	-5.91	-1.43	5.95	-0.001481	20.	760.
17.8	-2.0	151.3	259.8	0.0000159	11.80	-10.36	-0.99	-5.56	-1.14	5.53	-0.001609	20.	760.
17.8	-1.0	164.7	263.4	0.0000159	13.12	-12.66	-0.39	-3.41	-0.69	3.37	-0.001673	20.	760.
17.8	0.0	167.2	263.6	0.0000159	13.25	-12.92	-0.32	-2.91	0.00	2.92	-0.001352	20.	760.
17.8	1.0	173.5	259.4	0.0000159	13.93	-13.84	-0.28	-1.54	0.69	1.41	-0.001432	20.	760.
17.8	2.0	176.5	269.4	0.0000159	14.09	-14.07	-0.00	-0.84	0.74	0.39	-0.001425	20.	760.
17.8	3.0	167.7	80.0	0.0000159	17.38	-16.98	0.63	3.64	2.26	2.92	-0.002404	20.	760.
17.8	4.0	167.1	81.6	0.0000159	16.09	-15.69	0.52	3.54	2.51	2.55	-0.002375	20.	760.
17.8	5.0	171.6	85.3	0.0000159	8.74	-8.64	0.10	1.27	1.13	0.59	0.001500	20.	760.
17.8	6.0	155.9	90.6	0.0000159	12.76	-11.65	-0.05	5.20	3.13	4.15	0.000801	20.	760.
17.8	7.0	164.0	49.3	0.0000159	10.95	-10.52	1.96	2.29	2.43	1.77	0.000947	20.	760.
17.8	8.0	155.6	53.4	0.0000159	10.24	-9.33	2.52	3.40	2.97	3.00	0.001529	20.	760.
17.8	9.0	165.1	70.5	0.0000159	8.01	-7.74	0.68	1.94	1.82	0.95	0.001247	20.	760.
17.8	10.0	33.6	232.7	0.0000159	19.60	16.31	-6.58	-8.65	7.00	8.31	-0.000833	20.	760.
17.8	11.0	50.1	269.0	0.0000159	22.58	14.47	-0.29	-17.33	7.95	15.43	-0.001162	20.	760.
17.8	12.0	52.0	276.3	0.0000159	26.69	16.40	2.34	-20.93	9.79	18.65	-0.001762	20.	760.
17.8	13.0	54.6	281.5	0.0000159	27.95	16.17	4.56	-22.34	10.48	20.24	-0.001619	20.	760.
17.8	14.0	55.7	287.2	0.0000159	27.05	15.20	6.63	-21.37	10.54	19.73	-0.000844	20.	760.
17.8	15.0	59.6	288.3	0.0000159	27.00	13.65	7.34	-22.10	10.31	20.88	-0.000748	20.	760.
17.8	20.0	48.1	303.2	0.0000159	12.99	8.67	5.30	-8.09	6.86	6.81	0.001105	20.	760.
17.8	25.0	18.7	240.6	0.0000159	4.68	4.43	-0.73	-1.30	1.46	0.35	0.001929	20.	760.
17.8	30.0	41.9	191.2	0.0000159	3.76	2.79	-2.46	-0.49	2.21	1.18	0.002175	20.	760.

Table II-55. COMPUTER-REDUCED DATA FOR THE SWIRL BURNER (Swirl Number, S = 0.8) AT THE 30.5-cm AXIAL POSITION

MOVEABLE BLOCK BURNER SET FOR INTERMEDIATE SWIRL - COLD MODEL

RESULTS

AP	RP	FI	DELTA	RHO	V	VX	VY	VZ	VT	VR	PST	T	PB
30.5	-30.0	25.0	264.1	0.0000159	6.90	6.25	-0.29	-2.90	-2.64	1.25	0.001047	20.	760.
30.5	-25.0	34.1	249.0	0.0000159	4.05	3.36	-0.81	-2.12	-1.75	1.45	0.001178	20.	760.
30.5	-20.0	80.2	220.1	0.0000159	8.40	1.42	-6.32	-5.34	-0.92	8.23	0.002824	20.	760.
30.5	-18.0	46.6	234.4	0.0000159	15.62	10.72	-6.61	-9.24	-5.52	9.93	0.002146	20.	760.
30.5	-16.0	47.7	234.6	0.0000159	16.26	10.93	-6.96	-9.81	-5.18	10.86	0.002192	20.	760.
30.5	-14.0	53.6	241.2	0.0000159	17.79	10.55	-6.89	-12.55	-4.58	13.56	0.002731	20.	760.
30.5	-12.0	62.3	249.2	0.0000159	17.82	8.26	-5.59	-14.77	-3.18	15.46	0.002739	20.	760.
30.5	12.0	165.3	350.0	0.0000159	8.57	-8.29	2.13	-0.37	1.80	1.20	0.002138	20.	760.
30.5	10.0	167.0	344.6	0.0000159	9.00	-8.77	1.94	-0.53	1.65	1.15	0.002098	20.	760.
30.5	8.0	160.2	327.8	0.0000159	7.99	-7.52	2.28	-1.43	1.59	2.17	0.001299	20.	760.
30.5	6.0	169.3	350.9	0.0000159	9.58	-9.41	1.74	-0.27	1.28	1.22	0.001051	20.	760.
30.5	4.0	172.6	331.0	0.0000159	9.96	-9.87	1.12	-0.62	0.91	0.90	0.001193	20.	760.
30.5	2.0	168.4	287.9	0.0000159	9.43	-9.23	0.58	-1.80	0.57	1.80	0.001246	20.	760.
30.5	0.0	166.0	281.6	0.0000159	9.69	-9.40	0.47	-2.29	0.00	2.34	0.001342	20.	760.
30.5	-2.0	164.9	278.5	0.0000159	9.19	-8.87	0.35	-2.36	-0.56	2.32	0.001207	20.	760.
30.5	-4.0	161.8	277.9	0.0000159	8.89	-8.45	0.38	-2.75	-1.02	2.57	0.001047	20.	760.
30.5	-6.0	160.2	273.8	0.0000159	8.02	-7.55	0.18	-2.71	-1.30	2.38	0.001042	20.	760.
30.5	-8.0	160.9	282.1	0.0000159	8.33	-7.88	0.56	-2.65	-1.64	2.16	0.000848	20.	760.
30.5	-10.0	162.3	299.8	0.0000159	6.29	-6.00	0.94	-1.65	-1.36	1.32	-0.000141	20.	760.
30.5	14.0	41.6	91.0	0.0000159	10.80	8.07	-0.12	7.17	3.29	6.37	0.001362	20.	760.
30.5	16.0	33.3	77.9	0.0000159	13.90	11.61	1.60	7.47	4.76	5.97	0.000897	20.	760.
30.5	18.0	43.0	68.2	0.0000159	16.47	12.02	4.17	10.45	6.00	9.51	0.001402	20.	760.
30.5	20.0	39.7	59.7	0.0000159	16.51	12.69	5.32	9.12	6.53	8.30	0.001358	20.	760.
30.5	22.0	42.3	54.9	0.0000159	15.16	11.21	5.86	8.35	6.34	8.00	0.001476	20.	760.
30.5	24.0	44.2	52.5	0.0000159	13.25	9.48	5.62	7.34	5.80	7.20	0.001558	20.	760.
30.5	25.0	51.7	61.0	0.0000159	11.64	7.20	4.42	7.99	4.96	7.67	0.002055	20.	760.
30.5	30.0	51.2	42.4	0.0000159	7.40	4.63	4.25	3.89	3.57	4.53	0.001776	20.	760.

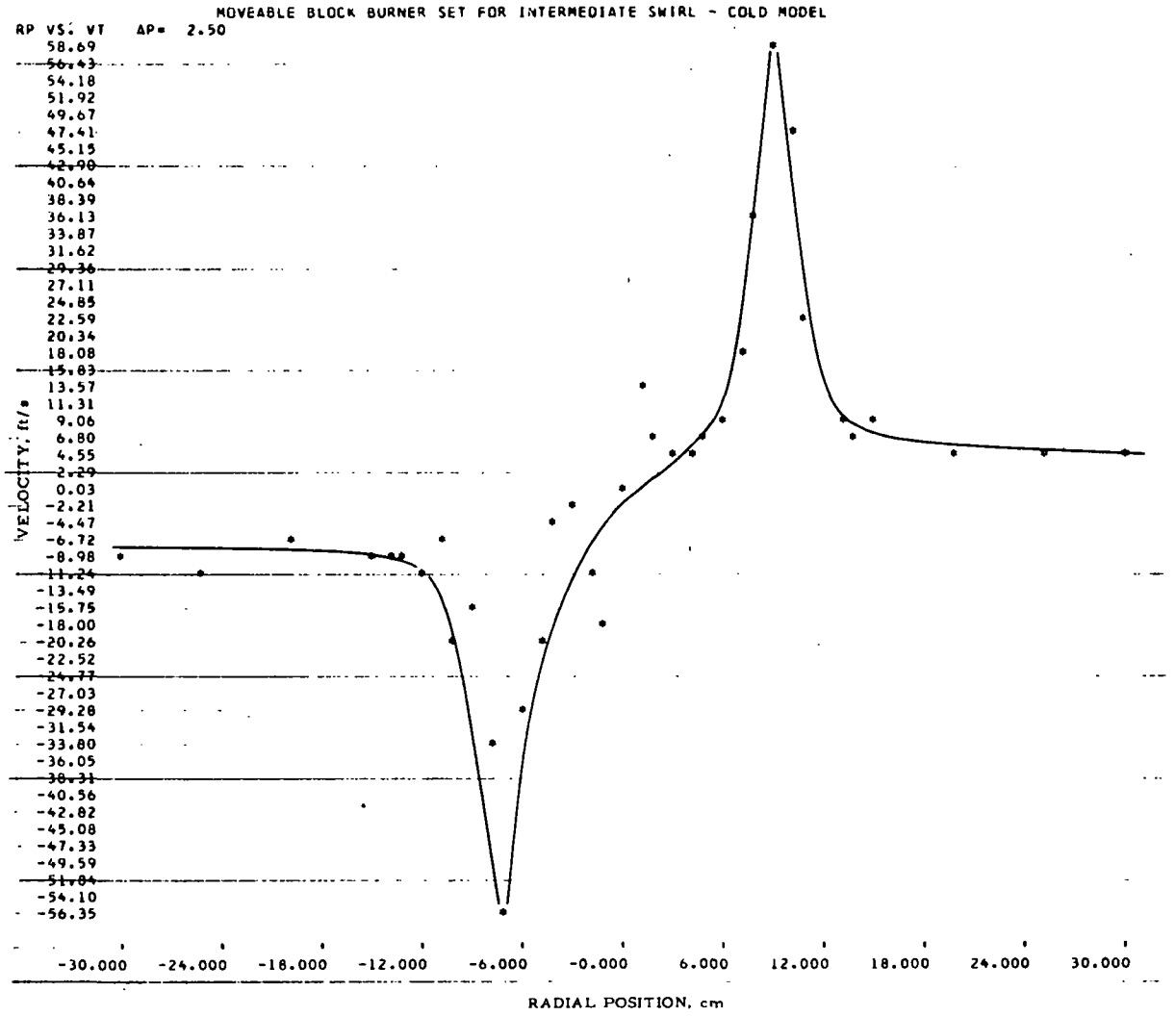

Figure II-224. TANGENTIAL VELOCITY PROFILE FOR THE SWIRL BURNER AT THE 2.5-cm AXIAL POSITION (Swirl Number, S = 0.8)

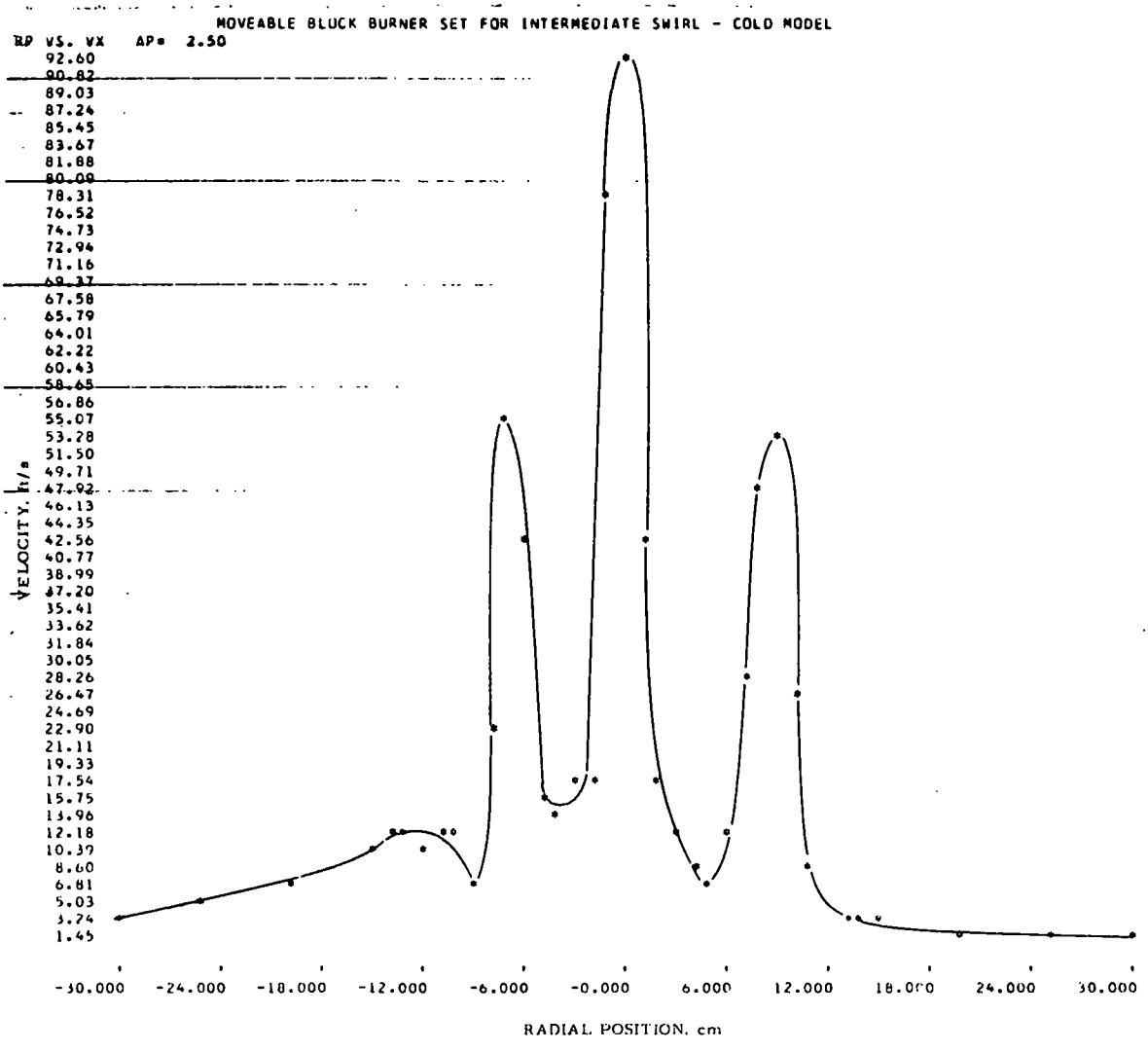

Figure II-225. AXIAL VELOCITY PROFILE FOR THE SWIRL BURNER AT THE 2.5-cm AXIAL POSITION (Swirl Number, S = 0.8)

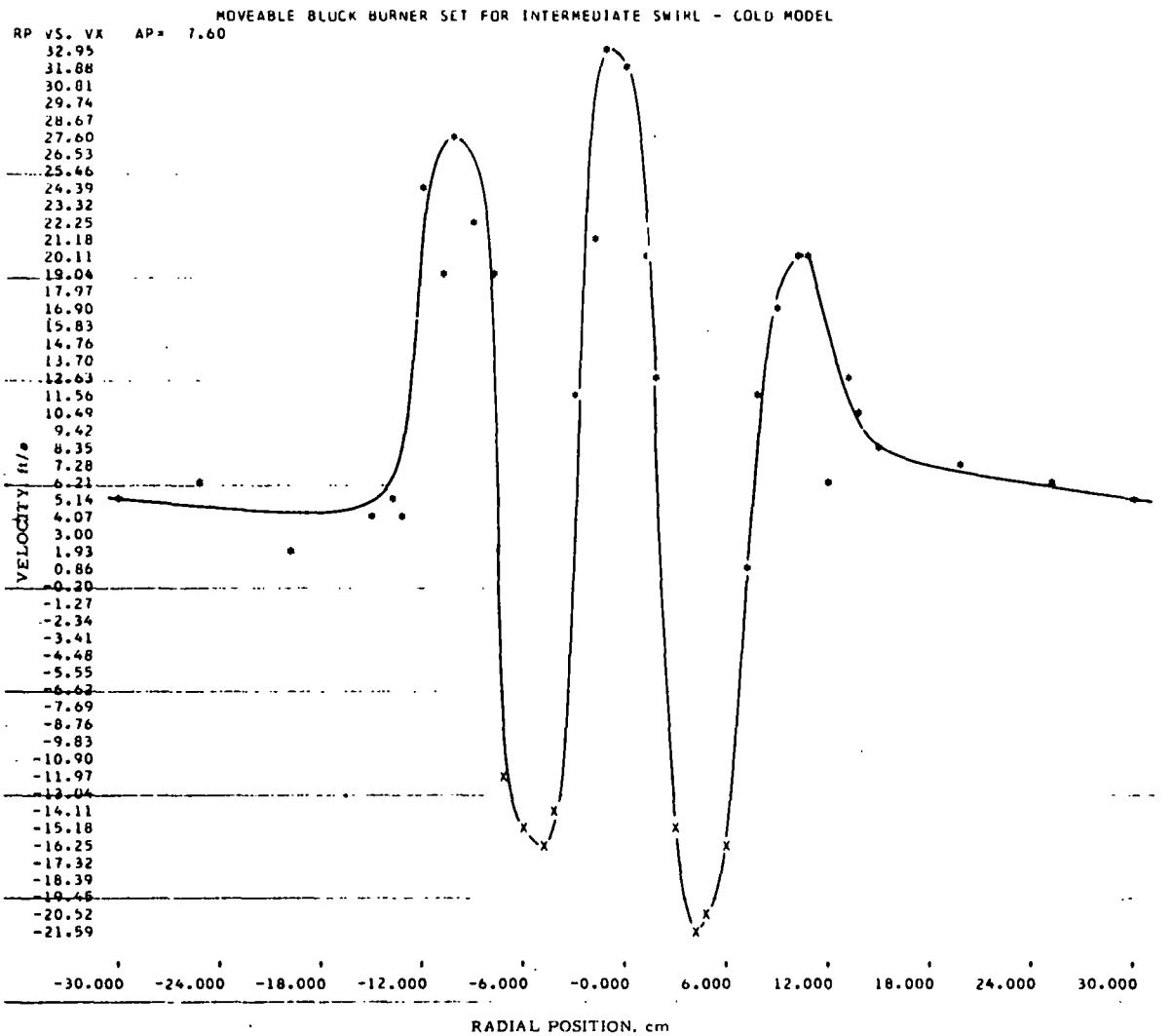

Figure II-226. AXIAL VELOCITY PROFILE FOR THE SWIRL BURNER AT THE 7.6-cm AXIAL POSITION (Swirl Number, S = 0.8)

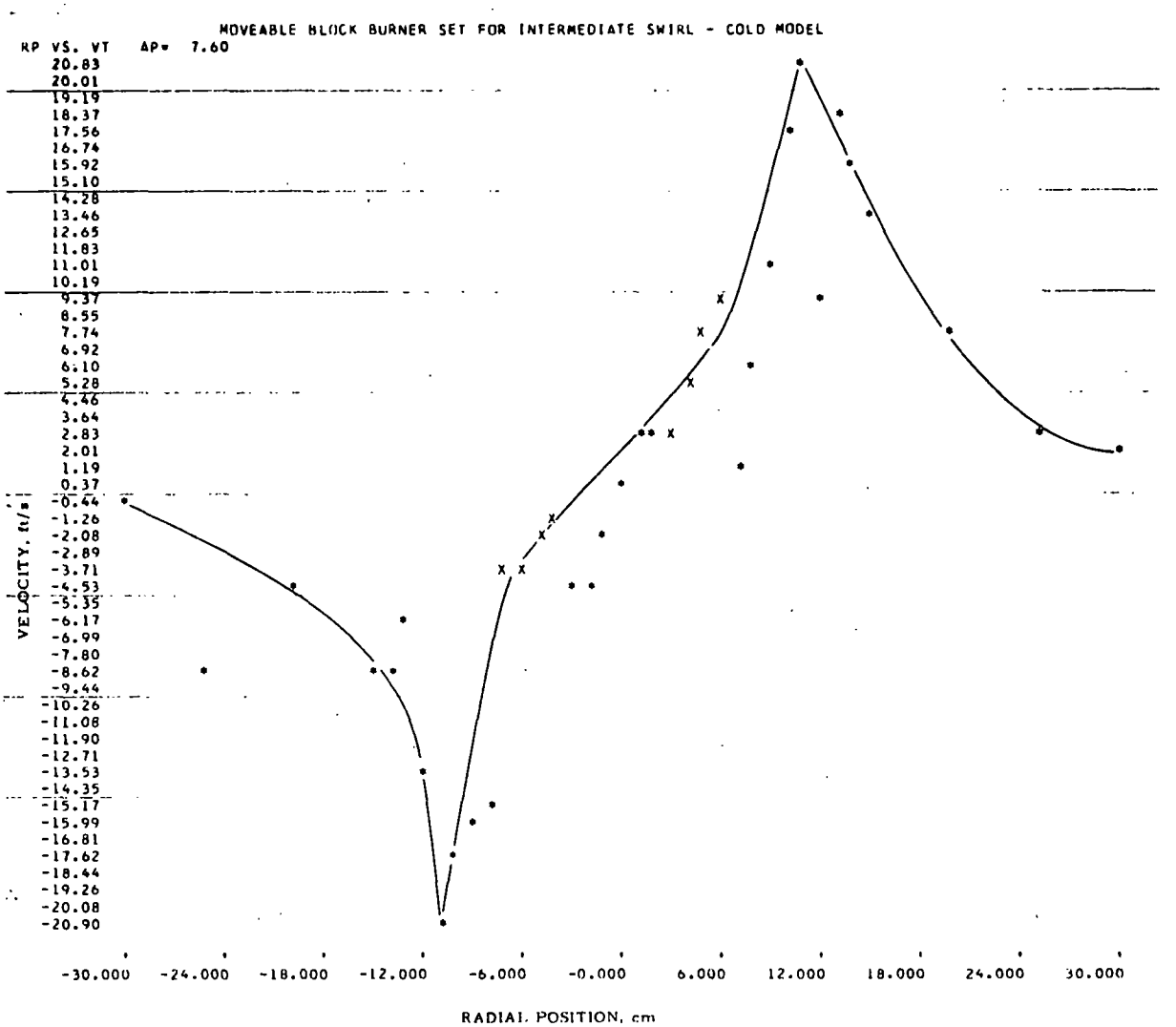

Figure II-227. TANGENTIAL VELOCITY PROFILE FOR THE SWIRL BURNER AT THE 7.6-cm AXIAL POSITION (Swirl Number, S = 0.8)

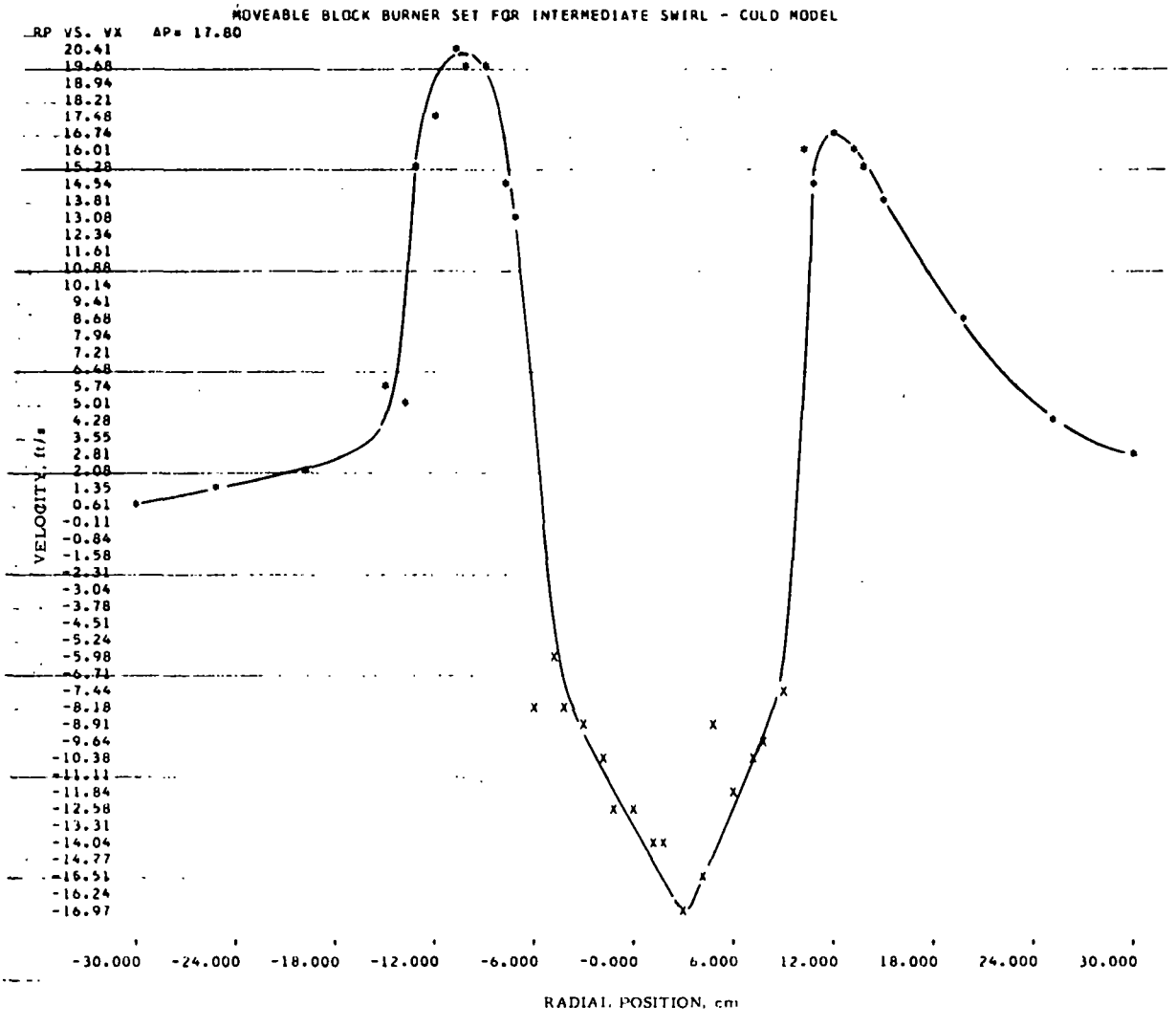

Figure II-228. AXIAL VELOCITY PROFILE FOR THE SWIRL BURNER AT THE 17.8-cm AXIAL POSITION (Swirl Number, S = 0.8)

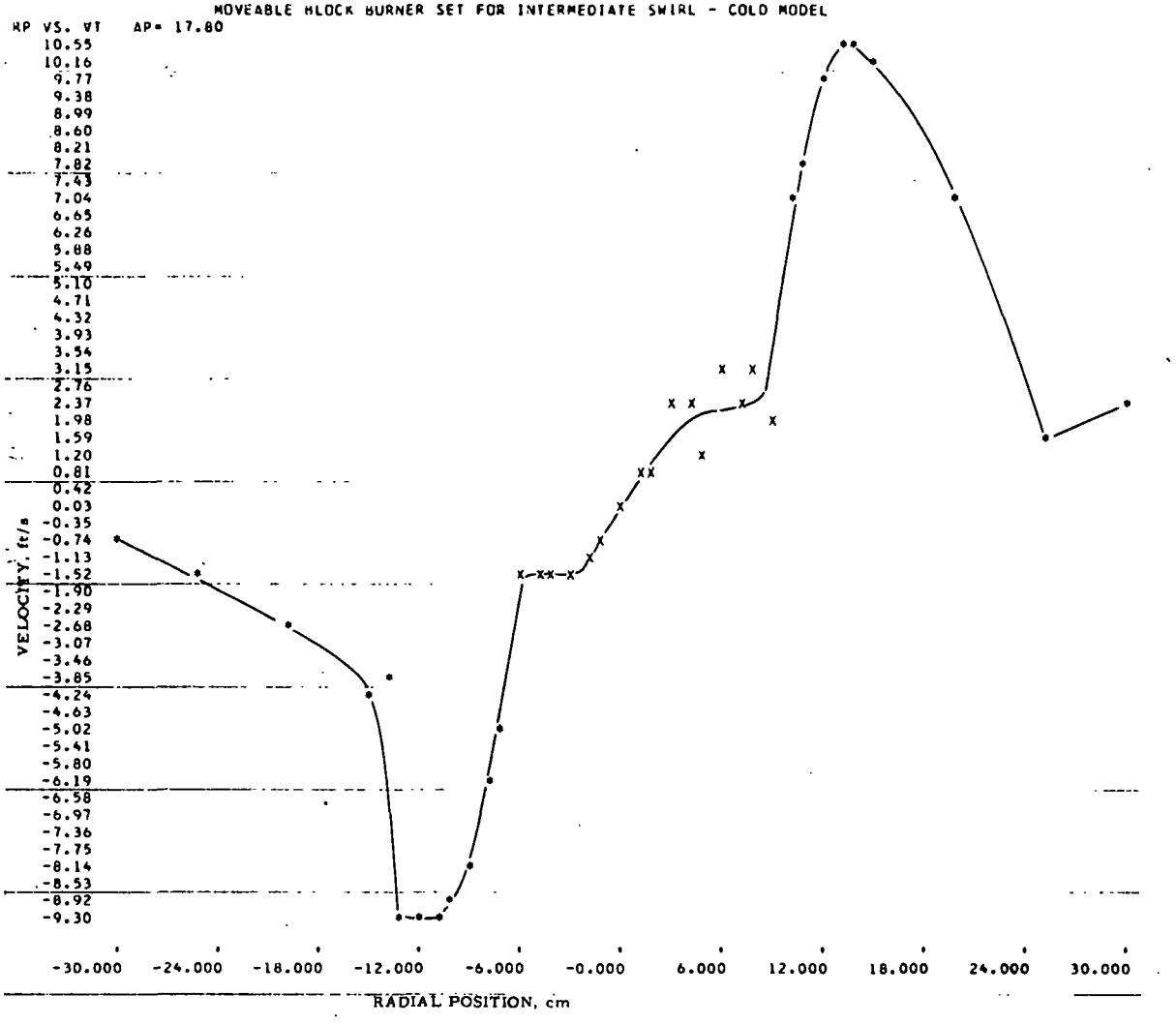

Figure II-229. TANGENTIAL VELOCITY PROFILE FOR THE SWIRL BURNER AT THE 17.8-cm AXIAL POSITION (Swirl Number, S = 0.8)

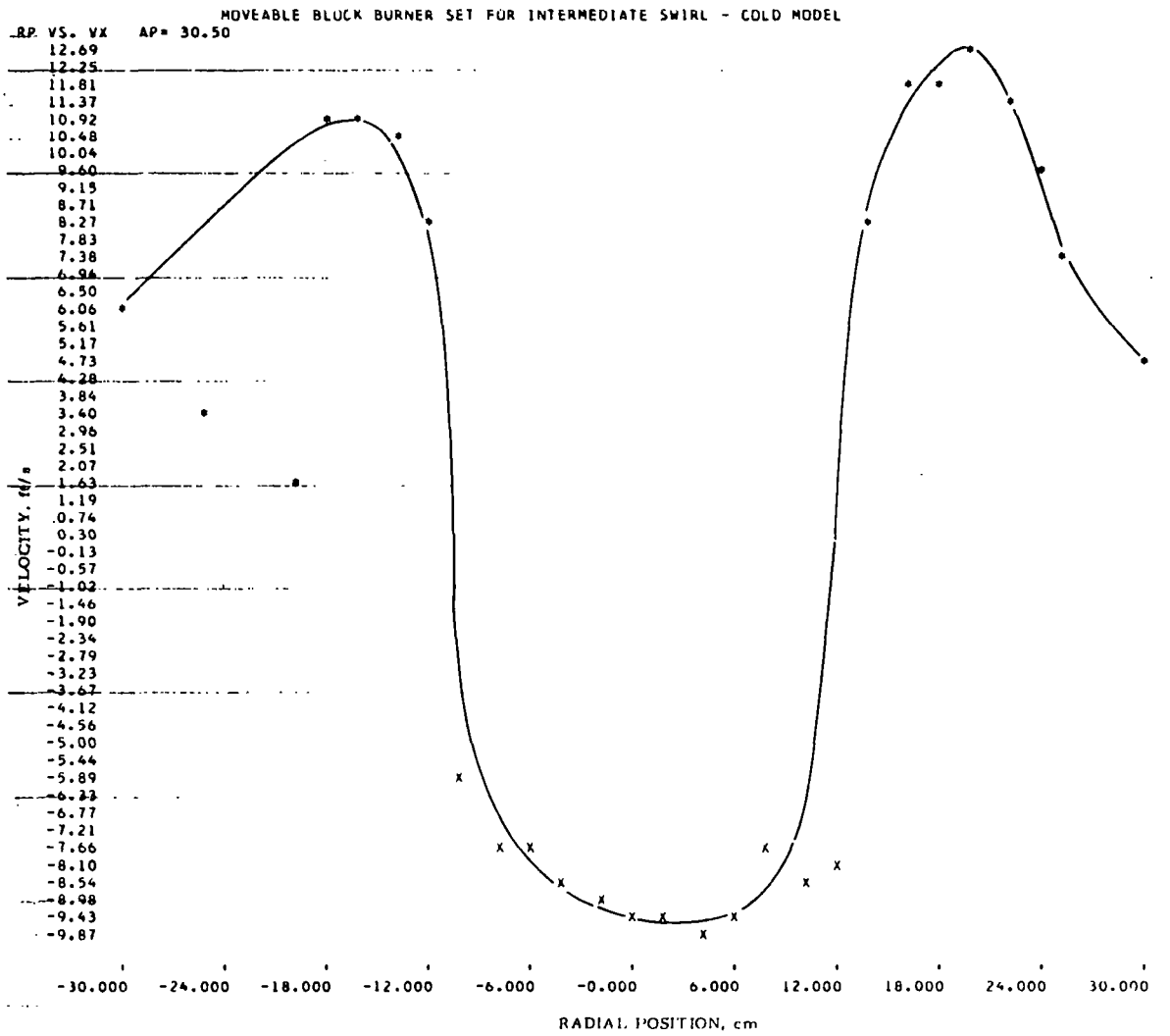

Figure II-230. AXIAL VELOCITY PROFILE FOR THE SWIRL BURNER AT THE 30.5-cm AXIAL POSITION (Swirl Number, S = 0.8)

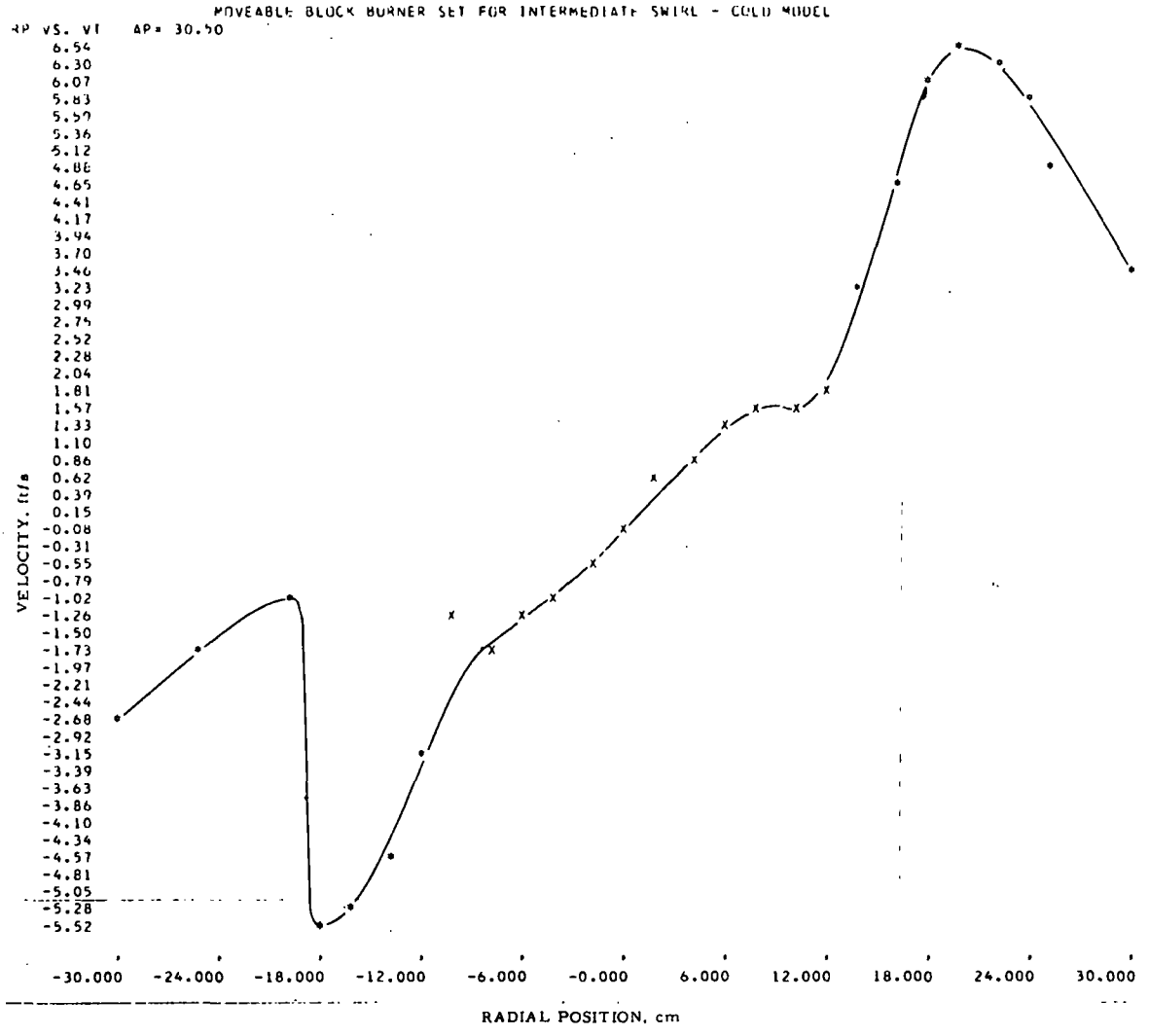

Figure II-231. TANGENTIAL VELOCITY PROFILE FOR THE SWIRL BURNER AT THE 30.5-cm AXIAL POSITION (Swirl Number, S = 0.8)

Figure II-224 represents the tangential velocity profile at an axial position of 2.5 cm. The graph is much the same as that obtained in the minimum swirl case, with one exception: The maximum magnitude of the velocity has increased by a factor of 3-1/2. There has, however, been a radical change in the shape of the axial profile, which can be seen by comparing Figure II-225 with Figure II-214. Two new peaks have appeared and are shown in Figure II-225. In the case of minimum swirl there was a constant velocity near 30 ft/s in the throat of the burner, while for intermediate swirl this region has a range of velocities from 8 to 56 ft/s. Comparing Tables II-40 and II-43, we see that the magnitude and the size of the region occupied by negative static pressure is greater for intermediate than for minimum swirl.

Although qualitative investigations indicate a narrow region of reverse flow in the throat of the burner occurring between the outside and central velocity peaks in the axial profile, it was impossible to make any quantitative measurements at the 2.5-cm axial position because of the 3-inch shepherd's-crook-shaped probe head. Thus, all data points for the 2.5-cm axial position are presented as representing forward flow.

Figure II-226 shows that, at an axial position of 7.6 cm, the axial velocity in the center peak has decreased by a factor of 3 from its value at 2.5 cm, while the outside peaks have decreased by only a factor of 2. There is recirculation on both sides of the central peak; these data points are represented by X rather than by an asterisk, and are shown with a negative velocity. Figure II-227 presents the tangential velocity. (Note that the reverse flow stream has no tangential velocity.) At an axial position of 17.8 cm, the central peak at axial velocity has disappeared and the entire burner region has reverse flow, as shown in Figure II-228. Figure II-229 shows that the forward tangential velocity has a magnitude of about one-half that of the forward axial velocity. Figures II-230 and II-231 present the axial and tangential velocity profiles at an axial position of 30.5 cm. The same general observations made for the profiles at 17.8 cm still persist with the addition of an expanding recirculation region.

4. Hot-Model Input-Output Data

The swirl burner was operated at three different swirl intensities for the input-output tests, with two gas nozzle positions for each swirl intensity. For the first gas nozzle position, the nozzle tip was located even with the inside edge of the burner wall (hot face) while in the second position the nozzle tip was withdrawn into the burner block, 6 inches from the hot face wall. (For the remainder of this report, these positions will be referred to as the "exit position" and "throat position," respectively.) The input-output tests were conducted at gas inputs of 1578 CF/hr, 1976 CF/hr, and 2382 CF/hr, with between 10 and 80% of excess air. Figures II-232 through II-238 show the input-output test results. The nitric oxide (NO) concentrations were normalized by dividing the weight of the flue products at the stoichiometric mixture of fuel and air into the measured concentration of NO, and multiplying this ratio by the weight of the flue products for the input conditions under which the measurements were taken.

Based on an analysis of the input-output data from the movable block swirl burner, we determined the following:

- The maximum measured NO concentration occurred at the lowest levels of gas input and swirl intensity.
- At excess oxygen levels below 6%, generally more NO was formed when the gas nozzle was in the throat position than when it was in the exit position. Insufficient data are available to evaluate the relative effect of burner nozzle position when operating with more than 6% excess oxygen.
- Increasing gas input (and consequently gas velocity) always reduced the normalized concentration of NO independent of swirl intensity and percent excess air, when the burner was in the throat position. However, when the nozzle was in the exit position, changing gas input had little or no effect on the normalized NO concentration. This was observed for intermediate and high swirl intensity. Insufficient data were obtainable for the case of low swirl intensity.

5. In-the-Flame Data Survey Results

Again, as part of this program, we mapped the concentrations of CO, CO_2, CH_4, O_2, and NO; the temperature; and the gas velocity in the flame. This information is obtained to gain insight into the mechanism and location of NO formation for different flame conditions and for use as input data to an NO_x computer modeling program, sponsored by EPA with Ultrasystems, Inc. The maps were obtained while operating the burner at conditions of intermediate swirl intensity and with the gas nozzle in the throat position. This was determined by the input-output tests to produce the maximum level of NO.

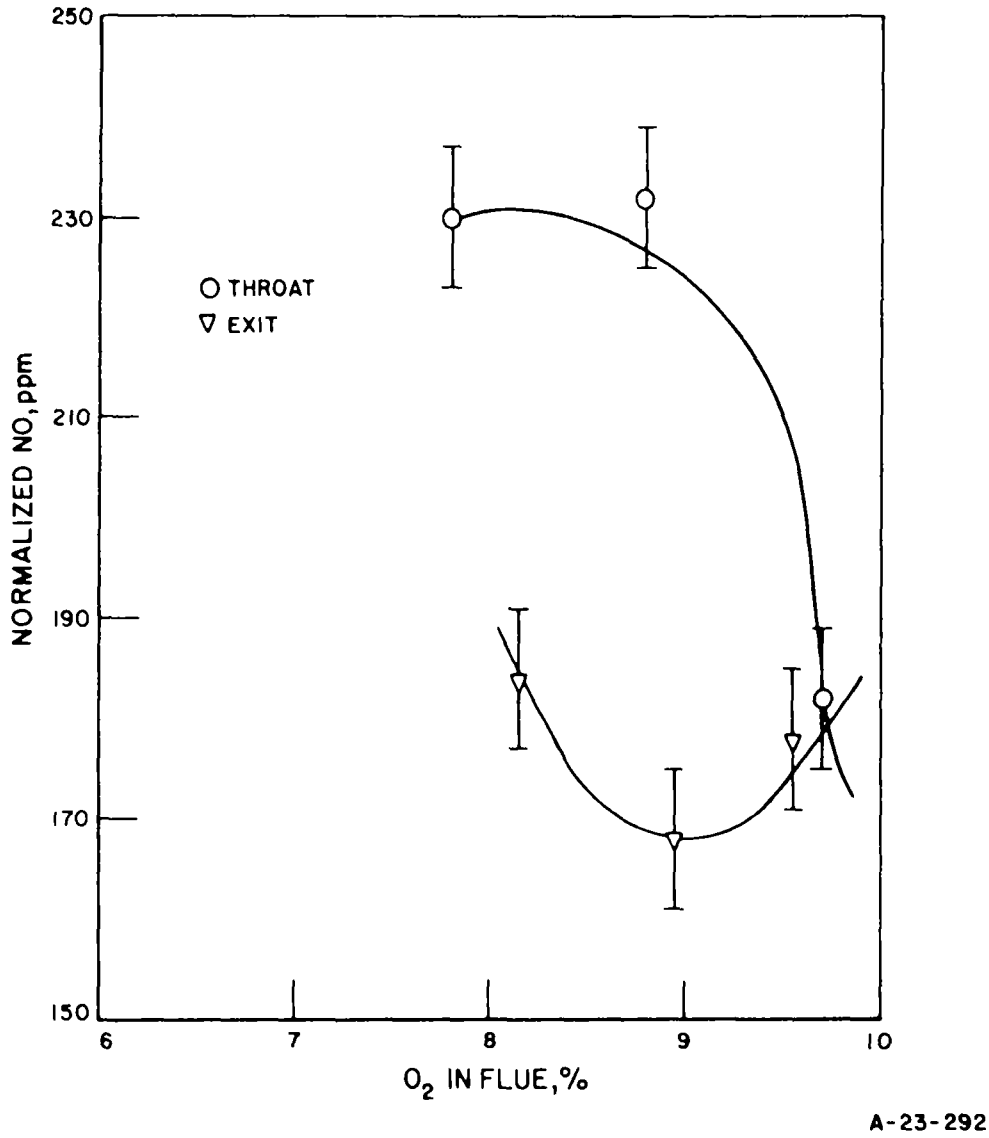

Figure II-232. NORMALIZED NO CONCENTRATION AS A FUNCTION OF EXCESS AIR (Movable-Block Swirl Burner — Low Swirl Intensity). GAS INPUT, 1578 CF/hr

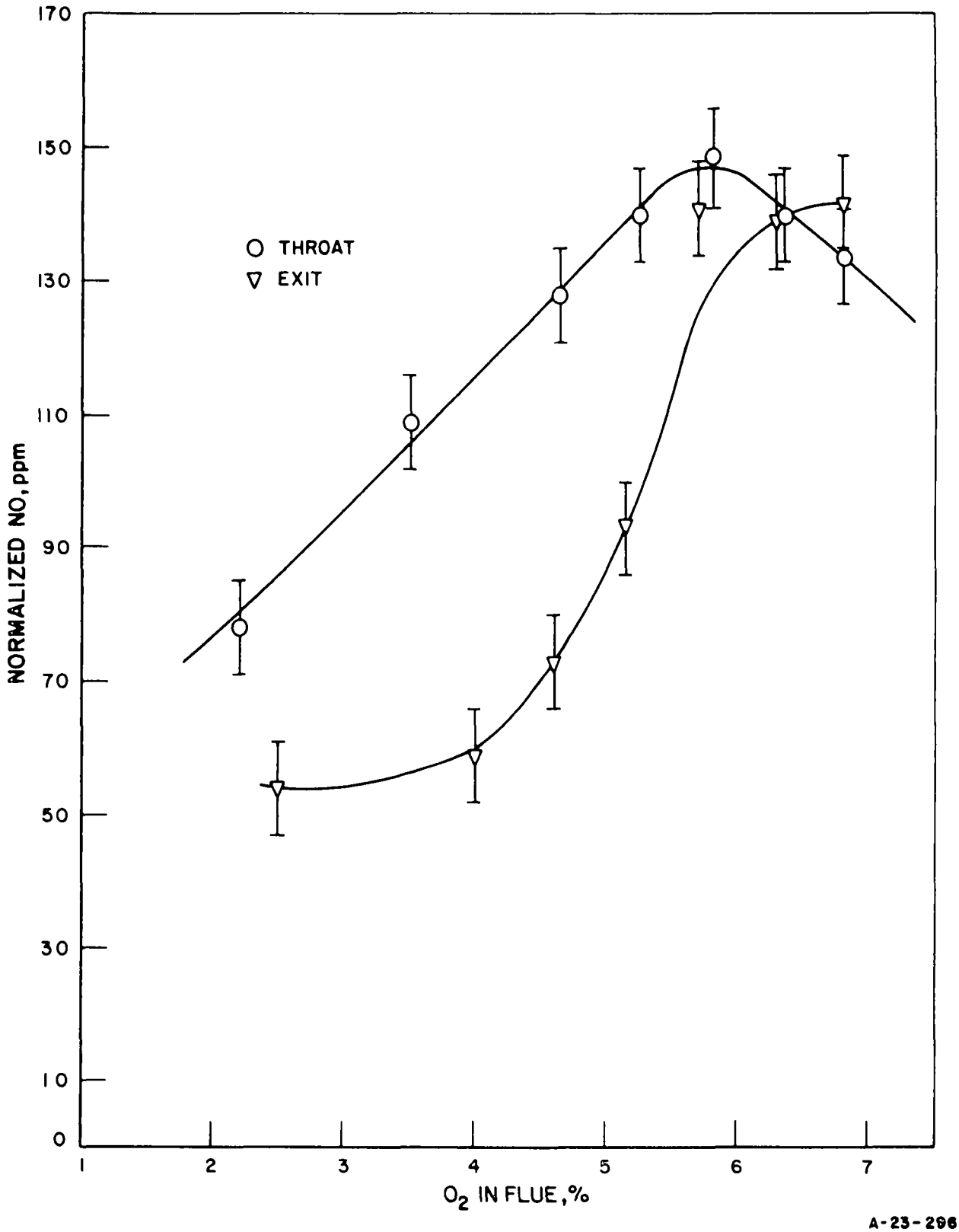

Figure II-233. NORMALIZED NO CONCENTRATION AS A FUNCTION OF EXCESS AIR (Movable-Block Swirl Burner – Low Swirl Intensity). GAS INPUT, 1976 CF/hr

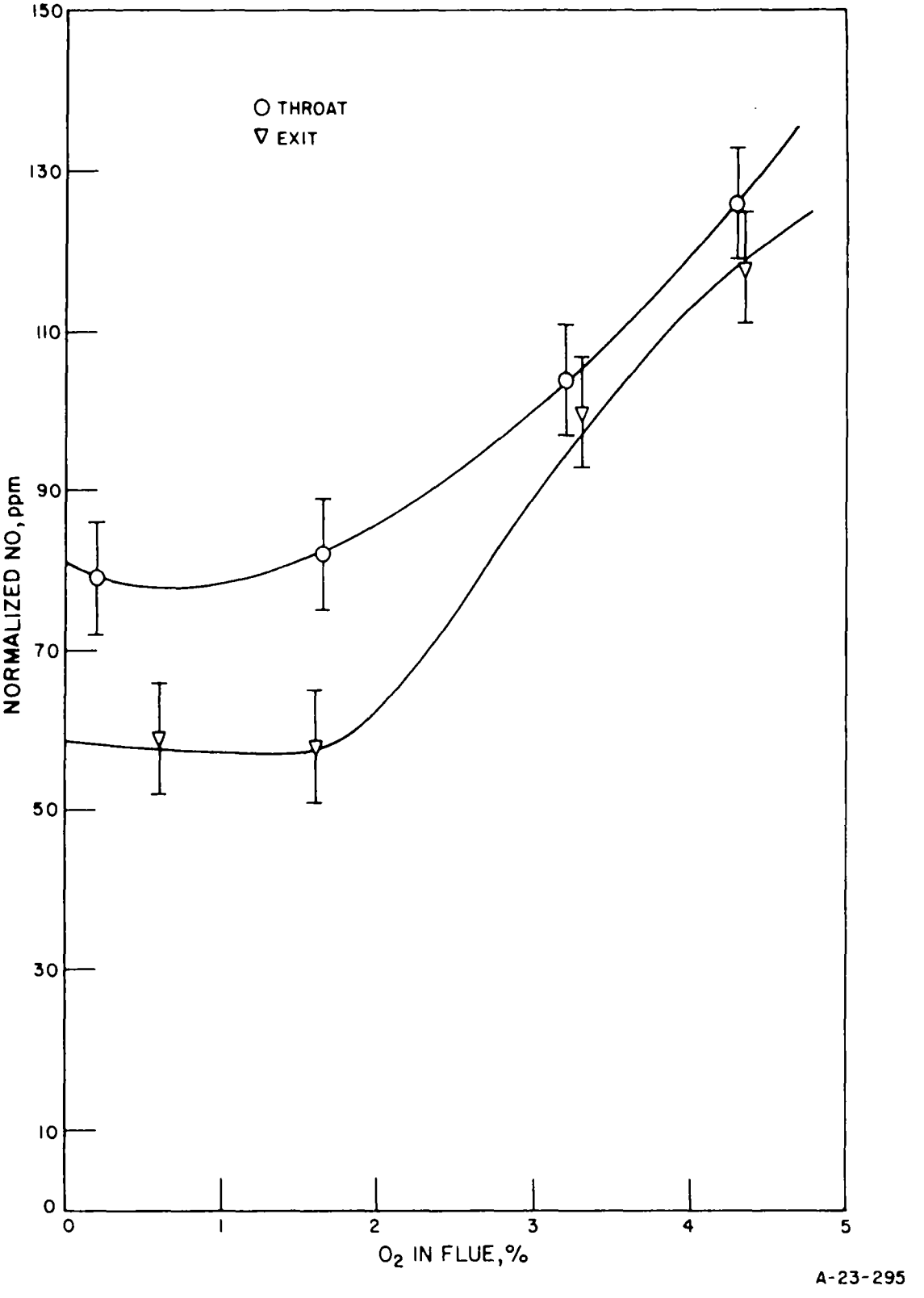

Figure II-234. NORMALIZED NO CONCENTRATION AS A FUNCTION OF EXCESS AIR (Movable-Block Swirl Burner – Low Swirl Intensity). GAS INPUT, 2382 CF/hr

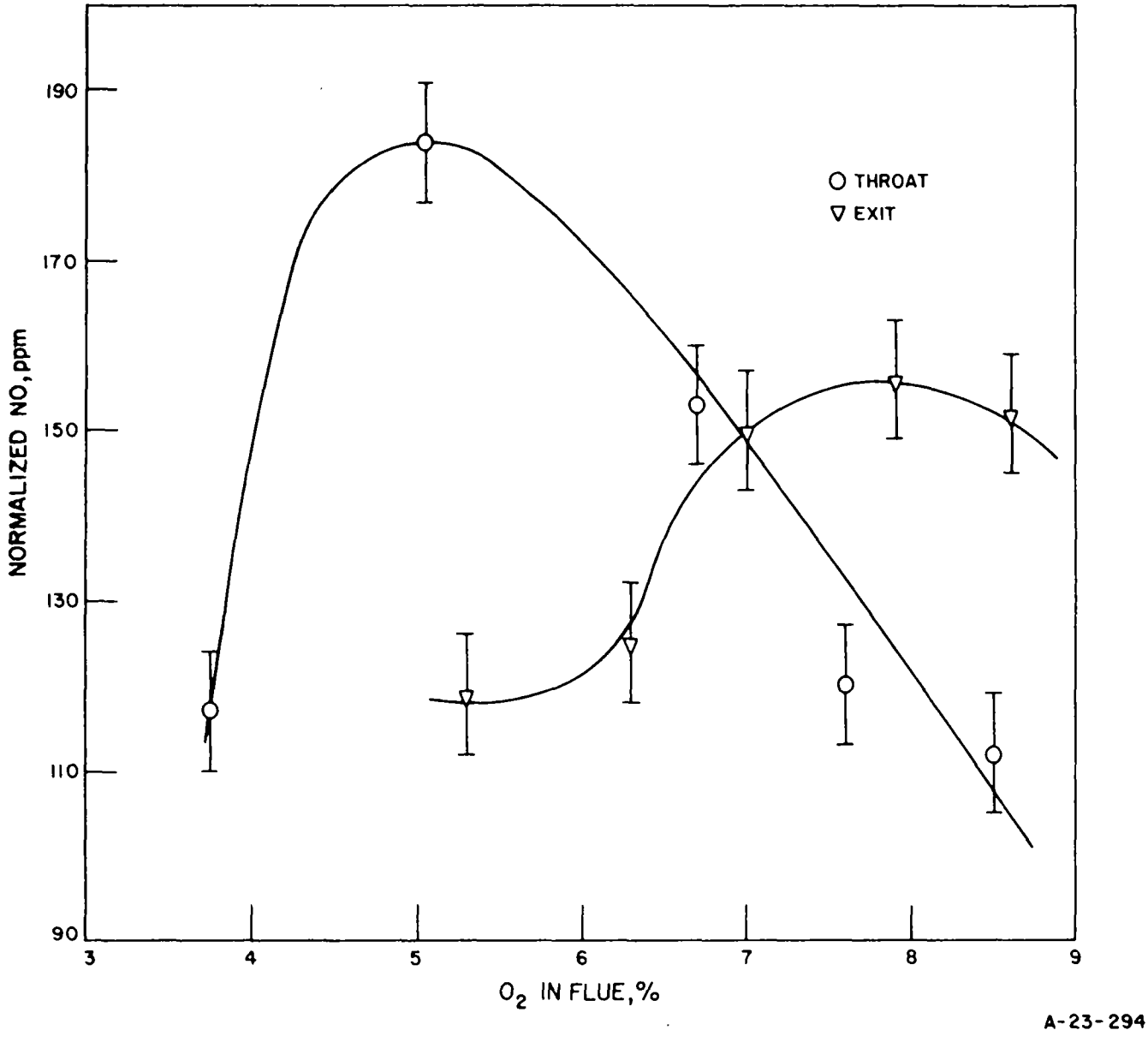

Figure II-235. NORMALIZED NO CONCENTRATION AS A FUNCTION OF EXCESS AIR (Movable-Block Swirl Burner – Intermediate Swirl Intensity). GAS INPUT, 1578 CF/hr

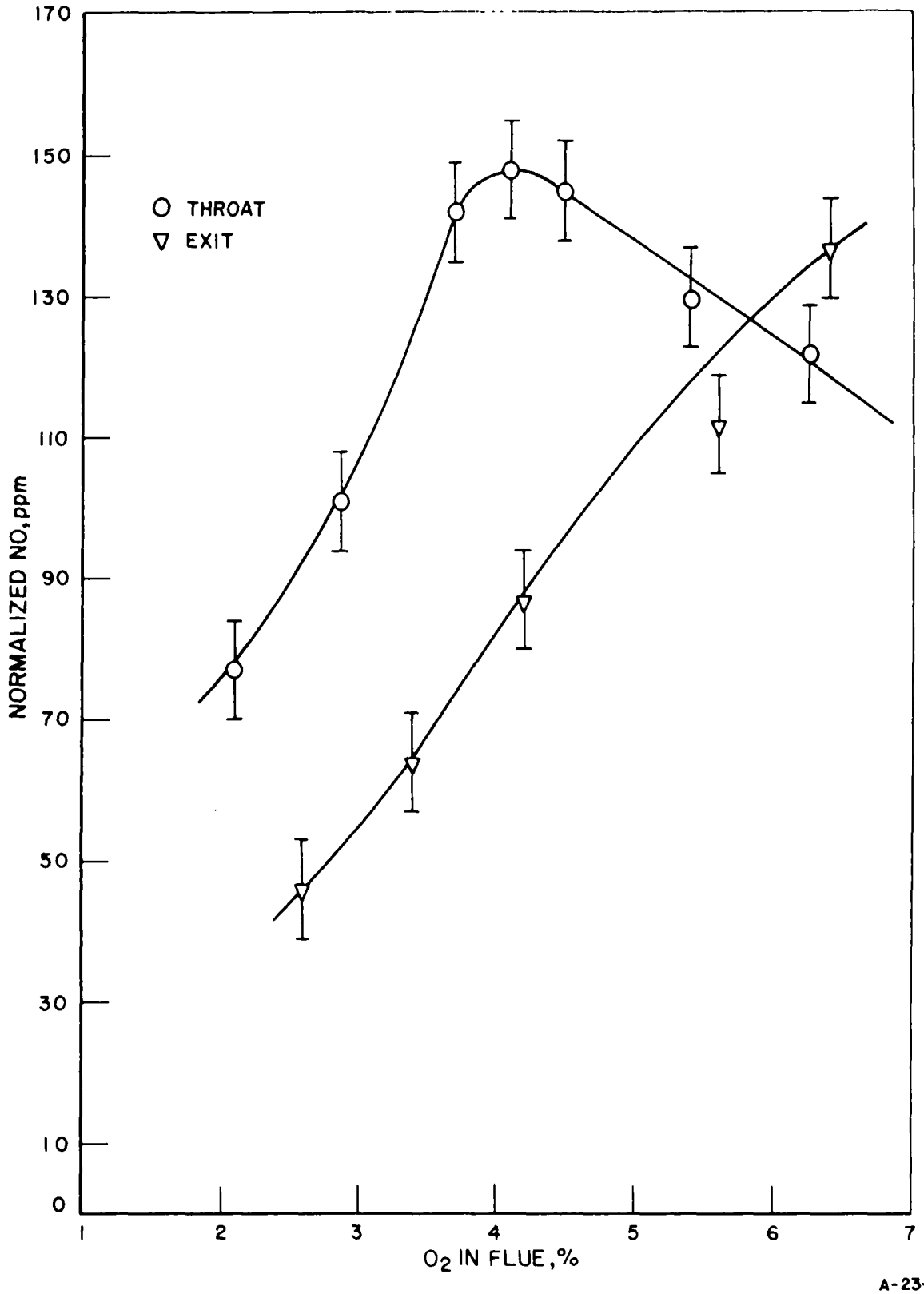

Figure II-236. NORMALIZED NO CONCENTRATION AS A FUNCTION OF EXCESS AIR (Movable-Block Swirl Burner — Intermediate Swirl Intensity). GAS INPUT, 1976 CF/hr

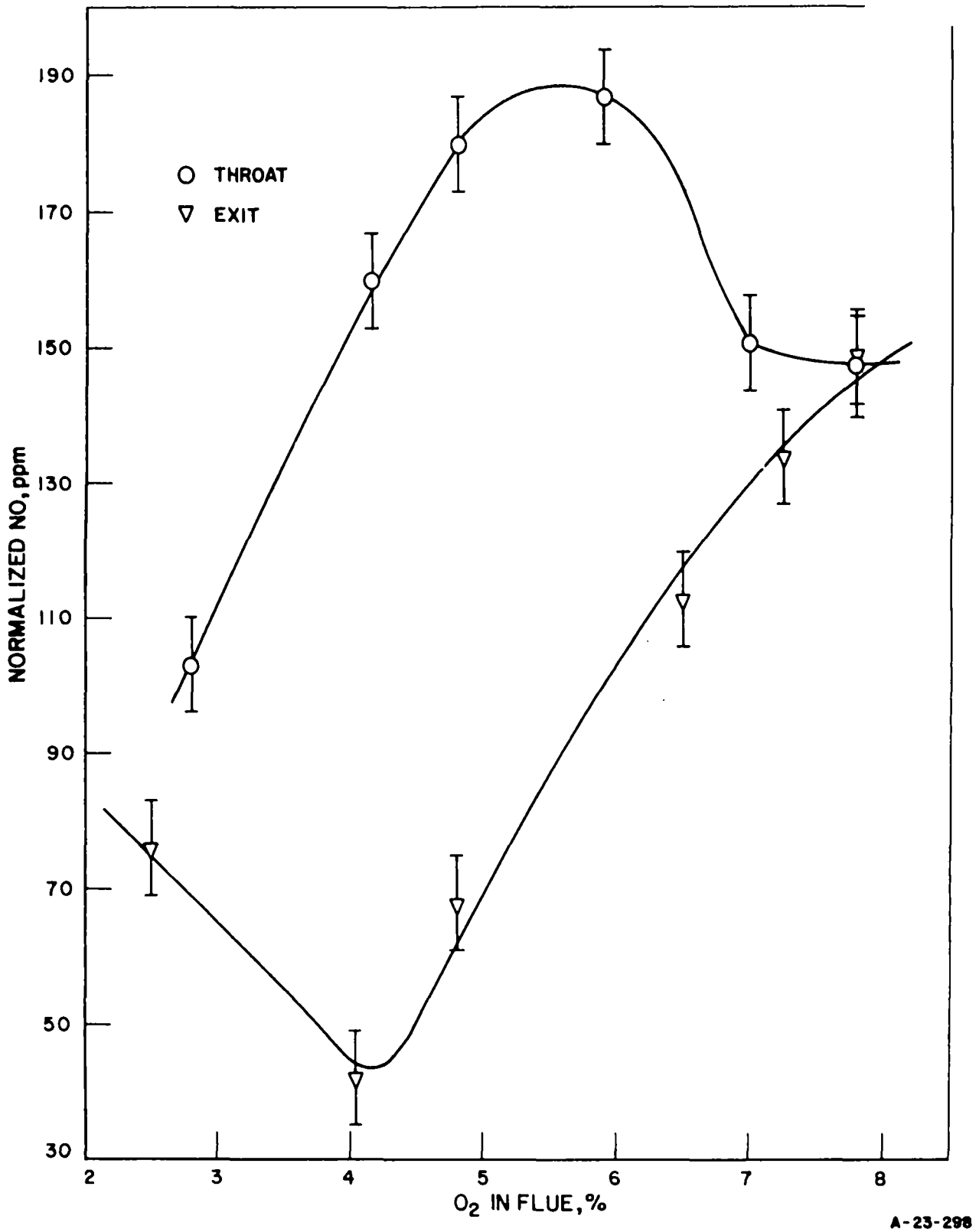

Figure II-237. NORMALIZED NO CONCENTRATION AS A FUNCTION OF EXCESS AIR (Movable-Block Swirl Burner – High Swirl Intensity). GAS INPUT, 1578 CF/hr

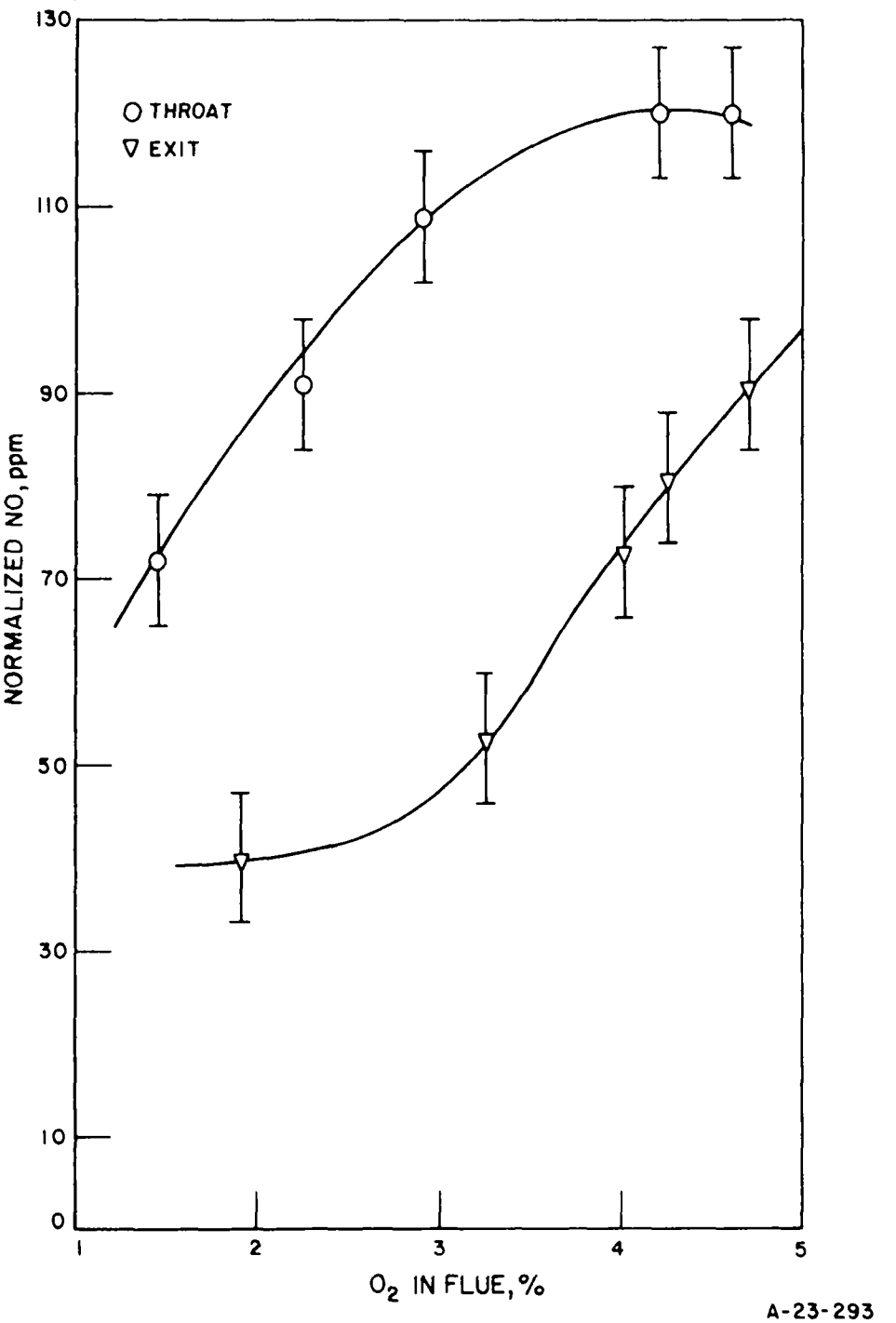

Figure II-238. NORMALIZED NO CONCENTRATION AS A FUNCTION OF EXCESS AIR (Movable-Block Swirl Burner – High Swirl Intensity). GAS INPUT, 1976 CF/hr

Profiles were first obtained by scanning radially at several axial positions. The gas sampling probe was moved at a constant velocity (approximately 1.5 cm/s), with the gas species concentrations continuously measured and displayed on a high-speed strip recorder. These scanning traverses were made at 30-cm axial intervals from the burner wall and the data inspected for the degree of primary and secondary combustion, as well as for the NO concentration and its variation with radial position. From these analyses, we determined that a point-by-point time-averaged measurement of the gas species, temperature, and velocity should be taken at axial positions of 12.7, 30.5, and 107 cm to obtain the maximum amount of information with the minimum amount of detailed surveys.

To determine the direction of flow in the flame front, continuous radial scans were made at axial positions of 12.7, 30.5, and 107 cm using the two-hole cylindrical Hubbard Probe. These scans are shown in Figures II-239, II-240, and II-241. A positive reading indicates flow moving away from the burner wall and a negative number indicates flow moving toward the burner wall. Although the Hubbard Probe scans give a qualitative illustration of the flow patterns, more quantitative information is required to determine the orientation for the five-hole pitot tube to measure velocities. Therefore, detailed point-by-point profiles were later taken at the appropriate axial position with the pressure differential integrated at each sample point. Table II-56 lists the data for the radial profile taken at the 12.7-cm axial position. Flow reversal occurs in six distinct radial regions, as exhibited by the negative time-averaged pressure differentials. The data obtained for the 30.5-cm and 107-cm axial positions are given in Tables II-57 and II-58.

The time-averaged gas species profiles were run on the swirl burner set for intermediate swirl intensity with a gas input of 2008 CF/hr, with the gas nozzle in the throat position, and with 3.6% excess oxygen. Figure II-242 shows a composite of the gas-sampling profiles taken at an axial position of 12.7 cm from the burner block face. These curves show that methane concentration (curve M) was in excess of 42% on the axis of the burner (0.0 cm). The carbon monoxide (curve C) varied between 0.4 and 2.4% in the region of the burner block (from +7 cm to −7 cm) to a minimum of 200 ppm near the sidewalls of the furnace.

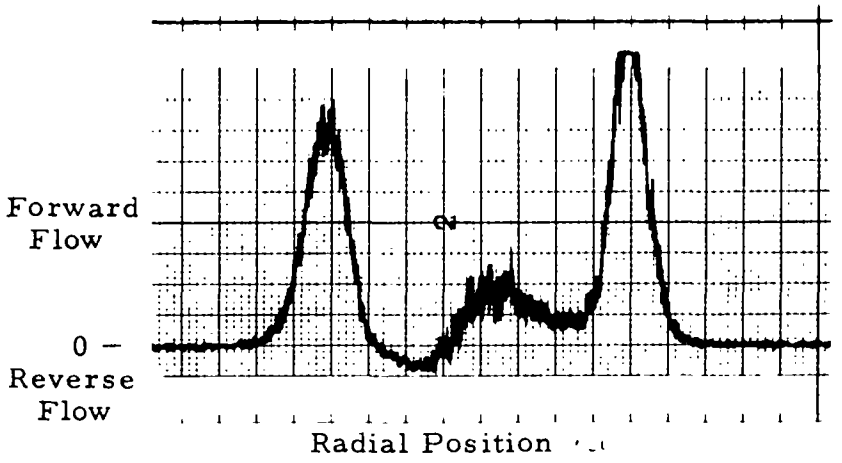

Figure II-239. SCAN OF FLOW DIRECTION AT THE 12.7-cm AXIAL POSITION (Movable-Block Swirl Burner – Intermediate Swirl Intensity). GAS INPUT, 2008 CF/hr; EXCESS OXYGEN, 3.6%; NOZZLE IN THROAT POSITION

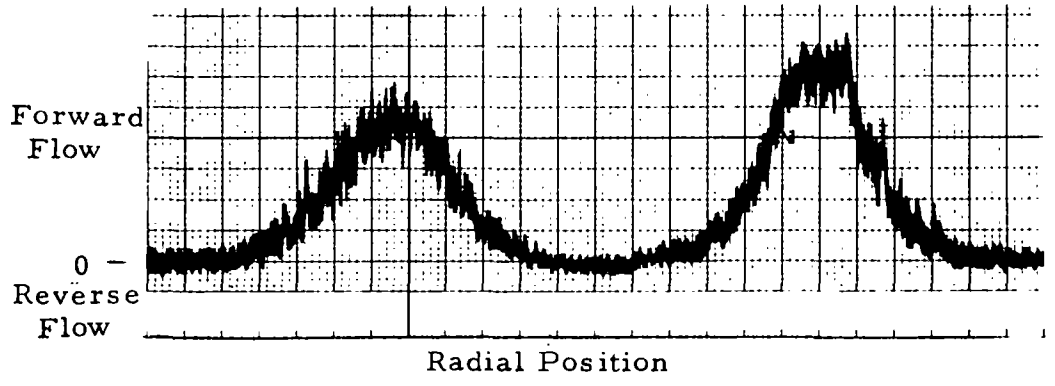

Figure II-240. SCAN OF FLOW DIRECTION AT THE 30.5-cm AXIAL POSITION (Movable-Block Swirl Burner – Intermediate Swirl Intensity). GAS INPUT, 2008 CF/hr; EXCESS OXYGEN, 3.6%; NOZZLE IN THROAT POSITION

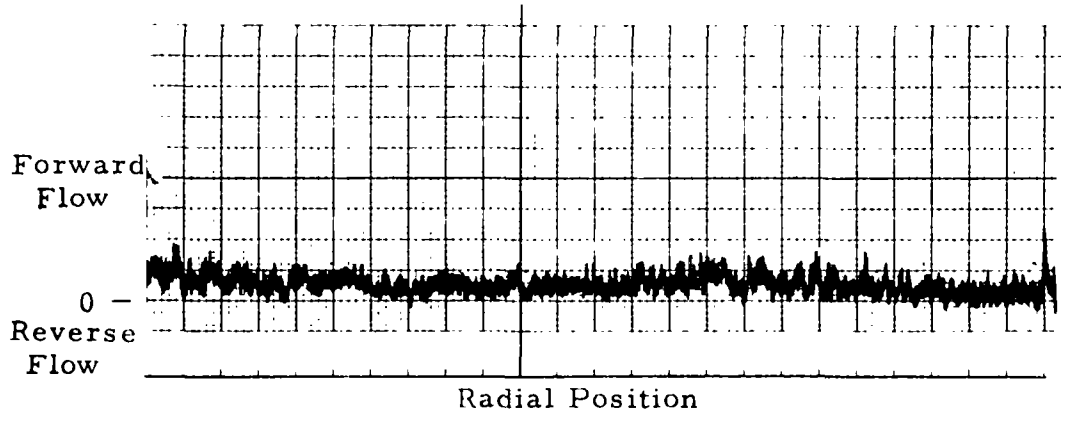

Figure II-241. SCAN OF FLOW DIRECTION AT THE 107-cm AXIAL POSITION (Movable-Block Swirl Burner – Intermediate Swirl Intensity). GAS INPUT, 2008 CF/hr; EXCESS OXYGEN, 3.6%; NOZZLE IN THROAT POSITION

Table II-56. TIME-AVERAGED DIRECTIONAL FLOW DATA OBTAINED AT THE 12.7-cm AXIAL POSITION (Movable-Block Swirl Burner – Intermediate Swirl Intensity). GAS INPUT, 2008 CF/hr; 3.6% EXCESS OXYGEN; NOZZLE IN THROAT POSITION

RP,* cm	Time-Averaged ΔP	RP,* cm	Time-Averaged ΔP	RP,* cm	Time-Averaged ΔP
20	−1.31	6	−7.59	−3	−26.37
17	−1.11	5	−7.5	−4	−20.93
15	0.00	4	−6.3	−5	−7.39
14	+6.87	3	+0.06	−6	+29.87
11	+202.0	2	+7.22	−7	+148.3
10	+204.8	1	+12.37	−8	+282.7
9	+40.6	0	+12.76	−9	+213.0
8	−0.1	−1	−4.51	−10	+91.56
7	−5.76	−2	−19.31	−13	−2.28

*Radial Position

Table II-57. TIME-AVERAGED DIRECTIONAL FLOW DATA AT THE 30.5-cm AXIAL POSITION AND OBTAINED USING A HUBBARD PROBE (Movable-Block Swirl Baffle – Intermediate Swirl Intensity). GAS INPUT, 2008 CF/hr; EXCESS OXYGEN, 3.6%; NOZZLE IN THROAT POSITION

RP,* cm	Time-Averaged ΔP	RP,* cm	Time-Averaged ΔP	RP,* cm	Time-Averaged ΔP
−13	+55.86	−1	−2.09	11	+17.21
−10	+59.82	2	−3.38	14	+42.63
−7	+31.52	5	−1.48	17	+33.37
−4	+4.77	6	−0.88	20	+8.59
−3	+1.58	7	−0.08	23	+1.08
−2	−0.94	8	+1.86	26	−0.53
				29	−0.77

*Radial Position

Table II-58. TIME-AVERAGED DIRECTIONAL FLOW DATA AT THE 107-cm AXIAL POSITION AND OBTAINED USING A HUBBARD PROBE (Movable-Block Swirl Burner – Intermediate Swirl Intensity). GAS INPUT, 2008 CF/hr; EXCESS OXYGEN, 3.6%; NOZZLE IN THROAT POSITION

RP,* cm	Time-Averaged ΔP	RP,* cm	Time-Averaged ΔP	RP,* cm	Time-Averaged ΔP
−13	+0.28	8	+2.21	29	+13.76
−10	+7.52	11	+2.06	32	+11.69
−7	+9.27	14	+3.27	35	+10.05
−4	+9.17	17	+5.27	40	+3.92
−1	+7.43	20	+7.62	45	−0.32
2	+4.71	23	+12.36	50	−0.68
5	+3.12	26	+13.64		

*Radial Position

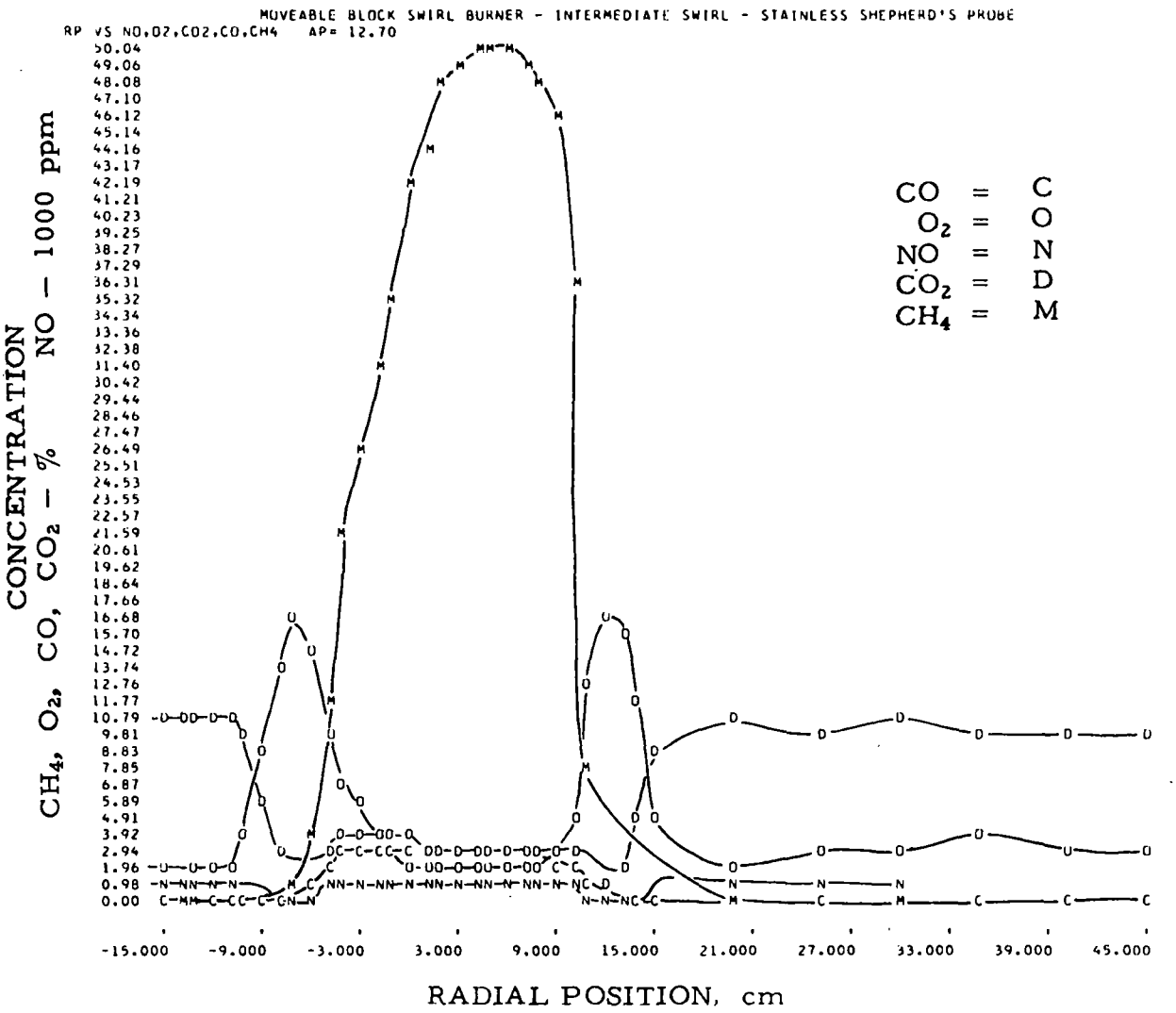

Figure II-242. COMPOSITE PLOT OF GAS SAMPLING PROFILES FOR CO, CO_2, CH_4, NO, AND O_2 AT THE 12.7-cm AXIAL POSITION (Movable-Block Swirl Burner – Intermediate Swirl Intensity). GAS INPUT, 2008 CF/hr; EXCESS OXYGEN, 3.6%; NOZZLE IN THROAT POSITION

Oxygen (curve O) varied from 1.6% at +4 cm to a maximum of 17.1% at a 12-cm radial position and to a recirculation value of 3.1%. Nitric oxide (curve N) had a maximum of 129 ppm at a radial position of 9 cm and a minimum of 0.0 ppm (no instrument reading) at a radial position of 12 cm. Carbon dioxide (curve D) varied from about 0.84% at a radial position of 12 cm to 10.5% in the recirculation zone.

The curves of Figure II-242 were plotted on a single 0-50% scale because of computer limitations. The following legend applies to this figure and some of the others (computer print-outs) that follow:

AP = axial position
RP = radial position

The actual data were collected over a range of concentrations that provided greater resolution of the measuring equipment. Plots of these data are given in Figures II-243 to II-247. The raw and reduced data from which these plots were made are presented in Table II-59. Table II-60 shows the coefficients and standard deviation of the mathematical fit for each gas.

Figure II-248 shows the temperature profile across the furnace at the 12.7-cm axial probe position. These data support the gas concentration analysis in that the "cold" region (temperatures below the 2453°F ambient) of the flame front corresponds to positions of high oxygen (12 cm and −7 cm) and methane (35 cm) concentrations, with the "hot" regions (temperatures above 2426°F ambient and positions of 11 cm and −4 cm) appearing at the point where the stoichiometric mixture between oxygen and methane is achieved.

Figure II-249 displays the tangential component of velocity as a function of radial position at a 12.7-cm axial probe position. Peaks occur in the forward velocity at −8 cm, 3 cm, and 13 cm. By comparing these peaks with the temperature and gas concentration analysis, we conclude that good agreement exists with the positions of the high concentrations of oxygen and methane. Figure II-250 shows the axial velocity component.

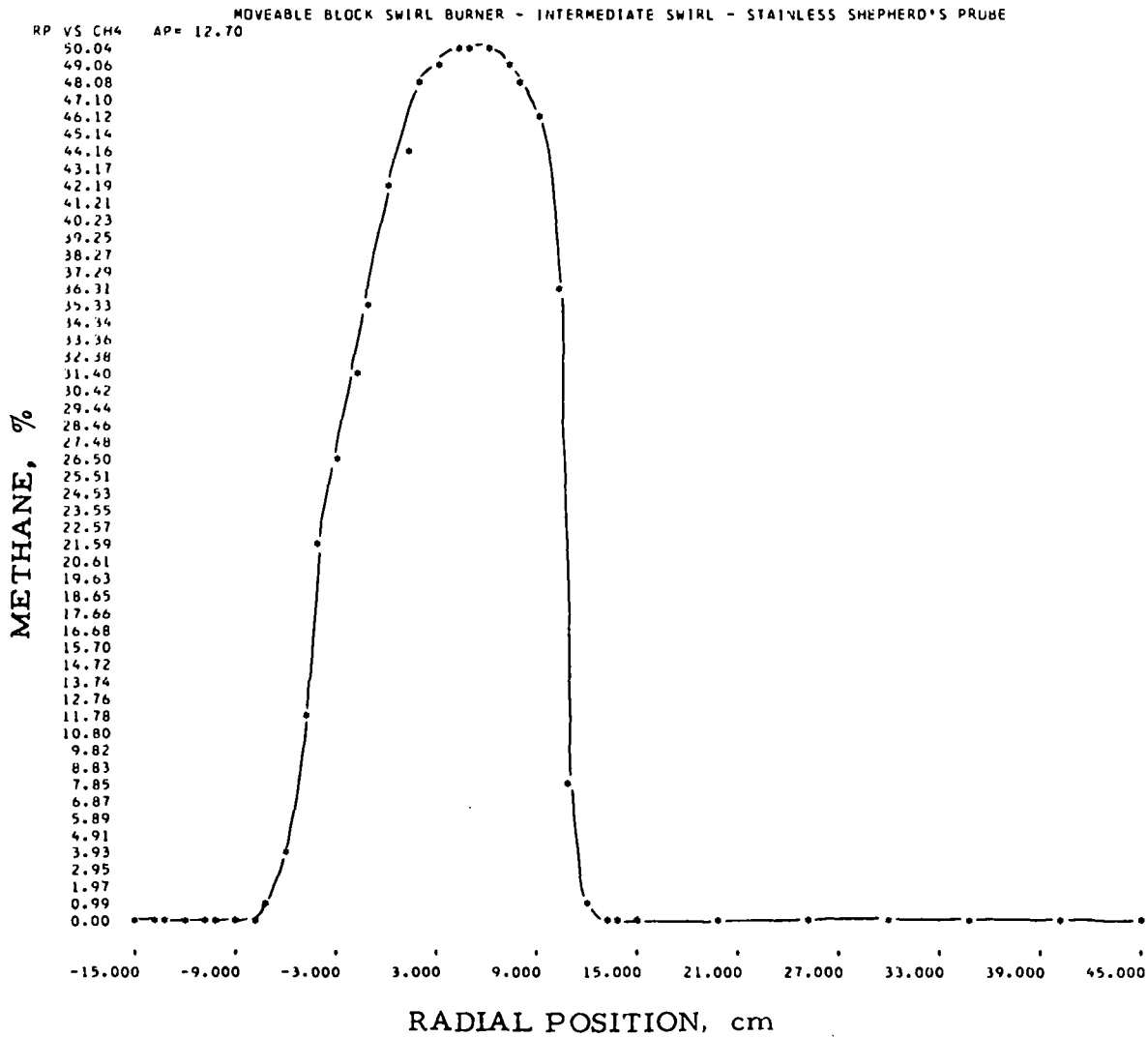

Figure II-243. RADIAL PROFILE FOR CH_4 AT THE 12.7-cm AXIAL POSITION (Movable-Block Swirl Burner – Intermediate Swirl Intensity). GAS INPUT, 2008 CF/hr; EXCESS OXYGEN, 3.6%; NOZZLE IN THROAT POSITION

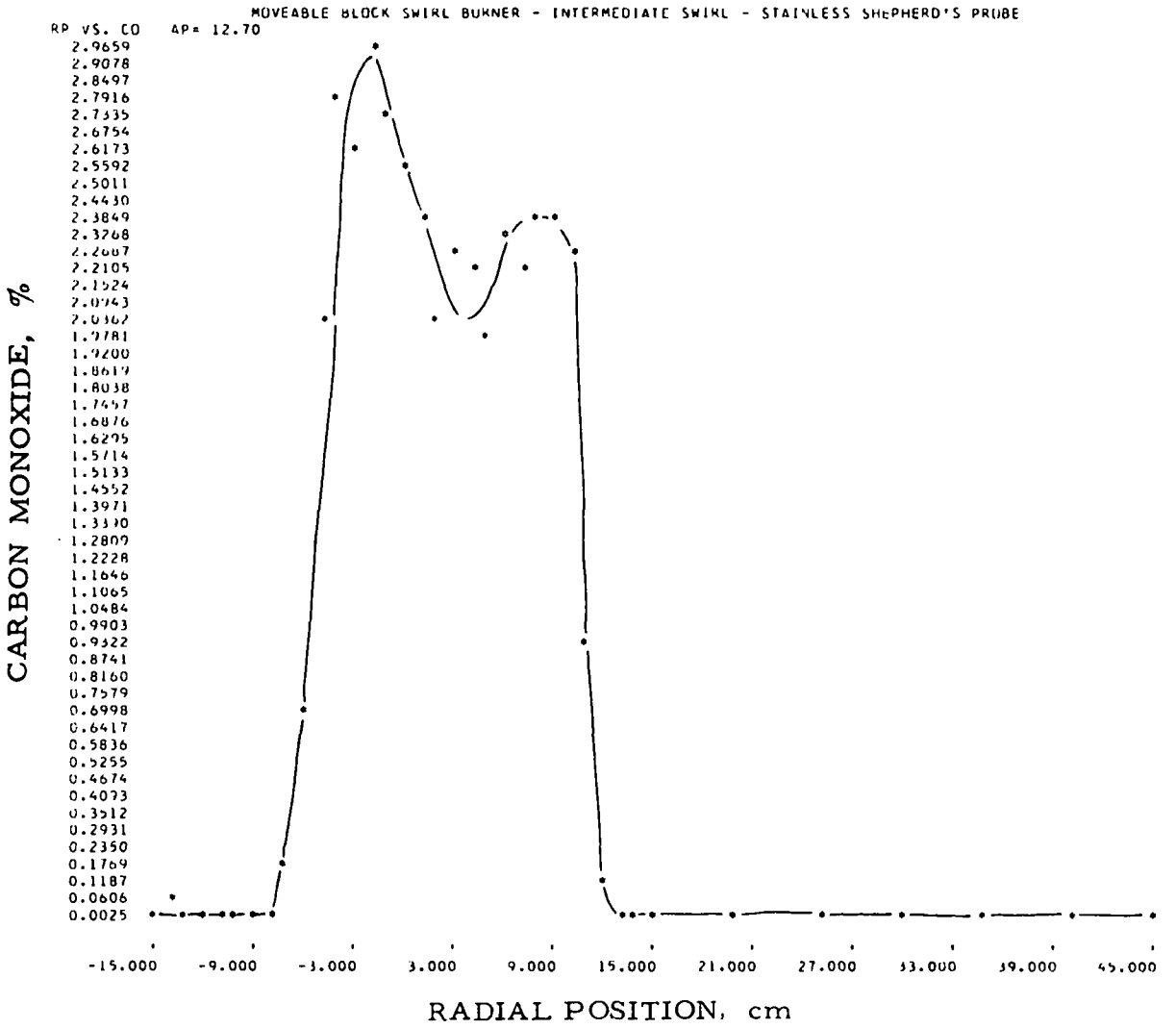

Figure II-244. RADIAL PROFILE FOR CO AT THE 12.7-cm AXIAL POSITION (Movable-Block Swirl Burner – Intermediate Swirl Intensity). GAS INPUT, 2008 CF/hr; EXCESS OXYGEN, 3.6% ; NOZZLE IN THROAT POSITION

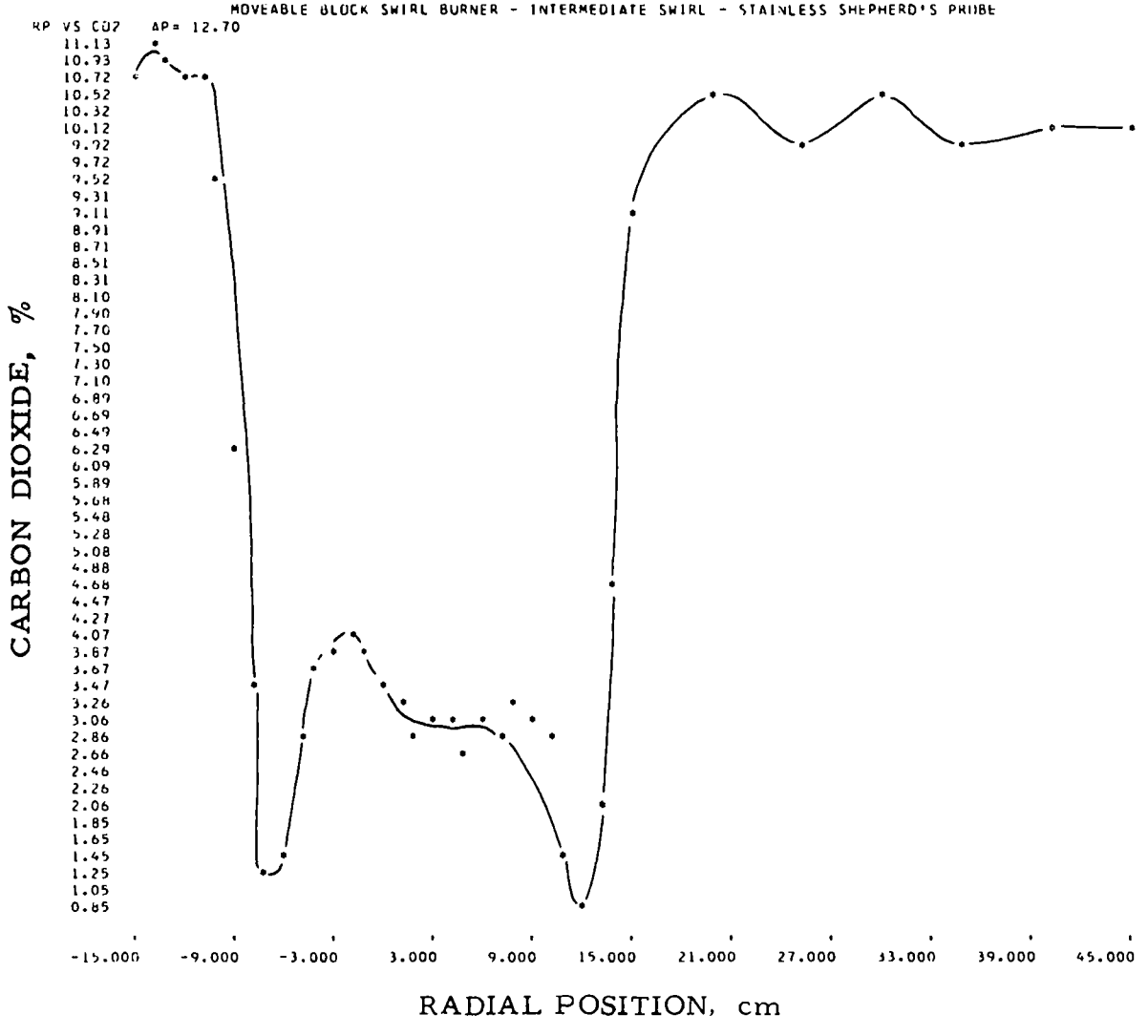

Figure II-245. RADIAL PROFILE FOR CO_2 AT THE 12.7-cm AXIAL POSITION (Movable-Block Swirl Burner — Intermediate Swirl Intensity). GAS INPUT, 2008 CF/hr; EXCESS OXYGEN, 3.6%; NOZZLE IN THROAT POSITION

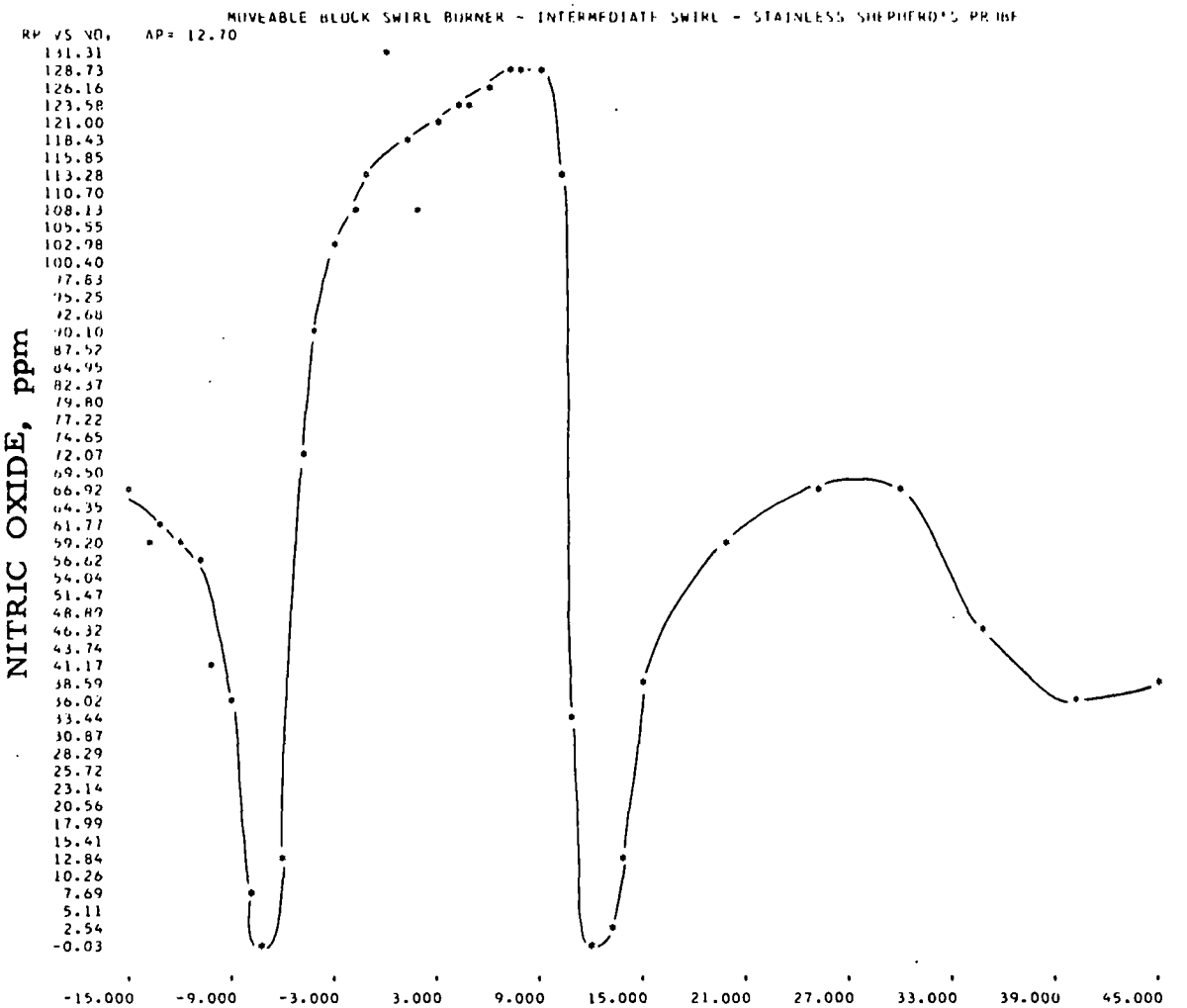

Figure II-246. RADIAL PROFILE FOR NO AT THE 12.7-cm AXIAL POSITION (Movable-Block Swirl Burner – Intermediate Swirl Intensity). GAS INPUT, 2008 CF/hr; EXCESS OXYGEN, 3.6%; NOZZLE IN THROAT POSITION

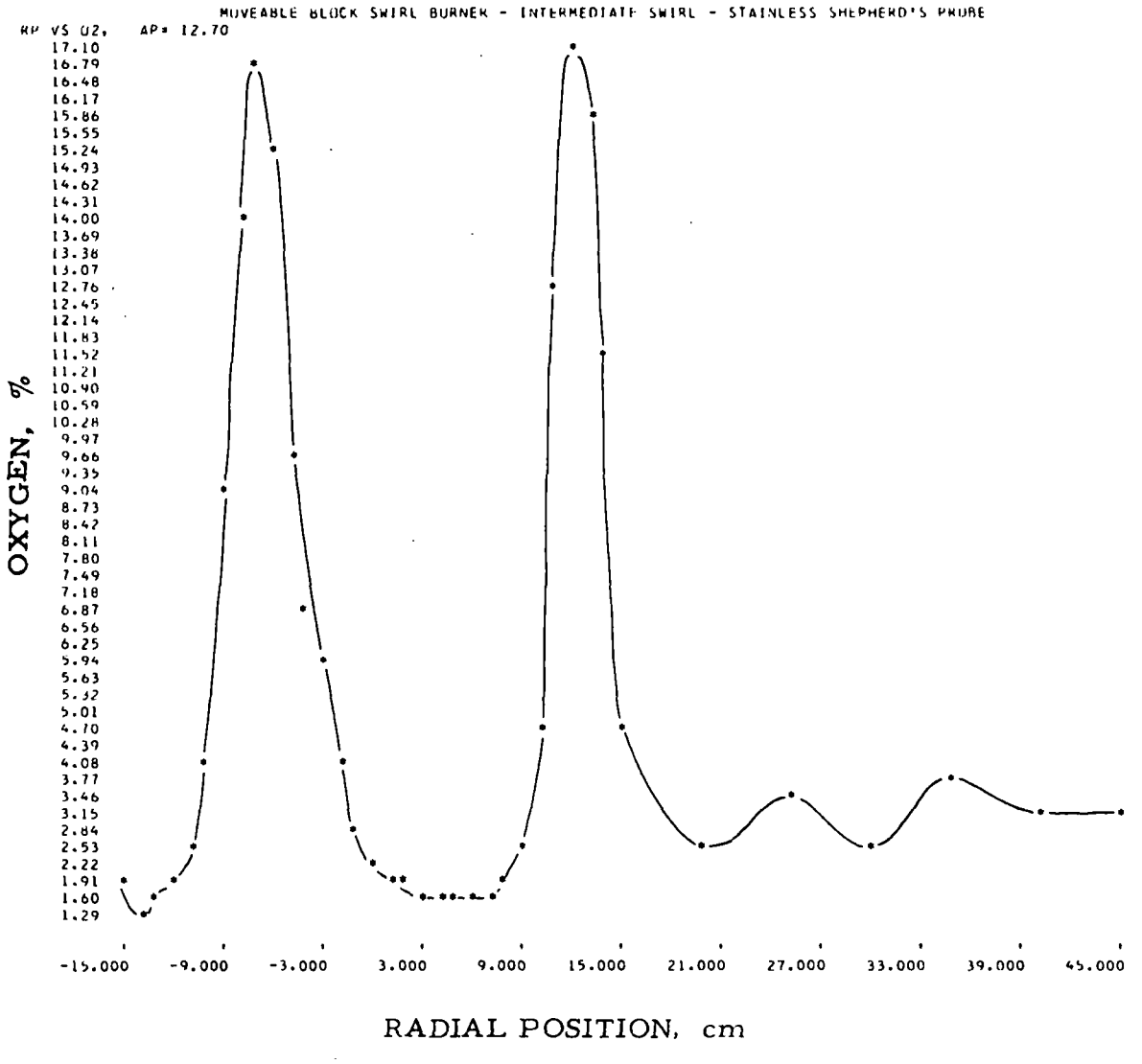

Figure II-247. RADIAL PROFILE FOR O_2 AT THE 12.7-cm AXIAL POSITION (Movable-Block Swirl Burner – Intermediate Swirl Intensity). GAS INPUT, 2008 CF/hr; EXCESS OXYGEN, 3.6% ; NOZZLE IN THROAT POSITION

Table II-59. TIME-AVERAGED RADIAL PROFILE OBTAINED AT THE 12.7-cm AXIAL POSITION

TRACER GAS STUDIES OF COMBUSTION BURNERS PROGRAM 2
MOVEABLE BLOCK SWIRL BURNER - INTERMEDIATE SWIRL - STAINLESS SHEPHERD'S PROBE

INPUT GAS 2008 WALL TEMPERATURE 2453 PREHEAT TEMPERATURE 0
OUTPUT ANALYSIS
NITROGEN OXIDE 56.70 PERCENT ON RANGE 3, 111.09 PPM OXYGEN 3.60 PERCENT
CARBON DIOXIDE 79.30 PERCENT ON RANGE 1, 9.96 PERCENT
CARBON MONOXIDE 10.40 PERCENT ON RANGE 3, 0.004 PERCENT
METHANE 0.00 PERCENT ON RANGE 0, 0.00 PERCENT

EXPERIMENTAL RESULTS

		NITROGEN OXIDE -NO			OXYGEN	CARBON DIOXIDE-CO2			CARBON MONOXIDE -CO			METHANE - CH4		
AP	RP	RANGE	X	Y	O2	RANGE	X	Y	RANGE	X	Y	RANGE	X	Y
12.70	-15.00	3	34.30	66.4	2.06	1	83.30	10.82	3	13.40	0.005	3	0.90	0.04
12.70	-14.00	3	31.20	60.3	1.29	1	84.70	11.12	3	69.50	0.032	3	0.30	0.01
12.70	-13.00	3	31.60	61.1	1.52	1	84.00	10.97	3	61.10	0.028	3	0.20	0.01
12.70	-12.00	3	30.80	59.6	1.87	1	83.00	10.75	3	51.20	0.022	3	0.50	0.02
12.70	-11.00	3	29.20	56.4	2.44	1	82.70	10.69	3	37.30	0.016	3	0.70	0.03
12.70	-10.00	3	21.50	41.4	4.14	1	77.00	9.49	3	46.40	0.020	3	2.00	0.08
12.70	-9.00	3	19.10	36.7	9.08	1	60.10	6.34	2	1.30	0.022	3	1.20	0.05
12.70	-8.00	3	3.60	6.8	13.90	1	40.30	3.42	3	66.80	0.031	3	3.40	0.14
12.70	-7.00	3	0.00	-0.0	16.80	1	19.20	1.23	2	10.50	0.172	3	22.50	0.96
12.70	-6.00	3	6.40	12.2	15.20	1	21.80	1.45	2	38.70	0.675	3	73.40	3.51
12.70	-5.00	3	36.70	71.2	9.60	1	36.00	2.90	1	53.80	2.019	1	73.80	12.12
12.70	-4.00	3	46.00	89.6	6.79	1	42.10	3.65	1	67.30	2.767	1	104.00	21.12
12.70	-3.00	3	52.60	102.8	5.86	1	43.70	3.86	1	65.00	2.633	1	120.00	26.84
12.70	-2.00	3	55.00	107.6	4.00	1	45.40	4.09	1	70.60	2.965	1	132.00	31.57
12.70	-1.00	3	58.20	114.1	2.90	1	43.00	3.77	1	66.70	2.732	1	142.00	35.60
12.70	0.00	3	66.70	131.3	2.17	1	40.40	3.43	1	63.30	2.535	1	156.00	42.15
12.70	1.00	3	60.70	119.1	1.94	1	39.10	3.27	1	61.00	2.406	1	160.00	44.06
12.70	2.00	3	55.60	108.8	1.83	1	35.60	2.85	1	54.60	2.060	1	168.00	48.00
12.70	3.00	3	61.40	120.5	1.61	1	37.40	3.06	1	58.00	2.241	1	170.00	49.02
12.70	4.00	3	63.40	124.6	1.56	1	37.00	3.02	1	57.90	2.236	1	172.00	50.04
12.70	5.00	3	62.80	123.4	1.68	1	33.70	2.63	1	52.90	1.972	1	172.00	50.04
12.70	6.00	3	63.90	125.6	1.58	1	37.70	3.10	1	59.30	2.312	1	172.00	50.04
12.70	7.00	3	65.90	129.6	1.74	1	35.60	2.85	1	57.30	2.203	1	170.00	49.02
12.70	8.00	3	65.10	128.0	1.93	1	38.20	3.16	1	60.40	2.372	1	168.00	48.00
12.70	9.00	3	65.70	129.2	2.60	1	38.10	3.15	1	60.50	2.378	1	164.00	46.01
12.70	10.00	3	57.40	112.5	4.70	1	36.30	2.93	1	58.00	2.241	1	144.00	36.68
12.70	11.00	3	17.20	33.0	12.80	1	21.70	1.44	1	29.30	0.910	1	56.00	7.92
12.70	12.00	3	0.00	-0.0	17.10	1	14.10	0.84	1	3.90	0.100	3	26.00	1.14
12.70	13.00	3	0.70	1.2	15.90	1	28.00	2.03	3	49.40	0.022	3	6.90	0.29
12.70	14.00	3	6.60	12.5	11.60	1	50.10	4.76	3	45.70	0.020	3	2.70	0.11
12.70	15.00	3	19.80	38.1	4.65	1	75.50	9.18	3	61.40	0.028	3	0.90	0.04
12.70	20.00	3	30.90	59.7	2.41	1	81.90	10.51	3	27.40	0.011	3	0.00	0.00
12.70	25.00	3	34.70	67.2	3.34	1	79.50	10.00	3	9.40	0.003	3	0.00	0.00
12.70	30.00	3	35.00	67.8	2.66	1	81.90	10.51	3	14.20	0.005	3	0.00	0.00
12.70	35.00	3	23.90	46.0	3.66	1	79.20	9.94	3	6.20	0.002	3	0.00	0.00
12.70	40.00	3	18.30	35.1	3.12	1	80.10	10.13	3	7.00	0.002	3	0.00	0.00
12.70	45.00	3	20.70	39.8	3.09	1	80.10	10.13	3	6.50	0.002	3	0.00	0.00

Table II-60. COEFFICIENTS AND STANDARD DEVIATIONS OF THE MATHEMATICAL FIT FOR EACH GAS

TRACER GAS STUDIES OF COMBUSTION BURNERS PROGRAM 2

NO-RANGE 1

X	OBSERVED Y	COMPUTED Y	STANDARD DEVIATION ON Y	COEFFICIENTS, Y=C(1)+C(2)*X+..+C(N+1)*X**
0.000	0.000	1.192	7.04546	C(1)= 1.1920803
28.000	250.000	245.365		C(2)= 8.2232437
55.000	500.000	507.189		C(3)= 0.0177582
77.500	750.000	745.154		
100.000	1000.000	1001.099		

NO-RANGE 3

X	OBSERVED Y	COMPUTED Y	STANDARD DEVIATION ON Y	COEFFICIENTS, Y=C(1)+C(2)*X+..+C(N+1)*X**
0.000	0.000	-0.038	0.34061	C(1)= -0.0388039
26.000	50.000	50.192		C(2)= 1.9082312
51.000	100.000	99.657		C(3)= 0.0009138
76.000	150.000	150.265		
100.000	200.000	199.922		

CO2 RANGE 1

X	OBSERVED Y	COMPUTED Y	STANDARD DEVIATION ON Y	COEFFICIENTS, Y=C(1)+C(2)*X+..+C(N+1)*X**
0.000	0.000	0.060	0.33791	C(1)= 0.0607462
41.200	3.750	3.540		C(2)= 0.0406835
67.000	7.500	7.555		C(3)= 0.0010623
87.000	11.300	11.641		
100.000	15.000	14.752		

CO2 RANGE 2

X	OBSERVED Y	COMPUTED Y	STANDARD DEVIATION ON Y	COEFFICIENTS, Y=C(1)+C(2)*X+..+C(N+1)*X**
0.000	0.000	0.008	0.04551	C(1)= 0.0086310
33.000	1.250	1.232		C(2)= 0.0305986
59.000	2.500	2.484		C(3)= 0.0001873
82.000	3.750	3.802		
100.000	5.000	4.972		

CO2 RANGE 3

X	OBSERVED Y	COMPUTED Y	STANDARD DEVIATION ON Y	COEFFICIENTS, Y=C(1)+C(2)*X+..+C(N+1)*X**
0.000	0.000	0.000	0.00285	C(1)= 0.0005971
32.000	0.125	0.123		C(2)= 0.0033220
58.000	0.250	0.248		C(3)= 0.0000165
81.000	0.375	0.378		
100.000	0.500	0.498		

CO RANGE 1

X	OBSERVED Y	COMPUTED Y	STANDARD DEVIATION ON Y	COEFFICIENTS, Y=C(1)+C(2)*X+..+C(N+1)*X**
0.000	0.000	0.007	0.02630	C(1)= 0.0074353
37.000	1.250	1.223		C(2)= 0.0229367
63.000	2.500	2.516		C(3)= 0.0002686
83.000	3.750	3.762		
100.000	5.000	4.987		

CO RANGE 2

X	OBSERVED Y	COMPUTED Y	STANDARD DEVIATION ON Y	COEFFICIENTS, Y=C(1)+C(2)*X+..+C(N+1)*X**
0.000	0.000	0.001	0.00766	C(1)= 0.0017783
29.100	0.500	0.497		C(2)= 0.0156220
55.000	1.000	0.996		C(3)= 0.0000411
79.000	1.500	1.508		
100.000	2.000	1.995		

CO RANGE 3

X	OBSERVED Y	COMPUTED Y	STANDARD DEVIATION ON Y	COEFFICIENTS, Y=C(1)+C(2)*X+..+C(N+1)*X**
0.000	0.000	0.000	0.00019	C(1)= 0.0000444
29.100	0.012	0.012		C(2)= 0.0003955
55.000	0.025	0.024		C(3)= 0.0000010
79.000	0.037	0.037		
100.000	0.050	0.049		

Table II-60, Cont. COEFFICIENTS AND STANDARD DEVIATIONS OF THE MATHEMATICAL FIT FOR EACH GAS

TRACER GAS STUDIES OF COMBUSTION BURNERS PROGRAM 2

CH4 RANGE 1

X	OBSERVED Y	COMPUTED Y	STANDARD DEVIATION ON Y	COEFFICIENTS, Y=C(1)+C(2)*X+..+C(N+1)*X**N
0.000	0.000	0.084	0.33885	C(1)= 0.0843171
39.100	5.000	4.701		C(2)= 0.0673895
66.000	10.000	10.181		C(3)= 0.0012968
85.200	15.000	15.240		
100.000	20.000	19.792		

CH4 RANGE 2

X	OBSERVED Y	COMPUTED Y	STANDARD DEVIATION ON Y	COEFFICIENTS, Y=C(1)+C(2)*X+..+C(N+1)*X**N
0.000	0.000	0.012	0.03837	C(1)= 0.0122515
32.500	2.500	2.467		C(2)= 0.0633469
58.800	5.000	5.007		C(3)= 0.0003571
81.000	7.500	7.534		
100.000	10.000	9.978		

CH4 RANGE 3

X	OBSERVED Y	COMPUTED Y	STANDARD DEVIATION ON Y	COEFFICIENTS, Y=C(1)+C(2)*X+..+C(N+1)*X**N
0.000	0.000	0.004	0.01073	C(1)= 0.0041916
28.000	1.250	1.240		C(2)= 0.0419261
54.000	2.500	2.500		C(3)= 0.0000797
78.000	3.750	3.759		
100.000	5.000	4.994		

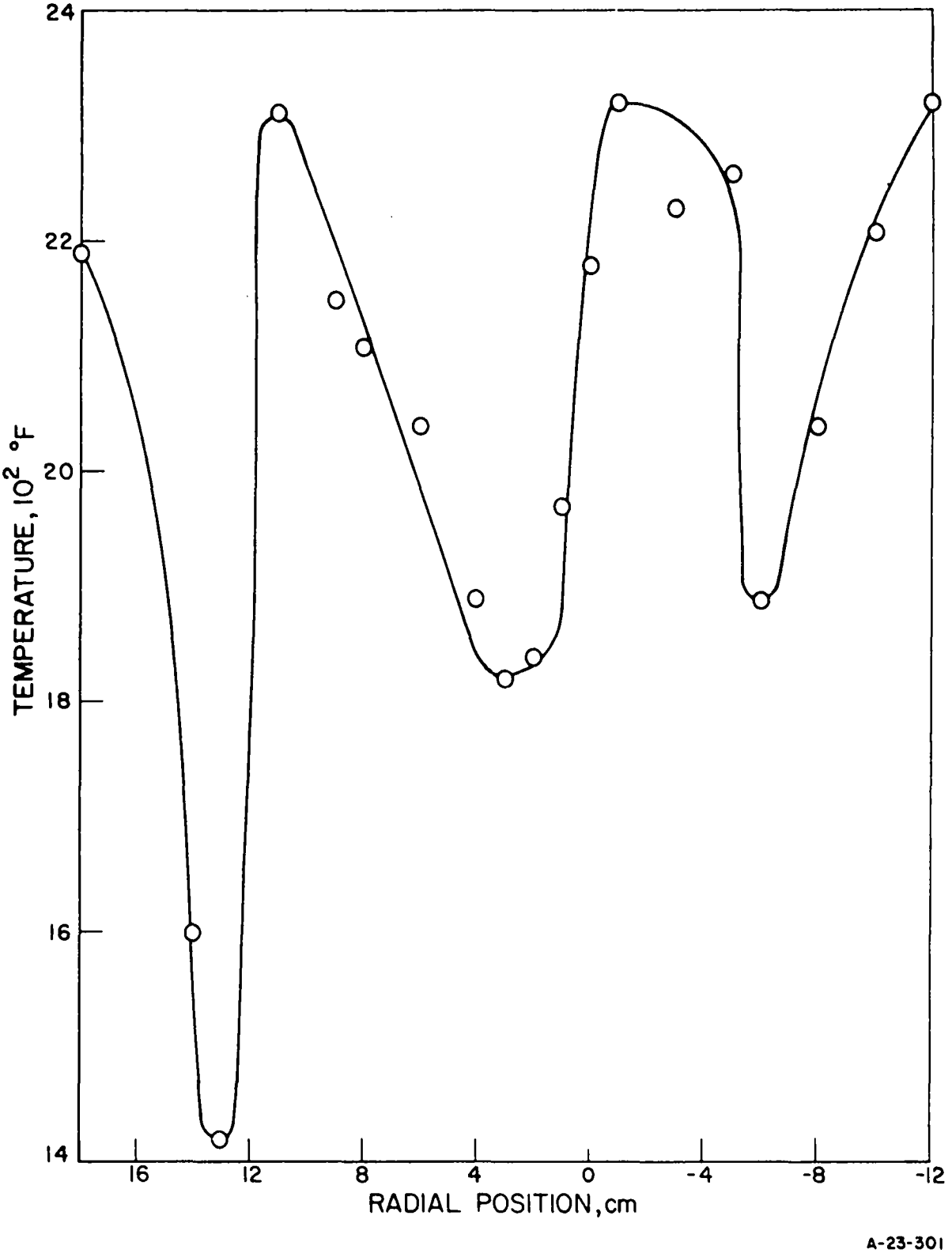

Figure II-248. RADIAL TEMPERATURE PROFILE AT THE 12.7-cm AXIAL POSITION (Movable-Block Swirl Burner – Intermediate Intensity). GAS INPUT, 2008 CF/hr; EXCESS OXYGEN; 3.6%, NOZZLE IN THROAT POSITION

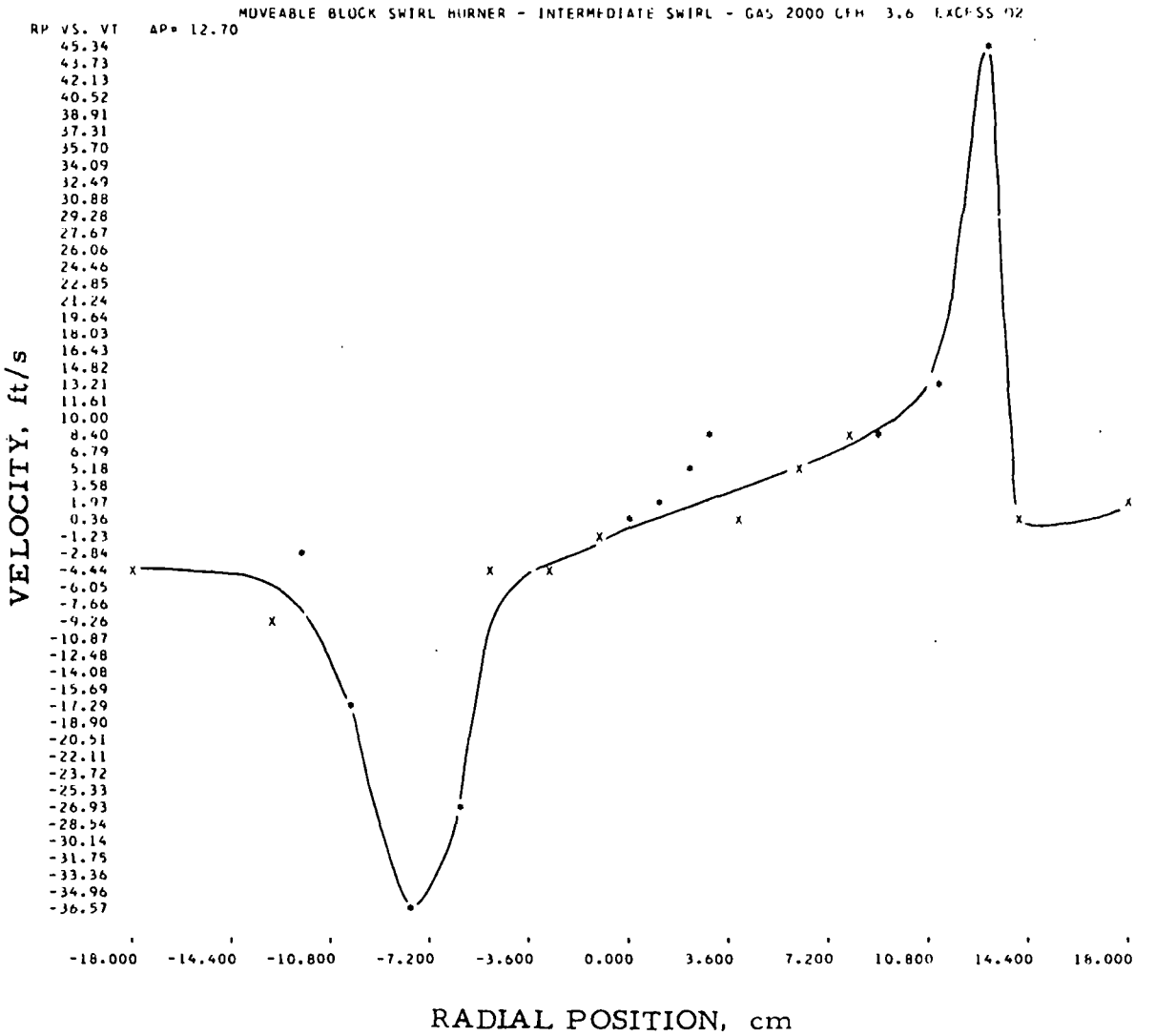

Figure II-249. TANGENTIAL VELOCITY PROFILE AT THE 12.7-cm AXIAL POSITION (Movable-Block Swirl Burner – Intermediate Swirl Intensity). GAS INPUT, 2000 CF/hr; EXCESS OXYGEN, 3.6%; NOZZLE IN THROAT POSITION

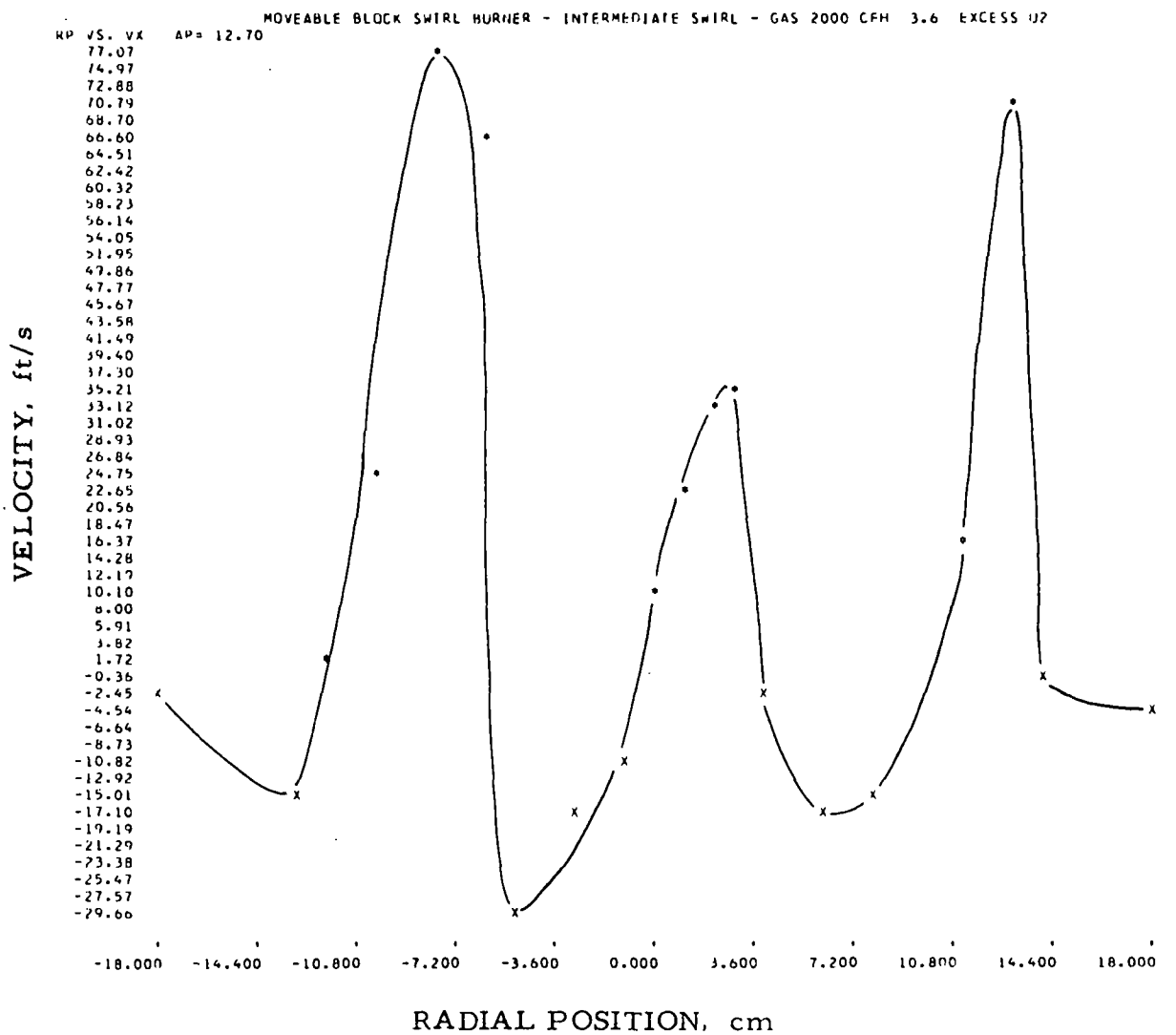

Figure II-250. AXIAL VELOCITY PROFILE AT THE 12.7-cm AXIAL POSITION (Movable-Block Swirl Burner – Intermediate Swirl Intensity). GAS INPUT, 2000 CF/hr; EXCESS OXYGEN, 3.6% ; NOZZLE IN THROAT POSITION

Figure II-251 shows a composite plot of the CO, CO_2, CH_4, NO, and O_2 at an axial position of 30.5 cm. The maximum methane concentration has decreased from more than 50 to 8.2%. In contrast, the CO has increased from 2 to 5% in the burner block region. The nitric oxide concentration ranges in values from a maximum of 103 ppm to a minimum of 32 ppm. The oxygen readings show that the peak concentrations of air are now at −12 cm and 26 cm, as compared with the previous positions of −8 cm and 13 cm at an axial position of 12.7 cm. Data plots with greater resolution are given in Figures II-252 to II-256. Raw data appear in Table II-61.

Figure II-257 shows the temperature profile at the 30.5-cm axial position. The central "cold" spot has moved to 10 cm, accompanied by a 600°F temperature increase, and the outside cold spots have disappeared. The "hot" regions are now at −7 cm and 21 cm, which corresponds nicely with the points where the stoichiometric mixture of CH_4 and O_2 are achieved (−7 cm and 20 cm).

Figure II-258 displays the axial component of velocity as a function of radial position at 30.5 cm. Interestingly, the central portion of the flame front (−2 cm to 7 cm) displays reverse flow. The magnitude of the peak axial velocity has decreased 40% from its value at the 12.7-cm axial position. The tangential velocity, shown in Figure II-259, displays a uniform peak of magnitude 18.6 ft/s about the 20-cm radial position.

The composite plot of the gas species concentrations for an axial position of 107 cm is given in Figure II-260. There is no trace of methane at this axial position. The oxygen (O curve) shows an average value of 1% in the region of the burner block, with a linear increase to 5.3% near the sidewall of the furnace. The nitric oxide (curve N) has an average value of 36 ppm in the burner block region, with a gradual decrease to 21.5 ppm near the furnace sidewall. The CO concentration (curve C) has a peak value of 2.8% near the axis of the burner and drops to 4200 ppm near the sidewalls.

The data plot of Figure II-260 is shown with greater resolution in Figures II-261 to II-264. The raw data from which these plots were made are given in Table II-62.

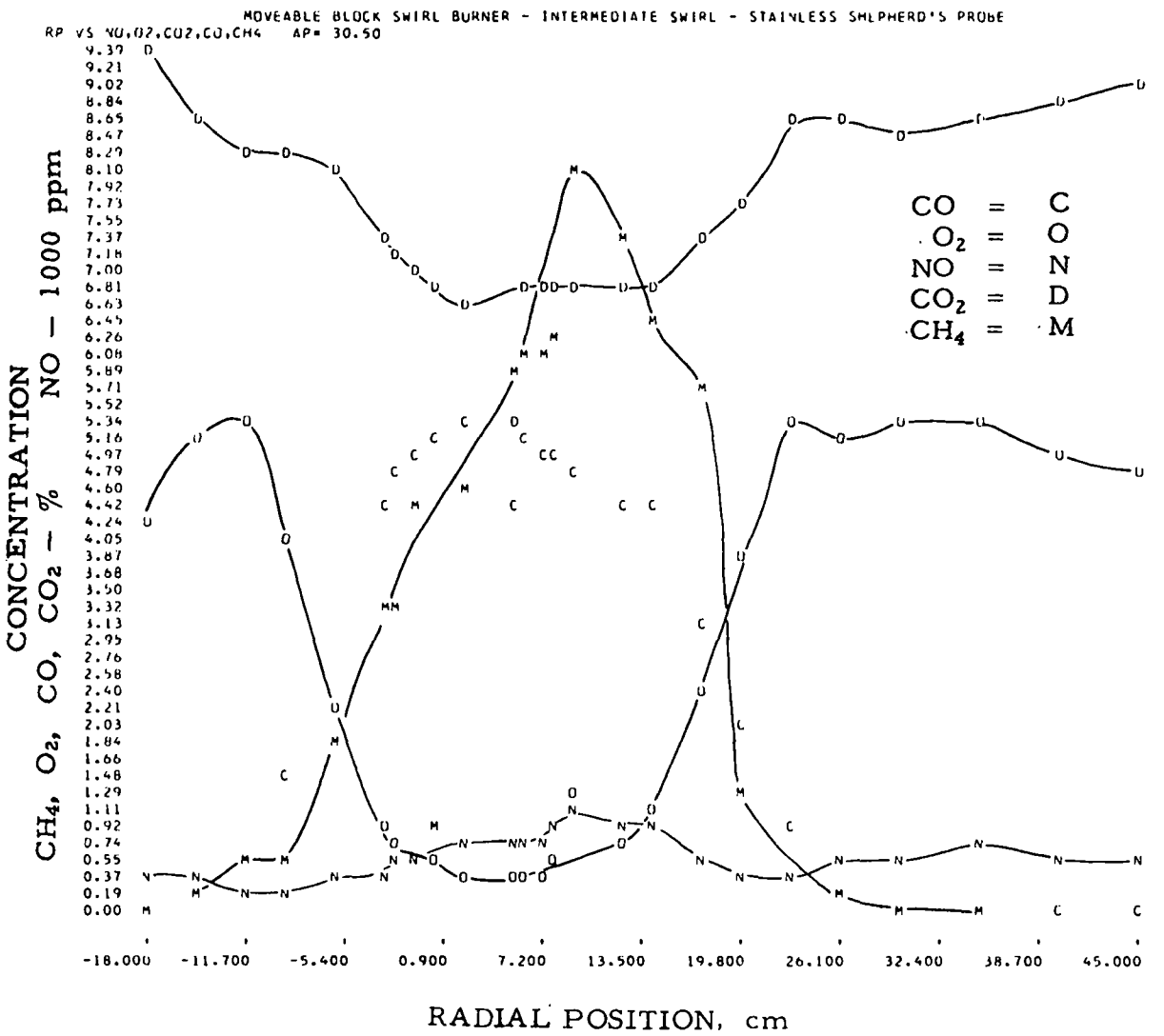

Figure II-251. COMPOSITE PLOT OF GAS SAMPLING PROFILES FOR CO, CO_2, CH_4, NO, AND O_2 AT THE 30.5-cm AXIAL POSITION (Movable-Block Swirl Burner – Intermediate Swirl Intensity). GAS INPUT, 2008 CF/hr; EXCESS OXYGEN, 3.6%; NOZZLE IN THROAT POSITION

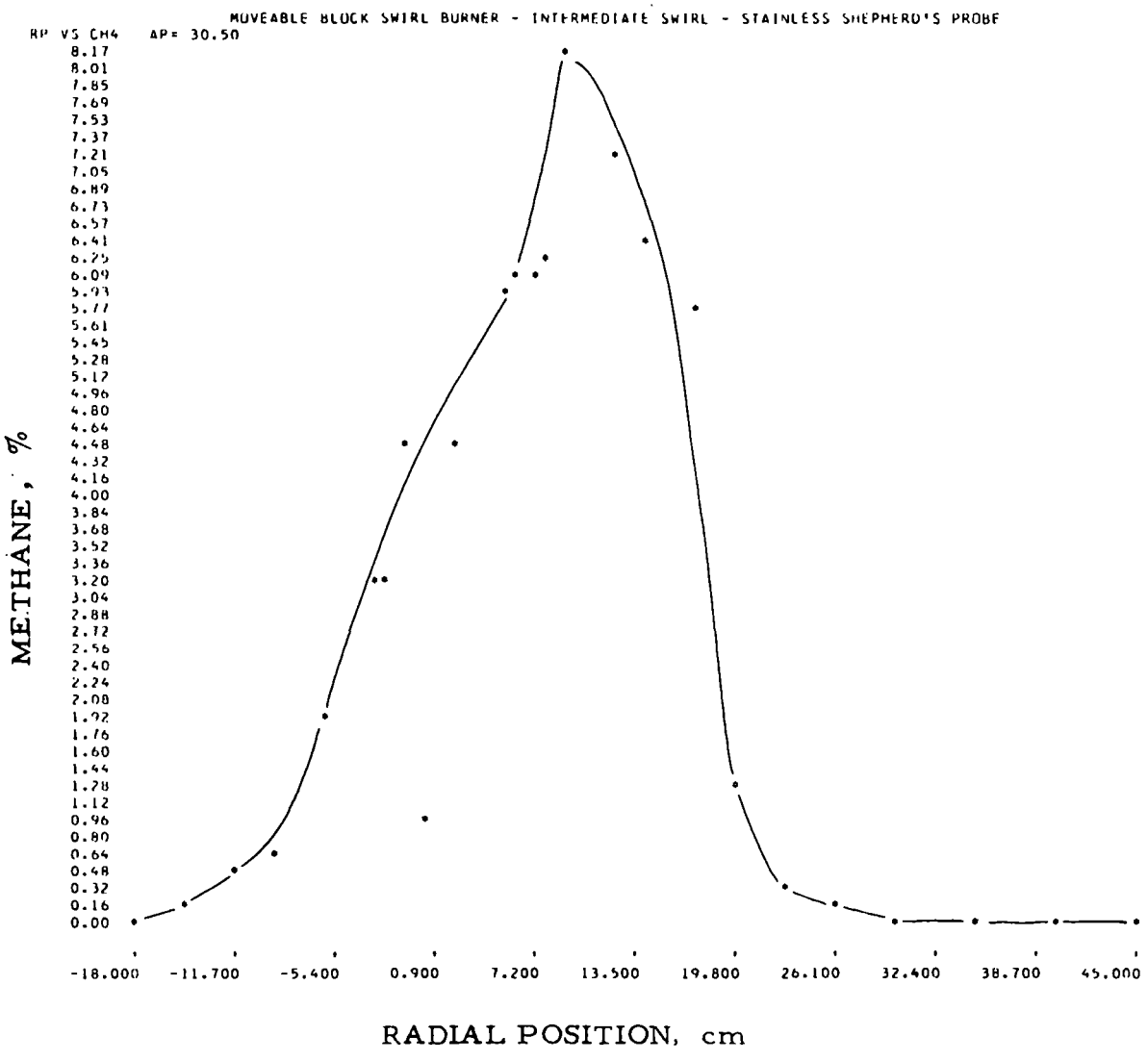

Figure II-252. RADIAL PROFILE FOR CH_4 AT THE 30.5-cm AXIAL POSITION (Movable-Block Swirl Burner – Intermediate Swirl Intensity). GAS INPUT, 2008 CF/hr; EXCESS OXYGEN, 3.6%; NOZZLE IN THROAT POSITION

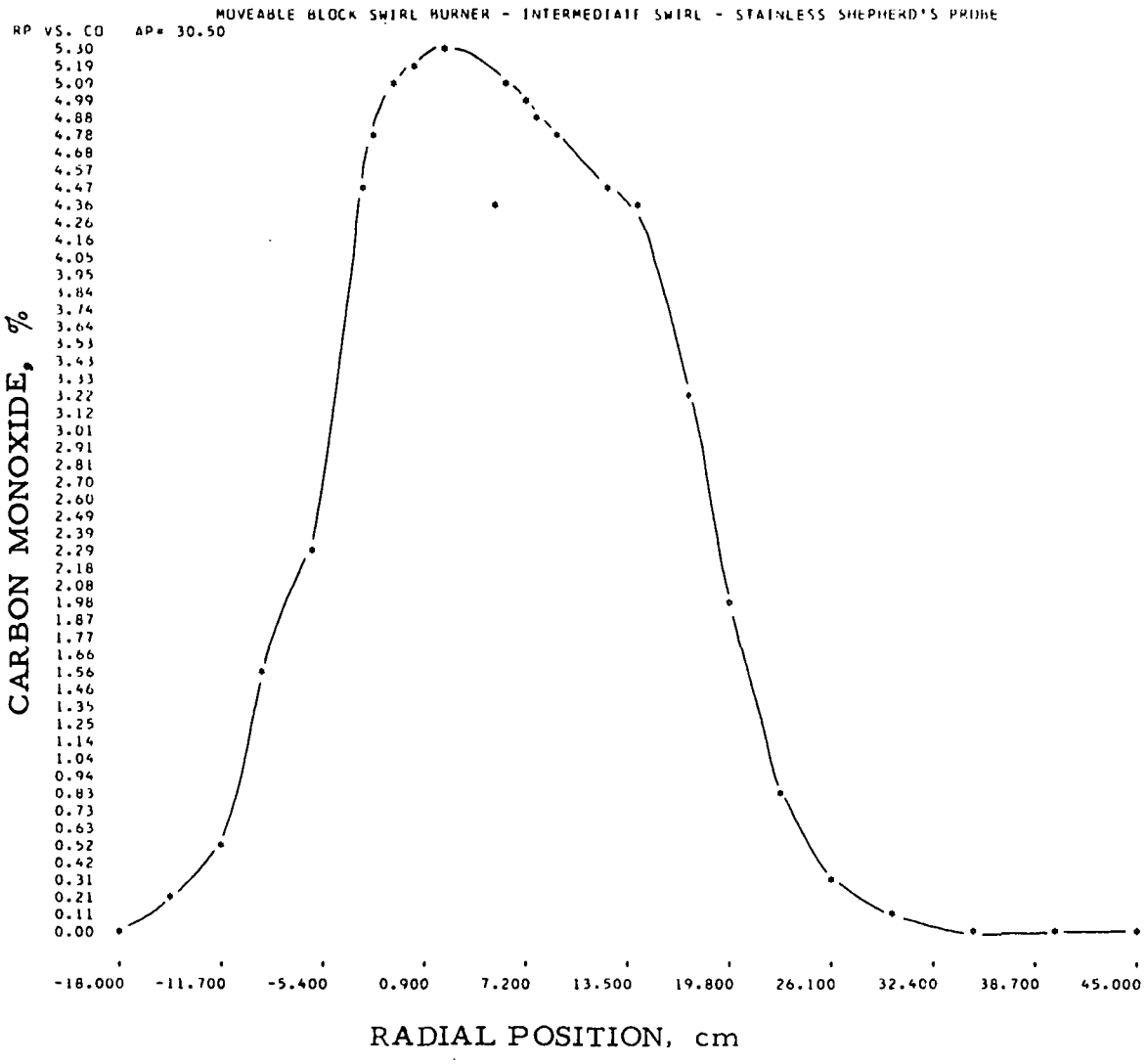

Figure II-253. RADIAL PROFILE FOR CO AT THE 30.5-cm AXIAL POSITION (Movable-Block Swirl Burner – Intermediate Swirl Intensity). GAS INPUT, 2008 CF/hr; EXCESS OXYGEN, 3.6% ; NOZZLE IN THROAT POSITION

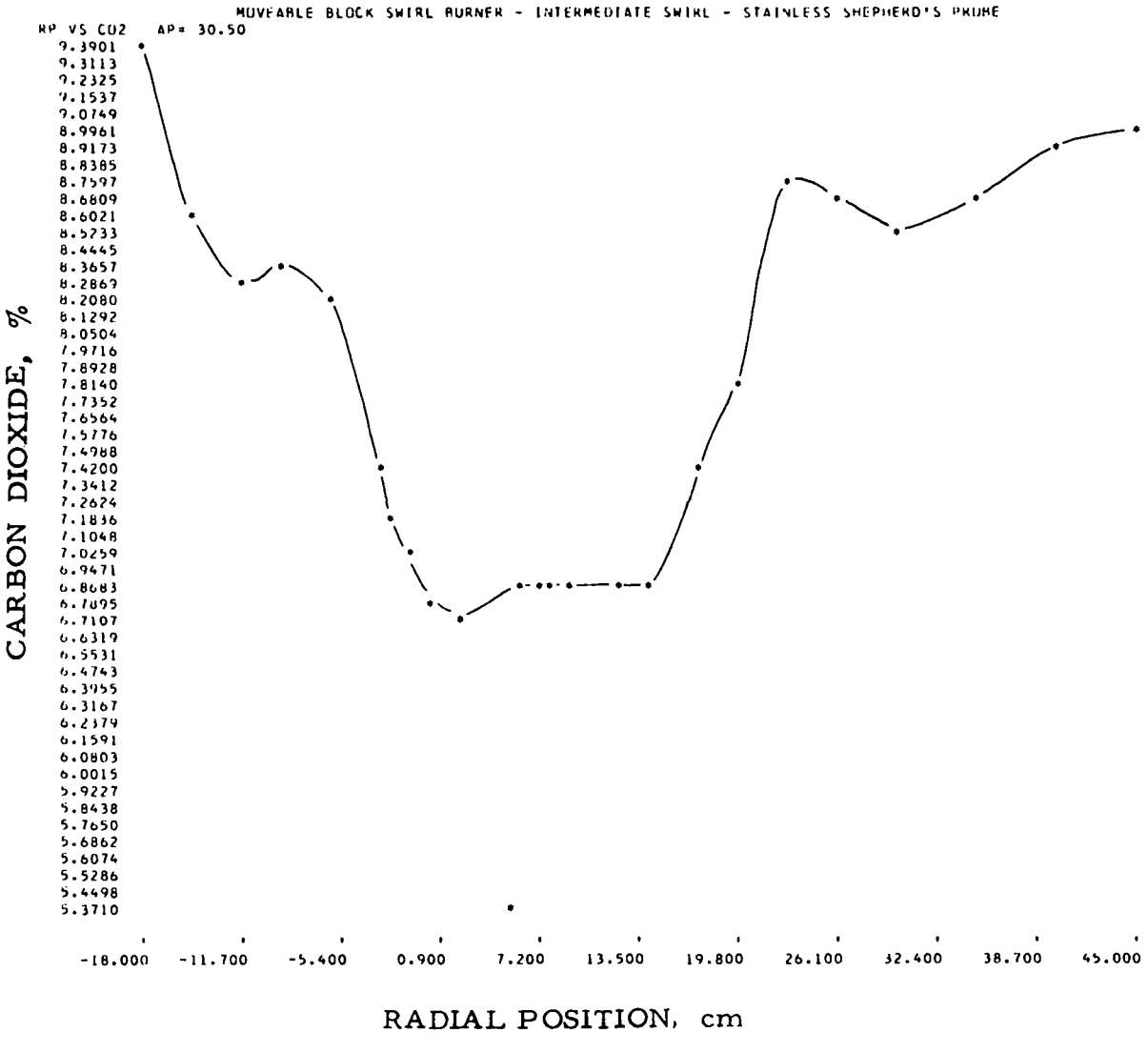

Figure II-254. RADIAL PROFILE FOR CO_2 AT THE 30.5-cm AXIAL POSITION (Movable-Block Swirl Burner – Intermediate Swirl Intensity). GAS INPUT, 2008 CF/hr; EXCESS OXYGEN, 3.6%; NOZZLE IN THROAT POSITION

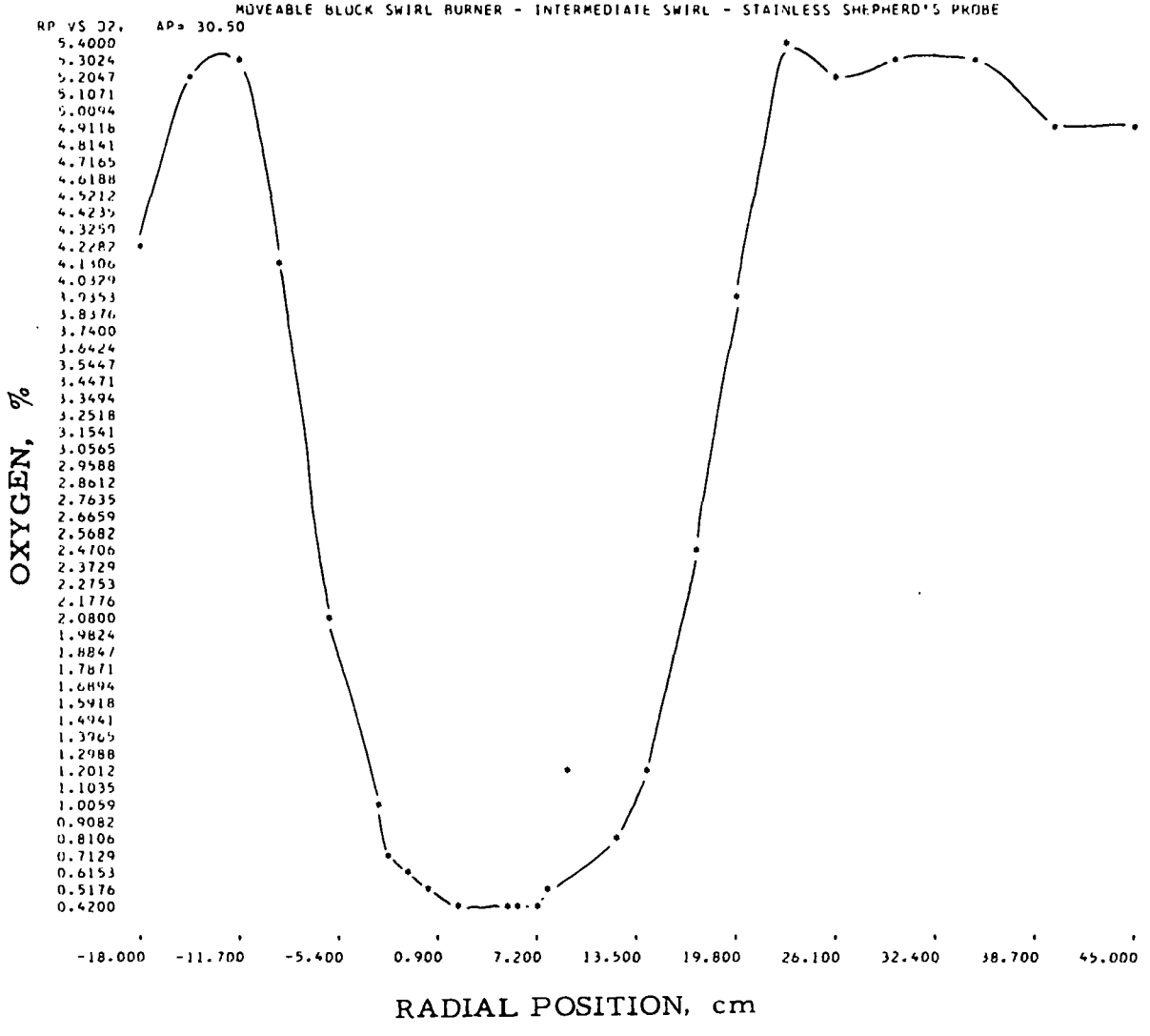

Figure II-255. RADIAL PROFILE FOR O_2 AT THE 30.5-cm AXIAL POSITION (Movable-Block Swirl Burner – Intermediate Swirl Intensity). GAS INPUT, 2008 CF/hr; EXCESS OXYGEN, 3.6%; NOZZLE IN THROAT POSITION

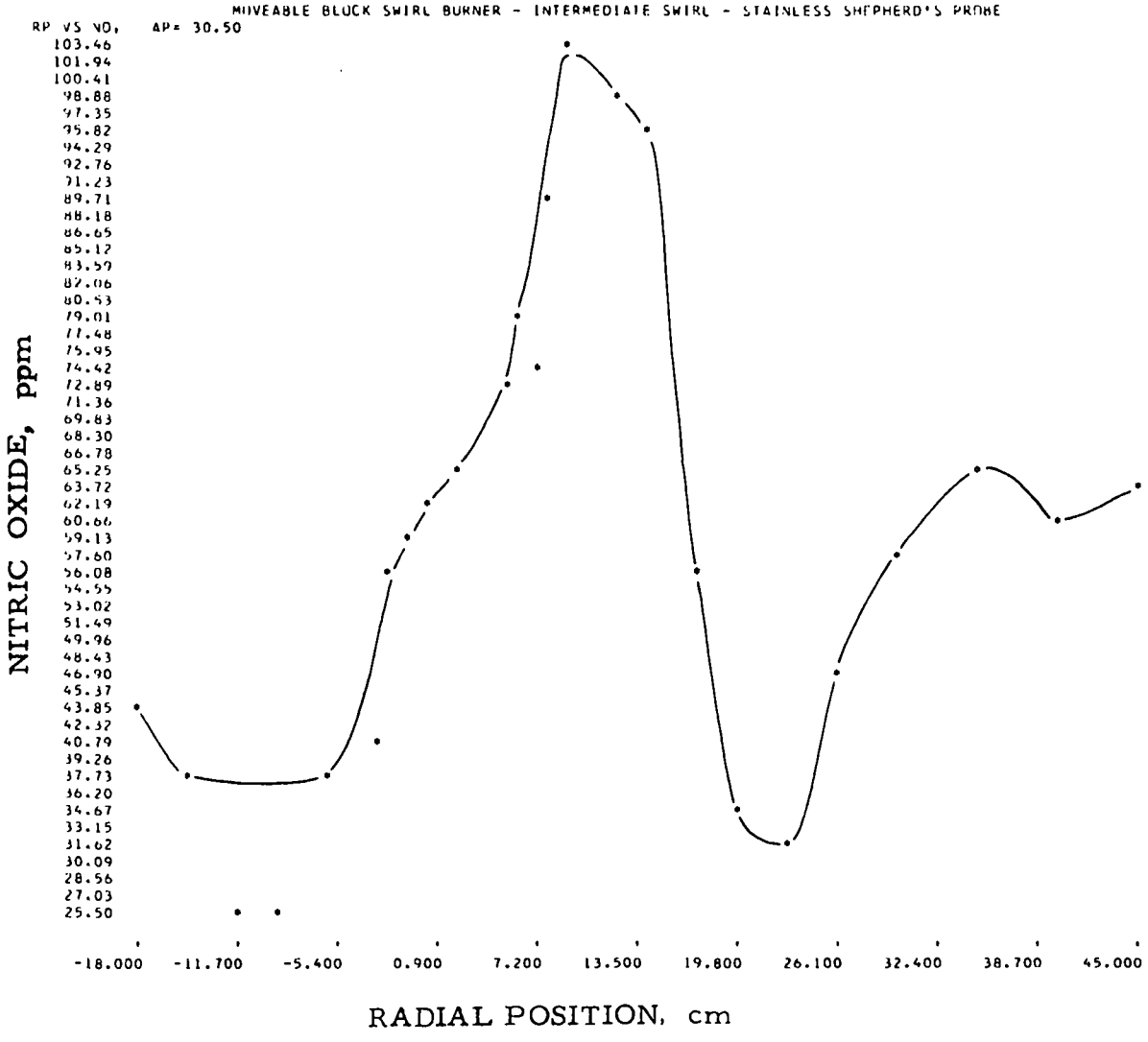

Figure II-256. RADIAL PROFILE FOR CH_4 AT THE 30.5-cm AXIAL POSITION (Movable-Block Swirl Burner – Intermediate Swirl Intensity). GAS INPUT, 2008 CF/hr; EXCESS OXYGEN, 3.6%; NOZZLE IN THROAT POSITION

Table II-61. DATA OBTAINED AT THE 30.5-cm AXIAL POSITION (Movable-Block Swirl Burner — Intermediate Swirl Intensity). GAS INPUT, 2008 CF/hr; EXCESS AIR, 3.6%; NOZZLE IN THROAT POSITION

TRACER GAS STUDIES OF COMBUSTION BURNERS PROGRAM 2
MOVEABLE BLOCK SWIRL BURNER - INTERMEDIATE SWIRL - STAINLESS SHEPHERD'S PROBE

INPUT GAS 2008 WALL TEMPERATURE 2453 PREHEAT TEMPERATURE 0
OUTPUT ANALYSIS
NITROGEN OXIDE 56.70 PERCENT ON RANGE 3, 111.09 PPM OXYGEN 3.60 PERCENT
CARBON DIOXIDE 79.30 PERCENT ON RANGE 1, 9.96 PERCENT
CARBON MONOXIDE 10.40 PERCENT ON RANGE 3, 0.004 PERCENT
METHANE 0.00 PERCENT ON RANGE 0, 0.00 PERCENT

EXPERIMENTAL RESULTS

		NITROGEN OXIDE -NO			OXYGEN	CARBON DIOXIDE-CO2			CARBON MONOXIDE -CO			METHANE - CH4		
AP	RP	RANGE	X	Y	O2	RANGE	X	Y	RANGE	X	Y	RANGE	X	Y
30.50	-18.00	3	22.50	43.3	4.23	1	76.50	9.39	3	100.20	0.050	3	0.80	0.03
30.50	-15.00	3	19.70	37.9	5.16	1	72.40	8.57	2	11.20	0.184	3	2.50	0.10
30.50	-12.00	3	13.40	25.6	5.26	1	70.80	8.26	2	31.40	0.539	3	11.30	0.46
30.50	-9.00	3	13.30	25.5	4.14	1	71.20	8.34	2	81.40	1.562	3	13.80	0.59
30.50	-6.00	3	19.40	37.3	2.12	1	70.30	8.17	2	111.80	2.285	3	41.60	1.88
30.50	-3.00	3	21.40	41.2	0.98	1	66.30	7.42	1	93.10	4.471	3	69.10	3.28
30.50	-2.00	3	28.80	55.6	0.74	1	64.90	7.17	1	97.70	4.812	3	82.40	3.24
30.50	-1.00	3	30.20	58.4	0.62	1	64.00	7.01	1	100.90	5.057	3	90.80	4.46
30.50	0.00	3	31.90	61.7	0.52	1	62.90	6.82	1	103.30	5.243	2	14.20	0.99
30.50	2.00	3	33.80	65.5	0.46	1	62.30	6.71	1	104.00	5.298	2	54.30	4.53
30.50	5.00	3	37.60	73.0	0.44	1	54.10	5.37	1	92.30	4.413	2	87.50	5.93
30.50	6.00	3	40.50	78.7	0.42	1	63.30	6.89	1	101.10	5.072	2	69.00	6.12
30.50	7.00	3	38.30	74.3	0.44	1	63.10	6.85	1	100.20	5.003	2	69.00	6.12
30.50	8.00	3	46.00	89.6	0.54	1	63.20	6.87	1	99.10	4.919	2	70.50	6.29
30.50	9.00	3	52.90	103.4	1.25	1	63.20	6.87	1	97.10	4.767	2	86.10	8.16
30.50	12.00	3	50.60	98.8	0.78	1	63.00	6.84	1	92.60	4.435	2	78.90	7.26
30.50	14.00	3	48.80	95.2	1.18	1	63.10	6.85	1	92.00	4.391	2	71.80	6.44
30.50	17.00	3	28.90	55.8	2.46	1	66.20	7.40	1	74.30	3.194	2	65.30	5.71
30.50	20.00	3	16.20	34.9	3.93	1	68.30	7.79	1	53.20	1.988	3	28.40	1.25
30.50	23.00	3	16.40	31.5	5.40	1	73.20	8.73	1	27.30	0.833	3	8.40	0.36
30.50	26.00	3	24.60	47.4	5.18	1	73.00	8.69	1	10.30	0.272	3	3.40	0.14
30.50	30.00	3	30.00	58.0	5.32	1	72.10	8.51	1	2.50	0.066	3	0.70	0.03
30.50	35.00	3	34.00	65.8	5.33	1	72.80	8.65	3	17.40	0.007	3	0.00	0.00
30.50	40.00	3	31.30	60.5	4.94	1	74.00	8.85	3	8.30	0.003	3	0.00	0.00
30.50	45.00	3	33.20	64.3	4.67	1	74.50	8.96	3	6.50	0.002	3	0.00	0.00

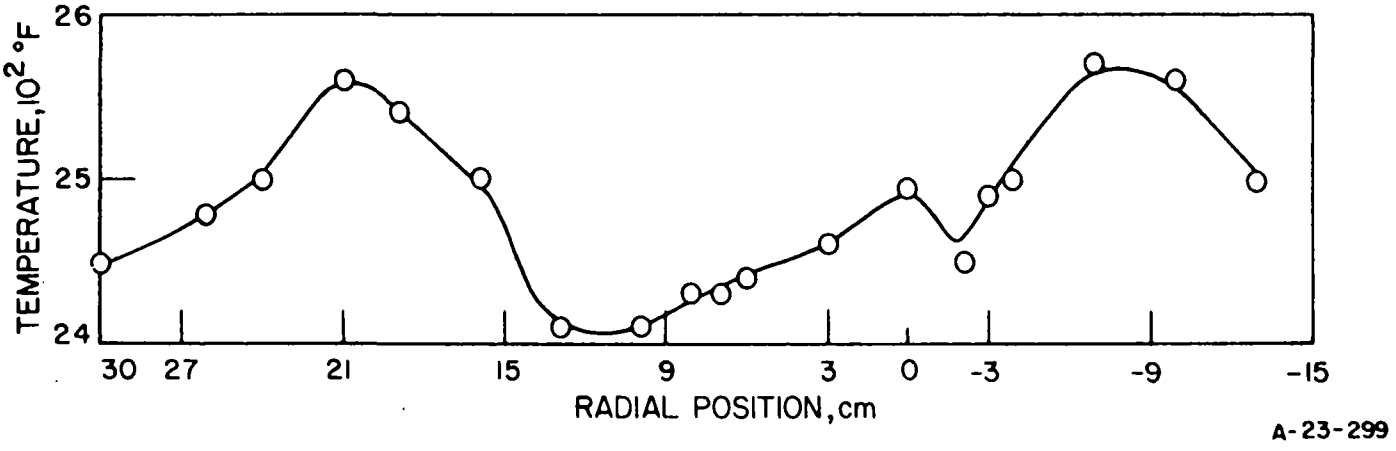

Figure II-257. RADIAL TEMPERATURE PROFILE AT THE 30.5-cm AXIAL POSITION (Movable-Block Swirl Burner — Intermediate Swirl Intensity). GAS INPUT, 2008 CF/hr; EXCESS OXYGEN, 3.6%; NOZZLE IN THROAT POSITION

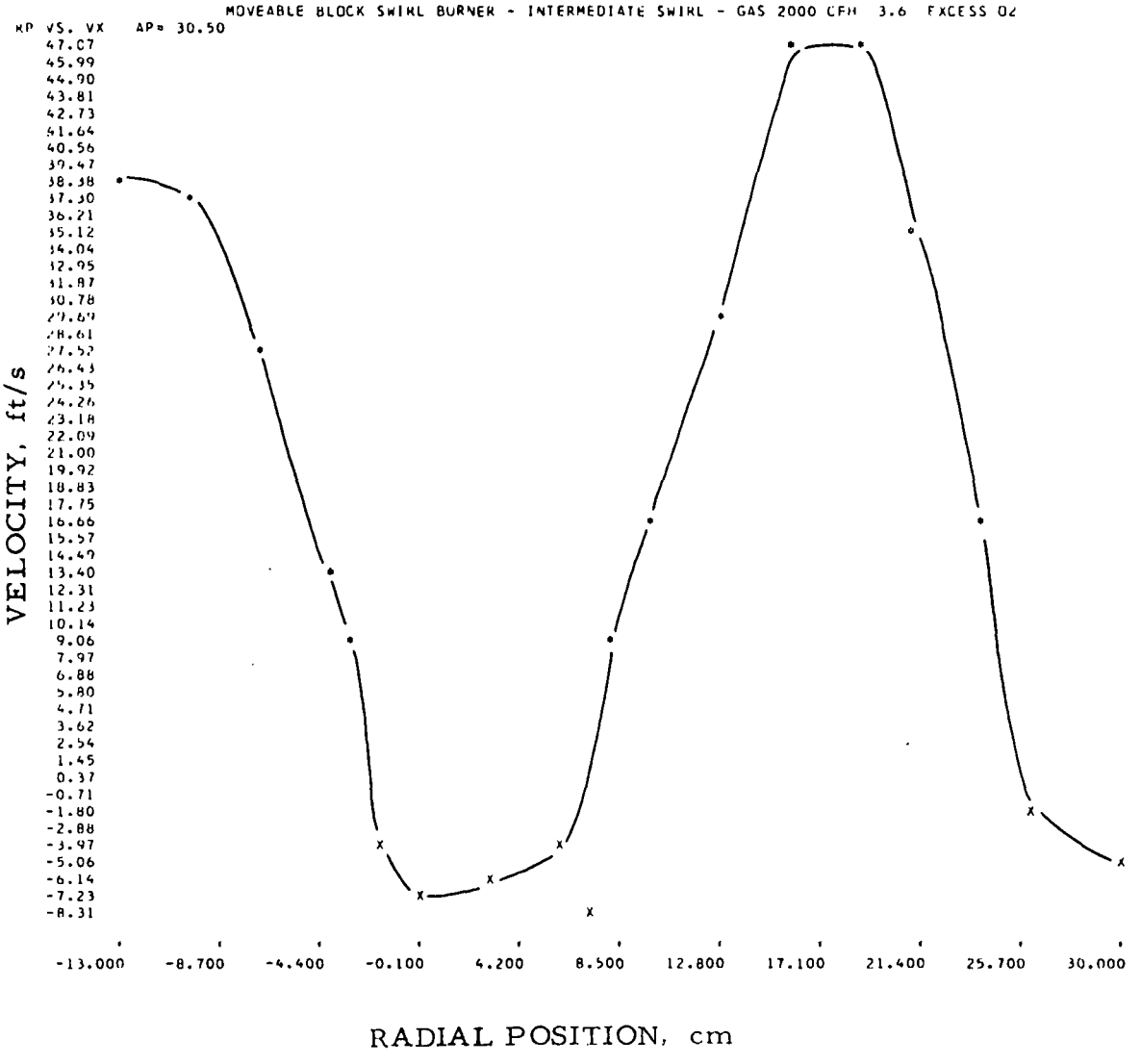

Figure II-258. AXIAL VELOCITY COMPONENT AT THE 30.5-cm AXIAL POSITION (Movable-Block Swirl Burner – Intermediate Swirl Intensity). GAS INPUT, 2000 CF/hr; EXCESS OXYGEN, 3.6%; NOZZLE IN THROAT POSITION.

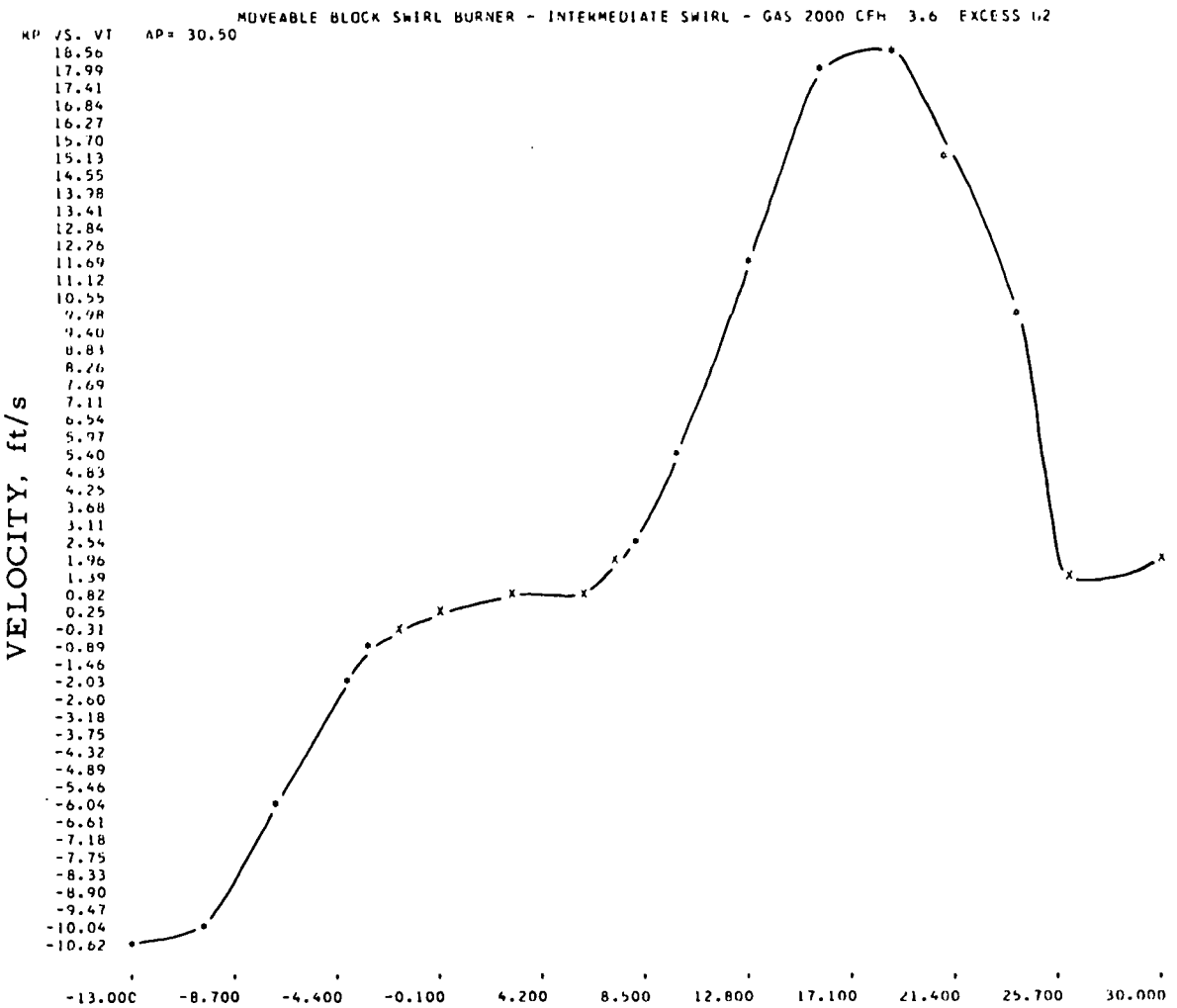

Figure II-259. TANGENTIAL VELOCITY COMPONENT AT THE 30.5-cm AXIAL POSITION (Movable-Block Swirl Burner — Intermediate Swirl Intensity). GAS INPUT, 2000 CF/hr; EXCESS OXYGEN, 3.6%; NOZZLE IN THROAT POSITION

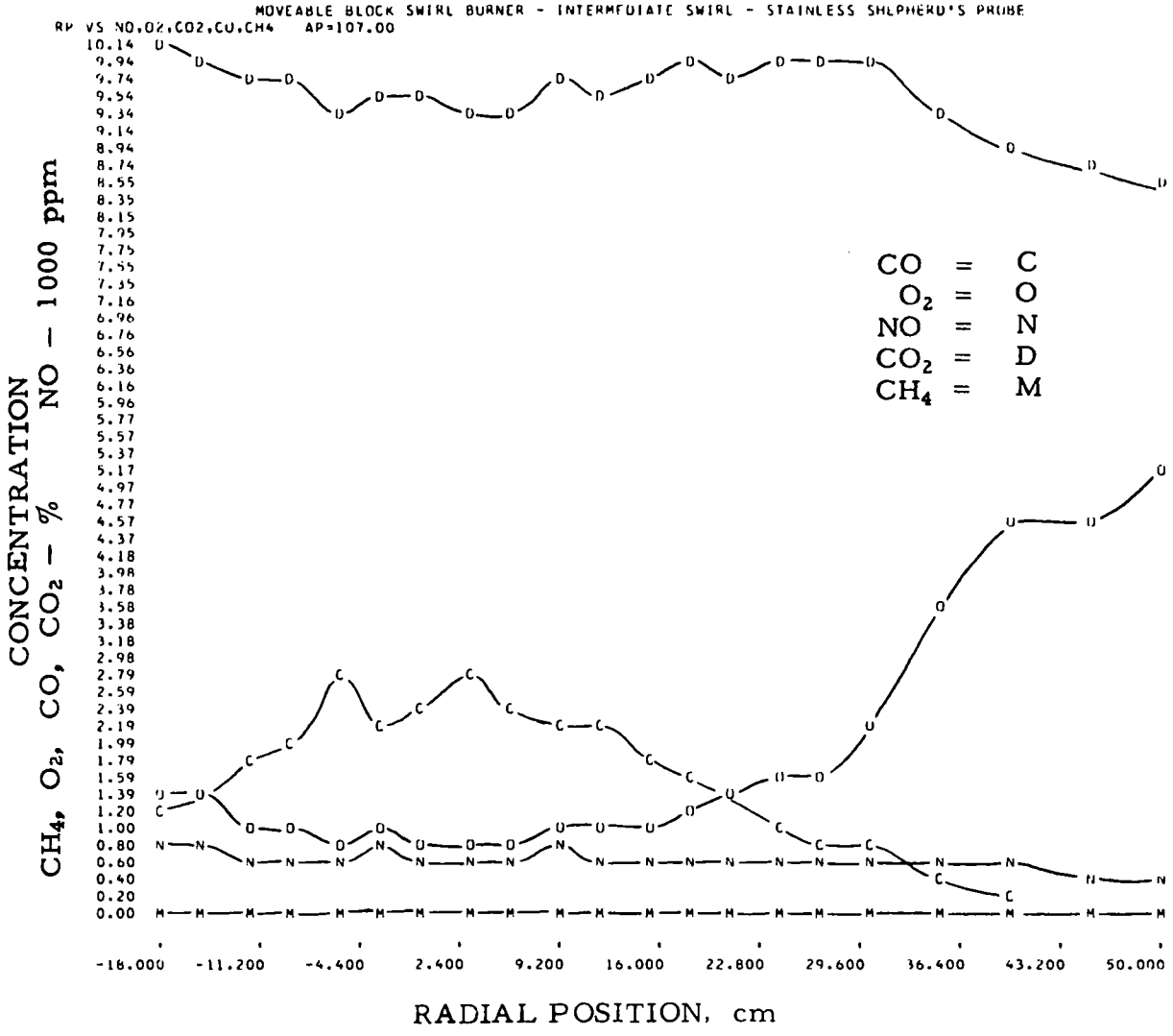

Figure II-260. COMPOSITE PLOT OF GAS SAMPLING PROFILES FOR CO, CO_2, CH_4, NO, AND O_2 AT THE 107-cm AXIAL POSITION (Movable-Block Swirl Burner – Intermediate Swirl Intensity). GAS INPUT, 2008 CF/hr; EXCESS OXYGEN, 3.6%; NOZZLE IN THROAT POSITION

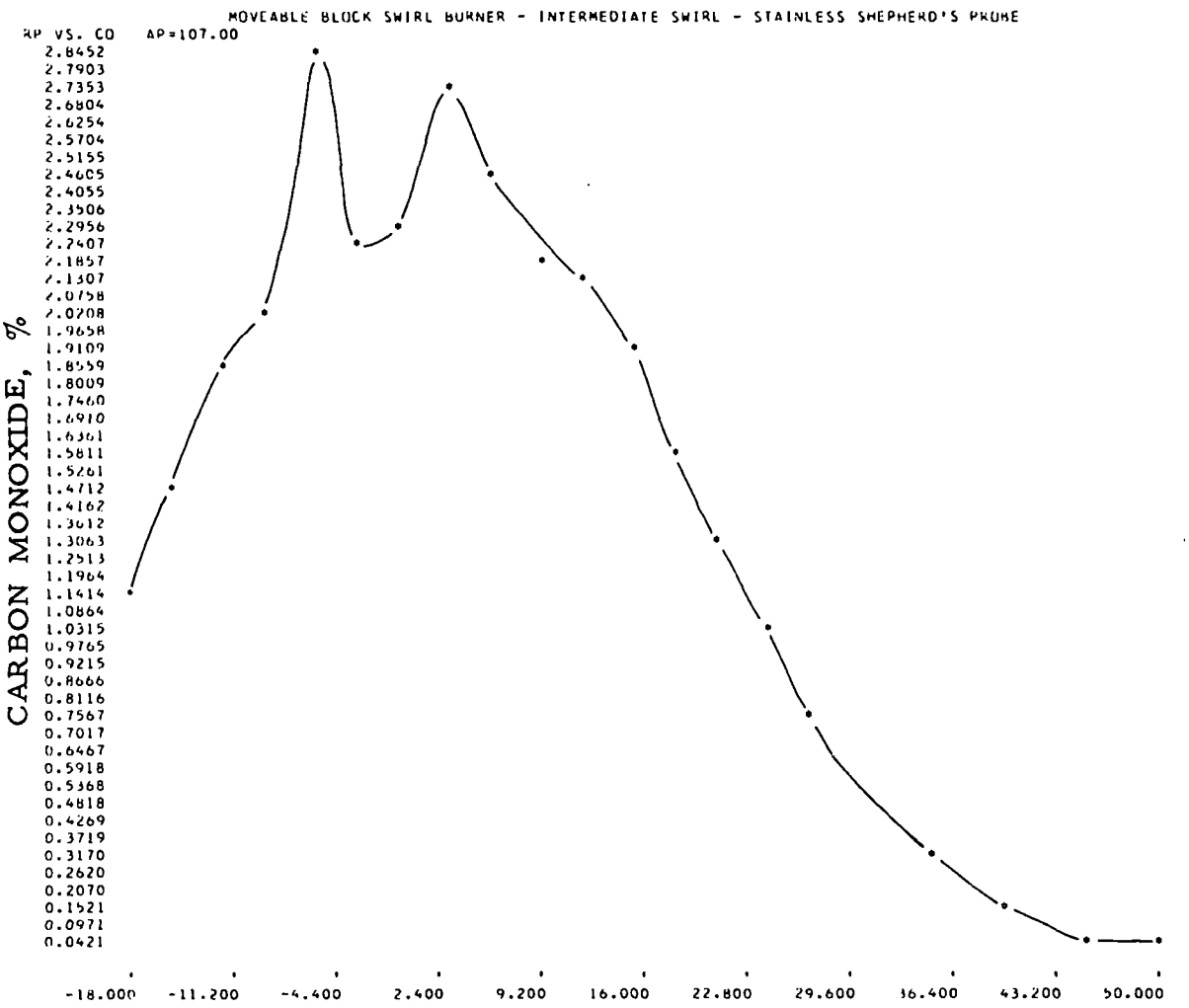

Figure II-261. RADIAL PROFILE FOR CO AT THE 107-cm AXIAL POSITION (Movable-Block Swirl Burner – Intermediate Swirl Intensity). GAS INPUT, 2008 CF/hr; EXCESS OXYGEN, 3.6%; NOZZLE IN THROAT POSITION

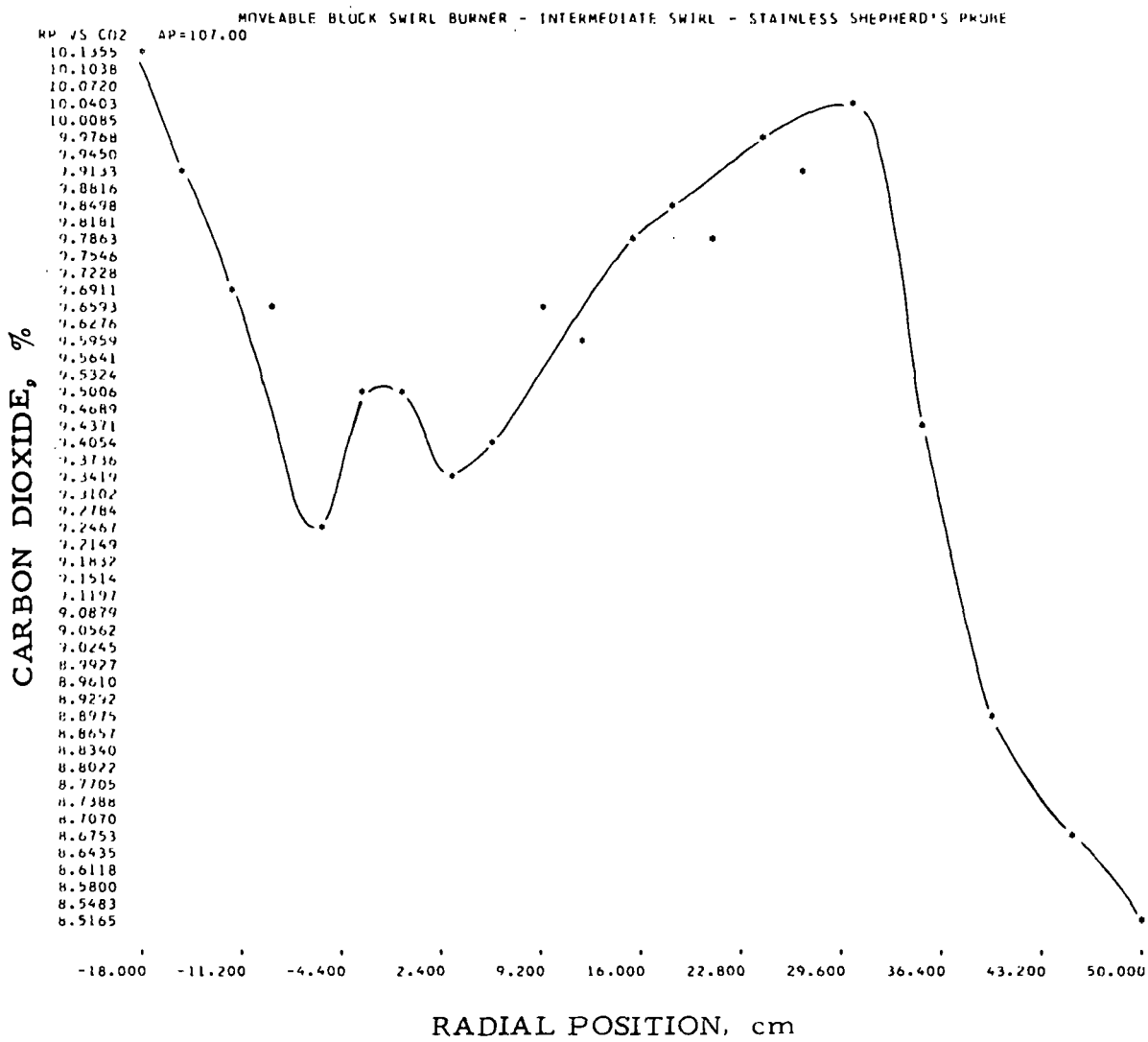

Figure II-262. RADIAL PROFILE FOR CO_2 AT THE 107-cm AXIAL POSITION (Movable-Block Swirl Burner – Intermediate Swirl Intensity). GAS INPUT, 2008 CF/hr; EXCESS OXYGEN, 3.6%; NOZZLE IN THROAT POSITION

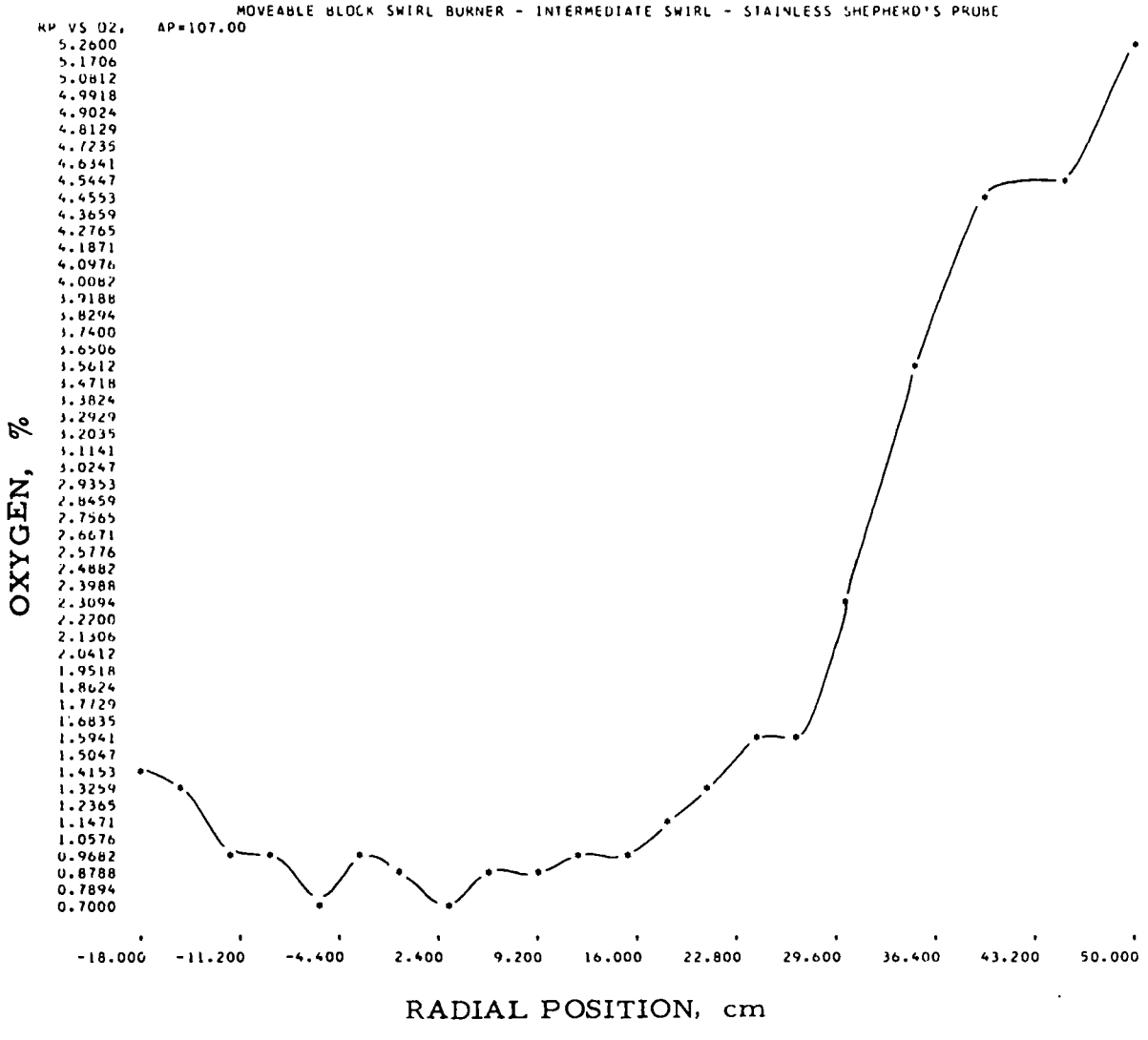

Figure II-263. RADIAL PROFILE FOR O_2 AT THE 107-cm AXIAL POSITION (Movable-Block Swirl Burner – Intermediate Swirl Intensity). GAS INPUT, 2008 CF/hr; EXCESS OXYGEN, 3.6% ; NOZZLE IN THROAT POSITION

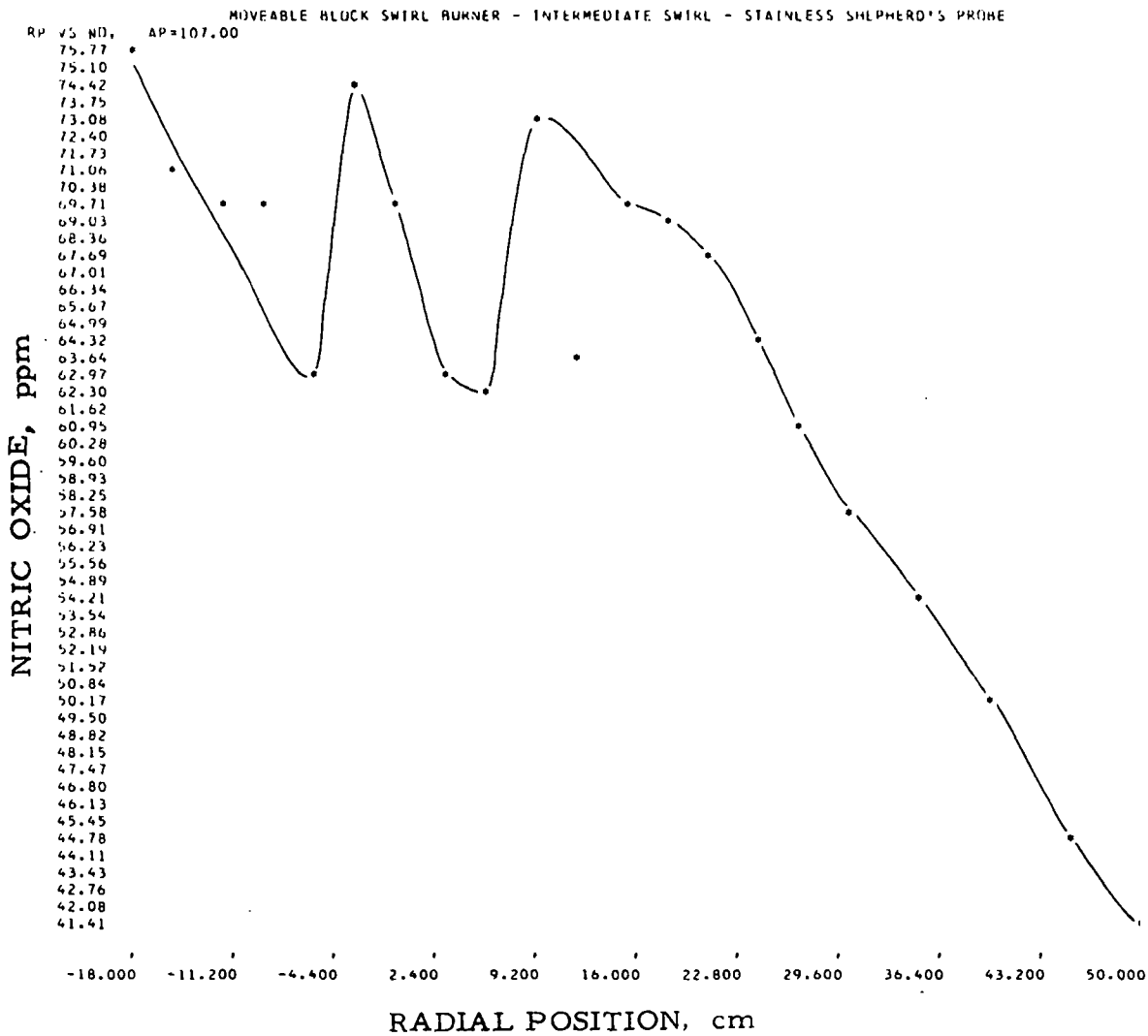

Figure II-264. RADIAL PROFILE FOR NO AT THE 107-cm AXIAL POSITION (Movable-Block Swirl Burner – Intermediate Swirl Intensity). GAS INPUT, 2008 CF/hr; EXCESS OXYGEN, 3.6%; NOZZLE IN THROAT POSITION

Table II-62. DATA OBTAINED AT THE 107-cm AXIAL POSITION (Movable-Block Swirl Burner – Intermediate Swirl Intensity). GAS INPUT, 2008 CF/hr; EXCESS AIR, 3.6%; NOZZLE IN THROAT POSITION

TRACER GAS STUDIES OF COMBUSTION BURNERS PROGRAM 2
MOVEABLE BLOCK SWIRL BURNER - INTERMEDIATE SWIRL - STAINLESS SHEPHERD'S PROBE

INPUT GAS 2008 WALL TEMPERATURE 2453 PREHEAT TEMPERATURE 0
OUTPUT ANALYSIS
NITROGEN OXIDE 56.70 PERCENT ON RANGE 3, 111.09 PPM OXYGEN 3.60 PERCENT
CARBON DIOXIDE 79.30 PERCENT ON RANGE 1, 9.96 PERCENT
CARBON MONOXIDE 10.40 PERCENT ON RANGE 3, 0.004 PERCENT
METHANE 0.00 PERCENT ON RANGE 0, 0.00 PERCENT

EXPERIMENTAL RESULTS

		NITROGEN OXIDE -NO			OXYGEN	CARBON DIOXIDE-CO2			CARBON MONOXIDE -CO			METHANE - CH4		
AP	RP	RANGE	X	Y	O2	RANGE	X	Y	RANGE	X	Y	RANGE	X	Y
107.00	-18.00	3	39.00	75.7	1.44	1	80.10	10.13	2	61.60	1.132	3	0.00	0.00
107.00	-15.00	3	36.70	71.2	1.31	1	79.10	9.92	2	77.60	1.477	3	0.00	0.00
107.00	-12.00	3	35.90	69.6	1.00	1	77.90	9.67	1	51.10	1.881	3	0.00	0.00
107.00	-9.00	3	35.80	69.4	0.95	1	77.80	9.65	1	53.60	2.008	3	0.00	0.00
107.00	-6.00	3	32.50	62.9	0.70	1	75.80	9.24	1	68.60	2.845	3	0.00	0.00
107.00	-3.00	3	38.40	74.5	0.96	1	77.10	9.51	1	57.50	2.214	3	0.00	0.00
107.00	0.00	3	35.80	69.4	0.84	1	77.10	9.51	1	59.40	2.317	3	0.00	0.00
107.00	3.00	3	32.50	62.9	0.71	1	76.30	9.34	1	66.60	2.726	3	0.00	0.00
107.00	6.00	3	32.30	62.5	0.86	1	76.50	9.39	1	62.00	2.462	3	0.00	0.00
107.00	9.00	3	37.80	73.3	0.90	1	77.80	9.65	1	56.60	2.166	3	0.00	0.00
107.00	12.00	3	32.80	63.5	0.96	1	77.50	9.59	1	55.60	2.113	3	0.00	0.00
107.00	15.00	3	35.90	69.6	1.00	1	78.50	9.80	1	51.20	1.886	3	0.00	0.00
107.00	18.00	3	35.60	69.0	1.16	1	78.70	9.84	1	45.00	1.583	3	0.00	0.00
107.00	21.00	3	34.80	67.4	1.30	1	78.50	9.80	1	39.00	1.310	3	0.00	0.00
107.00	24.00	3	33.30	64.5	1.56	1	79.30	9.96	1	32.70	1.044	3	0.00	0.00
107.00	27.00	3	31.60	61.1	1.63	1	79.00	9.90	2	42.70	0.752	3	0.00	0.00
107.00	30.00	3	29.90	57.8	2.26	1	79.60	10.03	2	45.00	0.797	3	0.00	0.00
107.00	33.00	3	28.00	54.1	3.53	1	76.70	9.43	2	18.30	0.305	3	0.00	0.00
107.00	40.00	3	26.10	50.3	4.49	1	74.00	8.88	2	8.60	0.140	3	0.00	0.00
107.00	45.00	3	23.20	44.7	4.56	1	72.90	8.67	3	98.70	0.049	3	0.00	0.00
107.00	50.00	3	21.50	41.4	5.26	1	72.10	8.51	3	86.80	0.042	3	0.00	0.00

The temperature profile for a 107-cm axial position maintains a constant value of $2550^0 \pm 20^0$F across the width of the furnace.

The axial component of velocity is shown in Figure II-265. The peaks occur at –4 cm and +40 cm, with recirculation appearing at 45 cm. Figure II-266 shows the tangential velocity at the 107-cm axial position.

We examined a gas sample from the center line of the burner at a 12.7-cm axial position to determine if higher hydrocarbons were being formed during the combustion process. Table II-63 lists the chemical components of the natural gas being used. Table II-64 lists the gas species analysis on the burner center line as determined by a mass spectrograph. The hydrocarbons formed in the combustion process were 0.4% ethylene, 0.2% propylene, and 0.4% acetylene.

To get an indication of the axial variation of the chemical species, an in-depth profile of the gas concentrations along the center line of the burner was made. The profile is presented in Figure II-267. The NO profile shows similar characteristics to that of the short-flame baffle burner; that is, it has its maximum value on the burner wall, reaches a minimum at an axial position of about 40 cm, and then asymptotically approaches a constant value which is less than the average concentration of NO measured in the flue.

By finding the point where the stoichiometric fuel/air ratio is achieved, it is possible to make a prediction of the flame length along the axis of the burner. In this case, it occurs near an axial position of 84 cm.

D. High-Intensity Flat-Flame Burner

1. Burner Design

The flat-flame high-intensity burner (cross-sectional view in Figure II-268) is constructed so that the fuel and air have a high swirl intensity and are then allowed to rapidly expand along the burner block walls. This arrangement causes combustion to occur in a thin layer over the burner-block surface. This flame has the visible appearance of being flat.

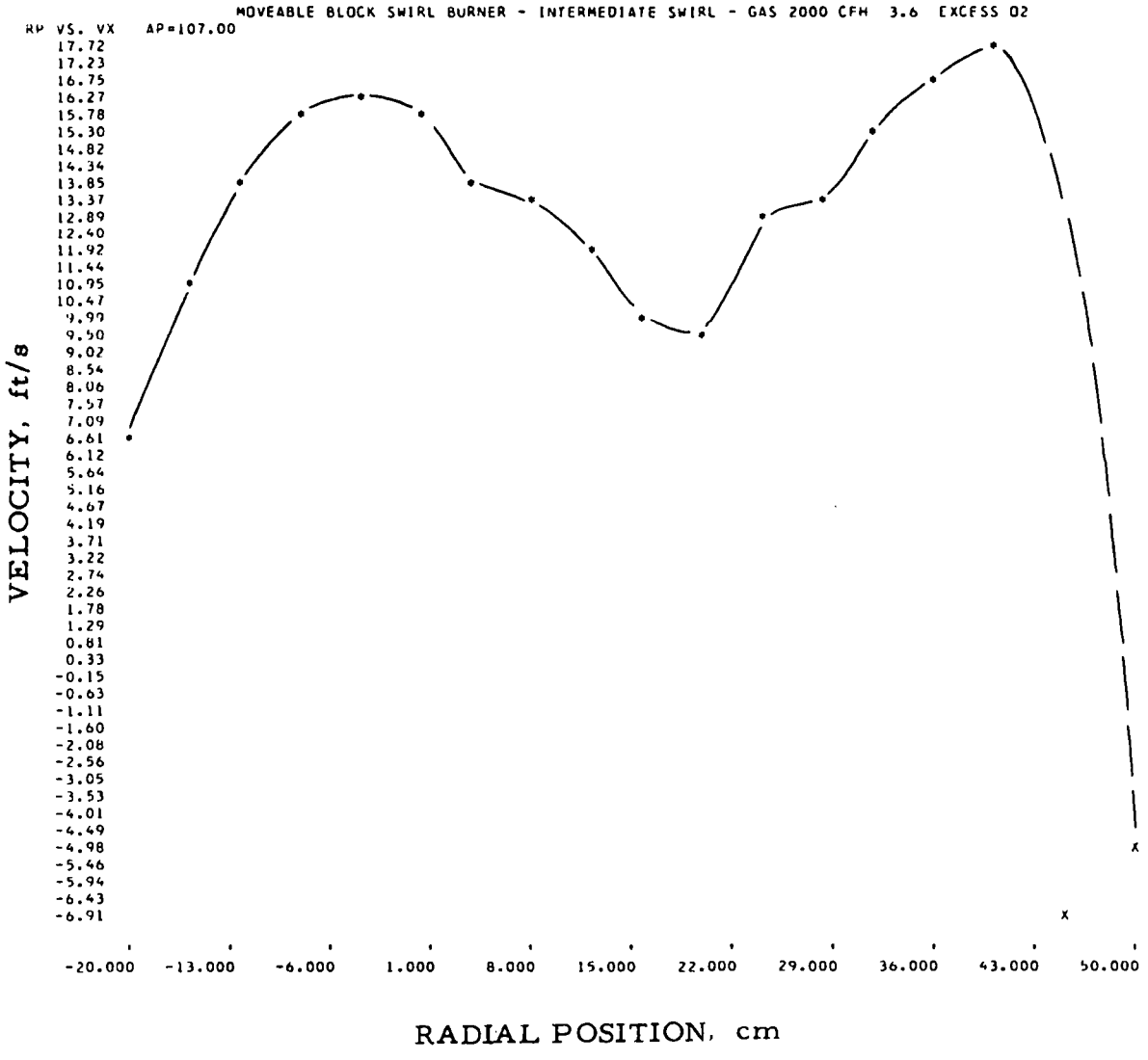

Figure II-265. AXIAL VELOCITY COMPONENT AT THE 107-cm AXIAL POSITION (Movable-Block Swirl Burner — Intermediate Swirl Intensity). GAS INPUT, 2000 CF/hr; EXCESS OXYGEN, 3.6%; NOZZLE IN THROAT POSITION

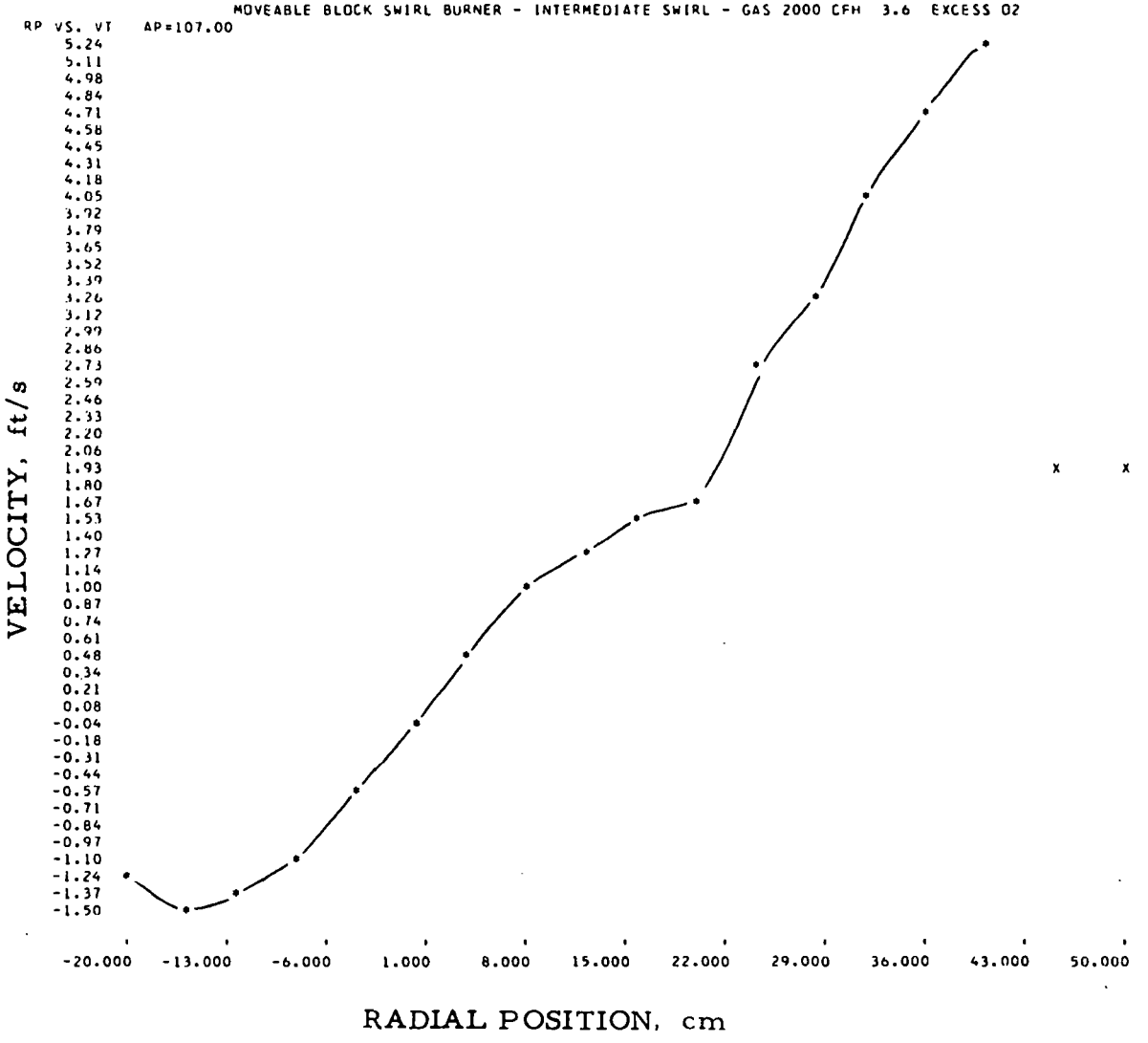

Figure II-266. TANGENTIAL VELOCITY COMPONENT AT THE 107-cm AXIAL POSITION (Movable-Block Swirl Burner — Intermediate Swirl Intensity). GAS INPUT, 2000 CF/hr; EXCESS OXYGEN, 3.6%; NOZZLE IN THROAT POSITION

Table II-63. MASS SPECTROMETER LABORATORY ANALYTICAL REPORT (Natural Gas Input)

Material 8933 Natural Gas Input — Date 1/11/73

Requested by — M. S. Run No. 3555

	Mol %		Mol %
Nitrogen	1.0	Ethylene	
Carbon Monoxide		Propylene	
Nitrogen+CO		Butenes	
Oxygen		Pentenes	
Carbon Dioxide	0.77	Hexenes	
Hydrogen			
Argon		1,3-Butadiene	
Water Vapor		Pentadienes	
Helium	0.04	Cyclopentadiene	
Methane	94.3	Acetylene	
Ethane	3.0	Diacetylene	
Propane	0.56	Methyl Acetylene	
n-Butane	0.10	+Propadiene	
Isobutane	0.10	Vinyl Acetylene	
Pentanes	0.05	Benzene	0.02
Hexanes	0.03	Toluene	0.03
Heptanes	0.02	Xylenes	
Octanes		Ethyl Benzene	
		Styrene	
		Indene	
		Napthalene	
		TOTAL	100.0

Calc. H. V., Btu SCF 1018 — Air Content 32.5%

Calc. sp gr (Air 1.000) .592 — Approved by

Table II-64. MASS SPECTROMETER LABORATORY ANALYTICAL REPORT (Furnace Product Gas)

8933 Furnace Product Gas

Material Radial Position – 0 cm Axial Position – 14 in. Date 1/11/73

Requested by _____ M. S. Run No. 3554

	Mol %		Mol %
Nitrogen	51.7	Ethylene	0.4
Carbon Monoxide	3.2	Propylene	0.2
Nitrogen+CO		Butenes	
Oxygen	2.8	Pentenes	
Carbon Dioxide	3.8	Hexenes	
Hydrogen	4.0		
Argon	0.6	1,3-Butadiene	
Water Vapor		Pentadienes	
Helium		Cyclopentadiene	
Methane	31.8	Acetylene	0.4
Ethane	1.0	Diacetylene	
Propane	0.1	Methyl Acetylene	
n-Butane		+Propadiene	
Isobutane		Vinyl Acetylene	
Pentanes		Benzene	
Hexanes		Toluene	
Heptanes		Xylenes	
Octanes		Ethyl Benzene	
		Styrene	
		Indene	
		Napthalene	
		TOTAL	100.0

Calc. H. V., Btu SCF _____ Air Content _____

Calc. sp gr (Air 1.000) _____ Approved by _____

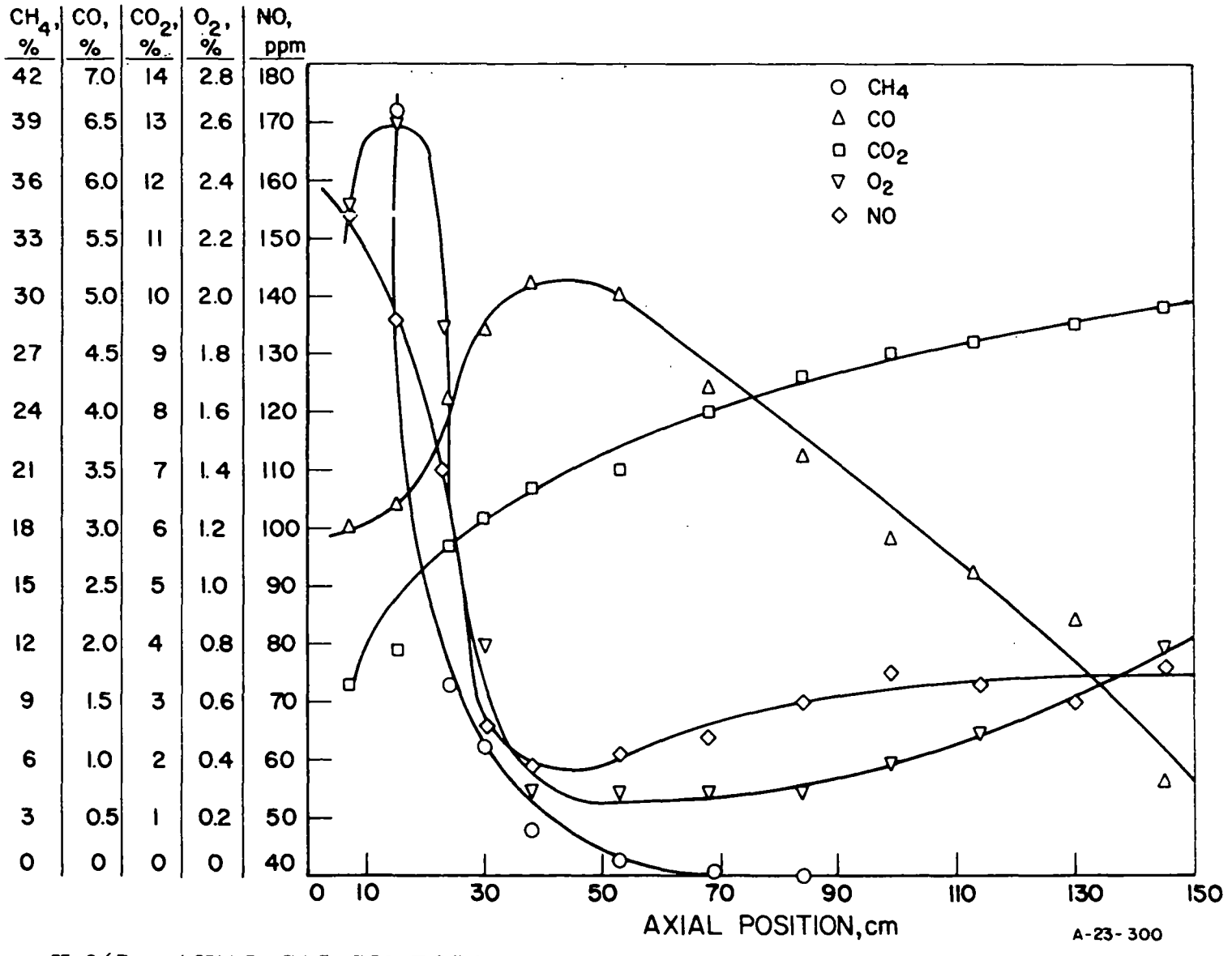

Figure II-267. AXIAL GAS COMPOSITION PROFILE AT THE 0.0-cm RADIAL POSITION (Movable-Block Swirl Burner – Intermediate Swirl Intensity). GAS INPUT, 2008 CF/hr; EXCESS OXYGEN, 3.6%; NOZZLE IN THROAT POSITION

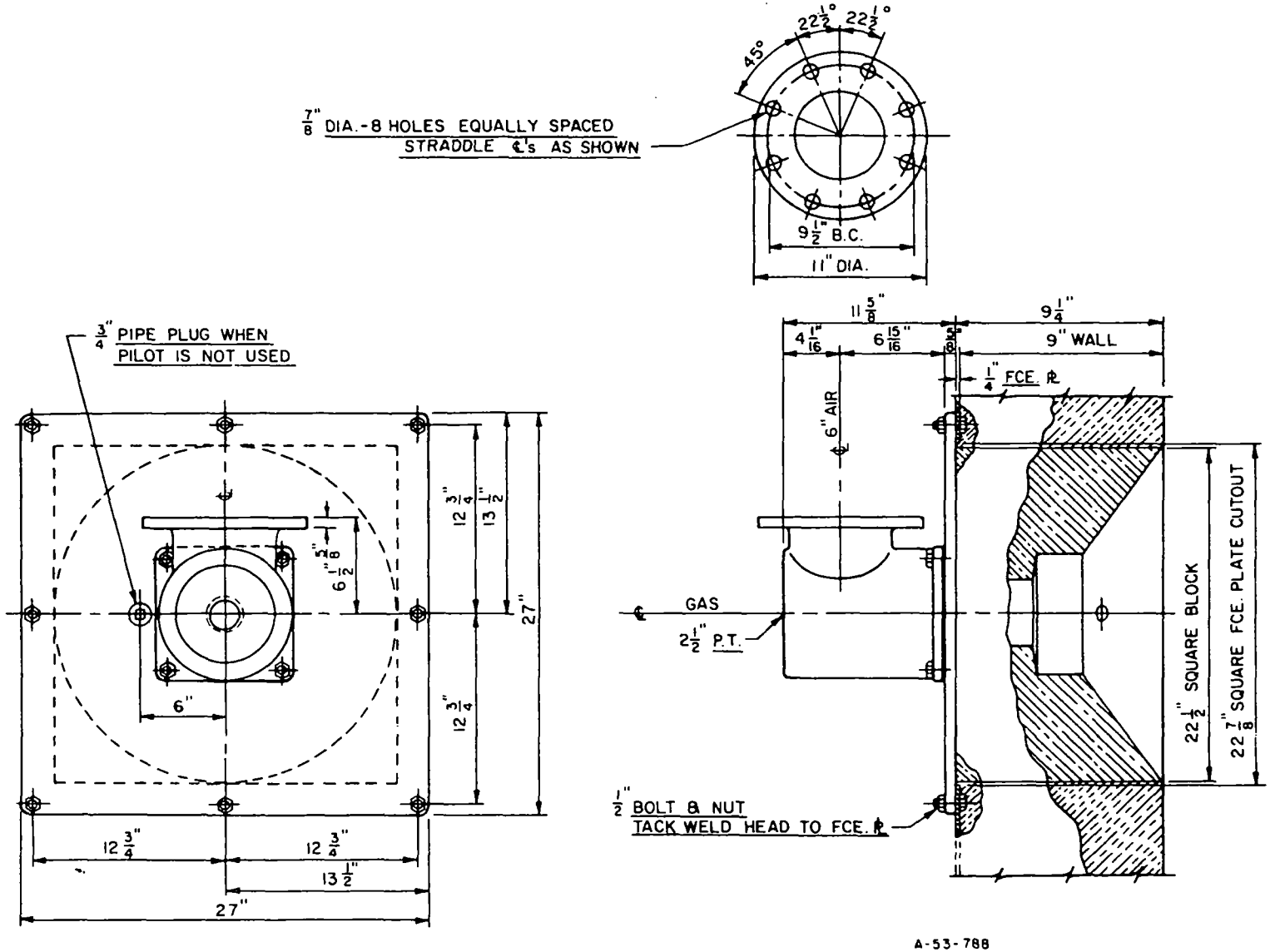

Figure II-268. CROSS-SECTIONAL VIEW OF HIGH-INTENSITY FLAT-FLAME BURNER

2. Hot-Model Input-Output Data

The flat-flame burner was operated at three different gas inputs, all over a range of fuel/air ratios expressed as percentage of oxygen in the flue. No changes were made in the burner nozzle position or the swirl vanes in the burner housing as these were fixed by design. The input-output tests were conducted at gas inputs of 1670, 2010, and 2394 CF/hr, with between 1.0 and 7.0% oxygen in the flue by volume. Figure II-269 shows the results of these runs. The nitric oxide (NO) concentrations were normalized by dividing the weight of the flue products at the stoichiometric mixture of fuel and air into the measured concentration of NO and multiplying this ratio by the weight of the flue products for the input conditions at which the measurements were taken. The input-output data for the other gas species (O_2, CO_2, and CO) are shown in Table II-65.

Based on the analysis of the input-output results we concluded that —

1. From 1.0 to about 3.75% excess oxygen in the flue, the gas input rate made little difference in the amount of NO formed so long as the flame had a visible appearance of being flat. Spot-check runs for NO in the flue gases at gas inputs below 1670 CF/hr (where the flame lost its flat appearance) showed differences as gas input was changed. However, the flame was very lazy and concentration readings erratic. Definite measurements could not be made, only gross differences observed. Consequently, measurements at gas inputs below 1670 CF/hr were not pursued further.

2. The amount of NO formed with more than 3.75% oxygen in the flue did change significantly with changes in the gas input. We observed that the shape and appearance of the flame also changed as the flue oxygen increased beyond 3.75%. The flame withdrew into the burner block and appeared as though combustion was completed before the gases could expand around the curvature of the burner block and form the characteristic flat appearance.

3 The NO concentration at all gas inputs and excess air levels tested was considerably lower for the flat-flame burner than any other "commercial type" burner tested. We postulate that the NO was relatively low because the flame tightly adhered to the burner block, which is a good heat sink. The heat-sink effect of the block lowered flame temperature and hence lowers NO formation.

3. In-the-Flame Survey Results

Again, as part of this program, we mapped the concentrations of CO, CO_2, CH_4, O_2, and NO; the temperature; and the gas velocity in the flame.

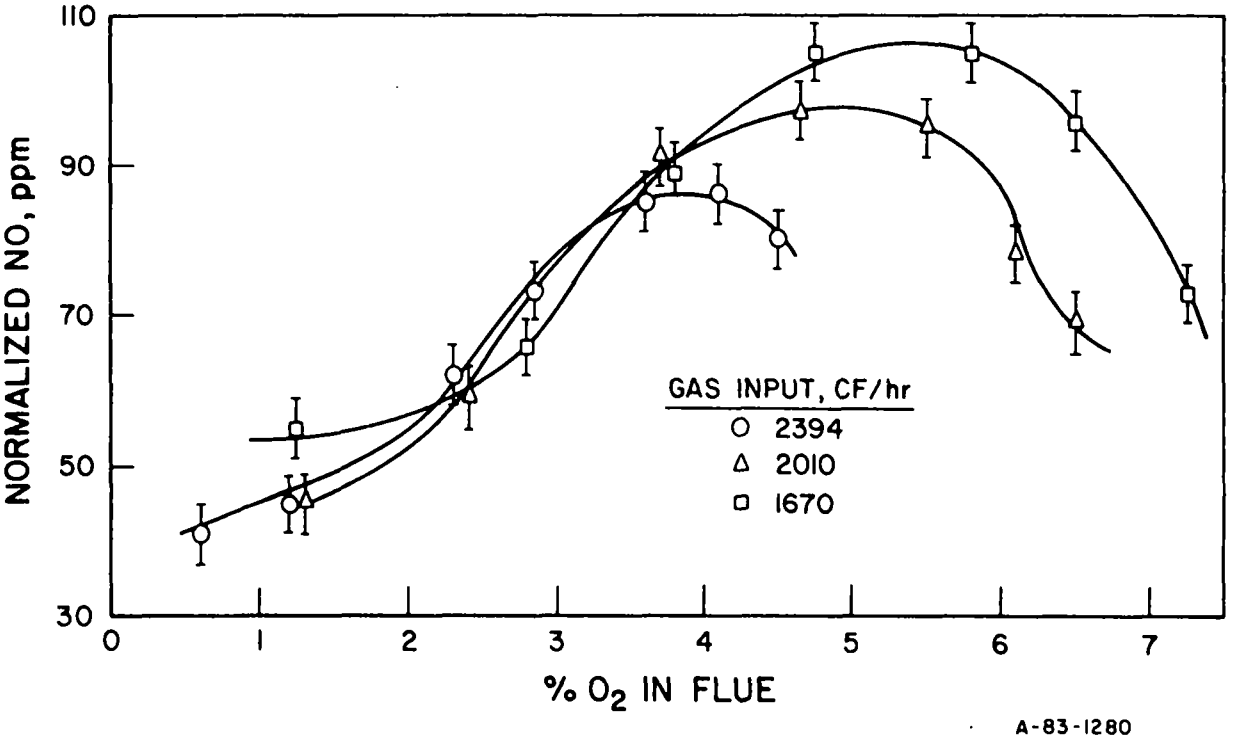

Figure II-269. NORMALIZED NO CONCENTRATION AS A FUNCTION OF EXCESS AIR FOR THE FLAT-FLAME BURNER AT THREE GAS INPUTS

Table II-65. INPUT-OUTPUT DATA FOR THE FLAT-FLAME BURNER

Run No.	Gas Input, CF/hr	Flue Analysis				Normalized NO, ppm
		NO, ppm	O_2, %	CO_2, %	CO, ppm	
1	2394	48	2.31	10.7	2.3	53
2	2394	39	0.63	11.5	7.6	41
3	2394	65	4.53	9.0	0.7	80
4	2394	71	4.13	9.2	0.3	86
5	2394	72	3.62	9.7	0.6	85
6	2394	65	2.86	10.2	0.7	73
7	2394	56	2.36	10.5	1.2	62
8	2394	42	1.21	11.2	44.5	45
9	2010	50	6.53	7.9	0.1	69
10	2010	58	6.13	8.2	1.3	78
11	2010	73	5.49	8.7	1.2	95
12	2010	78	4.66	9.1	0.6	97
13	2010	77	3.68	9.8	0.5	91
14	2010	53	2.37	10.5	4.8	59
15	2010	42	1.30	11.2	46.6	45
17	1670	58	2.82	10.1	3.6	66
18	1670	51	1.26	10.9	26.8	55
19	1670	85	4.49	9.1	1.2	105
20	1670	79	5.80	8.5	1.3	105
21	1670	70	6.48	8.1	0.8	96
22	1670	51	7.24	7.6	0.9	73
23	1670	40	7.84	7.2	0.3	60
24	1670	75	3.77	9.6	2.9	89

Both because gas input had little effect on the NO formed and the NO concentrations were relatively low, we ran only one set of conditions at a gas input of 2010 CF/hr and 4.4% oxygen in the flue. We also suspected that most of the flow patterns of interest occurred near the burner block because of the visible appearance of the flame. A radial scan of temperature at axial positions of 12, 69, and 130 cm substantiated that combustion is nearly complete very near the burner-block hot face (Figure II-270). At only 12 cm from the block, the temperature across the furnace width was already nearly uniform. The maximum deviation from the mean was only $\pm 40^{0}$F.

Flow direction was also looked at with a two-hole Hubbard Probe. Table II-66 shows a radial flow direction scan at 12.7 cm axially from the burner hot face. Flow was found to be up the furnace [toward the burner as indicated by the negative (–) ΔP readings] except at extreme radial positions of beyond ±30 cm. Farther out into the furnace, the flow direction was always away from the burner as shown in Tables II-67 and II-68 by positive (+) ΔP readings. The data of Tables II-67 and II-68 were taken at axial positions of 71 cm and 104 cm, respectively.

This initial work was followed by detailed in-the-flame scans for gas species at 12.7 cm, 68.6 cm, and 104.1 cm from the burner block. A composite of the results is shown in Figure II-271 for NO, O_2, CO_2, CO, and CH_4 at an axial position of only 12.7 cm. Interestingly, at an axial position relatively close to the burner, the methane concentration is already less than 1/4% with only small variations in concentration as a function of radial position. This is another indication of how fast and near the burner that combustion is completed. Because of the scale required to plot all of the species concentrations on the same graph, a great deal of resolution is lost. However, the data were collected in such a way as to obtain the required finer resolution as shown by the raw data given in Table II-69 and plotted in Figures II-272, II-273, II-274, II-275, and II-276.

Radial scans of species concentration were also taken farther down the furnace length at 68.6 cm and 104.1 cm. However, these were of only minor interest since combustion was complete and the concentration from one axial position to the next changed very little. The raw and

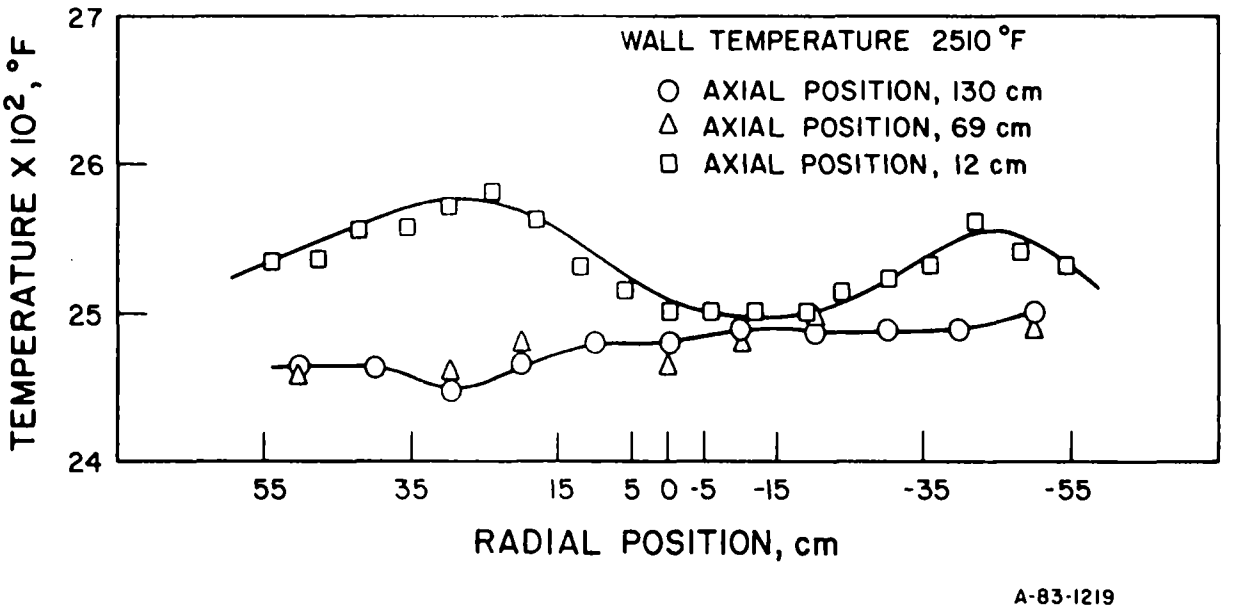

Figure II-270. RADIAL SCAN OF TEMPERATURE FOR THE FLAT-FLAME BURNER AT A GAS INPUT OF 2010 CF/hr AND 4.4% EXCESS OXYGEN IN THE FLUE

Table II-66. TIME-AVERAGED DIRECTIONAL FLOW DATA OBTAINED USING A TWO-HOLE PROBE AT AN AXIAL POSITION OF 12.7 cm (Flat-Flame Burner; 2010 CF/hr, Gas Input; 4.4% Excess Oxygen)

RP, cm	Time Avg, Δ P	RP, cm	Time Avg, Δ P	RP, cm	Time Avg, Δ P
50	2.173	15	−2.456	−20	−1.434
45	1.879	10	−2.644	−25	0.294
40	0.970	5	−3.082	−30	1.542
35	−0.206	0	−3.158	−35	2.532
30	−0.764	−5	−3.067	−40	1.701
25	−1.521	−10	−2.812	−45	1.306
20	−2.207	−15	−2.226		

Table II-67. TIME-AVERAGED DIRECTIONAL FLOW DATA OBTAINED USING A TWO-HOLE PROBE AT AN AXIAL POSITION OF 71 cm (Flat-Flame Burner; 2010 CF/hr, Gas Input; 4.4% Excess Oxygen)

RP, cm	Time Avg, Δ P	RP, cm	Time Avg, Δ P	RP, cm	Time Avg, Δ P
45	0.880	10	0.994	−25	0.763
40	0.849	5	0.973	−30	0.659
35	1.097	0	1.020	−35	0.645
30	1.071	−5	0.907	−40	0.518
25	1.150	−10	0.853	−45	0.329
20	1.089	−15	0.765		
15	1.043	−20	0.819		

Table II-68. TIME-AVERAGED DIRECTIONAL FLOW DATA OBTAINED USING A TWO-HOLE PROBE AT AN AXIAL POSITION OF 104 cm
(Flat-Flame Burner; 2010 CF/hr, Gas Input, 4.4% Excess Oxygen)

RP, cm	Time Avg, Δ P	RP, cm	Time Avg, Δ P	RP, cm	Time Avg, Δ P
45	0.398	10	0.234	−25	0.395
40	0.223	5	0.269	−30	0.421
35	0.302	0	0.259	−35	0.465
30	0.318	−5	0.295	−40	0.509
25	0.164	−10	0.323	−45	0.581
20	0.285	−15	0.375	−50	0.633
15	0.293	−20	0.375		

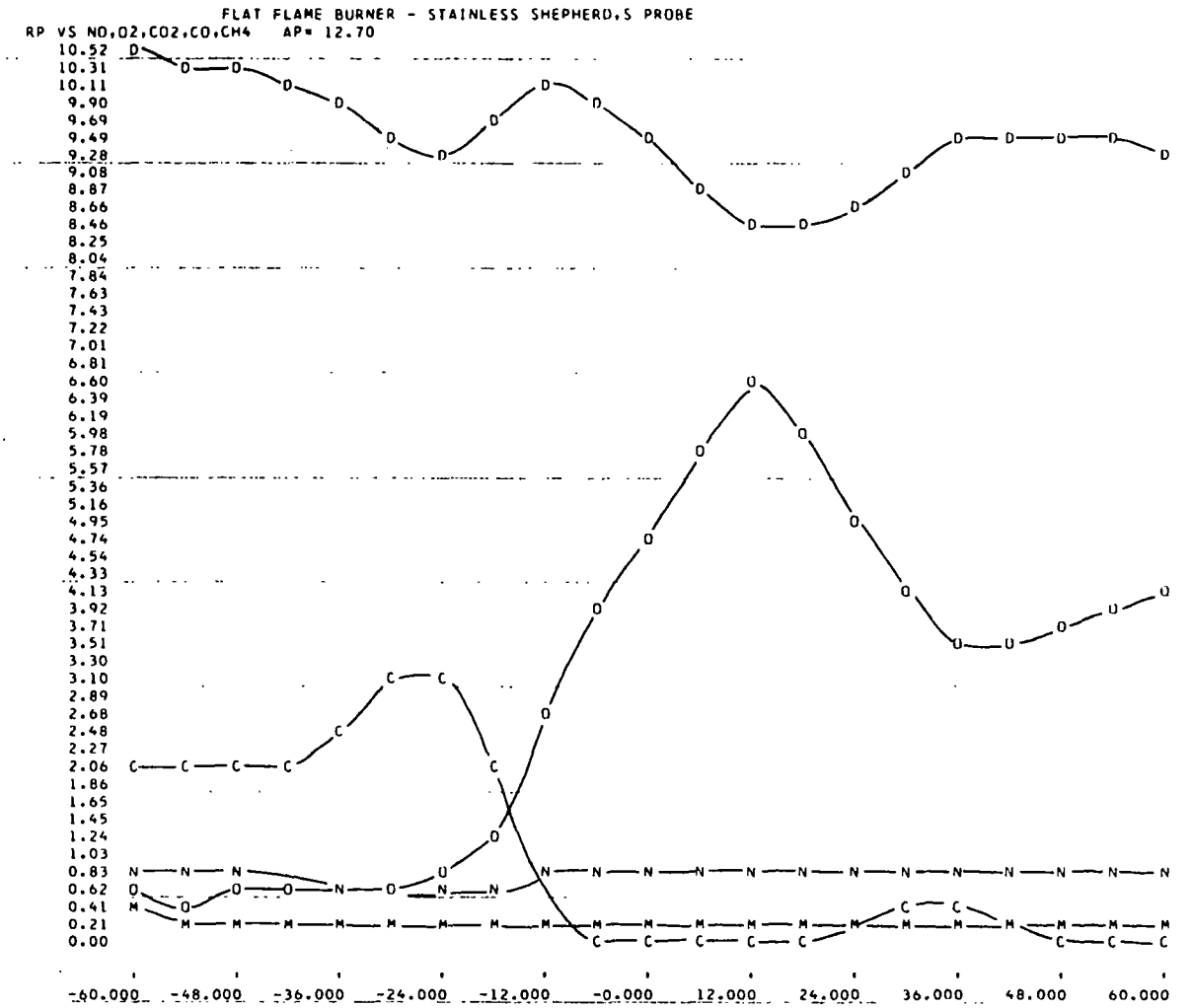

Figure II-271. COMPOSITE PLOT OF RADIAL GAS SPECIES CONCENTRATION AT A 12.7-cm AXIAL POSITION FOR A FLAT-FLAME BURNER OPERATING AT A GAS INPUT OF 2010 CF/hr AND 4.4% EXCESS OXYGEN IN THE FLUE

Table II-69. RAW AND REDUCED GAS SPECIES DATA FOR RADIAL SAMPLING SCANS AT AN AXIAL POSITION OF 12.7 cm FROM A FLAT-FLAME BURNER OPERATING AT A GAS INPUT OF 2010 CF/hr AND 4.4% EXCESS OXYGEN IN THE FLUE

TRACER GAS STUDIES OF COMBUSTION BURNERS PROGRAM 2
FLAT FLAME BURNER - STAINLESS SHEPHERD,S PROBE

INPUT GAS 2010 WALL TEMPERATURE 2480 PREHEAT TEMPERATURE 0
OUTPUT ANALYSIS
NITROGEN OXIDE 45.50 PERCENT ON RANGE 3, 88.67 PPM OXYGEN 4.40 PERCENT
CARBON DIOXIDE 75.70 PERCENT ON RANGE**, 177.73 PERCENT
CARBON MONOXIDE 1.60 PERCENT ON RANGE 3, 0.000 PERCENT
METHANE 0.00 PERCENT ON RANGE 0, 0.00 PERCENT

EXPERIMENTAL RESULTS

		NITROGEN OXIDE -NO			OXYGEN	CARBON DIOXIDE-CO2			CARBON MONOXIDE -CO			METHANE - CH4		
AP	RP	RANGE	X	Y	O2	RANGE	X	Y	RANGE	X	Y	RANGE	X	Y
12.70	-60.00	3	39.80	77.3	0.56	1	81.90	10.51	1	53.30	1.993	3	8.40	0.36
12.70	-54.00	3	40.70	79.1	0.50	1	81.10	10.34	1	52.80	1.967	3	5.70	0.24
12.70	-48.00	3	40.10	77.9	0.55	1	80.70	10.26	1	53.20	1.988	3	5.20	0.22
12.70	-42.00	3	36.70	71.2	0.57	1	80.10	10.13	1	54.80	2.071	3	5.10	0.22
12.70	-36.00	3	35.80	69.4	0.70	1	78.70	9.84	1	63.30	2.535	3	5.90	0.25
12.70	-30.00	3	36.50	70.8	0.65	1	77.00	9.49	1	73.00	3.113	3	6.20	0.26
12.70	-24.00	3	33.80	65.5	0.79	1	76.20	9.32	1	72.20	3.064	3	6.80	0.29
12.70	-18.00	3	33.30	64.5	1.29	1	78.20	9.73	1	54.10	2.034	3	6.90	0.29
12.70	-12.00	3	37.60	73.0	2.78	1	80.10	10.13	1	10.00	0.263	3	3.80	0.16
12.70	-6.00	3	41.90	81.5	3.90	1	78.50	9.80	3	64.10	0.029	3	3.50	0.15
12.70	0.00	3	40.70	79.1	4.83	1	76.60	9.41	3	8.60	0.003	3	4.30	0.18
12.70	6.00	3	38.50	74.7	5.80	1	74.20	8.92	3	5.70	0.002	3	3.10	0.13
12.70	12.00	3	41.10	79.9	6.59	1	72.00	8.49	3	6.90	0.002	3	2.60	0.11
12.70	18.00	3	41.10	79.9	6.05	1	71.90	8.47	3	98.30	0.048	3	6.10	0.26
12.70	24.00	3	41.10	79.9	5.00	1	73.30	8.75	2	12.90	0.212	3	4.80	0.20
12.70	30.00	3	38.50	74.7	4.05	1	75.40	9.16	2	24.80	0.419	3	5.40	0.23
12.70	36.00	3	40.70	79.1	3.52	1	76.70	9.43	2	26.50	0.449	3	4.60	0.19
12.70	42.00	3	41.80	81.3	3.56	1	77.00	9.49	2	13.60	0.224	3	4.00	0.17
12.70	48.00	3	42.20	82.1	3.80	1	76.80	9.45	2	4.70	0.077	3	2.80	0.12
12.70	54.00	3	47.30	92.2	3.92	1	76.90	9.47	2	0.70	0.012	3	3.60	0.15
12.70	60.00	3	46.60	90.8	4.19	1	76.00	9.28	3	74.00	0.034	3	4.70	0.20

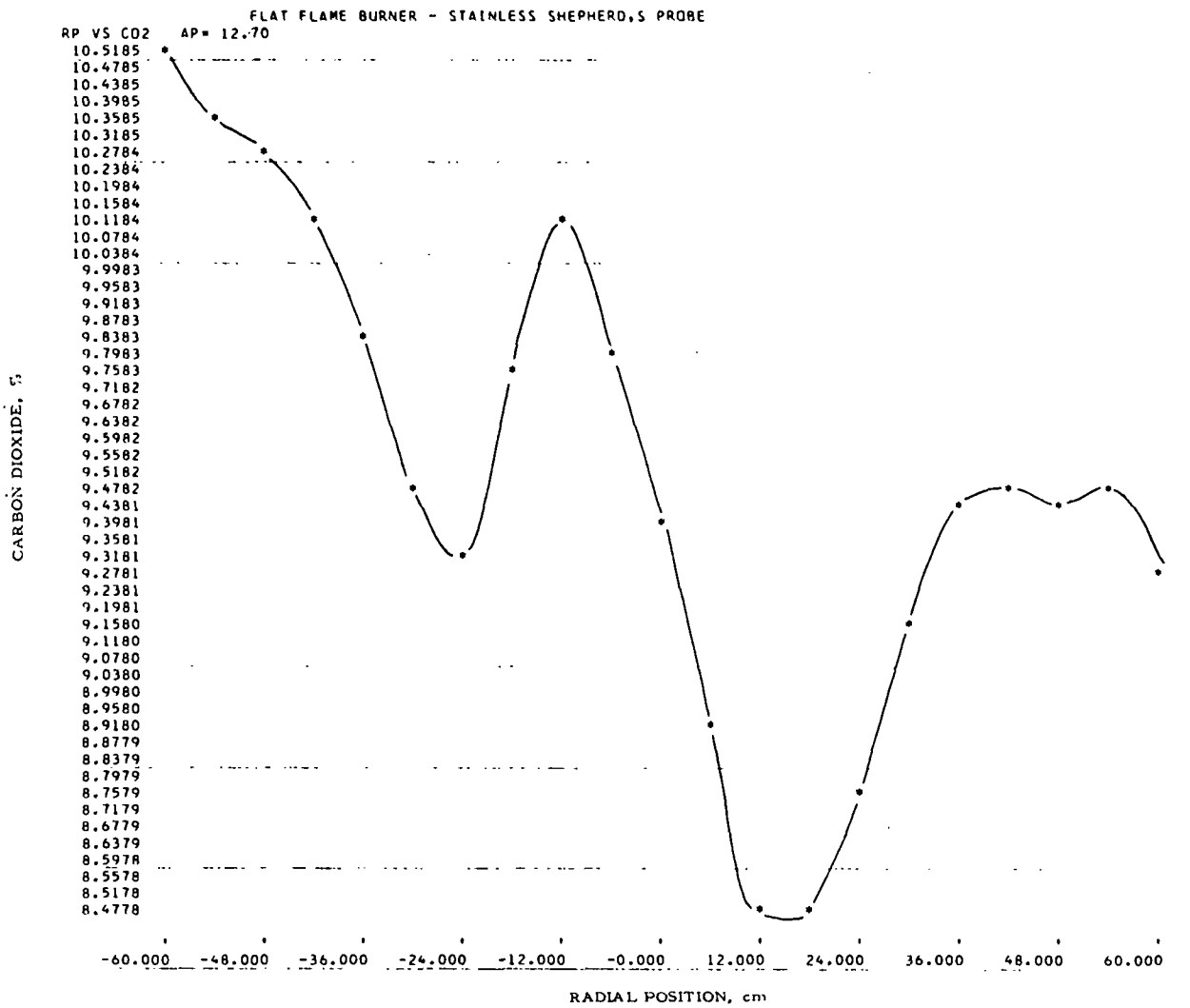

Figure II-272. RADIAL SCAN OF CARBON DIOXIDE FROM A FLAT-FLAME BURNER AT AN AXIAL POSITION OF 12.7 cm WHILE OPERATING AT A 2010 CF/hr GAS INPUT AND 4.4% EXCESS OXYGEN IN THE FLUE

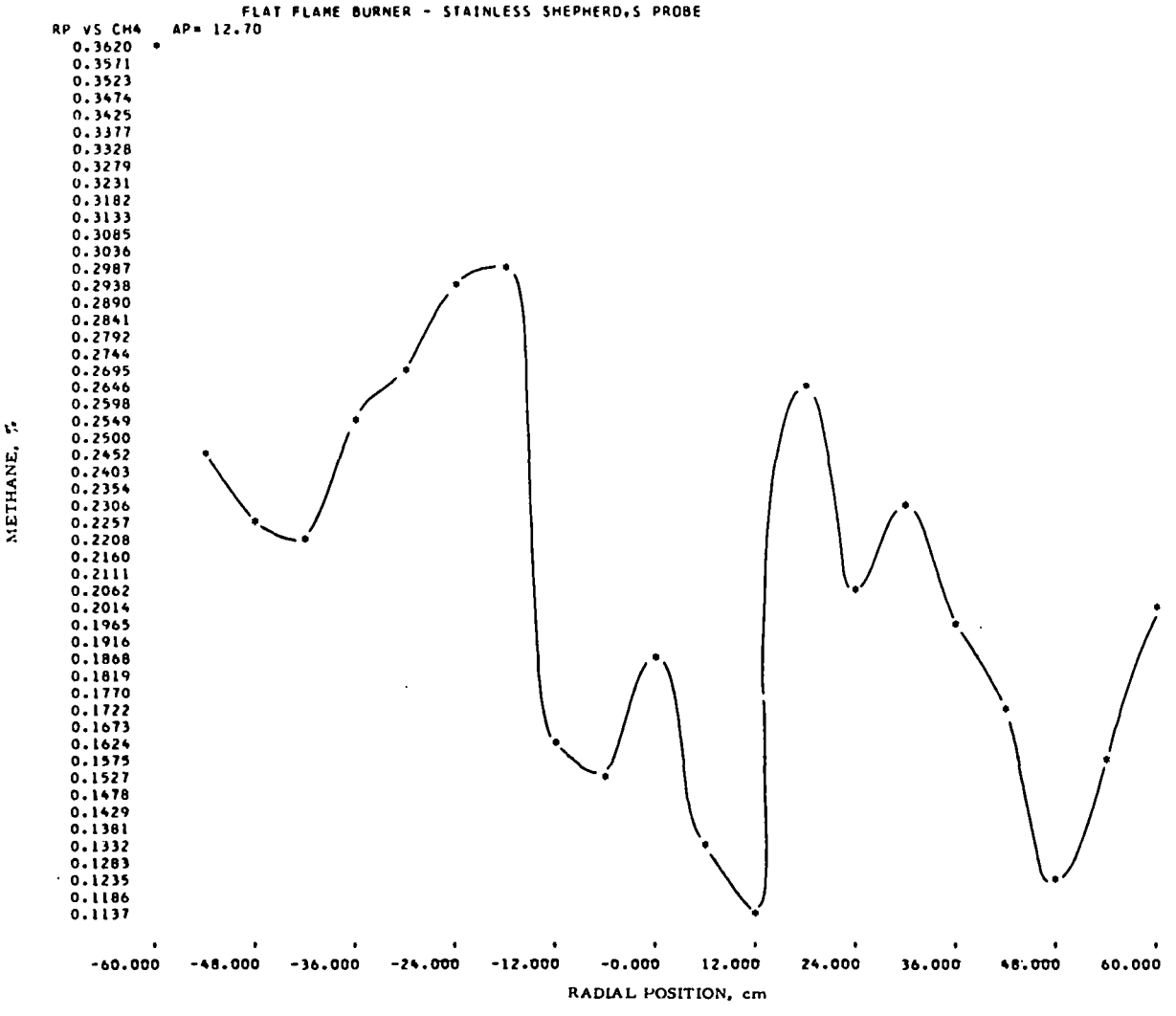

Figure II-273. RADIAL SCAN OF METHANE FROM A FLAT-FLAME BURNER AT AN AXIAL POSITION OF 12.7 cm WHILE OPERATING AT A 2010 CF/hr GAS INPUT AND 4.4% EXCESS OXYGEN IN THE FLUE

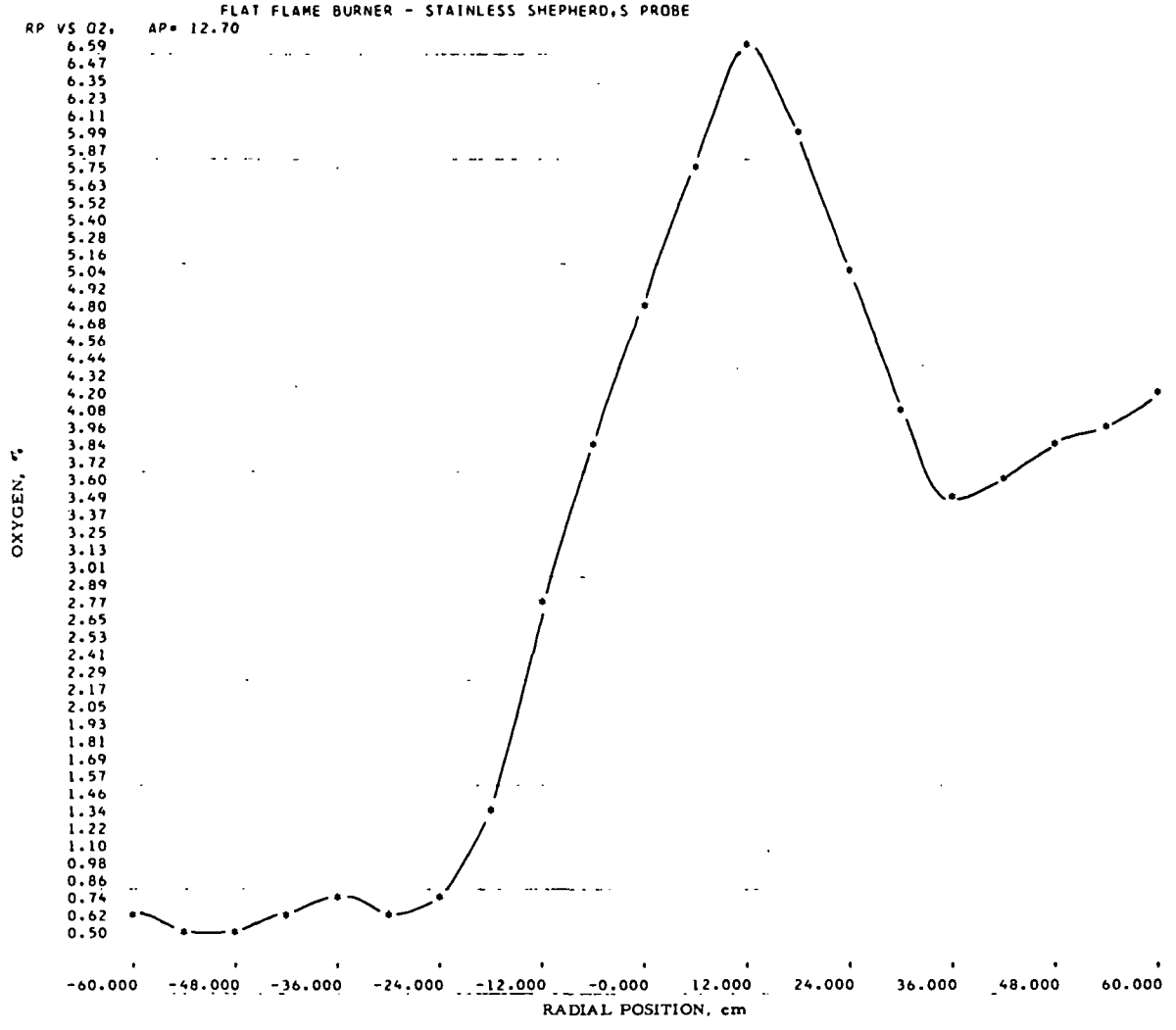

Figure II-274. RADIAL SCAN OF OXYGEN FROM A FLAT-FLAME BURNER AT AN AXIAL POSITION OF 12.7 cm WHILE OPERATING AT A 2010 CF/hr GAS INPUT AND 4.4% EXCESS OXYGEN IN THE FLUE

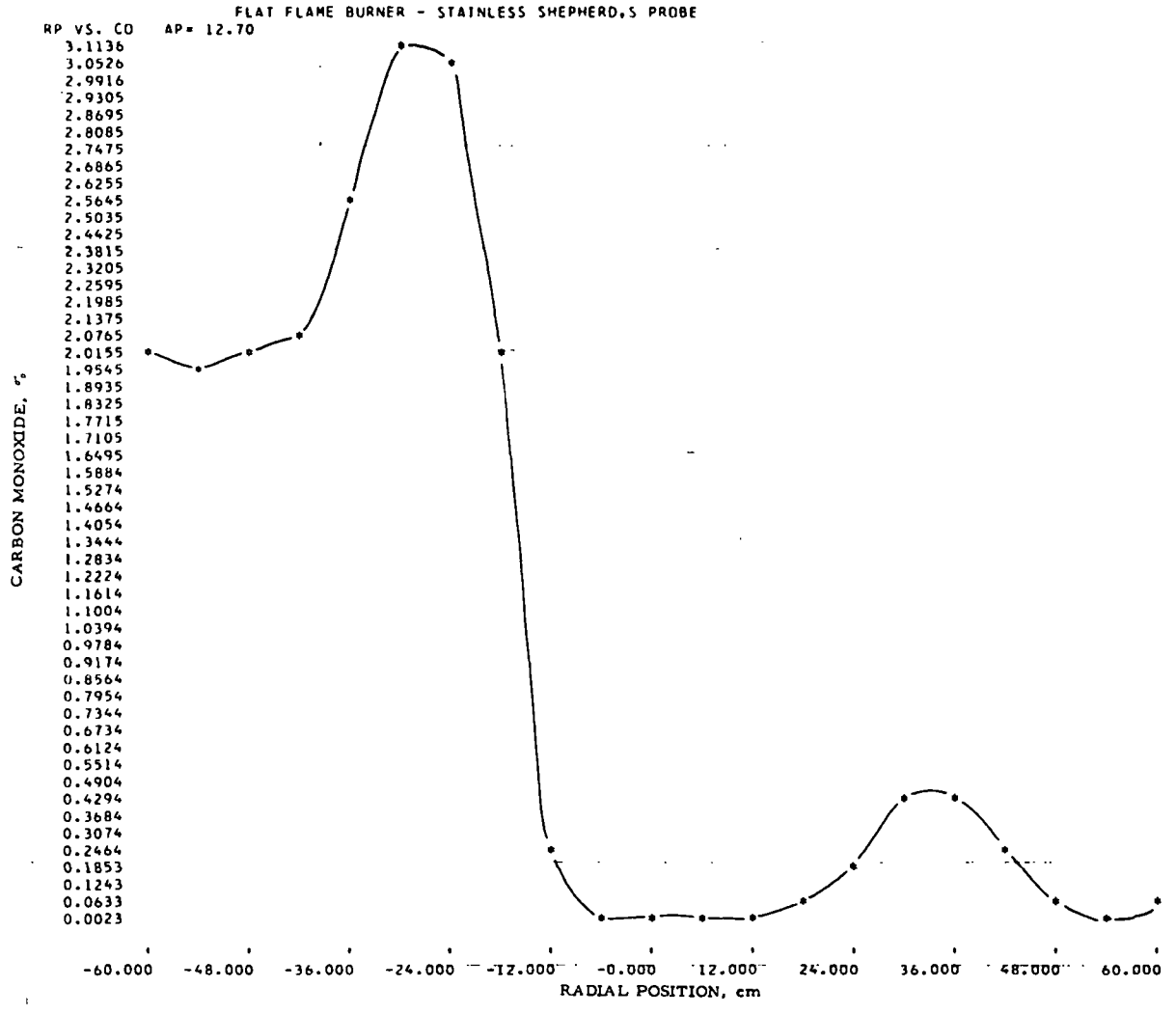

Figure II-275. RADIAL SCAN OF CARBON MONOXIDE FROM A FLAT-FLAME BURNER AT AN AXIAL POSITION OF 12.7 cm WHILE OPERATING AT A 2010 CF/hr GAS INPUT AND 4.4% EXCESS OXYGEN IN THE FLUE

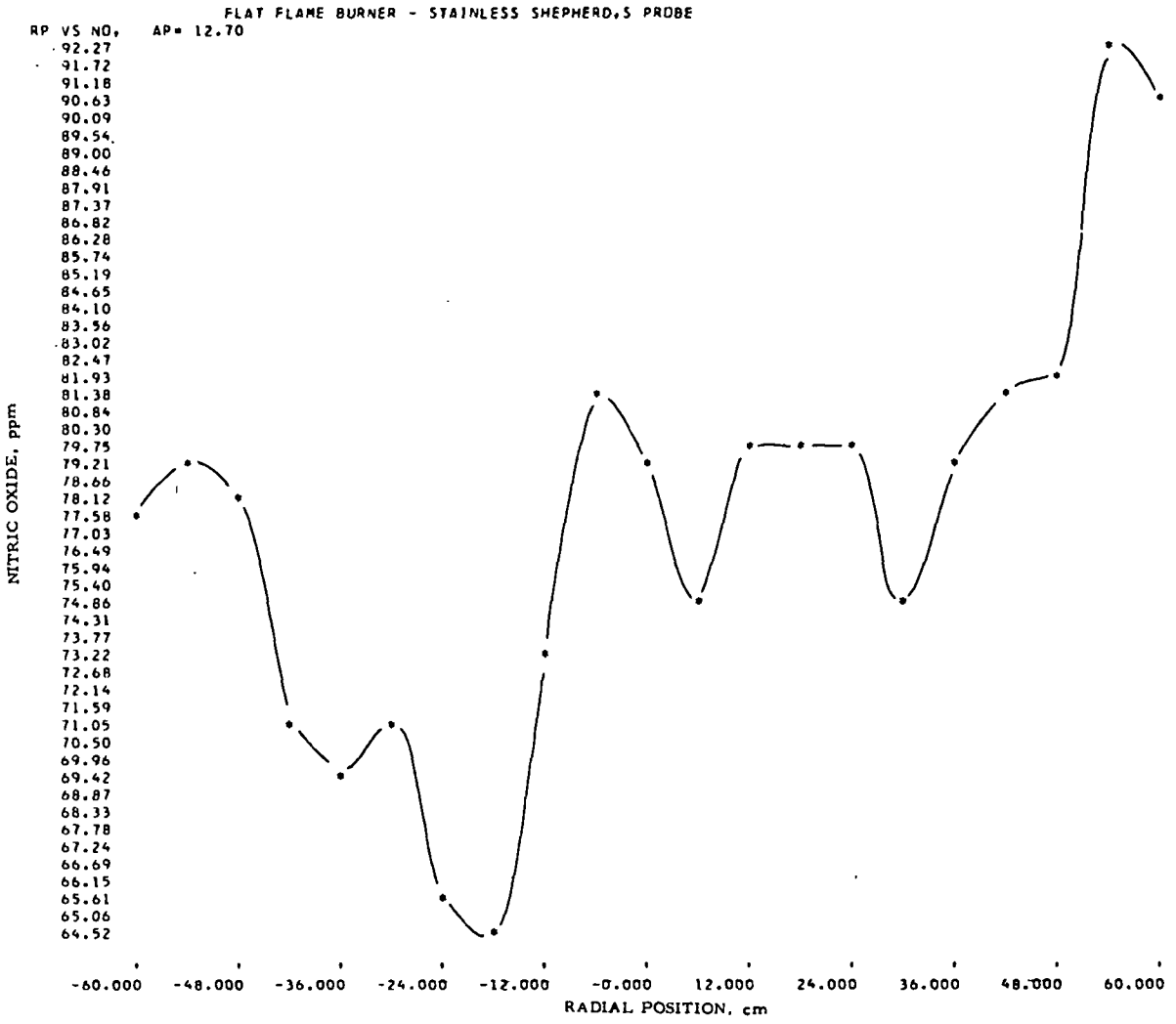

Figure II-276. RADIAL SCAN OF NITRIC OXIDE FROM A FLAT-FLAME BURNER AT AN AXIAL POSITION OF 12.7 cm WHILE OPERATING AT A 2010 CF/hr GAS INPUT AND 4.4% EXCESS OXYGEN IN THE FLUE

reduced data for an axial position of 68.6 cm are shown in Table II-70 and plotted as a composite graph in Figure II-277. Plots of each species with a greater resolution than in Figure II-277 are shown in Figures II-278, II-279, II-280, II-281, and II-282 for NO, O_2, CO_2, CO, and CH_4. The raw and reduced data for an axial position of 104.1 cm is shown in Table II-71 and plotted as a composite in Figure II-283. Again plots of each species at greater resolution are given in Figures II-284, II-285, II-286, II-287, and II-288.

E. Boiler Burner

1. Burner Design

The experimental burner used for these tests was a sealed-down (momentum) version of a typical vane-register boiler burner (Figure II-289). This design was selected because it generates the same type of swirl pattern and intensity as a large number of full-scale types from different major manufacturers. This type of vane arrangement is also readily mathematically modeled to describe the swirl intensity. The burner consists of eight air-guide vanes through which the air passes in parallel to the vane major area surfaces (Figure II-290). The vanes can be adjusted 90 degrees on their own axis from a full closed position to full open. At the full open position, the air stream is directed radially to the burner axis. By adjusting the angle of the vanes, the amount or intensity of swirl is changed. Gas is injected through a central tube located at the hot face of the burner block hole and on the axis of the burner. The end of the gas nozzle has a hemispherical head with eight gas ports drilled at a 45-degree angle to the burner axis. In this way the gas is injected slightly radially to the axis of the burner. The hole diameters in the end of the gas nozzle are 0.25 inch in diameter. The exit gas velocity is dependent on volumetric flow of gas. The design capacity of the burner is 4000 CF/hr for a gas velocity per nozzle of about 107 ft/s.

Table II-70. RAW AND REDUCED GAS SPECIES DATA FOR RADIAL SAMPLING SCANS AT AN AXIAL POSITION OF 68.6 cm FROM A FLAT-FLAME BURNER OPERATING AT A GAS INPUT OF 2010 CF/hr AND 4.4% EXCESS OXYGEN IN THE FLUE

TRACER GAS STUDIES OF COMBUSTION BURNERS PROGRAM 2
FLAT FLAME BURNER - STAINLESS SHEPHERD,S PROBE

INPUT GAS 2010 WALL TEMPERATURE 2480 PREHEAT TEMPERATURE 0

OUTPUT ANALYSIS

NITROGEN OXIDE	45.50 PERCENT	ON RANGE 3,	88.67 PPM	OXYGEN	4.40 PERCENT
CARBON DIOXIDE	75.70 PERCENT	ON RANGE**,	177.73 PERCENT		
CARBON MONOXIDE	1.60 PERCENT	ON RANGE 3,	0.000 PERCENT		
METHANE	0.00 PERCENT	ON RANGE 0,	0.00 PERCENT		

EXPERIMENTAL RESULTS

		NITROGEN OXIDE -NO			OXYGEN	CARBON DIOXIDE-CO2			CARBON MONOXIDE -CO			METHANE - CH4		
AP	RP	RANGE	X	Y	O2	RANGE	X	Y	RANGE	X	Y	RANGE	X	Y
68.60	-60.00	3	54.80	107.2	0.69	1	84.80	11.15	2	13.70	0.226	3	6.00	0.25
68.60	-50.00	3	50.80	99.2	0.77	1	85.50	11.30	2	9.20	0.150	3	5.60	0.24
68.60	-40.00	3	59.00	115.7	1.08	1	84.70	11.12	2	1.60	0.027	3	6.40	0.27
68.60	-30.00	3	56.10	109.8	1.65	1	86.20	11.46	3	104.30	0.052	3	6.20	0.26
68.60	-20.00	3	54.50	106.6	1.40	1	85.90	11.39	3	76.10	0.036	3	5.40	0.23
68.60	-10.00	3	48.70	95.0	2.28	1	83.30	10.82	3	52.70	0.023	3	5.00	0.21
68.60	0.00	3	49.40	96.4	3.08	1	80.90	10.30	3	9.70	0.003	3	4.70	0.20
68.60	10.00	3	47.90	93.4	3.81	1	78.90	9.88	3	0.60	0.000	3	4.40	0.19
68.60	20.00	3	44.40	86.4	4.84	1	76.00	9.28	3	1.20	0.000	3	3.80	0.16
68.60	30.00	3	43.90	85.4	4.92	1	75.40	9.16	3	0.50	0.000	3	4.10	0.17
68.60	40.00	3	42.70	83.1	5.08	1	75.10	9.10	3	1.40	0.000	3	4.70	0.20
68.60	50.00	3	39.10	75.9	5.23	1	74.00	8.88	3	2.60	0.001	3	3.80	0.16
68.60	60.00	3	36.30	70.4	6.01	1	72.00	8.49	3	1.10	0.000	3	4.50	0.19

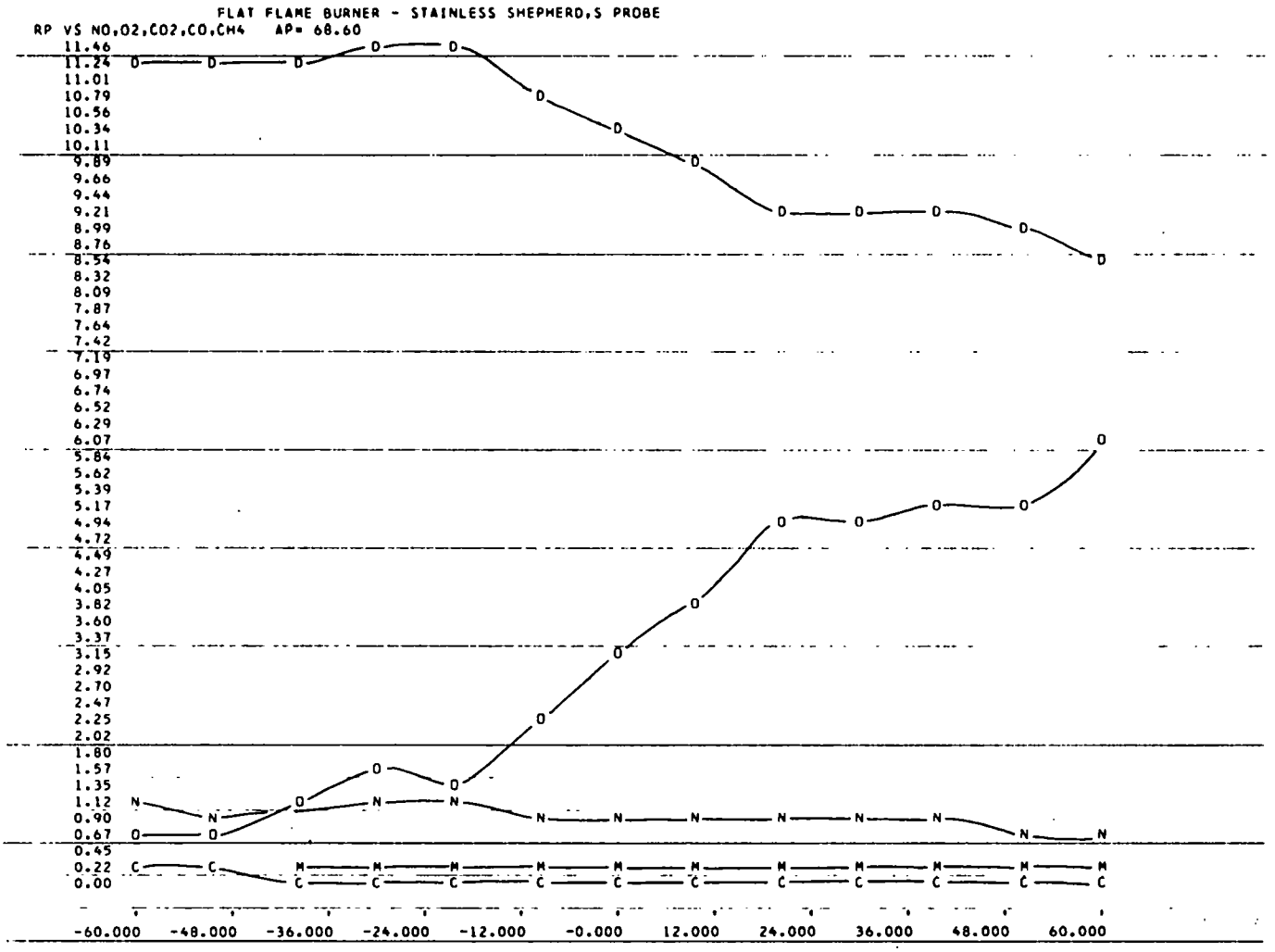

Figure II-277. COMPOSITE PLOT OF RADIAL GAS SPECIES CONCENTRATION AT A 68.6 cm AXIAL POSITION FOR A FLAT-FLAME BURNER OPERATING AT A GAS INPUT OF 2010 CF/hr AND 4.4% EXCESS OXYGEN IN THE FLUE

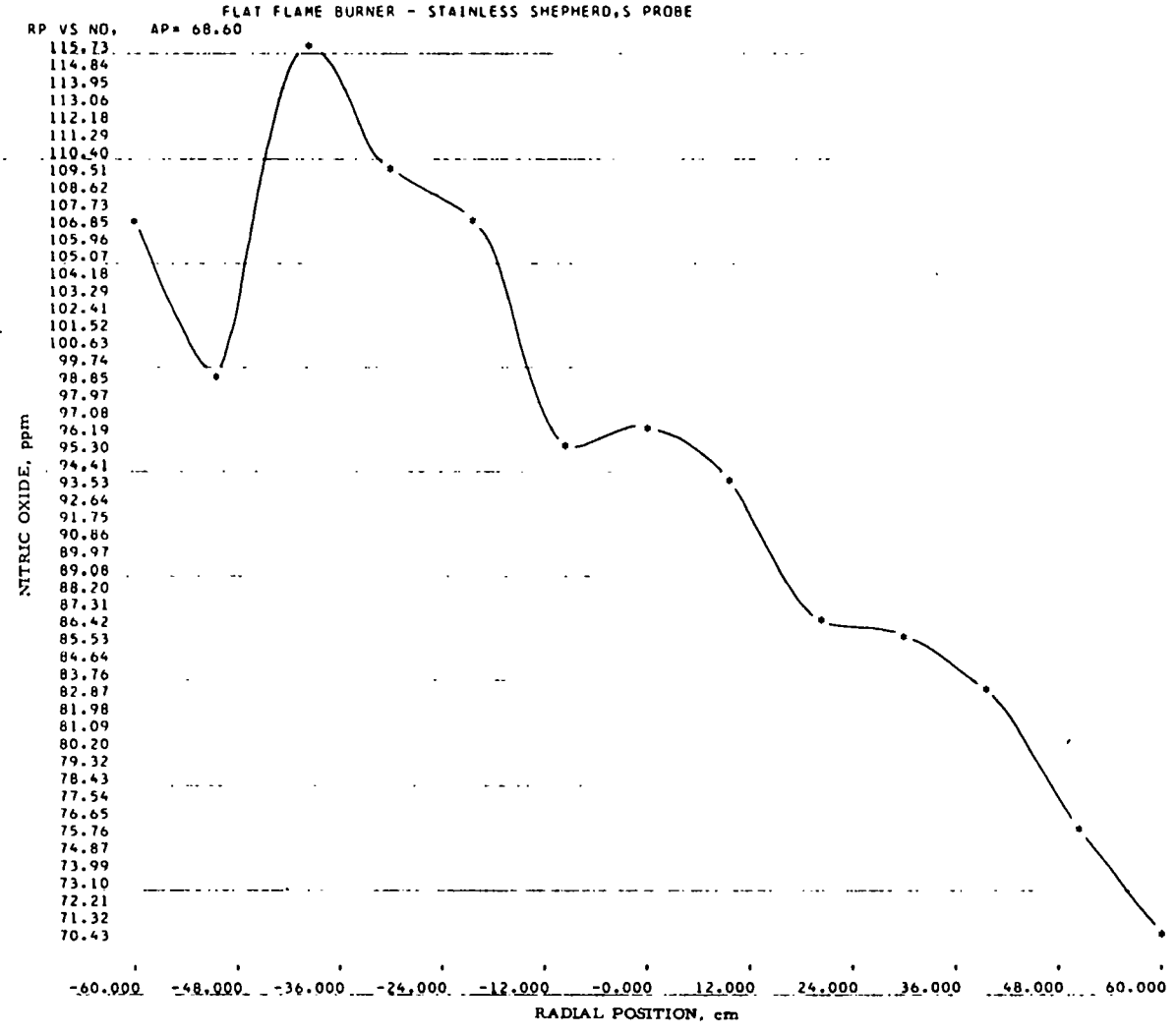

Figure II-278. RADIAL SCAN OF NITRIC OXIDE FROM A FLAT-FLAME BURNER AT AN AXIAL POSITION OF 68.6 cm WHILE OPERATING AT A 2010 CF/hr GAS INPUT AND 4.4% EXCESS OXYGEN IN THE FLUE

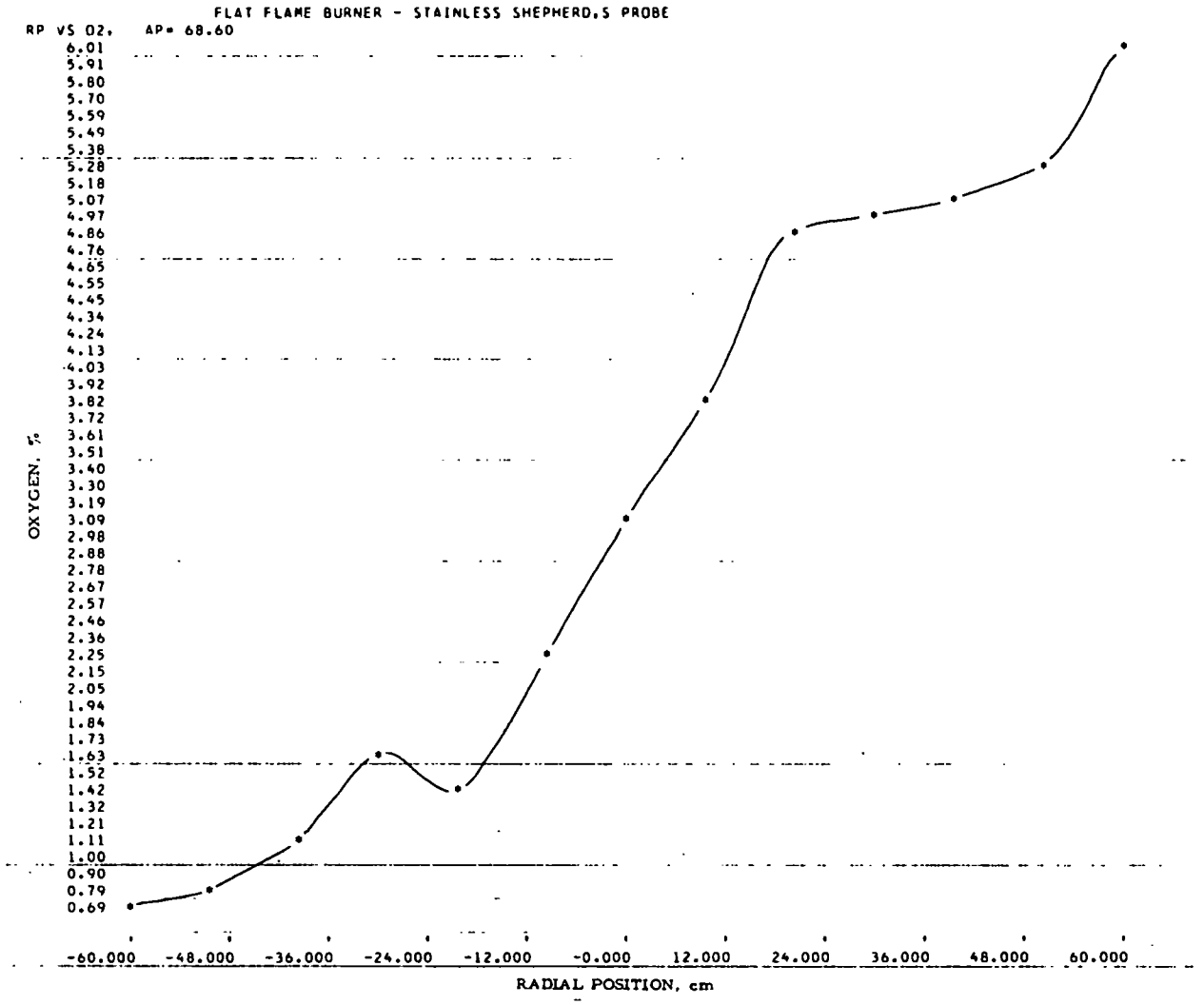

Figure II-279. RADIAL SCAN OF OXYGEN FROM A FLAT-FLAME BURNER AT AN AXIAL POSITION OF 68.6 cm WHILE OPERATING AT A 2010 CF/hr GAS INPUT AND 4.4% EXCESS OXYGEN IN THE FLUE

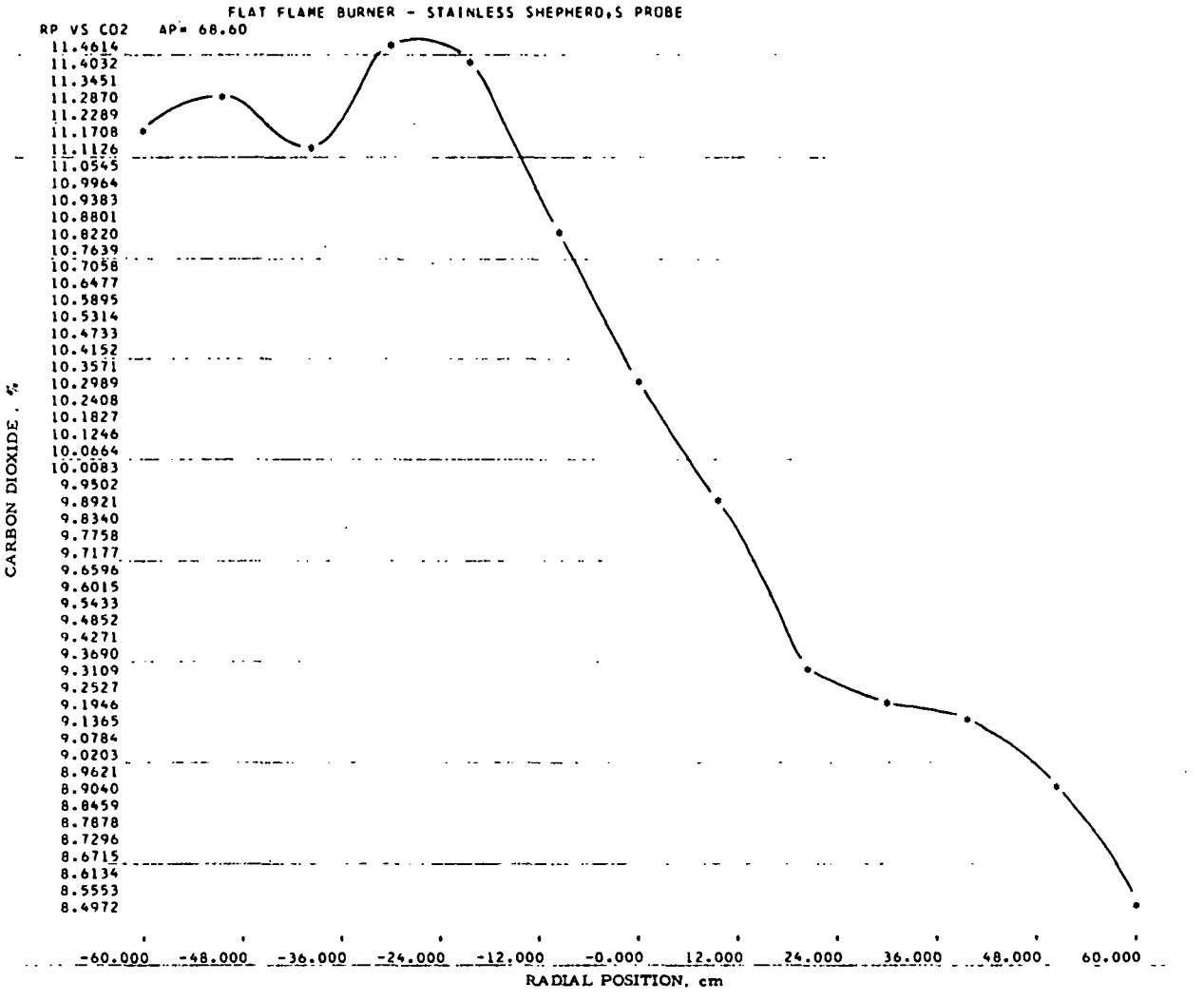

Figure II-280. RADIAL SCAN OF CARBON DIOXIDE FROM A FLAT-FLAME BURNER AT AN AXIAL POSITION OF 68.6 cm WHILE OPERATING AT A 2010 CF/hr GAS INPUT AND 4.4% EXCESS OXYGEN IN THE FLUE

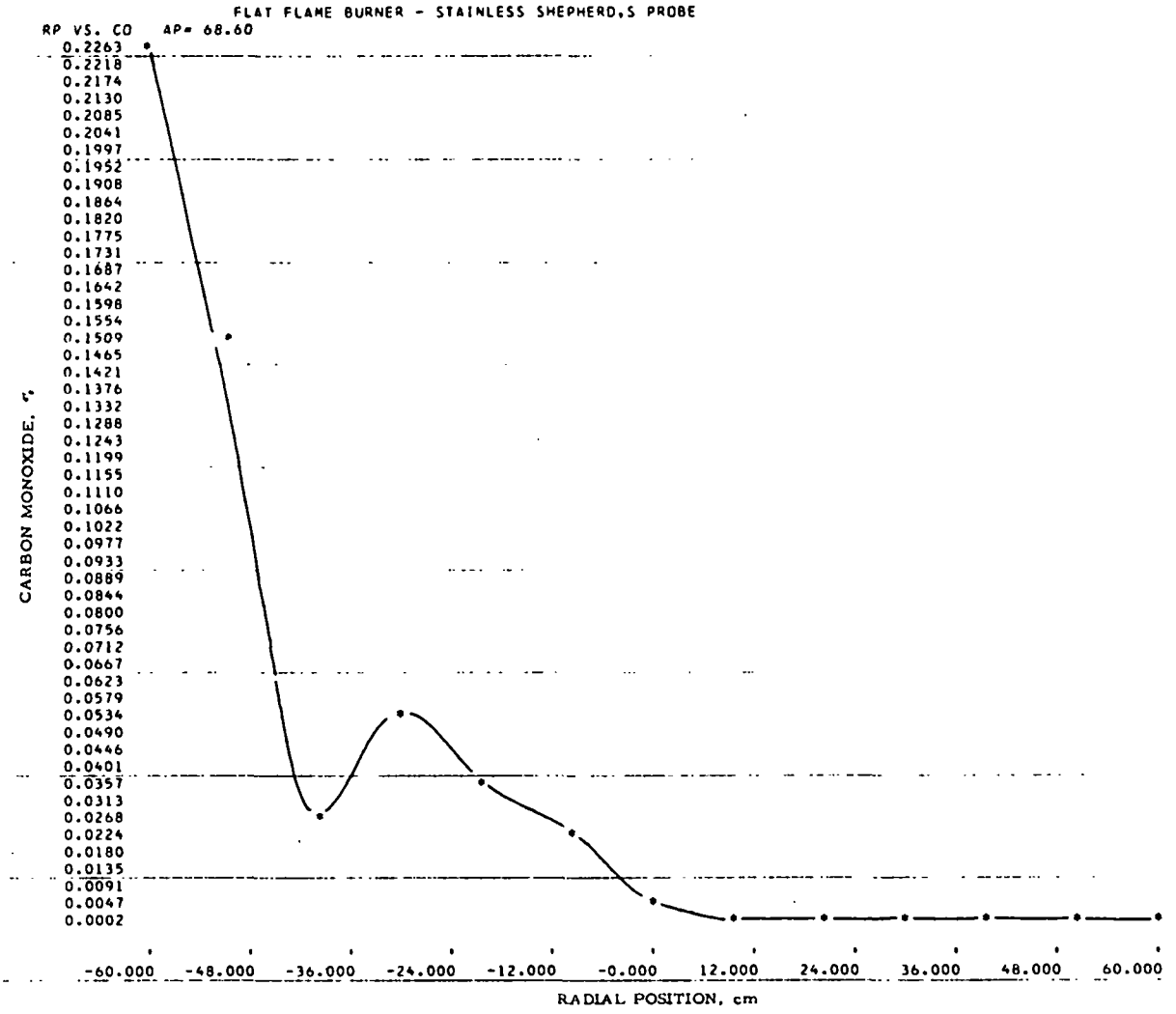

Figure II-281. RADIAL SCAN OF CARBON MONOXIDE FROM A FLAT-FLAME BURNER AT AN AXIAL POSITION OF 68.6 cm WHILE OPERATING AT A 2010 CF/hr GAS INPUT AND 4.4% EXCESS OXYGEN IN THE FLUE

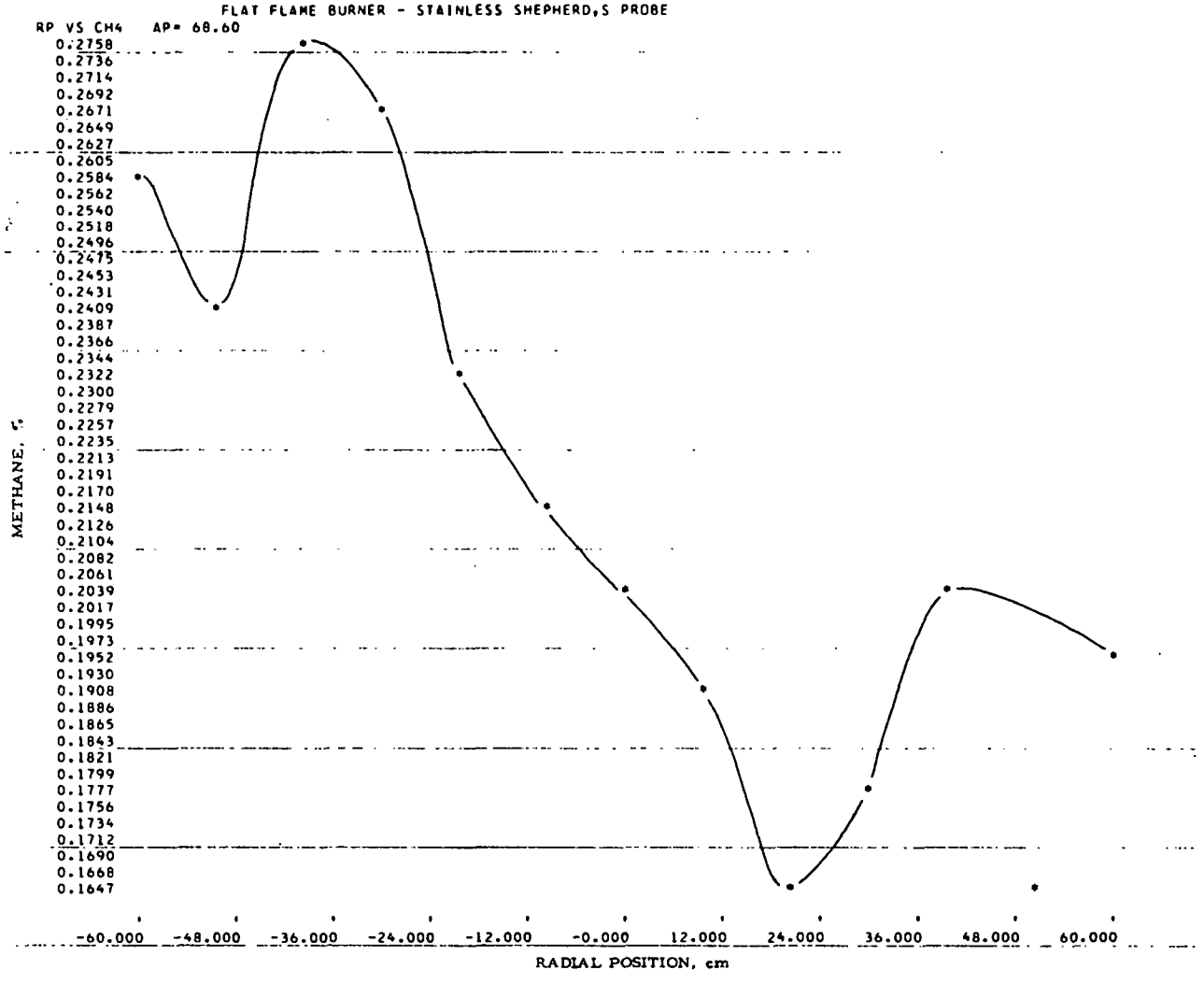

Figure II-282. RADIAL SCAN OF METHANE FROM A FLAT-FLAME BURNER AT AN AXIAL POSITION OF 68.6 cm WHILE OPERATING AT A 2010 CF/hr GAS INPUT AND 4.4% EXCESS OXYGEN IN THE FLUE

Table II-71. RAW AND REDUCED GAS SPECIES DATA FOR RADIAL SAMPLING SCANS AT AN AXIAL POSITION OF 104.1 cm FROM A FLAT-FLAME BURNER OPERATING AT A GAS INPUT OF 2010 CF/hr AND 4.4% EXCESS OXYGEN IN THE FLUE

TRACER GAS STUDIES OF COMBUSTION BURNERS PROGRAM 2
FLAT FLAME BURNER - STAINLESS SHEPHERD,S PROBE

INPUT GAS 2010 WALL TEMPERATURE 2480 PREHEAT TEMPERATURE 0

OUTPUT ANALYSIS

NITROGEN OXIDE	45.50 PERCENT ON RANGE 3,	88.67 PPM	OXYGEN 4.40 PERCENT
CARBON DIOXIDE	75.70 PERCENT ON RANGE**,	177.73 PERCENT	
CARBON MONOXIDE	1.60 PERCENT ON RANGE 3,	0.000 PERCENT	
METHANE	0.00 PERCENT ON RANGE 0,	0.00 PERCENT	

EXPERIMENTAL RESULTS

		NITROGEN OXIDE -NO			OXYGEN	CARBON DIOXIDE-CO2			CARBON MONOXIDE -CO			METHANE - CH4		
AP	RP	RANGE	X	Y	O2	RANGE	X	Y	RANGE	X	Y	RANGE	X	Y
104.10	-60.00	3	39.40	76.5	1.62	1	84.40	11.06	3	39.50	0.017	3	6.20	0.26
104.10	-50.00	3	38.80	75.3	1.57	1	84.50	11.08	3	35.80	0.015	3	5.30	0.22
104.10	-40.00	3	37.40	72.6	1.82	1	83.90	10.95	3	19.50	0.008	3	5.20	0.22
104.10	-30.00	3	37.40	72.6	1.92	1	83.60	10.88	3	12.50	0.005	3	4.90	0.21
104.10	-20.00	3	37.70	73.2	2.34	1	83.20	10.79	3	11.80	0.004	3	5.50	0.23
104.10	-10.00	3	35.10	68.0	2.82	1	80.10	10.13	3	7.00	0.002	3	4.60	0.19
104.10	0.00	3	34.00	65.8	3.07	1	79.80	10.07	3	3.50	0.001	3	4.10	0.17
104.10	10.00	3	33.20	64.3	3.60	1	79.30	9.96	3	2.70	0.001	3	4.50	0.19
104.10	20.00	3	33.90	65.7	4.37	1	77.50	9.59	3	1.70	0.000	3	4.90	0.21
104.10	30.00	3	33.60	65.1	4.80	1	76.00	9.28	3	0.60	0.000	3	4.20	0.18
104.10	40.00	3	30.50	59.0	5.09	1	74.80	9.04	3	0.50	0.000	3	4.00	0.17
104.10	50.00	3	31.40	60.7	5.38	1	73.90	8.86	3	1.70	0.000	3	4.80	0.20
104.10	60.00	3	29.50	57.0	5.88	1	72.10	8.51	3	2.00	0.000	3	3.40	0.14

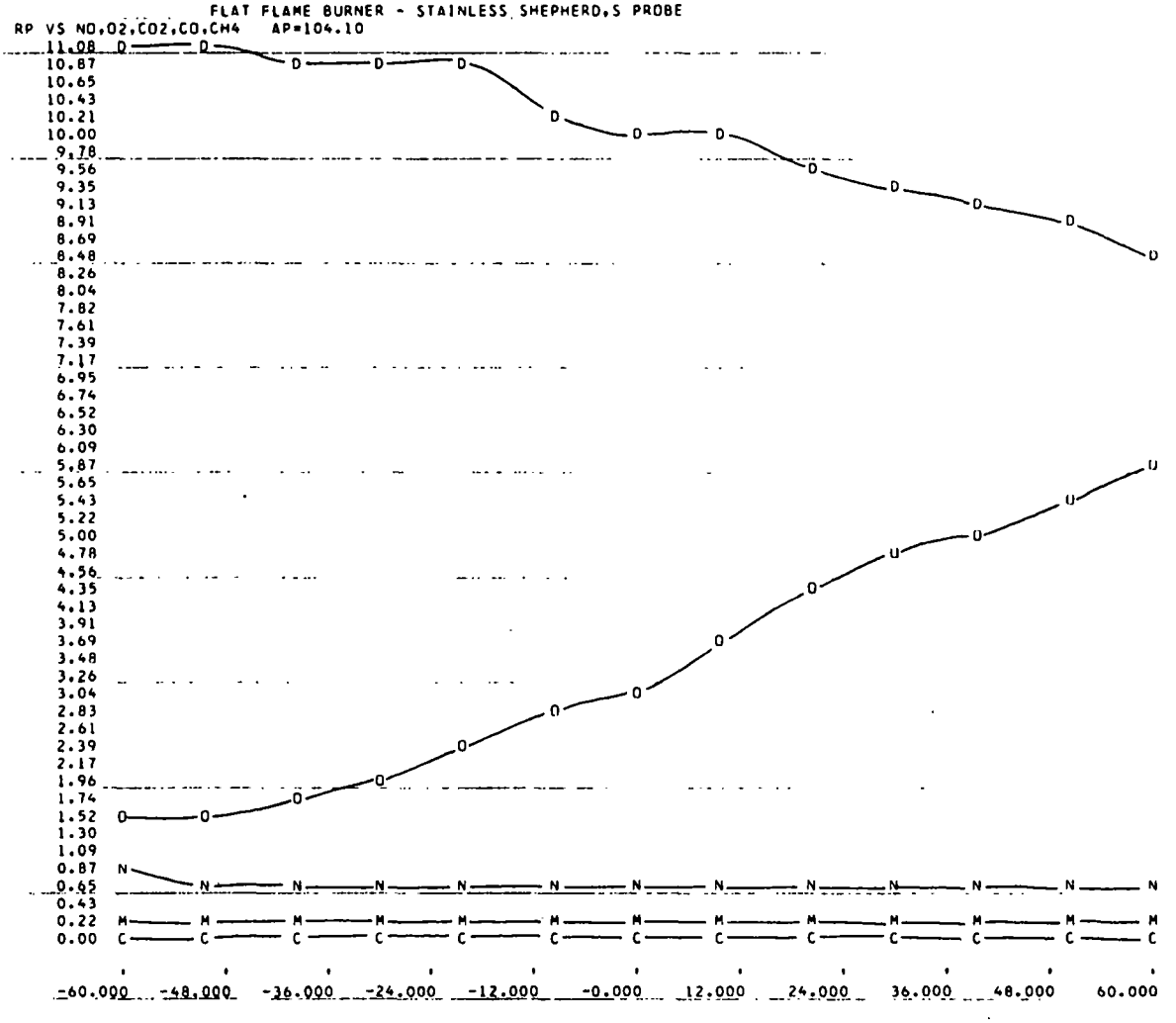

Figure II-283. COMPOSITE PLOT OF RADIAL GAS SPECIES CONCENTRATION AT A 104.1 cm AXIAL POSITION FOR A FLAT-FLAME BURNER OPERATING AT A GAS INPUT OF 2010 CF/hr AND 4.4% EXCESS OXYGEN IN THE FLUE

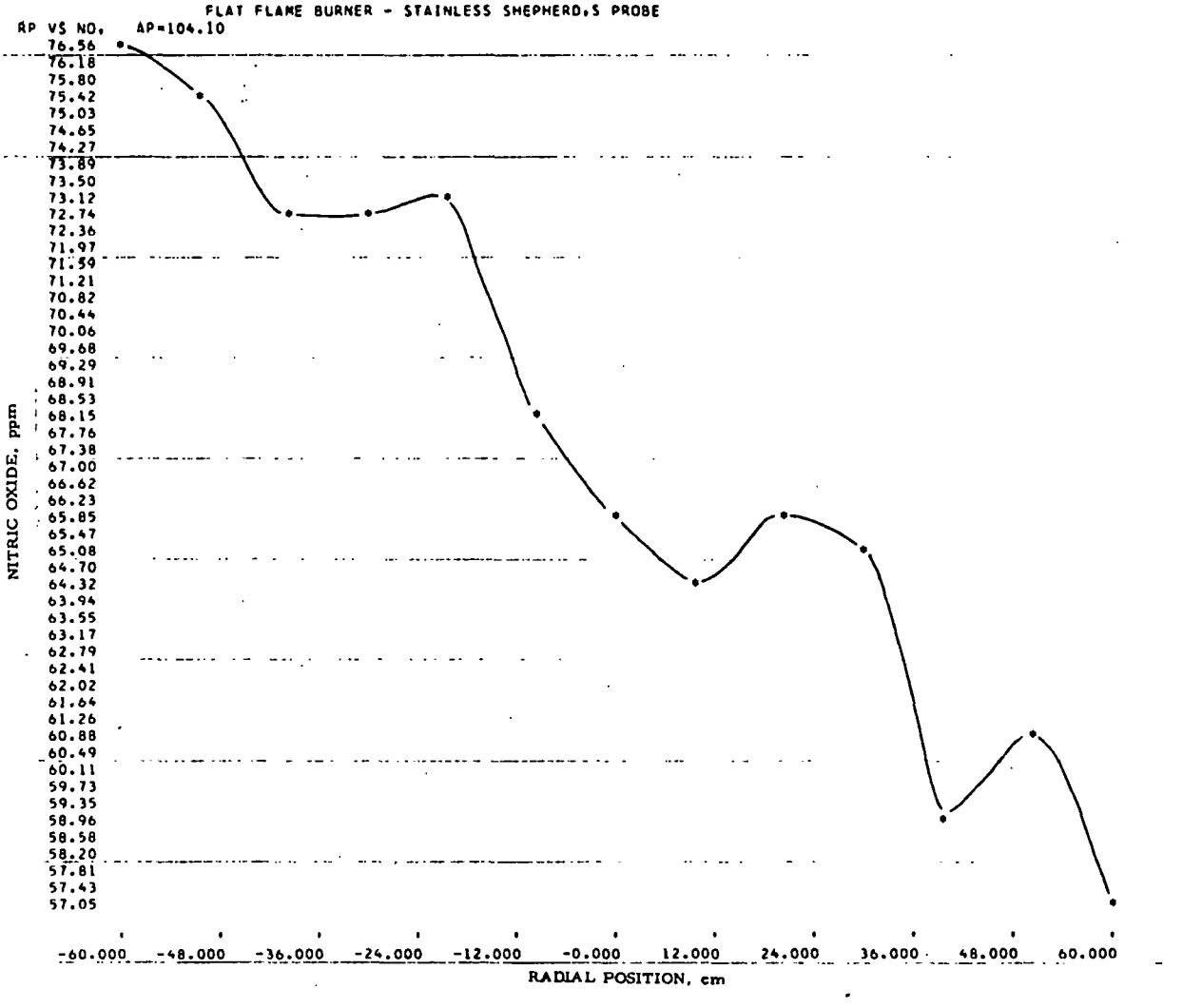

Figure II-284. RADIAL SCAN OF NITRIC OXIDE FROM A FLAT-FLAME BURNER AT AN AXIAL POSITION OF 104.1 cm WHILE OPERATING AT A 2010 CF/hr GAS INPUT AND 4.4% EXCESS OXYGEN IN THE FLUE

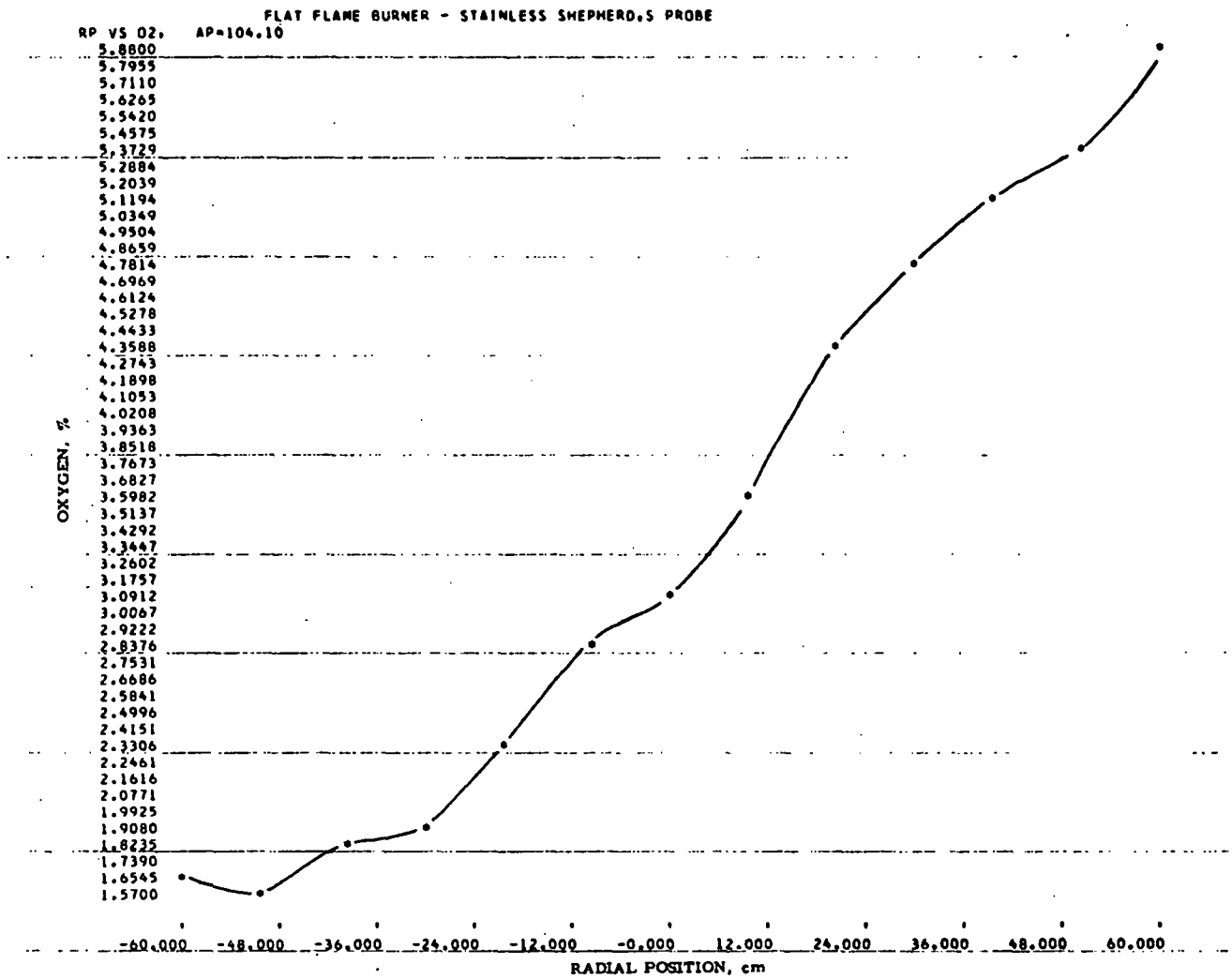

Figure II-285. RADIAL SCAN OF OXYGEN FROM A FLAT-FLAME BURNER AT AN AXIAL POSITION OF 104.1 cm WHILE OPERATING AT A 2010 CF/hr GAS INPUT AND 4.4% EXCESS OXYGEN IN THE FLUE

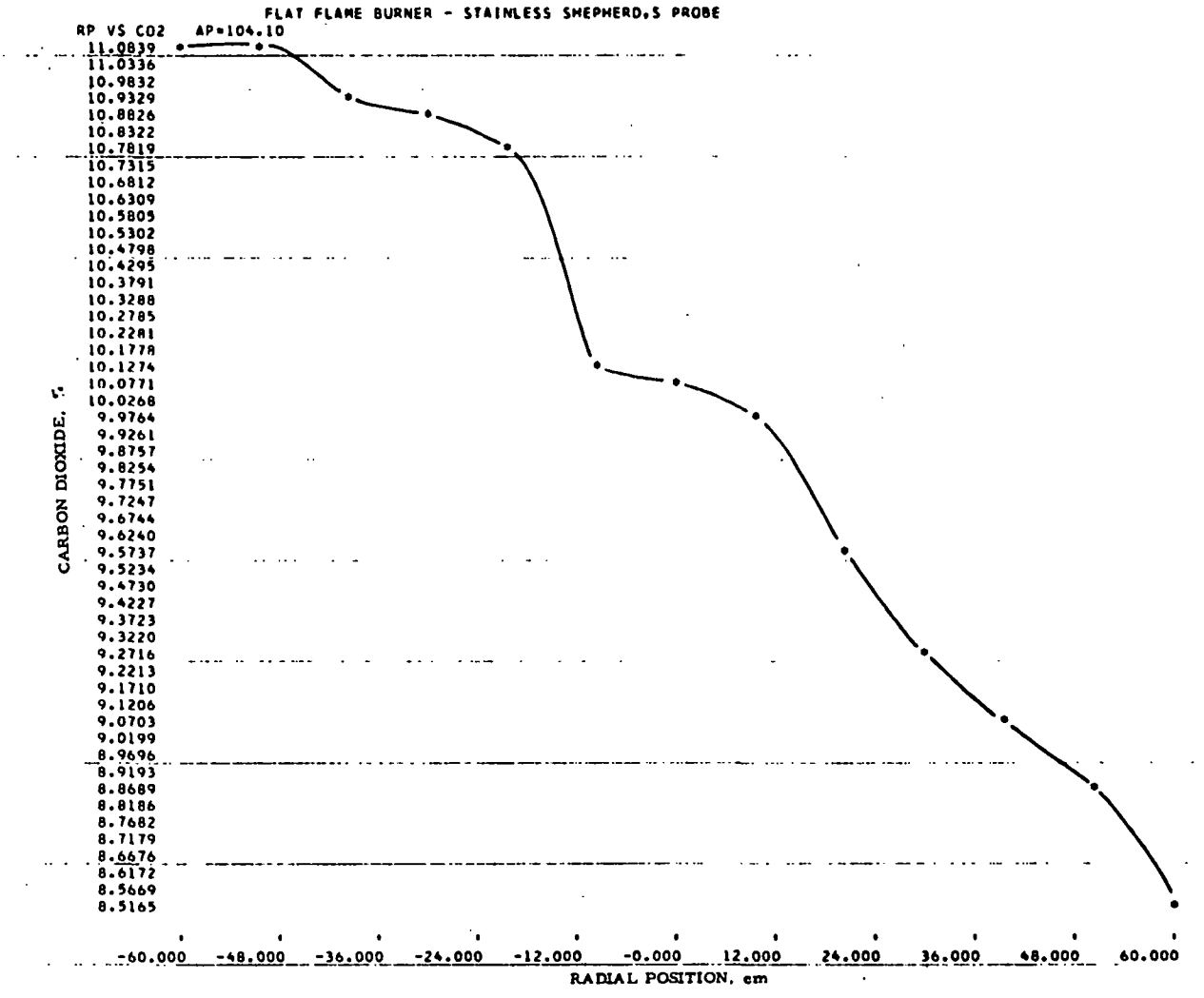

Figure II-286. RADIAL SCAN OF CARBON DIOXIDE FROM A FLAT-FLAME BURNER AT AN AXIAL POSITION OF 104.1 cm WHILE OPERATING AT A 2010 CF/hr GAS INPUT AND 4.4% EXCESS OXYGEN IN THE FLUE

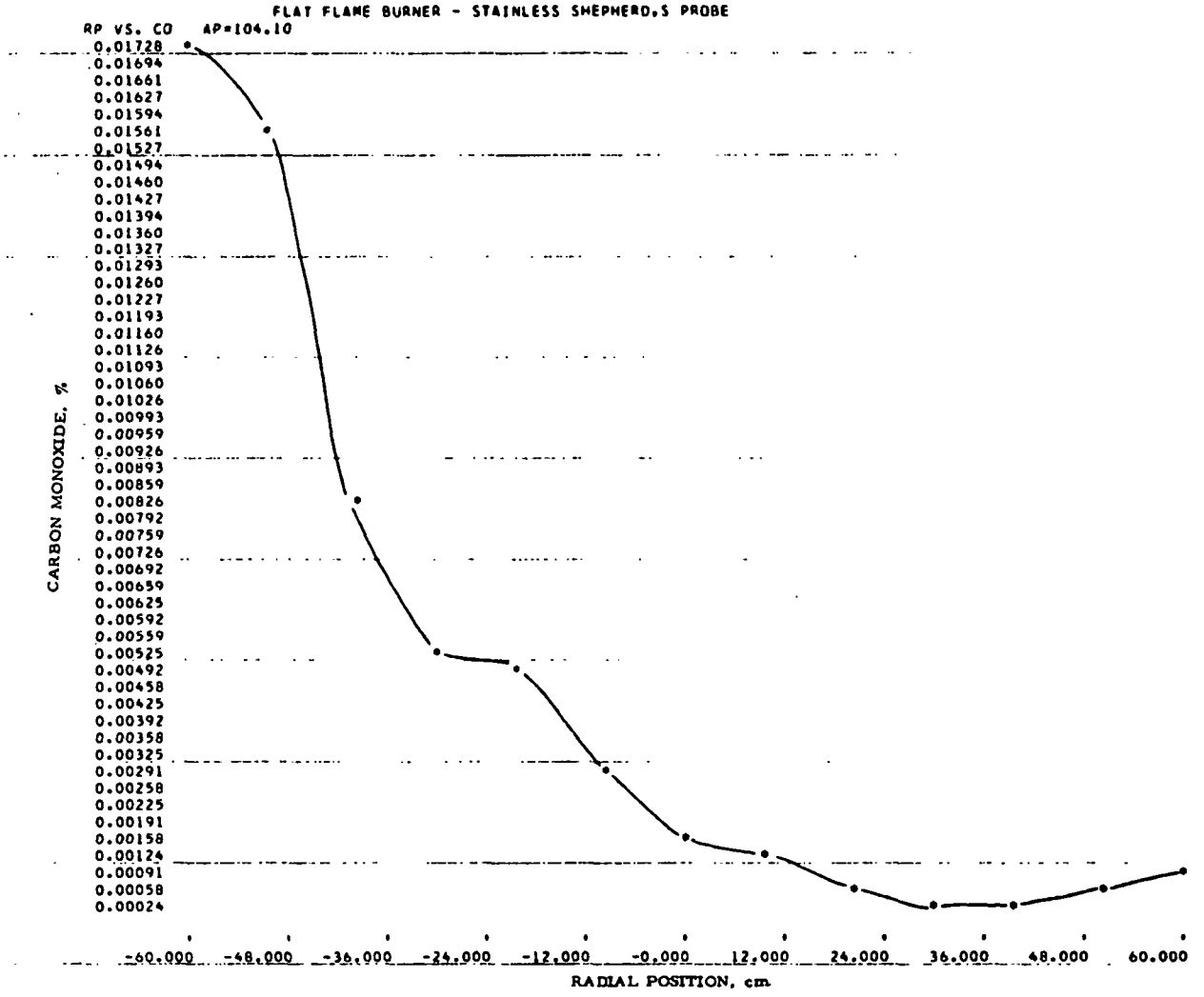

Figure II-287. RADIAL SCAN OF CARBON MONOXIDE FROM A FLAT-FLAME BURNER AT AN AXIAL POSITION OF 104.1 cm WHILE OPERATING AT A 2010 CF/hr GAS INPUT AND 4.4% EXCESS OXYGEN IN THE FLUE

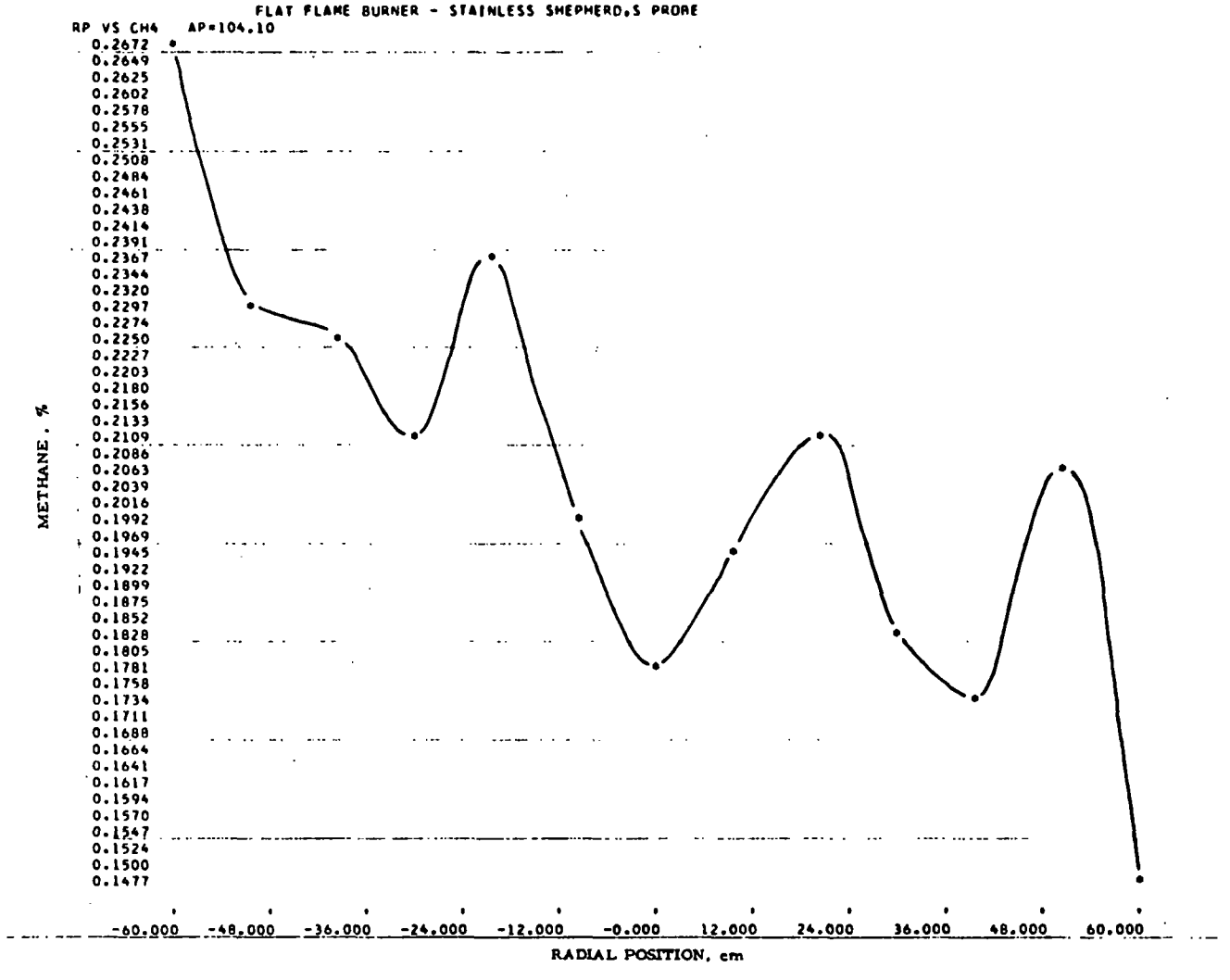

Figure II-288. RADIAL SCAN OF METHANE FROM A FLAT-FLAME BURNER AT AN AXIAL POSITION OF 104.1 cm WHILE OPERATING AT A 2010 CF/hr GAS INPUT AND 4.4% EXCESS OXYGEN IN THE FLUE

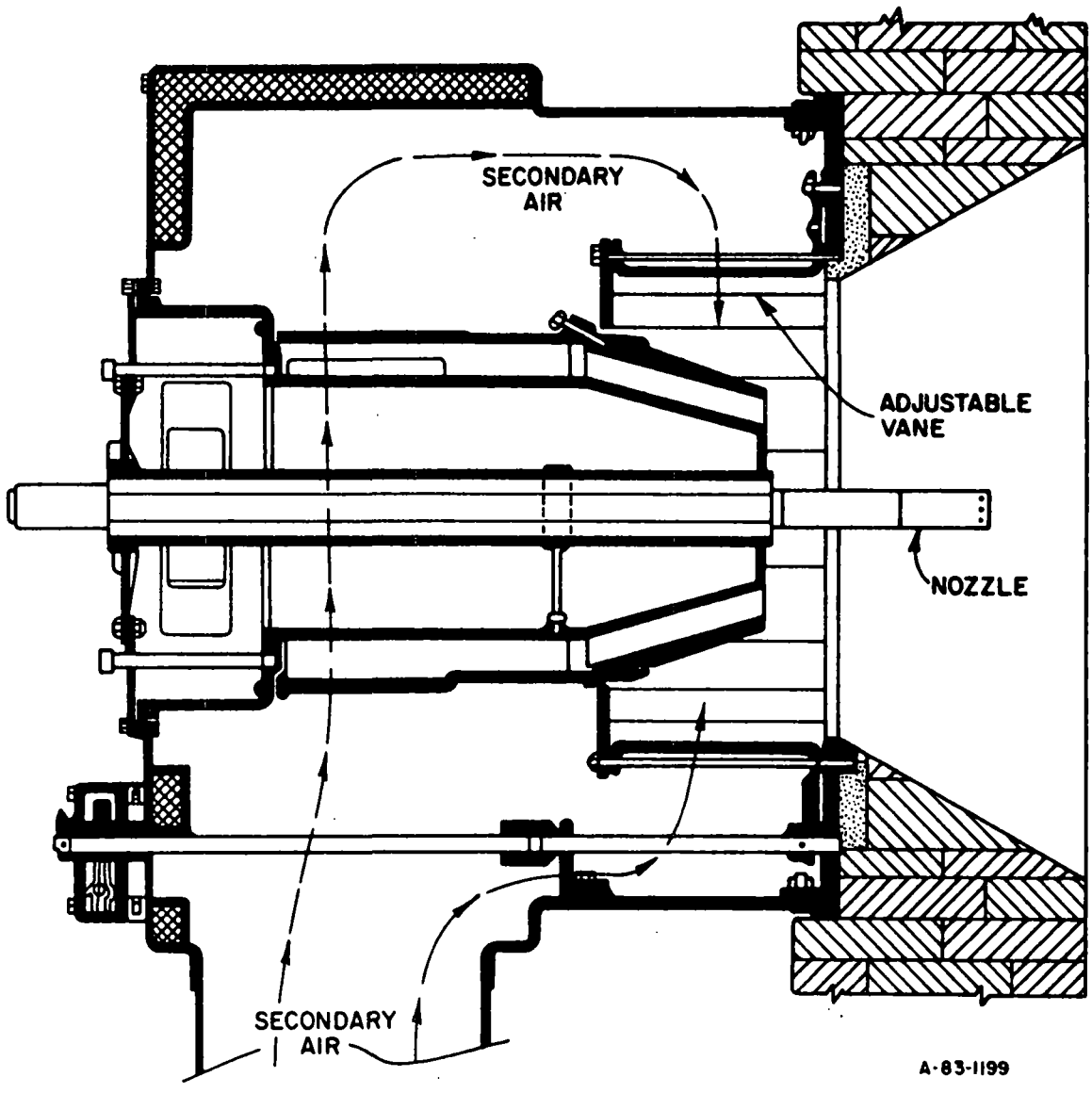

Figure II-289. BOILER BURNER

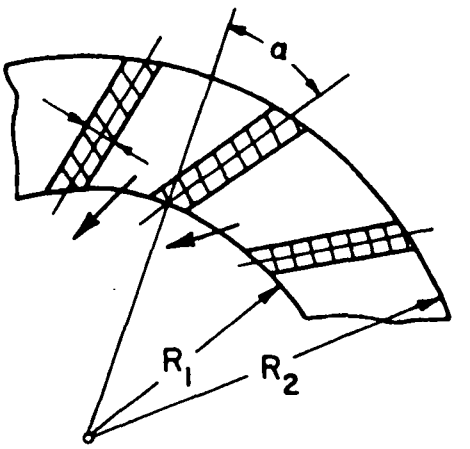

A-53-787

Figure II-290. GUIDE VANES

2. Hot-Model Input-Output Data

The boiler burner was operated at only one gas input during these tests. The characteristic stability of the burner occurred at 75% of rated input or 3020 CF/hr of natural gas. Gas inputs of less than 3000 CF/hr prevented good control of excess air level and fuel oxygen concentrations below 5%. Burning more than 3020 CF/hr resulted in excessively long flames and instability of the flame pattern. This occurred because the gas velocity from the nozzles was high enough to push through the swirling air stream. Drilling larger ports in the gas nozzle to lower velocity was not possible because of the overall nozzle diameter. A new burner design with a large gas nozzle is needed to give greater flexibility to the gas input.

Figures II-291, II-292, and II-293 show the results of the input-output tests as a function of combustion air temperature and amount of excess air (excess oxygen in the flue) for three different vane angles. Changing the combustion air temperature had about the same effect for the boiler burner as other burners studied, particularly the intermediate baffle burner. Increasing air temperature increased the amount of NO and shifted the location of the peak NO to higher amounts of excess air. Changing the vane angle (changing the swirl intensity) also had an effect on the NO formed. Increasing the vane angle, which increases the swirl intensity,

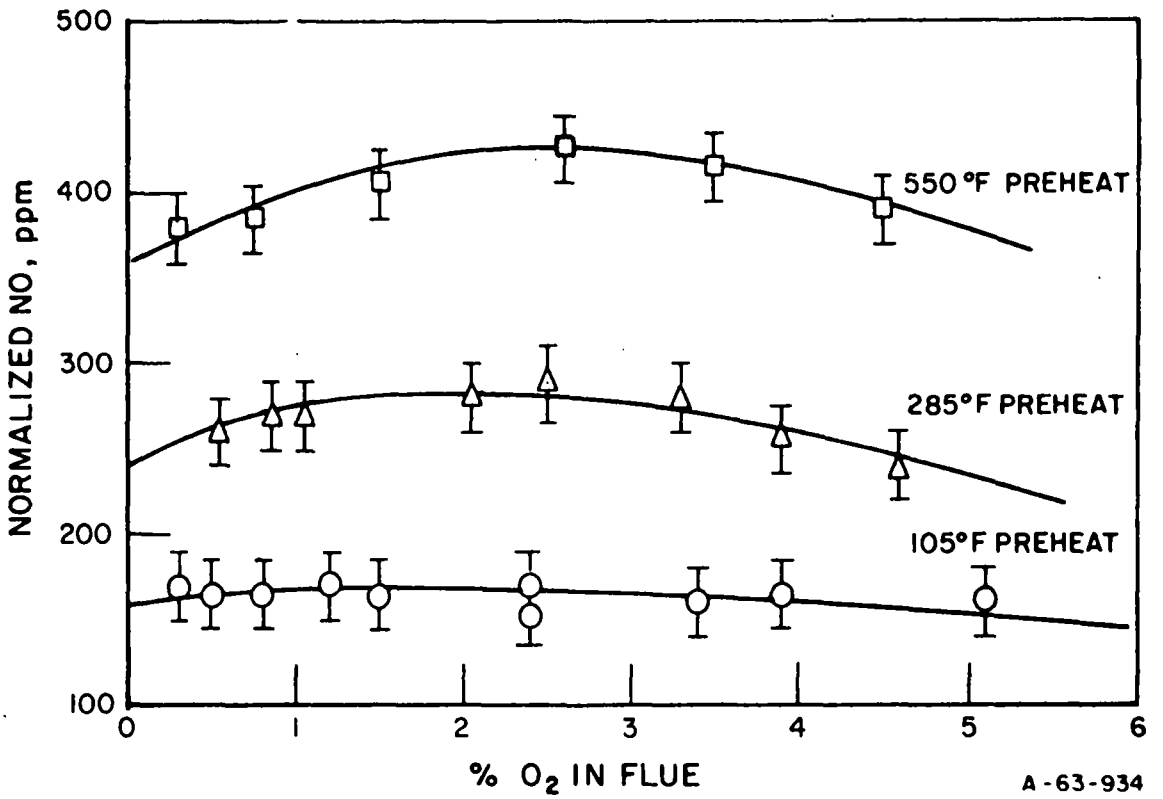

Figure II-291. NORMALIZED NO CONCENTRATION AS A FUNCTION OF EXCESS AIR (Boiler Burner With 30-deg Vane Setting; Gas Input, 3020 CF/hr) AND COMBUSTION AIR TEMPERATURE

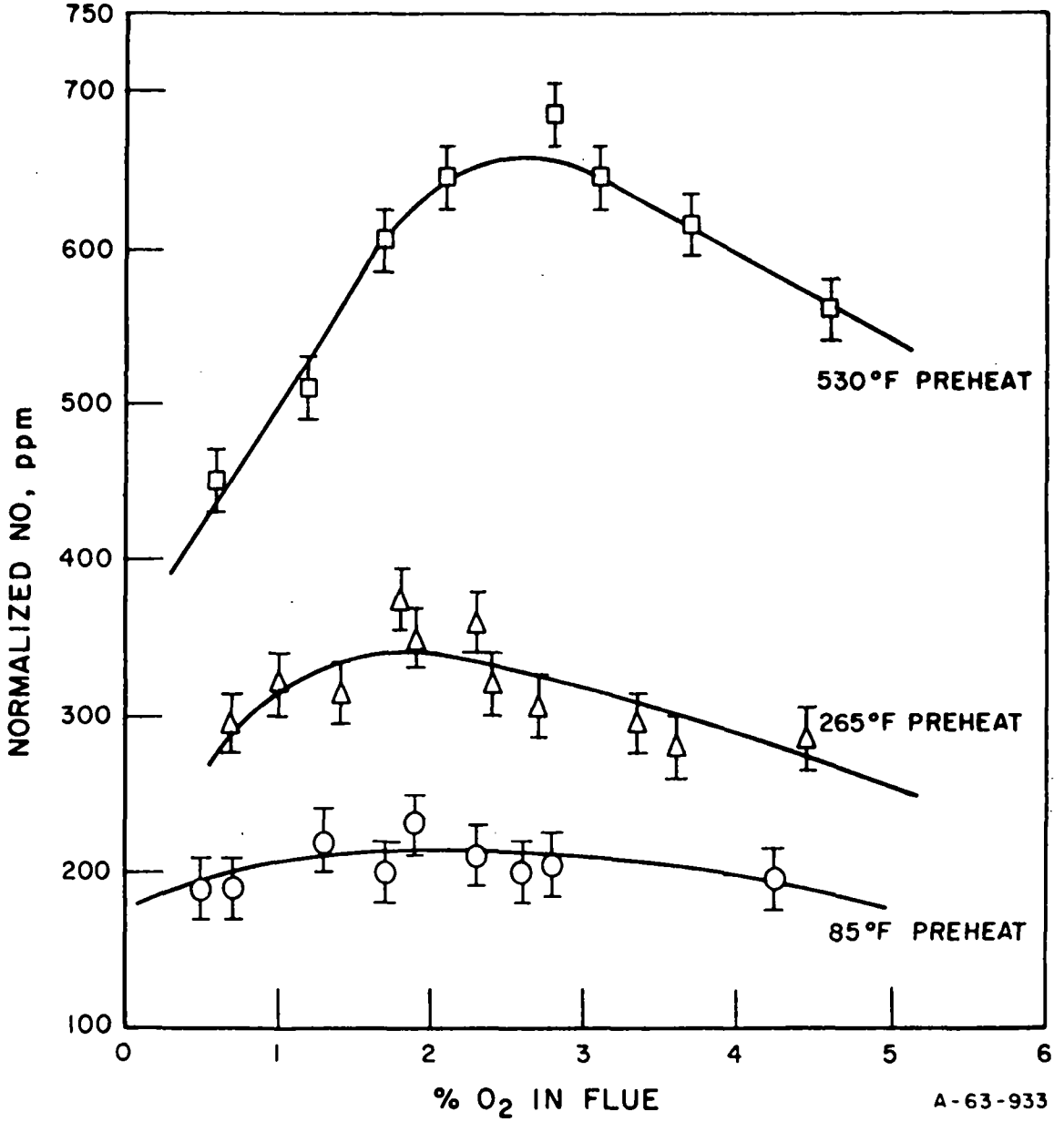

Figure II-292. NORMALIZED NO CONCENTRATION AS A FUNCTION OF EXCESS AIR (Boiler Burner With 40-deg Angle Vane Setting; Gas Input, 3040 CF/hr) AND COMBUSTION AIR TEMPERATURE

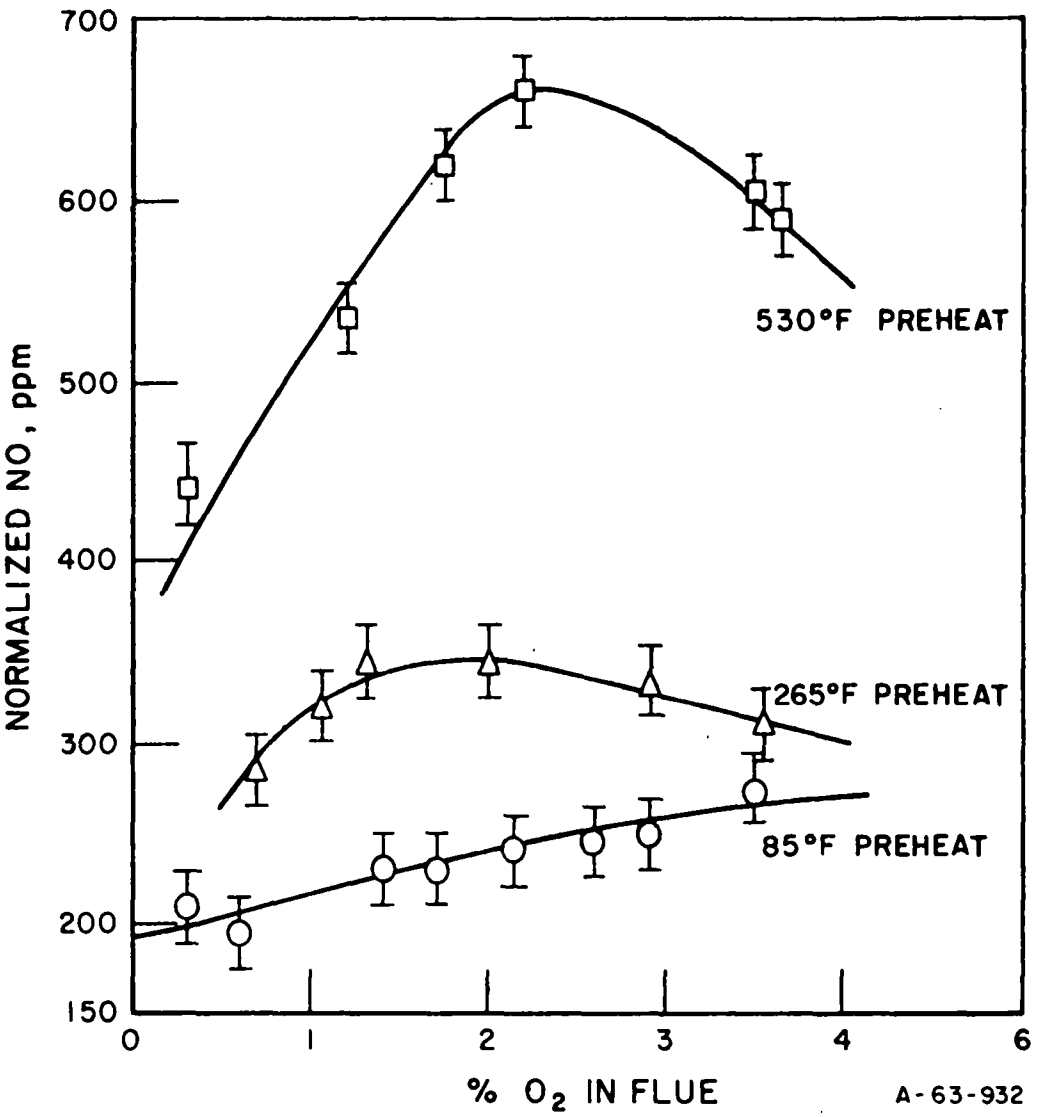

Figure II-293. NORMALIZED NO CONCENTRATION AS A FUNCTION OF EXCESS AIR (Boiler Burner With 60-deg Angle Vane Setting; Gas Input 3040 CF/hr) AND COMBUSTION AIR TEMPERATURE

generally increased the amount of NO formed. However, the magnitude of the change in NO varied with the preheat temperature of the air and the total amount the vanes were open. The greatest increase in NO occurred, for any change in vane angle, at the higher air temperatures. At near ambient air temperatures, changing the vane angle had relatively little effect on the amount of NO observed in the flue. The amount the vanes were open prior to any vane change also affected the magnitude of change of NO. At a preheat temperature of about 530°F, increasing the vane angle from 30 to 40 degrees increased NO from 425 to 630 ppm at a 2% concentration of oxygen in the flue. This is an increase of 205 ppm. However, increasing the vane angle from 40 to 60 degrees at the same level of air preheat temperature only increased the NO from 630 to 650 ppm or 20 ppm. The same was true for lower preheated air temperatures, but the changes were of a smaller amount.

Tables II-72 to II-76 show the raw and reduced data for Figures II-291, II-292, and II-293.

3. In-the-Flame Survey Results

Again, as part of this program, we mapped the species concentration in the flame for CO, CO_2, CH_4, O_2, and NO. Profiles were obtained at the same gas input (3040 CF/hr) as the input-output data for 20% excess air and at two combustion air temperatures of 100° and 270°F. Higher air temperatures produced flame temperatures excessive for the sampling probes. Tables II-77 and II-78 show the raw and reduced data for air temperatures of 100° and 270°F. Figures II-294 and II-295 show a composite plot of the raw data of Tables II-77 and II-78. While the input-output data showed a great similarity to the baffle burners run earlier, the detailed profiles are similar to the flat-flame data. That is, most of the methane is burned very near the burner at an axial position of 12.7 cm. The effect of increasing preheat temperature can also be seen both on the nitric oxide and carbon monoxide levels while it is not clear for methane. When the air temperature is increased from 100° to 270°F, the NO increases and the CO concentration decreases significantly. This effect is caused by the increased air velocity associated with a higher volumetric flow at higher temperatures increasing the gas-air mixing rate. While the effect of increased air temperature cannot be seen on

Table II-72. INPUT-OUTPUT DATA FOR THE BOILER BURNER WITH A RADIAL NOZZLE
(30-deg Vane Angle; Gas Input, 3020 CF/hr;
Preheated Air Temperatures of 104°, 285°, and 550°F Average)

Run No.	Preheat Temperature, °F	Flue Analysis				Normalized NO, ppm
		NO, ppm	O_2, %	CO_2, %	CO, ppm	
1	104	155	2.43	10.6	45	172
2	104	126	5.08	9.0	30	161
3	104	139	3.89	9.7	33	166
4	104	171	0.30	11.6	8300	174
5	104	135	3.41	9.97	25	157
6	104	138	2.39	10.7	27	153
7	104	153	1.47	11.3	45	164
8	104	159	0.52	11.9	225	163
9	104	162	0.82	11.6	82	168
10	104	160	1.17	11.4	52	170
11	300	252	0.55	11.6	195	259
12	310	275	2.05	10.8	37	281
13	300	241	3.32	9.95	26	278
14	270	192	4.68	9.2	20	240
15	320	262	0.78	11.9	100	272
16	280	211	3.91	9.9	58	252
17	315	257	1.04	11.3	67	270
18	310	260	2.46	10.7	31	289
19	540	379	2.63	10.5	40	424
20	525	354	3.48	10.2	32	414
21	510	314	4.49	9.6	28	386
22	550	378	1.49	11.2	57	404
23	590	368	0.74	11.5	90	381
24	550	361	3.83	9.8	35	430
25	620	375	0.35	11.7	12	383

Table II-73. INPUT-OUTPUT DATA FOR THE BOILER BURNER WITH A RADIAL NOZZLE (40-deg Vane Angle; Gas Input, 3040 CF/hr)

Run No.	Preheat Temperature, °F	Flue Analysis				Normalized NO, ppm
		NO, ppm	O_2, %	CO_2, %	CO, ppm	
1	85	212	1.88	10.9	45	231
2	85	179	2.78	10.3	50	202
3	88	159	4.24	9.6	20	194
4	85	174	2.81	10.4	25	197
5	85	191	2.33	10.7	30	211
6	85	207	1.29	11.2	55	220
7	85	147	0.44	10.7	16.0×10^3	151
8	85	186	4.64	9.3	30	232
9	85	179	2.61	10.4	45	200
10	85	187	1.68	11.0	65	202
11	85	186	0.70	11.4	25	193
12	85	188	0.52	11.2	11.1×10^3	193
13	87	227	1.32	11.3	75	242
14	87	208	3.57	11.1	50	244
15	245	232	4.46	9.3	35	287
16	260	244	3.62	9.8	25	289
17	275	269	2.70	10.4	25	302
18	250	257	3.35	10.0	20	298
19	265	291	2.36	10.6	35	322
20	240	296	1.40	11.2	55	316
21	250	289	0.70	11.7	200	298
22	260	325	1.89	11.0	35	353
23	245	307	3.56	9.9	40	359
24	265	328	2.30	10.6	52	362
25	290	312	1.00	11.4	145	328
26	260	324	4.08	9.6	27	392
27	270	345	1.82	10.9	65	374
28	525	482	1.22	11.2	105	511
29	500	564	3.09	10.3	50	646
30	575	561	1.70	11.2	65	606
31	550	607	2.78	10.6	51	686
32	500	520	3.73	10.2	40	614
33	470	449	4.61	9.5	30	557
34	590	439	0.60	11.1	800	452
35	550	591	2.12	10.7	60	647
36	510	547	2.90	10.5	57	621
37	475	469	4.19	9.8	46	570

B-83-1218

Table II-74. INPUT-OUTPUT DATA FOR THE BOILER BURNER WITH A RADIAL NOZZLE (60-deg Vane Angle; Gas Input, 3040 CF/hr; Air Preheat Temperature, 85°F)

Run No.	Preheat Temperature, °F	Flue Analysis				Normalized NO, ppm
		NO, ppm	O_2, %	CO_2, %	CO, ppm	
1	85	218	2.14	10.6	35	240
2	85	232	3.51	10.2	25	271
3	85	217	1.39	11.2	50	231
4	85	210	1.69	10.9	40	227
5	85	217	2.56	10.3	30	242
6	85	184	0.59	11.6	370	192
7	85	204	2.85	10.4	25	231
8	85	218	2.91	10.1	25	247
9	85	229	0.75	11.4	115	240
10	85	204	0.26	11.3	130	212

Table II-75. INPUT-OUTPUT DATA FOR THE BOILER BURNER WITH A RADIAL NOZZLE (60-deg Vane Angle; Gas Input, 3040 CF/hr; Air Preheat Temperature, 265°F Average)

Run No.	Preheat Temperature, °F	Flue Analysis				Normalized NO, ppm
		NO, ppm	O_2, %	CO_2, %	CO, ppm	
1	235	262	3.55	10.0	20	308
2	245	296	2.87	10.3	25	334
3	260	318	1.97	10.9	35	347
4	270	325	1.29	11.3	55	346
5	285	270	0.70	11.7	155	284
6	310	244	0.32	11.5	3800	322
7	300	318	1.06	11.3	70	317

Table II-76. INPUT-OUTPUT DATA FOR THE BOILER BURNER WITH A RADIAL NOZZLE (60-deg Vane Angle; Gas Input, 3040 CF/hr; Air Preheat Temperature, 530°F Average)

Run No.	Preheat Temperature, °F	Flue Analysis				Normalized NO, ppm
		NO, ppm	O_2, %	CO_2, %	CO, ppm	
1	560	507	1.21	11.1	70	537
2	575	424	0.58	11.5	215	443
3	555	575	1.74	10.9	50	621
4	530	598	2.24	10.6	35	658
5	515	571	2.77	10.3	30	579
6	490	522	3.49	9.8	25	611
7	480	498	3.63	9.7	20	588

Table II-77. RAW AND REDUCED GAS CONCENTRATION RADIAL SCAN DATA FOR THE BOILER BURNER OPERATED AT A 3040 CF/hr GAS INPUT, 1.9% EXCESS OXYGEN IN THE FLUE, AND A COMBUSTION AIR TEMPERATURE OF 100°F

TRACER GAS STUDIES OF COMBUSTION BURNERS PROGRAM 2
BOILER BURNER - RADIAL GAS NOZZLE - BLUNT STAINLESS PROBE

INPUT GAS 3039 WALL TEMPERATURE 2534 PREHEAT TEMPERATURE 0

OUTPUT ANALYSIS

NITROGEN OXIDE	32.00 PERCENT	ON RANGE 1,	282.52 PPM	OXYGEN	1.92 PERCENT
CARBON DIOXIDE	83.70 PERCENT	ON RANGE 1,	10.90 PERCENT		
CARBON MONOXIDE	18.00 PERCENT	ON RANGE 3,	0.007 PERCENT		
METHANE	0.00 PERCENT	ON RANGE 0,	0.00 PERCENT		

EXPERIMENTAL RESULTS

		NITROGEN OXIDE -NO			OXYGEN	CARBON DIOXIDE-CO2			CARBON MONOXIDE -CO			METHANE - CH4		
AP	RP	RANGE	X	Y	O2	RANGE	X	Y	RANGE	X	Y	RANGE	X	Y
12.70	-12.00	1	15.30	131.1	3.06	1	79.50	10.00	2	4.60	0.075	3	0.70	0.03
12.70	-9.00	1	15.10	129.4	2.47	1	81.50	10.43	2	7.00	0.114	3	0.80	0.03
12.70	-6.00	1	15.60	133.7	2.15	1	82.10	10.56	2	9.00	0.147	3	0.40	0.02
12.70	-3.00	1	15.50	132.9	2.17	1	82.10	10.56	2	12.00	0.197	3	0.80	0.03
12.70	0.00	1	15.40	132.0	2.14	1	81.50	10.43	2	13.00	0.214	3	0.60	0.02
12.70	3.00	1	15.80	135.5	2.06	1	81.90	10.51	2	24.00	0.405	3	0.60	0.02
12.70	6.00	1	15.80	135.5	1.65	1	82.30	10.60	2	34.00	0.587	3	0.60	0.02
12.70	9.00	1	14.90	127.6	1.73	1	81.60	10.45	2	59.00	1.078	3	0.90	0.04
12.70	12.00	1	14.70	125.9	1.87	1	81.00	10.32	2	42.00	0.738	3	1.40	0.06
12.70	15.00	1	13.20	112.8	2.45	1	79.70	10.05	2	38.00	0.662	3	1.50	0.06
12.70	18.00	1	13.60	116.3	2.38	1	80.20	10.15	2	42.00	0.738	3	1.40	0.06
12.70	21.00	1	16.10	138.1	1.47	1	82.00	10.54	2	56.00	1.016	3	1.70	0.07
12.70	24.00	1	17.90	154.0	0.82	1	81.50	10.43	1	49.00	1.776	3	3.00	0.13
12.70	27.00	1	13.90	118.9	0.21	1	76.40	9.36	1	78.00	3.431	3	4.10	0.17
12.70	30.00	1	12.90	110.2	0.19	1	69.90	8.09	1	104.00	5.298	3	5.20	0.22
12.70	33.00	1	13.90	118.9	0.18	1	63.50	6.92	1	116.00	6.283	3	7.60	0.32
12.70	36.00	1	20.10	173.6	0.41	1	76.30	9.34	1	78.00	3.431	3	5.10	0.22

Table II-78. RAW AND REDUCED GAS CONCENTRATION RADIAL SCAN DATA FOR THE BOILER BURNER OPERATED AT A 3040 CF/hr GAS INPUT, 1.9% EXCESS OXYGEN IN THE FLUE, AND A COMBUSTION AIR TEMPERATURE OF 270°F

TRACER GAS STUDIES OF COMBUSTION BURNERS PROGRAM 2
BOILER BURNER - RADIAL GAS NOZZLE - BLUNT STAINLESS PROBE

INPUT GAS 3039 WALL TEMPERATURE 2534 PREHEAT TEMPERATURE 270
OUTPUT ANALYSIS
NITROGEN OXIDE 32.00 PERCENT ON RANGE 1, 282.52 PPM OXYGEN 1.92 PERCENT
CARBON DIOXIDE 83.70 PERCENT ON RANGE 1, 10.90 PERCENT
CARBON MONOXIDE 18.00 PERCENT ON RANGE 3, 0.007 PERCENT
METHANE 0.00 PERCENT ON RANGE 0, 0.00 PERCENT

EXPERIMENTAL RESULTS

		NITROGEN OXIDE -NO			OXYGEN	CARBON DIOXIDE-CO2			CARBON MONOXIDE -CO			METHANE - CH4		
AP	RP	RANGE	X	Y	O2	RANGE	X	Y	RANGE	X	Y	RANGE	X	Y
12.70	60.00	1	31.20	275.0	4.68	1	76.10	9.30	3	11.00	0.004	3	0.00	0.00
12.70	55.00	1	29.50	259.2	5.01	1	74.40	8.96	3	10.00	0.004	3	0.00	0.00
12.70	50.00	1	29.50	259.2	4.78	1	75.80	9.24	3	8.00	0.003	3	0.00	0.00
12.70	45.00	1	30.10	264.8	4.73	1	75.90	9.26	3	8.00	0.003	3	0.00	0.00
12.70	40.00	1	29.70	261.0	4.75	1	76.40	9.36	3	8.00	0.003	3	0.00	0.00
12.70	35.00	1	28.00	245.3	3.81	1	78.10	9.71	2	19.00	0.317	3	0.00	0.00
12.70	30.00	1	18.80	162.0	0.30	1	73.90	8.86	1	86.00	3.967	3	2.60	0.11
12.70	27.00	1	15.80	135.5	0.23	1	70.80	8.26	1	99.80	4.972	3	3.30	0.14
12.70	24.00	1	18.90	162.9	0.23	1	75.90	9.26	1	82.00	3.694	3	2.70	0.11
12.70	21.00	1	21.10	182.6	0.23	1	79.30	9.96	1	66.00	2.691	3	2.10	0.09
12.70	18.00	1	24.20	210.5	1.03	1	82.10	10.56	1	28.00	0.860	3	1.20	0.05
12.70	15.00	1	23.30	202.4	1.30	1	81.40	10.41	2	64.00	1.183	3	1.20	0.05
12.70	12.00	1	25.10	218.7	0.84	1	82.30	10.60	2	83.00	1.598	3	1.10	0.05
12.70	9.00	1	25.80	225.1	0.45	1	82.70	10.69	1	39.00	1.310	3	1.10	0.05
12.70	6.00	1	28.50	249.9	0.43	1	84.00	10.97	1	31.00	0.976	3	1.50	0.06
12.70	3.00	1	28.70	251.8	0.48	1	84.00	10.97	2	63.00	1.162	3	1.60	0.07
12.70	0.00	1	27.60	241.6	0.57	1	84.50	11.08	2	51.00	0.915	3	1.20	0.05
12.70	-3.00	1	25.50	222.4	1.01	1	84.40	11.06	2	27.00	0.458	3	0.50	0.02
12.70	-6.00	1	24.80	216.0	1.17	1	84.00	10.97	2	21.00	0.352	3	0.60	0.02
12.70	-9.00	1	23.80	206.9	1.50	1	83.80	10.93	2	15.00	0.248	3	0.50	0.02
12.70	-12.00	1	22.60	196.1	2.14	1	82.30	10.60	2	5.00	0.081	3	0.10	0.00

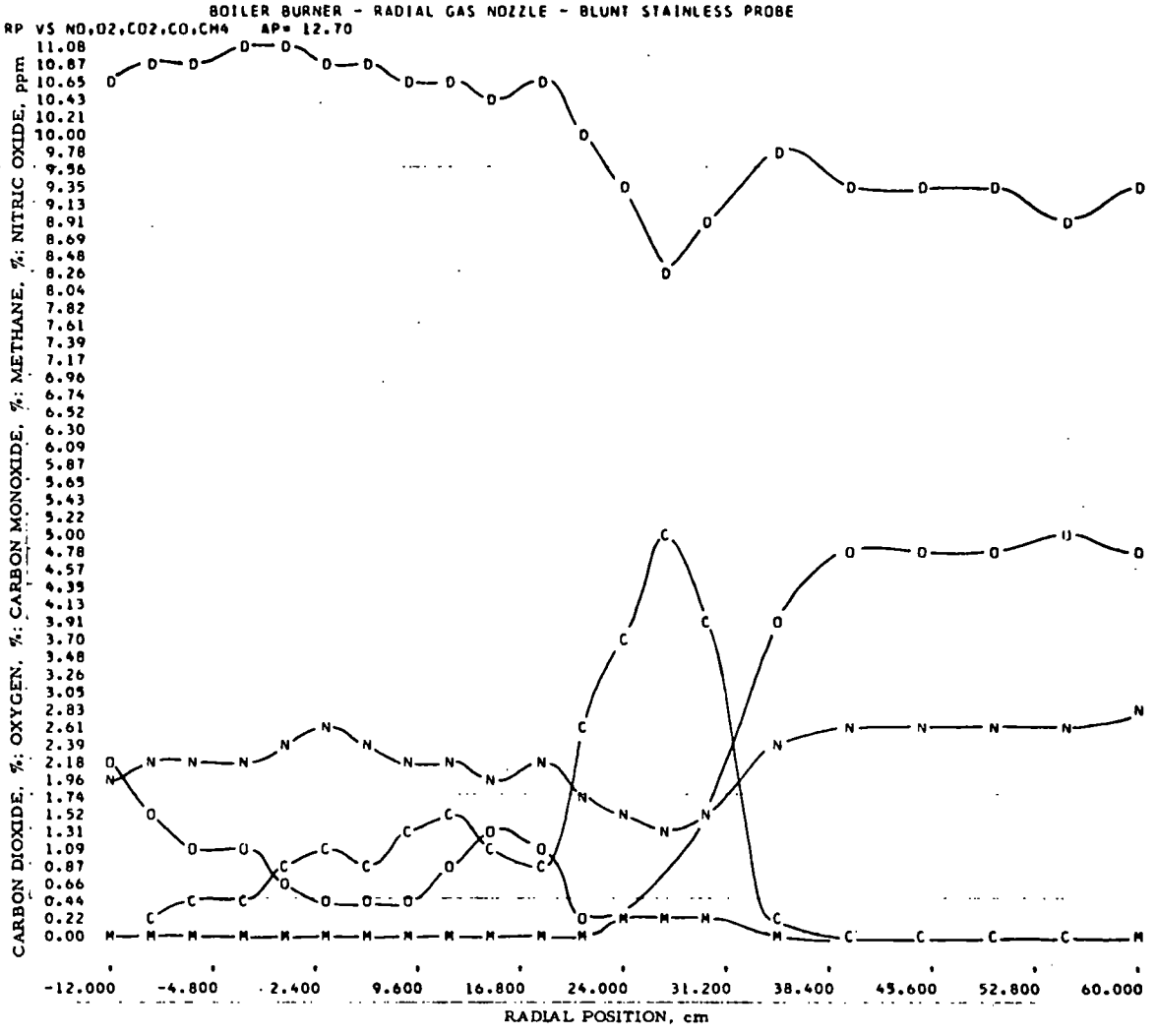

Figure II-294. COMPOSITE RADIAL SCAN OF GAS SPECIES FROM A BOILER BURNER WITH A 60-deg VANE ANGLE SETTING AT AN AXIAL POSITION OF 12.7 cm WHILE OPERATING AT A 3040 CF/hr GAS INPUT, 1.9% EXCESS OXYGEN, AND A 100°F PREHEATED AIR TEMPERATURE

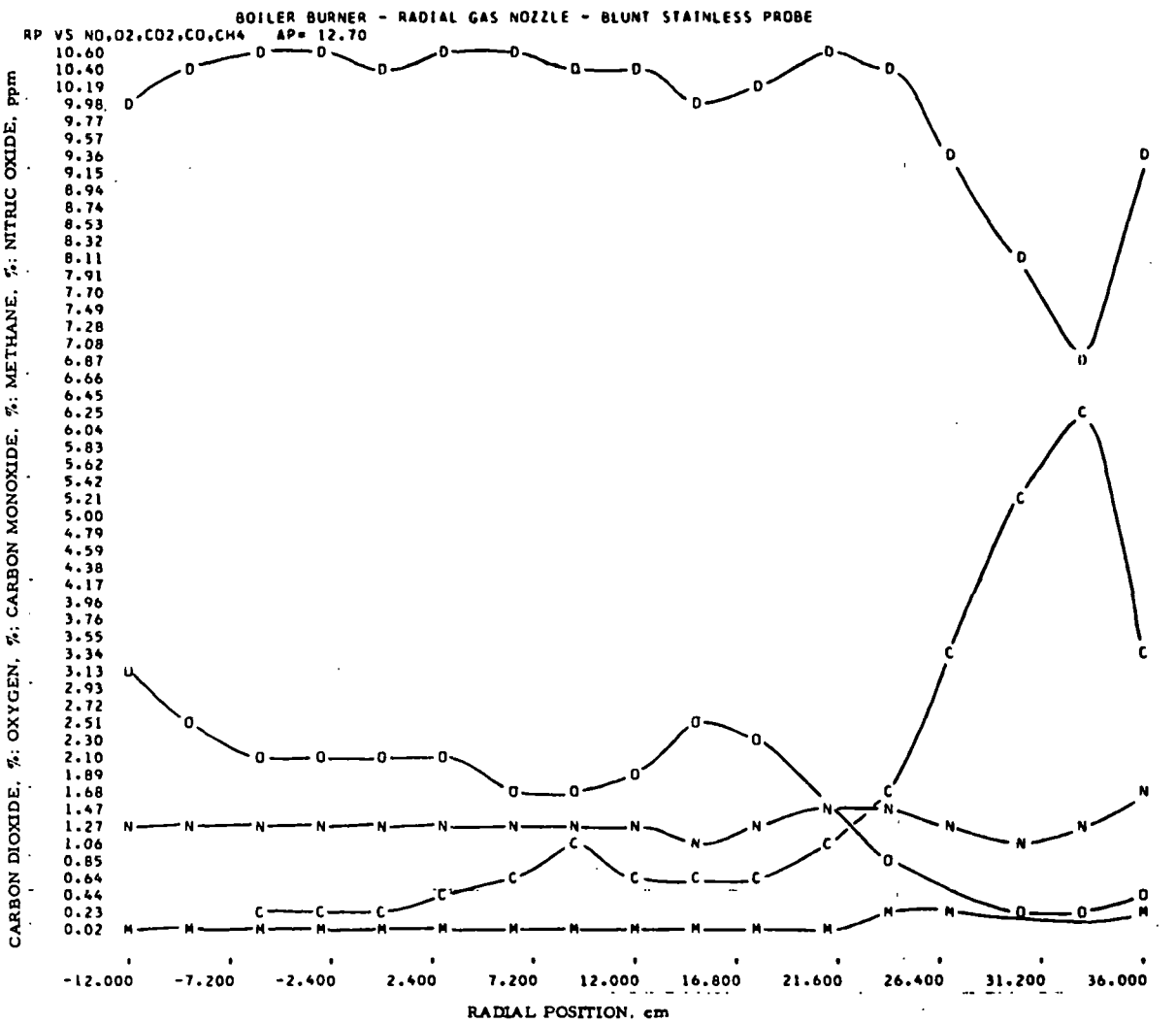

Figure II-295. COMPOSITE RADIAL SCAN OF GAS SPECIES FROM A BOILER BURNER WITH A 60-deg VAN ANGLE SETTING AT AN AXIAL POSITION OF 12.7 cm WHILE OPERATING AT A 3040 CF/hr GAS INPUT, 1.9% EXCESS OXYGEN, AND A 270°F PREHEATED AIR TEMPERATURE

the composite plots (Figures II-294 and II-295), it is clearly seen in Figures II-296 and II-297, which have greater resolution. As air temperature and hence volumetric flow and mixing rate increase, the average methane concentration decreases at an axial position of 12.7 cm. Gas species scans with greater resolution are shown in Figures II-298 to II-301 for a 100°F air temperature and in Figures II-302 to II-305 for a 2700°F air temperature.

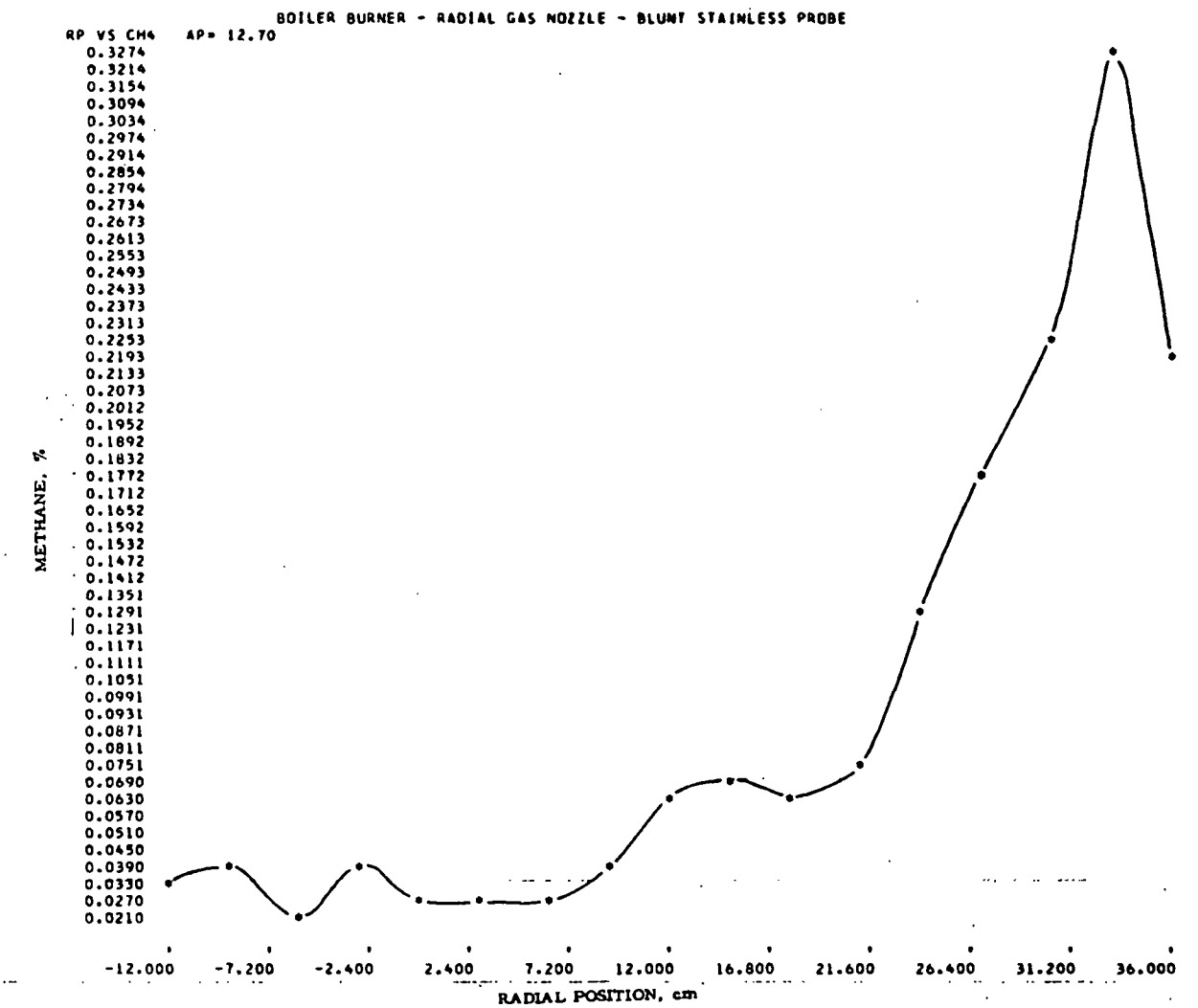

Figure II-296. RADIAL SCAN OF METHANE FROM A BOILER BURNER WITH A 60-deg VANE ANGLE SETTING AT AN AXIAL POSITION OF 12.7 cm WHILE OPERATING AT A 3040 CF/hr GAS INPUT, 1.9% EXCESS OXYGEN, AND A 100°F PREHEATED AIR TEMPERATURE

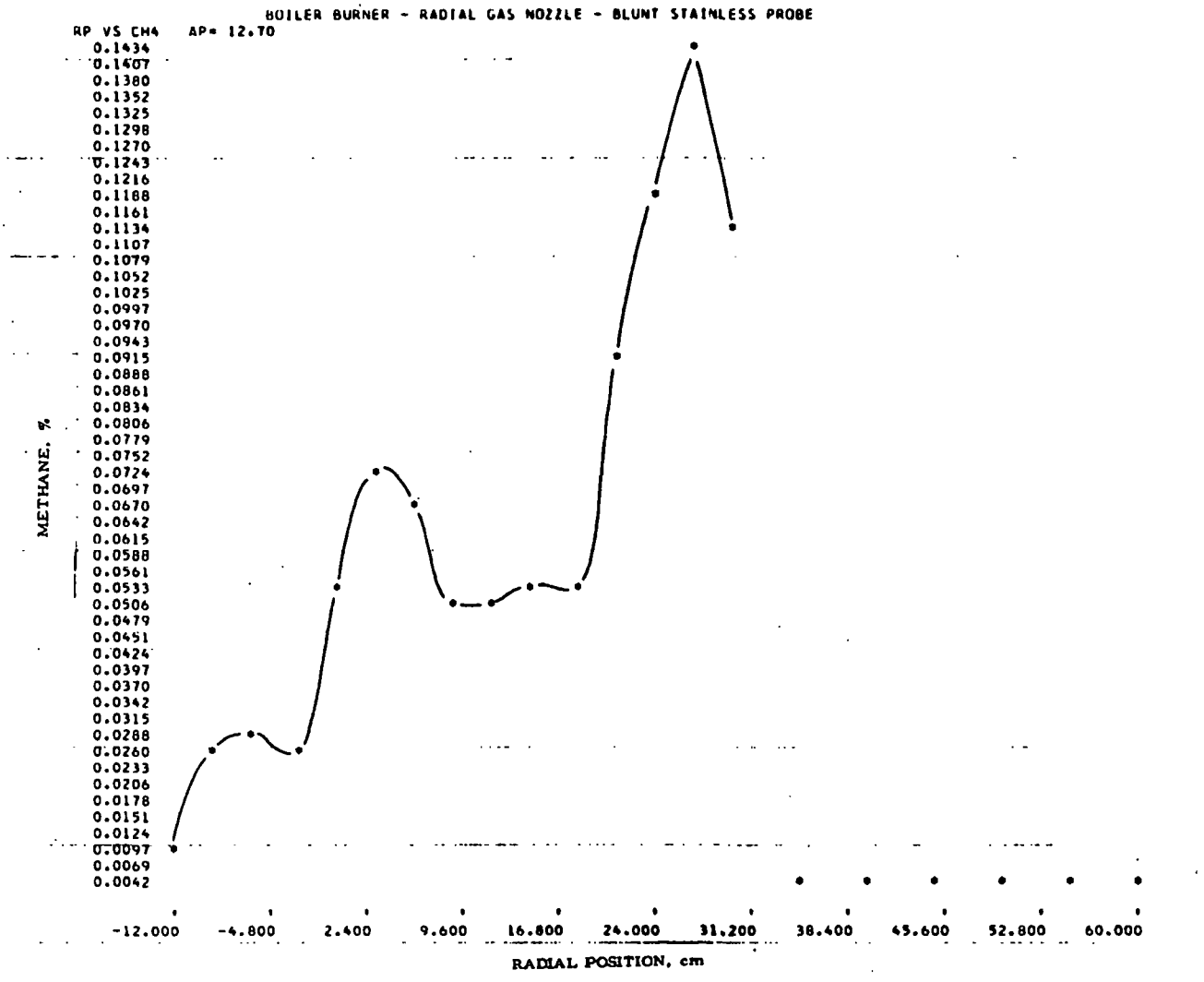

Figure II-297. RADIAL SCAN OF METHANE FROM A BOILER BURNER WITH A 60-deg VANE ANGLE SETTING AT AN AXIAL POSITION OF 12.7 cm WHILE OPERATING AT A 3040 CF/hr GAS INPUT, 1.9% EXCESS OXYGEN, AND A 270°F PREHEATED AIR TEMPERATURE

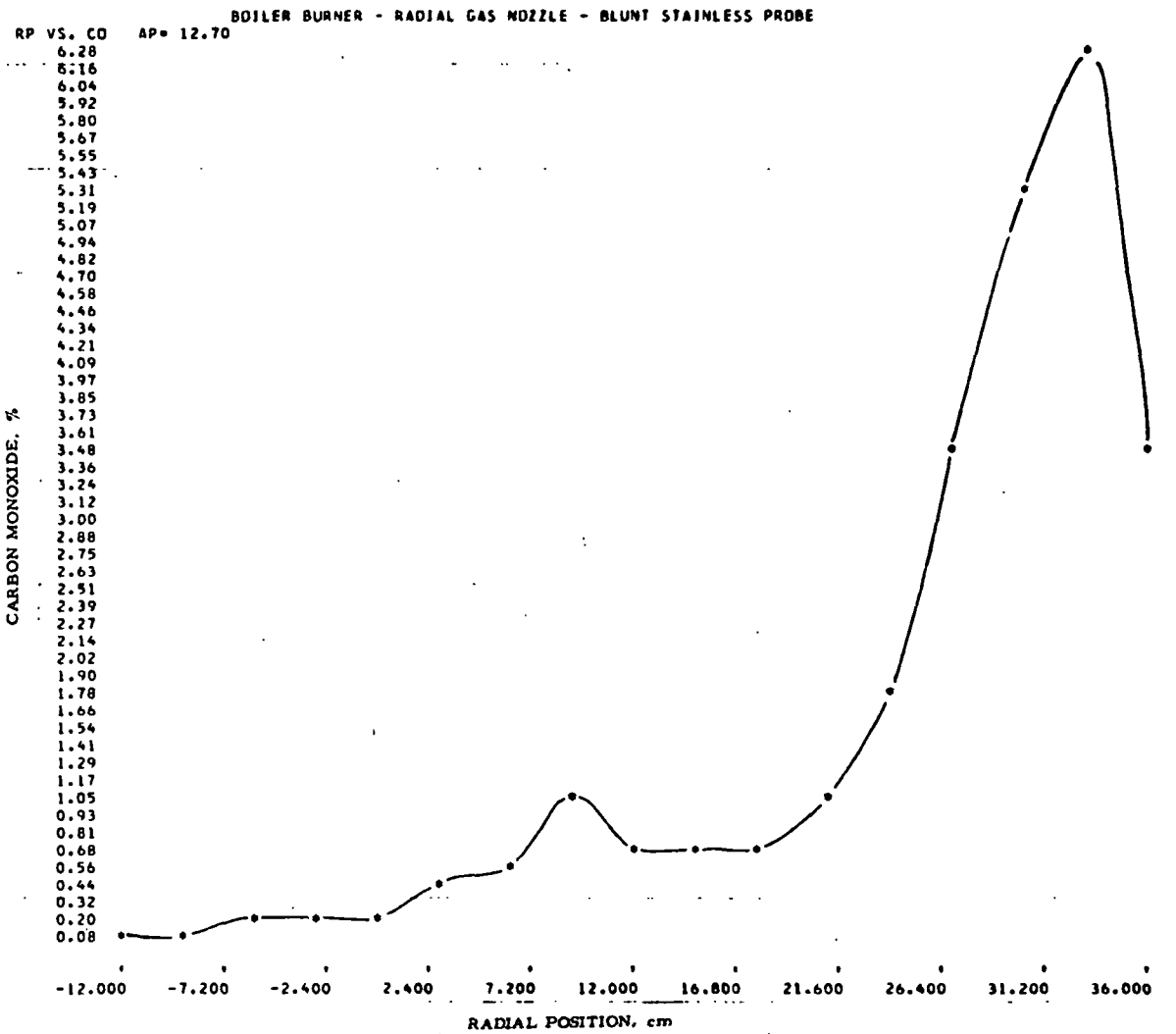

Figure II-298. RADIAL SCAN OF CARBON MONOXIDE FROM A BOILER BURNER WITH A 60-deg VANE ANGLE SETTING AT AN AXIAL POSITION OF 12.7 cm WHILE OPERATING AT A 3040 CF/hr GAS INPUT, 1.9% EXCESS OXYGEN, AND A 100°F PREHEATED AIR TEMPERATURE

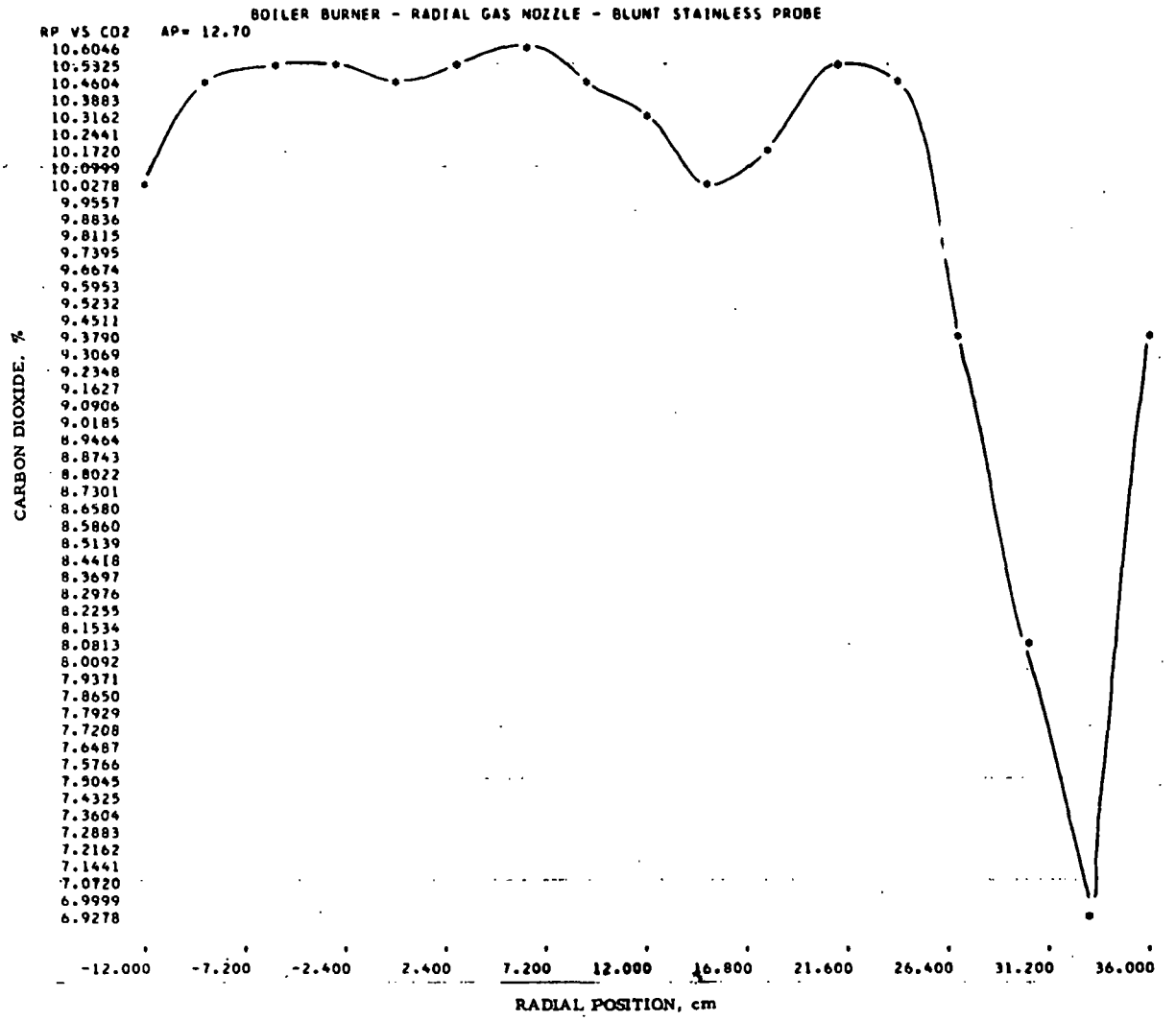

Figure II-299. RADIAL SCAN OF CARBON DIOXIDE FROM A BOILER BURNER WITH A 60-deg VANE ANGLE SETTING AT AN AXIAL POSITION OF 12.7 cm WHILE OPERATING AT A 3040 CF/hr GAS INPUT, 1.9% EXCESS OXYGEN, AND A 100°F PREHEATED AIR TEMPERATURE

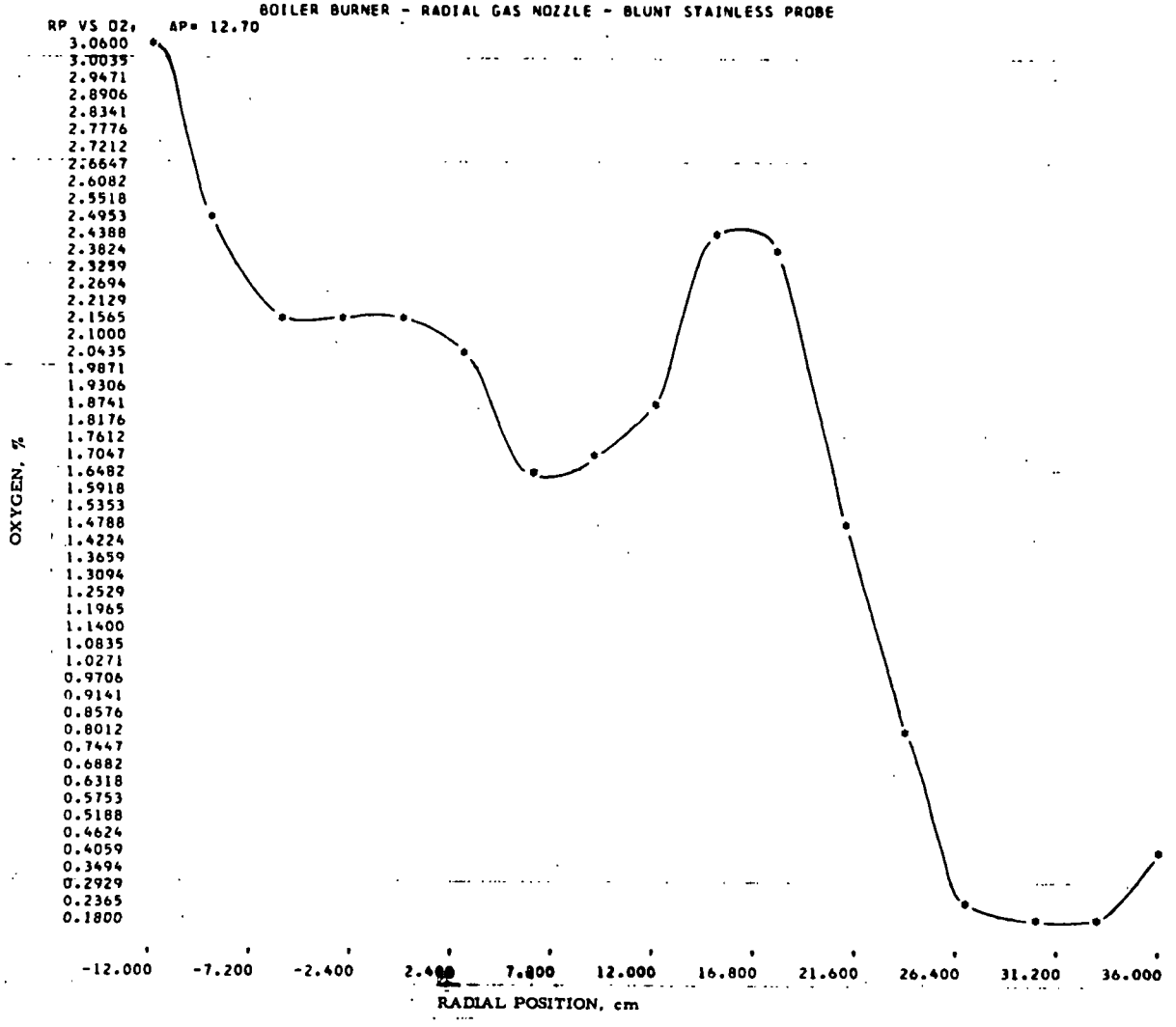

Figure II-300. RADIAL SCAN OF OXYGEN FROM A BOILER BURNER WITH A 60-deg VANE ANGLE SETTING AT AN AXIAL POSITION OF 12.7 cm WHILE OPERATING AT A 3040 CF/hr GAS INPUT, 1.9% EXCESS OXYGEN, AND A 100°F PREHEATED AIR TEMPERATURE

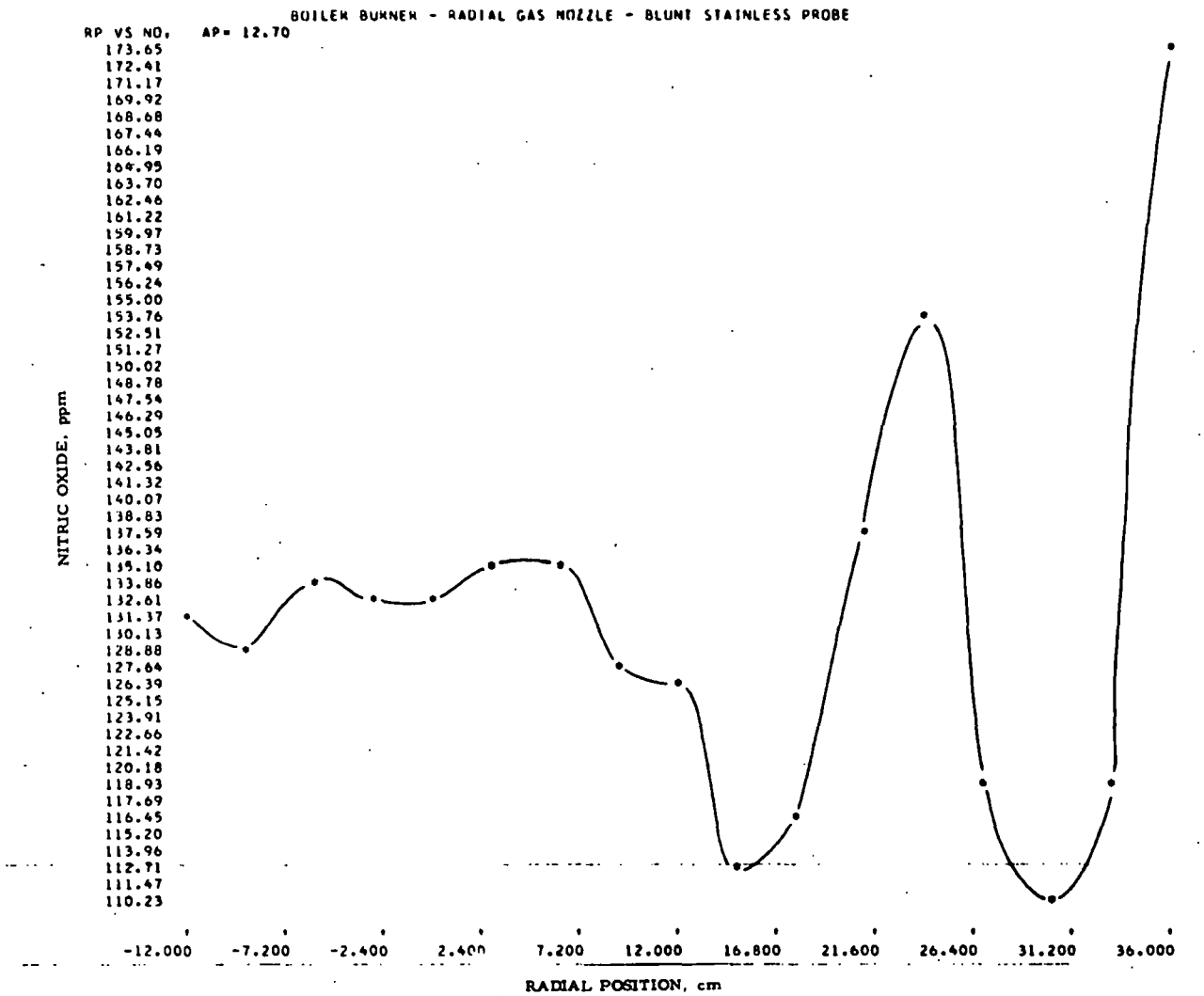

Figure II-301. RADIAL SCAN OF NITRIC OXIDE FROM A BOILER BURNER WITH A 60-deg VANE ANGLE SETTING AT AN AXIAL POSITION OF 12.7 cm WHILE OPERATING AT A 3040 CF/hr GAS INPUT, 1.9% EXCESS OXYGEN, AND A 100^{0}F PREHEATED AIR TEMPERATURE

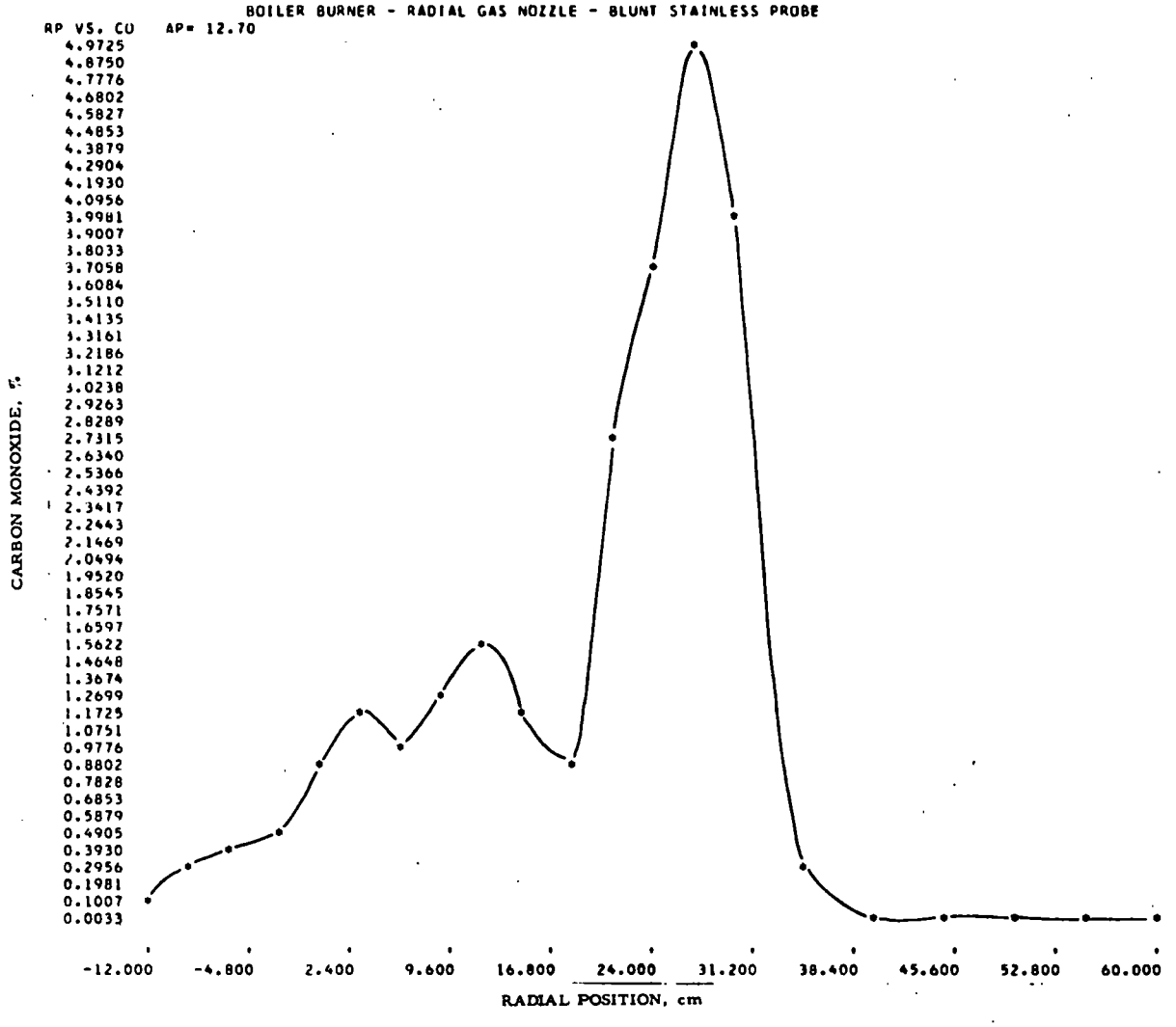

Figure II-302. RADIAL SCAN OF CARBON MONOXIDE FROM A BOILER BURNER WITH A 60-deg VANE ANGLE SETTING AT AN AXIAL POSITION OF 12.7 cm WHILE OPERATING AT A 3040 CF/hr GAS INPUT, 1.9% EXCESS OXYGEN, AND A 270°F PREHEATED AIR TEMPERATURE

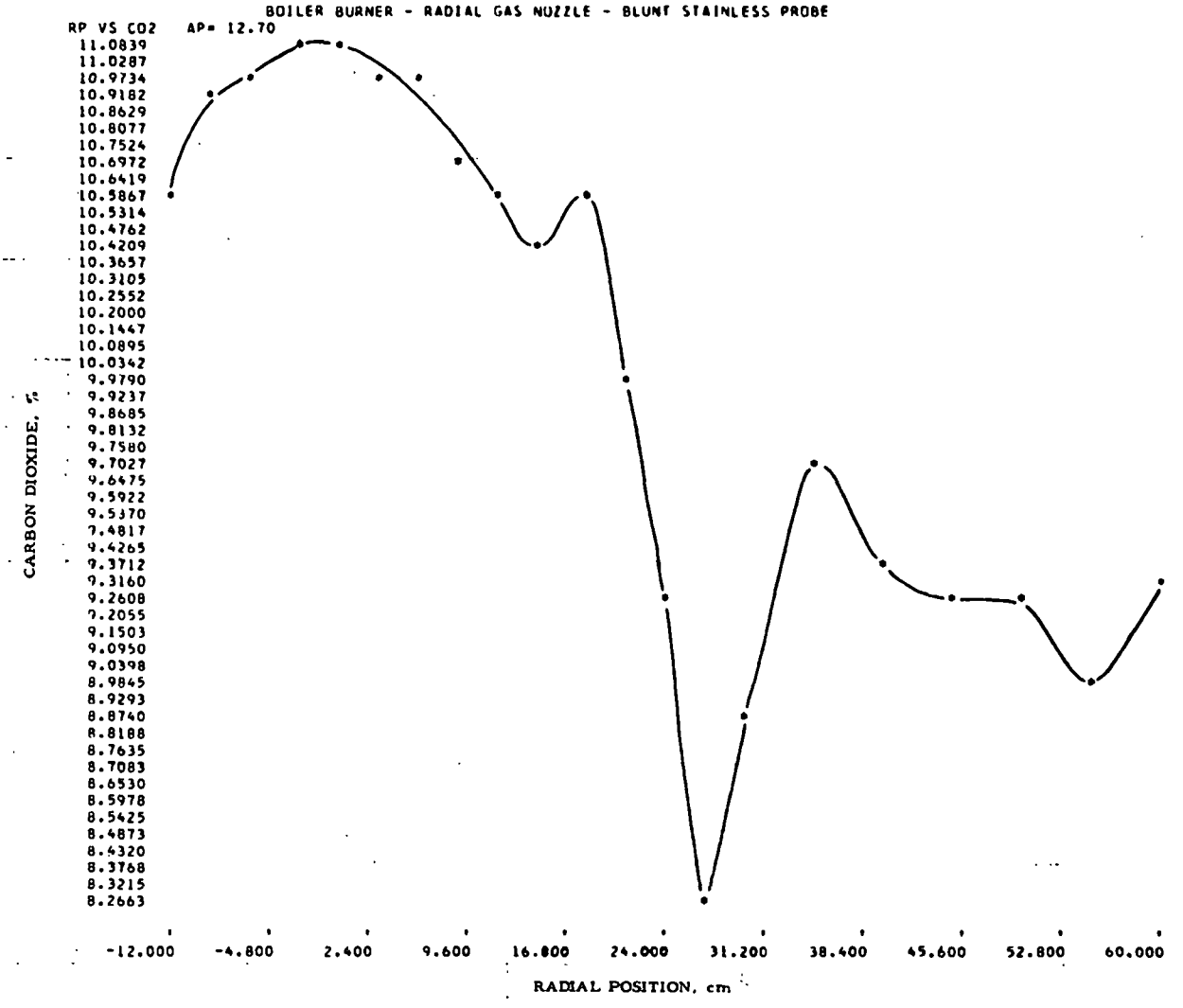

Figure II-303. RADIAL SCAN OF CARBON DIOXIDE FROM A BOILER BURNER WITH A 60-deg VANE ANGLE SETTING AT AN AXIAL POSITION OF 12.7 cm WHILE OPERATING AT A 3040 CF/hr GAS INPUT, 1.9% EXCESS OXYGEN, AND A 270°F PREHEATED AIR TEMPERATURE

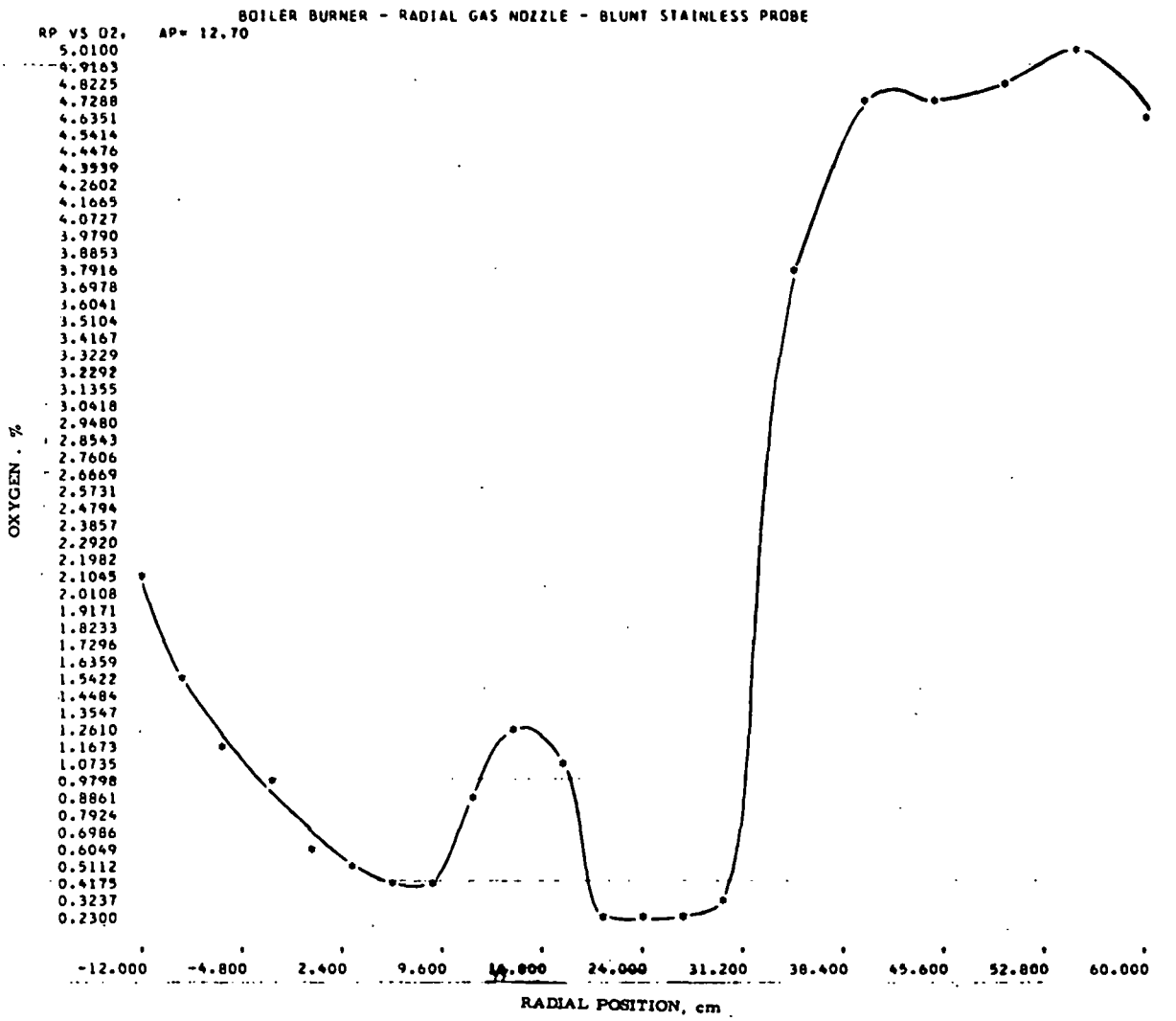

Figure II-304. RADIAL SCAN OF OXYGEN FROM A BOILER BURNER WITH A 60-deg VANE ANGLE SETTING AT AN AXIAL POSITION OF 12.7 cm WHILE OPERATING AT A 3040 CF/hr GAS INPUT, 1.9% EXCESS OXYGEN, AND A 270^{0}F PREHEATED AIR TEMPERATURE

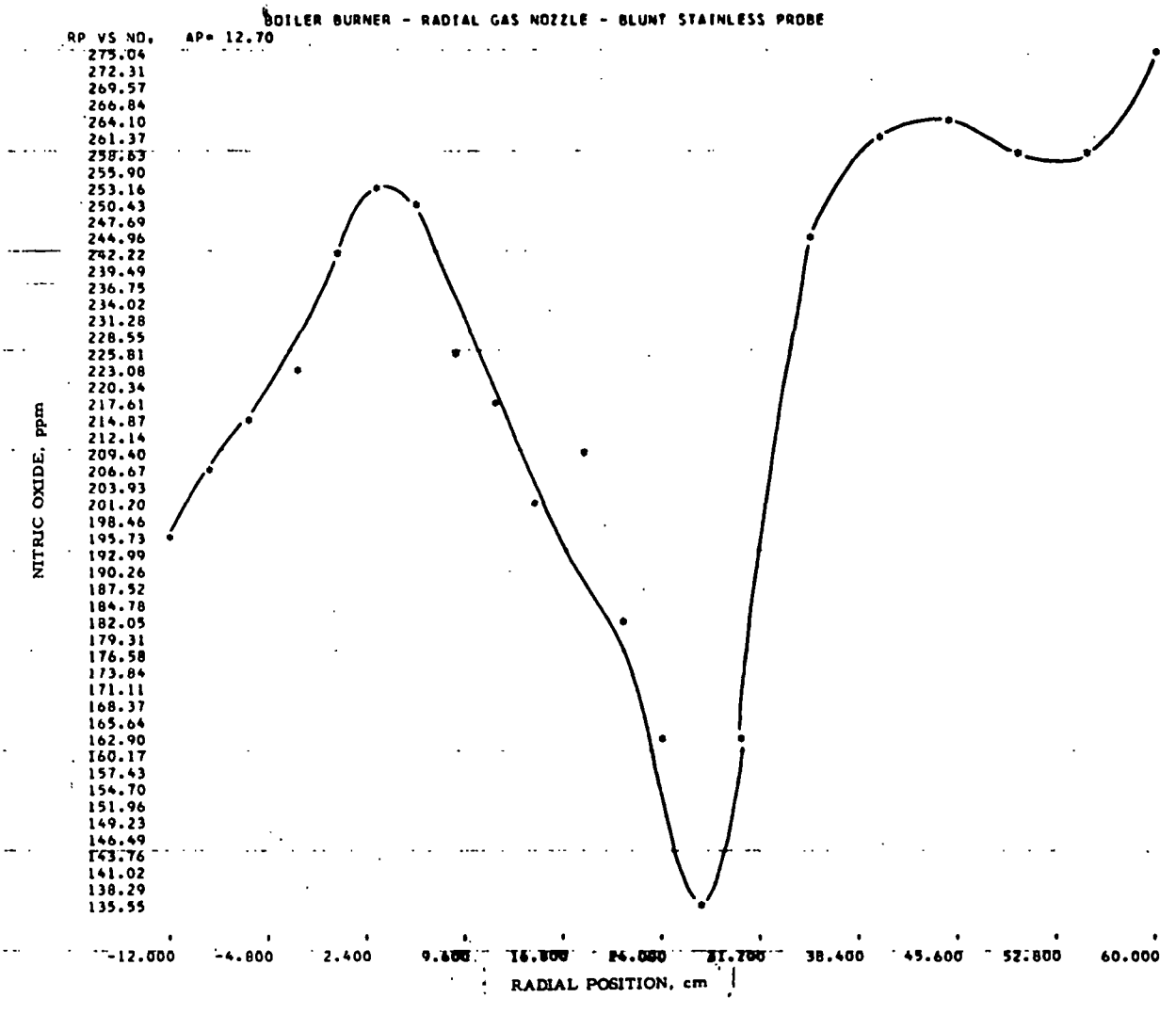

Figure II-305. RADIAL SCAN OF NITRIC OXIDE FROM A BOILER BURNER WITH A 60-deg VANE ANGLE SETTING AT AN AXIAL POSITION OF 12.7 cm WHILE OPERATING AT A 3040 CF/hr GAS INPUT, 1.9% EXCESS OXYGEN, AND A 270^{0}F PREHEATED AIR TEMPERATURE

APPENDIX II-A. Computer Program for Reduction Velocity Data

The following computer program was written to transform the raw pressure difference data from the hot- and cold-model five-hole pitot probe into axial and tangential velocity profiles.

Table II-A-1

```
// JOB     0001 2801 2603            0001 2603 0001 2M10,101

LOG DRIVE    CART SPEC    CART AVAIL   PHY DRIVE
  0000         0001         0001         0000
  0001         2801         2801         0001
  0002         2603         2603         0002

V2 M10   ACTUAL 16K  CONFIG 16K

// FOR
*LIST ALL
*ONE WORD INTEGERS
*EXTENDED PRECISION
*IOCS(CARD,1403 PRINTER,DISK)
C       MARCH 24,1972
C       A1,A2,A3,B0,B2,B4,C,D& ARE CALIBRATION COEFFICIENTS
C       THETA ANGLE THRU WHICH THE PROBE IS ROTATED ABOUT THE Y AXIS
C       AP AXIAL POSITION, RP RADIAL POSITION, T TEMP IN DEGREES C
C       PB IS ATMOSPHERIC PRESS IN MM OF HG, FI CONICAL ANGLE, DELTA IS DIHEDRAL
C       VT TANGENTIAL VELOCITY, VR RADIAL VELOCITY
      DIMENSION X1(200),Y1(200),Y2(200),        MARK(200)
       DIMENSION MARK2(200)
      DIMENSION ID(40)
      DEFINE FILE 1(201,45,U,IFILE)
       INPUT = 2
       IOUT = 5
      READ (2,5) A1,A2,A3,B0,B2,B4,C,D
    5 FORMAT (8F10.0)
  801 INDEX=1
       IPAGE=45
C      IPAGE -CONSTANT FOR SKIPPING TO NEW PAGE ON INPUT PRINTOUT
       IOPGE =  52
C      IOPGE -CONSTANT FOR SKIPPING TO NEW PAGE ON OUTPUT
       IC = 0
       READ(INPUT,912)ID
    4 READ (2,6) THETA,AP,RP,P13,P03,P24,P04,P0A,T,PB
       RP =-1.*RP
       IF(T)805,803,804
  805 CALL EXIT
  803 WRITE(IOUT,918)ID
       WRITE(IOUT,919)
       IC = 0
       NO=INDEX-1
       DO 1008 I=1,NO
       IF(IC-IOPGE)1007,1007,1006
 1006 WRITE(IOUT,917)
       IC = 0
       WRITE(IOUT,919)
 1007 READ(1'I)AP,RP,FI,DELTA,RHO,V,VX,VY,VZ,VT,VR,PST,T,PB
       WRITE(5,920)  AP,RP,FI,DELTA,RHO,V,VX,VY,VZ,VT,VR,PST,T,PB
       IC = IC+1
 1008 CONTINUE
       WRITE(IOUT,903)ID,APST
       CALL  PTSE9(X1,Y1,MARK,NO)
       WRITE(IOUT,904)ID,APST
       CALL PTSE9(X1,Y2,MARK2,NO)
       GO TO 801
```

Table II-A-2

```
 904 CONTINUE
     IF(INDEX-1)500,1000,1002
 500 WRITE(IOUT,911)
     CALL EXIT
1000 WRITE(IOUT,913)A1,A2,A3,B0,B2,B4,C,D
     WRITE(IOUT,914)ID
     WRITE(IOUT,915)
1002 IF(IC-IPAGE)1003,1003,1004
1004 WRITE(IOUT,917)
     WRITE(IOUT,915)
     IC = 0
     IF(IPAGE-40)1015,1015,1016
1015 IPAGE=IPAGE+6
1016 CONTINUE
1003 CONTINUE
     WRITE(IOUT,916)THETA,AP,RP,P13,P03,P24,P04,P0A,T,PB
     IC = IC+1
   6 FORMAT (3F5.0,5F10.0,2F5.0)
 901 FORMAT(10(F10.2,2X))
     P13=0.98/P13
     P03=0.98/P03
     P24=0.98/P24
     P04=0.98/P04
     P0A=0.98/P0A
     P01=P03-P13
     P02=P04-P24
     PR=SQRT(P01*P01+P02*P02+P03*P03+P04*P04)
     XF=1.-(P01+P02+P03+P04)*.5/PR
     IF (XF) 70,71,71
  70 WRITE (5,72) AP,RP,PR
  72 FORMAT (2F5.1,17H KPHI IS NEGATIVE,56X,F12.4)
     GO TO 4
  71 FI=SQRT(XF)
     FI=((A3*XF+A2)*XF+A1)*FI
     DELTA=ABS(P24/P13)
     DELTA=ATAN(DELTA)
     IF (P13) 10,16,11
  10 IF (P24/P13) 12,13,13
  13 DELTA=6.28318-DELTA
     GO TO 12
  11 IF (P24/P13) 14,15,15
  14 DELTA=DELTA+3.14159
     GO TO 12
  16 IF (P24-0.) 18,18,17
  17 DELTA=1.5707963
     GO TO 12
  18 DELTA=4.712389
     GO TO 12
  15 DELTA=3.14159-DELTA
  12 RHO=(0.002458*PB/760.*273./(273.+T))/(12.*12.)
     FIS=FI*FI
     XKV=((FIS*B4+B2)*FIS+B0)*PR
     V=SQRT(2.*XKV/RHO)
     VT=V*SIN(FI)
     VX=V*COS(FI)
     VY=VT*COS(DELTA)
     VZ=VT*SIN(DELTA)
```

Table II-A-3

```
      XKP=1.+C*(EXP(-D*FI*FI)-1.)
      PST=P0A-XKP*XKV
      IF (THETA) 20,21,20
   20 THETA=THETA*0.0174533
      VXP=VX
      VZP=VZ
      VX=VXP*COS(THETA)-VZP*SIN(THETA)
      VZ=VZP*COS(THETA)+VXP*SIN(THETA)
      A=ABS(VX/V)
      DEN=SQRT(1.-(A*A))
      FI=ATAN(DEN/A)
      IF (VX) 50,51,51
   50 FI=3.14159-FI
   51 A=ABS(VZ/(V*SIN(FI)))
      DEN=SQRT(1.-(A*A))
      DELTA=ATAN(A/DEN)
      IF (VZ) 52,53,53
   52 IF (VY) 54,55,55
   55 DELTA=6.28318-DELTA
      GO TO 21
   54 DELTA=3.14159+DELTA
      GO TO 21
   53 IF (VY) 56,57,57
   56 DELTA=3.14159-DELTA
      GO TO 21
   57 DELTA=DELTA
   21 X2=AP*AP
      RO=RP*RP
      DEN=SQRT(RO*COS(FI)*COS(FI)+X2*SIN(FI)*SIN(FI))
      VT=(V*RP*SIN(FI)*COS(FI))/DEN
      VR=(V*AP*SIN(FI)*SIN(FI))/DEN
      DELTA=DELTA*57.295777
      FI=FI*57.29577
      WRITE(1'INDEX)AP,RP,FI,DELTA,RHO,V,VX,VY,VZ,VT,VR,PST,T,PB
      IF(FI-90.)806,807,807
  806 MARK(INDEX)  =23616
      MARK2(INDEX)=23616
      GO TO 808
  807 MARK(INDEX)=-6336
      MARK2(INDEX)=-6336
  808 CONTINUE
      X1(INDEX)=RP
      Y1(INDEX)=VT
      Y2(INDEX)=VX
      INDEX=INDEX+1
      IF(INDEX-200)809,809,811
  811 WRITE(5,910)
      CALL EXIT
  809 CONTINUE
      APST=AP
      GO TO 4
   40 FORMAT (3(F5.1,1X),F6.1,E9.2,6(2X,F6.2),2F9.6,2X,F6.0,2X,F6.0)
  903 FORMAT( 1H1,20X,40A2/10H RP VS. VT,3X,3HAP=F6.2)
  904 FORMAT( 1H1,20X,40A2/10H RP VS. VX,3X,3HAP=F6.2)
  905 FORMAT( 1H1,20X,40A2/10H RP VS. VR,3X,3HAP=F6.2)
  909 FORMAT(1H1)
  910 FORMAT('  INDEX GREATER THAN 200')
```

```
  911 FORMAT(15H ERROR IN LOGIC )
  912 FORMAT(40A2)
  913 FORMAT(1H1,30X,42HAERODYNAMIC MODELING OF COMBUSTION BURNERS //
     142H CALIBRATION COEFFICIENTS FOR FORWARD FLOW /
     25H A1 = F11.6,3X, 4HA2 = F11.6,3X,4HA3 = F11.6/
     35H B0 = F11.6,3X, 4HB2 = F11.6,3X,4HB4 = F11.6/
     45H C  = F11.6,3X, 4HD  = F11.6)
  914 FORMAT(72CX,40A2/17H TOTAL DATA INPUT  )
  915 FORMAT(/6H THETA,4X, 2HAP, 5X, 2HRP,12X, 3HP13, 13X, 3HP03,13X,3HP
     124, 13X, 3HP04, 13X, 3HP0A,  7X, 1HT, 6X,2HPB)
  916 FORMAT(1H ,F5.0,2F7.1,5(2X,F14.2),F8.0,F7.0)
  917 FORMAT(1H1)
  918 FORMAT(1H1,20X,40A2/ 8H RESULTS/)
  919 FORMAT(/ 5H   AP,5X, 2HRP, 6X, 2HFI,4X,5HDELTA, 5X, 3HRHO, 10X,
     11HV, 7X, 2HVX, 7X,2HVY, 7X,2HVZ, 7X,2HVT, 7X,2HVR, 6X, 3HPSI,9X,
     21HT,5X, 2HPB)
  920 FORMAT(F6.1,F7.1,2F8.1,F12.7,6F9.2,F11.6,F8.0,F6.0)
      END
VARIABLE ALLOCATIONS
    X1(R )=025C-0007     Y1(R )=04B4-025F     Y2(R )=07CC-04B7     A1(R )=C70F          A2(R )=C712          A3(R )=C715
    B0(R )=0718          B2(R )=071B          B4(R )=071E          C(R )=0721           D(R )=0724         THETA(R )=0727
    AP(R )=072A          RP(R )=072D         P13(R )=0730         P03(R )=0733         P24(R )=0736         P04(R )=0739
   P0A(R )=073C          T(R )=073F           PB(R )=0742          FI(R )=0745        DELTA(R )=0748       RHO(R )=074B
     V(R )=074E          VX(R )=0751          VY(R )=0754          VZ(R )=0757          VT(R )=075A          VR(R )=075D
   PST(R )=0760        APST(R )=0763        P01(R )=0766         P02(R )=0769         PR(R )=076C          XF(R )=076F
   FIS(R )=0772         XKV(R )=0775         XKP(R )=0778         VXP(R )=077B         VZP(R )=077E          A(R )=0781
   DEN(R )=0784          X2(R )=0787          R0(R )=078A       MARK(I )=0860-0799 MARK2(I )=0928-0861     I(I )=0995-0
 IFILE(I )=0951       INPUT(I )=0952       IOUT(I )=0953       INDEX(I )=0954       IPAGE(I )=0955       IPSF(I )=0956
    IC(I )=0957          NO(I )=0958          I(I )=0959

UNREFERENCED STATEMENTS
 901     40      905     909

STATEMENT ALLOCATIONS
 5    =099A  6    =09DD  901  =09A4  72   =09A9  40   =09B8  903  =09C3  904  =09D6  905  =09EB  907  =09FF  910  =0A12
 911  =0A10  912  =0A1A  913  =0A19  914  =0A7A  915  =0A8A  916  =0AB9  917  =0ABC  918  =0ABF  919  =0ACC  920  =0AD5
 801  =0B3C  4    =0B52  805  =0B77  803  =0B78  1006 =0B97  1007 =0BA3  1008 =0BEB  804  =0C11  809  =0C19  1010 =0C1C
 1002 =0C3D  1004 =0C43  1015 =0C55  1016 =0C58  1003 =0C5B  70   =0CD8  71   =0CE7  10   =0D11  13   =0D16  11   =0D2
 14   =0D27  16   =0D2F  17   =0D36  18   =0D3C  15   =0D42  12   =0D48  20   =0DCC  50   =0E16  51   =0E1C  52   =0E47
 55   =0E4C  54   =0E54  53   =0E5C  56   =0E61  57   =0E69  21   =0E6D  806  =0EF3  807  =0F0C  808  =0F1D  811  =0F4E
 809  =0F43

FEATURES SUPPORTED
 ONE WORD INTEGERS
 EXTENDED PRECISION
 IOCS

CALLED SUBPROGRAMS
 PTSE9   ESQRT   EABS    EATAN   ESIN    ECOS    EEXP    EADD    ESUB    EMPY    EDIV    ELT     FSIN    ESTOP   CS=3
 EDVR    CARDZ   SRED    SWRT    SCOMP   SFIO    SIOAI   SIOF    SUBSC   PRNZ    SNR     SDFIO   SORED   SDWRT   SOC
 SDF

REAL CONSTANTS
   .100000000E 01=095C     .980000000E 00=095F     .500000000E 00=0962     .628318000E 01=0965     .314159000E 01=0968
   .000000000E 00=096B     .157079630E 01=096E     .471238900E 01=0971     .245800000E-02=0974     .76[illegible]E 03=0977
   .273000000E 03=097A     .120000000E 02=097D     .200000000E 01=0980     .174533000E-01=0983     .57[illegible]E 02=0986
   .572957700E 02=0989     .900000000E 02=098C
```

Table II-A-5

```
// FOR
*ONE WORD INTEGERS
*LIST SOURCE PROGRAM
* EXTENDED PRECISION
      SUBROUTINE PTSET(XPLOT,YPLOT,MARK,NO)
C     PROGRAMMER  -  LOTTIE TOCZYCKI                DATE - MAY 1971
      DIMENSION XPLOT(2),YPLOT(2),MARK(2)
      DIMENSION L(1501)
      DIMENSION LINE(101),XP(11)
C     XPLOT = ARRAY FOR X-COORDINATES
C     YPLOT = ARRAY FOR Y-COORDINATES
C     NO    = NUMBER OF POINTS,  MAXIMUM NUMBER OF POINTS=801
C     XLINE = NUMBER OF STEP SIZES DX INTO WHICH X AXIS IS DIVIDED
C     YLINE = NUMBER OF STEP SIZES DY INTO WHICH Y AXIS IS DIVIDED
      DATA IBLK/' '/
C     LOGICAL UNIT NUMBERS FOR INPUT/OUTPUT
      IOUT =5
      IF(NO-1500)92,92,93
   93 WRITE(IOUT,919)NO
  919 FORMAT(' SIZE OF THE ARRAYS TO BE PLOTTED IS GREATER THAN ALLOWED
     1'/ ' CHANGE THE DIMENSION OF L TO ' I6)
      CALL EXIT
   92 DO 94 I=1,NO
   94 L(I)=I
      XLINE = 100.0
      YLINE=51.0
C     LINEX = NUMBER OF POINTS PLOTTED ON X AXIS
C     LINEY = NUMBER OF POINTS PLOTTED ON Y AXIS
      LINEX = XLINE +1.0
      LINEY = YLINE+1.0
C     **************************
C     ARRANGE THE Y-VALUES IN DESCENDING ORDER
      LIM = NO-1
    1 INT = 1
      DO 4 I=1,LIM
      I1  = I+1
      IF(YPLOT(I1)-YPLOT(I))4,4,2
    2 TEMP1 = YPLOT(I1)
      TEMP2=XPLOT(I1)
      IT3 = L(I1)
      IT4=MARK(I1)
      YPLOT(I1)=YPLOT(I)
      XPLOT(I1)=XPLOT(I)
      L(I1)=L(I)
      MARK(I1)=MARK(I)
      YPLOT(I) = TEMP1
      XPLOT(I)= TEMP2
      L(I)=IT3
      MARK(I)=IT4
      INT   =I
    4 CONTINUE
      IF(INT -1)6,6,5
    5 LIM=INT
      GO TO 1
C     DY= STEP SIZE FOR Y-AXIS
    6 DY =(YPLOT(1)-YPLOT(NO))/YLINE
      POWR = 10000.0
      DO 50 LD=1,9
      IF(DY-POWR)41,79,79
```

Table II-A-6

```
   79 IPRNT=9
      GO TO 51
   41 POWR = POWR*0.10
      IF (DY-POWR) 50,42,42
   42 IPRNT = 10
      GO TO 51
   50 CONTINUE
      IPRNT = 9
   51 CONTINUE
C     ************************
C     FIND THE RANGE OF X AND THE STEP SIZE FOR X-AXIS, DX
      XMAX = XPLOT(1)
      DO 30 I=2,NO
      IF(XMAX-XPLOT(I))27,30,30
   27 XMAX= XPLOT(I)
   30 CONTINUE
      XMIN = XPLOT(1)
      DO 40 I=2,NO
      IF(XMIN-XPLOT(I))40,40,39
   39 XMIN=XPLOT(I)
   40 CONTINUE
      DX = (XMAX-XMIN)/XLINE
C     PLOT X,Y
      I=1
      Y = YPLOT(I)
   90 DO 7 J=1,LINEX
    7 LINE(J)= IBLK
   10 IF(YPLOT(I)- Y+0.5  *ABS(DY))14,11,11
   11 J = (XPLOT(I)-XMIN)/DX +1.5
  128 LINE(J) =  MARK(I)
      I = I+1
      IF (I-NO)10,10,14
   14 GO TO(61,61,61,64,64,66,66,68,69),IPRNT
   61 WRITE (IOUT,911) Y,LINE
      GO TO 20
   64 YPRNT = Y+0.005
      WRITE (IOUT,912) YPRNT,LINE
      GO TO 20
   66 YPRNT = Y+0.00005
      WRITE (IOUT,913) YPRNT,LINE
  913 FORMAT(1H ,F8.4,2X,101A1)
      GO TO 20
   68 YPRNT = Y+0.000005
      WRITE (IOUT,914) YPRNT,LINE
      GO TO 20
   69 WRITE (IOUT,915) Y,LINE
   20 Y  =  Y-DY
      IF(I-NO)90,90,91
   91 CONTINUE
      K  =  0
      DO 21 I=1,11
      XP(I)= XMIN+DX*K
   21 K=K+10
      IF(XP(11)-10000.)70,74,74
   74 IF(XP(11)-1.E7)72,71,71
   72 DELX=0.5
      DO 81 I=1,11
      IF(XP(I))76,81,77
   76 XP(I)=XP(I)-DELX
```

Table II-A-7

```
      GO TO 81
   77 XP(I)=XP(I)+DELX
   81 CONTINUE
      WRITE(IOUT,918)XP
      GO TO 99
   71 WRITE(IOUT,915)XP
      GO TO 99
   70 IF(XP(11)-0.01)71,75,75
   75 DELX=0.0005
      DO 82 I=1,11
      IF(XP(I))78,82,83
   78 XP(I)=XP(I)-DELX
      GO TO 82
   83 XP(I)=XP(I)+DELX
   82 CONTINUE
      WRITE(IOUT,902)XP
      GO TO 99
   99 CONTINUE
      LIM=NO
  201 INT=1
      DO 96 I=1,LIM
      J=L(I)
      IF(J-I)97,96,97
   97 TEMP1 = YPLOT(I)
      TEMP2 = XPLOT(I)
      IT3 = L(I)
      YPLOT(I) = YPLOT(J)
      XPLOT(I) = XPLOT(J)
      L(I) = L(J)
      YPLOT(J) = TEMP1
      XPLOT(J) = TEMP2
      L(J) = IT3
      INT=I
   96 CONTINUE
      IF(INT-1)205,205,202
  202 LIM=INT
      GO TO 201
  205 RETURN
  902 FORMAT(/2H  ,11(9X,1H')/2H  ,11F10.3)
  911 FORMAT(1H ,F8.0,2X,101A1)
  912 FORMAT(1H ,F8.2,2X,101A1)
  914 FORMAT(1H ,F8.5,2X,101A1)
  915 FORMAT(E10.2 ,1X, 101A1)
  916 FORMAT(/2H  ,11(9X,1H')/2H  ,11E10.2)
  917 FORMAT(/2H  ,11(9X,1H')/2H  ,11F10.5)
  918 FORMAT(/2H  ,11(9X,1H')/2H  ,11F10.0)
      END
```

APPENDIX II-B. Cold-Model Studies of an Axial Flow Burner With an ASTM Flow Nozzle*

Burner Design

Axial flow burners are typically used on high-temperature, large-scale applications such as steel mill soaking pits and slab heaters and large car bottom and rotary hearth furnaces, where burner inputs are in the 5-30 million Btu/hr range. Numerous individual designs of axial flow burners are in use. Surface Combustion has two designs. The first was used over a 15-20 year period (1950 to 1965) and installed on about 1200 soaking pits in the United States (Figure II-B-1).

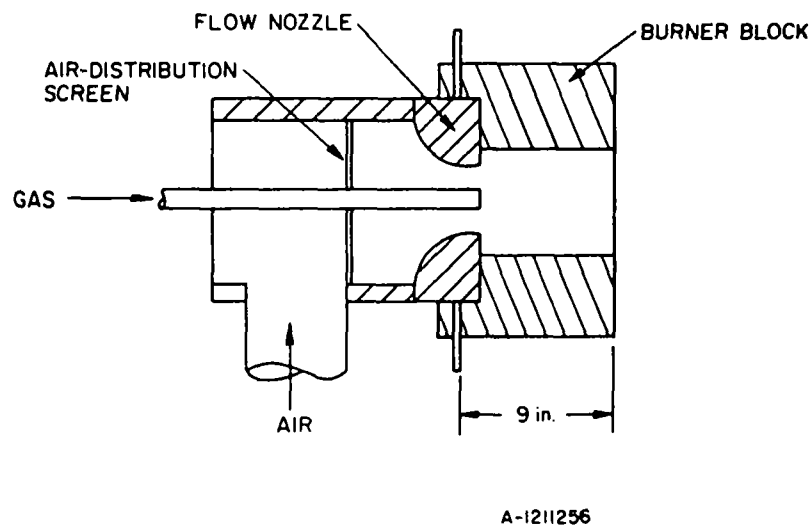

Figure II-B-1. SURFACE COMBUSTION AXIAL BURNER DESIGN

The major design feature is the use of an ASME flow nozzle contour for air discharge at the air-gas mixing point. This not only provides control over velocity and velocity distribution of the mixing point, but also precision air metering for burner-input control. An axial flow gas nozzle is located at the flow nozzle throat for long-flame applications. An even longer flame can be obtained if the gas nozzle is positioned at a point of lower velocity differential.

---

* This burner had a flame longer than our experimental furnace. Therefore, it was not studied in hot-modeling conditions.

Flame length must usually be tailored for heating-chamber dimensions, and this is accomplished by using additional gas nozzles. Nozzle patterns are usually 1, 2, or 4. Additional flame-length control can be achieved by introducing swirl into the gas nozzles. With multiple nozzles, 2 or 4, swirls can be in opposite directions.

The second burner design is being used on installations built since the 1963-1964 period and uses the same air-side design contours including the flow nozzle. The major improvement is in the gas nozzle system, which incorporates both radial and axial gas mixing for flame-length control. This gas mixing system can be installed on existing old-style burners (Figure II-B-2).

The experimental burner is designed to simulate both of the above burner designs through the use of removable inserts. The gas input of the experimental burner is limited by our furnace to 3.5 million Btu/hr. Therefore, it has to be scaled down from the 30 million Btu/hr input of a full-sized burner using velocity scaling techniques. Velocity scaling is the most widely used technique of burner equipment manufacturers. The basic operating characteristics of the experimental burner are given in Table II-B-1 and represent the conditions found in a full-sized commercial burner.

Table II-B-1. OPERATING CHARACTERISTICS OF EXPERIMENTAL AXIAL FLOW BURNER

Gas Input (Maximum)	4000 CF/hr
Air Input at 10% Excess Air	44,000 CF/hr (STP)
Air Preheat Temperature	800^0-900^0F
Air Duct Velocity at 900^0F	30 ft/s
Air Housing Velocity at 900^0F	30 ft/s
Air Velocity at Throat	160 ft/s
Burner Block Velocity at 900^0F	40 ft/s
Gas Nozzle Velocity at 60^0F (Maximum Flame Length)	160 ft/s

Based on the above design information, the following scaled-down burner dimensions were calculated.

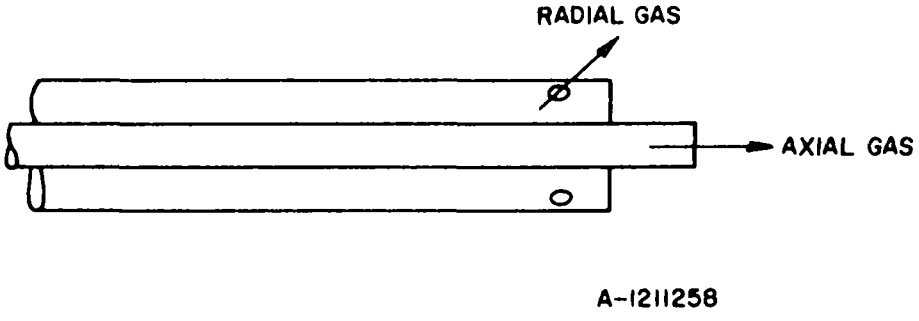

Figure II-B-2. COMBINATION RADIAL-AXIAL GAS BURNER

1. Air Housing Diameter

Air at 44,000 CF/hr (STP), raised to a 900°F preheat temperature while maintaining a 30 ft/s chamber velocity, requires a housing diameter of 14 inches as determined from Equation II-B-1.

$$D^2 = 4Q(T_2/T_1)/V\pi(3600) \qquad \text{(II-B-1)}$$

where —

D = diameter, ft
Q = air flow at STP, CF/hr
T_2 = preheat temperature, °R = 1360
T_1 = temperature at STP, °R = 520
V = velocity, ft/s (30 ft/s)

2. Surface Combustion Flow Nozzle Diameter

Air again at 44,000 CF/hr (STP), raised to 900°F preheat temperature while maintaining a 160 ft/s velocity, requires a nozzle diameter of 6 inches using Equation II-B-1. The pressure drop through the nozzle was calculated at 2.4 inches of water per velocity head using the following relationships:

Pressure drop, h_v, in feet of fluid flowing is given by Equation II-B-2:

$$h_v = \frac{V^2}{2g_c} \qquad \text{(II-B-2)}$$

To express h_v in feet of water column, it is corrected for the density difference between water and the flowing fluid, air, where —

V^2 = velocity, ft/s at STP
g_c = gravity constant, 32.17 ft-lb/$lb_f s^2$
ρ(water) = 62.4 lb/cu ft
ρ(air) = 0.0763 lb/CF

Therefore,

$$h_v(\text{feet of water}) = \frac{V^2}{2g_c}\left(\frac{\rho_{air}}{\rho_{water}}\right) \qquad \text{(II-B-3)}$$

3. Surface Combustion Gas Nozzle Diameter

For longest flame operation the velocity of the gas should equal the velocity of the air or be 160 ft/s. Again using Equation II-B-1 and assuming $T_1 = T_2$, the nozzle diameter was calculated at 1.12 inches. The pressure drop in the nozzle will be 5.0 inches of water using Equation II-B-3.

4. Axial Flow Burner Operation for Cold Flow Studies

The burner designed for use on the hot furnace (Figure II-B-3) will also be used on the cold model with adjustments made to the volumetric flow to scale mixing for the lower air temperature (70°F) in the cold model. We decided that momentum flux scaling would be better than either Reynolds number or velocity scaling for obtaining the data required from the cold model for this program. To scale from the hot burner (900°F preheated air) to the cold burner (70°F air), momentum flux is held constant according to Equation II-B-4.

$$\rho_H V_H^2 = \rho_c V_c^2 \qquad \text{(II-B-4)}$$

where –

ρ_H = air density at 900°F, lb/CF

ρ_c = air density at 70°F, lb/CF

V_H = air velocity (hot system), ft/s

V_c = air velocity (cold system), ft/s

Once the air velocity is determined for the cold system, the volumetric flow is adjusted to obtain this velocity with the fixed burner dimensions (Figure II-B-3). Table II-B-2 shows the results of our scaling calculations for the burner using both 900°F and 70°F air.

In both the hot and cold test work, a pressure-drop screen was used in the burner to distribute flow evenly across the burner housing diameter. These screens are designed for a 3.0 inches of water column pressure drop. For the hot operation, this is a screen having about 13% open area.

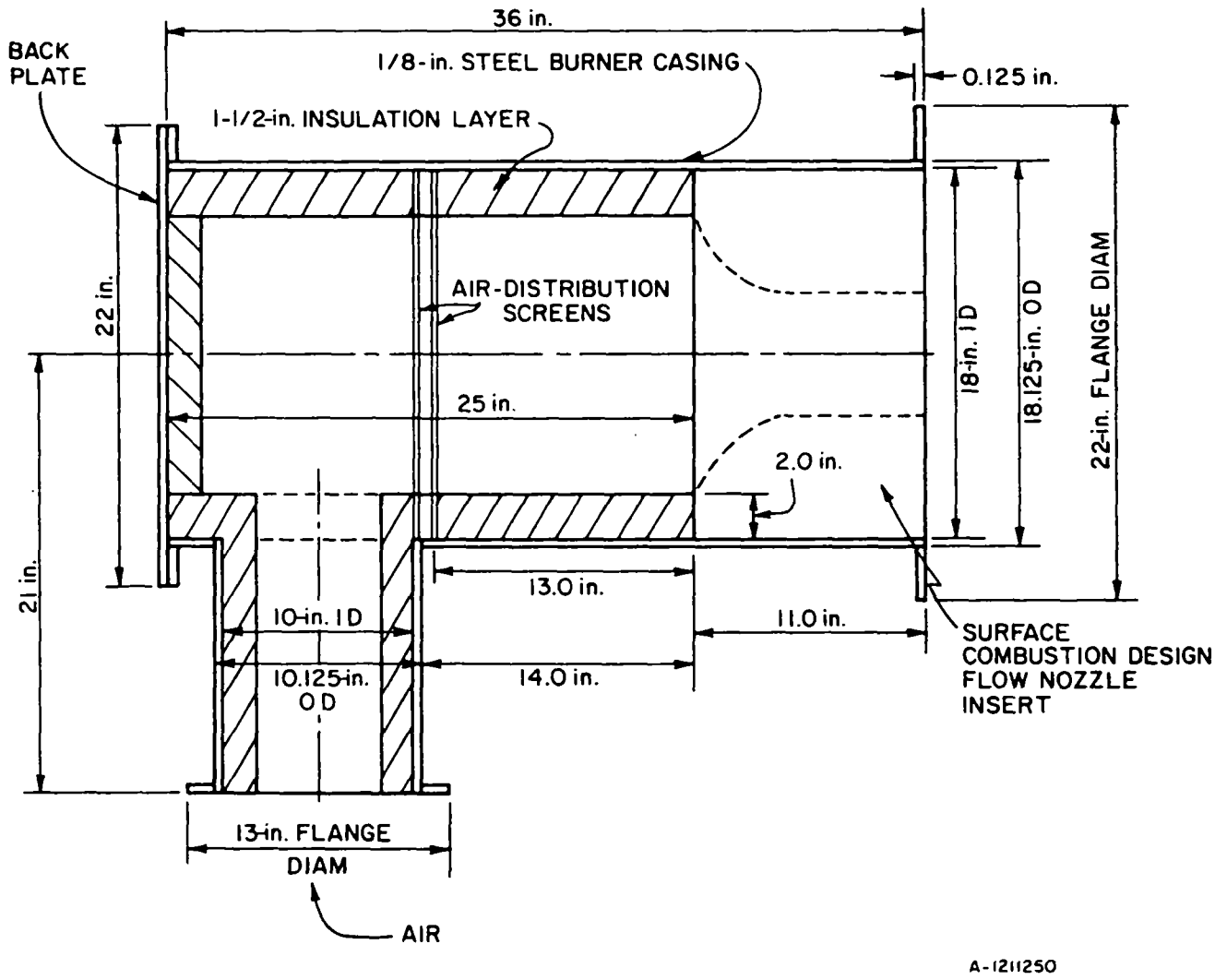

Figure II-B-3. AXIAL FLOW BURNER OUTSIDE CASING ASSEMBLY

Table II-B-2. OPERATING VARIABLES AND BURNER DIMENSIONS FOR AXIAL FLOW BURNER USING 900°F AND 70°F AIR

	Air Temperature	
	900°F	70°F
Gas Nozzle Input, SCF/hr	4,000	6,420
Air Input, SCF/hr	44,000	70,500
Air Duct Velocity, ft/s	30	<30
Nozzle Diameter, inches	6	6
Nozzle Pressure Drop, in. H_2O	2.4	2.4
Gas Nozzle Diameter, inches	1-1/8	1-3/4
Gas Nozzle Pressure Drop, in. H_2O	5	3.6

In both the hot and cold test work, a pressure-drop screen was used in the burner to distribute flow evenly across the burner housing diameter. These screens are designed for a 3.0 inches of water column pressure drop. For the hot operation, this is a screen having about 13% open area.

Tracer-Gas Mixing Studies

Table II-B-3 and Figure II-B-4 show the raw data input, the reduced data, and a graphical presentation of the data for the axial flow burner fitted with the ASTM flow nozzle at a 5.1-cm axial sampling position. The following is an explanation of the headings listed in Table II-B-3: Y-observed is a carbon monoxide value on the calibration curve for a given value of x; Y-computed is the value of Y-calculated from a polynomial fit of the calibration curve for the same value of x; difference is the numerical difference between Y-observed and Y-computed; SD is the standard deviation of Y-computed. The coefficients of the fitted calibration curve are listed next as C(1), C(2)...C(N). Under experimental results we list AP, the axial position of the data point in centimeters; RP, the radial position of the data point in centimeters; X(V), the experimentally time-averaged voltage corresponding to the unknown concentration; and CO, the value of the carbon monoxide concentration in parts per million (ppm). Figure II-B-4 shows the graphical output of Table II-B-3. The carbon monoxide concentration above the ambient level of approximately 70 ppm occurs between ±2 cm from the axis of the burner; in the throat of the burner the concentration falls to 8 ppm. Figure

Table II-B-3. TRACER-GAS MIXING DATA FOR THE AXIAL BURNER WITH THE ASTM FLOW NOZZLE AT THE 5.1-cm AXIAL POSITION

TRACER GAS STUDIES OF COMBUSTION BURNERS
AXIAL BURNER WITH SURFACE COMBUSTION NOZZLE - COLD MODEL (CO TRACER GAS)

Y OBSERVED	Y COMPUTED	DIFFERENCE
0.00	0.44	0.44457
125.00	124.26	-0.73118
250.00	249.14	-0.85674
375.00	377.18	2.18748
500.00	498.95	-1.04412

SD Y= 0.19159E 01

COEFFICIENTS FOR Y= C(1)+C(2)*X+...+C(N+1)*X**N
C(1)= 0.4445
C(2)= 395.5515
C(3)= 102.9597

EXPERIMENTAL RESULTS

AP	RP	X(V)	CO
5.10	-25.00	0.172	71.52
5.10	-20.00	0.170	70.66
5.10	-15.00	0.172	71.52
5.10	-14.00	0.171	71.09
5.10	-13.00	0.171	71.09
5.10	-12.00	0.171	71.09
5.10	-10.00	0.171	71.09
5.10	-9.00	0.171	71.09
5.10	-8.00	0.169	70.23
5.10	-7.00	0.080	32.74
5.10	-6.00	0.030	12.40
5.10	-5.00	0.020	8.39
5.10	-4.00	0.019	7.99
5.10	-3.00	0.018	7.59
5.10	-2.00	0.645	298.40
5.10	-1.00	1.410	762.86
5.10	0.00	1.600	896.90
5.10	1.00	1.720	985.38
5.10	2.00	0.690	322.39
5.10	3.00	0.021	8.79
5.10	4.00	0.019	7.99
5.10	5.00	0.020	8.39
5.10	6.00	0.021	8.79
5.10	7.00	0.021	8.79
5.10	8.00	0.065	26.59
5.10	9.00	0.146	60.38
5.10	10.00	0.169	70.23
5.10	11.00	0.172	71.52
5.10	12.00	0.172	71.52
5.10	13.00	0.172	71.52
5.10	14.00	0.172	71.52
5.10	15.00	0.172	71.52
5.10	20.00	0.171	71.09
5.10	25.00	0.172	71.52

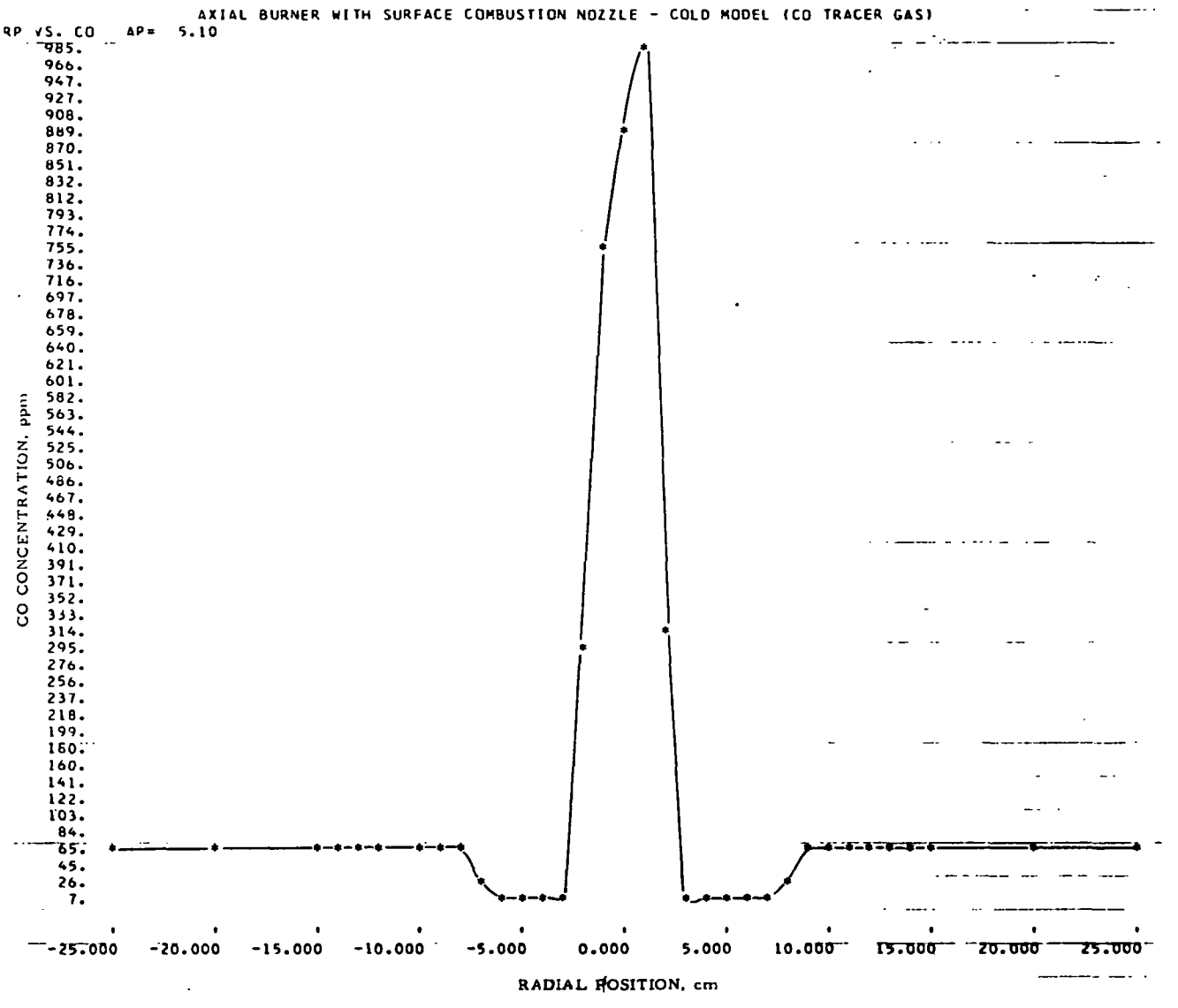

Figure II-B-4. TRACER-GAS MIXING PROFILE FOR THE AXIAL BURNER WITH THE ASTM FLOW NOZZLE AT THE 5.1-cm AXIAL POSITION

II-B-5 shows the tracer-gas studies made at an axial position of 25.4 cm. We found that there is little difference in the qualitative structure of the concentration profile: Only the magnitude of the carbon monoxide concentration at the center of the peak has decreased. The tracer-gas profile taken at an axial position of 45.7 cm is shown in Figure II-B-6. The concentration in the peak is one-half the concentration measured at 5.1 cm, and the width of the peak has increased by 2 cm. Figure II-B-7 shows the tracer-gas data gathered at an axial position of 66.0 cm. The peak concentration has again decreased, accompanied by an increase in the width of the peak. The difference between the ambient carbon monoxide concentration and the concentration in the throat of the burner is now 20 ppm, compared with 62 ppm at an axial position of 5.1 cm. A profile taken at an axial position of 86.7 cm showed that the central peak has vanished; therefore, we considered the mixing complete and did not run full profiles beyond this point. Data taken at axial positions farther from the burner only showed experimental fluctuations about the ambient concentration. The raw and computed data for the axial burner fitted with the ASTM flow nozzle are presented in Tables II-B-4 to II-B-6.

Cold-Model Velocity Data for the Axial Burner

Point-by-point velocity profile data were collected for the axial burner, fitted with the ASTM flow nozzle, by using a multidirectional impact tube (MDIT). A typical set of raw data obtained from the axial flow burner fitted with the ASTM nozzle is shown in Table II-B-7. The rotational angle of the probe in the x-z plane is represented by θ. AP is the axial position of the probe in centimeters, and RP is its radial position in centimeters. PB is the atmospheric pressure in millimeters of mercury and P_{xy} is the pressure differential between pressure holes, x and y, expressed in terms of time. The pressure differentials are expressed in terms of time because of the integration method used to collect the data. The pressure differentials we are attempting to measure are constantly changing since we are dealing with a turbulent system. To determine the mean value of these transient pressure differentials, we electronically integrate. These experimentally determined mean pressure differentials yield the velocity (magnitude and direction) of the air stream by means of the techniques outlined earlier in this report.

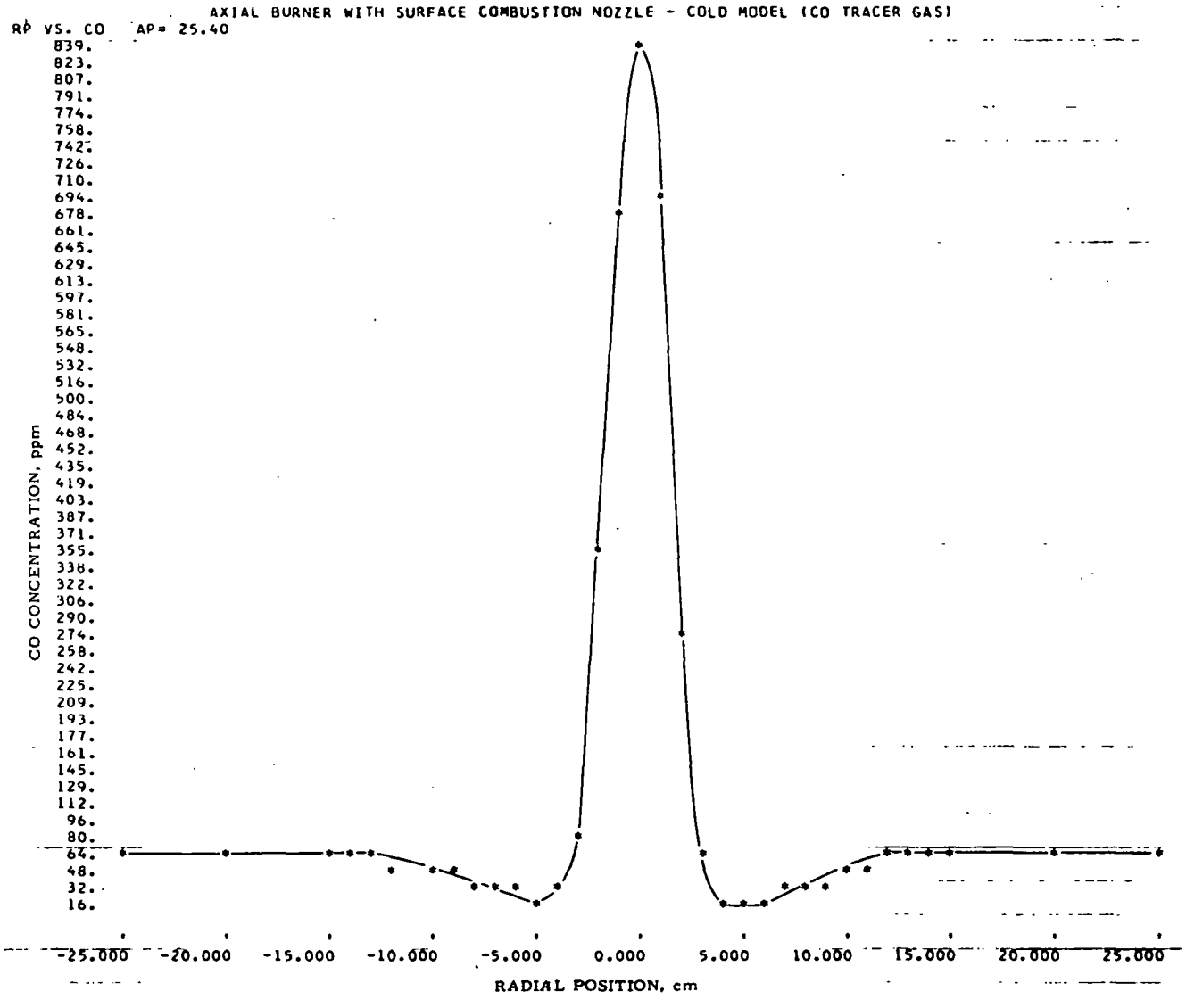

Figure II-B-5. TRACER-GAS MIXING PROFILE FOR THE AXIAL BURNER WITH THE ASTM FLOW NOZZLE AT THE 25.4-cm AXIAL POSITION

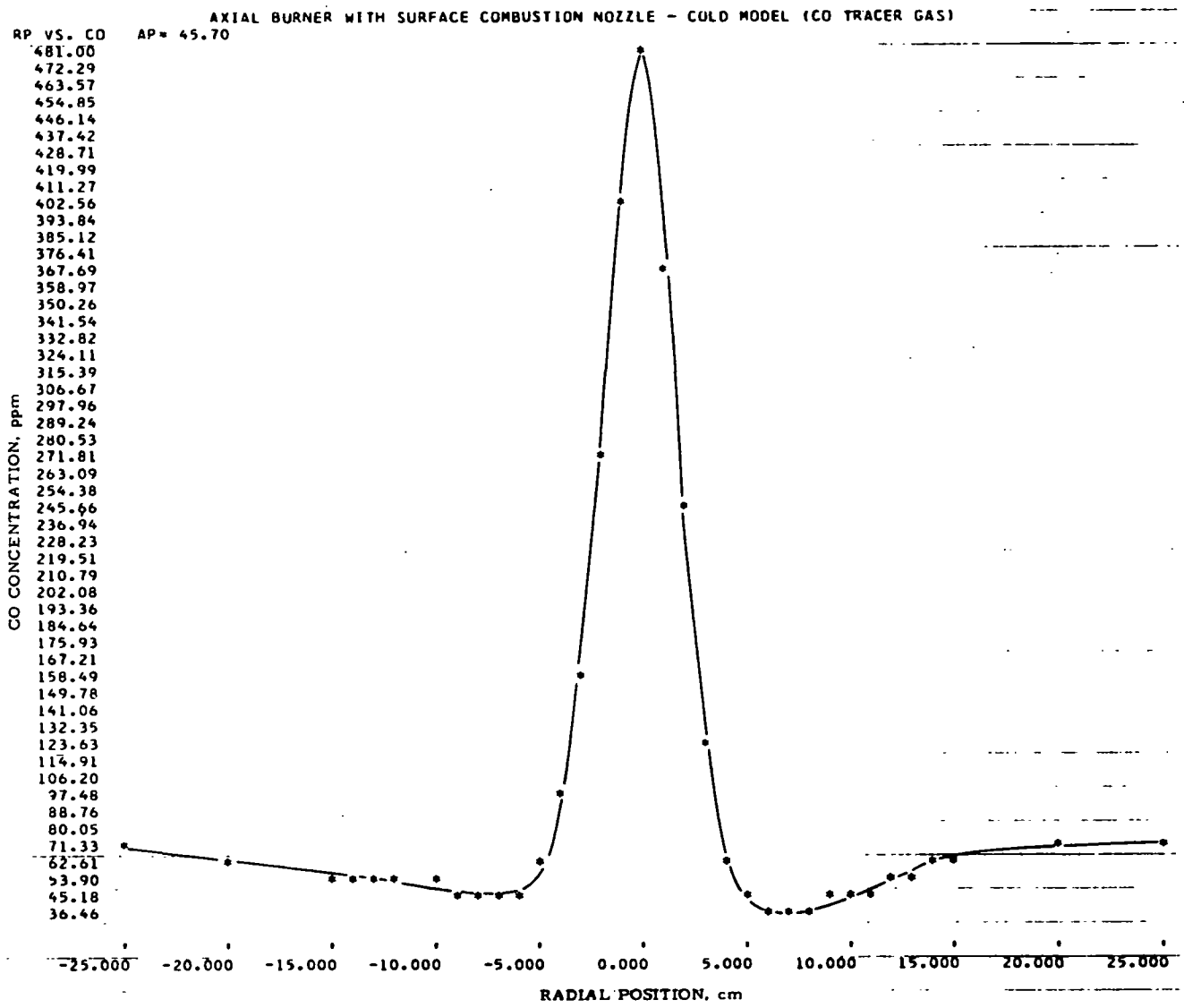

Figure II-B-6. TRACER-GAS MIXING PROFILE FOR THE AXIAL BURNER WITH THE ASTM FLOW NOZZLE AT THE 45.7-cm AXIAL POSITION

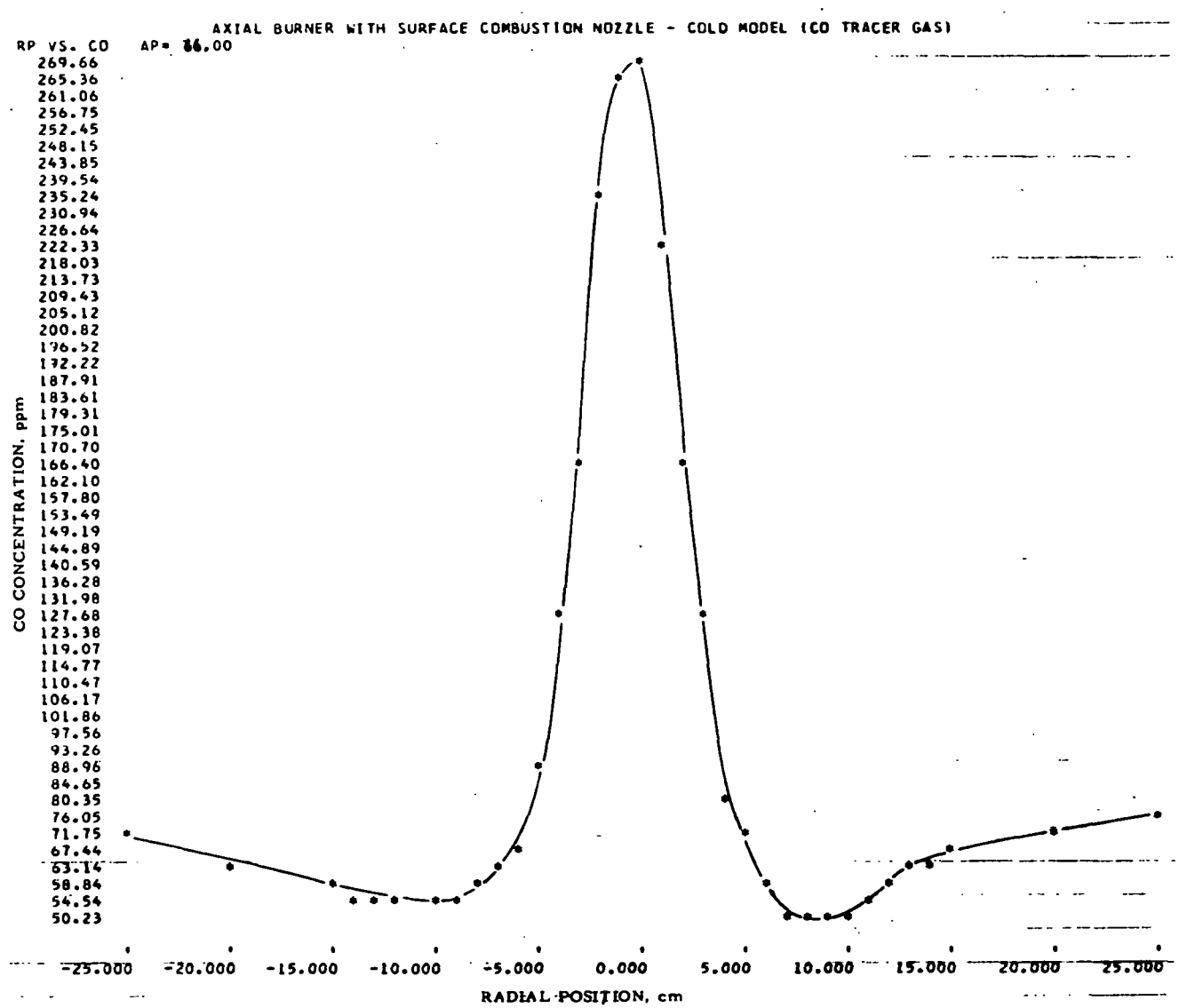

Figure II-B-7. TRACER-GAS MIXING PROFILE FOR THE AXIAL BURNER WITH THE ASTM FLOW NOZZLE AT THE 66.0-cm AXIAL POSITION

Table II-B-4. TRACER-GAS MIXING DATA FOR THE AXIAL BURNER WITH THE ASTM FLOW NOZZLE AT THE 25.4-cm AXIAL POSITION

TRACER GAS STUDIES OF COMBUSTION BURNERS
AXIAL BURNER WITH SURFACE COMBUSTION NOZZLE - COLD MODEL (CO TRACER GAS)

Y OBSERVED	Y COMPUTED	DIFFERENCE
0.00	0.44	0.44457
125.00	124.26	-0.73118
250.00	249.14	-0.85674
375.00	377.18	2.18748
500.00	498.95	-1.04412

SD Y= 0.19159E 01

COEFFICIENTS FOR Y= C(1)+C(2)*X+...+C(N+1)*X**N

C(1)= 0.4445
C(2)= 395.5515
C(3)= 102.9597

EXPERIMENTAL RESULTS

AP	RP	X(V)	CO
25.40	-25.00	0.171	71.09
25.40	-20.00	0.165	68.51
25.40	-15.00	0.163	67.65
25.40	-14.00	0.157	65.08
25.40	-13.00	0.145	59.96
25.40	-12.00	0.133	54.87
25.40	-10.00	0.120	49.39
25.40	-9.00	0.102	41.86
25.40	-8.00	0.091	37.29
25.40	-7.00	0.077	31.51
25.40	-6.00	0.067	27.40
25.40	-5.00	0.058	23.73
25.40	-4.00	0.070	28.63
25.40	-3.00	0.206	86.29
25.40	-2.00	0.748	353.92
25.40	-1.00	1.290	682.04
25.40	0.00	1.520	839.56
25.40	1.00	1.300	688.66
25.40	2.00	0.590	269.66
25.40	3.00	0.141	58.26
25.40	4.00	0.042	17.23
25.40	5.00	0.039	16.02
25.40	6.00	0.054	22.10
25.40	7.00	0.065	26.59
25.40	8.00	0.084	34.39
25.40	9.00	0.097	39.78
25.40	10.00	0.108	44.36
25.40	11.00	0.127	52.34
25.40	12.00	0.147	60.81
25.40	13.00	0.162	67.22
25.40	14.00	0.165	68.51
25.40	15.00	0.170	70.66
25.40	20.00	0.171	71.09
25.40	25.00	0.170	70.66

Table II-B-5. TRACER-GAS MIXING DATA FOR THE AXIAL BURNER WITH THE ASTM FLOW NOZZLE AT THE 45.7-cm AXIAL POSITION

TRACER GAS STUDIES OF COMBUSTION BURNERS
AXIAL BURNER WITH SURFACE COMBUSTION NOZZLE - COLD MODEL (CO TRACER GAS)

Y OBSERVED	Y COMPUTED	DIFFERENCE
0.00	0.44	0.44457
125.00	124.26	-0.73118
250.00	249.14	-0.85674
375.00	377.18	2.18748
500.00	498.95	-1.04412

SD Y= 0.19159E 01

COEFFICIENTS FOR Y= C(1)+C(2)*X+...+C(N+1)*X**N
C(1)= 0.4445
C(2)= 395.5515
C(3)= 102.9597

EXPERIMENTAL RESULTS

AP	RP	X(V)	CO
45.70	-25.00	0.169	70.23
45.70	-20.00	0.155	64.22
45.70	-15.00	0.138	56.99
45.70	-14.00	0.135	55.72
45.70	-13.00	0.130	53.60
45.70	-12.00	0.125	51.49
45.70	-10.00	0.125	51.49
45.70	-9.00	0.109	44.78
45.70	-8.00	0.105	43.11
45.70	-7.00	0.104	42.69
45.70	-6.00	0.118	48.55
45.70	-5.00	0.145	59.96
45.70	-4.00	0.232	97.75
45.70	-3.00	0.359	155.71
45.70	-2.00	0.600	274.84
45.70	-1.00	0.835	402.51
45.70	0.00	0.970	481.00
45.70	1.00	0.780	371.61
45.70	2.00	0.538	243.05
45.70	3.00	0.282	120.17
45.70	4.00	0.149	61.66
45.70	5.00	0.109	44.78
45.70	6.00	0.090	36.87
45.70	7.00	0.089	36.46
45.70	8.00	0.095	38.95
45.70	9.00	0.108	44.36
45.70	10.00	0.102	41.86
45.70	11.00	0.110	45.20
45.70	12.00	0.131	54.02
45.70	13.00	0.137	56.56
45.70	14.00	0.149	61.66
45.70	15.00	0.153	63.37
45.70	20.00	0.170	70.66
45.70	25.00	0.169	70.23

Table II-B-6. TRACER-GAS MIXING DATA FOR THE AXIAL BURNER WITH THE ASTM FLOW NOZZLE AT THE 66.0-cm AXIAL POSITION

TRACER GAS STUDIES OF COMBUSTION BURNERS
AXIAL BURNER WITH SURFACE COMBUSTION NOZZLE - COLD MODEL (CO TRACER GAS)

Y OBSERVED	Y COMPUTED	DIFFERENCE
0.00	0.44	0.44457
125.00	124.26	-0.73118
250.00	249.14	-0.85674
375.00	377.18	2.18748
500.00	498.95	-1.04412

SD Y= 0.19159E 01

COEFFICIENTS FOR Y= C(1)+C(2)*X+...+C(N+1)*X**N
C(1)= 0.4445
C(2)= 395.5515
C(3)= 102.9597

EXPERIMENTAL RESULTS

AP	RP	X(V)	CO
66.00	-25.00	0.168	69.80
66.00	-20.00	0.149	61.66
66.00	-15.00	0.142	58.68
66.00	-14.00	0.137	56.56
66.00	-13.00	0.136	56.14
66.00	-12.00	0.136	56.14
66.00	-10.00	0.131	54.02
66.00	-9.00	0.135	55.72
66.00	-8.00	0.138	56.99
66.00	-7.00	0.150	62.09
66.00	-6.00	0.159	65.94
66.00	-5.00	0.210	88.05
66.00	-4.00	0.303	129.74
66.00	-3.00	0.378	164.67
66.00	-2.00	0.525	236.48
66.00	-1.00	0.580	264.50
66.00	0.00	0.590	269.66
66.00	1.00	0.500	223.96
66.00	2.00	0.383	167.04
66.00	3.00	0.303	129.74
66.00	4.00	0.189	78.88
66.00	5.00	0.170	70.66
66.00	6.00	0.141	58.26
66.00	7.00	0.124	51.07
66.00	8.00	0.122	50.23
66.00	9.00	0.125	51.49
66.00	10.00	0.125	51.49
66.00	11.00	0.133	54.87
66.00	12.00	0.145	59.96
66.00	13.00	0.156	64.65
66.00	14.00	0.155	64.22
66.00	15.00	0.164	68.08
66.00	20.00	0.175	72.81
66.00	25.00	0.182	75.84

Table II-B-7. RAW VELOCITY DATA FOR THE AXIAL BURNER WITH THE ASTM FLOW NOZZLE AT THE 5.1-cm AXIAL POSITION

AERODYNAMIC MODELING OF COMBUSTION BURNERS

CALIBRATION COEFFICIENTS FOR FORWARD FLOW

A1 =	0.770590	A2 =	0.272353	A3 =	-0.059818
B0 =	0.737720	B2 =	-0.158821	B4 =	0.129246
C =	4.464660	D =	0.394812		

AXIAL BURNER WITH SURFACE COMBUSTION NOZZLE - COLD MODEL

TOTAL DATA INPUT

THETA	AP	RP	P13	P03	P24	P04	POA	T	PB
0.	5.1	-25.0	28000.00	32800.00	55000.00	43200.00	420.00	20.	760.
0.	5.1	-20.0	25600.00	69400.00	84000.00	180400.00	440.00	20.	760.
0.	5.1	-15.0	20000.00	97000.00	999999999.50	-152400.00	455.00	20.	760.
0.	5.1	-14.0	17900.00	-70000.00	-121000.00	-41000.00	480.00	20.	760.
0.	5.1	-13.0	15100.00	-87000.00	-120000.00	-43000.00	455.00	20.	760.
0.	5.1	-12.0	14000.00	-118000.00	-58900.00	-57200.00	501.00	20.	760.
0.	5.1	-11.0	12400.00	-204000.00	-56800.00	-48000.00	475.00	20.	760.
0.	5.1	-10.0	10400.00	-43400.00	-16800.00	-26600.00	504.00	20.	760.
0.	5.1	-9.0	6120.00	107000.00	-17100.00	-18700.00	492.00	20.	760.
0.	5.1	-8.0	-1200.00	-3240.00	-2750.00	-6800.00	486.00	20.	760.
0.	5.1	-7.0	-320.00	4770.00	-2530.00	448.00	200.00	20.	760.
0.	5.1	-6.0	-417.00	212.00	300.00	152.00	94.00	20.	760.
0.	5.1	-5.0	-4420.00	162.00	456.00	139.00	88.80	20.	760.
0.	5.1	-4.0	4720.00	155.00	730.00	144.00	86.00	20.	760.
0.	5.1	-3.0	1880.00	154.00	592.00	142.00	88.00	20.	760.
0.	5.1	-2.0	1550.00	153.00	488.00	136.00	86.80	20.	760.
0.	5.1	-1.0	534.00	113.00	544.00	114.00	41.20	20.	760.
0.	5.1	0.0	-672.00	162.00	1180.00	135.00	78.00	20.	760.
0.	5.1	1.0	2730.00	116.00	930.00	113.00	70.40	20.	760.
0.	5.1	2.0	4670.00	136.00	1600.00	150.00	90.20	20.	760.
0.	5.1	3.0	-3540.00	154.00	512.00	134.00	76.40	20.	760.
0.	5.1	4.0	-2668.00	167.00	-2308.00	172.00	87.20	20.	760.
0.	5.1	5.0	-11120.00	152.00	1090.00	147.00	85.60	20.	760.
0.	5.1	6.0	11720.00	156.00	392.00	162.00	87.20	20.	760.
0.	5.1	7.0	439.00	141.00	358.00	143.00	76.80	20.	760.
0.	5.1	8.0	301.00	274.00	1860.00	374.00	179.00	20.	760.
0.	5.1	9.0	2380.00	38880.00	-23620.00	49000.00	445.00	20.	760.
0.	5.1	10.0	-294000.00	-18400.00	-24000.00	-52000.00	386.00	20.	760.
0.	5.1	25.0	16400.00	-77200.00	-63000.00	-68800.00	442.00	20.	760.
0.	5.1	20.0	10000.00	-76400.00	-53200.00	-52000.00	414.00	20.	760.
0.	5.1	15.0	8200.00	-66000.00	-92000.00	-32800.00	380.00	20.	760.

A typical set of reduced velocity data is given in Table II-B-8. The direction of the velocity is defined by FI, the conical angle measured about the x-axis, and by Δ, the dihedral angle measured from the positive y-axis in the y-z plane. The magnitude of the velocity in ft/s is given by V; RHO is the density of the air in slugs/ft-sq in.; and VX, VY, and VZ are the velocity components in ft/s. Both VT, the tangential velocity, and VR, the radial velocity, are expressed in ft/s. PST is the static pressure in psig.

Figure II-B-8 shows the axial velocity at an axial position of 5.1 cm. The central peak occurs in the region of the throat of the burner. Figure II-B-9 shows the axial velocity profile at an axial position of 25.4 cm. The most noticeable structural change in the curve from the profile at 5.1 cm is the increase in radial length of the shear region between the combustion air and surrounding recirculation region radially from 4 to 6 cm. Figure II-B-10 presents the axial velocity profile at 45.7 cm. The central peak and the constant-velocity plateau have blended together with the shear layer to give a smooth bell-shaped velocity distribution. The structure of the axial velocity profile at 66.0 cm, shown in Figure II-B-11, is very similar to the profile at 45.7 cm. The maximum velocity at the peak is 31.5 ft/s, a slight decrease from the 39.0 ft/s measured at an axial position of 5.1 cm.

The raw pressure data for the case of the axial burner fitted with the ASTM nozzle are given in Tables II-B-9 to II-B-11. The reduced profile data are listed in Tables II-B-12 to II-B-14.

Initial runs on the hot furnace with the axial burner fitted with the ASTM nozzle showed that the flame was longer than the furnace. Consequently, further work was not undertaken.

Table II-B-8. COMPUTER REDUCED DATA FOR THE AXIAL BURNER WITH THE ASTM FLOW NOZZLE AT THE 5.1-cm AXIAL POSITION

AXIAL BURNER WITH SURFACE COMBUSTION NOZZLE - COLD MODEL

RESULTS

AP	RP	FI	DELTA	RHO	V	VX	VY	VZ	VT	VR	PST	T	PB
5.1	-25.0	27.3	153.0	0.0000159	1.84	1.63	-0.75	0.38	-0.84	0.08	0.002316	20.	760.
5.1	-20.0	62.9	163.0	0.0000159	1.64	0.74	-1.39	0.42	-1.30	0.65	0.002242	20.	760.
5.1	-15.0	73.4	179.9	0.0000159	2.06	0.58	-1.98	0.00	-1.30	1.49	0.002192	20.	760.
5.1	-14.0	82.2	188.4	0.0000159	3.02	0.40	-2.96	-0.43	-1.05	2.80	0.002149	20.	760.
5.1	-13.0	81.0	187.1	0.0000159	3.10	0.48	-3.04	-0.38	-1.14	2.84	0.002263	20.	760.
5.1	-12.0	77.7	193.3	0.0000159	2.99	0.63	-2.84	-0.67	-1.33	2.60	0.002048	20.	760.
5.1	-11.0	77.7	192.3	0.0000159	3.10	0.65	-2.96	-0.64	-1.28	2.74	0.002163	20.	760.
5.1	-10.0	76.6	211.7	0.0000159	3.71	0.85	-3.07	-1.90	-1.52	3.27	0.002083	20.	760.
5.1	-9.0	76.0	199.6	0.0000159	4.15	1.00	-3.80	-1.36	-1.61	3.69	0.002162	20.	760.
5.1	-8.0	48.0	336.4	0.0000159	7.50	5.01	5.11	-2.23	-4.55	3.23	0.002053	20.	760.
5.1	-7.0	16.2	352.7	0.0000159	20.72	19.89	5.75	-0.72	-5.67	1.20	0.001962	20.	760.
5.1	-6.0	8.7	54.2	0.0000159	31.91	31.54	2.82	3.92	-4.79	0.62	0.002656	20.	760.
5.1	-5.0	3.9	84.1	0.0000159	33.67	33.59	0.23	2.30	-2.31	0.16	0.002095	20.	760.
5.1	-4.0	2.4	98.7	0.0000159	33.89	33.86	-0.22	1.42	-1.43	0.07	0.002287	20.	760.
5.1	-3.0	3.1	107.4	0.0000159	33.68	33.63	-0.55	1.76	-1.83	0.17	0.002161	20.	760.
5.1	-2.0	3.7	107.4	0.0000159	33.87	33.80	-0.67	2.13	-2.20	0.37	0.002234	20.	760.
5.1	-1.0	3.6	135.5	0.0000159	37.97	37.89	-1.73	1.70	-2.30	0.75	0.012402	20.	760.
5.1	0.0	2.7	29.6	0.0000159	35.60	35.56	1.46	0.83	0.00	1.68	0.002521	20.	760.
5.1	1.0	1.5	108.8	0.0000159	39.04	39.02	-0.33	0.97	1.02	0.13	0.001813	20.	760.
5.1	2.0	2.3	108.9	0.0000159	35.20	35.17	-0.45	1.34	1.41	0.14	0.001037	20.	760.
5.1	3.0	3.3	81.7	0.0000159	34.62	34.56	0.28	1.99	2.00	0.19	0.003350	20.	760.
5.1	4.0	1.1	310.8	0.0000159	33.32	33.31	0.41	-0.48	0.63	0.01	0.002414	20.	760.
5.1	5.0	1.7	84.4	0.0000159	34.35	34.34	0.09	1.01	1.02	0.03	0.002075	20.	760.
5.1	6.0	6.3	91.9	0.0000159	32.29	32.09	-0.12	3.59	3.58	0.34	0.003126	20.	760.
5.1	7.0	6.8	129.1	0.0000159	32.74	32.51	-2.48	3.04	3.91	0.34	0.004448	20.	760.
5.1	8.0	16.1	170.8	0.0000159	21.17	20.33	-5.82	0.94	5.80	1.07	0.002402	20.	760.
5.1	9.0	68.7	185.7	0.0000159	6.19	2.24	-5.74	-0.57	3.26	4.75	0.002487	20.	760.
5.1	10.0	77.4	274.6	0.0000159	2.94	0.64	0.23	-2.86	1.15	2.63	0.002628	20.	760.
5.1	25.0	77.9	194.5	0.0000159	2.88	0.60	-2.73	-0.71	2.04	1.95	0.002304	20.	760.
5.1	20.0	77.2	190.6	0.0000159	3.53	0.77	-3.38	-0.63	2.28	2.57	0.002494	20.	760.
5.1	15.0	79.5	185.0	0.0000159	4.00	0.72	-3.91	-0.34	1.88	3.45	0.002754	20.	760.

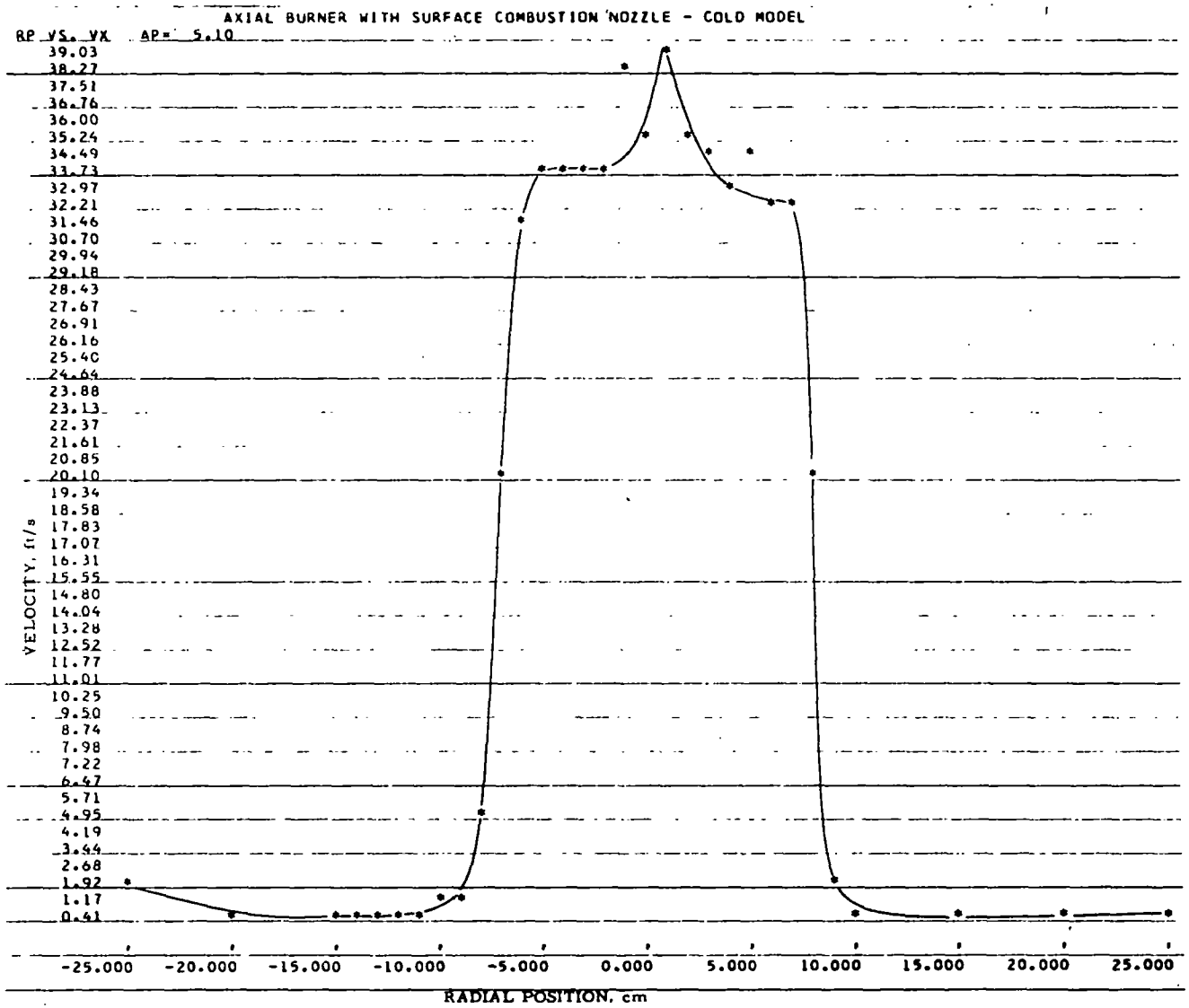

Figure II-B-8. AXIAL VELOCITY PROFILE FOR THE AXIAL BURNER WITH THE ASTM FLOW NOZZLE AT THE 5.1-cm AXIAL POSITION

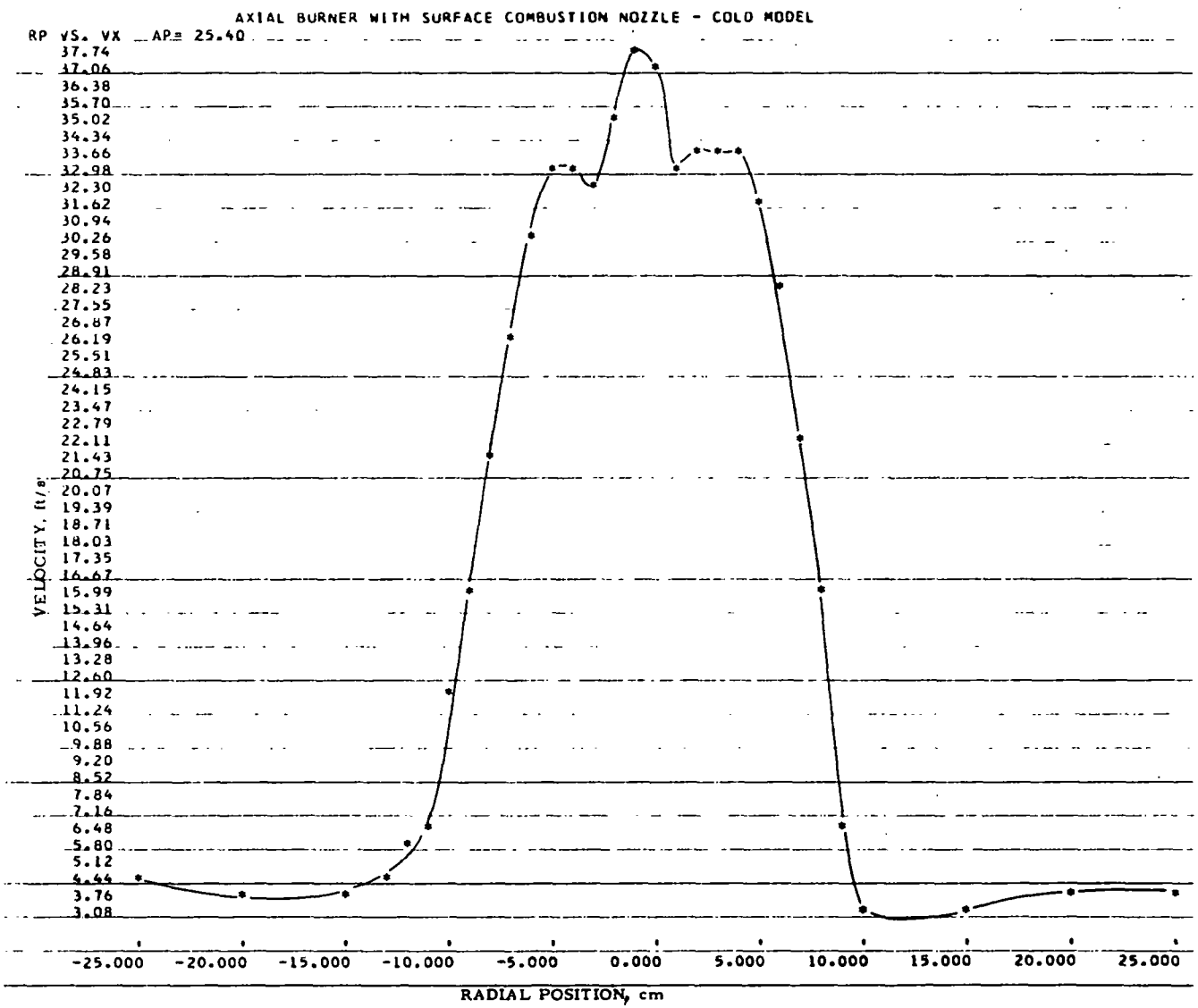

Figure II-B-9. AXIAL VELOCITY PROFILE FOR THE AXIAL BURNER WITH THE ASTM FLOW NOZZLE AT THE 25.4-cm AXIAL POSITION

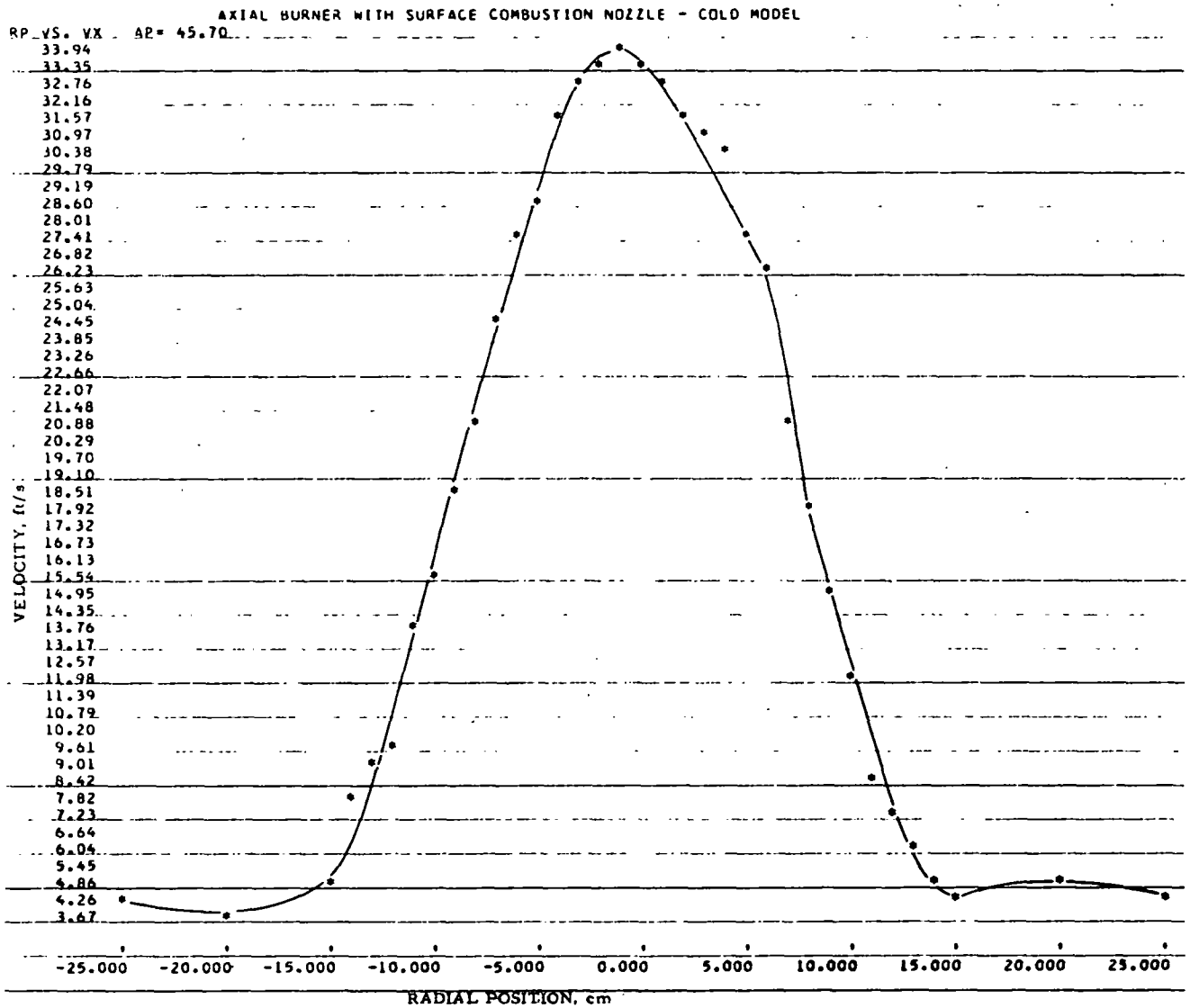

Figure II-B-10. AXIAL VELOCITY PROFILE FOR THE AXIAL BURNER WITH THE ASTM FLOW NOZZLE AT THE 45.7-cm AXIAL POSITION

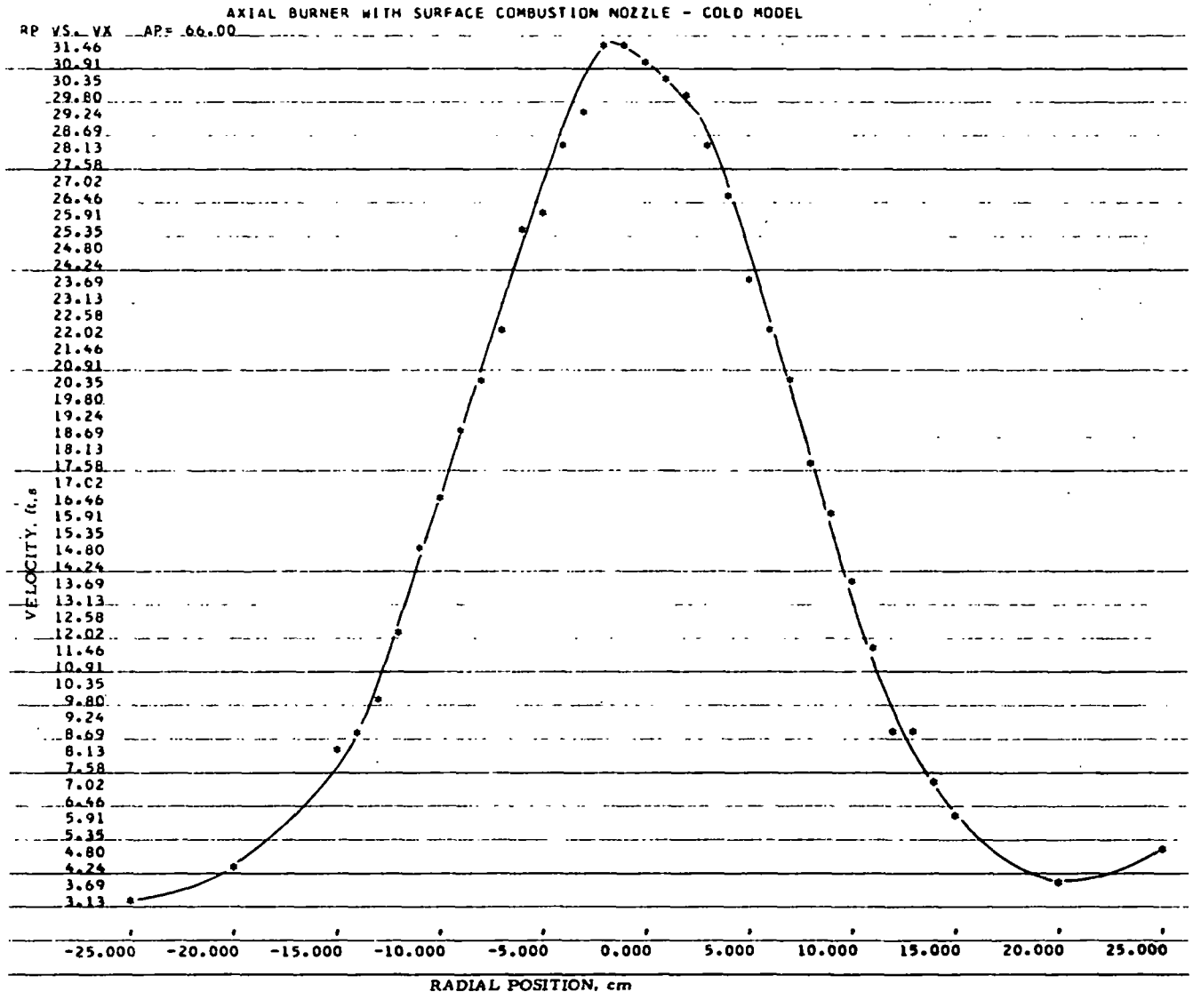

Figure II-B-11. AXIAL VELOCITY PROFILE FOR THE AXIAL BURNER WITH THE ASTM FLOW NOZZLE AT THE 66.0-cm AXIAL POSITION

Table II-B-9. RAW VELOCITY DATA FOR THE AXIAL BURNER WITH THE ASTM FLOW NOZZLE AT THE 25.4-cm AXIAL POSITION

AERODYNAMIC MODELING OF COMBUSTION BURNERS

CALIBRATION COEFFICIENTS FOR FORWARD FLOW

A1 =	0.770590	A2 =	0.272353	A3 =	-0.059818
B0 =	0.737720	B2 =	-0.158821	B4 =	0.129246
C =	4.464660	D =	0.394812		

AXIAL BURNER WITH SURFACE COMBUSTION NOZZLE - COLD MODEL

TOTAL DATA INPUT

THETA	AP	RP	P13	P03	P24	P04	POA	T	PB
0.	25.4	25.0	-41500.00	12300.00	12100.00	12300.00	351.00	20.	760.
0.	25.4	20.0	-215200.00	11800.00	13800.00	12600.00	355.00	20.	760.
0.	25.4	15.0	374800.00	11600.00	11400.00	12700.00	353.00	20.	760.
0.	25.4	10.0	1830.00	16100.00	-20700.00	11300.00	336.00	20.	760.
0.	25.4	9.0	1120.00	4080.00	-69300.00	1860.00	299.00	20.	760.
0.	25.4	8.0	-677.00	1480.00	3340.00	620.00	214.00	20.	760.
0.	25.4	7.0	-558.00	534.00	3020.00	355.00	152.00	20.	760.
0.	25.4	6.0	-421.00	324.00	-6800.00	231.00	125.00	20.	760.
0.	25.4	5.0	-510.00	218.00	25240.00	186.00	83.70	20.	760.
0.	25.4	4.0	-847.00	174.00	1560.00	156.00	84.60	20.	760.
0.	25.4	3.0	-1920.00	165.00	770.00	153.00	83.00	20.	760.
0.	25.4	2.0	-3300.00	160.00	563.00	146.00	84.00	20.	760.
0.	25.4	1.0	-970.00	181.00	648.00	148.00	88.00	20.	760.
0.	25.4	0.0	-756.00	147.00	624.00	122.00	72.00	20.	760.
0.	25.4	-1.0	-628.00	134.00	610.00	122.00	74.00	20.	760.
0.	25.4	-2.0	1050.00	139.00	1002.00	139.00	83.00	20.	760.
0.	25.4	-3.0	5760.00	174.00	-4540.00	176.00	85.20	20.	760.
0.	25.4	-4.0	-36200.00	163.00	4740.00	164.00	84.80	20.	760.
0.	25.4	-5.0	4200.00	162.00	1280.00	159.00	87.20	20.	760.
0.	25.4	-6.0	980.00	173.00	604.00	178.00	106.00	20.	760.
0.	25.4	-7.0	556.00	207.00	660.00	227.00	127.00	20.	760.
0.	25.4	-8.0	594.00	294.00	876.00	336.00	166.00	20.	760.
0.	25.4	-9.0	680.00	473.00	1164.00	557.00	218.00	20.	760.
0.	25.4	-10.0	1720.00	874.00	1350.00	980.00	270.00	20.	760.
0.	25.4	-15.0	-53000.00	11400.00	19400.00	11600.00	343.00	20.	760.
0.	25.4	-20.0	-42400.00	11100.00	11400.00	11000.00	338.00	20.	760.
0.	25.4	-25.0	-48000.00	11100.00	98400.00	10600.00	342.00	20.	760.
0.	25.4	-11.0	2440.00	2780.00	29600.00	3490.00	330.00	20.	760.
0.	25.4	-12.0	7200.00	3160.00	3200.00	4350.00	335.00	20.	760.
0.	25.4	-13.0	10600.00	5380.00	6500.00	5900.00	340.00	20.	760.

Table II-B-10. RAW VELOCITY DATA FOR THE AXIAL BURNER WITH THE ASTM FLOW NOZZLE AT THE 45.7-cm AXIAL POSITION

AERODYNAMIC MODELING OF COMBUSTION BURNERS

CALIBRATION COEFFICIENTS FOR FORWARD FLOW

A1 =	0.770590	A2 =	0.272353	A3 =	-0.059818
B0 =	0.737720	B2 =	-0.158821	B4 =	0.129246
C =	4.464660	D =	0.394812		

AXIAL BURNER WITH SURFACE COMBUSTION NOZZLE - COLD MODEL

TOTAL DATA INPUT

THETA	AP	RP	P13	P03	P24	P04	POA	T	PB
0.	45.7	25.0	-20000.00	7840.00	8160.00	7900.00	346.00	20.	760.
0.	45.7	20.0	-25000.00	7230.00	8900.00	7720.00	347.00	20.	760.
0.	45.7	15.0	-20000.00	7600.00	9980.00	8800.00	335.00	20.	760.
0.	45.7	14.0	-13900.00	7640.00	12200.00	6470.00	328.00	20.	760.
0.	45.7	13.0	-12700.00	6460.00	42400.00	5470.00	322.00	20.	760.
0.	45.7	12.0	-4880.00	5640.00	23800.00	3260.00	310.00	20.	760.
0.	45.7	11.0	-2580.00	4340.00	-36200.00	2730.00	298.00	20.	760.
0.	45.7	10.0	-1220.00	2540.00	4300.00	1170.00	274.00	20.	760.
0.	45.7	9.0	-804.00	1530.00	10900.00	860.00	234.00	20.	760.
0.	45.7	8.0	-633.00	890.00	2630.00	568.00	198.00	20.	760.
0.	45.7	7.0	-630.00	617.00	2370.00	389.00	165.00	20.	760.
0.	45.7	6.0	-585.00	302.00	2190.00	272.00	147.00	20.	760.
0.	45.7	5.0	-552.00	313.00	2380.00	239.00	124.00	20.	760.
0.	45.7	4.0	-664.00	233.00	1300.00	182.00	106.00	20.	760.
0.	45.7	3.0	-840.00	214.00	1210.00	182.00	106.00	20.	760.
0.	45.7	2.0	-1000.00	196.00	980.00	168.00	99.00	20.	760.
0.	45.7	1.0	-1150.00	184.00	960.00	159.00	93.00	20.	760.
0.	45.7	0.0	-900.00	173.00	880.00	151.00	88.00	20.	760.
0.	45.7	-1.0	-4380.00	159.00	850.00	146.00	80.20	20.	760.
0.	45.7	-2.0	7300.00	156.00	910.00	158.00	83.00	20.	760.
0.	45.7	-3.0	3680.00	162.00	950.00	159.00	97.60	20.	760.
0.	45.7	-4.0	1380.00	172.00	1070.00	171.00	100.00	20.	760.
0.	45.7	-5.0	1140.00	199.00	1010.00	199.00	114.00	20.	760.
0.	45.7	-6.0	1070.00	211.00	1070.00	225.00	130.00	20.	760.
0.	45.7	-7.0	930.00	268.00	1220.00	273.00	139.00	20.	760.
0.	45.7	-8.0	798.00	341.00	1490.00	374.00	170.00	20.	760.
0.	45.7	-9.0	1080.00	415.00	2620.00	486.00	203.00	20.	760.
0.	45.7	-10.0	1190.00	574.00	2310.00	620.00	234.00	20.	760.
0.	45.7	-11.0	1680.00	746.00	4430.00	914.00	266.00	20.	760.
0.	45.7	-12.0	2130.00	1330.00	2760.00	1500.00	292.00	20.	760.
0.	45.7	-13.0	4290.00	1800.00	4880.00	1980.00	293.00	20.	760.
0.	45.7	-14.0	5190.00	2520.00	6280.00	2190.00	314.00	20.	760.
0.	45.7	-15.0	18000.00	6670.00	12400.00	4990.00	332.00	20.	760.
0.	45.7	-20.0	-52800.00	13400.00	13900.00	10300.00	334.00	20.	760.
0.	45.7	-25.0	-17300.00	10100.00	10700.00	9400.00	328.00	20.	760.

Table II-B-11. RAW VELOCITY DATA FOR THE AXIAL BURNER WITH THE ASTM FLOW NOZZLE AT THE 66.0-cm AXIAL POSITION

AERODYNAMIC MODELING OF COMBUSTION BURNERS

CALIBRATION COEFFICIENTS FOR FORWARD FLOW

A1 =	0.770590	A2 =	0.272353	A3 =	-0.059818
B0 =	0.737720	B2 =	-0.158821	B4 =	0.129246
C =	4.464660	D =	0.394812		

AXIAL BURNER WITH SURFACE COMBUSTION NOZZLE - COLD MODEL

TOTAL DATA INPUT

THETA	AP	RP	P13	P03	P24	P04	POA	T	PB
0.	66.0	25.0	-22300.00	6570.00	10600.00	6760.00	356.00	20.	760.
0.	66.0	20.0	-14900.00	11200.00	12000.00	16400.00	457.00	20.	760.
0.	66.0	15.0	-4090.00	8440.00	11800.00	5900.00	344.00	20.	760.
0.	66.0	14.0	-4010.00	5580.00	11160.00	3180.00	338.00	20.	760.
0.	66.0	13.0	-2250.00	4410.00	200000.00	2620.00	316.00	20.	760.
0.	66.0	12.0	-2350.00	4160.00	35800.00	2370.00	323.00	20.	760.
0.	66.0	11.0	-1780.00	2100.00	15600.00	1460.00	290.00	20.	760.
0.	66.0	10.0	-1140.00	1960.00	9600.00	900.00	256.00	20.	760.
0.	66.0	9.0	-980.00	1270.00	6800.00	692.00	232.00	20.	760.
0.	66.0	8.0	-738.00	960.00	2620.00	559.00	208.00	20.	760.
0.	66.0	7.0	-828.00	593.00	2620.00	415.00	201.00	20.	760.
0.	66.0	6.0	-740.00	496.00	1840.00	349.00	184.00	20.	760.
0.	66.0	5.0	-658.00	419.00	1010.00	292.00	152.00	20.	760.
0.	66.0	4.0	-582.00	324.00	1090.00	244.00	135.00	20.	760.
0.	66.0	3.0	-726.00	277.00	980.00	209.00	118.00	20.	760.
0.	66.0	2.0	-970.00	228.00	816.00	179.00	108.00	20.	760.
0.	66.0	1.0	-1120.00	210.00	720.00	176.00	107.00	20.	760.
0.	66.0	0.0	-1650.00	199.00	636.00	168.00	93.80	20.	760.
0.	66.0	-1.0	-2620.00	183.00	680.00	168.00	92.10	20.	760.
0.	66.0	-2.0	21190.00	183.00	682.00	167.00	99.00	20.	760.
0.	66.0	-3.0	3600.00	205.00	674.00	181.00	104.00	20.	760.
0.	66.0	-4.0	1240.00	205.00	825.00	208.00	115.00	20.	760.
0.	66.0	-5.0	1090.00	240.00	894.00	246.00	133.00	20.	760.
0.	66.0	-6.0	1280.00	241.00	1190.00	261.00	139.00	20.	760.
0.	66.0	-7.0	1170.00	323.00	1090.00	325.00	160.00	20.	760.
0.	66.0	-8.0	1330.00	391.00	1440.00	379.00	182.00	20.	760.
0.	66.0	-9.0	1300.00	428.00	1680.00	447.00	198.00	20.	760.
0.	66.0	-10.0	1660.00	558.00	2110.00	589.00	220.00	20.	760.
0.	66.0	-11.0	1380.00	648.00	2990.00	777.00	261.00	20.	760.
0.	66.0	-12.0	1740.00	980.00	2500.00	1030.00	259.00	20.	760.
0.	66.0	-13.0	2000.00	1350.00	2590.00	1400.00	277.00	20.	760.
0.	66.0	-14.0	3280.00	1700.00	4830.00	1960.00	304.00	20.	760.
0.	66.0	-15.0	3440.00	1910.00	6800.00	2480.00	309.00	20.	760.
0.	66.0	-20.0	20400.00	10600.00	9380.00	6520.00	341.00	20.	760.
0.	66.0	-25.0	194400.00	13500.00	12000.00	13800.00	345.00	20.	760.

Table II-B-12. COMPUTER REDUCED DATA FOR THE AXIAL BURNER WITH THE ASTM FLOW NOZZLE AT THE 25.4-cm AXIAL POSITION

AXIAL BURNER WITH SURFACE COMBUSTION NOZZLE - COLD MODEL

RESULTS

AP	RP	FI	DELTA	RHO	V	VX	VY	VZ	VT	VR	PST	T	PB
25.4	25.0	17.6	73.7	0.0000159	3.73	3.55	0.31	1.08	1.07	0.34	0.002699	20.	760.
25.4	20.0	15.3	86.3	0.0000159	3.62	3.49	0.06	0.95	0.90	0.31	0.002669	20.	760.
25.4	15.0	19.0	91.7	0.0000159	3.57	3.37	-0.03	1.16	1.00	0.59	0.002693	20.	760.
25.4	10.0	63.1	185.0	0.0000159	6.83	3.08	-6.07	-0.53	1.19	5.97	0.003177	20.	760.
25.4	9.0	43.3	180.9	0.0000159	9.38	6.81	-6.44	-0.10	2.26	6.03	0.003210	20.	760.
25.4	8.0	11.2	11.4	0.0000159	16.63	16.31	3.18	0.64	2.74	1.73	0.002527	20.	760.
25.4	7.0	7.3	10.4	0.0000159	22.46	22.28	2.83	0.52	2.60	1.22	0.002549	20.	760.
25.4	6.0	6.0	356.4	0.0000159	28.31	28.15	2.96	-0.18	2.71	1.21	0.001588	20.	760.
25.4	5.0	3.9	1.1	0.0000159	31.62	31.55	2.20	0.04	2.07	0.73	0.003822	20.	760.
25.4	4.0	2.4	28.4	0.0000159	33.65	33.62	1.27	0.69	1.39	0.38	0.002604	20.	760.
25.4	3.0	2.7	68.1	0.0000159	33.37	33.33	0.59	1.49	1.48	0.60	0.002987	20.	760.
25.4	2.0	3.3	80.3	0.0000159	33.61	33.55	0.33	1.96	1.59	1.19	0.002738	20.	760.
25.4	1.0	3.4	56.2	0.0000159	33.15	33.09	1.09	1.63	1.08	1.64	0.002451	20.	760.
25.4	0.0	3.0	50.4	0.0000159	36.83	36.78	1.26	1.52	0.00	1.98	0.002877	20.	760.
25.4	-1.0	3.6	45.8	0.0000159	37.81	37.73	1.68	1.73	-1.26	2.05	0.001952	20.	760.
25.4	-2.0	2.2	133.6	0.0000159	34.96	34.93	-0.95	1.00	-1.23	0.62	0.002114	20.	760.
25.4	-3.0	0.6	231.7	0.0000159	32.27	32.26	-0.22	-0.28	-0.36	0.03	0.003223	20.	760.
25.4	-4.0	0.5	82.5	0.0000159	33.22	33.22	0.04	0.32	-0.32	0.02	0.002779	20.	760.
25.4	-5.0	1.5	106.9	0.0000159	32.98	32.97	-0.26	0.85	-0.89	0.12	0.002599	20.	760.
25.4	-6.0	4.5	121.6	0.0000159	30.37	30.28	-1.25	2.02	-2.26	0.75	0.001985	20.	760.
25.4	-7.0	6.8	139.8	0.0000159	26.52	26.33	-2.43	2.04	-2.91	1.27	0.002261	20.	760.
25.4	-8.0	8.9	145.8	0.0000159	21.62	21.36	-2.78	1.88	-3.00	1.50	0.002343	20.	760.
25.4	-9.0	13.1	149.7	0.0000159	16.41	15.98	-3.23	1.88	-3.12	2.06	0.002550	20.	760.
25.4	-10.0	13.8	128.1	0.0000159	12.19	11.84	-1.80	2.29	-2.47	1.55	0.002566	20.	760.
25.4	-15.0	10.3	69.8	0.0000159	3.87	3.81	0.23	0.65	-0.66	0.20	0.002744	20.	760.
25.4	-20.0	16.6	74.9	0.0000159	3.91	3.74	0.29	1.08	-1.04	0.39	0.002795	20.	760.
25.4	-25.0	3.2	26.0	0.0000159	4.16	4.15	0.21	0.10	-0.23	0.01	0.002728	20.	760.
25.4	-11.0	20.7	175.2	0.0000159	6.83	6.39	-2.41	0.19	-1.82	1.59	0.002682	20.	760.
25.4	-12.0	24.8	113.9	0.0000159	6.19	5.62	-1.05	2.37	-1.85	1.82	0.002717	20.	760.
25.4	-13.0	17.1	121.5	0.0000159	4.89	4.67	-0.75	1.22	-1.23	0.74	0.002721	20.	760.

Table II-B-13. COMPUTER REDUCED DATA FOR THE AXIAL BURNER WITH THE ASTM FLOW NOZZLE AT THE 45.7-cm AXIAL POSITION

AXIAL BURNER WITH SURFACE COMBUSTION NOZZLE - COLD MODEL

RESULTS

AP	RP	FI	DELTA	RHO	V	VX	VY	VZ	VT	VR	PST	T	PB
45.7	25.0	17.1	67.8	0.0000159	4.74	4.53	0.52	1.29	1.22	0.68	0.002680	20.	760.
45.7	20.0	15.3	70.4	0.0000159	4.83	4.66	0.42	1.20	1.08	0.67	0.002661	20.	760.
45.7	15.0	16.3	63.4	0.0000159	4.74	4.55	0.59	1.19	0.99	0.88	0.002771	20.	760.
45.7	14.0	10.2	48.7	0.0000159	5.16	5.08	0.60	0.68	0.78	0.46	0.002787	20.	760.
45.7	13.0	5.3	16.6	0.0000159	5.79	5.77	0.51	0.15	0.51	0.16	0.002780	20.	760.
45.7	12.0	8.0	11.5	0.0000159	7.27	7.20	0.99	0.20	0.89	0.48	0.002755	20.	760.
45.7	11.0	10.5	355.9	0.0000159	8.76	8.61	1.60	-0.11	1.26	0.98	0.002713	20.	760.
45.7	10.0	11.9	15.8	0.0000159	12.21	11.95	2.42	0.68	1.81	1.74	0.002479	20.	760.
45.7	9.0	11.3	4.2	0.0000159	15.17	14.87	2.98	0.22	2.09	2.13	0.002482	20.	760.
45.7	8.0	10.4	13.5	0.0000159	18.23	17.93	3.23	0.77	2.28	2.41	0.002459	20.	760.
45.7	7.0	7.5	14.8	0.0000159	21.09	20.91	2.66	0.70	2.09	1.80	0.002506	20.	760.
45.7	6.0	5.8	14.9	0.0000159	26.51	26.37	2.62	0.70	2.13	1.67	0.001179	20.	760.
45.7	5.0	5.0	13.0	0.0000159	27.25	27.14	2.35	0.54	1.87	1.52	0.002079	20.	760.
45.7	4.0	3.6	27.0	0.0000159	30.47	30.41	1.73	0.88	1.57	1.15	0.001912	20.	760.
45.7	3.0	3.1	34.7	0.0000159	30.74	30.69	1.38	0.95	1.29	1.07	0.001769	20.	760.
45.7	2.0	2.8	45.5	0.0000159	31.74	31.70	1.11	1.14	1.04	1.20	0.001920	20.	760.
45.7	1.0	2.5	50.1	0.0000159	32.57	32.54	0.94	1.12	0.64	1.32	0.002128	20.	760.
45.7	0.0	2.9	45.6	0.0000159	33.62	33.58	1.19	1.22	0.00	1.70	0.002185	20.	760.
45.7	-1.0	2.1	79.0	0.0000159	33.96	33.94	0.23	1.23	-0.63	1.07	0.003067	20.	760.
45.7	-2.0	2.4	97.1	0.0000159	33.24	33.21	-0.17	1.42	-1.02	1.01	0.003048	20.	760.
45.7	-3.0	2.1	104.4	0.0000159	32.78	32.76	-0.30	1.19	-1.07	0.61	0.001513	20.	760.
45.7	-4.0	2.4	127.7	0.0000159	31.42	31.39	-0.81	1.04	-1.19	0.57	0.001972	20.	760.
45.7	-5.0	3.2	131.5	0.0000159	28.85	28.81	-1.06	1.20	-1.43	0.73	0.002011	20.	760.
45.7	-6.0	3.6	134.9	0.0000159	27.46	27.41	-1.25	1.25	-1.58	0.78	0.001582	20.	760.
45.7	-7.0	4.6	142.6	0.0000159	24.32	24.24	-1.55	1.18	-1.73	0.91	0.002398	20.	760.
45.7	-8.0	6.6	151.8	0.0000159	20.75	20.61	-2.13	1.14	-2.01	1.34	0.002421	20.	760.
45.7	-9.0	5.7	157.5	0.0000159	18.75	18.66	-1.75	0.72	-1.68	0.86	0.002079	20.	760.
45.7	-10.0	7.6	152.7	0.0000159	15.92	15.78	-1.88	0.96	-1.80	1.10	0.002233	20.	760.
45.7	-11.0	6.9	159.2	0.0000159	13.71	13.61	-1.54	0.58	-1.47	0.74	0.002227	20.	760.
45.7	-12.0	12.6	142.3	0.0000159	9.89	9.65	-1.71	1.32	-1.64	1.40	0.002644	20.	760.
45.7	-13.0	8.1	138.6	0.0000159	8.87	8.78	-0.94	0.82	-1.12	0.56	0.002740	20.	760.
45.7	-14.0	8.7	140.4	0.0000159	7.98	7.88	-0.93	0.77	-1.08	0.54	0.002634	20.	760.
45.7	-15.0	8.5	124.5	0.0000159	5.14	5.09	-0.43	0.63	-0.69	0.32	0.002749	20.	760.
45.7	-20.0	11.9	75.2	0.0000159	3.75	3.66	0.19	0.75	-0.69	0.33	0.002830	20.	760.
45.7	-25.0	16.2	58.2	0.0000159	4.37	4.20	0.64	1.04	-1.08	0.57	0.002856	20.	760.

Table II-B-14. COMPUTER REDUCED DATA FOR THE AXIAL BURNER WITH THE ASTM FLOW NOZZLE AT THE 66.0-cm AXIAL POSITION

AXIAL BURNER WITH SURFACE COMBUSTION NOZZLE - COLD MODEL

RESULTS

AP	RP	FI	DELTA	RHO	V	VX	VY	VZ	VT	VR	PST	T	PB
66.0	25.0	11.5	64.5	0.0000159	5.15	5.04	0.44	0.92	0.90	0.48	0.002556	20.	760.
66.0	20.0	24.3	51.1	0.0000159	4.10	3.73	1.05	1.31	0.94	1.40	0.002051	20.	760.
66.0	15.0	17.1	19.1	0.0000159	6.16	5.89	1.71	0.59	1.07	1.46	0.002592	20.	760.
66.0	14.0	10.1	19.7	0.0000159	7.38	7.27	1.22	0.44	0.99	0.83	0.002489	20.	760.
66.0	13.0	11.7	0.6	0.0000159	8.94	8.75	1.82	0.02	1.25	1.32	0.002511	20.	760.
66.0	12.0	10.7	3.7	0.0000159	9.07	8.91	1.69	0.11	1.17	1.22	0.002419	20.	760.
66.0	11.0	8.9	6.5	0.0000159	11.52	11.38	1.79	0.20	1.30	1.24	0.002368	20.	760.
66.0	10.0	9.6	6.7	0.0000159	13.79	13.59	2.30	0.27	1.53	1.73	0.002390	20.	760.
66.0	9.0	8.4	8.2	0.0000159	15.82	15.65	2.30	0.33	1.57	1.71	0.002308	20.	760.
66.0	8.0	9.2	15.7	0.0000159	17.70	17.46	2.74	0.77	1.69	2.28	0.002334	20.	760.
66.0	7.0	6.1	17.5	0.0000159	20.41	20.30	2.09	0.66	1.53	1.56	0.001627	20.	760.
66.0	6.0	6.0	21.9	0.0000159	22.10	21.97	2.16	0.87	1.51	1.77	0.001518	20.	760.
66.0	5.0	6.6	33.0	0.0000159	23.73	23.57	2.29	1.49	1.49	2.29	0.002073	20.	760.
66.0	4.0	5.7	28.0	0.0000159	26.45	26.32	2.34	1.25	1.36	2.27	0.001792	20.	760.
66.0	3.0	4.3	36.5	0.0000159	28.03	27.95	1.72	1.27	1.09	1.85	0.002117	20.	760.
66.0	2.0	3.5	49.9	0.0000159	30.04	29.99	1.20	1.43	0.81	1.68	0.001942	20.	760.
66.0	1.0	3.6	57.2	0.0000159	30.53	30.47	1.04	1.62	0.44	1.87	0.001796	20.	760.
66.0	0.0	3.5	68.9	0.0000159	30.97	30.91	0.69	1.79	0.00	1.92	0.002869	20.	760.
66.0	-1.0	3.3	75.4	0.0000159	31.51	31.46	0.45	1.76	-0.46	1.76	0.002788	20.	760.
66.0	-2.0	3.0	91.8	0.0000159	31.24	31.20	-0.05	1.67	-0.82	1.45	0.002172	20.	760.
66.0	-3.0	3.4	100.6	0.0000159	29.50	29.44	-0.33	1.76	-1.07	1.44	0.002546	20.	760.
66.0	-4.0	3.8	123.6	0.0000159	28.17	28.11	-1.04	1.56	-1.26	1.39	0.002257	20.	760.
66.0	-5.0	4.4	129.3	0.0000159	25.72	25.64	-1.27	1.55	-1.39	1.45	0.002162	20.	760.
66.0	-6.0	3.8	132.9	0.0000159	25.61	25.55	-1.16	1.25	-1.37	1.01	0.001873	20.	760.
66.0	-7.0	5.2	132.9	0.0000159	22.05	21.96	-1.36	1.46	-1.51	1.30	0.002312	20.	760.
66.0	-8.0	5.0	137.2	0.0000159	20.28	20.20	-1.31	1.21	-1.44	1.06	0.002158	20.	760.
66.0	-9.0	5.4	142.2	0.0000159	18.93	18.84	-1.43	1.10	-1.47	1.04	0.002144	20.	760.
66.0	-10.0	5.7	141.8	0.0000159	16.50	16.41	-1.28	1.01	-1.36	0.90	0.002327	20.	760.
66.0	-11.0	7.6	155.2	0.0000159	14.65	14.52	-1.76	0.81	-1.51	1.21	0.002100	20.	760.
66.0	-12.0	10.0	145.1	0.0000159	11.96	11.77	-1.71	1.19	-1.49	1.46	0.002708	20.	760.
66.0	-13.0	13.2	142.3	0.0000159	9.97	9.70	-1.81	1.40	-1.46	1.76	0.002821	20.	760.
66.0	-14.0	9.5	145.8	0.0000159	8.93	8.80	-1.22	0.83	-1.15	0.91	0.002620	20.	760.
66.0	-15.0	10.1	153.1	0.0000159	8.20	8.07	-1.29	0.65	-1.13	0.89	0.002665	20.	760.
66.0	-20.0	15.3	114.6	0.0000159	4.14	3.99	-0.45	0.99	-0.81	0.73	0.002754	20.	760.
66.0	-25.0	19.9	93.5	0.0000159	3.33	3.13	-0.06	1.13	-0.82	0.78	0.002770	20.	760.

APPENDIX II-C. Investigation of Velocity Measurement Dependence on Five-Hole Pitot Probe Orientation

We completed an investigation to determine if the experimentally determined velocities depend on the orientation of the multidirectional impact tube's (MDIT) sensing head of the probe, relative to the air jet. The MDIT's sensing head or probe tip was placed at a position in the swirl burner's air stream, where we already knew that the direction of flow was at an approximate angle of 45 degrees to the axis of the burner. This position was 1 inch from the burner wall and 3 inches out, radially, from the burner axis. We collected data at this point in the test chamber with the probe rotated 0, 45, and 90 degrees relative to the burner axis, with 45 degrees being the approximate known direction of flow. Since the MDIT probe head can measure the velocity and direction of a stream so long as the stream approaches it from a direction less than ±60 degrees from the probe head axis, the values of velocity and flow direction obtained at the three rotational probe positions should be the same.

Table II-C-1 shows the results of these measurements. The error introduced by the position of the MDIT head relative to the direction of flow is about ±5%.

Table II-C-1. VELOCITY ANALYSIS FOR VARIOUS PROBE ORIENTATIONS RELATIVE TO A FIXED DIRECTION OF FLOW

	Rotational Orientation, degrees		
	0	45	90
Velocity, V, ft/s	20.8	22.1	20.8
Conical Angle, φ	43°49'	45°04'	41°36'
Dihedral Angle, δ	76°06'	75°03'	70°28'
V_x, ft/s	15.9	15.3	15.1
V_y, ft/s	3.2	4.3	5.9
V_z, ft/s	14.1	15.2	12.9

Care must be taken in calculating the values as presented in Table II-C-1. They are relative to the coordinate system of the burner, shown in Figure II-C-1; however, the raw data obtained from the sensing head are relative to the coordinate system of the head itself, also shown in

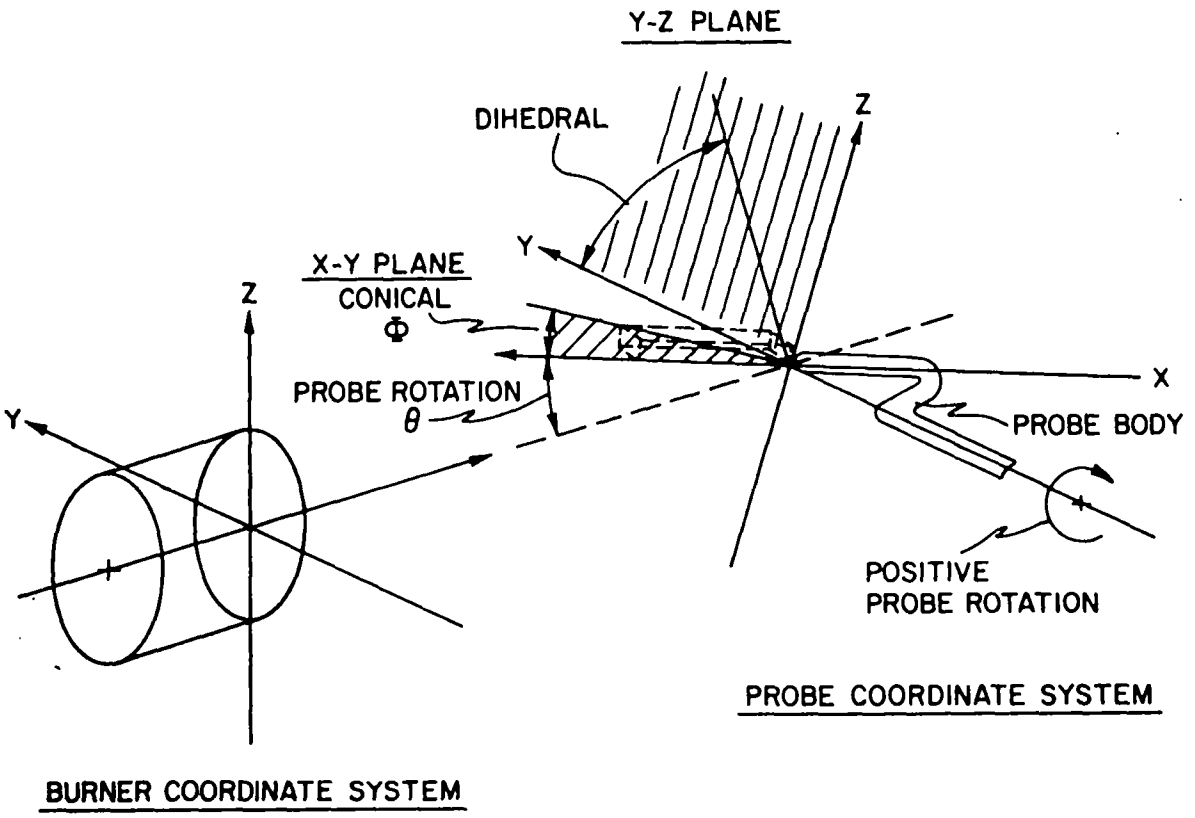

Figure II-C-1. BURNER AND PROBE COORDINATE SYSTEMS

Figure II-C-1. Therefore, the raw data must be related to the burner's coordinate system before any analysis is made. For a rotational orientation of the probe other than zero degrees, the raw data are translated from the probe to the burner coordinate system by the transformation Equations II-C-1, II-C-2, II-C-3, and II-C-4.

$$V_x = V_x' \cos\theta - V_z' \sin\theta \qquad \text{(II-C-1)}$$

$$V_z = V_z' \cos\theta + V_x' \sin\theta = V \sin\theta \sin\nu \qquad \text{(II-C-2)}$$

$$\Phi \text{ (conical angle)} = \cos^{-1}\frac{V_x}{V} \qquad \text{(II-C-3)}$$

$$\nu \text{ (dihedral angle)} = \sin^{-1}\frac{V_z}{V \sin\Phi} \qquad \text{(II-C-4)}$$

where –

V_x, V_z = velocities relative to the burner coordinate system, ft/s

V_x', V_z' = velocities relative to the probe head coordinate system, ft/s

APPENDIX II-D. Method of Calculating Swirl Number

In swirling free jets or flames both the axial flux of the angular momentum, G_s, and of the linear momentum, G_x, are conserved. G_s and G_x are expressed by Equations II-D-1 and II-D-2:

$$G_x = \int_{r_1}^{r_2} V_x \rho V_x 2\pi r dr + \int_0^{r_0} P 2\pi r dr \qquad \text{(II-D-1)}$$

$$G_s = \int_{r_1}^{r_2} V_t r^2 \rho V_x 2\pi dr \qquad \text{(II-D-2)}$$

where V_x, V_t, V_r, and P are the axial, tangential, and radial components of the velocity and static pressure in a jet enclosed by an annular disk of outer radius, r_2, and inner radius, r_1. Since both of these momentum fluxes are characteristics of the aerodynamic behavior of the jet, a nondimensional characteristic based on these quantities is used as a criterion of swirl intensity, defined as —

$$S = \frac{G_s}{G_x R_2} \qquad \text{(II-D-3)}$$

To define V_t, the tangential velocity, in terms of the quantities measured by the multidirectional impact tube, the geometrical scheme shown in Figure II-D-1 was used. The angle Φ corresponds to the measured conical angle, x is the distance of the sensing head from the burner wall, and r_0 is the radius of the burner. From geometrical arguments, which can be directly deduced from Figure II-D-1, the tangential velocity is shown to be —

$$V_t = V \sin \Phi \sin \varphi = \frac{V r_0 \sin \Phi \cos \Phi}{\sqrt{r_0^2 \cos^2 \Phi + X^2 \sin^2 \Phi}} \qquad \text{(II-D-4)}$$

The radial velocity equals —

$$V_r = V \sin \Phi \cos \varphi = \frac{V r_0 \sin^2 \Phi}{\sqrt{r_0^2 \cos^2 \Phi + X^2 \sin^2 \Phi}} \qquad \text{(II-D-5)}$$

These equations were first presented by Thring.[2] All the quantities needed to determine the swirl can be measured.

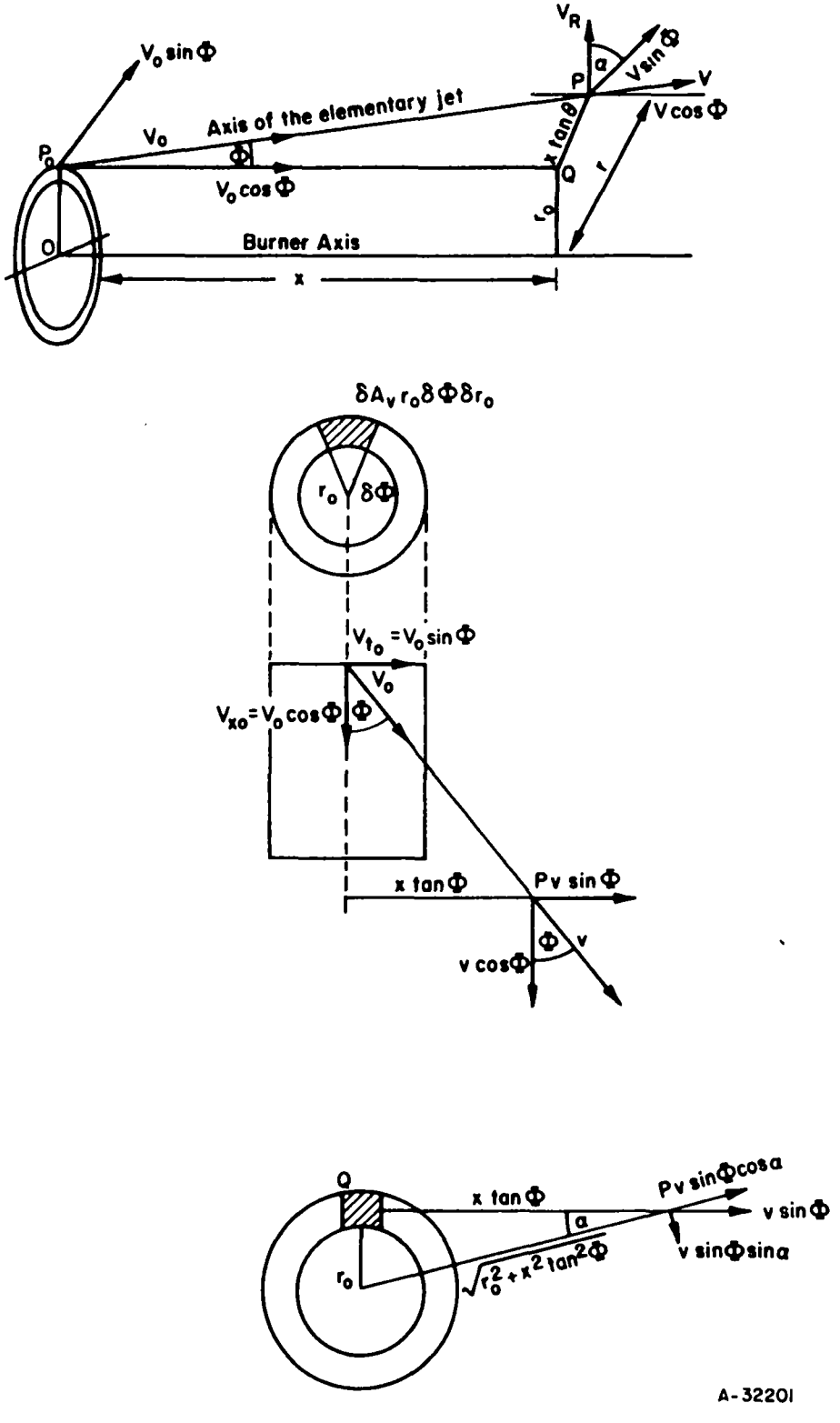

Figure II-D-1. GEOMETRIC RELATIONS DESCRIBING DEFINITION OF TANGENTIAL AND RADIAL VELOCITY

In a paper published by Beer and Leuckel,[1] the swirl number, S, is calculated from the input velocity distribution in the swirl generator rather than from the velocity distribution in the jet. Thus, the static pressure term is omitted and a good approximation of the swirl number is —

$$S' = \frac{G_s}{G_x' R_2} \qquad \text{(II-D-6)}$$

where

$$G_x' = 2\pi \int_{r_1}^{r_2} \rho (V_x')^2 \, r dr \qquad \text{(II-D-7)}$$

and V_x' represents the axial velocity in the swirl generator. Using this approximation, they derived the following general relationship for the swirl number, S', of flow through a cylindrical or annular duct attached to a movable-block swirler:

$$S' = \sigma \frac{R}{2\beta} \left[1 - \left(\frac{R_h}{R}\right)^2\right] \qquad \text{(II-D-8)}$$

The dimensionless coefficient, σ, can be interpreted as the ratio of the average tangential and radial velocity components at the swirler exit. β is the channel width in the axial direction, R is the radius of the throat of the burner, and R_h is the inner radius of the air duct at the throat of the burner. The values for these parameters used in the movable-block-type swirl generator are shown in Figure II-178 of the text. For the movable-block swirler the coefficient as a function of the swirler adjustment $\xi / \xi m$, where ξ is the angle of adjustment of the swirler ($0 < \xi < \xi m$), is shown in Figure II-178.

Table II-D-1 compares the swirl numbers for our burner and operating conditions as calculated from experimental data, from the semi-empirical equations of Beer and Leuckel,[1] and from the values obtained by the International Flame Research Foundation and published in IFRF Document No. G01/9/18. The agreement between the three sources is quite good.

Table II-D-1. COMPARISON OF SWIRL NUMBERS CALCULATED FOR SWIRL BURNER WITH INTERMEDIATE VANE SETTING AND 28 ft/s THROAT VELOCITY

Method	Swirl Number, S
IGT Experimental	0.82
Beer and Leuckel	0.78
IFRF Measured*	0.79

References Cited

1. Beer, J. M. and Leuckel, W., "Turbulent Flames in Rotating Flow Systems." Paper No. F-NAFTC-7 presented at the North American Fuel Technology Conference, Ottawa, Canada, May 31-June 3, 1970.

2. Thring, M. W., "Study of Burners With Air Vortex," Riv. Combust. 24, 53-59 (1970) February (Italian text with English summary).

* Corrected for small-dimensional differences between IFRF and IGT burners.

APPENDIX II-E. Computer Program for Data Transformation and Plotting Tracer-Gas Mixing Results

Table II-E-1

```
// JOB T

LOG DRIVE   CART SPEC   CART AVAIL  PHY DRIVE
  0000        0001        0001        0000
                          2801        0001
                          2603        0002

V2 M10   ACTUAL 16K  CONFIG 16K

// FOR
*ONE WORD INTEGERS
*EXTENDED PRECISION
*LIST SOURCE PROGRAM
      SUBROUTINE CUFIH(C,X,Y,N,M)
C      MARCH 28,1972
C     N = ORDER OF FIT
C     M = NUMBER OF DATA POINTS
C     C = COEFFICIENTS
C     X = INDEPENDENT VARIABLE
C     Y = DEPENDENT   VARIABLE      Y=C(1)+C(2)*X+...+C(N+1)*X**N
      DIMENSION C(10),X(100),Y(100),A(10,10)
      IOUT = 5
      DO 155 I=1,10
      C(I)=0.0
  155 CONTINUE
      L = N+1
      IF(L-10)157,157,156
  156 CALL EXIT
  157 CONTINUE
      LL= N+2
      DO 8 J=1,L
      DO 8 K=1,LL
    8 A(J,K) = C.0
      DO 12 I=1,M
      DO 11 J=1,L
      DO 10 K=1,L
   10 A(J,K) = A(J,K)+ X(I)**(J+K-2)
   11 A(J,LL)= A(J,LL)+X(I)**(J-1)*Y(I)
   12 CONTINUE
      A(1,1)=M
      A(1,LL)=0.0
      DO 114 I=1,M
  114 A(1,LL)=A(1,LL)+Y(I)
      DO 13 I=1,L
      C(I) = A(I,LL)
   13 CONTINUE
      I = 0
  105 I = I+1
  106 J = I
      DD = A(I,J)
      IF(A(I,J))120,107,120
  107 IF(J-L)108,150,108
  108 K = I
  109 IF(A(K+1,J))111,110,111
  110 K = K+1
      IF(J-L)109,150,109
  111 DO 121 J=1,L
```

Table II-E-2

```
  121 A(K,J) = A(K,J)+A(K+1,J)
      C(K) = C(K)+C(K+1)
      GO TO 106
  120 DO 112 J=1,L
  112 A(I,J) = A(I,J)/DD
      C(I) = C(I)/DD
      DO 133 K=1,L
      IF(K-I)131,133,131
  131 AC = A(K,I)
      DO 115 J=1,L
  115 A(K,J) = A(K,J)-AC*A(I,J)
      C(K)= C(K)-AC*C(I)
  133 CONTINUE
      IF(I-L)105,150,105
  150 CONTINUE
      S = 0.0
      WRITE(IOUT,902)
      DO 18 I=1,M
      YZ=C(1)
      DO 16 J=2,L
   16 YZ = YZ+C(J)*X(I)**(J-1)
      D = YZ-Y(I)
      S = S+D*D
   18 WRITE (IOUT,900) Y(I),YZ,D
      VARY=S/(M-N-1)
      IF(VARY)303,304,304
  303 WRITE(IOUT,909)
      CALL EXIT
  304 SDY=VARY**0.5
      WRITE(IOUT,910)SDY
      WRITE(IOUT,901) (I,C(I),I=1,L)
      RETURN
  900 FORMAT(F7.2,6X,F7.2,6X,F8.5)
  901 FORMAT( /48H COEFFICIENTS FOR Y= C(1)+C(2)*X+...+C(N+1)*X**N
     1( 3H C(I2,2H)= F9.4))
  902 FORMAT(/11H Y OBSERVED,2X,10HY COMPUTED,3X, 10HDIFFERENCE)
  909 FORMAT(' NEGATIVE VARIANCE')
  910 FORMAT(' SD Y='E13.5)
      END

FEATURES SUPPORTED
 ONE WORD INTEGERS
 EXTENDED PRECISION

CORE REQUIREMENTS FOR COFIH
 COMMON       0  VARIABLES    332  PROGRAM     812

RELATIVE ENTRY POINT ADDRESS IS 01AA (HEX)

END OF COMPILATION

// DUP

*STORE       WS  UA  COFIH
CART ID 0001   DB ADDR  4202   DB CNT   0036

// FOR
```

Table II-E-3

```
C       MARCH 28,1972
        DIMENSION MARK(200)
        DIMENSION X(200),CON(200),ID(40)
        DIMENSION CF(10),XCF(100),YCF(100)
        DATA ISTAR/'*'/
        CALL OVERFL(IOVFL)
        CALL DVCHK(IDVCK)
    5   CONTINUE
        INPUT=2
        IOUT=5
        READ(INPUT,902)ID
        WRITE(IOUT,905)ID
        INDEX=0
        XCF(1)=0.0
        YCF(1)=0.0
        XCF(2)=.291
        YCF(2)=125.
        XCF(3)=.55
        YCF(3)=250.
        XCF(4)=.79
        YCF(4)=375.
        XCF(5)=1.
        YCF(5)=500.
        M=5
        N=M-3
        CALL COFIH(CF,XCF,YCF,N,M)
        WRITE(IOUT,904)
    1   READ(INPUT,900) AP,RP,V
        IF(AP)500,20,2
    2   INDEX=INDEX+1
        IF(INDEX-200)3,3,500
    3   MARK(INDEX)=ISTAR
        X(INDEX)=RP
        CON(INDEX)=CF(1)+CF(2)*V+CF(3)*V*V+CF(4)*V**3
        WRITE(IOUT,901)AP,RP,V,CON(INDEX)
        APST=AP
        GO TO 1
   20   WRITE(IOUT,903)ID
        WRITE(IOUT,909)APST
        CALL PTSE9(X,CON,MARK,INDEX)
        CALL OVERFL(IOVFL)
        GO TO(201,202,202),IOVFL
  201   WRITE(IOUT,908)
  202   CALL DVCHK(IDVCK)
        GO TO (201,203),IDVCK
  203   CONTINUE
        GO TO 5
  500   CALL EXIT
  900   FORMAT(10F8.3)
  901   FORMAT(F6.2,F8.2,F9.3,F9.2)
  902   FORMAT(40A2)
  903   FORMAT(1H1,/20X,40A2)
  904   FORMAT(/' EXPERIMENTAL RESULTS'/5H    AP,5X,2HRP,7X,4HX(V),5X,2HCO)
  905   FORMAT(1H1,25X,'TRACER GAS STUDIES OF COMBUSTION BURNERS'/20X40A2)
  908   FORMAT(' OVERFLOW OR DIVISION BY ZERO')
  909   FORMAT(10H RP VS. CO ,3X,3HAP=F6.2)
        END
```